



**HAL**  
open science

# Ruthenium (II) and Manganese (I) Catalyzed Organic Transformations via Hydrogen Transfer Reactions

Akash Kaithal

► **To cite this version:**

Akash Kaithal. Ruthenium (II) and Manganese (I) Catalyzed Organic Transformations via Hydrogen Transfer Reactions. Catalysis. Université de Lyon; Rheinisch-westfälische technische Hochschule (Aix-la-Chapelle, Allemagne), 2020. English. NNT: 2020LYSE1069 . tel-03210491

**HAL Id: tel-03210491**

**<https://theses.hal.science/tel-03210491>**

Submitted on 28 Apr 2021

**HAL** is a multi-disciplinary open access archive for the deposit and dissemination of scientific research documents, whether they are published or not. The documents may come from teaching and research institutions in France or abroad, or from public or private research centers.

L'archive ouverte pluridisciplinaire **HAL**, est destinée au dépôt et à la diffusion de documents scientifiques de niveau recherche, publiés ou non, émanant des établissements d'enseignement et de recherche français ou étrangers, des laboratoires publics ou privés.

N°d'ordre NNT : 2020LYSE1069

# **THESE de DOCTORAT DE L'UNIVERSITE DE LYON**

opérée au sein de

**l'Université Claude Bernard Lyon 1**

**Ecole Doctorale de Lyon**

**N° ED206**

**Spécialité de doctorat : Chimie**

**Discipline : Chimie Industrielle Durable**

Soutenue publiquement le 27/04/2020, par:

**Akash Kaithal**

---

## **Ruthenium(II) and Manganese(I) Catalyzed Organic Transformations via Hydrogen Transfer Reactions**

---

Devant le jury composé de:

Prof. Carmen Claver	<b>Rapporteur</b>	Université Rovira i Virgili Tarragona
Prof. David Cole-Hamilton	<b>Rapporteur</b>	Université de St Andrews (Royaume-Uni)
Prof. Carsten Bolm	<b>Rapporteur</b>	Université RWTH – Aachen
Dr. Hélène Bourbigou	<b>Examinatrice</b>	IFPEN - Solaize
Prof. Regina Palkovits	<b>Examinatrice</b>	Université RWTH – Aachen
Prof. Bruno Andrioletti	<b>Examineur</b>	Université Lyon 1 UMR 5246 - ICBMS
Prof. Dieter Vogt	<b>Examineur</b>	Université Technique de Dortmund
Prof. Walter Leitner	<b>Directeur de thèse</b>	Université RWTH – Aachen
Dr. Elsje Quadrelli	<b>Directrice de thèse</b>	CNRS Lyon UMR 5265 – C2P2
Dr. Clément Camp	<b>Invité</b>	CNRS Lyon UMR 5265 – C2P2

# UNIVERSITE CLAUDE BERNARD - LYON 1

Président de l'Université	M. Frédéric FLEURY
Président du Conseil Académique	M. Hamda BEN HADID
Vice-président du Conseil d'Administration	M. Didier REVEL
Vice-président du Conseil Formation et Vie Universitaire	M. Philippe CHEVALIER
Vice-président de la Commission Recherche	M. Fabrice VALLÉE
Directeur Général des Services	M. Damien VERHAEGHE

## **COMPOSANTES SANTE**

Faculté de Médecine Lyon-Est-Claude Bernard	Doyen : M. Gilles RODE
Faculté de Médecine et de Maïeutique Lyon Sud – Charles Mérieux	Doyenne: Mme Carole BURILLON
Faculté d'Odontologie	Doyenne Mme Dominique SEUX
Institut des Sciences Pharmaceutiques et Biologiques	Directrice : Mme Christine VINCIGUERRA
Institut des Sciences et Techniques de la Réadaptation	Directeur : M. Xavier PERROT
Département de formation et Centre de Recherche en Biologie Humaine	Directeur : Mme Anne-Marie SCHOTT

## **COMPOSANTES ET DEPARTEMENTS DE SCIENCES ET TECHNOLOGIE**

UFR Biosciences	Directrice : Mme Kathrin GIESELER
Département Génie Electrique et des Procédés (GEP)	Directrice : Mme Rosaria FERRIGNO
Département Informatique	Directeur : M. Behzad SHARIAT
Département Mécanique	Directeur : M. Marc BUFFAT
UFR - Faculté des Sciences	Administrateur Provisoire : M. Bruno ANDRIOLETTI
UFR (STAPS)	Directeur : M. Yannick VANPOULLE
Observatoire de Lyon	Directeur : Mme Isabelle DANIEL
Ecole Polytechnique Universitaire Lyon 1	Directeur : Emmanuel PERRIN
Ecole Supérieure de Chimie, Physique, Electronique (CPE Lyon)	Directeur : Bernard BIGOT
Institut Universitaire de Technologie de Lyon 1	Directeur : M. Christophe VITON
Institut de Science Financière et d'Assurances ESPE	Directeur : M. Nicolas LEBOISNE Administrateur Provisoire : M. Pierre CHAREYRON

# **Ruthenium(II) and Manganese(I) Catalyzed Organic Transformations via Hydrogen Transfer Reactions**

Von der Fakultät für Mathematik, Informatik und Naturwissenschaften der RWTH  
Aachen University zur Erlangung des akademischen Grades eines  
Doktors der Naturwissenschaften genehmigte Dissertation

vorgelegt von

**Akash Kaithal, M.Sc.**

aus Kanpur, Indien

Berichter: *Prof. Dr. Walter Leitner*  
*Dr. Elsje Alessandra Quadrelli*

Tag der mündlichen Prüfung: 27/04/2020

Diese Dissertation ist auf den Internetseiten der Universitätsbibliothek verfügbar.





## DECLARATION

---

The present dissertation was written in the period from 2<sup>nd</sup> of October 2016 to 1<sup>st</sup> of October 2019 under the scientific guidance of Prof. Dr. Walter Leitner and Prof. Elsje Alessandra Quadrelli (Host supervisor: Dr Clément Camp) at the Institut für Technische und Makromolekulare Chemie (ITMC) der RWTH Aachen University (Home University) and Université Lyon 1, UMR5265 – C2P2 (CNRS, CPE Lyon, Université' Claude Bernard Lyon 1) (Host University), respectively. The whole project was funded by the European Doctoral Programme on Sustainable Industrial Chemistry (SINCHEM). The dissertation time-period was divided into two sections where the candidate stayed two and a half years in the home university (2<sup>nd</sup> October 2016 – 11<sup>th</sup> November 2018 and 14<sup>th</sup> May 2019 – 1<sup>st</sup> of October 2019) and six months (12<sup>th</sup> of November 2018 – 13<sup>th</sup> May 2019) in the host university.

## DECLARATION

I, Akash Kaithal, hereby declare that the investigation presented in the dissertation has been carried out by me. This dissertation was completed entirely in the above-mentioned time. If any part of this work was previously used for an academic degree or any other studies at present or other institutes, this was indicated and well-mentioned. All major sources of support have been designated. If the part of the dissertation was performed in collaboration with other groups or institutes, it is mentioned what the other groups have done. Parts of this dissertation are published and all the publications are mentioned in the text and in annexes.

**Akash Kaithal**



*To my parents*



## Abstract

The present dissertation focuses on new organic transformations enabled by hydrogen transfer reactions using Mn(I) and Ru(II) pincer complexes. The primary focus deals with the study of Mn(I) and Ru(II) complexes and their similar reactivity in hydrogen transfer reactions which includes hydrogen borrowing and reduction reactions.

Chapter 1 is a general introduction of hydrogen-transfer reactions reported for Mn(I) complexes and their similar reactivity with the Ru(II) complexes that are well-established for the hydrogen-transfer reactions.

Chapter 2 focuses on the utilization of MeOH as a C1 source for the synthesis of fine chemicals, pharmaceuticals and alternative fuels. The selective  $\beta$ -methylation of alcohols was achieved using methanol as a C1 source. Various ruthenium complexes were investigated for this transformation and a Ru-MACHO-BH pincer complex revealed the best catalytic results. Mechanistic studies and DFT calculations confirmed that the reaction proceeds via “Hydrogen borrowing pathways” and involved metal-ligand cooperation on the ruthenium metal center.

Chapter 3 also deals with the selective  $\beta$ -methylation of alcohols using methanol as a C1 source. However, in this chapter, earth-abundant and air-stable manganese pincer complexes were investigated. The reactivity of Mn(I) pincer complexes with Ru(II) pincer complexes was compared. Numerous manganese pincer complexes were synthesized and checked for this process where the Mn-MACHO-<sup>*i*</sup>Pr complex demonstrates the optimum results with high selectivity and high yield to the corresponding desired product.

Chapter 4 demonstrates the formation of substituted cycloalkanes using secondary alcohols or ketones and diols as initial substrates employing Mn-MACHO-<sup>*i*</sup>Pr complex as pre-catalyst. The reaction studies showed that the Mn-MACHO-<sup>*i*</sup>Pr complex revealed better reactivity in comparison to the Ru-MACHO-BH complex. Various substituted cycloalkane rings such as substituted cyclopentane, cyclohexane, and cycloheptane rings were synthesized employing the Mn-MACHO-<sup>*i*</sup>Pr complex. Mechanistic studies revealed that the reaction proceeds via “hydrogen borrowing pathways”.

Chapter 5 addresses the selective deuteration of primary and aliphatic alcohols using D<sub>2</sub>O as a deuterium source. The already established Mn-MACHO-*i*Pr complex was investigated for this transformation which showed selective deuterations of benzylic alcohols at the alpha positions and alpha and beta deuteration for aliphatic alcohols.

Chapter 6 deals with the selective hydrogenation of cyclic carbonates to the analogous methanol and diols. Several manganese pincer complexes were synthesized to confirm the activity towards this transformation. Air-stable Mn-MACHO-*i*Pr pincer complex showed the best catalytic activity with high turnover numbers and selective preparation to the corresponding methanol and diols.

Chapter 7 discusses the preparation of methoxy-borane and boronate-diols via selective reduction of cyclic and linear carbonates and CO<sub>2</sub> using pinacolborane as a reducing agent. A newly synthesized manganese pincer complex was explored for this process which revealed the high efficiency and selectivity towards this transformation.

## Zusammenfassung

Die vorliegende Dissertation befasst sich mit der Umsetzung neuer organischer Umwandlungen mittels Wasserstoff-Transfer-Reaktionen unter Verwendung von Mn(I)- und Ru(II)-Komplexen. Hauptaugenmerk liegt in der Untersuchung von Mn(I)- und Ru(II)-Komplexen und ihrem ähnlichen Reaktionsverhalten in Wasserstoff-Transfer-Reaktionen, sowie dem „Hydrogen Borrowing“-Konzept und Reduktions-Reaktionen.

Kapitel 1 gibt einen Überblick über den aktuellen Stand der Technik für Wasserstoff-Transfer-Reaktionen mit Mn(I)-Komplexen und ihrem ähnlichen Reaktionsverhalten zu Ru(II)-Komplexen, welche bereits für diese Reaktionen etabliert sind.

Kapitel 2 beschreibt die selektive  $\beta$ -Methylierung von Alkoholen unter Verwendung von Methanol als C1 Baustein für die Synthese von Feinchemikalien, Arzneimitteln und alternativen Brennstoffen. Verschiedene Ruthenium-Komplexe wurden für diese Reaktion getestet, wobei sich der Ru-MACHO-BH-Pincer-Komplex als der geeignetste Katalysator herausstellte. Mechanistische Untersuchungen und DFT-Computerrechnungen bestätigten, dass die Reaktion über „Hydrogen Borrowing“-Reaktionspfade und mit Metall-Ligand-Kooperationen am Ruthenium Metallcenter verläuft.

Kapitel 3 fokussiert ebenfalls auf die  $\beta$ -Methylierung von Alkoholen unter Verwendung von Methanol als C1 Baustein. Allerdings wurden luftstabile 3d-Übergangsmetall-Mangan-Pincer-Komplexe verwendet. Die Reaktivitäten der Mn(I)- und Ru(II)-Pincer-Komplexe wurden miteinander verglichen. Ausgewählte Mangan-Pincer-Komplexe wurden synthetisiert und in der Reaktion getestet, wobei der Mn-MACHO-<sup>i</sup>Pr-Komplex ausgezeichnete Ergebnisse mit höchster Selektivität und Ausbeute zum gewünschten Produkt aufwies.

Kapitel 4 stellt die Umsetzung von substituierten Cycloalkanen mit sekundären Alkoholen oder Ketonen und Diolen als Ausgangsstoffe dar. Dabei wurden die Ru-MACHO-BH- und Mn-MACHO-<sup>i</sup>Pr-Komplexe als Präkatalysatoren eingesetzt. Untersuchungen zeigten, dass der Mn-MACHO-<sup>i</sup>Pr-Komplex eine bessere Reaktivität aufwies als der Ru-MACHO-BH-Komplex. Unter Verwendung des Mn-MACHO-<sup>i</sup>Pr-Katalysators konnten verschieden substituierte Cycloalkane, wie substituierte Cyclopentane, Cyclohexane sowie Cycloheptane, synthetisiert



werden. Mechanistische Untersuchungen ergaben, dass die Reaktion über „Hydrogen Borrowing“-Reaktionswege verläuft.

In Kapitel 5 wird die selektive Deuterierung von primären, aliphatischen Alkoholen mit D<sub>2</sub>O als Deuteriumquelle herausgestellt. Der bereits etablierte Mn-MACHO-<sup>i</sup>Pr-Komplex wurde für die Reaktion untersucht und zeigte die selektive Deuterierung von Benzylalkohol an  $\alpha$ -Position, sowie die  $\alpha$ - und  $\beta$ -Deuterierungen bei aliphatischen Alkoholen.

Kapitel 6 erläutert die selektive Hydrierung von cyclischen Carbonaten zu den entsprechenden Diolen und Methanol. Ausgewählte Mangan Pincer Komplexe wurden synthetisiert und für die Reaktion getestet, wobei der luftstabile Mn-MACHO-<sup>i</sup>Pr Pincer Komplex die höchste katalytische Produktivität und Selektivität aufwies.

Das letzte Kapitel beschreibt die Herstellung von Methoxyboronatester mittels selektiver Reduktion von organischen, cyclischen und linearen Carbonaten, sowie CO<sub>2</sub> mit Pinakolboran als Reduktionsmittel. Ein neuer Mangan Pincer Komplex wurde entwickelt und ermöglicht die effiziente, selektive Umsetzung der Reaktion.

## Résumé

La dissertation suivante se focalise sur de nouvelles transformations organiques, à travers des transferts d'hydrogènes, en utilisant des complexes en tenaille Mn(I) et Ru(II). L'objectif principal est l'étude des complexes Mn(I) et Ru(II) et leur réactivité similaire lors des réactions de transferts d'hydrogènes, comprenant les réactions d'échanges d'hydrogènes et réductions.

Le chapitre 1 est une introduction générale sur les réactions de transferts d'hydrogènes reportées dans la littérature pour les complexes Mn(I) et leur réactivité similaire à celle des complexes Ru(II), connus pour leur capacité à réaliser des transferts d'hydrogènes.

Le chapitre 2 traite de l'utilisation de MeOH comme une source de carbone C1 pour la synthèse de produits de chimie fine, pharmaceutiques et carburants alternatifs. La  $\beta$ -méthylation sélective des alcools a été conduite avec succès en utilisant MeOH comme source de carbone C1. Différents complexes de ruthénium ont été investigués pour cette transformation et le complexe en tenaille Ru-MACHO-BH s'est révélé être le meilleur en termes de résultats catalytiques. Des études mécanistiques et calculs DFT ont confirmé la voie par transferts d'hydrogènes « Hydrogen Borrowing Reaction » et la coopération métal-ligand sur le centre métallique ruthénium.

Le chapitre 3, lui aussi, concerne la  $\beta$ -méthylation sélective des alcools à l'aide de MeOH comme source de carbone C1. Cependant, dans ce chapitre, les complexes étudiés sont des complexes en tenaille, stables à l'air, à base d'un métal abondant : le manganèse. La réactivité des deux complexes Mn(I) et Ru(II) a été comparée. De nombreux complexes de manganèse en tenaille ont été synthétisés et testés pour la  $\beta$ -méthylation sélective des alcools à l'aide de MeOH. Pour cette réaction, le complexe Mn-MACHO-<sup>i</sup>Pr a montré les meilleurs résultats avec d'excellentes sélectivités et de très bons rendements.

Le chapitre 4 démontre la formation de cycloalcanes substitués en utilisant des alcools secondaires ou des cétones ainsi que des diols comme réactifs de départ, avec les complexes Ru-MACHO-BH ou Mn-MACHO-<sup>i</sup>Pr comme pré-catalyseurs. L'analyse de ces réactions a mis en évidence la meilleure réactivité du complexe Mn-MACHO-<sup>i</sup>Pr en comparaison avec le complexe Ru-MACHO-BH. Différents cycloalcanes substitués comme des cyclopentanes, des cyclohexanes et des cycloheptanes ont été synthétisés avec ce complexe de manganèse. Des

études mécanistiques ont révélé que la réaction procède *via* transfert d'hydrogène « Hydrogen Borrowing reaction ».

Le chapitre 5 concerne la deutération sélective d'alcools primaires et aliphatiques en utilisant D<sub>2</sub>O comme source de deutérium et le complexe précédemment établi Mn-MACHO-<sup>i</sup>Pr comme catalyseur. Les analyses ont montré la deutération sélective d'alcools benzyliques en position alpha et la deutération d'alcools aliphatiques en position alpha et béta.

Le chapitre 6 concerne l'hydrogénation sélective de carbonates cycliques en méthanol et diols correspondants. Différents complexes de manganèse en tenaille ont été synthétisés pour confirmer l'activité envers cette transformation. Le complexe stable à l'air Mn-MACHO-<sup>i</sup>Pr a montré la meilleure activité catalytique avec des TON élevés ainsi qu'une très bonne sélectivité concernant la formation de méthanol et diols.

Le chapitre 7 traite de la préparation de méthoxy-boranes and boronate-diols *via* réduction sélective de carbonates organiques cycliques et linéaires, ainsi que du CO<sub>2</sub>, en utilisant le pinacolborane comme agent réducteur. Un nouveau complexe de manganèse en tenaille synthétisé a été exploré et a révélé une grande efficacité et sélectivité pour cette transformation.

**Table of Contents**

1. Motivation and structure of the thesis .....	1
1.1. Pincer complexes and their reactivity in hydrogen transfer reactions .....	1
1.2. Manganese(I) pincer complexes and their analogous reactivity compared to ruthenium(II) complexes .....	2
1.2.1. Diagonal relationship between Ru(II) and Mn(I) complexes .....	4
1.2.2. Catalyst activation, stability and hydride formation: Mn(I) vs Ru(II) pincer complexes .....	5
1.3. C–C bond formation via hydrogen transfer: Mn(I) versus Ru(II).....	7
1.4. Comparison of catalytic hydrogenation reaction: Mn(I) versus Ru(II) complexes .....	12
1.5. Conclusion and outlook.....	18
1.6. Structure of the thesis .....	20
References .....	23
2. Ruthenium catalyzed $\beta$ -methylation of alcohols using MeOH as a C1 source .....	27
2.1. Objective .....	33
2.2. Catalyst optimization.....	34
2.3. Temperature and base optimization .....	36
2.4. Ru-catalyzed $\beta$ -methylation of secondary aryl alcohols with MeOH.....	37
2.5. Ru-catalyzed $\beta$ -methylation of 2-arylethanol with MeOH.....	38
2.6. Ru-catalyzed $\beta$ -methylation of aliphatic alcohols with MeOH.....	39
2.7. Mechanistic studies .....	41
2.7.1. Conversion/time profile .....	41
2.7.2. Estimation of the Gibbs free energy of activation using the Eyring equation .....	43
2.7.3. Observation of <i>in situ</i> formed intermediates and labeling experiments.....	43
2.7.4. Stoichiometric reaction of Ru-MACHO-BH with alcohols.....	45
2.7.5. Computed catalytic cycle.....	46
2.8. Conclusion and Outlook.....	51
2.9. Experimental .....	51
2.9.1. General Experimental .....	51
2.9.2. General procedure for screening of Ru-catalysts.....	52

## Table of Contents

---

2.9.3.	General procedure for the screening of different bases at various temperatures ....	52
2.9.4.	General procedure for catalytic selective $\beta$ -methylation of secondary alcohols ....	53
2.9.5.	General procedure for catalytic selective $\beta$ -methylation of 2-aryl ethanols.....	56
2.9.6.	General procedure for catalytic selective $\beta$ -methylation of aliphatic alcohols.....	58
2.9.7.	Labeling experiments and observation of potential intermediates .....	62
2.10.	General procedure for the calculation of Gibbs free activation energy.....	69
2.11.	DFT calculated reaction mechanism .....	70
2.11.1.	Estimation of the Gibbs free activation energy (i.e. the energy span) of activation using the Eyring Equation .....	70
2.11.2.	Computational Details.....	71
	References .....	74
3.	Manganese(I) catalyzed selective $\beta$ -methylation of alcohols using MeOH as the C1 source.....	77
3.1.	Objective .....	81
3.2.	Reaction optimization .....	82
3.3.	Mn(I) catalyzed $\beta$ -methylation of 2-arylethanols with methanol.....	83
3.4.	Mn(I) catalyzed $\beta$ -methylation of secondary alcohols with methanol.....	85
3.5.	Mn(I) catalyzed $\beta$ -methylation of aliphatic alcohols and diols with methanol.....	86
3.6.	Mechanistic investigation.....	88
3.6.1.	Conversion/time profile .....	88
3.6.2.	Labeling experiments.....	89
3.6.3.	Stoichiometric reaction of complex Mn-2 with alcohols.....	90
3.7.	Proposed catalytic cycle .....	91
3.8.	Conclusion and outlook.....	92
3.9.	Experimental .....	92
3.9.1.	General experimental .....	92
3.9.2.	Synthesis of manganese pincer complexes .....	93
3.9.3.	General procedure for screening of Mn-catalysts .....	95
3.9.4.	General procedure for the catalytic selective $\beta$ -methylation of 2-aryl ethanols ....	95
3.9.5.	General procedure for the catalytic selective $\beta$ -methylation of secondary alcohols . .....	99
3.9.6.	General procedure for catalytic selective $\beta$ -methylation of aliphatic alcohols.....	103

## Table of Contents

---

3.9.7.	General procedure for the catalytic selective $\beta$ -methylation of diols .....	106
3.9.8.	Conversion/time profile from experiments for the $\beta$ -methylation of 8a with MeOH at different time intervals.....	107
3.9.9.	Labeling experiments and observation of potential intermediates .....	108
	References .....	115
4.	Direct synthesis of cycloalkanes from diols and secondary alcohols or ketones using a homogeneous manganese catalyst .....	118
4.1.	Objective .....	121
4.2.	Reaction optimization .....	122
4.3.	Selective preparation of substituted cyclohexanes from 3-methylpentane-1,5-diol 20b .. .....	124
4.4.	Selective preparation of substituted cyclohexanes from a variety of secondary alcohols and substituted pentanediols .....	126
4.5.	Selective preparation of substituted cycloalkanes from ketones and diols .....	127
4.6.	Observation of in situ formed intermediates and labeling experiments.....	129
4.7.	Proposed catalytic pathway.....	130
4.8.	Conclusion and outlook.....	133
4.9.	Experimental .....	134
4.9.1.	General experimental.....	134
4.9.2.	Synthesis of manganese pincer complex .....	134
4.9.3.	Preparation of starting materials .....	134
4.9.4.	General procedure for reaction optimization .....	136
4.9.5.	General procedure for the preparation of substituted cyclohexanes from secondary alcohols and diols .....	136
4.9.6.	General procedure for the preparation of substituted cycloheptanes from ketone and diols .....	147
4.9.7.	General procedure for the preparation of substituted cyclohexane from ketone and diols .....	149
4.9.8.	General procedure for the preparation of substituted cyclopentanes from ketone and diols .....	150
4.9.9.	Control experiments and labeling studies .....	152
4.9.10.	Characterization of major diastereomer in compound 21b .....	154
4.9.11.	Computation of the relative stability for different isomers of 21b.....	159

## Table of Contents

---

References .....	160
5. Manganese catalyzed selective $\alpha$ - and $\alpha$ , $\beta$ -deuteration of primary alcohols using deuterium oxide.....	163
5.1. Objective .....	166
5.2. Reaction optimization .....	167
5.3. Selective $\alpha$ -deuteration of aryl Methanols .....	168
5.4. Selective $\alpha$ -, and $\beta$ - deuteration of 2-aryl ethanols .....	169
5.5. Selective $\alpha$ -, and $\beta$ - deuteration of aliphatic alcohols .....	169
5.6. Mechanistic Studies.....	171
5.6.1. Stoichiometric reaction of complex Mn-2 with water and alcohols .....	171
5.6.2. Kinetic experiments .....	172
5.7. Catalytic cycle based on DFT calculation.....	173
5.8. Conclusion.....	174
5.9. Experimental .....	174
5.9.1. General experimental.....	174
5.9.2. General procedure for catalytic H/D exchange reaction for aryl methyl alcohol .	175
5.9.3. General procedure for catalytic H/D exchange reaction for aliphatic alcohol.....	175
5.9.4. Stoichiometric reaction of complex Mn-2 with H <sub>2</sub> O in the presence of a base....	176
5.9.5. Reaction after 10 h at 60 °C temperature .....	176
5.9.6. Stoichiometric reaction of complex Mn-2 with benzyl alcohol 27a.....	177
5.9.7. Dehydrogenation of benzyl alcohol 27a using complex Mn-2.....	179
5.9.8. Eyring-Plot.....	180
5.9.9. Computational Details .....	183
References .....	185
6. Catalytic hydrogenation of cyclic carbonates using manganese complexes .....	187
6.1. Objective .....	193
6.2. Catalyst screening .....	194
6.3. Mn(I) catalyzed hydrogenation of various cyclic Carbonates .....	196
6.4. Mechanistic Investigation .....	198
6.5. Catalytic Cycle .....	199
6.6. Conclusion.....	201

## Table of Contents

---

6.7. Experimental .....	201
6.7.1. General experimental .....	201
6.7.2. Synthesis of manganese complexes .....	202
6.7.3. General procedure for screening of Mn-catalysts .....	202
6.7.4. General procedure for the hydrogenation of cyclic carbonates 6 using complex MN-2 .....	202
6.7.5. General procedure for the hydrogenation of ethylene carbonate 34a using the pre-activated complex 14 .....	204
References .....	210
7. Manganese(I) catalyzed selective hydroboration of organic carbonates and carbon dioxide ....	212
7.1. Objective .....	216
7.2. Synthesis of a manganese precatalyst .....	217
7.3. Reaction optimization for the reduction of organic carbonates using Mn complex Mn-24 .....	219
7.4. Mn(I)-catalyzed selective hydroboration of Organic carbonates .....	220
7.5. Catalytic reactivity of complex Mn-24 in CO <sub>2</sub> hydroboration .....	222
7.6. Mechanistic Studies .....	223
7.7. Catalytic Cycle .....	225
7.8. Conclusion .....	226
7.9. Experimental .....	227
7.9.1. General experimental .....	227
7.9.2. Synthesis of the ligand (Si-PNP) .....	227
7.9.3. Synthesis of manganese complex Mn-24 .....	228
7.9.4. Optimization of the reaction conditions for the hydroboration of ethylene carbonate .....	228
7.9.5. General procedure for the hydroboration of carbonates .....	229
7.9.6. General procedure for catalytic hydroboration of carbon dioxide .....	232
7.9.7. Observation of catalytic intermediates .....	232
References .....	237
8. General Conclusion .....	239
9. Summary .....	242
9. Sommaire .....	252



## Table of Contents

---

Acknowledgements.....	265
Annexes.....	268
List of synthesized complexes.....	268
List of publications.....	269
Curriculum Vitae .....	271

## Abbreviation Index

NHC	<i>N</i> -heterocyclic carbene
MeOH	Methanol
DCM	Dichloromethane
THF	Tetrahydrofuran
[D <sub>8</sub> ]-Toluene	<sup>2</sup> H-labeled toluene
[D <sub>8</sub> ]-THF	<sup>2</sup> H-labeled Tetrahydrofuran
°C	Celsius
DMF	Dimethylformamide
DMFA	Dimethylammonium formate
PEHA	Pentaethylenehexamine
NCs	Nanoclusters
TON	Turnover Number
TOF	Turnover Frequency
Conv.	Conversion
<i>T</i>	Temperature
<i>o</i> -	<i>Ortho</i> -
<i>p</i> -	<i>Para</i> -
<i>m</i> -	<i>Meta</i> -
equiv.	Equivalent
GC	Gas Chromatography
FID	Flame ionization detector
NMR	Nuclear magnetic resonance
HRMS	High resolution mass spectrometry
Hz	Hertz
ppm	Parts per million
K	Kelvin
DFT	Density functional theory
TS	Transition state
ΔG <sup>‡</sup>	Gibbs free activation energy

## Abbreviation Index

---

R	Organic substituent
<sup>t</sup> Bu	<i>tert</i> -Butyl
MPO	2-methyl-1,3-propanediol
HNTf <sub>2</sub>	Trifluoromethanesulfonimide
rt	Room temperature
TMS	Tetramethylsilane
PTFE	Polytetrafluoroethylene
RCM	Ring close metathesis
EDG	Electron donating group
EWG	Electron withdrawing group

## 1. Motivation and structure of the thesis

### 1.1. Pincer complexes and their reactivity in hydrogen transfer reactions

The transformation of organic compounds involving the transfer of hydrogen comprises a broad range of chemicals in the industry as well as in pharmaceutical chemistry.<sup>[1]</sup> Hydrogen is one of the effective, green and cleanest reducing agents and is also being considered central to future fuel energy and mobility systems.<sup>[2]</sup> Employing suitable catalysts, hydrogen shuffling can be attained in its molecular form or the form of hydrides and protons.<sup>[3]</sup> A variety of metal-complexes can perform both reactions including the addition and subtraction of hydrogen to and from the organic molecules, respectively. Moreover, extending this concept can also lead to the multistep reactions involving de-hydrogenation, re-hydrogenation and the formation of C–C or C–N bonds in a single synthetic process.<sup>[1a]</sup> Considering these points, molecular homogeneous metal complexes can be a powerful tool for the production of various organic molecules via multistep catalytic processes.

In this chapter, the focus is on the critical analysis of recent developments in hydrogen transfer reactions reported by Mn(I) complexes, mostly pincer complexes and their similar reactivities with Ru(II) complexes.

Pincer complexes are used in a variety of organic transformations which make them efficient complexes in homogeneous catalysis. In general, the pincer ligands can be synthesized in a few steps and can easily be tuned to their steric and electronic properties (Figure 1.1).<sup>[4]</sup> The pincer ligands consist of a well-defined tridentate framework which upon coordination with the metal center provides an environment around the metal and increases the complex stability. A distinct pincer complex can be synthesized by the modification of steric and electronic effects of the coordinating atoms granting fine-tuning and advancing their catalytic reactivity and selectivity towards the formation of the desired product.



**Figure 1.1:** Common structure for pincer complexes.

In the last few decades, several studies have been reported for the transfer of hydrogen focusing on noble-metal complexes such as ruthenium, rhodium, iridium and palladium pincer complexes.<sup>[1a, 3, 5]</sup> Especially, most of these reaction developments were reported using ruthenium or iridium complexes. Recently, the earth-abundant 3d-metals such as iron, cobalt, and nickel pincer complexes also have gained an increasing interest in these organic transformations.<sup>[1b, 6]</sup> Notably, the Mn(I) pincer complexes captivated the catalytic community because of its earth abundance, cheap, biocompatibility and similar reactivity to the Ru(II) complexes.<sup>[7]</sup>

## 1.2. Manganese(I) pincer complexes and their analogous reactivity compared to ruthenium(II) complexes

Ruthenium pincer complexes are well-established complexes and their reactivity towards de-hydrogenations/hydrogenations of polar substrates is well-known. Metal-ligand cooperation plays an important role to accomplish such organic transformations.<sup>[3]</sup> In the presence of a base, pincer complexes with the lutidine backbone are deprotonated at the methylene linker which leads to the de-aromatization of the hetero-aromatic ring providing a catalytically active complex (Figure 1.2, structure (a)). Similarly, complexes with an aliphatic backbone comprising secondary amine functionality near the metal center can act as amines/amides by protonating/deprotonating the N–H bond (Figure 1.2, structure (b)).

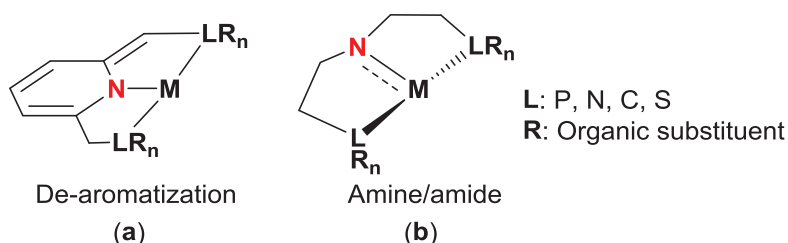


**Figure 1.2:** Activated form of de-aromatized lutidine based (a) and aliphatic based (b) pincer complexes.

In the past, pioneer efforts have been reported by the group of Milstein using the pincer complexes for the hydrogen transfer reactions and also for the activation of small molecules and difficult bonds.<sup>[3, 8]</sup> Lately, our group focused on the PNP pincer complexes containing the aliphatic backbone comprising secondary amine co-operativity in the metal-ligand complex to accomplish new organic transformations (Figure 1.2, structure (b)).<sup>[9]</sup> These complexes are well-established involving noble metal complexes of Ru, Ir, and Pd. In the last few years, several studies using these complexes were also reported for non-noble metal complexes, for instance, Fe, Co, and Mn complexes.<sup>[6a, 7b, 8b]</sup>

Initial studies reported for Fe(II) pincer complexes on hydrogen transfer reactions showed good reactivities in de-hydrogenation/re-hydrogenation and hydrogenation reactions.<sup>[6a, 10]</sup> Based on these results, it was speculated that iron can be a new congener of ruthenium in molecular homogeneous catalysis.<sup>[11]</sup> However, recent developments achieved by Mn(I) pincer complexes show more similarities with the analogous Ru(II) complexes in comparison to the Fe(II) complexes. Employing Mn(I) pincer complexes, various hydrogen transfer reactions were reported and showed better reactivity with respect to the previously established Fe(II) pincer complexes.<sup>[7]</sup>

The first synthesis of Mn-pincer complexes was reported by the group of van Koten<sup>[12]</sup> and Wieghardt.<sup>[13]</sup> However, these individual groups mainly focused on coordination chemistry with no catalytic applications. The first Mn-PNP pincer complexes were reported by the group of Ozerov and Nocera, who prepared a variety of diarylamido-PNP complexes containing tricarbonyl manganese as a central moiety in the metal-complex.<sup>[14]</sup> Inspired by these complexes, Boncella and Tondreau also reported several Mn(I) pincer complexes starting from Mn(CO)<sub>5</sub>Br and different PNP pincer ligands.<sup>[15]</sup> Our group also synthesized a new silane-based Mn-PNP pincer complex which was used for the reduction of difficult carbonyl substrates such as CO<sub>2</sub> and carbonic acid derivative using pinacolborane as a reducing agent.<sup>[9c]</sup> Further details of this transformation are discussed in chapter 7. Manganese is well-known for its variable oxidation state. Remarkably, it was found that high-valent Mn-pincer complexes did not show reactivity towards hydrogen borrowing reactions. Manganese pincer complexes comprising oxidation state +1 are reactive in such transformations. The detailed discussion is described in the next sections.

### 1.2.1. Diagonal relationship between Ru(II) and Mn(I) complexes

It is well established previously that a diagonal relationship in the periodic table occurs between the element pairs which are situated diagonally adjacent in the second and third periods.<sup>[16]</sup> The diagonal relationship between the elements occurs mostly because of their similarity in their atomic radii, electronegativity and charge density. In the periodic table, as we move rightward across the period, atomic radii of the atoms decrease and moving downward in the group, atomic radii of the atoms increase. Similarly, in the periodic table, less basic character, more covalent, and electronegative nature were observed as we move rightward. However, moving downward in the group, the elements result in more basic, more ionic and less electronegative. Therefore, the second-period elements and diagonally to the lower right element in the third-period, the changes in elements “eliminate” one another out. Thus, we see similar chemical properties between these elements.

Alike the similar chemical properties between the elements of second and third periods, recently it was assumed that the  $\text{Ru}^{2+}$  and  $\text{Mn}^{1+}$  ions also comprise the diagonal relationship in the periodic table. In the past, various organic transformations such as de-hydrogenation,<sup>[17]</sup> hydrogenation,<sup>[18]</sup> and hydrogen borrowing reactions<sup>[17b, 19]</sup> were reported where Mn(I) complexes showed similar reactivities with the previously established Ru(II) complexes. Similarly, the complexes of these ions exhibited similar stability, high-temperature tolerance and revealed identical pathways for the activation of small molecules and organic molecules.

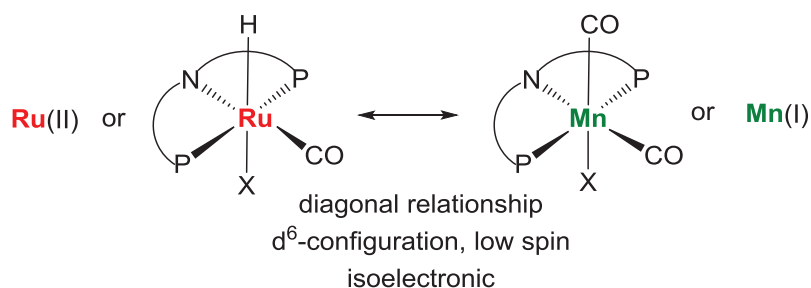


**Figure 1.3:** Similar properties between Ru(II) and Mn(I) complexes.

Apart from the diagonal relationship, other similarities were also observed between these two ions. Both ions are isoelectronic and contain  $d_6$ -configuration. Additionally, these ions form low spin complexes while coordinating with the tridentate pincer ligands and other strong ligands such as  $\text{NH}_3$ ,  $\text{CH}_3\text{CN}$ , or  $\text{CO}$ , etc. (Figure 1.3).

In the table 1.1, some of the electronic and physical properties of manganese and ruthenium are shown.

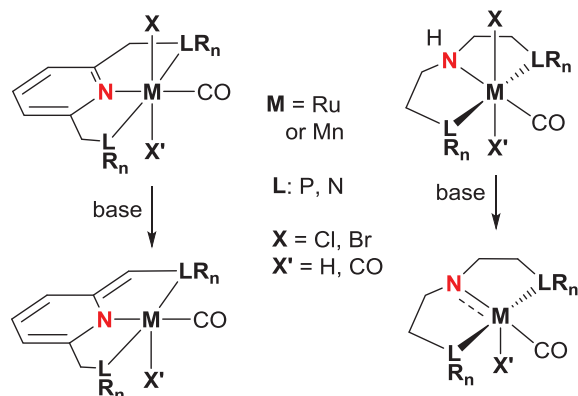
Properties	Mangaense	Ruthenium
Electronic configuration	[Ar] 3d <sup>5</sup> , 4s <sup>2</sup>	[Ar] 4d <sup>7</sup> , 5s <sup>1</sup>
1+	d6	d7
2+	d5	d6
3+	d4	d5
Electronegativity	Mn <sup>2+</sup> (1s): 1.343	Ru <sup>3+</sup> : 1.576
Atomic radii	127 pm	134 pm
Ion radii	Mn <sup>2+</sup> (1s): 81 pm	Ru <sup>3+</sup> : 82 pm
Price per kg (2018)	<5.0 €	>9000 €

**Table 1.1:** Electronic and physical properties of manganese and ruthenium.<sup>[20]</sup>

### 1.2.2. Catalyst activation, stability and hydride formation: Mn(I) vs Ru(II) pincer complexes

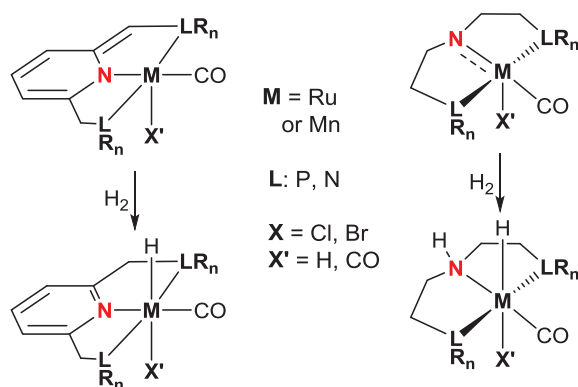
The catalytically active species for both Mn(I) and Ru(II)-pincer complexes are generated in a similar fashion from the catalyst precursors when the ligands contain a lutidine backbone or an aliphatic backbone with secondary amine PNP or PNN units (Scheme 1.1). Both metal-pincer complexes exhibit metal-ligand cooperation while activating the organic molecules. As discussed earlier, Mn(I) or Ru(II) pincer complexes consisting of lutidine or aliphatic secondary amine backbone activate via de-aromatization/aromatization and amine/amide pathways, respectively. Considering the stability of manganese(I) pincer complexes, these complexes showed high robustness and long term stability toward harsh reaction conditions which are in comparison with the early-established ruthenium(II) pincer complexes. Several works were reported where de-aromatization and aromatization were observed for lutidine based pincer complexes and intermediates incorporated with these processes were isolated for Ru(II) and Mn(I)-pincer complexes both.<sup>[3, 21]</sup> Similarly, the activated intermediate of the aliphatic backbone with secondary amine based pincer complexes comprising amine/amide formation was also isolated and characterized.<sup>[22]</sup>





**Scheme 1.1:** Activation of Mn(I) and Ru(II) pincer complexes by deprotonating at the ligand backbone.

In the hydrogen transfer reactions, the formation of hydride is one of the crucial steps in the catalytic cycle. Interestingly, Ru(II) and Mn(I) pincer complexes show comparable reactivity in reaction with hydrogen or hydrogen source (Scheme 1.2). Alike, previously established Ru(II)-hydride pincer complexes, Mn(I) pincer complexes comprising lutidine backbone or secondary amine incorporated aliphatic backbone revealed high reactivity towards hydride formation on reaction with hydrogen or hydrogen source.<sup>[9a, 23]</sup> In the past, several works have been reported where Mn(I) pincer complexes can form hydride easily and transfer the hydride to another organic molecule alike Ru(II) pincer complexes.



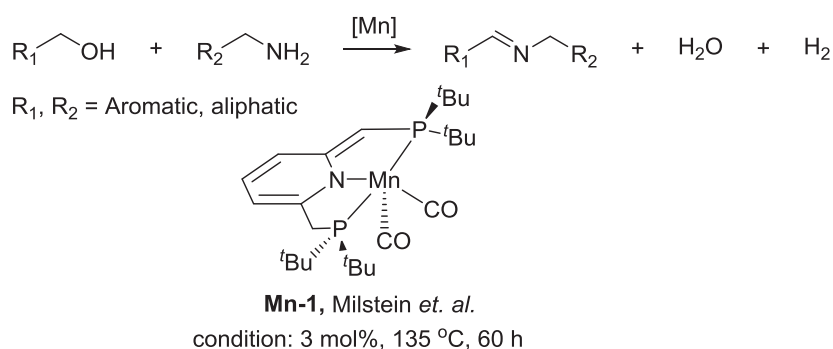
**Scheme 1.2:** Hydride formation for Ru(II) and Mn(I) pincer complexes.

### 1.3. C–C bond formation via hydrogen transfer: Mn(I) versus Ru(II)

The formation of C–C bonds is one of the fundamental and important methods to prepare new organic molecules, natural products and pharmaceuticals.<sup>[1a, 24]</sup> In this section, we will discuss the C–C bond formation via “Hydrogen borrowing reactions”.

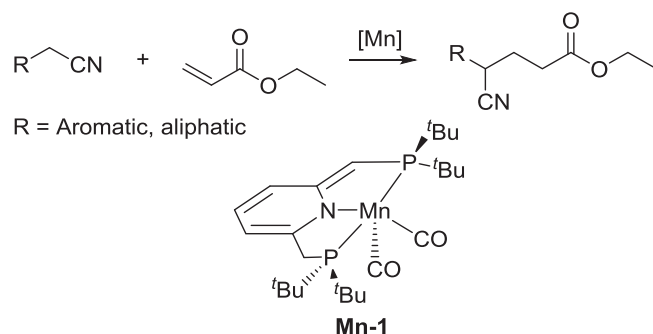
Ruthenium is an eminent metal and its molecular complexes are well-known as catalysts for C–C bond formations using hydrogen borrowing reactions, which comprises high reactivity and high selectivity.<sup>[25]</sup> Recently, several studies were shown where Mn(I) complexes also exhibited good reactivity towards these organic transformations.<sup>[7b, 7c]</sup> In the case of manganese as a metal center, most of these transformations were performed using Mn(I)-pincer complexes, but in some cases bidentate complexes were also used.

The motivation to employ Mn complexes as a hydrogen borrowing catalyst emerged by the first Mn(I) catalyzed hydrogen transfer reaction reported by the group of Milstein. The reaction showed the coupling of alcohols and amines to the corresponding aldimines by using the lutidine-based Mn-PNP pincer complex **Mn-1**.<sup>[21]</sup> The reaction was performed by using a catalyst loading of 3 mol% at 135 °C for 60 h in benzene as a solvent (Scheme 1.3). These results revealed that Mn(I) complexes may be a potential candidates for hydrogen borrowing reactions to generate C–C bonds as these reactions resulted in high reactivity towards the dehydrogenation of alcohols.



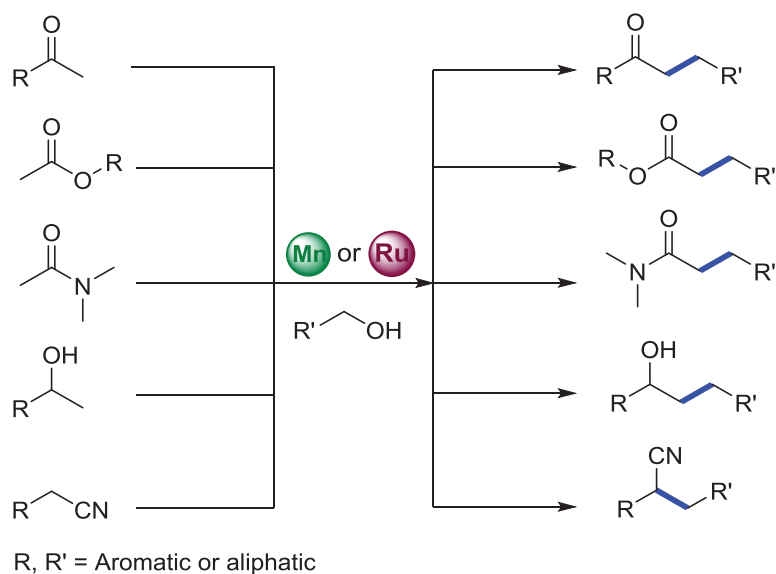
**Scheme 1.3:** Synthesis of imines using Mn(I) pincer complexes.<sup>[21]</sup>

Afterwards, the group of Milstein also demonstrated Mn(I) catalyzed C–C bond formation via a Michael-addition reaction (Scheme 1.4).<sup>[26]</sup> Employing the de-aromatized lutidine Mn(I) pincer complex **Mn-1**, the C–C bond formation was performed between the non-active aliphatic nitriles and ethyl acrylate as substrates.



**Scheme 1.4:** First C–C bond formation report using a Mn(I)-pincer complex by Milstein *et. al.*<sup>[26]</sup>

The group of Beller first reported the formation of C–C bonds via the hydrogen borrowing method using the Mn(I) pincer complex **Mn-2** as a precatalyst (Scheme 1.5, Figure 1.4).<sup>[27]</sup> The selective alkylation of ketones using primary alcohols as an alkylating reagents was reported employing Mn(I) pincer complex. The used Mn(I) complex consists of an aliphatic backbone, a secondary amine and two phosphorus atoms as a coordinating ligand to the metal center. The group of Milstein also showed the alkylation of ketones, esters, and amides using primary alcohols as an alkylating reagents and Mn-PNP pincer complex as a precatalyst **Mn-3** (Scheme 1.5, Figure 1.4).<sup>[17c]</sup> After these initial studies, several groups reported a number of alkylation reactions using Mn(I) pincer complexes.<sup>[17d]</sup> Various alkylation reactions for several functional groups such as ketones,<sup>[17g]</sup> alcohols,<sup>[17b, 28]</sup> amines,<sup>[29]</sup> esters,<sup>[17c, 17f]</sup> amides,<sup>[17c, 17f]</sup> and nitriles<sup>[17d, 30]</sup> were reported by using the Mn(I) complexes. The brief description and reaction conditions for the alkylation reactions using Mn(I) complexes are shown in scheme 1.5 and Figure 1.4-1.7.



**Scheme 1.5:** Alkylation reactions using primary alcohols as an alkylating reagent.

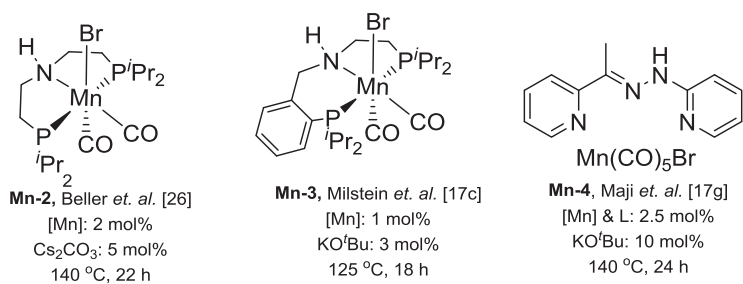


**Figure 1.4:** Mn(I)-pincer complexes used for the alkylation of ketones.

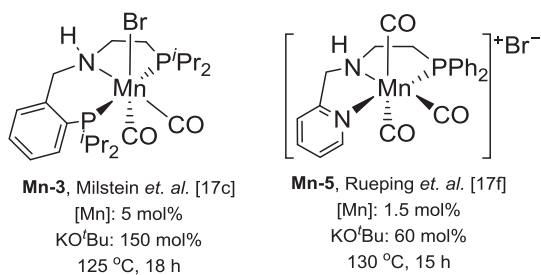


**Figure 1.5:** Mn(I)-pincer complexes used for the alkylation of esters and amides.

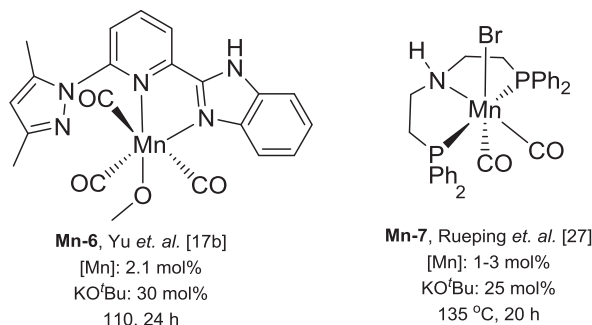


**Figure 1.6:** Mn(I)-pincer complexes used for the alkylation of secondary alcohols.

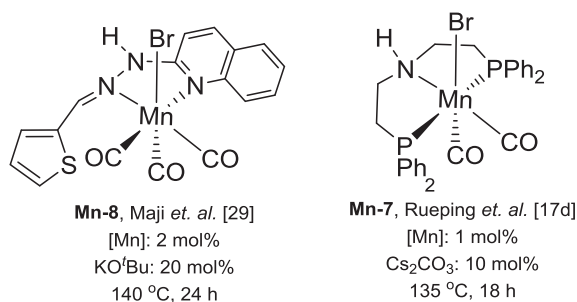
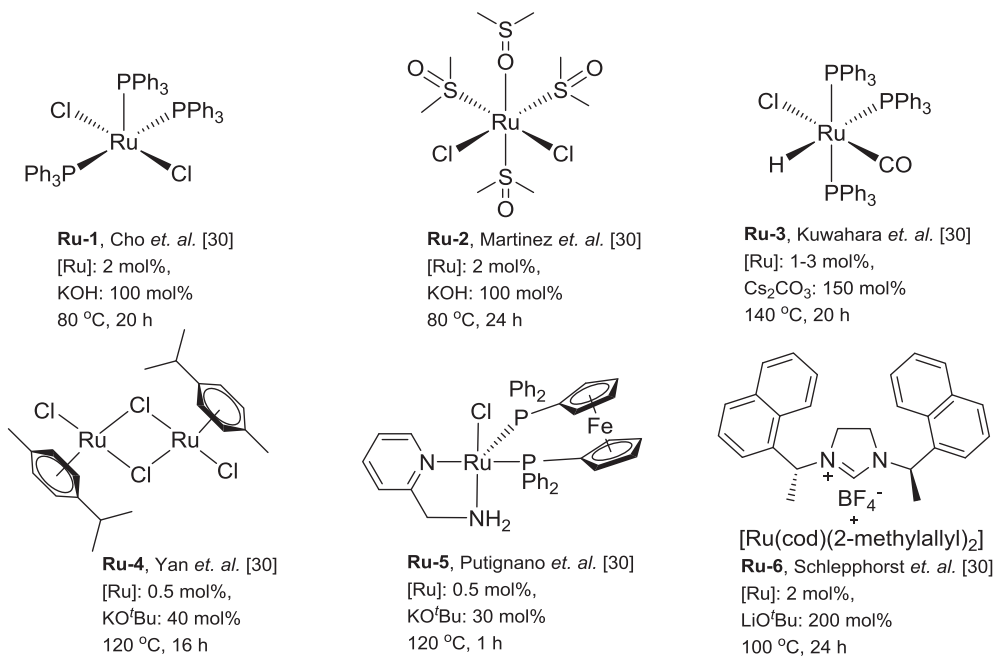


**Figure 1.7:** Mn(I)-pincer complexes used for the alkylation of nitriles.

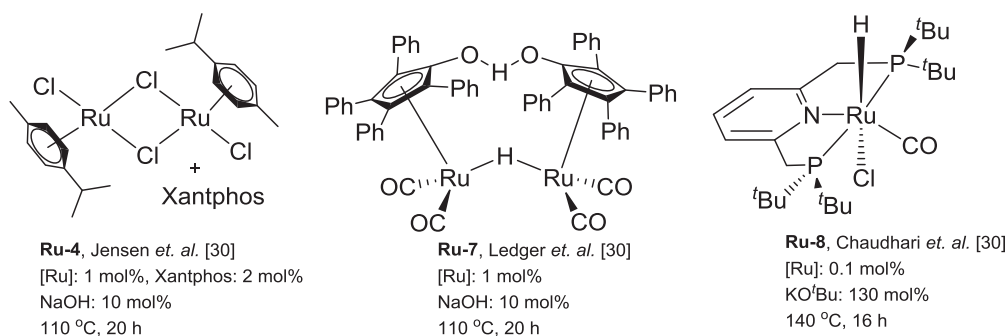
The results obtained from alkylation reactions nicely showed the similarities between manganese and ruthenium complexes. The brief description and reaction conditions for alkylation reactions using Ru(II) complexes are shown in scheme 1.5 and Figure 1.8 - 1.11. However, an aspect that seems to be important is that the alkylation reactions using ruthenium complexes can be performed employing commercially available ruthenium precursors as well as with various ligands such as monodentate, bidentate ligand embedded complexes, along with well-defined tridentate pincer complexes.<sup>[22b, 25, 31]</sup> However, in the case of manganese, most of the transformations are restricted to the pincer complexes. Only in a few cases bidentate complexes were used.<sup>[17b]</sup> Considering the reactivities, manganese complexes revealed similar reactivity as compared to the ruthenium complexes. In some of the cases, ruthenium displayed a better reactivity than manganese. However, considering the environmental aspect, manganese is an economic, biocompatible and earth-abundant metal. Therefore, utilizing manganese complexes as a metal-precursor is positive in organic transformations.

Recently, our group established catalytic systems for the selective  $\beta$ -methylation of alcohols using methanol as a C1 source. In this work, the reactivity of Ru(II)-PNP complex

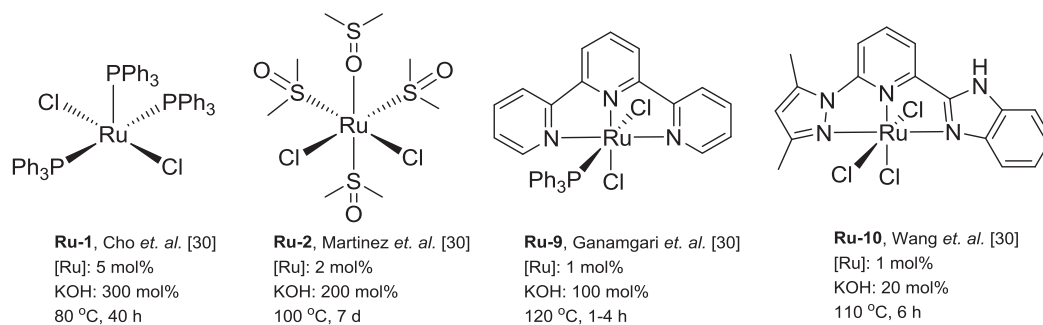
and Mn(I)-PNP complex was studied.<sup>[9b, 32]</sup> Interestingly, it was found that the Mn(I) pincer complex enabled analogous organic transformations as the Ru(II) pincer complex. However, in the case of the ruthenium system, the reaction could be performed using only low loadings of catalyst. The detailed discussion is shown in the next chapters 2 and 3.



**Figure 1.8:** Selected Ru(II)-complexes used for alkylation of ketones.



**Figure 1.9:** Selected Ru(II)-complexes used for the alkylation of amides.



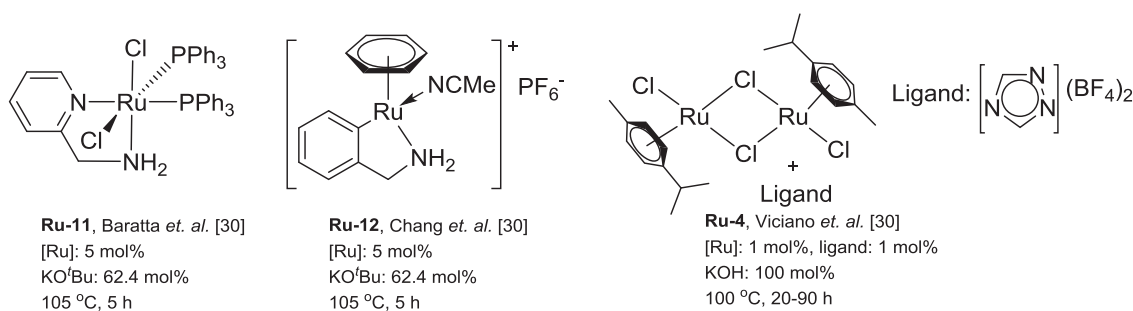


**Figure 1.10:** Selected Ru(II) complexes used for the alkylation of alcohols.

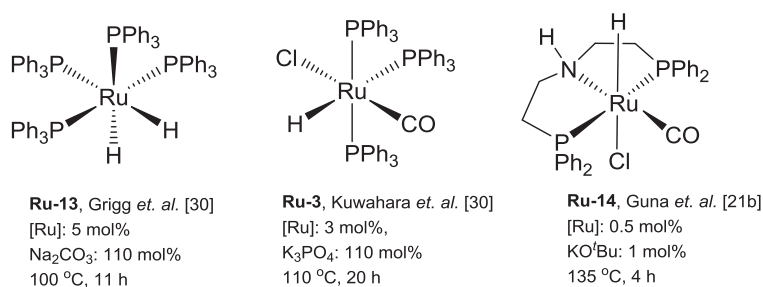


**Figure 1.11:** Selected Ru(II)-complexes used for the alkylation of nitriles.

## 1.4. Comparison of catalytic hydrogenation reaction: Mn(I) versus Ru(II) complexes

The reduction of carbonyl functionalities is an important transformation in organic synthesis. Traditionally, the reduction is performed using reducing agents such as lithium aluminum hydride or sodium borohydride in stoichiometric amount which produces a copious amount of inorganic waste. Substituting these reducing agents with hydrogen can be beneficial since hydrogen generates no waste and can be produced from sustainable sources.<sup>[33]</sup> In the past, Ru(II) complexes were shown to hydrogenate various carbonyl functional groups.<sup>[3]</sup> Functional groups containing carbonyl functionality such as aldehydes,<sup>[34]</sup> ketones,<sup>[34-35]</sup> nitriles,<sup>[36]</sup> esters,<sup>[34, 37]</sup> and amides<sup>[38]</sup> were hydrogenated using these complexes. Similarly, the difficult substrates comprising of carbonic acid derivatives and CO<sub>2</sub> were also hydrogenated.<sup>[39]</sup> Recently, alike, Ru(II) complexes, Mn(I) complexes were also found to be the potential candidate for the hydrogenation reactions.<sup>[7b, 7c]</sup>

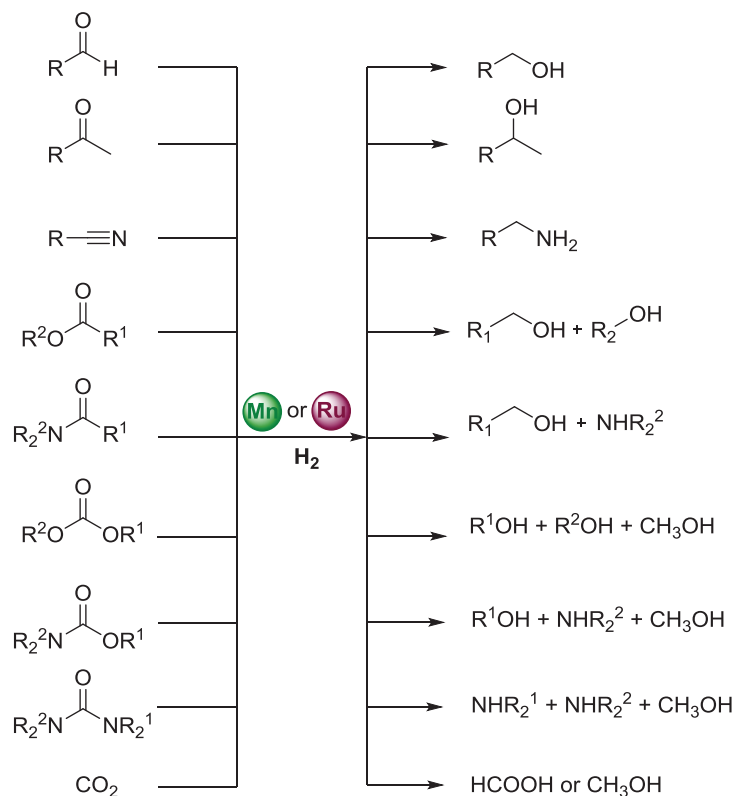
In 2016, the first studies using manganese complexes as hydrogenation catalyst were reported by the group of Beller and Kempe (Scheme 1.6, Figure 1.12).<sup>[18a, 40]</sup> The group of Beller reported the

hydrogenation of aldehydes, ketones, and nitriles using the Mn(I)-pincer complex (Mn-MACHO-<sup>i</sup>Pr, **Mn-2**). The pincer complex consisted of an aliphatic backbone, a secondary amine as a cooperative functionality and manganese as the metal center was used.<sup>[18a]</sup> In the same year, the group of Kempe also published a catalytic system for the hydrogenation of aldehydes and ketones using a Mn-PN<sub>5</sub>P pincer complex **Mn-9** consisting of a substituted 1,3,5-triazine-2,4-diamine as a backbone.<sup>[40]</sup>

After these preliminary studies, the group of Beller investigated the hydrogenation of esters using another manganese pincer complex **Mn-13** where the *iso*-propyl or phenyl groups at the phosphorous atoms were replaced by ethyl groups (Scheme 1.6, Figure 1.14).<sup>[23]</sup> The hydrogenation with pre-established manganese complexes such as Mn-MACHO-<sup>i</sup>Pr, Mn-MACHO-Cy or Mn-MACHO-Ph revealed low activities for the hydrogenation. However, the less-hindered Mn-MACHO-Et **Mn-13** complex showed the best reactivity and selectivity to the final alcohol products. Subsequently, the same group also reported the hydrogenation of amides using the Mn-PNN complex **Mn-16**.<sup>[41]</sup> The already established Mn-MACHO type pincer complexes showed a very low reactivity towards the hydrogenation of amides. Nevertheless, they synthesized a new air-stable imidazole based Mn(I)-PNN-pincer complex which showed a good reactivity towards the hydrogenation of the secondary amides and primary amides (Scheme 1.6, Figure 1.15).

Furthermore, several groups reported the hydrogenation of carbonyl functionalities such as ketones,<sup>[42]</sup> esters,<sup>[18e, 18g]</sup> and nitriles<sup>[43]</sup> to the corresponding hydrogenation product (Scheme 1.6, Figure 1.12 – 1.14). Interestingly, carbon dioxide originated carbonic acid derivatives were also hydrogenated using the well-established Mn(I)-complexes. Difficult substrates such as carbonates,<sup>[9a, 18c, 18d]</sup> carbamates,<sup>[18f]</sup> and urea derivatives<sup>[18f]</sup> were hydrogenated using the Mn-PNN and Mn-PNP complexes (Scheme 1.6, Figure 1.16, 1.17). The hydrogenation of CO<sub>2</sub> to formate was also made possible using the bipyridine Mn(I) complex<sup>[44]</sup> and Mn-PN<sub>3</sub>P complex (Scheme 1.6, Figure 1.18).<sup>[45]</sup> However, the direct conversion of CO<sub>2</sub> to methanol was not explored explicitly. Prakash *et. al.* reported the catalytic system for the stepwise hydrogenation of CO<sub>2</sub> to methanol using the Mn-PNP complex **Mn-2**.<sup>[46]</sup> However, the reaction was performed in two individual steps (Scheme 1.6, Figure 1.18). The brief description and reaction conditions for the hydrogenation reaction using the Mn(I) complexes are shown in scheme 1.6 and figures 1.12 – 1.18.





**Scheme 1.6:** Hydrogenation of carbonyl functionalities using Mn(I) vs Ru(II) complexes.

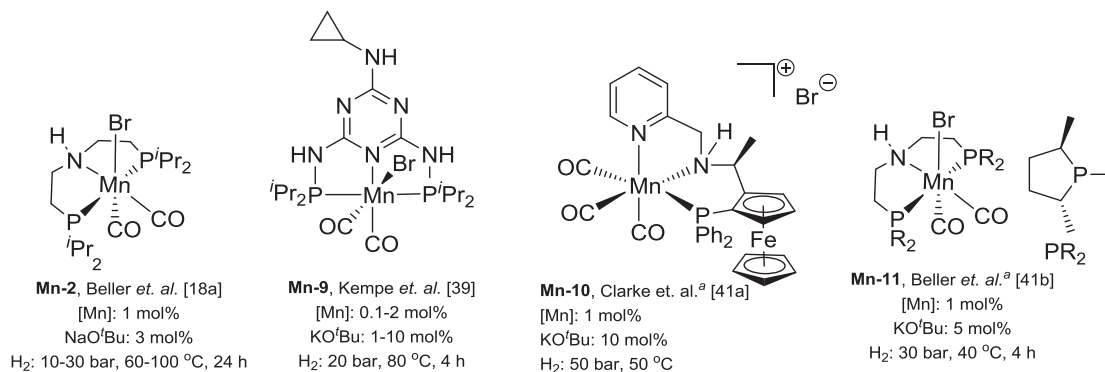


**Figure 1.12:** Mn(I) complexes used for the hydrogenation of aldehydes and ketones. <sup>a</sup>Mn(I) complexes used for asymmetric hydrogenation of ketones.

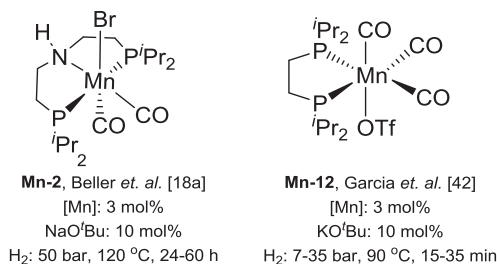


**Figure 1.13:** Mn(I) complexes used for the hydrogenation of nitriles.

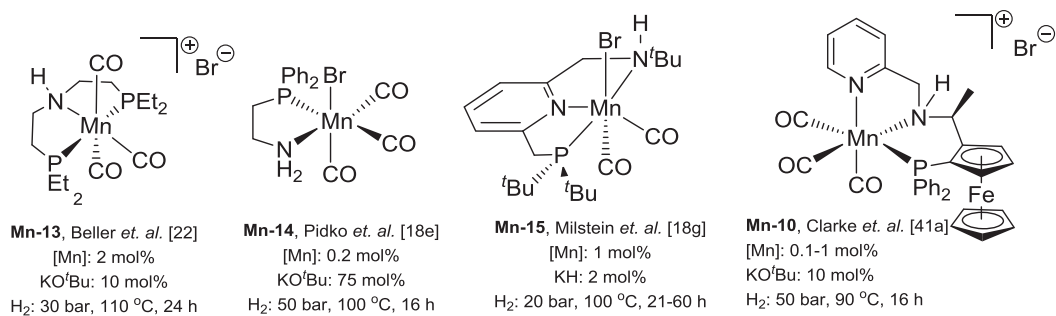


**Figure 1.14:** Mn(I) complexes used for the hydrogenation of esters.

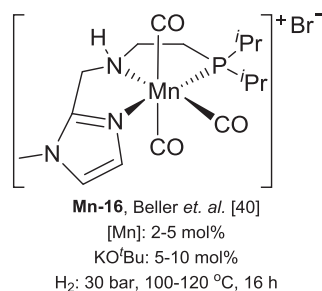


**Figure 1.15:** Mn(I) complexes used for the hydrogenation of amides.

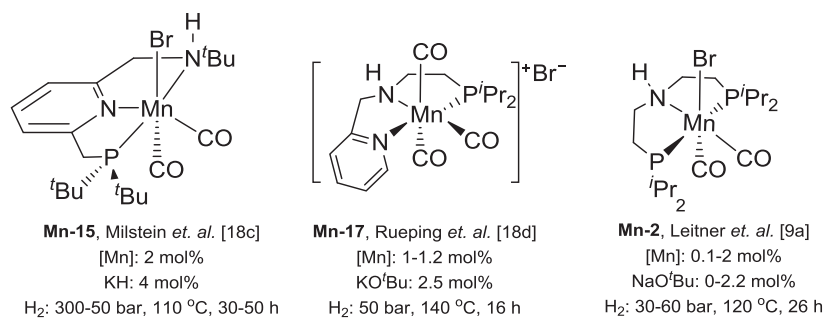


**Figure 1.16:** Mn(I) complexes used for the hydrogenation of carbonates.

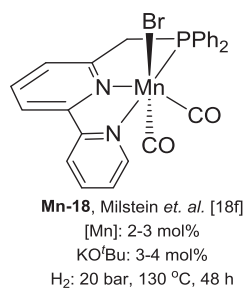


**Figure 1.17:** Mn(I) complex used for the hydrogenation of carbamates and urea.

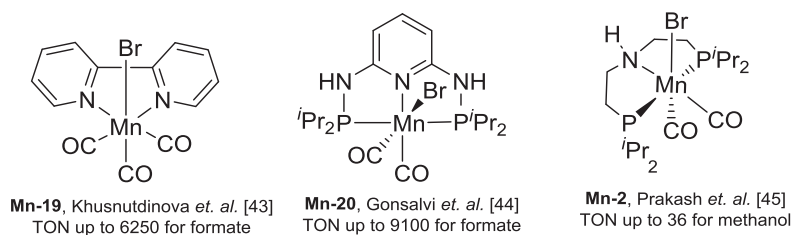


**Figure 1.18:** Mn(I) complexes used for the hydrogenation of CO<sub>2</sub> to formate and methanol

The results relevant for the hydrogenations comprising Mn(I) or Ru(II) pincer complexes or bidentate complexes confirmed that the activation of hydrogen and assistance of substrate in the complex is accompanied by metal-ligand cooperation which is a crucial step for these transformations. The brief description and reaction conditions for the hydrogenation reactions using Ru(II) pincer complexes are shown in scheme 1.6 and figures 1.19 – 1.23.<sup>[34-36, 37e, 37f, 38, 47]</sup> The reactions using other Ru(II) tridentate, bidentate and monodentate complexes were also reported, previously.<sup>[48]</sup> However, in this section, the reactivity of Ru(II) pincer complexes will be discussed because of their similarity with the Mn(I) pincer complexes.

The hydrogenation reactions using Ru(II) complexes had shown that the hydrogenation of carbonyl functionalities such as aldehydes, ketones, nitriles, esters, and amides could be performed under mild conditions employing low catalyst loading, low temperature, and low hydrogen-pressure.<sup>[3]</sup> Similarly, these complexes showed high reactivity towards the hydrogenation of difficult organic substrates such as carbonates, carbamates, and CO<sub>2</sub>. These substrates were hydrogenated with impressive TONs to the corresponding C1 product employing the Ru(II) pincer complexes. Interestingly, Ru(II) complexes also catalyzed the direct hydrogenation of CO<sub>2</sub> to methanol with high TONs and high selectivity.<sup>[49]</sup>

Therefore, it can be stated that Mn complexes are active catalysts for hydrogenations. Various carbonyl functionalities were reduced using these complexes showing moderate to good reactivity. Ruthenium complexes are currently more active in catalytic hydrogenation reactions in comparison to the manganese complexes. The direct hydrogenation of CO<sub>2</sub> to methanol is possible using Ru-complexes which is still not yet explored explicitly using the Mn-complexes.

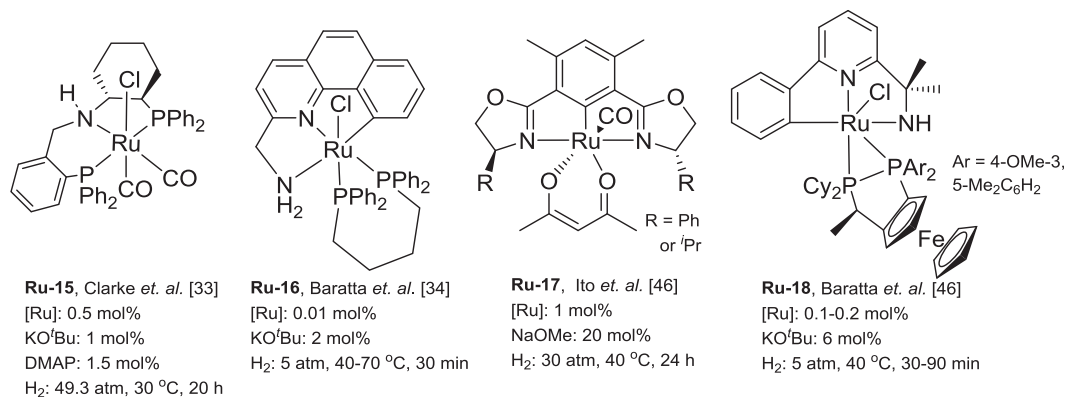


**Figure 1.19:** Ru(II) complexes used for the hydrogenation of ketones and aldehydes.

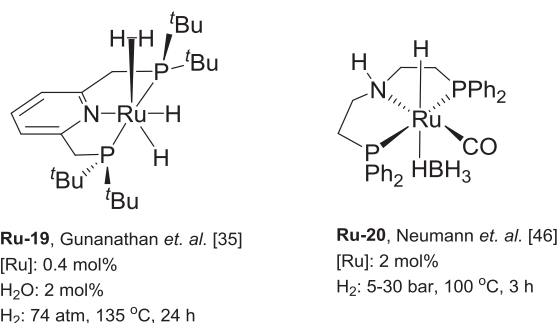


**Figure 1.20:** Selected Ru(II) complexes used for the hydrogenation of nitriles to amine.

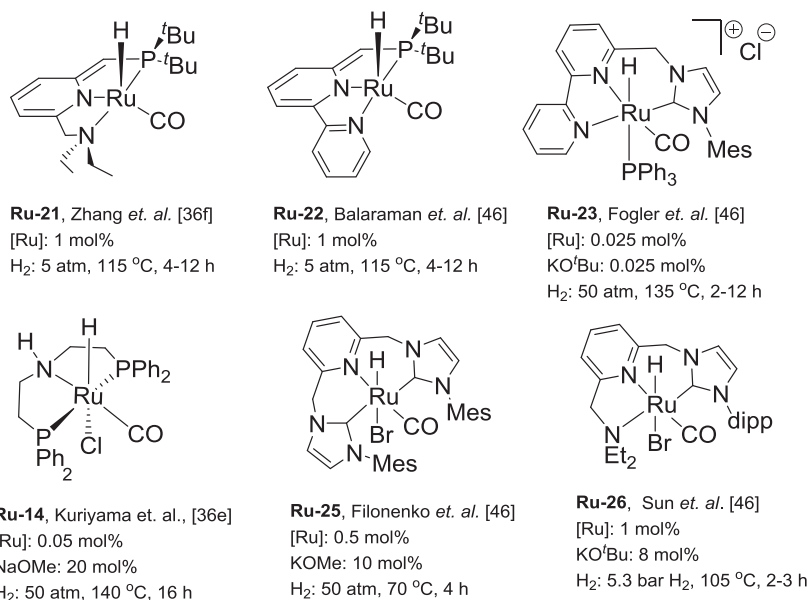


**Figure 1.21:** Selected Ru(II) complexes used for the hydrogenation of esters.

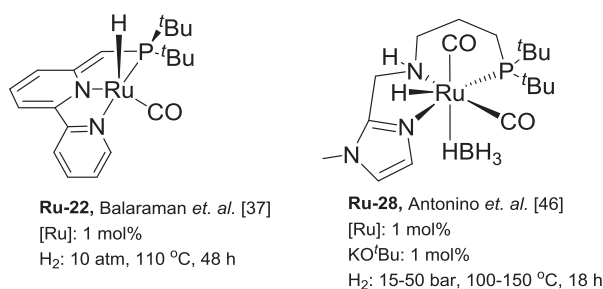


**Figure 1.22:** Selected Ru(II) complexes used for the hydrogenation of amides.

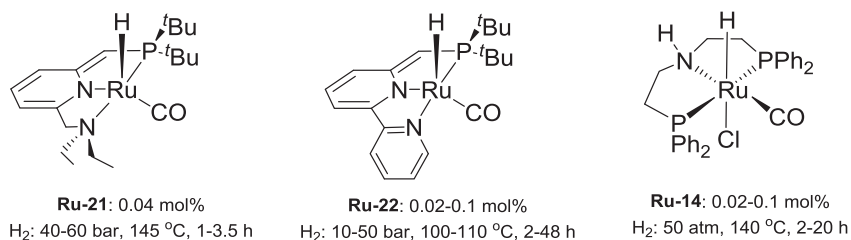


**Figure 1.23:** Selected Ru(II) complexes used for the hydrogenation of carbonates, carbamates, and urea.

## 1.5. Conclusion and outlook

The synthesis of new complexes containing non-noble metals and their applications in organic transformation represents an important and developing field in catalysis. Manganese is an emerging metal which successfully showed good reactivities in de-hydrogenations/hydrogenations. It is important to note that the reactivity of Mn(I) complexes is not a result of the metal center only. Instead the ligand which contains a heterocyclic ring or N–H functionality close to the metal center in the currently known systems plays important roles. Through metal-ligand cooperation, these complexes have shown good reactivity for several hydrogen-transfer reactions. The similar reactivities between the Ru(II) and Mn(I) pincer complexes can be explained because of their diagonal relationship in the periodic table and same  $d_6$  electronic configuration. Alike Ru(II) pincer complexes, Mn(I) pincer complexes also feasible to prepare the hydride on reaction with hydrogen or hydride source and can transfer the hydride easily to another organic molecules. Due to formation of hydride, these complexes can perform the hydrogen transfer reactions and various organic transformations such as small molecule activation, hydrogenation and hydrogen borrowing reactions are possible. At present, it can be stated that Mn(I)-complexes possess important and appealing catalytic features which define

their versatile reactivity and can be used in various difficult organic transformations. The possibility of modulating their electronic structure, ligand transformation and altering the steric properties may be a good option to make them competitive to the well-established Ru(II) complexes. Overall, manganese(I) pincer complexes already revealed a broad scope in organic transformations, in some cases the activities and productivities are even competitive to the well-established Ru(II) complexes. In terms of future developments, chiral manganese(I) pincer complexes for enantioselective catalysis and asymmetric hydrogenation reactions are still in early stage and need to be focused. Moreover, for organic transformations, functional group tolerance, mild reaction conditions, and high TONs and TOFs should be targeted.

## 1.6. Structure of the thesis

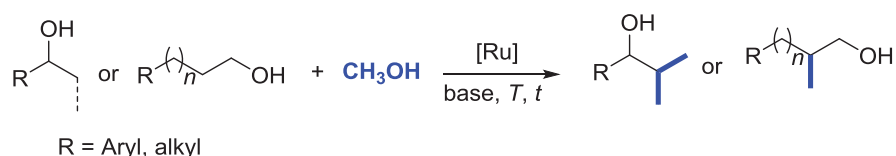
This thesis mainly focuses on hydrogen transfer reactions to perform organic transformations by using ruthenium(II) and manganese(I) pincer complexes. In the past, using noble metal complexes, especially ruthenium pincer complexes, several hydrogen transfer reactions were reported and used for the C–C bond formation employing the hydrogen borrowing reaction pathways. Similarly, reduction reactions were also reported using ruthenium complexes employing metal-ligand cooperation.

Recently, manganese has become an emerging metal that showed a similar reactivity towards hydrogen transfer and reduction reactions in comparison with the ruthenium. In this dissertation, a variety of manganese and ruthenium complexes were investigated with regard to their catalytic performance in hydrogen transfer reactions.

The dissertation is divided into two sections; the first section reports on ruthenium(II) and manganese(I) catalyzed hydrogen borrowing reactions. The first section is divided into four chapters where several hydrogen borrowing reactions were studied and the reactivities of Ru(II) and Mn(I)-pincer complexes were compared. The second section comprises two chapters where reduction reactions catalyzed by Mn(I) pincer complexes were examined. In this section, reduction of difficult substrates such as CO<sub>2</sub> and carbon dioxide generated carbonates were investigated.

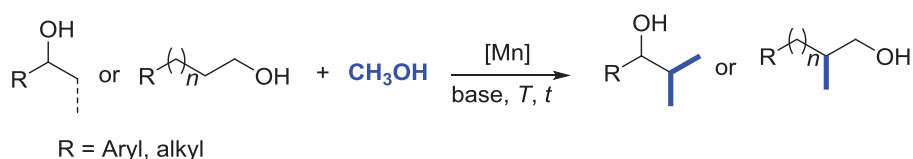
### First Section

The second chapter discusses the selective  $\beta$ -methylation of a variety of alcohols using methanol as a C1 source. In this transformation, various Ru(II) complexes were investigated. Among all studied Ru(II) complexes, the best ruthenium complex was chosen and further used for substrates scope. Control experiments were performed to investigate the catalytic cycle. Based on these results, DFT calculation was performed and a detailed catalytic cycle was proposed.



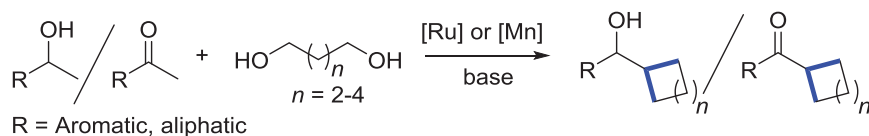
**Scheme 1.7:** Ru(II)-catalyzed  $\beta$ -methylation of alcohols using MeOH as a C1 source.

In the third chapter, one more time we studied the same reaction. However, in this case, ruthenium(II) complexes were substituted with manganese(I) complexes. Several manganese(I) complexes were investigated to perform the selective  $\beta$ -methylation of alcohols using methanol as a C1 source. Among all studied complexes, the best complex was used as a catalyst for the substrates scope. Control experiments and stoichiometric reactions with Mn-complex were performed. Based on these results, a catalytic cycle was proposed.



**Scheme 1.8:** Mn(I)-catalyzed  $\beta$ -methylation of alcohols using MeOH as a C1 source.

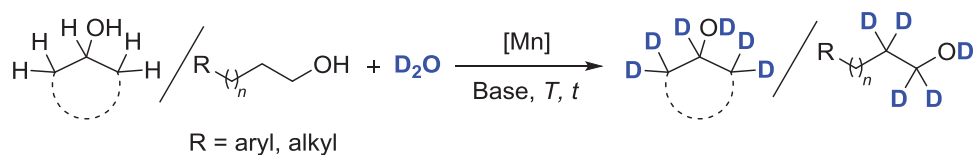
The fourth chapter deals with the formation of substituted cycloalkanes using secondary alcohols or ketones and diols as starting materials. Ru(II) and Mn(I) complexes were investigated for this transformation. Among all studied complexes, the complex which revealed good reactivity was used for the preparation of substituted cycloalkanes. Various substituted cyclopentanes, cyclohexanes and cycloheptanes were prepared using this methodology. Control experiments and mechanistic studies were performed and catalytic cycle was proposed.



**Scheme 1.9:** Synthesis of cycloalkanes from alcohols and diols using Mn(I) complex.

In the fifth chapter, we focused on the selective deuteration of alcohols using deuterium oxide ( $D_2O$ ) as a deuterium source. Previously reported literature showed that ruthenium(II) molecular complexes are well-established to perform this transformation. To compare the reactivity of Ru(II) versus Mn(I), this reaction was performed using manganese(I) pincer complex. Various benzylic alcohols and aliphatic alcohols were investigated for the selective deuteration. Detailed kinetic studies and DFT calculations were performed. Based on the results, the catalytic cycle was proposed.

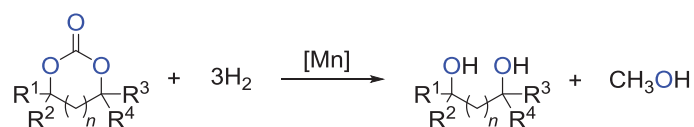




**Scheme 1.10:** Deuteration of alcohols using D<sub>2</sub>O as a deuterium source and Mn(I) complex as a precatalyst

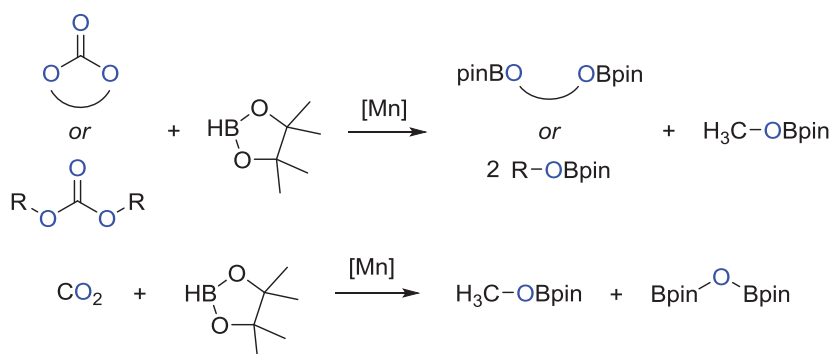
## Second Section

In chapter six, we discussed the hydrogenation of cyclic carbonates to the analogous methanol and diols. A variety of Mn(I)-pincer complexes were used for this transformation. The best catalytic was employed for the reduction of various cyclic carbonates. Control experiments were performed and based on the results, a catalytic cycle was proposed.



**Scheme 1.11:** Hydrogenation of cyclic carbonates using Mn(I) complex

Chapter seven addresses the selective reduction of CO<sub>2</sub> to the corresponding methoxy borane and CO<sub>2</sub> generated carbonates to the corresponding methoxy borane and boronate diols or alkoxy borane using pinacolborane as a reducing agent and Mn(I) pincer complex as a pre-catalyst. Control experiments were performed to get the reaction insight. Based on these experiments and results, a catalytic cycle was proposed.



**Scheme 1.12:** Hydroboration of CO<sub>2</sub> and organic carbonates using Mn(I) complex.

## References

- [1] a) A. Corma, J. Navas, M. J. Sabater, *Chem. Rev.* **2018**, *118*, 1410-1459; b) D. Wang, D. Astruc, *Chem. Rev.* **2015**, *115*, 6621-6686.
- [2] a) S. Luidold, H. Antrekowitsch, *JOM* **2007**, *59*, 20-26; b) I. Staffell, D. Scamman, A. Velazquez Abad, P. Balcombe, P. E. Dodds, P. Ekins, N. Shah, K. R. Ward, *Energy & Environmental Science* **2019**, *12*, 463-491.
- [3] C. Gunanathan, D. Milstein, *Chem. Rev.* **2014**, *114*, 12024-12087.
- [4] E. Peris, R. H. Crabtree, *Chem. Soc. Rev.* **2018**, *47*, 1959-1968.
- [5] a) T. Suzuki, *Chem. Rev.* **2011**, *111*, 1825-1845; b) P. Etayo, A. Vidal-Ferran, *Chem. Soc. Rev.* **2013**, *42*, 728-754; c) Q.-A. Chen, Z.-S. Ye, Y. Duan, Y.-G. Zhou, *Chem. Soc. Rev.* **2013**, *42*, 497-511.
- [6] a) E. Balaraman, A. Nandakumar, G. Jaiswal, M. K. Sahoo, *Catal. Sci. Technol.* **2017**, *7*, 3177-3195; b) R. A. Farrar-Tobar, B. Wozniak, A. Savini, S. Hinze, S. Tin, J. G. de Vries, *Angew. Chem. Int. Ed.* **2019**, *58*, 1129-1133; c) G. Wienhöfer, I. Sorribes, A. Boddien, F. Westerhaus, K. Junge, H. Junge, R. Llusar, M. Beller, *J. Am. Chem. Soc.* **2011**, *133*, 12875-12879; d) W. Ai, R. Zhong, X. Liu, Q. Liu, *Chem. Rev.* **2019**, *119*, 2876-2953.
- [7] a) N. Gorgas, K. Kirchner, *Acc. Chem. Res.* **2018**, *51*, 1558-1569; b) M. Garbe, K. Junge, M. Beller, *Eur. J. Org. Chem.* **2017**, *2017*, 4344-4362; c) G. A. Filonenko, R. van Putten, E. J. M. Hensen, E. A. Pidko, *Chem. Soc. Rev.* **2018**, *47*, 1459-1483.
- [8] a) J. R. Khusnutdinova, D. Milstein, *Angew. Chem. Int. Ed.* **2015**, *54*, 12236-12273; b) A. Mukherjee, D. Milstein, *ACS Catal.* **2018**, *8*, 11435-11469.
- [9] a) A. Kaithal, M. Hölscher, W. Leitner, *Angew. Chem. Int. Ed.* **2018**, *57*, 13449-13453; b) A. Kaithal, M. Schmitz, M. Hölscher, W. Leitner, *ChemCatChem* **2019**, DOI: 10.1002/cctc.201900788; c) A. Kaithal, S. Sen, C. Erken, T. Weyhermüller, M. Hölscher, C. Werlé, W. Leitner, *Nat. Commun.* **2018**, *9*, 4521.
- [10] R. Langer, G. Leitus, Y. Ben-David, D. Milstein, *Angew. Chem. Int. Ed.* **2011**, *50*, 2120-2124.
- [11] G. Bauer, K. A. Kirchner, *Angew. Chem. Int. Ed.* **2011**, *50*, 5798-5800.
- [12] J. G. Donkervoort, J. L. Vicario, J. T. B. H. Jastrzebski, G. van Koten, G. Cahiez, *Recl. Trav. Chim. Pays-Bas* **1996**, *115*, 547-548.
- [13] B. de Bruin, E. Bill, E. Bothe, T. Weyhermüller, K. Wieghardt, *Inorg. Chem.* **2000**, *39*, 2936-2947.
- [14] A. T. Radosevich, J. G. Melnick, S. A. Stoian, D. Bacciu, C.-H. Chen, B. M. Foxman, O. V. Ozerov, D. G. Nocera, *Inorg. Chem.* **2009**, *48*, 9214-9221.
- [15] A. M. Tondreau, J. M. Boncella, *Polyhedron* **2016**, *116*, 96-104.
- [16] T. P. Hanusa, *J. Chem. Educ.* **1987**, *64*, 686.
- [17] a) S. Elangovan, J. Neumann, J.-B. Sortais, K. Junge, C. Darcel, M. Beller, *Nat. Commun.* **2016**, *7*, 12641; b) T. Liu, L. Wang, K. Wu, Z. Yu, *ACS Catal.* **2018**, *8*, 7201-7207; c) S. Chakraborty, P. Daw, Y. Ben David, D. Milstein, *ACS Catal.* **2018**, *8*, 10300-10305; d) J. C. Borghs, M. A. Tran, J. Sklyaruk, M. Rueping, O. El-Sepelgy, *J. Org. Chem.* **2019**, *84*, 7927-7935; e) J. Rana, V. Gupta, E. Balaraman, *Dalton Trans.* **2019**, *48*, 7094-7099; f) Y. K. Jang, T. Krückel, M. Rueping, O. El-Sepelgy, *Org. Lett.* **2018**, *20*, 7779-7783; g) M. K. Barman, A. Jana, B. Maji, *Adv. Synth. Catal.* **2018**, *360*, 3233-3238.

- [18] a) S. Elangovan, C. Topf, S. Fischer, H. Jiao, A. Spannenberg, W. Baumann, R. Ludwig, K. Junge, M. Beller, *J. Am. Chem. Soc.* **2016**, *138*, 8809-8814; b) A. Kaithal, M. Hölscher, W. Leitner, *Angew. Chem. Int. Ed.* **2018**, *130*, 13637-13641; c) A. Kumar, T. Janes, N. A. Espinosa-Jalapa, D. Milstein, *Angew. Chem. Int. Ed.* **2018**, *57*, 12076-12080; d) V. Zubar, Y. Lebedev, L. M. Azofra, L. Cavallo, O. El-Sepelgy, M. Rueping, *Angew. Chem. Int. Ed.* **2018**, *57*, 13439-13443; e) R. van Putten, E. A. Uslamin, M. Garbe, C. Liu, A. Gonzalez-de-Castro, M. Lutz, K. Junge, E. J. M. Hensen, M. Beller, L. Lefort, E. A. Pidko, *Angew. Chem. Int. Ed.* **2017**, *56*, 7531-7534; f) U. K. Das, A. Kumar, Y. Ben-David, M. A. Iron, D. Milstein, *J. Am. Chem. Soc.* **2019**, *141*, 12962-12966; g) N. A. Espinosa-Jalapa, A. Nerush, L. J. W. Shimon, G. Leitus, L. Avram, Y. Ben-David, D. Milstein, *Chem. Eur. J.* **2017**, *23*, 5934-5938; h) M. B. Widegren, M. L. Clarke, *Org. Lett.* **2018**, *20*, 2654-2658.
- [19] a) R. Fertig, T. Irrgang, F. Freitag, J. Zander, R. Kempe, *ACS Catal.* **2018**, *8*, 8525-8530; b) B. G. Reed-Berendt, K. Polidano, L. C. Morrill, *Org. Biomol. Chem.* **2019**, *17*, 1595-1607.
- [20] a) R. Shannon, *Acta Crystallogr. A* **1976**, *32*, 751-767; b) K. Li, D. Xue, *J. Phys. Chem. A* **2006**, *110*, 11332-11337.
- [21] A. Mukherjee, A. Nerush, G. Leitus, L. J. W. Shimon, Y. Ben David, N. A. Espinosa Jalapa, D. Milstein, *J. Am. Chem. Soc.* **2016**, *138*, 4298-4301.
- [22] a) B. Chatterjee, C. Gunanathan, *Org. Lett.* **2015**, *17*, 4794-4797; b) S. Thiyagarajan, C. Gunanathan, *ACS Catal.* **2017**, *7*, 5483-5490; c) S. Fu, Z. Shao, Y. Wang, Q. Liu, *J. Am. Chem. Soc.* **2017**, *139*, 11941-11948.
- [23] S. Elangovan, M. Garbe, H. Jiao, A. Spannenberg, K. Junge, M. Beller, *Angew. Chem. Int. Ed.* **2016**, *55*, 15364-15368.
- [24] M. G. Edwards, R. F. R. Jazzar, B. M. Paine, D. J. Shermer, M. K. Whittlesey, J. M. J. Williams, D. D. Edney, *Chem. Commun.* **2004**, 90-91.
- [25] G. Chelucci, *Coord. Chem. Rev.* **2017**, *331*, 1-36.
- [26] A. Nerush, M. Vogt, U. Gellrich, G. Leitus, Y. Ben-David, D. Milstein, *J. Am. Chem. Soc.* **2016**, *138*, 6985-6997.
- [27] M. Peña-López, P. Piehl, S. Elangovan, H. Neumann, M. Beller, *Angew. Chem. Int. Ed.* **2016**, *55*, 14967-14971.
- [28] O. El-Sepelgy, E. Matador, A. Brzozowska, M. Rueping, *ChemSusChem* **2019**, *12*, 3099-3102.
- [29] a) V. G. Landge, A. Mondal, V. Kumar, A. Nandakumar, E. Balaraman, *Org. Biomol. Chem.* **2018**, *16*, 8175-8180; b) S. Elangovan, J. Neumann, J.-B. Sortais, K. Junge, C. Darcel, M. Beller, *Nat. Commun.* **2016**, *7*, 12641; c) L. Homberg, A. Roller, K. C. Hultsch, *Org. Lett.* **2019**, *21*, 3142-3147.
- [30] A. Jana, C. B. Reddy, B. Maji, *ACS Catal.* **2018**, *8*, 9226-9231.
- [31] a) C. S. Cho, B. T. Kim, T.-J. Kim, S. Chul Shim, *Tetrahedron Lett.* **2002**, *43*, 7987-7989; b) R. Martínez, D. J. Ramón, M. Yus, *Tetrahedron* **2006**, *62*, 8982-8987; c) T. Kuwahara, T. Fukuyama, I. Ryu, *Org. Lett.* **2012**, *14*, 4703-4705; d) F.-X. Yan, M. Zhang, X.-T. Wang, F. Xie, M.-M. Chen, H. Jiang, *Tetrahedron* **2014**, *70*, 1193-1198; e) E. Putignano, G. Bossi, P. Rigo, W. Baratta, *Organometallics* **2012**, *31*, 1133-1142; f) C. Schlepphorst, B. Maji, F. Glorius, *ACS Catal.* **2016**, *6*, 4184-4188; g) C. S. Cho, B. T. Kim, H.-S. Kim, T.-J. Kim, S. C. Shim, *Organometallics* **2003**, *22*, 3608-3610; h) D. Gnanamgari, C. H. Leung, N. D. Schley, S. T. Hilton, R. H. Crabtree, *Org. Biomol. Chem.* **2008**, *6*, 4442-4445; i) Q. Wang, K. Wu, Z.

- Yu, *Organometallics* **2016**, *35*, 1251-1256; j) W. Baratta, E. Herdtweck, K. Siega, M. Toniutti, P. Rigo, *Organometallics* **2005**, *24*, 1660-1669; k) X. Chang, L. W. Chuan, L. Yongxin, S. A. Pullarkat, *Tetrahedron Lett.* **2012**, *53*, 1450-1455; l) M. Viciano, M. Sanaú, E. Peris, *Organometallics* **2007**, *26*, 6050-6054; m) R. Grigg, T. R. B. Mitchell, S. Sutthivaiyakit, N. Tongpenyai, *Tetrahedron Lett.* **1981**, *22*, 4107-4110; n) T. Kuwahara, T. Fukuyama, I. Ryu, *Chem. Lett.* **2013**, *42*, 1163-1165; o) T. Jensen, R. Madsen, *J. Org. Chem.* **2009**, *74*, 3990-3992; p) M. B. Chaudhari, G. S. Bisht, P. Kumari, B. Gnanaprakasam, *Org. Biomol. Chem.* **2016**, *14*, 9215-9220.
- [32] A. Kaithal, P. v. Bonn, M. Hölscher, W. Leitner, *Angew. Chem. Int. Ed.* **2019**, DOI: 10.1002/anie.201909035.
- [33] S. E. Hosseini, M. A. Wahid, *Renew. Sust. Energ. Rev.* **2016**, *57*, 850-866.
- [34] M. L. Clarke, M. B. Díaz-Valenzuela, A. M. Z. Slawin, *Organometallics* **2007**, *26*, 16-19.
- [35] W. Baratta, L. Fanfoni, S. Magnolia, K. Siega, P. Rigo, *Eur. J. Inorg. Chem.* **2010**, *2010*, 1419-1423.
- [36] C. Gunanathan, M. Hölscher, W. Leitner, *Eur. J. Inorg. Chem.* **2011**, *2011*, 3381-3386.
- [37] a) D. Spasyuk, S. Smith, D. G. Gusev, *Angew. Chem. Int. Ed.* **2013**, *52*, 2538-2542; b) S. Takebayashi, S. H. Bergens, *Organometallics* **2009**, *28*, 2349-2351; c) J. Zhang, E. Balaraman, G. Leitus, D. Milstein, *Organometallics* **2011**, *30*, 5716-5724; d) D. Spasyuk, S. Smith, D. G. Gusev, *Angew. Chem. Int. Ed.* **2012**, *51*, 2772-2775; e) W. Kuriyama, T. Matsumoto, O. Ogata, Y. Ino, K. Aoki, S. Tanaka, K. Ishida, T. Kobayashi, N. Sayo, T. Saito, *Org. Process Res. Dev.* **2012**, *16*, 166-171; f) J. Zhang, G. Leitus, Y. Ben-David, D. Milstein, *Angew. Chem. Int. Ed.* **2006**, *45*, 1113-1115; g) W. Kuriyama, Y. Ino, O. Ogata, N. Sayo, T. Saito, *Adv. Synth. Catal.* **2010**, *352*, 92-96.
- [38] E. Balaraman, B. Gnanaprakasam, L. J. W. Shimon, D. Milstein, *J. Am. Chem. Soc.* **2010**, *132*, 16756-16758.
- [39] a) E. Balaraman, C. Gunanathan, J. Zhang, L. J. W. Shimon, D. Milstein, *Nat. Chem* **2011**, *3*, 609; b) Z. Han, L. Rong, J. Wu, L. Zhang, Z. Wang, K. Ding, *Angew. Chem. Int. Ed.* **2012**, *51*, 13041-13045; c) E. Balaraman, Y. Ben-David, D. Milstein, *Angew. Chem. Int. Ed.* **2011**, *50*, 11702-11705; d) M. Vogt, M. Gargir, M. A. Iron, Y. Diskin-Posner, Y. Ben-David, D. Milstein, *Chem. Eur. J.* **2012**, *18*, 9194-9197; e) G. A. Filonenko, M. P. Conley, C. Copéret, M. Lutz, E. J. M. Hensen, E. A. Pidko, *ACS Catal.* **2013**, *3*, 2522-2526; f) C. A. Huff, M. S. Sanford, *ACS Catal.* **2013**, *3*, 2412-2416.
- [40] F. Kallmeier, T. Irrgang, T. Dietel, R. Kempe, *Angew. Chem. Int. Ed.* **2016**, *55*, 11806-11809.
- [41] V. Papa, J. R. Cabrero-Antonino, E. Alberico, A. Spanneberg, K. Junge, H. Junge, M. Beller, *Chem. Sci.* **2017**, *8*, 3576-3585.
- [42] a) M. B. Widegren, G. J. Harkness, A. M. Z. Slawin, D. B. Cordes, M. L. Clarke, *Angew. Chem. Int. Ed.* **2017**, *56*, 5825-5828; b) M. Garbe, K. Junge, S. Walker, Z. Wei, H. Jiao, A. Spanneberg, S. Bachmann, M. Scalone, M. Beller, *Angew. Chem. Int. Ed.* **2017**, *56*, 11237-11241.
- [43] J. A. Garduño, J. J. García, *ACS Catal.* **2019**, *9*, 392-401.
- [44] A. Dubey, L. Nencini, R. R. Fayzullin, C. Nervi, J. R. Khusnutdinova, *ACS Catal.* **2017**, *7*, 3864-3868.

- [45] F. Bertini, M. Glatz, N. Gorgas, B. Stöger, M. Peruzzini, L. F. Veiros, K. Kirchner, L. Gonsalvi, *Chem. Sci.* **2017**, *8*, 5024-5029.
- [46] S. Kar, A. Goepfert, J. Kothandaraman, G. K. S. Prakash, *ACS Catal.* **2017**, *7*, 6347-6351.
- [47] a) J.-i. Ito, S. Ujiiie, H. Nishiyama, *Chem. Commun.* **2008**, 1923-1925; b) W. Baratta, M. Bosco, G. Chelucci, A. Del Zotto, K. Siega, M. Toniutti, E. Zangrando, P. Rigo, *Organometallics* **2006**, *25*, 4611-4620; c) J. Neumann, C. Bornschein, H. Jiao, K. Junge, M. Beller, *Eur. J. Org. Chem.* **2015**, *2015*, 5944-5948; d) E. Balaraman, E. Fogler, D. Milstein, *Chem. Commun.* **2012**, *48*, 1111-1113; e) E. Fogler, E. Balaraman, Y. Ben-David, G. Leitun, L. J. W. Shimon, D. Milstein, *Organometallics* **2011**, *30*, 3826-3833; f) G. A. Filonenko, E. Cosimi, L. Lefort, M. P. Conley, C. Copéret, M. Lutz, E. J. M. Hensen, E. A. Pidko, *ACS Catal.* **2014**, *4*, 2667-2671; g) Y. Sun, C. Koehler, R. Tan, V. T. Annibale, D. Song, *Chem. Commun.* **2011**, *47*, 8349-8351; h) J. R. Cabrero-Antonino, E. Alberico, H.-J. Drexler, W. Baumann, K. Junge, H. Junge, M. Beller, *ACS Catal.* **2016**, *6*, 47-54.
- [48] a) R. Reguillo, M. Grellier, N. Vautravers, L. Vendier, S. Sabo-Etienne, *J. Am. Chem. Soc.* **2010**, *132*, 7854-7855; b) J. R. Cabrero-Antonino, E. Alberico, K. Junge, H. Junge, M. Beller, *Chem. Sci.* **2016**, *7*, 3432-3442; c) C. Federsel, R. Jackstell, A. Boddien, G. Laurency, M. Beller, *ChemSusChem* **2010**, *3*, 1048-1050.
- [49] a) J. Kothandaraman, A. Goepfert, M. Czaun, G. A. Olah, G. K. S. Prakash, *J. Am. Chem. Soc.* **2016**, *138*, 778-781; b) S. Kar, R. Sen, A. Goepfert, G. K. S. Prakash, *J. Am. Chem. Soc.* **2018**, *140*, 1580-1583; c) S. Wesselbaum, T. vom Stein, J. Klankermayer, W. Leitner, *Angew. Chem. Int. Ed.* **2012**, *51*, 7499-7502; d) N. M. Rezayee, C. A. Huff, M. S. Sanford, *J. Am. Chem. Soc.* **2015**, *137*, 1028-1031; e) S. Wesselbaum, V. Moha, M. Meuresch, S. Brosinski, K. M. Thenert, J. Kothe, T. v. Stein, U. Englert, M. Hölscher, J. Klankermayer, W. Leitner, *Chem. Sci.* **2015**, *6*, 693-704.

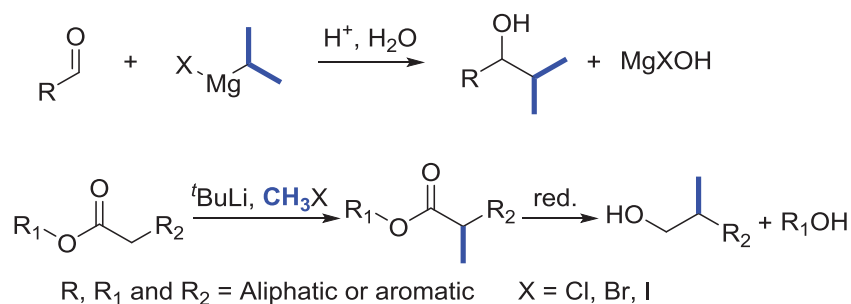
## 2. Ruthenium catalyzed $\beta$ -methylation of alcohols using MeOH as a C1 source

Parts of this chapter have been published:

A. Kaithal, M. Schmitz, M. Hölscher, W. Leitner, *ChemCatChem*, **2019**, *11*, 5287-5291.

A. Kaithal, M. Schmitz, M. Hölscher, W. Leitner, *ChemCatChem*. **2020**, *12*, 781-787.

The introduction of a methyl group into alkyl chains using C–C bond formation strategies is an essential methodology in medicinal chemistry, fuel production and fine chemical synthesis.<sup>[1]</sup> At present, 67% of all drug molecules comprise of at least one methyl group.<sup>[2]</sup> The functionalization of C–H bonds in methyl groups can also lead to the construction of a variety of bonds such as C–C, C–O, and C–X (X = Cl, Br, I) bonds. Therefore, the development of new sustainable methods for the methylation of organic molecules is an important topic. Traditionally, the methylation is carried out using highly toxic and flammable reagents such as Grignard reagents or methylation reagents (e.g. methyl iodide, methyl sulfate or diazomethane, Scheme 2.1).<sup>[3]</sup> Reactions with these compounds generate a stoichiometric amount of waste and require cumbersome workup procedures.

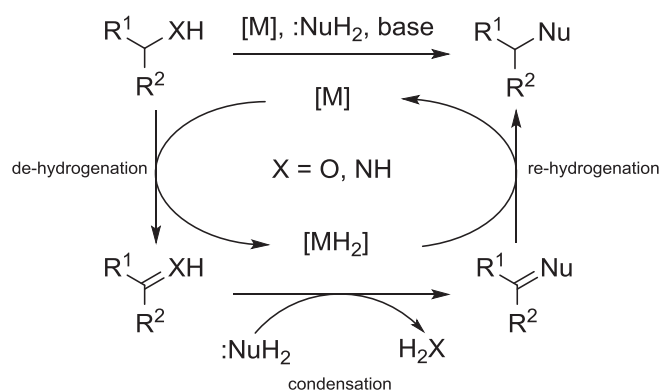


**Scheme 2.1:** Traditional approach for the preparation of  $\beta$ -methylated alcohols.

To alleviate these problems, a less toxic and easy to apply compound which can be used as a methylation reagent in organic synthesis should be used. In this regard, methanol would be an ideal choice as a sustainable C1 building block. Presently, bio-methanol or green methanol is produced from biomass or from CO<sub>2</sub> and H<sub>2</sub> confirming the usage of renewable carbon and renewable energy to synthesize organic products.<sup>[4]</sup>



Hydrogen borrowing reactions, also known as hydrogen auto-transfer can be seen as one important catalytic concept in green chemistry.<sup>[5]</sup> This reaction integrates a transfer hydrogenation process with a parallel reaction by reacting *in situ* generated intermediates (Scheme 2.2). Hydrogen borrowing reactions allow not only the formation of C–C bonds; they can also form other linkages including C–N bonds while reaction of amines or amides and alcohols as an alkylating reagent. In this way the toolbox for atom-economical syntheses of bulk and fine chemicals is extended.

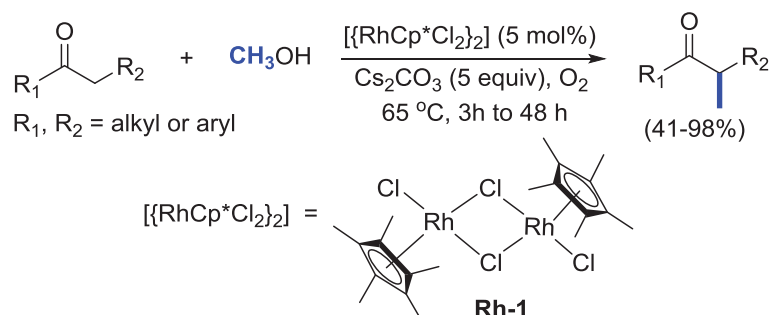


**Scheme 2.2:** Metal-catalyzed alkylation reaction via “hydrogen borrowing methodology”.

Using the hydrogen borrowing methods, methanol could be potentially used as an alkylating C1-reagent. The use of methanol is well known for the high-temperature gas-phase methylation of ethanol and propanol to *iso*-butanol.<sup>[6]</sup> However, the usage of methanol in combination with molecular catalysts for selective methylations of aromatic and aliphatic alcohols is not well explored. Iridium, rhodium, and ruthenium complexes are known catalysts for de-hydrogenations of higher alcohols for use as alkylating reagents.<sup>[7]</sup> The  $\alpha$ -methylation of ketones was reported using molecular Ir-, Rh- and Ru-complexes with high catalyst loadings.<sup>[1d, 8]</sup> However, the homogeneously metal-catalyzed selective  $\beta$ -methylation of alcohols using methanol as a C1 source is still not fully explored. It is assumed that the alkylation with methanol is difficult due to its high de-hydrogenation energy with respect to other alcohols.<sup>[9]</sup>

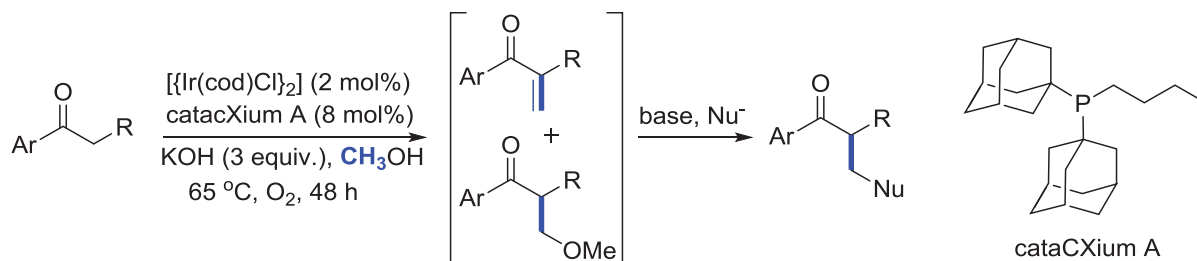
In 2014, the group of Donohoe showed an example for the selective  $\alpha$ -methylation of ketones using methanol as a C1 source (Scheme 2.3).<sup>[8a]</sup> The reaction was performed at 65 °C employing the molecular rhodium catalyst [ $\{Cp^*RhCl_2\}_2$ ] **Rh-1** and a stoichiometric amount of  $Cs_2CO_3$  as a base. This reaction was performed with a high catalyst loading (5 mol%) and an excess amount of a base (5 equivalents of base with respect to the ketone) to accomplish moderate to high

conversions. A range of aromatic and aliphatic ketones was selectively  $\alpha$ -methylated using methanol as the C1 source. The reaction showed good reactivity for mono-methylations of a variety of aromatic and aliphatic ketones while the reactivity for the di-methylation of ketones remained low. Mechanistic studies showed that the reaction proceeds via “hydrogen borrowing reaction pathways”.



**Scheme 2.3:**  $\alpha$ -methylation of ketones using methanol reported by Donohoe *et. al.*<sup>[8a]</sup>

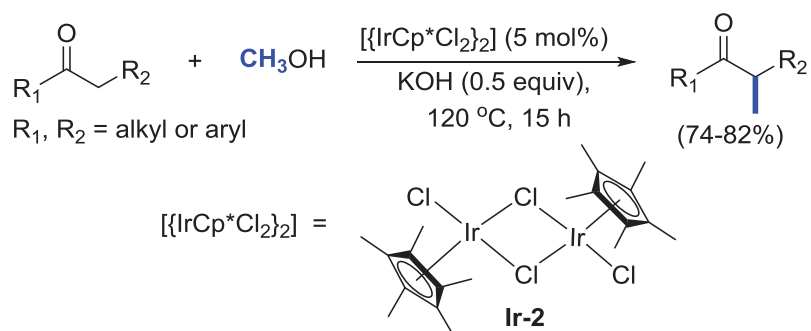
Later, in 2015, Donohoe’s group developed a similar procedure whereupon the reaction of methanol with the ketone provided a stabilized enone intermediate which subsequently reacted with nucleophiles to generate alkylated ketones as products (Scheme 2.4).<sup>[8c]</sup> This work was carried out using molecular iridium complex  $[\{\text{Ir}(\text{cod})\text{Cl}\}_2]$  **Ir-1** as a pre-catalyst, cataCXium A (a bulky mono-dentate phosphine ligand) as a co-catalyst and a stoichiometric amount of KOH. CataCXium A was used to interrupt the catalytic cycle and prevent an enone reduction in the reaction. Interestingly, this reaction was performed in the presence of oxygen atmosphere and somehow the presence of oxygen accelerates the reaction rate. A variety of aromatic and aliphatic ketones were successfully alkylated using methanol and different nucleophiles resulting in yields of up to 94%.



**Scheme 2.4:**  $\alpha$ -alkylation of ketones using methanol and nucleophile reported by Donohoe *et. al.*<sup>[8c]</sup>



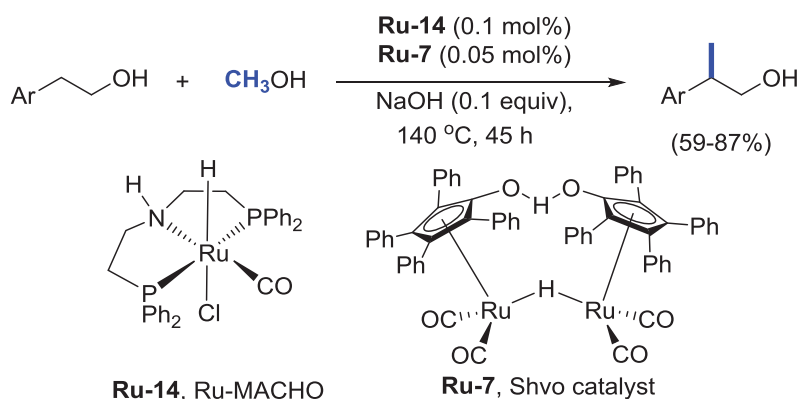
Similarly, in 2014, the group of Obora reported the selective methylation of ketones using a dimeric iridium complex and methanol as a methylating reagent (Scheme 2.5).<sup>[8b]</sup> The reaction was performed using iridium complex  $[\{\text{Cp}^*\text{IrCl}_2\}_2]$  **Ir-2** as a precatalyst and base as a co-catalyst. This catalyst system showed a good selectivity for both mono-methylation and di-methylation. Additionally, this work also introduced the three components cross  $\alpha$ -alkylation using methanol and a primary alcohol as an alkylating reagent. Apart from alcohols, they showed the selective  $\alpha$ -methylation of arylacetonitriles using the same iridium complex.



**Scheme 2.5:**  $\alpha$ -methylation of ketones using methanol reported by Obora *et. al.*<sup>[8b]</sup>

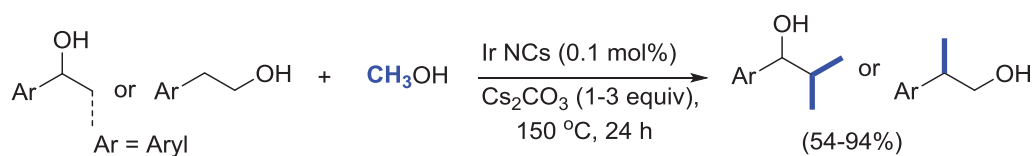
Concerning the selective  $\beta$ -methylation of alcohols using methanol as a C1 source, only a handful of reports for this challenging transformation are available. In 2014 Beller *et. al.* reported the currently only available molecular catalytic system for the selective  $\beta$ -methylation of alcohols (Scheme 2.6).<sup>[10]</sup> This work was carried out using the combination of two ruthenium complexes and base as a co-catalyst. The Ru-MACHO complex **Ru-14** showed little catalytic activity in this transformation, however, the combination of two distinct molecular catalysts, namely Ru-MACHO **Ru-14** and Ru-Shvo **Ru-7** catalyst revealed the best catalytic activity for this transformation.

The drawback of this catalytic system is the restriction of the reaction system to 2-arylethanol as substrates and an extended reaction time of 40 h, including the de-pressurization of the reaction setup to remove the extra  $\text{H}_2$  formation at least twice. Reaction with other alcohols was also investigated. However, the catalyst system did not exhibit a good reactivity to the desired products. The highest catalytic turnover number for 2-arylethanol as a substrate achieved was 500.



**Scheme 2.6:**  $\beta$ -methylation of alcohols using methanol reported by Beller *et. al.*<sup>[10]</sup>

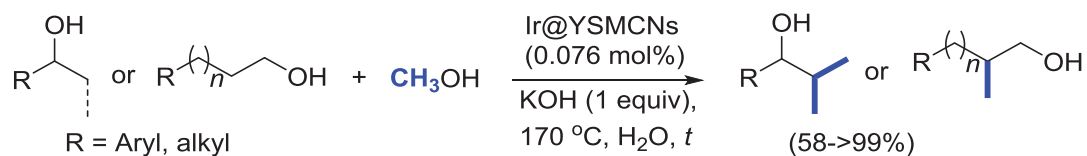
Apart from the homogeneous catalytic system, few heterogeneous catalytic systems were also reported for this particular transformation. In 2017, Obora *et. al.* reported a heterogeneous catalytic system which catalyzes the selective  $\beta$ -methylation of alcohols employing iridium nanoclusters using methanol as the C1 source (Scheme 2.7).<sup>[11]</sup> The preparation of nanoclusters (NCs) was carried out using  $\text{IrCl}_3$  as a metal precursor, which upon heating in DMF at  $140\text{ }^\circ\text{C}$  resulted in the formation of iridium nanoclusters (Ir NCs) after 10 h. The Ir NCs were stabilized using DMF as a solvent. These nanoclusters were employed for catalysis, and reactions of secondary alcohols and 2-aryl ethanols with methanol were carried out using Ir NCs and a stoichiometric amount of base. The reaction resulted in a yield of up to 94% to the corresponding desired  $\beta$ -methylated product. However, this catalytic system was restricted to aromatic alcohols only and remained unreactive towards aliphatic alcohols.



**Scheme 2.7:**  $\beta$ -methylation of alcohols using methanol reported by Obora *et. al.*<sup>[11]</sup>

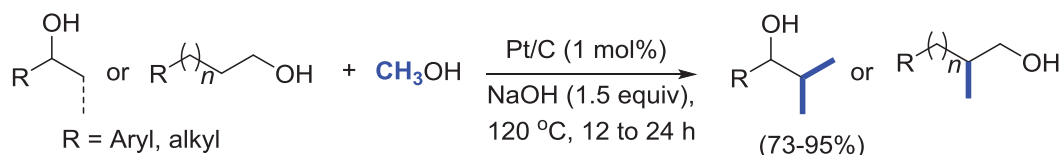
In the same year, Liu *et. al.* showed that this particular transformation can also be achieved using another type of heterogeneous iridium catalyst (Scheme 2.8).<sup>[12]</sup> The nanocatalyst was prepared using  $\text{IrCl}_3$  as a metal precursor which was encapsulated in mesoporous yolk-shell-structured carbon nanosphere (Ir@YSMCNs). This catalyst revealed the best catalytic activity for the methylation reaction of alcohols. The catalyst system, comprising of a low loading of Ir@YSMCNs (0.076 mol%) and a base (1 equiv. with respect to the substrate), showed a high

tolerance towards a variety of aromatic and aliphatic alcohols at 170 °C. The highest turnover number for this transformation was 9259, starting from ethanol to the corresponding *iso*-butanol.



**Scheme 2.8:**  $\beta$ -methylation of alcohols using methanol reported by Liu *et. al.*<sup>[12]</sup>

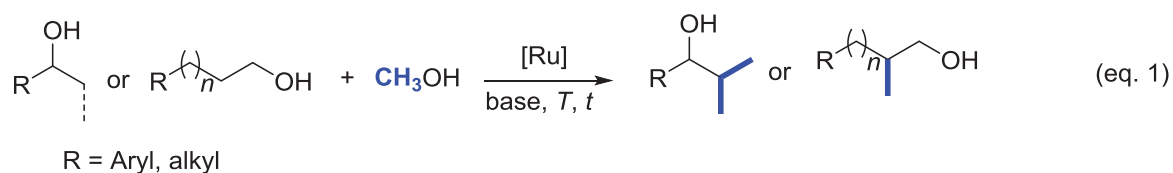
While the work of this thesis was in progress, in 2018, the group of Shimizu succeeded in this transformation using a heterogeneous platinum catalyst supported on charcoal and a stoichiometric amount of base (Scheme 2.9).<sup>[13]</sup> Numerous primary alcohols and secondary alcohols were selective  $\beta$ -methylated employing MeOH as a C1 source. For 2-phenylethanol as a substrate, the reaction resulted in a TON of 3280 to the corresponding  $\beta$ -methylated product.



**Scheme 2.9:**  $\beta$ -methylation of alcohols using methanol reported by Shimizu *et. al.*<sup>[13]</sup>

## 2.1. Objective

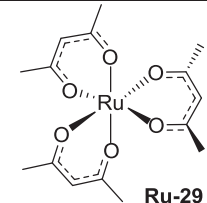
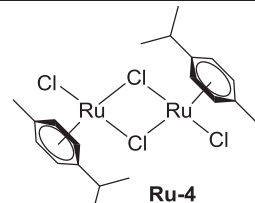
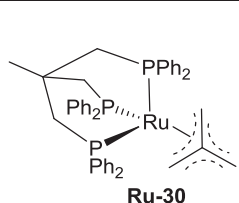
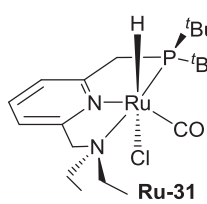
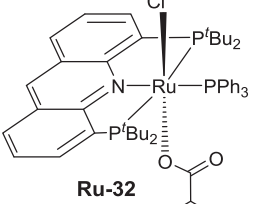
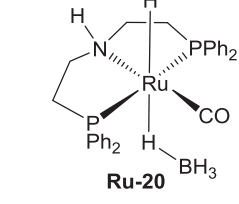
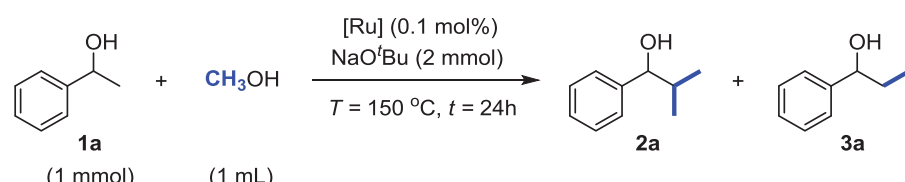
The development of an active and selective molecular catalyst system for the utilization of methanol as a C1 source is the main objective of this work. The aim is the implementation of methyl branches into the carbon chains of alcohol, selectively at  $\beta$ -position (eq 1). At present, very few examples are known which can accomplish this transformation using a homogeneous molecular catalyst and methanol as a methylating agent. Various ruthenium complexes will be chosen as precatalysts for this transformation. The best catalyst will be selected and further used for substrates scope. To investigate the catalytic cycle, control experiments and stoichiometric reactions will be performed. Based on these results, the DFT calculation will be carried out to propose a detailed catalytic cycle.



## 2.2. Catalyst optimization

At the outset, 1-phenylethan-1-ol **1a** was chosen as a benchmark substrate to identify an effective catalyst for this transformation. Various ruthenium complexes were screened which had been shown to be reactive in “hydrogen borrowing reactions”. The initial reaction was performed using substrate **1a** (1 mmol), MeOH (1 mL), NaO<sup>t</sup>Bu (2 mmol) and a series of various Ru-precatalysts (0.1 mol%) at 150 °C for 24 h. Under these conditions, a simple and unmodified complex, namely ruthenium(III) acetylacetonate already revealed moderate activity showing 51% conversion and 33% yield to the di-methylated product **2a** and 11% yield to the mono-methylated product **3a** (Table 2.1, entry 1). Ruthenium complexes bearing the *p*-cymene groups as ligands were also investigated. The reaction of commercially available Dichloro(*p*-cymene)ruthenium(II) dimer revealed only a low activity in this transformation (Table 2.1, entry 2). In a similar manner, the reaction of a proline substituted ruthenium *p*-cymene complex also exhibited low product formation (Table 2.1, entry 3). Interestingly, incorporation of phosphine ligands into the ruthenium coordination sphere enhanced the reactivity and resulted in high product formation. The reaction of a commercially available ruthenium phosphine complex such as [RuHCl(CO)(PPh<sub>3</sub>)<sub>3</sub>] revealed a good conversion of 88% with a yield of 50% of **2a** and 6% for **3a** (Table 2.1, entry 4). However, substituting the phenyl group to *iso*-propyl at the phosphine moieties decreased the catalytic activity to 40% (Table 2.1, entry 5). Based on these results, various ruthenium complexes with phosphine ligands were investigated. Using the same reaction conditions, 86% conversion was obtained using the ruthenium-triphos-TMM complex with 65% yield of **2a** and only 5% yield of **3a** (Table 2.1, entry 6). The reaction revealed a major selectivity to the di-methylated product **2a** formation. Appealingly, ruthenium pincer complexes such as basic lutidine based ruthenium PNN complex and ruthenium-Acriphos complex also showed product formation with good conversion and yield (Table 2.1, entry 7, 8). In this regard, the best catalytic activity was found when the Ru-MACHO-BH pincer complex was used as a pre-catalyst in the reaction. Using the same reaction condition, this complex resulted in >99% conversion with a 75% yield of **2a** and 11% yield of **3a** (Table 2.1, entry 9).

**Table 2.1:**  $\beta$ -methylation of 1-phenyl ethanol **1a** with various ruthenium precatalysts.<sup>[a, b]</sup>

			
Ruthenium(III) acetylacetonate	[Ru( <i>p</i> -cymene)Cl] <sub>2</sub> Cl <sub>2</sub>	[Ru-(triphos)(tmm)]	
			
[RuHCl(CO)(PNN)]	[Ru(Acriphos)(PPh <sub>3</sub> )(Cl)(PhCO <sub>2</sub> )]	Ru-MACHO-BH	
			
Entry	Catalyst	Conv.(%)	Yield ( <b>2a/3a</b> )
1	Ruthenium(III) acetylacetonate	51	33/11
2	[Ru( <i>p</i> -cymene)Cl] <sub>2</sub> Cl <sub>2</sub>	33	13/11
3	[Ru( <i>p</i> -cymene)Cl(proline)]	36	28/3
4	RuHCl(CO)(PPh <sub>3</sub> ) <sub>3</sub>	88	50/6
5	RuHCl(CO)(P <sup><i>i</i></sup> Pr) <sub>3</sub>	40	21/9
6	[Ru-(triphos)(tmm)]	86	65/5
7	[RuHCl(CO)(PNN)] <sup>b</sup>	89	40/22
8	[Ru(Acriphos)(PPh <sub>3</sub> )(Cl)(PhCO <sub>2</sub> )]	64	47/16
9	Ru-MACHO-BH	97	75/11

[a] Conditions: **1a** (1 mmol), MeOH (1 mL as a reagent and solvent), Ru precatalyst (0.1 mol%), and NaO<sup>*t*</sup>Bu (2 mmol) at 150 °C for 24 h. [b] Conversions and yields were determined by <sup>1</sup>H-NMR analysis using mesitylene as internal standard. PNN = 2-(di-*tert*-butylphosphinomethyl)-6-(diethylaminomethyl)pyridine, tmm = trimethylene methane.

### 2.3. Temperature and base optimization

Based on the previously optimized reaction conditions, Ru-MACHO-BH complex **Ru-20** was used for further investigation. Next, the effect of temperature was examined (Table 2.2, entry 1–4). Decreasing the temperature from 150 °C to 125 °C or 100 °C resulted in product formation albeit with low selectivity and low yield only. The reaction at a temperature of 100 °C showed almost no reactivity at all. At 125 °C, the reaction revealed good conversion but low selectivity to the corresponding di-methylated product was observed. Increasing the reaction temperature above 150 °C did not enhance the product formation and selectivity.

Considering the base optimization, inorganic bases such as  $\text{Cs}_2\text{CO}_3$  and KOH were less effective in this transformation (Table 2.2, entry 5, 6). However, using NaOMe as a base, a comparable activity was observed as  $\text{NaO}^t\text{Bu}$ . Applying the NaOMe as a base, the reaction showed 97% conversion with a 75% yield for **2a** and 6% yield for **3a** (Table 2.2, entry 7). The best reaction condition was found when the amount of methanolate was increased to 3 equivalents instead of 2 equivalents. The results confirmed that the yield was increased and the overall selectivity was shifted to the dimethylated product **2a** (Table 2.2, entry 8).

**Table 2.2:**  $\beta$ -methylation of 1-phenyl ethanol **1a** at various temperatures and different bases<sup>[a, b]</sup>

#	Base	T [°C]	Conv. (%)	Yield (%) ( <b>2a</b> / <b>3a</b> )
1	$\text{NaO}^t\text{Bu}$	100	21	2 / 10
2	$\text{NaO}^t\text{Bu}$	125	85	50 / 27
3	$\text{NaO}^t\text{Bu}$	150	>99	75 / 11
4	$\text{NaO}^t\text{Bu}$	175	>99	73 / 6
5	KOH	150	67	13 / 48
6	$\text{Cs}_2\text{CO}_3$	150	91	0 / 2
7	NaOMe	150	97	75 / 6
8 <sup>#</sup>	NaOMe	150	92	84 / 8

[a] Conditions: **1a** (1 mmol), MeOH (1 mL as a reagent and solvent), Ru precatalyst (0.1 mol%), and base (2 mmol) for 24 h. [b] Conversions and yields were determined by  $^1\text{H-NMR}$  analysis using mesitylene as an internal standard.  
<sup>#</sup>3 mmol of NaOMe was used.

## 2.4. Ru-catalyzed $\beta$ -methylation of secondary aryl alcohols with MeOH

Based on the aforementioned optimized conditions, several secondary alcohols were tested in the  $\beta$ -methylation (Table 2.3). Initially, the focus was on the selective di-methylation of secondary alcohols. Using the standard optimized reaction condition, 1-naphthylethanol **1b** was selectively di-methylated with 78% yield and showed 67% yield to the isolated product. Electron-donating methyl-substituted 1-*p*-tolylethanol **1c** was well tolerated showing good selectivity to the di-methylated product with a yield of 84% to **2c**. Similarly, an electron-withdrawing chloro-substituent in *para*-position of the phenyl moiety **1d** also revealed good conversion. However, moderate selectivity was observed resulting in 52% yield of the di-methylated product **2d** and 30% yield to mono-methylated product **3d**.

Next, the mono-methylation of 1-arylpropanols and cyclic secondary alcohols was investigated. The mono-methylation can be performed using a low base loading with 1.5 equivalents of methanolate and a reaction time of 20 h. Using the optimized reaction conditions, 1-phenyl propanol **1e** resulted in 83% yield to the corresponding  $\beta$ -methylated product. Similarly, a methyl substituent in *para*-position in 1-phenyl propanol **1f** gave the corresponding product **2f** in 79% yield. Cyclic alcohols such as aryl-substituted five-membered **1g** and six-membered **1h** rings confirmed the product formation with 72% and 90% yield, respectively. Increasing the ring size to seven-membered ring in **1i** somehow decreased the reactivity and showed a moderate yield of 61% to the corresponding product. In five and six-membered rings, the methyl group was preferentially installed in the *trans*-position. However, in the case of a seven-member ring, no stereo-selectivity was observed.

Furthermore, to check the robustness of the catalyst, the catalyst loading was decreased to 0.005 mol%. For a reaction time of 36 h using **1e** as a substrate, product **2e** was obtained with a yield of 89% and 90% in two independent experiments, respectively which corresponds to a TON of ca. 18,000 (details are described in the experimental section). These reactions clearly showed the high reactivity and stability of the complex **Ru-20** and the robustness of the current catalytic method.



**Table 2.3:** Ru-catalyzed reactions of secondary aryl alcohols **1** with MeOH.<sup>[a, b]</sup>

		 <b>Ru-20</b>
Conversion (%) / Yield (2:3) <sup>d</sup> / Isolated Yield of dimethylated product 2 <sup>e</sup>		
 <b>2a</b> 92/(84:8)/74	 <b>2b</b> 82/(78:4)/67	 <b>2c</b> 94/(84:10)/73
 <b>2d</b> 82/(52:30)	 <b>2e<sup>c</sup></b> 83 %	 <b>2f<sup>c</sup></b> 79%
 <b>2g<sup>c</sup></b> 72/ <i>cis:trans</i> (18:54)	 <b>2h<sup>c</sup></b> 90/ <i>cis:trans</i> (37:53)	 <b>2i<sup>c</sup></b> 61/ <i>cis:trans</i> (25:36)

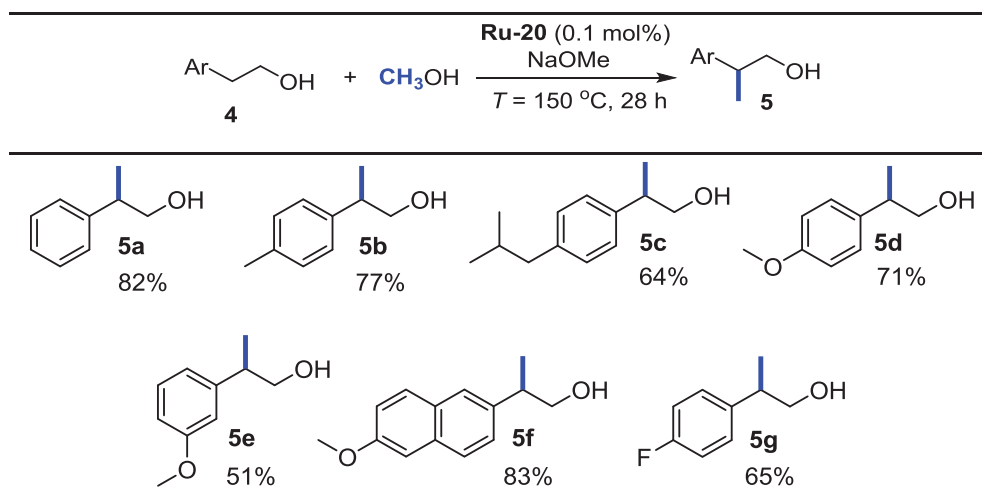
[a] Conditions: **1** (1 mmol), MeOH (1 mL as a reagent and solvent), **Ru-20** (0.1 mol%), and NaOMe (3 mmol) at 150 °C for 24 h. [b] Yields were determined by <sup>1</sup>H NMR analysis using mesitylene as internal standard. [c] **1** (1 mmol), MeOH (1 mL as a reagent and solvent), **Ru-20** (0.1 mol%) and NaOMe (1.5 mmol) at 150 °C for 20 h. [d] Number in parentheses show the yield of **2** and **3**. [e] Yield of the isolated dimethylated product **2**.

## 2.5. Ru-catalyzed $\beta$ -methylation of 2-arylethanol with MeOH

2-arylethanol are important molecules in pharmaceutical chemistry. Important pharmaceutical molecules such as ibuprofen and naproxen can be directly prepared using these substrates. Considering these points, next the selective  $\beta$ -methylation of 2-arylethanol was studied (Table 2.4). For this substrate class, 2-phenylethanol **4a** was chosen as a parent substrate. Interestingly, for this particular class, the methanolate amount could be decreased to 1 equiv. due to the high acidity of the  $\beta$ -CH proton in the benzylic position of 2-aryl ethanol. The reaction required 28 h and resulted in a selective mono-methylation. Using the optimized reaction

condition, **4a** reacted in 82% yield to mono-methylated **5a**. Interestingly, electron-donating substituents such as methyl and methoxy groups in *para*-position in 2-phenylethanols led to product formation with 77% and 71% yield, respectively. However, the reaction with methoxy substituent in *meta*-position **4e** and fluoro substituent in *para*-position **4g** in 2-arylethanols showed low reactivity with 51% and 65% yield, respectively. This low reactivity can be explained due to the electron-deficient aromatic ring of the substrates. Gratifyingly, using this methodology, pharmaceutical important molecules such as ibuprofen alcohol **5c** and naproxen alcohol **5f** were also directly prepared with good yield and selectivity.

**Table 2.4:** Ru-catalyzed reactions of 2-arylethanols **4** with MeOH.<sup>[a,b]</sup>



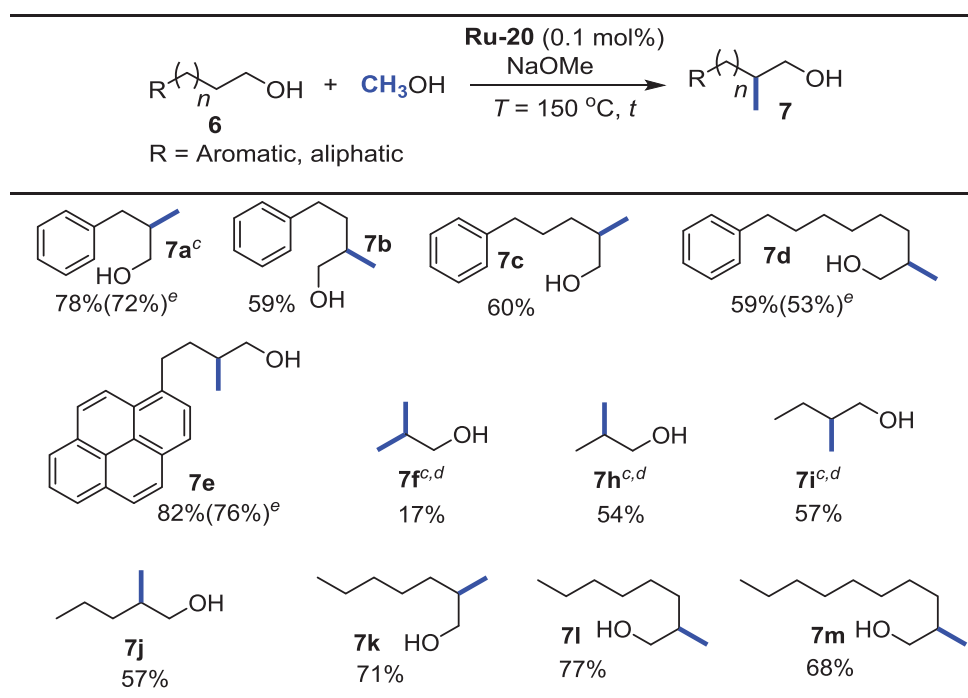
[a] Conditions: **4** (1 mmol), MeOH (1 mL as a reagent and solvent), **Ru-20** (0.1 mol%) and NaOMe (1 mmol) at 150 °C for 28 h. [b] Yields were determined by <sup>1</sup>H NMR analysis using mesitylene as internal standard.

## 2.6. Ru-catalyzed $\beta$ -methylation of aliphatic alcohols with MeOH

Aliphatic alcohols are challenging substrates to activate as they require a strong base to generate the appreciable amounts of the alcoholate anion and will, therefore, be much less nucleophilic. Therefore, the transformation of aliphatic alcohols to the corresponding  $\beta$ -methylated alcohol is more challenging than the transformation of other alcohols. Considering these points, the selective  $\beta$ -methylation of aliphatic alcohols was investigated (Table 2.5). Initially, 3-phenylpropan-1-ol **6a** was chosen as a benchmark substrate. In the presence of 1 equiv. of the base, the reactivity was low with regard to the formation of the corresponding methylated product and also a mixture of products was obtained. A change of reaction parameters confirmed

that a higher amount of methanolate (2 equiv.) was necessary to perform this reaction. Using the optimized conditions **6a** (1 mmol), NaOMe (2 mmol), Ru-MACHO-BH **Ru-20** (0.1 mol%) and MeOH (1 mL), the reaction led to the selective formation of the  $\beta$ -monomethylated product with 78% yield after 30 h. The yield of the isolated product was 72%. Increasing the carbon chain between the aryl and alcohol functionality resulted in a reduced reactivity. The reaction of 4-phenylbutan-1-ol **6b**, 5-phenylpentan-1-ol **6c** and 8-phenyloctan-1-ol **6d** with methanol showed product formation with yields of 59%, 60%, and 59%, respectively. Interestingly, 4-(pyren-1-yl)butan-1-ol **6e**, which is commonly used in photochemistry was also selectively  $\beta$ -methylated showing 82% yield and 76% yield after isolation.<sup>[14]</sup>

**Table 2.5:** Ru-catalyzed reactions of aliphatic alcohol **6** with MeOH.<sup>[a,b]</sup>



[a] Conditions: **6** (1 mmol), MeOH (1 mL as a reagent and solvent), **Ru-20** (0.1 mol%) and NaOMe (2 mmol) at 150 °C for 28 h. [b] Yields were determined by <sup>1</sup>H NMR analysis using mesitylene as internal standard. [c] Reaction time: 30 h. [d] Yields were measured by GC analysis. [e] Yield of the isolated monomethylated product **7**.

Encouraged by these results, next, the most challenging type of substrates, pure aliphatic alcohols were investigated. At first, short chain aliphatic alcohols such as ethanol, 1-propanol, 1-butanol and 1-pentanol were investigated in the selective  $\beta$ -methylation. Using the same optimized conditions, the reaction of ethanol with methanol to the corresponding di-methylated product *iso*-butanol revealed a low yield of 17%. Interestingly, the reaction of C3–C5 aliphatic

alcohols revealed the corresponding mono-methylated product in respectable yields between 54% and 57%. Furthermore, longer chain alcohols such as 1-heptanol, 1-octanol and 1-decanol were also investigated. Longer chain aliphatic alcohols showed good reactivity in comparison to small chain aliphatic alcohols. The reaction of 1-heptanol with MeOH using the same optimized conditions confirmed the corresponding mono-methylated product with a yield of 71%. Similarly, 1-octanol and 1-decanol also revealed the high activity and confirmed the product formation with 77% and 68% yields, respectively.

## 2.7. Mechanistic studies

### 2.7.1. Conversion/time profile

The conversion/time profile was mapped out using 1-phenylpropanol **1e** as a benchmark substrate. Individual experiments were performed over different reaction times. Two different kinetic regimes were observed from the data depicted in Figure 2.1. In the starting phase, the reaction was very fast reaching a conversion of up to 40% after 15 minutes. In this phase, the desired methylated product **2e** was formed in a yield of 24% accompanied by the significant formation of ketone **2e'** ( $^1\text{H}$  NMR at  $\delta = 1.13$  ppm (d,  $J = 8$  Hz)). Over time, ketone **2e'** was consumed, which suggests that the ketone is acting as an intermediate in the reaction.

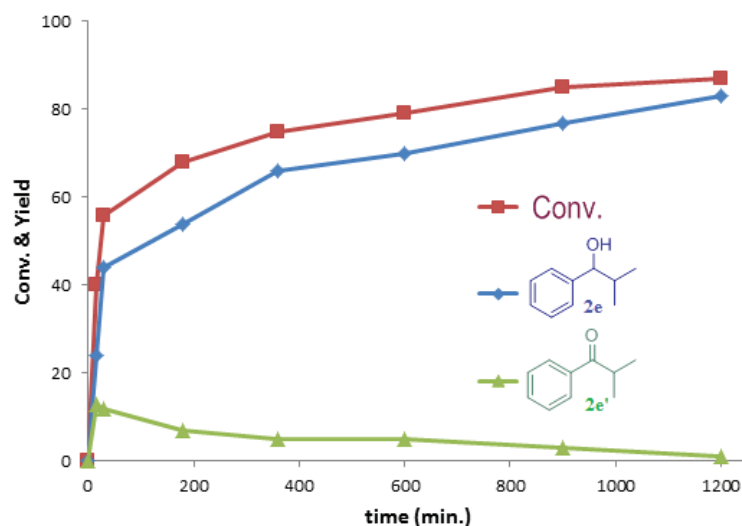
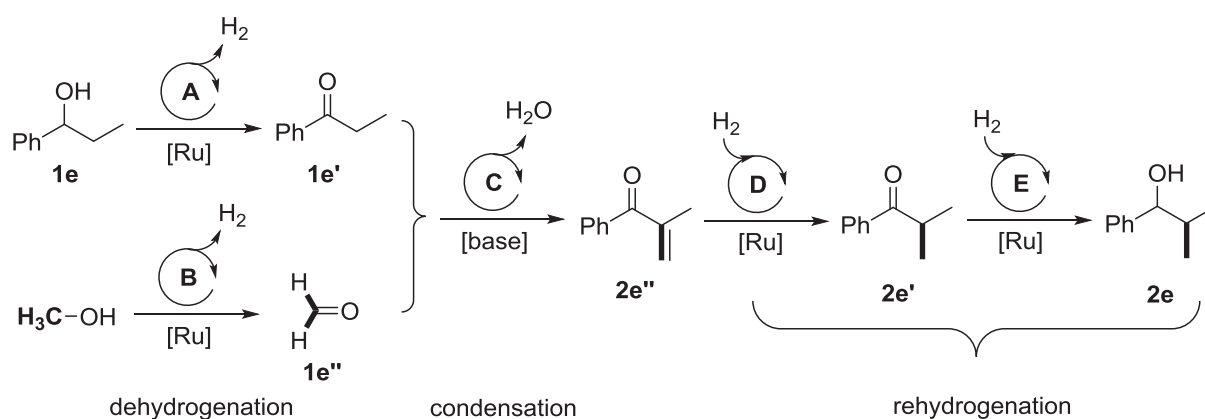


**Figure 2.1:** Reaction progress based on  $^1\text{H}$  NMR. **1e** (1 mmol), MeOH (1 mL as a reagent and solvent), Ru pre-catalyst **Ru-20** (0.1 mol%), and NaOMe (1.5 mmol) at 150 °C.

After 30 minutes, the reaction showed 60% conversion and 42% yield to **2e**. After 30 minutes, the reaction decelerated significantly but steadily continued to reach 83% of the selective mono-methylated product **2e**.

Two distinct kinetic regimes can be explained due to a sequence of de-hydrogenation and re-hydrogenation coupled with an aldol condensation process, which can plausibly be explained by a “hydrogen borrowing mechanism”. The generalized catalytic network for the metal-catalyzed de-hydrogenation/re-hydrogenation and base mediated aldol condensation is depicted in scheme 2.10.



**Scheme 2.10:** Postulated generalized reaction network for the selective mono-methylation of alcohol.

The conversion/time profile showed that the reaction proceeds fast in the initial 30 minutes. In the early stage of the reaction, the catalyst performs the de-hydrogenation of **1e** and methanol to the corresponding dehydrogenated products **1e'** and formaldehyde. In the presence of a base, an aldol-condensation takes place between the molecules **1e'** and formaldehyde which generates the corresponding enone **2e''**. In the initial phase of the reaction, the availability of hydrogen generated from the de-hydrogenation of alcohols is the limiting factor to re-hydrogenate the *in situ* formed ketone **2e'** to **2e** because of low partial pressure in the closed system. Therefore, re-hydrogenation is not complete and the formation of intermediate **2e'** was seen in the reaction mixture. Over time, the concentration of **1e** decreased in the reaction mixture. However, the liberation of the increased amount of H<sub>2</sub> generated from excess methanol accelerates the hydrogenation of ketone **2e'** to the final product **2e**. In the same time, due to the excess amount of hydrogen, it also reverses the equilibrium and re-hydrogenates the *in situ* formed ketone/aldehyde (**1e'**) to the corresponding alcohol **1e** and decrease the overall reaction rate.

This hypothesis was confirmed by the detection of the hydrogen in the reaction mixture when 1-phenylpropanol **1e** was reacted with an equimolar amount of MeOH under the standard reaction conditions. Furthermore, when the same reaction was performed under hydrogen pressure (10 bar), after 2 h, **2e** was present in the reaction mixture in a yield of 13%. In the absence of hydrogen, the yield of **2e** after 2 h was 47%.

### 2.7.2. Estimation of the Gibbs free energy of activation using the Eyring equation

To calculate the Gibbs free activation energy for the selective  $\beta$ -methylation, the Eyring equation was used (eq. 2).

$$k = \frac{k_B \cdot T}{h} \cdot e^{\frac{-\Delta G^\ddagger}{R \cdot T}} \quad (\text{eq. 2})$$

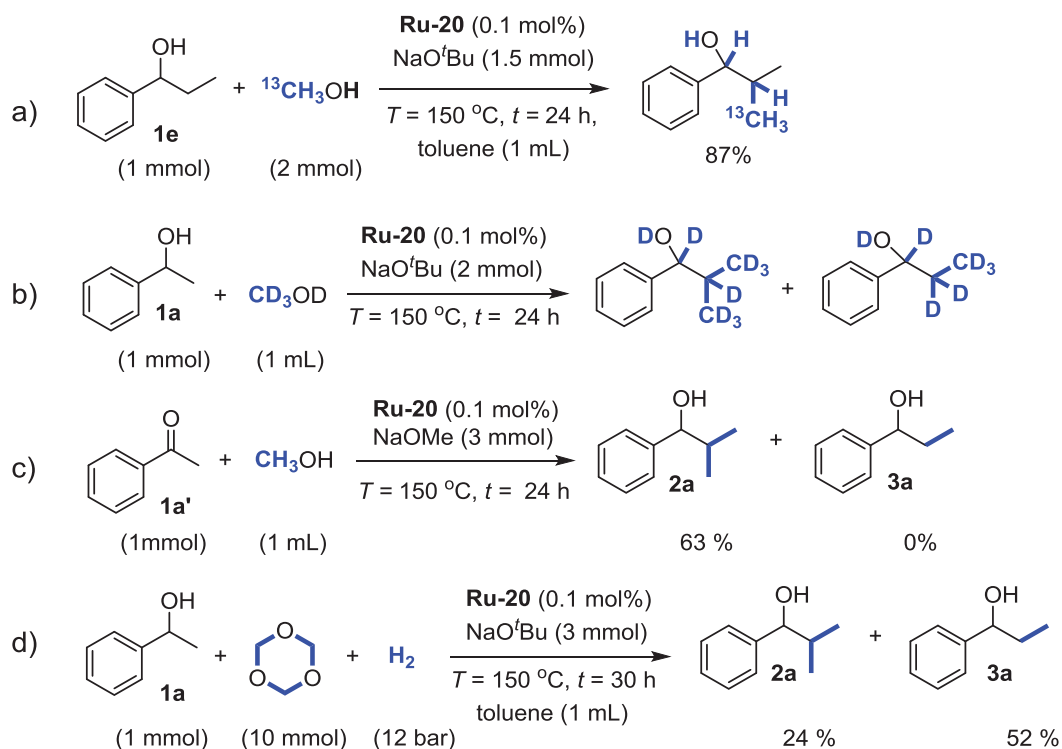
1-phenyl-propan-1-ol **1e** was chosen a benchmark substrate. All experiments were conducted at a reaction temperature of 90 °C (363 K). At this temperature, no side reactions were observed. At different time-intervals, the turn over frequency (TOF) was calculated which was further used for the calculation of the Gibbs free activation energy. Using equation 2, the Gibbs free activation energy for the  $\beta$ -methylation of **1e** was obtained with a value of  $\Delta G^\ddagger = 26.11 \pm 0.5 \text{ kcal} \cdot \text{mol}^{-1}$ . The detailed calculations are described in the experimental section.

### 2.7.3. Observation of *in situ* formed intermediates and labeling experiments

It was postulated earlier in Scheme 2.10 that the reaction is proceeding via several dehydrogenation and re-hydrogenation pathways. A variety of control and labeling experiments were performed, summarized in scheme 2.11. While performing the labeling experiments, NaO<sup>t</sup>Bu was used as a base instead of NaOMe. Using the standard reaction conditions, the reaction of 1-phenylpropanol **1e** with <sup>13</sup>C-labeled methanol in the presence of toluene as a solvent led to the methylated product with a yield of 87% and showed the incorporation of <sup>13</sup>C isotope in the newly formed methyl group. In a similar manner, the reaction of **1a** with CD<sub>3</sub>OD using the standard reaction condition showed the incorporation of deuterium at the

newly formed methyl group as well as in  $\alpha$ - and  $\beta$ - position of the alcohol. These results confirmed that methanol is acting as a C1 source in the reaction and also the incorporation of deuterium in the aliphatic region of alcohols affirmed that the reaction is proceeding via “hydrogen borrowing mechanism”.

Next, to confirm the intermediates formed from alcohols and methanol to the corresponding ketone or aldehyde and formaldehyde, some reactions were performed. At first, acetophenone **1a'** was reacted with methanol using the same standard reaction condition. The selective transformation to the dimethylated product **2a** was achieved with a yield of 63% after 24 h. The reaction of paraformaldehyde with 1-phenylethanol **1a** in the presence of 12 bar of hydrogen and toluene as a solvent, showed a very low product formation. This may reflect the poor solubility of polymeric material. Interestingly, when the same reaction was performed using 1,3,5-trioxane (which generates formaldehyde *in situ*) and 12 bar of hydrogen pressure, 24% yield was obtained to **2a** and a 52% yield to **3a**. Considering these results, it can be stated that the reaction is proceeding via the dehydrogenation of alcohols.

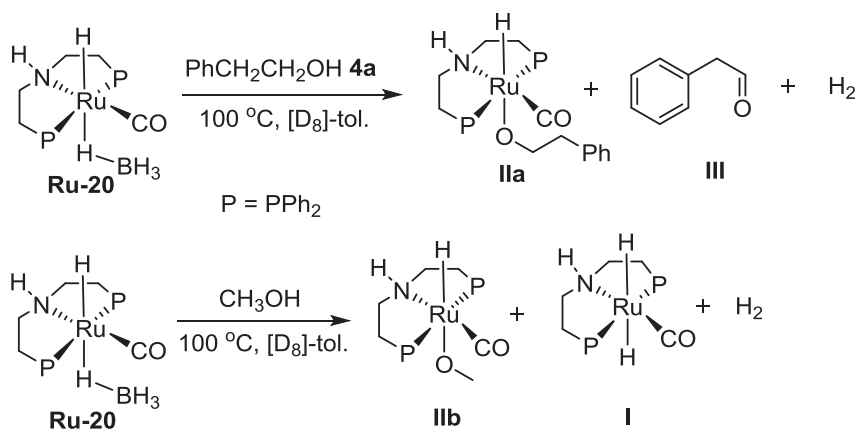


**Scheme 2.11:** Reactivity of plausible intermediates and labeling experiments.

### 2.7.4. Stoichiometric reaction of Ru-MACHO-BH with alcohols

In order to get further insight into the reaction mechanism, stoichiometric reactions between complex **Ru-20** and alcohols were undertaken (Scheme 2.12). At first, the reaction of complex **Ru-20** with 2-phenylethanol **4a** in  $[D_8]$ -toluene at 100 °C led to alcoholate complex **IIa**, observed by  $^1H$ NMR spectroscopy ( $\delta = -16.96$  ppm, t,  $J = 18$  Hz). Additionally, the formation of aldehyde **III** and  $H_2$  was also observed in the  $^1H$  NMR spectrum considering the characteristic peak at 9.20 ppm (t,  $J = 3$  Hz) and 4.50 ppm, respectively (details are described in the experimental section).

Similarly, the reaction of methanol with **Ru-20** in  $[D_8]$ -toluene at room temperature revealed the formation of methoxy alcoholate species **IIb** after 12 h. The characteristic hydride peak for **IIb** has a chemical shift of  $\delta = -17.08$  ppm (t, 1H,  $J = 20$  Hz, RuH) in the  $^1H$  NMR spectrum while in the  $^{31}P$ -NMR shift of the P-atoms occurs at 55.82 ppm. Interestingly, increasing the temperature to 100 °C generated the dihydride species **I**, and hydrogen gas. Complex **I** was observed in the  $^1H$ -NMR spectrum at a chemical shift of  $\delta = -6.14$  ppm (t, 2H,  $J = 16$  Hz, RuH). It is important to note that in both cases, the formation of  $H_2$  is observed. These data show that complex **Ru-20** is active for the dehydrogenation of alcohols (details are described in the experimental section).



**Scheme 2.12:** Ru(II)-complexes relevant as possible intermediates obtained by stoichiometric reactions of Ru-MACHO-BH **Ru-20**.



### 2.7.5. Computed catalytic cycle

Based on the experimental results and the above monitored intermediates, DFT calculations were carried out. The DFT calculations were performed by Dr. Markus Hölscher. The DFT computation (B97-D3BJ/def2-TZVP) for the selective  $\beta$ -methylation of alcohols was performed where 1-phenyl-propane-1-ol **1e** and methanol employing ruthenium dihydride **I** as the catalytic active species were chosen. The geometries of the local minima and transition states were optimized in the condensed phase (SMD model was applied to implicitly include the solvent methanol).

The whole catalytic cycle is divided into the subcycles A-E (Scheme 2.10 and figure 2.2). The brief description is shown earlier in Scheme 2.10. In the first two subcycles A and B, the dehydrogenation of the alcohol substrate and methanol is described, while in the subcycle C, the aldol condensation to form the C–C bond between the dehydrogenated products from the alcohols is discussed. In the subcycle D and E, the re-hydrogenation to the final methylated product is presented.

In subcycle A, the first step consists of the formation of a hydrogen bridge between the alcohol-functionality of substrate **1e** and the N–H proton of the active Ru species **I** generating **II**. The O–H proton of **1e** aligns towards one of the hydrides of the Ru-center. The formation of the new bond via **TSII-III** (12.0 kcal/mol) between the O–H proton and the Ru-hydride leads to the formation of a non-classical hydrogen co-ordinated to the Ru-metal center in **III**. Next, the dissociation of the hydrogen molecule takes place forming complex **IV**. The hydrogen bridged alcohol reorients towards the Ru-center and reacts to the endergonic Ru-alcoholate compound **V**. Next, the alcoholate dissociates, reorients and then the hydride from the carbonyl atom is transferred to the metal centre via **TSV-I'** (6.9 kcal/mol), leading to the reformation of active species **I** (**I'**) and the corresponding de-hydrogenated ketone product **A**.

In subcycle B, the dehydrogenation of methanol to formaldehyde **B** and H<sub>2</sub> takes place with the regeneration of the catalytic active species **I'** analogous to subcycle A. The energy barrier was not high and thus the facile de-hydrogenation reaction can be performed at moderate temperatures (Subcycle B). The subcycle A and subcycle B comprises the formation of the two carbonyl species, ketone and formaldehyde, respectively including the two molecules of H<sub>2</sub>. At this stage, the reaction system resides at a height of 13.3 kcal/mol on the hyper surface.

Subcycle C comprises the aldol condensation between the ketone and formaldehyde which were formed in subcycles A and subcycle B, respectively. The base-catalyzed aldol condensation between the carbonyl functionalities leads to the formation of the enone species **D** with the elimination of one molecule of H<sub>2</sub>O. This reaction also holds the rate-determining transition state (TDTS) which is shown in the figure 2.3 from intermediate A/B to intermediate C.

In Figure 2.3, the detailed aldol-condensation part (subcycle C) is shown. The optimization was performed using the same density functional; however, in contrast to the metal containing compounds, the def2-TZVPD basis set/ECP was operated here (def2-TZVP basis set was used for the subcycle A, B, D and E). The def2-TZVPD basis set was used because of diffuse functions to properly describe anionic systems as *tert*-butoxide anion is a part of the subcycle. The energies of these compounds are shown in the experimental section in Table 2.7. All compounds of this subcycle were also described to be minima or transition states by frequency calculations and as before the thermochemical parameters were computed for a temperature of T = 423 K and a pressure of 603 atm.

As a direct comparison of the energies of compounds computed with different basis sets is not valid, the energies obtained for subcycle C in Figure 2.3 cannot be compared directly to the energies compared for subcycle C shown in Figure 2.4; also they cannot be compared directly to all other computed values shown in subcycles A-E. Therefore, the Gibbs free energy reference point in Figure 2.4 was chosen to be the sum of the energies of ketone **A**, formaldehyde **B** and *tert*-butanolate. However, as an orientation an energy comparison between the TZVP and the TZVPD derived structures can still be made: As can be seen from Figure 2.3 the start of subcycle C resides at a TZVP-derived energy value of 13.3 kcal/mol. In the TZVPD-derived results as shown in Figure 2.4 this is the reference point (0.0 kcal/mol). For orientation the value of 13.3 kcal/mol was added to all TZVPD-derived energies of the compounds in subcycle C. At the end of subcycle C this leads to energy of 4.4 kcal/mol, while the TZVP-hypersurface at this point has an energy value of 5.0 kcal/mol. This is a small energy difference with regard to the questions addressed in this work. It also suggests the energy difference for all other species occurring in subcycle C to have similarly small energy differences when computed with the one or the other basis set. It is therefore plausible to conclude that the computation of the energy span is reasonably accurate. As a counter check the reference point of the overall cycle (I) as well as the TDI (XIX) (TDI is discussed in the next paragraph) and the associated molecules (e.g.

substrate, methanol) were re-optimized using the def2-TZVPD(ECP) basis set to re-compute the energy span on the TZVD-level (computed values shown in Table 2.7). This leads to a Gibbs free energy value of -15.5 kcal/mol for the TDI, which compared to the TZVP-derived energy (-15.4 kcal/mol) is a negligible difference. Accordingly, also the energy span only rises by 0.1 kcal/mol when going from the def2-TZVP to the def2-TZVPD hyper surface.

Subcycle D for re-hydrogenation begins with the interaction of the active species **I<sup>6</sup>** and the *in situ* formed enone **D** corresponding to intermediate **XI**. The hydrogen bridge between the N–H of species **I<sup>6</sup>** and the oxygen of enone **D** as well as the hydride interaction from the Ru-centre to the carbon atom of the carbonyl group corresponds to the species **XII**. Subsequently, the hydride transfer leads to the formation of the intermediate species **XIII**, which on later addition of H<sub>2</sub> (formed from one of the subcycles A and B), undergoes the transformation to intermediate species **XIV**. Hydrogen splitting to a proton and hydride from the oxygen of N–H alcoholate and Ru-center leads to the formation of intermediate species **XV**. Next, the dissociation of enol **E** from intermediate species **XV** regenerates the active species **I<sup>6</sup>**. In presence of a base, enol **E** undergoes an allyl isomerization and generates ketone **F**.

In subcycle E, the hydrogenation of the carbonyl group of ketone **F** occurs alike the subcycle D which leads to the final mono-methylated product. In the context of the Gibbs free energy, it can be noted that in whole catalytic cycle, all single barriers are either low or moderate height which can be easily performed. However, the stability of complex **XIX** is high (-15.4 kcal/mol) and comprises a turnover determining intermediate (TDI). As already discussed before, the TDTS from the subcycle consists of a height of 26.9 kcal/mol on the hypersurface. In accordance with this, the activation energy should be the addition of TDTS and TDI (15.4 + 26.9 kcal/mol) subtracted by the Gibbs free activation energy (-13.1 kcal/mol) resulting in the total value of 29.2 kcal/mol. This value compares well with the experimentally calculated value of 26.1 +/- 0.5 kcal/mol calculated from conversion/time-experiments and in this way supports the derived mechanism.



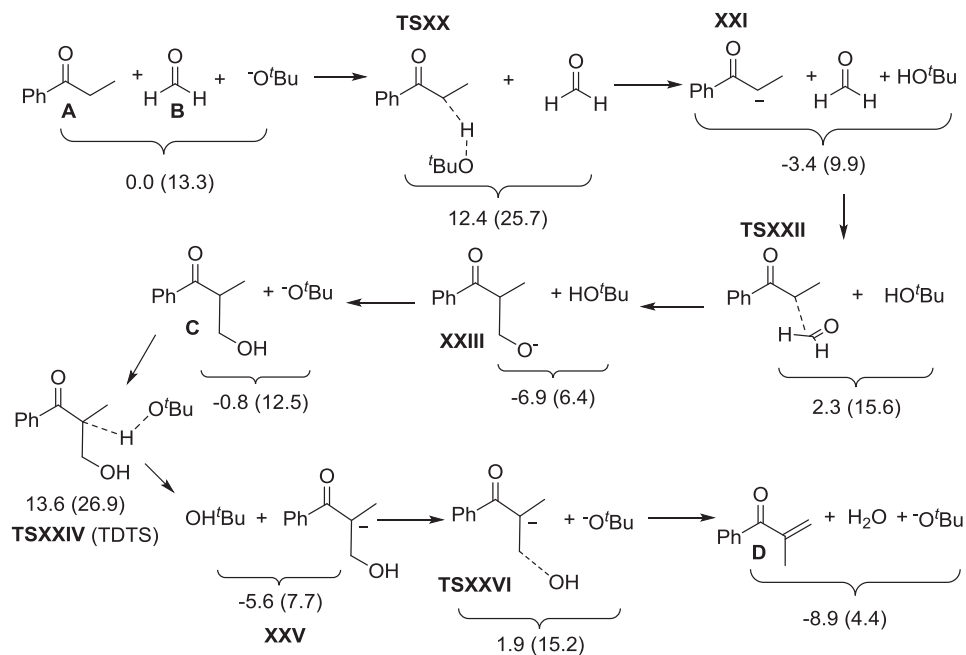


**Figure 2.3:** B97D3-BJ/def2-TZVPD(SMD) optimized structures of the aldol condensation of subcycle C with relative Gibbs free energies (kcal/mol). Values in parenthesis are derived by adding 13.3 kcal/mol to the def2-TZVPD derived values to obtain an estimate of the energy position of the compounds on the def2-TZVP hyper surface.

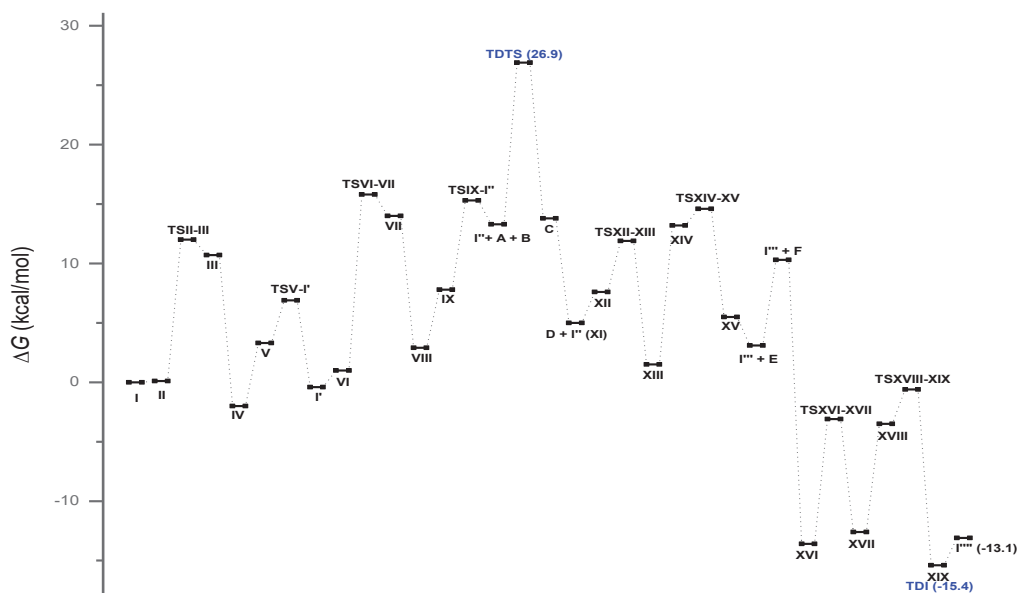


**Figure 2.4:** Abbreviated energy profile for the complete catalytic cycle showing TDI and TDTS.

## 2.8. Conclusion and Outlook

In conclusion, the ruthenium-catalyzed selective  $\beta$ -methylation of a variety of primary and secondary alcohols was achieved using methanol as a C1 source. A number of ruthenium complexes were investigated and among the precatalysts studied the commercially available Ru-MACHO-BH complex **Ru-20** showed the best catalytic activity. Complex **Ru-20** enabled TONs for this process resulting in values of up to 18000. This surpasses the other reported homogeneous and heterogeneous catalytic system. Biomass generated aliphatic alcohols such as ethanol, propanol, and butanol were also selectively  $\beta$ -methylated. The mechanistic studies confirmed that the reaction proceeds via a “hydrogen borrowing mechanism”. The ruthenium complex mediates the de-hydrogenation and re-hydrogenation processes and the base performs the C–C bond formation via an aldol-condensation reaction. Furthermore, the DFT calculations showed that N–H functionality at the Ru complex played an important role for the proton shuffling and similarly the ruthenium center showed high reactivity for the hydride transfer. Even employing this methodology, MeOH can be easily transformed to the corresponding formaldehyde and hydrogen. The computed Gibbs free activation energy of 29.2 kcal/mol for the overall reaction is in reasonable agreement with the experimentally estimated value of  $26.1 \pm 0.5$  kcal/mol. The DFT calculation shows that all the subcycles in the whole catalytic cycle comprise barriers with low or moderate height. The rate-determining transition state in the reaction is the base-catalyzed aldol condensation reaction while the turnover determining intermediate is the complex formed between the final methylated product and Ru-hydride complex **I**.

## 2.9. Experimental

### 2.9.1. General Experimental

All catalytic and stoichiometric reactions were performed under argon atmosphere using a combination of Schlenk and glove box techniques. Chemicals were purchased from Sigma-Aldrich, Alfa-Aesar, TCI chemicals and used without further purification. Dry solvents were prepared according to standard procedures. Glasswares were dried under vacuum at high temperatures, evacuated, and refilled with argon at least three times.  $^1\text{H}$ ,  $^{13}\text{C}$ , and  $^{31}\text{P}$  NMR spectra were recorded with spectrometers Bruker AV300 or AV400 at room temperature. The

solvent signals were used as references and the chemical shifts converted to the TMS scale (CDCl<sub>3</sub>:  $\delta_{\text{H}}$  = 7.26 ppm,  $\delta_{\text{C}}$  = 77.3 ppm; C<sub>6</sub>D<sub>6</sub>:  $\delta_{\text{H}}$  = 7.16 ppm,  $\delta_{\text{C}}$  = 127.6 ppm; [D<sub>8</sub>]-THF:  $\delta_{\text{H}}$  = 1.72 ppm,  $\delta_{\text{C}}$  = 24.2 ppm; [D<sub>8</sub>]-Toluene:  $\delta_{\text{H}}$  = 2.1 ppm,  $\delta_{\text{C}}$  = 21.4 ppm). Chemical shifts for <sup>31</sup>P are reference against H<sub>3</sub>PO<sub>4</sub> as external standard. Multiplicity is abbreviated as: s, singlet; d, doublet; t, triplet; q, quartet; m, multiplet; br, broad.

GC analyses were performed on a Trace GC Ultra (Thermo Scientific) using a packed CP-WAX-58-CB column (length = 50 m, diameter = 0.25 mm) isothermally at 50 °C for 5 min, then heated to 200 °C at 8 °C min<sup>-1</sup>. A constant 1.5 bar pressure of N<sub>2</sub> was applied. The gas chromatograph was equipped with a FID detector.

**Safety advice:** High-pressure experiments represent a significant risk and must be conducted with appropriate safety procedures and in conjunction with the use of suitable equipment.

### 2.9.2. General procedure for screening of Ru-catalysts

The Ru-precursor (0.1 mol%) and NaO<sup>t</sup>Bu (192.2 mg, 2 mmol) were weighed into a glass inlet equipped with a stirring bar inside a glovebox. The glass inlet was transferred to a 10 mL stainless steel autoclave that was evacuated and refilled with argon at least three times. 1-phenyl ethanol **1a** (120  $\mu$ L, 1 mmol) and methanol (1 mL) were added at room temperature through a valve under argon. The autoclave was sealed and heated to 150 °C temperature. After 24 h, the autoclave was cooled to room temperature and slowly vented while stirring continued. Mesitylene was added as an internal standard to the reaction mixture that was then passed through a short path of acidic alumina before the composition was analyzed by NMR spectroscopy.

### 2.9.3. General procedure for the screening of different bases at various temperatures

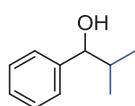
Ru-MACHO-BH **Ru-20** (0.59 mg, 0.1 mol%) and base (2 mmol) were weighed into a glass inlet equipped with a stirring bar inside a glovebox. The glass inlet was transferred to a 10 mL stainless steel autoclave that was evacuated and refilled with argon at least three times. 1-phenyl ethanol **1a** (1 mmol, 120  $\mu$ L) and methanol (1 mL) were added at room temperature through a valve under argon. The autoclave was sealed and heated to the desired reaction temperature. After 24 h, the autoclave was cooled to room temperature and slowly vented while

stirring continued. Mesitylene was added as an internal standard to the reaction mixture that was then passed through a short path of acidic alumina before the composition was analyzed by NMR spectroscopy.

#### 2.9.4. General procedure for catalytic selective $\beta$ -methylation of secondary alcohols

Ru-MACHO-BH **Ru-20** (0.59 mg, 0.1 mol%) and NaOMe were weighed into a glass inlet equipped with a stirring bar inside a glovebox. The glass inlet was transferred to a 10 mL stainless steel autoclave that was evacuated and refilled with argon at least three times. The secondary alcohol **1** (1 mmol) and methanol (1 mL) were added at room temperature through a valve under argon. The autoclave was sealed and heated to 150 °C temperature. After 24 h, the autoclave was cooled to room temperature and slowly vented while stirring continued. Mesitylene was added as an internal standard to the reaction mixture that was then passed through a short path of acidic alumina before the composition was analyzed by NMR spectroscopy.

**2-methyl-1-phenylpropan-1-ol (2a)**: Prepared by following the general experimental procedure

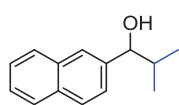


with: **Ru-20** (0.59 mg, 0.1 mol%), 1-phenylethan-1-ol **1a** (122.2 mg, 1 mmol), NaOMe (162.1 mg, 3 mmol), MeOH (1 mL). Yield was determined by  $^1\text{H}$  NMR spectrum using mesitylene (127 mg, 1.06 mmol) as an internal standard ( $\delta_{\text{Mesitylene(standard)}} = 6.71$  (s, 3H),  $\delta_{\text{product}} = 4.35$  (d, 1H)). Compound **2a** was isolated by column chromatography.  $^1\text{H}$  NMR (300 MHz,  $\text{CDCl}_3$ , 298 K)  $\delta = 7.16$ - $7.28$  (m, 5H, ArCH), 4.25 (d, 1H,  $J = 6.9$  Hz, CH), 1.82-1.93 (m, 1H, CH), 1.78 (br s, 1H, OH), 0.92 (d, 3H,  $J = 6.7$  Hz,  $\text{CH}_3$ ), 0.71 (d, 3H,  $J = 6.8$  Hz,  $\text{CH}_3$ ).  $^{13}\text{C}$ - $\{^1\text{H}\}$  NMR (101 MHz,  $\text{CDCl}_3$ , 298 K)  $\delta = 143.86$  (quat-C), 128.41 (ArCH), 127.63 (ArCH), 126.79 (ArCH), 80.27 (CH), 35.48 (CH), 19.22 ( $\text{CH}_3$ ), 18.47 ( $\text{CH}_3$ ). Yield of the isolated product: 74%. The obtained analytical data is consistent with those previously reported in the literature.<sup>[15]</sup>

**2-methyl-1-(naphthalen-2-yl)propan-1-ol (2b)**: Prepared by following the general experimental procedure with: **Ru-20** (0.59 mg, 0.1 mol%), 1-(naphthalen-2-yl)ethan-1-ol **1b** (172.2 mg, 1 mmol), NaOMe (162.1 mg, 3 mmol), MeOH (1 mL). Yield was determined by

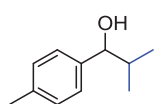


$^1\text{H}$  NMR spectrum using mesitylene (119 mg, 0.99 mmol) as an internal standard



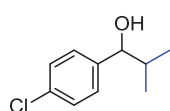
( $\delta_{\text{Mesitylene(standard)}} = 6.71$  (s, 3H),  $\delta_{\text{product}} = 4.45$  (d, 1H)). Compound **2b** was isolated by column chromatography.  $^1\text{H}$  NMR (400 MHz,  $\text{CDCl}_3$ , 298 K)  $\delta = 7.73$ -7.76 (m, 3H, ArCH), 7.67 (s, 1H, ArCH), 7.36-7.41 (m, 3H, ArCH), 4.45 (d, 1H,  $J = 6.9$  Hz, CH), 1.97-2.03 (m, 1H, CH), 1.83 (br s, 1H, OH), 0.96 (d, 3H,  $J = 6.7$  Hz,  $\text{CH}_3$ ), 0.76 (d, 3H,  $J = 6.8$  Hz,  $\text{CH}_3$ ).  $^{13}\text{C}\{-^1\text{H}\}$  NMR (75 MHz,  $\text{CDCl}_3$ , 298 K)  $\delta = 141.35$  (quat-C), 133.40 (quat-C), 133.19 (quat-C), 128.20 (ArCH), 128.16 (ArCH), 127.89 (ArCH), 126.30 (ArCH), 125.97 (ArCH), 125.64 (ArCH), 124.87 (ArCH), 80.40 (CH), 35.43 (CH), 19.38 (CH<sub>3</sub>), 18.47 (CH<sub>3</sub>). Yield of the isolated product: 67%. The obtained analytical data is consistent with those previously reported in the literature.<sup>[15]</sup>

**2-methyl-1-(*p*-tolyl)propan-1-ol (2c):** Prepared by following the general experimental



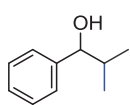
procedure with: **Ru-20** (0.59 mg, 0.1 mol%), 1-(*p*-tolyl)ethan-1-ol **1c** (136.1 mg, 1 mmol), NaOMe (162.1 mg, 3 mmol), MeOH (1 mL). Yield was determined by  $^1\text{H}$  NMR spectrum using mesitylene (125 mg, 1.04 mmol) as an internal standard ( $\delta_{\text{Mesitylene(standard)}} = 6.71$  (s, 3H),  $\delta_{\text{product}} = 4.24$  (d, 1H)). Compound **2c** was isolated by column chromatography.  $^1\text{H}$  NMR (400 MHz,  $\text{CDCl}_3$ , 298 K)  $\delta = 7.13$  (d, 2H,  $J = 8.0$  Hz, ArCH), 7.07 (d, 2H,  $J = 8.0$  Hz, ArCH), 4.24 (d, 1H,  $J = 7.0$  Hz, CH), 2.27 (s, 3H,  $\text{CH}_3$ ), 1.83-1.91 (m, 1H, CH), 1.68 (br s, 1H, OH), 0.93 (d, 3H,  $J = 6.7$  Hz,  $\text{CH}_3$ ), 0.71 (d, 3H,  $J = 6.8$  Hz,  $\text{CH}_3$ ).  $^{13}\text{C}\{-^1\text{H}\}$  NMR (75 MHz,  $\text{CDCl}_3$ , 298 K)  $\delta = 140.93$  (quat-C), 137.28 (quat-C), 129.11 (ArCH), 126.74 (ArCH), 80.20 (CH), 35.44 (CH), 21.35 (CH<sub>3</sub>), 19.24 (CH<sub>3</sub>), 18.60 (CH<sub>3</sub>). Yield of the isolated product: 73%. The obtained analytical data is consistent with those previously reported in the literature.<sup>[15]</sup>

**1-(4-chlorophenyl)-2-methylpropan-1-ol (2d):** Prepared by following the general experimental



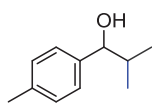
procedure with: **Ru-20** (0.59 mg, 0.1 mol%), 1-(4-chlorophenyl)ethan-1-ol **1d** (156.6 mg, 1 mmol), NaOMe (162.1 mg, 3 mmol), MeOH (1 mL). Yield was determined by  $^1\text{H}$  NMR spectrum using mesitylene (123 mg, 1.02 mmol) as an internal standard ( $\delta_{\text{Mesitylene(standard)}} = 6.71$  (s, 3H),  $\delta_{\text{product}} = 4.26$  (d, 1H)).  $^1\text{H}$  NMR (300 MHz,  $\text{CDCl}_3$ , 298 K)  $\delta = 7.14$ -7.27 (m, 4H, ArCH), 4.26 (d, 1H,  $J = 6.7$  Hz, CH), 1.91 (br s, 1H, OH), 1.80-1.89 (m, 1H, CH), 0.89 (d, 3H,  $J = 6.7$  Hz,  $\text{CH}_3$ ), 0.72 (d, 3H,  $J = 6.8$  Hz,  $\text{CH}_3$ ). The obtained analytical data is consistent with those previously reported in the literature.<sup>[16]</sup>

**2-methyl-1-phenylpropan-1-ol (2e):** Prepared by following the general experimental procedure



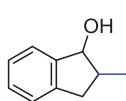
with: **Ru-20** (0.59 mg, 0.1 mol%), 1-phenylpropan-1-ol **1e** (136.2 mg, 1 mmol), NaOMe (81.03 mg, 1.5 mmol), MeOH (1 mL). Yield was determined by  $^1\text{H NMR}$  (300 MHz,  $\text{CDCl}_3$ , 298 K) spectrum using mesitylene (118 mg, 0.98 mmol) as an internal standard standard ( $\delta_{\text{Mesitylene(standard)}} = 6.71$  (s, 3H),  $\delta_{\text{product}} = 4.35$  (d, 1H)). The obtained analytical data is consistent with those previously reported in the literature.<sup>[15]</sup>

**2-methyl-1-(*p*-tolyl)propan-1-ol (2f):** Prepared by following the general experimental



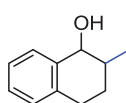
procedure with: **Ru-20** (0.59 mg, 0.1 mol%), 1-(*p*-tolyl)propan-1-ol **2f** (50.2 mg, 1 mmol), NaOMe (81.03 mg, 1.5 mmol), MeOH (1 mL). Yield was determined by  $^1\text{H NMR}$  (300 MHz,  $\text{CDCl}_3$ , 298 K) spectrum using mesitylene (119 mg, 0.99 mmol) as an internal standard ( $\delta_{\text{Mesitylene(standard)}} = 6.71$  (s, 3H),  $\delta_{\text{product}} = 4.24$  (d, 1H)). The obtained analytical data is consistent with those previously reported in the literature.<sup>[15]</sup>

**2-methyl-2,3-dihydro-1H-inden-1-ol (2g):** Prepared by following the general experimental



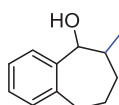
procedure with: **Ru-20** (0.59 mg, 0.1 mol%), 2,3-dihydro-1H-inden-1-ol **1g** (134.2 mg, 1 mmol), NaOMe (81.03 mg, 1.5 mmol), MeOH (1 mL). Yield was determined by  $^1\text{H NMR}$  (300 MHz,  $\text{CDCl}_3$ , 298 K) spectrum using mesitylene (120 mg, 1 mmol) as an internal standard ( $\delta_{\text{Mesitylene(standard)}} = 6.71$  (s, 3H),  $\delta_{\text{product}} = 4.65$  (d, 1H),  $\delta_{\text{product}} = 4.93$ ). The obtained analytical data is consistent with those previously reported in the literature.<sup>[17]</sup>

**2-methyl-1,2,3,4-tetrahydronaphthalen-1-ol (2h):** Prepared by following the general



experimental procedure with: **Ru-20** (0.59 mg, 0.1 mol%), 1,2,3,4-tetrahydronaphthalen-1-ol **1h** (148.2 mg, 1 mmol), NaOMe (81.03 mg, 1.5 mmol), MeOH (1 mL). Yield was determined by  $^1\text{H NMR}$  (300 MHz,  $\text{CDCl}_3$ , 298 K) spectrum using mesitylene (110 mg, 0.92 mmol) as an internal standard ( $\delta_{\text{Mesitylene(standard)}} = 6.71$  (s, 3H),  $\delta_{\text{product}} = 4.24$  (d, 1H),  $\delta_{\text{product}} = 4.47$  (d, 1H)). The obtained analytical data is consistent with those previously reported in the literature.<sup>[18]</sup>

**6-methyl-6,7,8,9-tetrahydro-5H-benzo[7]annulen-5-ol (2i):** Prepared by following the general



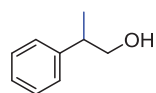
experimental procedure with: **Ru-20** (0.59 mg, 0.1 mol%), 6,7,8,9-tetrahydro-5H-benzo[7]annulen-5-ol **1i**, 162.2 mg, 1 mmol), NaOMe (81.03 mg, 1.5 mmol), MeOH

(1 mL). Yield was determined by  $^1\text{H}$  NMR (300 MHz,  $\text{CDCl}_3$ , 298 K) spectrum using mesitylene (158 mg, 1.32 mmol) as an internal standard ( $\delta_{\text{Mesitylene(standard)}} = 6.71$  (s, 3H),  $\delta_{\text{product}} = 4.65$  (d, 1H),  $\delta_{\text{product}} = 4.97$  (d, 1H)). The obtained analytical data is consistent with those previously reported in the literature.<sup>[17b]</sup>

### 2.9.5. General procedure for catalytic selective $\beta$ -methylation of 2-aryl ethanols

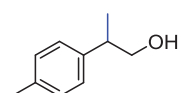
Ru-MACHO-BH **Ru-20** (0.59 mg, 0.1 mol%) and NaOMe (54.02 mg, 1 mmol) were weighed into a glass inlet equipped with a stirring bar inside a glovebox. The glass inlet was transferred to a 10 mL stainless steel autoclave that was evacuated and refilled with argon at least three times. 2-aryl ethanol **4** (1 mmol) and methanol (1 mL) were added at room temperature through a valve under argon. The autoclave was sealed and heated to 150 °C temperature for 28 h. After completion of the reaction, the autoclave was cooled to room temperature and slowly vented while stirring continued. Mesitylene was added as an internal standard to the reaction mixture that was then passed through a short path of acidic alumina before the composition was analyzed by NMR spectroscopy.

**2-phenylpropan-1-ol (5a)**: Prepared by following the general experimental procedure with:



**Ru-20** (0.59 mg, 0.1 mol%), 2-phenylethan-1-ol **4a** (122.2 mg, 1 mmol), NaOMe (54.02 mg, 1 mmol), MeOH (1 mL). Yield was determined by  $^1\text{H}$  NMR spectrum using mesitylene (122 mg, 1.02 mmol) as an internal standard ( $\delta_{\text{Mesitylene(standard)}} = 6.71$  (s, 3H),  $\delta_{\text{product}} = 3.63$  (d, 2H)).  $^1\text{H}$  NMR (300 MHz,  $\text{CDCl}_3$ , 298 K)  $\delta = 7.15$ -7.28 (m, 5H, ArCH), 3.63 (d, 2H,  $\text{CH}_2$ ), 2.84-2.91 (m, 1H, CH), 1.20 (d, 3H,  $J = 9.0$  Hz,  $\text{CH}_3$ ). The obtained analytical data is consistent with those previously reported in the literature.<sup>[15]</sup>

**2-(*p*-tolyl)propan-1-ol (5b)**: Prepared by following the general experimental procedure with:



**Ru-20** (0.59 mg, 0.1 mol%), 2-(*p*-tolyl)ethan-1-ol **4b** (136.2 mg, 1 mmol), NaOMe (54.02 mg, 1 mmol), MeOH (1 mL). Yield was determined by  $^1\text{H}$  NMR spectrum using mesitylene (120 mg, 1 mmol) as an internal standard ( $\delta_{\text{Mesitylene(standard)}} = 6.71$  (s, 3H),  $\delta_{\text{product}} = 3.59$  (d, 2H)).  $^1\text{H}$  NMR (300 MHz,  $\text{CDCl}_3$ , 298 K)  $\delta = 7.02$ -7.08 (m, 4H, ArCH), 3.59 (d, 2H,  $J = 6.9$  Hz,  $\text{CH}_2$ ), 2.79-2.86 (m, 1H, CH), 1.17 (d, 3H,  $J = 9$  Hz,  $\text{CH}_3$ ). The obtained analytical data is consistent with those previously reported in the literature.<sup>[15]</sup>

**2-(4-isobutylphenyl)propan-1-ol (5c):** Prepared by following the general experimental procedure with: **Ru-20** (0.59 mg, 0.1 mol%), 2-(4-isobutylphenyl)ethan-1-ol **4c** (178.3 mg, 1 mmol), NaOMe (54.02 mg, 1 mmol), MeOH (1 mL). Yield was determined by  $^1\text{H}$  NMR spectrum using mesitylene (124 mg, 1.03 mmol) as an internal standard ( $\delta_{\text{Mesitylene(standard)}} = 6.71$  (s, 3H),  $\delta_{\text{product}} = 3.62$  (d, 2H)).  $^1\text{H}$  NMR (400 MHz,  $\text{CDCl}_3$ , 298 K)  $\delta = 7.14$  (d, 2H,  $J = 8.0$  Hz, ArCH), 7.10 (d, 2H,  $J = 12$  Hz, ArCH), 3.71 (d, 2H,  $J = 8$  Hz,  $\text{CH}_2$ ), 2.89-3.01 (m, 1H, CH), 2.48 (d, 2H,  $J = 8$  Hz,  $\text{CH}_2$ ), 1.84-1.95 (m, 1H, CH), 1.29 (d, 3H,  $J = 12$  Hz,  $\text{CH}_3$ ), 0.94 (d, 6H,  $J = 8$  Hz,  $\text{CH}_3$ ). The obtained analytical data is consistent with those previously reported in the literature.<sup>[19]</sup>

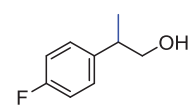
**2-(4-methoxyphenyl)propan-1-ol (5d):** Prepared by following the general experimental procedure with: **Ru-20** (0.59 mg, 0.1 mol%), 2-(4-methoxyphenyl)ethan-1-ol **4d** (152.2 mg, 1 mmol), NaOMe (54.02 mg, 1 mmol), MeOH (1 mL). Yield was determined by  $^1\text{H}$  NMR spectrum using mesitylene (120 mg, 1 mmol) as an internal standard ( $\delta_{\text{Mesitylene(standard)}} = 6.71$  (s, 3H),  $\delta_{\text{product}} = 3.58$  (d, 2H)).  $^1\text{H}$  NMR (400 MHz,  $\text{CDCl}_3$ , 298 K)  $\delta = 7.07$  (d, 2H,  $J = 8.6$  Hz, ArCH), 6.79 (d, 2H,  $J = 8.6$  Hz, ArCH), 3.58 (d, 2H,  $J = 7.1$  Hz,  $\text{CH}_2$ ), 2.79-2.84 (m, 1H, CH), 1.16 (d, 3H,  $J = 8$  Hz,  $\text{CH}_3$ ). The obtained analytical data is consistent with those previously reported in the literature.<sup>[15]</sup>

**2-(3-methoxyphenyl)propan-1-ol (5e):** Prepared by following the general experimental procedure with: **Ru-20** (0.59 mg, 0.1 mol%), 2-(3-methoxyphenyl)ethan-1-ol **4e** (152.2 mg, 1 mmol), NaOMe (54.02 mg, 1 mmol), MeOH (1 mL). Yield was determined by  $^1\text{H}$  NMR spectrum using mesitylene (120 mg, 1 mmol) as an internal standard ( $\delta_{\text{Mesitylene(standard)}} = 6.71$  (s, 3H),  $\delta_{\text{product}} = 3.62$  (d, 2H)).  $^1\text{H}$  NMR (400 MHz,  $\text{CDCl}_3$ , 298 K)  $\delta = 7.15$ -7.18 (m, 1H, ArCH), 6.69-6.76 (m, 3H, ArCH), 3.62 (d, 2H,  $J = 6.8$  Hz,  $\text{CH}_2$ ), 2.82-2.87 (m, 1H, CH), 1.18 (d, 3H,  $J = 8$  Hz,  $\text{CH}_3$ ). The obtained analytical data is consistent with those previously reported in the literature.<sup>[19]</sup>

**2-(6-methoxynaphthalen-2-yl)propan-1-ol (5f):** Prepared by following the general experimental procedure with: **Ru-20** (0.59 mg, 0.1 mol%), 2-(6-methoxynaphthalen-2-yl)ethan-1-ol **4f** (202.3 mg, 1 mmol), NaOMe (54.02 mg, 1 mmol), MeOH (1 mL). Yield was determined by  $^1\text{H}$  NMR spectrum using mesitylene (120 mg, 1 mmol) as an internal standard ( $\delta_{\text{Mesitylene(standard)}} = 6.71$  (s, 3H),  $\delta_{\text{product}} =$

3.66 (d, 2H)).  $^1\text{H NMR}$  (400 MHz,  $\text{CDCl}_3$ , 298 K)  $\delta$  = 7.50-7.63 (m, 2H, ArCH), 7.50 (s, 1H, ArCH), 7.24 (dd, 1H,  $J_1 = 8$  Hz,  $J_2 = 4$  Hz, ArCH), 7.02-7.07 (m, 2H, ArCH), 3.81 (s, 3H,  $\text{OCH}_3$ ), 3.66 (d, 2H,  $J = 6$  Hz,  $\text{CH}_2$ ), 2.94-3.01 (m, 1H, CH), 1.25 (d, 3H,  $J = 8$  Hz,  $\text{CH}_3$ ). The obtained analytical data is consistent with those previously reported in the literature.<sup>[20]</sup>

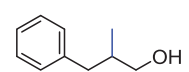
**2-(4-fluorophenyl)propan-1-ol (5g):** Prepared by following the general experimental procedure

 with: **Ru-20** (0.59 mg, 0.1 mol%), 2-(4-fluorophenyl)ethan-1-ol **4g** (140.2 mg, 1 mmol), NaOMe (54.02 mg, 1 mmol), MeOH (1 mL). Yield was determined by  $^1\text{H NMR}$  spectrum using mesitylene (124 mg, 1.03 mmol) as an internal standard ( $\delta_{\text{Mesitylene(standard)}} = 6.71$  (s, 3H),  $\delta_{\text{product}} = 3.58$ -3.61 (m, 2H)).  $^1\text{H NMR}$  (400 MHz,  $\text{CDCl}_3$ , 298 K)  $\delta$  = 7.08-7.14 (d, 2H, ArCH), 6.89-6.96 (m, 2H, ArCH), 3.58-3.61 (m, 2H,  $\text{CH}_2$ ), 2.82-2.89 (m, 1H, CH), 1.18 (d,  $J = 8$  Hz, 3H). The obtained analytical data is consistent with those previously reported in the literature.<sup>[10]</sup>

### 2.9.6. General procedure for catalytic selective $\beta$ -methylation of aliphatic alcohols

Ru-MACHO-BH **Ru-20** (0.59 mg, 0.1 mol%) and NaOMe (108.04 mg, 2 mmol) were weighed into a glass inlet equipped with a stirring bar inside a glovebox. The glass inlet was transferred to a 10 mL stainless steel autoclave that was evacuated and refilled with argon at least three times. Aliphatic alcohol (1 mmol) and methanol (1 mL) were added at room temperature through a valve under argon. The autoclave was sealed and heated to 150 °C temperature. After the desired reaction time, the autoclave was cooled to room temperature and slowly vented while stirring continued. Mesitylene was added as an internal standard to the reaction mixture that was then passed through a short path of acidic alumina before the composition was analyzed by NMR spectroscopy.

**2-methyl-3-phenylpropan-1-ol (7a):** Prepared by following the general experimental procedure with: **Ru-20** (0.59 mg, 0.1 mol%), 3-phenylpropan-1-ol **6a** (136.2 mg, 1 mmol), NaOMe

 (108.04 mg, 2 mmol), MeOH (1 mL). Yield was determined by  $^1\text{H NMR}$  spectrum using mesitylene (120 mg, 1 mmol) an internal standard ( $\delta_{\text{Mesitylene(standard)}} = 6.71$  (s, 3H),  $\delta_{\text{product}} = 0.84$  (d, 3H)). Compound **7a** was isolated by column chromatography.  $^1\text{H NMR}$  (300 MHz,  $\text{CDCl}_3$ , 298 K)  $\delta$  = 7.18-7.24 (m, 2H, ArCH), 7.09-7.14

(m, 3H, ArCH), 3.37-3.49 (dq, 2H,  $J = 10.6, 6.0$  Hz,  $CH_2$ ), 2.31-2.71 (ddd, 2H,  $J = 21.5, 13.4, 7.2$  Hz,  $CH_2$ ), 1.83-1.91 (m, 1H, CH), 1.52 (br s, 1H, OH), 0.84 (d, 3H,  $J = 6.7$  Hz,  $CH_3$ ).  $^{13}C$  { $^1H$ } NMR (75 MHz,  $CDCl_3$ , 298 K):  $\delta = 140.85$  (quat-C), 129.38 (ArCH), 128.50 (ArCH), 126.11 (ArCH), 67.89 (CH), 39.93 ( $CH_2$ ), 38.01 ( $CH_2$ ), 16.69 ( $CH_3$ ). Yield of the isolated product: 72%. The obtained analytical data is consistent with those previously reported in the literature.<sup>[21]</sup>

**2-methyl-4-phenylbutan-1-ol (7b):** Prepared by following the general experimental procedure with: **Ru-20** (0.59 mg, 0.1 mol%), 4-phenylbutan-1-ol **6b** (150.2 mg, 1 mmol), NaOMe (108.04 mg, 2 mmol), MeOH (1 mL). Yield was determined by  $^1H$  NMR spectrum using mesitylene (125 mg, 1.04 mmol) as an internal standard ( $\delta_{\text{Mesitylene(standard)}} = 6.71$  (s, 3H),  $\delta_{\text{product}} = 3.46-3.57$  (dq, 2H)).  $^1H$  NMR (400 MHz,  $CDCl_3$ , 298 K)  $\delta = 7.29-7.32$  (m, 2H, ArCH), 7.18-7.24 (m, 3H, ArCH), 3.46-3.57 (dq, 2H,  $J = 32, 4$  Hz,  $CH_2$ ), 2.60-2.77 (m, 2H,  $CH_2$ ), 1.65-1.82 (m, 2H,  $CH_2$ ), 1.43-1.50 (m, 1H, CH), 1.01 (d, 3H,  $J = 6.7$  Hz,  $CH_3$ ). The obtained analytical data is consistent with those previously reported in the literature.<sup>[22]</sup>

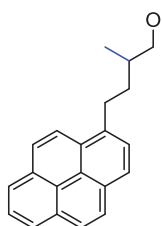
**2-methyl-5-phenylpentan-1-ol (7c):** Prepared by following the general experimental procedure with: **Ru-20** (0.59 mg, 0.1 mol%), 5-phenylpentan-1-ol **6c** (164.2 mg, 1 mmol), NaOMe (108.04 mg, 2 mmol), MeOH (1 mL). Yield was determined by  $^1H$  NMR spectrum using mesitylene (123 mg, 1.03 mmol) as an internal standard ( $\delta_{\text{Mesitylene(standard)}} = 6.71$  (s, 3H),  $\delta_{\text{product}} = 3.30-3.42$  (m, 2H)).  $^1H$  NMR (400 MHz,  $CDCl_3$ , 298 K)  $\delta = 7.17-7.20$  (m, 2H, ArCH), 7.08-7.10 (m, 3H, ArCH), 3.30-3.42 (m, 2H,  $CH_2$ ), 2.49-2.55 (m, 2H,  $CH_2$ ), 1.49-1.60 (m, 3H,  $CH_2$  & CH), 1.28-1.41 (m, 2H,  $CH_2$ ), 0.83 (d, 3H,  $J = 6.7$  Hz,  $CH_3$ ). The obtained analytical data is consistent with those previously reported in the literature.<sup>[23]</sup>

**2-methyl-8-phenyloctan-1-ol (7d):** Prepared by following the general experimental procedure with: **Ru-20** (0.59 mg, 0.1 mol%), 8-phenyloctan-1-ol **6d** (206.3 mg, 1 mmol), NaOMe (108.04 mg, 2 mmol), MeOH (1 mL). Yield was determined by  $^1H$  NMR spectrum using mesitylene (120 mg, 1 mmol) as an internal standard ( $\delta_{\text{Mesitylene(standard)}} = 6.71$  (s, 3H),  $\delta_{\text{product}} = 3.28-3.42$  (m, 2H)). Compound **7d** was isolated by column chromatography.  $^1H$  NMR (400 MHz,  $CDCl_3$ , 298 K)  $\delta = 7.16-7.20$  (m, 2H, ArCH), 7.06-7.12 (m, 3H, ArCH), 3.28-3.42 (m, 2H,  $CH_2$ ), 2.51 (m, 2H,  $CH_2$ ), 1.48-1.53 (m, 3H,  $CH_2$  &



CH), 1.17-1.30 (m, 8H, CH<sub>2</sub>), 0.81 (d, 3H, *J* = 6.9 Hz, CH<sub>3</sub>). <sup>13</sup>C-<sup>1</sup>H NMR (101 MHz, CDCl<sub>3</sub>, 298 K)  $\delta$  = 142.90 (quat-C), 128.42 (ArCH), 128.25 (ArCH), 125.60 (ArCH), 68.40 (CH<sub>2</sub>), 36.00 (CH), 35.76 (CH<sub>2</sub>), 33.15 (CH<sub>2</sub>), 31.53 (CH<sub>2</sub>), 29.82 (CH<sub>2</sub>), 29.32 (CH<sub>2</sub>), 26.92 (CH<sub>2</sub>), 16.61 (CH<sub>3</sub>). Yield of the isolated product: 53%.

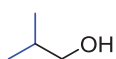
**2-methyl-4-(pyren-1-yl)butan-1-ol (7e):** Prepared by following the general experimental



procedure with: **Ru-20** (0.59 mg, 0.1 mol%), 4-(pyren-1-yl)butan-1-ol **6e** (274.4 mg, 1 mmol), NaOMe (108.04 mg, 2 mmol), MeOH (1 mL). Yield was determined by <sup>1</sup>H NMR spectrum using mesitylene (122 mg, 1.02 mmol) as an internal standard ( $\delta_{\text{Mesitylene(standard)}} = 6.71$  (s, 3H),  $\delta_{\text{product}} = 0.98$  (d, 3H)).

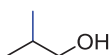
Compound **7e** was isolated by column chromatography. <sup>1</sup>H NMR (300 MHz, CDCl<sub>3</sub>, 298 K)  $\delta$  = 8.13 (d, 1H, *J* = 9 Hz, ArCH), 8.02 (d, 2H, *J* = 9 Hz, 2H, ArCH), 7.94-7.97 (m, 2H, ArCH), 7.82-7.90 (m, 3H, ArCH), 7.72 (d, 1H, *J* = 9 Hz, ArCH). 3.38-3.50 (m, 2H, CH<sub>2</sub>), 3.11-3.30 (m, 2H, CH<sub>2</sub>), 1.66-1.87 (m, 2H, CH<sub>2</sub>), 1.49-1.57 (m, 1H, CH), 0.98 (d, 3H, *J* = 6.6 Hz, CH<sub>3</sub>). <sup>13</sup>C-<sup>1</sup>H NMR (75 MHz, CDCl<sub>3</sub>, 298 K):  $\delta$  = 137.04 (quat-C), 131.48 (quat-C), 130.95 (quat-C), 129.81 (quat-C), 128.57 (quat-C), 127.56 (quat-C), 127.29 (quat-C), 127.14 (ArCH), 126.60 (ArCH), 125.83 (ArCH), 125.15 (ArCH), 125.08 (ArCH), 124.89 (ArCH), 124.72 (ArCH), 123.36 (ArCH), 68.19 (CH<sub>2</sub>), 35.96 (CH<sub>2</sub>), 35.44 (CH), 31.04 (CH<sub>2</sub>), 16.72 (CH<sub>2</sub>). Yield of the isolated product: 76%.

**2-methylpropan-1-ol (7f)** Prepared by following the general experimental procedure with:



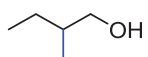
**Ru-20** (1.18 mg, 0.1 mol%), ethanol **6f** (92.1 mg, 2 mmol), NaOMe (216.08 mg, 4 mmol), MeOH (1 mL). Yield was determined by gas chromatography analysis.

**2-methylpropan-1-ol (7g):** Prepared by following the general experimental procedure with:



**Ru-20** (0.59 mg, 0.1 mol%), propan-1-ol **6g** (60.1 mg, 1 mmol), NaOMe (108.04 mg, 2 mmol), MeOH (1 mL). Yield was determined by gas chromatography analysis.

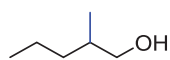
**2-methylbutan-1-ol (7h):** Prepared by following the general experimental procedure with:



**Ru-20** (0.59 mg, 0.1 mol%), butan-1-ol **6h** (74.1 mg, 1 mmol), NaOMe (108.04 mg, 2 mmol), MeOH (1 mL). Yield was determined by gas

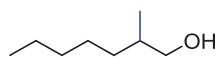
chromatography analysis.

**2-methylpentan-1-ol (7i):** Prepared by following the general experimental procedure with:



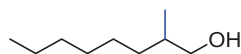
**Ru-20** (0.59 mg, 0.1 mol%), pentan-1-ol **6i** (88.2 mg, 1 mmol), NaOMe (108.04 mg, 2 mmol), MeOH (1 mL). Yield was determined by  $^1\text{H NMR}$  spectrum using mesitylene (124 mg, 1.03 mmol) as an internal standard ( $\delta_{\text{Mesitylene(standard)}} = 6.71$  (s, 3H),  $\delta_{\text{product}} = 3.31\text{-}3.46$  (dq, 2H)).  $^1\text{H NMR}$  (300 MHz,  $\text{CDCl}_3$ , 298 K)  $\delta = 3.31\text{-}3.46$  (dq, 2H,  $J = 29.8, 6.2$  Hz,  $\text{CH}_2$ ), 1.52-1.58 (m, 2H,  $\text{CH}$  and  $\text{OH}$ ), 1.18-1.32 (m, 4H,  $\text{CH}_2$ ), 0.81-0.85 (m, 6H,  $\text{CH}_3$ ). The obtained analytical data is consistent with those previously reported in the literature.<sup>[24]</sup>

**2-methylheptanol (7j):** Prepared by following the general experimental procedure with:



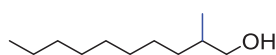
**Ru-20** (0.59 mg, 0.1 mol%), heptan-1-ol **6j** (116.2 mg, 1 mmol), NaOMe (108.04 mg, 2 mmol), MeOH (1 mL). Yield was determined by  $^1\text{H NMR}$  spectrum using mesitylene (118 mg, 0.98 mmol) as an internal standard ( $\delta_{\text{Mesitylene(standard)}} = 6.71$  (s, 3H),  $\delta_{\text{product}} = 3.39$  (dq, 2H)).  $^1\text{H NMR}$  (300 MHz,  $\text{CDCl}_3$ , 298 K)  $\delta = 3.39$  (dq, 2H,  $J = 29.4, 6.2$  Hz,  $\text{CH}_2$ ), 1.49-1.57 (m, 1H,  $\text{CH}$ ), 1.20-1.29 (m, 8H,  $\text{CH}_2$ ) 0.79-0.85 (m, 6H,  $\text{CH}_3$ ). The obtained analytical data is consistent with those previously reported in the literature.<sup>[25]</sup>

**2-methyloctan-1-ol (7k):** Prepared by following the general experimental procedure with:



**Ru-20** (0.59 mg, 0.1 mol%), 1-octanol **6k** (130.2 mg, 1 mmol), NaOMe (108.04 mg, 2 mmol), MeOH (1 mL). Yield was determined by  $^1\text{H NMR}$  spectrum using mesitylene (118 mg, 0.98 mmol) as an internal standard ( $\delta_{\text{Mesitylene(standard)}} = 6.71$  (s, 3H),  $\delta_{\text{product}} = 3.37$  (dq, 2H)).  $^1\text{H NMR}$  (300 MHz,  $\text{CDCl}_3$ , 298 K)  $\delta = 3.37$  (dq, 2H,  $J = 30, 6$  Hz,  $\text{CH}_2$ ), 1.47-1.55 (m, 1H,  $\text{CH}$ ), 1.20-1.27 (m, 10H,  $\text{CH}_2$ ), 1-1.07 (m, 1H), 0.79-0.84 (m, 6H,  $\text{CH}_3$ ). The obtained analytical data is consistent with those previously reported in the literature.<sup>[26]</sup>

**2-methyldecan-1-ol (7l):** Prepared by following the general experimental procedure with:



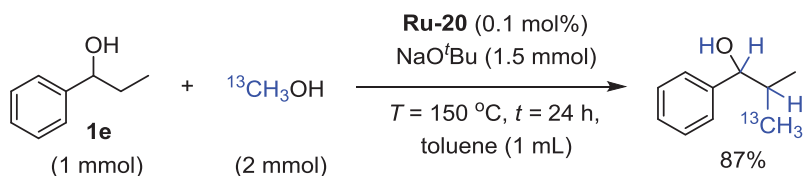
**Ru-20** (0.59 mg, 0.1 mol%), 1-decanol **6l** (158.3 mg, 1 mmol), NaOMe (108.04 mg, 2 mmol), MeOH (1 mL). Yield was determined by  $^1\text{H NMR}$  spectrum using mesitylene (120 mg, 1 mmol) as an internal standard ( $\delta_{\text{Mesitylene(standard)}} = 6.71$  (s, 3H),  $\delta_{\text{product}} = 3.37$  (dq, 2H)).  $^1\text{H NMR}$  (400 MHz,  $\text{CDCl}_3$ , 298 K)  $\delta = 3.37$  (dq, 2H,  $J = 30, 6$  Hz,  $\text{CH}_2$ ), 1.44-1.54 (m, 2H,  $\text{CH}_2$ ), 1.19-1.28 (m, 13H,  $\text{CH}_2$  &  $\text{CH}$ ), 0.98-1.05 (m, 1H,



OH), 0.82 (m, 6H,  $CH_3$ ). The obtained analytical data is consistent with those previously reported in the literature.<sup>[27]</sup>

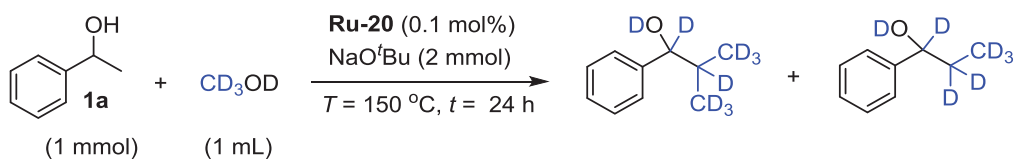
## 2.9.7. Labeling experiments and observation of potential intermediates

### 2.9.7.1 Procedure for $\beta$ -methylation of **1e** with $^{13}CH_3OH$



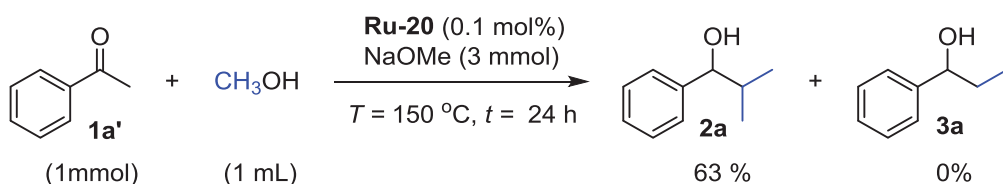
Ru-MACHO-BH **Ru-20** (0.59 mg, 0.1 mol%) and NaO<sup>t</sup>Bu (144.2 mg, 1.5 mmol) were weighed into a glass inlet equipped with a stirring bar inside a glovebox. The glass inlet was transferred to a 10 mL stainless steel autoclave that was evacuated and refilled with argon at least three times. **1e** (136.2 mg, 1 mmol),  $^{13}CH_3OH$  (66.06 mg, 2 mmol) and toluene (1 mL) were added at room temperature through a valve under argon. The autoclave was sealed and heated to 150 °C temperature for 24 h. After completion of the reaction, the autoclave was cooled to room temperature and slowly vented while stirring continued. Mesitylene (120 mg, 1 mmol) was added as an internal standard to the reaction mixture that was then passed through a short path of acidic alumina before the composition was analyzed by NMR spectroscopy. Yield was determined by  $^1H$  NMR spectrum using mesitylene (120.2 mg, 1 mmol) as an internal standard ( $\delta_{\text{Mesitylene(standard)}} = 6.71$  (s, 3H),  $\delta_{\text{product}} = 4.40$  (dd, 1H)).  $^1H$  NMR (400 MHz,  $CDCl_3$ , 298 K) (mixture of diastereomers)  $\delta = 7.34$ - $7.40$  (m, 5H, ArCH), 4.42 (d,  $J = 4$  Hz, CH), 4.41 (d,  $J = 4$  Hz, CH), 1.97-2.07 (m, 1H, CH), 1.01-1.23 (d, 3H,  $J = 81.35, 6.75$ ,  $CH_3$ ), 1.05-1.08 (dd, 3H,  $J = 6.66, 5.20$ ,  $CH_3$ ), 0.70-0.92 (dd, 3H,  $J = 81.25, 6.75$ ,  $CH_3$ ), 0.85-0.88 (m, 3H,  $J = 6.81, 5.17$ ).  $^{13}C$ - $\{^1H\}$  NMR (101 MHz,  $CDCl_3$ , 298 K)  $\delta = 143.79$  (quat-C), 128.31 (ArCH), 127.53 (ArCH), 126.69 (ArCH), 80.16 (CH), 35.40 (d,  $J = 35.47$ ), 19.12 ( $CH_3$ ), 18.34 ( $CH_3$ ). NMR yield: 87%, d.r.: 50:50.

### 2.9.7.2 Procedure for selective $\beta$ -methylation of **1a** with $\text{CD}_3\text{OD}$



Ru-MACHO-BH **Ru-20** (0.59 mg, 0.1 mol%) and  $\text{NaO}^t\text{Bu}$  (288.3 mg, 3 mmol) were weighed into a glass inlet equipped with a stirring bar inside a glovebox. The glass inlet was transferred to a 10 mL stainless steel autoclave that was evacuated and refilled with argon at least three times. **1a** (122.2 mg, 1 mmol) and  $\text{CD}_3\text{OD}$  (1 mL) were added at room temperature through a valve under argon. The autoclave was sealed and heated to 150 °C temperature for 24 h. After 24 h, the autoclave was cooled to room temperature and slowly vented while stirring continued. Mesitylene (120 mg, 1 mmol) was added as an internal standard to the reaction mixture that was then passed through a short path of acidic alumina before the composition was analyzed by NMR spectroscopy.  $^1\text{H}$  NMR (300 MHz,  $\text{CDCl}_3$ , 298 K)  $\delta = 7.18\text{-}7.30$  (m, 5H, ArCH), 4.26 (t, 0.08 H,  $J = 3\text{ Hz}$ , CH), 1.84 (br s, 0.09 H, CH), 0.92 (t, 0.24 H,  $J = 3\text{ Hz}$ ,  $\text{CH}_3$ ), 0.72 (t, 0.24 H,  $J = 3\text{ Hz}$ ,  $\text{CH}_3$ ).  $^{13}\text{C}\{^1\text{H}\}$  NMR (75 MHz,  $\text{CDCl}_3$ , 298 K)  $\delta = 143.85$  (quat-C), 128.39 (ArCH), 127.42 (ArCH), 126.11 (ArCH), 79.07-79.86 (m, CH), 34.05-35.01 (m, CH), 17.06-18.81 (m,  $\text{CH}_3$ ).

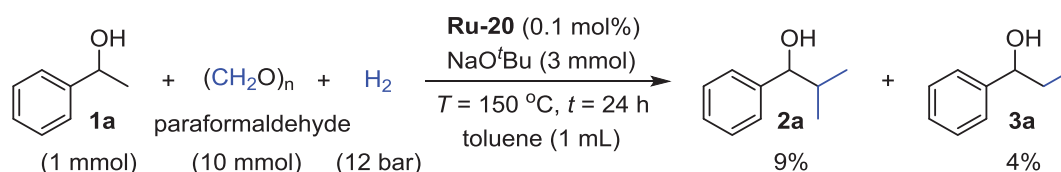
### 2.9.7.3 Procedure for $\beta$ -methylation of acetophenone **1a'** with methanol



Ru-MACHO-BH **Ru-20** (0.59 mg, 0.1 mol%) and  $\text{NaOMe}$  (162.1 mg, 3 mmol) were weighed into a glass inlet equipped with a stirring bar inside a glovebox. The glass inlet was transferred to a 10 mL stainless steel autoclave that was evacuated and refilled with argon at least three times. Acetophenone **1a'** (120.2 mg, 1 mmol) and methanol (1 mL) was added at room temperature through a valve under argon. The autoclave was sealed and heated to 150 °C temperature for 24 h. After 24 h, the autoclave was cooled to room temperature and slowly vented while stirring continued. Mesitylene (124 mg, 1.03 mmol) was added as an internal standard to the reaction mixture that was then passed through a short path of acidic alumina before the composition was

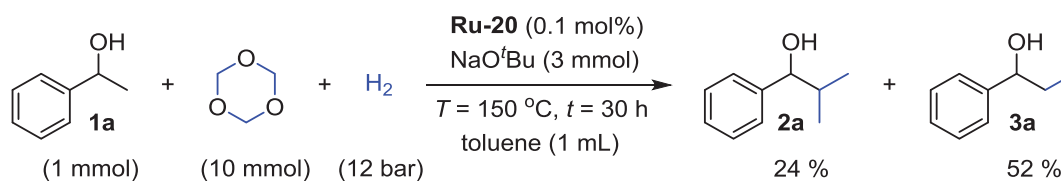
analyzed by NMR spectroscopy. Yield was determined by  $^1\text{H}$  NMR spectrum using mesitylene (120.2 mg, 1 mmol) as an internal standard ( $\delta_{\text{Mesitylene(standard)}} = 6.73$  (s, 3H),  $\delta_{\text{product}} = 4.28$  (d, 1H)).  $^1\text{H}$  NMR (300 MHz,  $\text{CDCl}_3$ , 298 K)  $\delta = 7.17$ - $7.26$  (m, 5H, ArCH), 4.28 (d, 1H,  $J = 6$  Hz, CH), 1.83-2.20 (m, 1H, CH), 0.92 (d, 3H,  $J = 6.65$  Hz,  $\text{CH}_3$ ), 0.72 (d, 3H,  $J = 6.80$  Hz,  $\text{CH}_3$ ). Yield of **2a**: 63%.

#### 2.9.7.4 Procedure for $\beta$ -methylation of **1a** with paraformaldehyde and $\text{H}_2$



Ru-MACHO-BH **Ru-20** (0.59 mg, 0.1 mol%),  $\text{NaO}^t\text{Bu}$  (288.30 mg, 3 mmol) and paraformaldehyde (300.30 mg, 10.0 mmol) were weighed into a glass inlet equipped with a stirring bar inside a glovebox. The glass inlet was transferred to a 10 mL stainless steel autoclave that was evacuated and refilled with argon at least three times. **1a** (122.2 mg, 1 mmol) and toluene (1 mL) were added at room temperature through a valve under argon. The autoclave was sealed and pressurized with 12 bar of hydrogen. The autoclave was heated to 150  $^\circ\text{C}$  temperature for 24 h. After 24 h, the autoclave was cooled to room temperature and slowly vented while stirring continued. Mesitylene (120 mg, 1 mmol) was added as an internal standard to the reaction mixture that was then passed through a short path of acidic alumina before the composition was analyzed by NMR spectroscopy. Yield of **2a**: 9%, Yield of **3a**: 4%.

#### 2.9.7.5 Procedure for $\beta$ -methylation of **1a** with 1,3,5 trioxane and $\text{H}_2$



Ru-MACHO-BH **Ru-20** (0.59 mg, 0.1 mol%),  $\text{NaO}^t\text{Bu}$  (288.3 mg, 3 mmol) and 1,3,5 trioxane (900.8 mg, 10 mmol) were weighed into a glass inlet equipped with a stirring bar inside a glovebox. The glass inlet was transferred to a 10 mL stainless steel autoclave that was evacuated and refilled with argon at least three times. **1a** (122.2 mg, 1 mmol), and toluene (1 mL) were

added at room temperature through a valve under argon. The autoclave was sealed and pressurized with 12 bar of hydrogen. The autoclave was heated to 150 °C temperature for 30 h. After 30 h, the autoclave was cooled to room temperature and slowly vented while stirring continued. Mesitylene (125 mg, 1.04 mmol) was added as an internal standard to the reaction mixture that was then passed through a short path of acidic alumina before the composition was analyzed by NMR spectroscopy. Yield was determined by  $^1\text{H}$  NMR spectrum using mesitylene (120.2 mg, 1 mmol) as an internal standard ( $\delta_{\text{Mesitylene(standard)}} = 6.70$  (s, 3H),  $\delta_{\text{product 2a}} = 4.23$  (d, 1H)),  $\delta_{\text{product 3a}} = 4.46$  (t, 1H)).  $^1\text{H}$  NMR (300 MHz,  $\text{CDCl}_3$ , 298 K) for **2a**,  $\delta = 7.06$ -7.24 (m, 5H, ArCH), 4.23 (d, 1H,  $J = 6$  Hz, CH), 1.79-1.92 (m, 1H, CH), 0.90 (d, 3H,  $J = 6.66$  Hz,  $\text{CH}_3$ ), 0.69 (d, 3H,  $J = 6.81$  Hz,  $\text{CH}_3$ ).  $^1\text{H}$  NMR (300 MHz,  $\text{CDCl}_3$ , 298 K) for **3a**,  $\delta = 7.06$ -7.24 (m, 5H, ArCH), 4.46 (t, 1H,  $J = 6.58$  Hz, CH), 1.58-1.73 (m, 1H, CH), 0.81 (t, 3H,  $J = 7.42$  Hz,  $\text{CH}_3$ ). NMR yield of **2a**: 24%, NMR yield of **3a**: 52%.

#### **2.9.7.6 Conversion/time profile experiments for the $\beta$ -methylation of **1e** with MeOH at different time intervals**

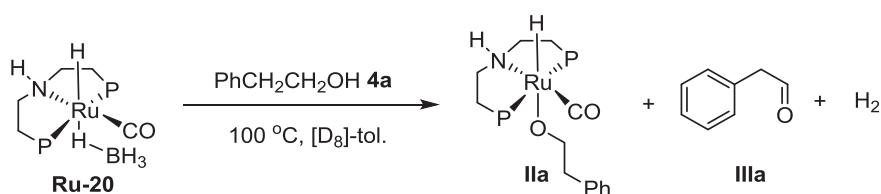
Seven reactions were performed for the reaction progress experiments at different time intervals. Ru-MACHO-BH **Ru-20** (0.59 mg, 0.1 mol%) and NaOMe (81.03 mg, 1.5 mmol) were weighed into a glass inlet equipped with a stirring bar inside a glovebox. The glass inlet was transferred to a 10 mL stainless steel autoclave that was evacuated and refilled with argon at least three times. **1e** (136.2 mg, 1 mmol), and MeOH (1 mL) were added at room temperature through a valve under argon. The autoclave was sealed and heated to 150 °C temperature. After a certain reaction time, the autoclave was fast cooled in ice bath, brings it to room temperature and slowly vented while stirring continued. Mesitylene was added as an internal standard to the reaction mixture that was then passed through a short path of acidic alumina before the composition was analyzed by NMR spectroscopy.

#### **2.9.7.7 Reaction of **1e** with methanol with low loading of catalyst**

Ru-MACHO-BH **Ru-20** (0.29 mg, 0.005 mol%) and NaOMe (810.3 mg, 15 mmol) were weighed into a glass inlet equipped with a stirring bar inside a glovebox. The glass inlet was transferred to a 20 mL stainless steel autoclave that was evacuated and refilled with argon at least three times. 1-Phenyl propanol **1e** (1.36 g, 10 mmol) and methanol (2 mL) were added at room temperature

through a valve under argon. The autoclave was sealed and heated to 150 °C temperature. After 36 h, the autoclave was cooled to room temperature and slowly vented while stirring continued. Mesitylene (120.19 mg, 1 mmol) was added as an internal standard to the reaction mixture that was then passed through a short path of acidic alumina before the composition was analyzed by NMR spectroscopy.

### 2.9.7.8 Reaction of Ru-MACHO-BH with 2-phenyl ethanol **4a**



2-Phenyl ethanol **4a** (1.22 mg, 0.01 mmol), Ru-MACHO-BH **Ru-20** (5.86 mg, 0.01 mmol) and [D<sub>8</sub>]-toluene (0.4 ml as a deuterated solvent) were charged in a Teflon tapped NMR tube under argon atmosphere. The NMR tube was heated at 100 °C temperature. <sup>1</sup>H NMR of the reaction mixture of **Ru-20** and **4a** were measured at different time intervals which confirmed the formation of Ru(II) intermediate **IIa** and **IIIa**. <sup>1</sup>H NMR (300 MHz, [D<sub>8</sub>]-toluene, 298 K) for **IIa**,  $\delta = -16.92$  (t, 1H,  $J = 19.07$  hz, RuH). <sup>1</sup>H NMR (300 MHz, [D<sub>8</sub>]-toluene-*d*<sub>8</sub>, 298 K) for phenylacetaldehyde **IIIa**,  $\delta = 9.24$  (t, 1H,  $J = 3$  Hz, HCO).

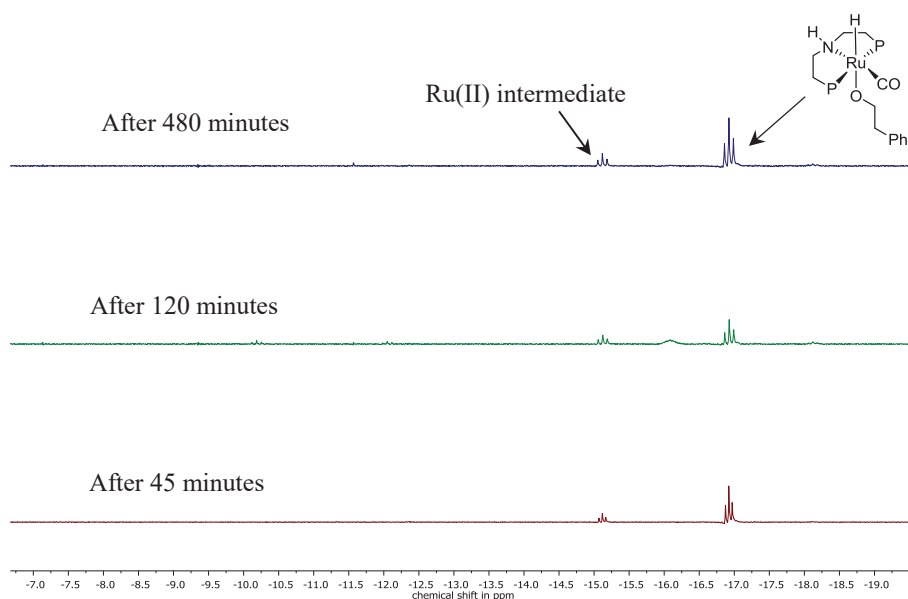


**Figure 2.5:** <sup>1</sup>H-NMR (300 MHz, [D<sub>8</sub>]-toluene, 298 K) spectra of intermediate **IIa** at different time intervals

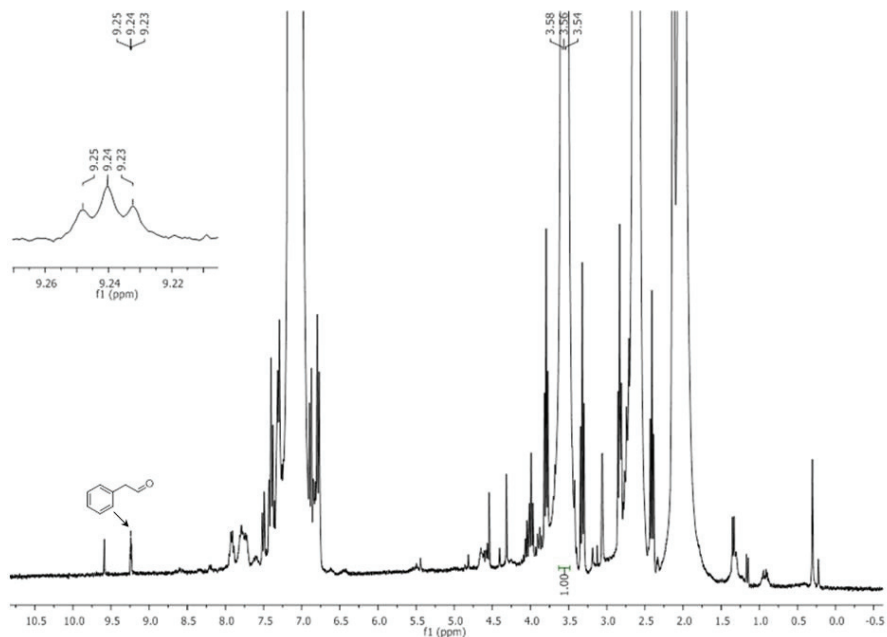
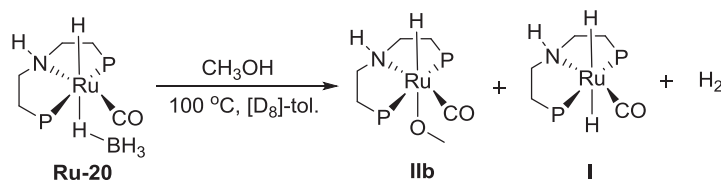


**Figure 2.6:**  $^1\text{H}$ -NMR (300 MHz,  $[\text{D}_8]$ -toluene, 298 K) spectrum of the solution obtained by reaction of Ru-MACHO-BH **Ru-20** with **4a**.

### 2.9.7.9 Reaction of Ru-MACHO-BH with methanol



Ru-MACHO-BH **Ru-20** (5.86 mg, 0.01 mmol), MeOH (1.6 mg, 0.05 mmol) and  $[\text{D}_8]$ -toluene (0.4 ml as a deuterated solvent) was charged in a teflon tapped NMR tube under argon atmosphere. The NMR tube was heated at certain temperature.  $^1\text{H}$  NMR of the reaction mixture of **Ru-20** and methanol were measured at different time intervals which confirmed the formation of Ru(II) intermediates **IIb**, and **I**.  $^1\text{H}$  NMR (400 MHz,  $[\text{D}_8]$ -toluene, 298 K) for **IIb**,  $\delta = -17.93$  (t, 1H,  $J = 17.90$  Hz, RuH),  $^{31}\text{P}\{^1\text{H}\}$  NMR (162 MHz,  $[\text{D}_8]$ -toluene, 298 K) for **IIb**,  $\delta = 55.82$  ppm.  $^1\text{H}$  NMR (400 MHz,  $[\text{D}_8]$ -toluene, 298 K) for **I**,  $\delta = -6.14$  (t, 2H,  $J = 16$  Hz, RuH). In figure 2.9,  $^{31}\text{P}\{^1\text{H}\}$  NMR revealed that the intensity of **Ru-20** increases overtime. The increase in intensity of **Ru-20** can be explained because of solubility of **Ru-20** in toluene rises as the temperature is increased.

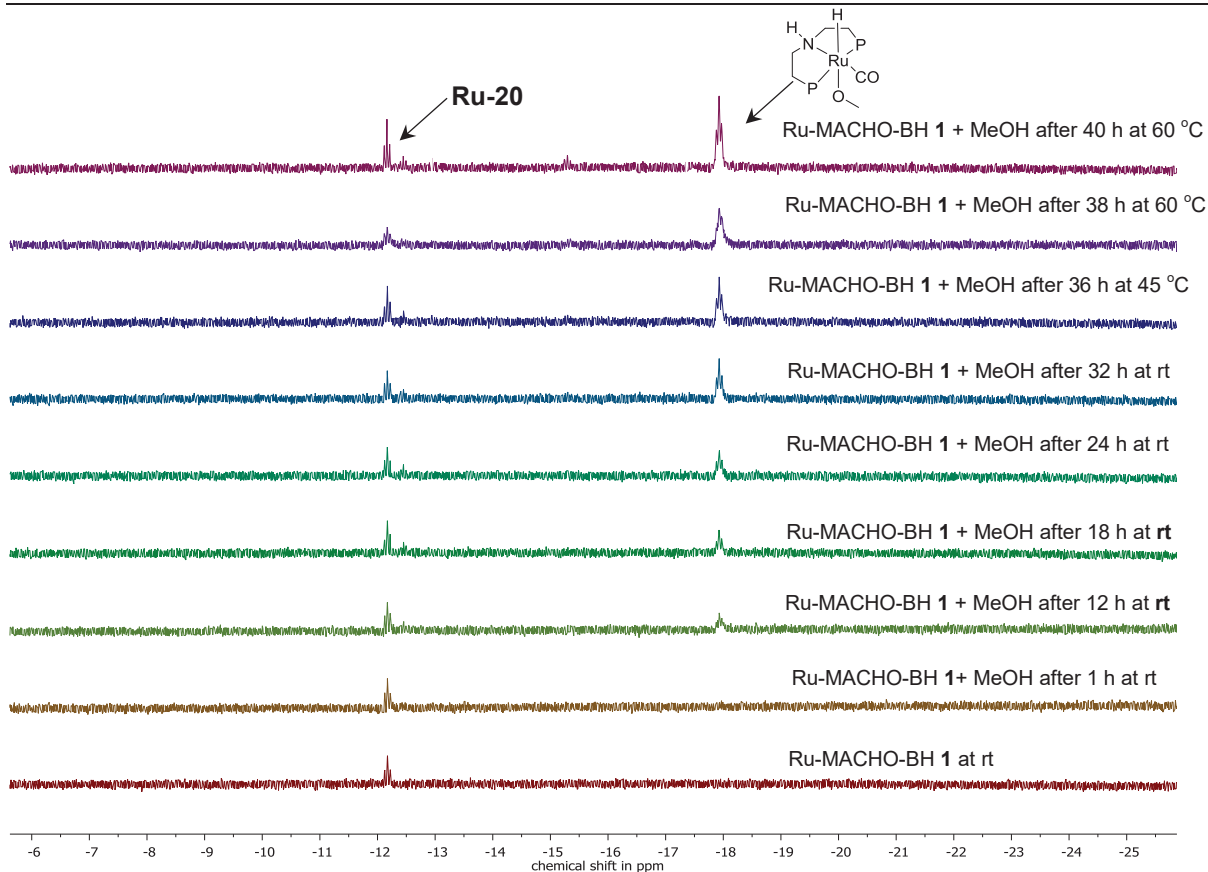


Figure 2.7:  $^1\text{H}$ -NMR (400 MHz,  $[\text{D}_8]$ -toluene, 298 K) spectra of intermediate **IIb** at different time intervals

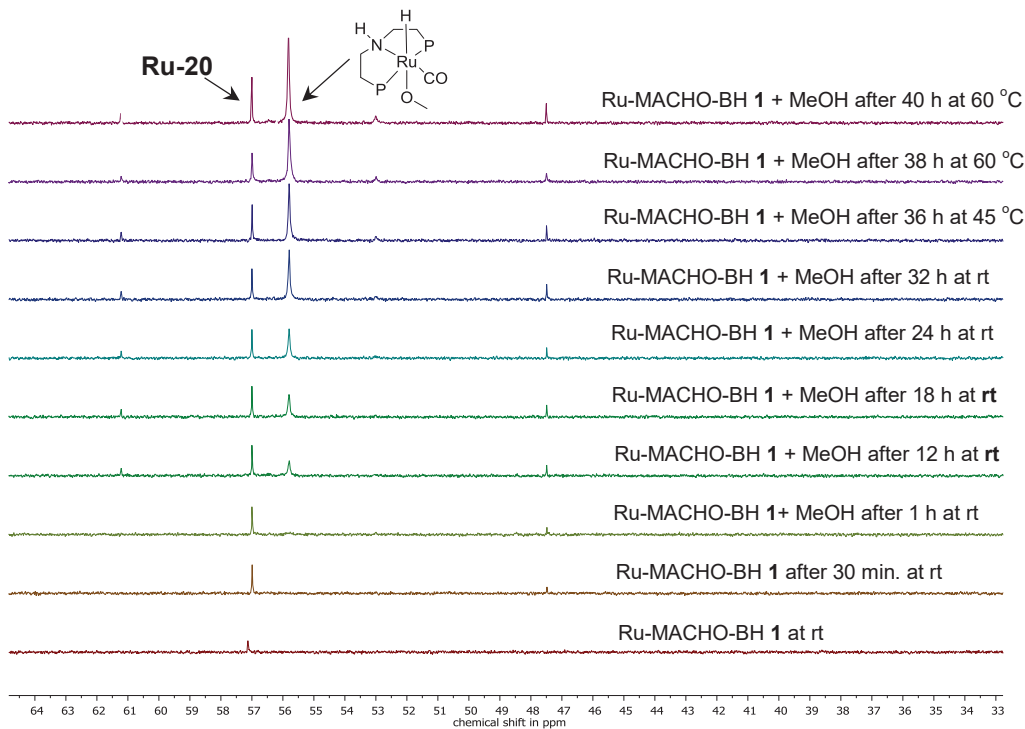


Figure 2.8:  $^{31}\text{P}\{^1\text{H}\}$ -NMR (162 MHz,  $[\text{D}_8]$ -toluene, 298 K) spectra of intermediate **IIb** at different time intervals

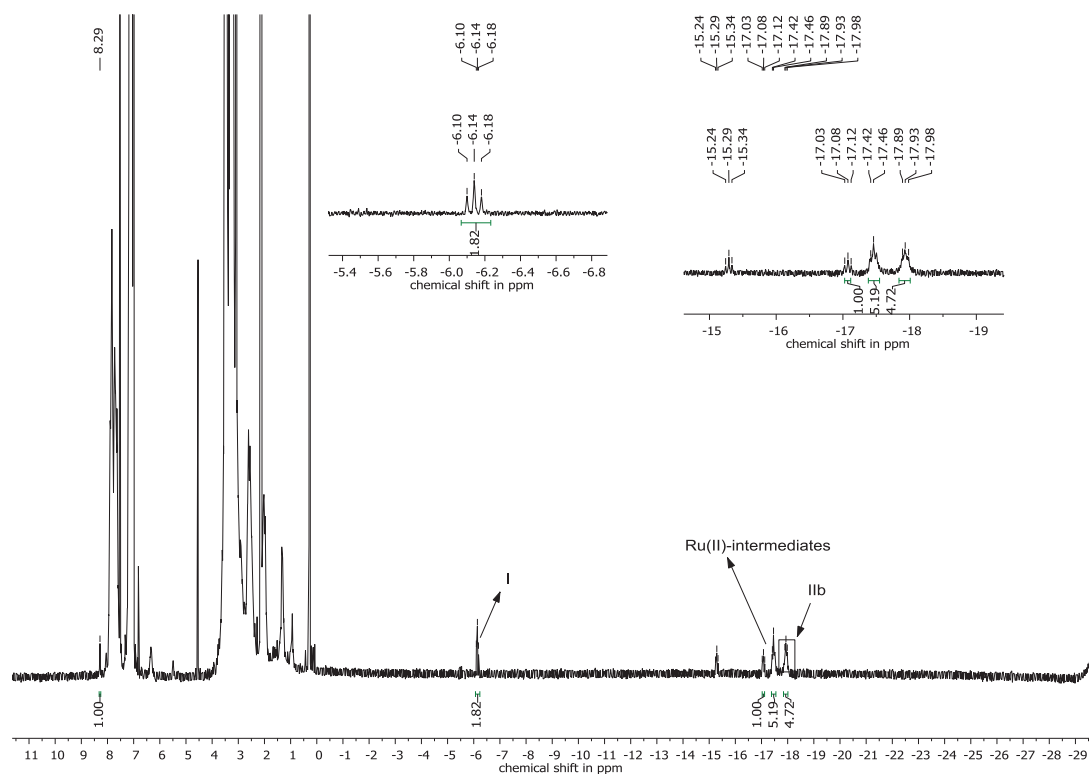
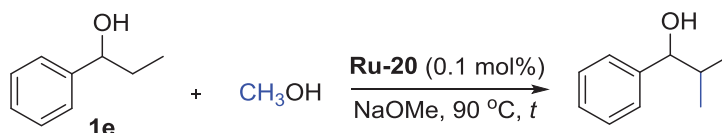


Figure 2.9:  $^1\text{H-NMR}$  (400 MHz,  $[\text{D}_8]$ -toluene, 298 K) spectrum of intermediates **IIb**, and **I** at 90 °C

## 2.10. General procedure for the calculation of Gibbs free activation energy



Several reactions were performed for the investigation of this process. Ru-MACHO-BH **Ru-20** (0.59 mg, 0.1 mol%) and NaOMe (216.12 mg, 4 mmol) were weighed into a glass inlet equipped with a stirring bar inside a glovebox. The glass inlet was transferred to a 10 mL stainless steel autoclave that was evacuated and refilled with argon at least three times. The 1-phenyl-propane-1-ol **1e** (136.2 mg, 1 mmol) and methanol (1 mL) were added at room temperature through a valve under argon. The autoclave was sealed and heated to 90 °C temperature. After certain reaction time, the autoclave was cooled to room temperature and slowly vented while stirring continued. Mesitylene was added as an internal standard to the



reaction mixture that was then passed through a short path of acidic alumina before the composition was analyzed by NMR spectroscopy.

## 2.11. DFT calculated reaction mechanism

### 2.11.1. Estimation of the Gibbs free activation energy (i.e. the energy span) of activation using the Eyring Equation

#### Eyring equation

$$k = \frac{k_B \cdot T}{h} \cdot e^{\frac{-\Delta G^\ddagger}{R \cdot T}} \quad (\text{eq. 2})$$

$h$  = Planck's constant =  $6.6262 \cdot 10^{-34}$  Js

$k_B$  = Boltzmann's constant =  $1,3807 \cdot 10^{-23}$  JK<sup>-1</sup>

$R$  = Gas constant =  $0.00198588$  kcalK<sup>-1</sup>mol<sup>-1</sup>

$T$  = Temperature = 363 K

$k$  = reaction rate constant

While calculating the Gibbs free activation energy (i.e. the energy span), we used turnover frequency. TOF does not rely on the rate-determining step or other factors and can be used as an integrated “rate function” of the entire cycle. At a given temperature, the energy span can be corroborated using an Eyring-type equation and TOF can be used as a rate function.

$$\text{TOF} = \frac{k_B \cdot T}{h} \cdot e^{\frac{-\Delta G^\ddagger}{R \cdot T}} \quad (\text{eq. 3})$$

To calculate the reaction rate constant, the turnover frequency (TOF) was determined at three different times. All experiments were performed at least two times.

After 15 hours, analysis of the reaction mixture using NMR spectroscopy confirmed the product formation with a yield of 6% which corresponds to a TOF of  $1.1 \times 10^{-3}$  s<sup>-1</sup>.

Based on this value, the Gibbs free activation energy was determined:

$$\Delta G_1^\ddagger = 26.28 \text{ kcal} \cdot \text{mol}^{-1}$$

Similarly after 20 hours, TOF was also determined. The reaction showed the yield of 10% to the desired product which corresponds to a TOF of  $1.4 \times 10^{-3}$  s<sup>-1</sup>.

Based on this value, the Gibbs free activation energy was determined:

$$\Delta G_2^\ddagger = 26.12 \text{ kcal} \cdot \text{mol}^{-1}$$

After 25 hours, reaction confirmed the product formation with 16% yield which corresponds to a TOF of  $1.8 \times 10^{-3} \text{ s}^{-1}$ .

Based on this value, the Gibbs free activation energy was determined:

$$\Delta G_3^\ddagger = 25.92 \text{ kcal} \cdot \text{mol}^{-1}$$

In conclusion, the three independent experiments showed the Gibbs free activation energy:

$$\Delta G_1^\ddagger = 26.28 \text{ kcal} \cdot \text{mol}^{-1}$$

$$\Delta G_2^\ddagger = 26.12 \text{ kcal} \cdot \text{mol}^{-1}$$

$$\Delta G_3^\ddagger = 25.92 \text{ kcal} \cdot \text{mol}^{-1}$$

Calculation of final Gibbs free activation energy with standard deviation and experimental error revealed the final  $\Delta G^\ddagger = 26.11 \pm 0.5 \text{ kcal} \cdot \text{mol}^{-1}$ .

### 2.11.2. Computational Details

The DFT calculations in this work were carried out by Dr. Markus Hölscher using the Gaussian09 program package (Revision E.01).<sup>[28]</sup> All compounds shown in Figure 2.3 (subcycles A-E) were optimized using the B97 density functional augmented with Grimmes D3 dispersion correction in combination with the Becke-Johnson (BJ) damping (B97D3-BJ).<sup>[29]</sup> The def2-TZVP basis set<sup>[30]</sup> was used for all elements together with the associated ECP for ruthenium.<sup>[31]</sup> The automatic density fitting approximation was activated.<sup>[32]</sup> The optimizations were carried out using an implicit solvent model (IEF-PCM) with the SMD radii model.<sup>[33]</sup> The solvent used was methanol. Corrections for standard state were applied by setting the pressure to 603 atm, while the thermochemical parameters were computed for a temperature of  $T = 423 \text{ K}$ . The nature of all local minima and all transition states was characterized by performing frequency calculations showing no ( $i = 0$ ) or one ( $i = 1$ ) imaginary frequencies, respectively. In selected cases intrinsic reaction coordinate (IRC) computations were carried out to prove the localized transition states to connect the independently optimized preceding/following minima. Energy values reported in figures and text are Gibbs free energies unless otherwise noted. The energies are listed in Table 2.6.

**Table 2.6:** DFT-computed energies (Hartree) and relative Gibbs free energies (kcal/mol) of compounds shown in Figure 2.3 of the main text.<sup>[a]</sup>

Compd.	<i>E</i>	<i>Ezpe</i>	<i>H</i>	<i>G</i>	Grel
I	-2031,444234	-2030,931304	-2030,866473	-2031,038234	0,0
II	-2456,774798	-2456,074939	-2455,988525	-2456,21005	0,1
TS II-III	-2456,751813	-2456,058159	-2455,972067	-2456,191032	12,0
III	-2456,756601	-2456,059888	-2455,973242	-2456,193168	10,7
IV	-2455,583241	-2454,899315	-2454,815006	-2455,030815	-2,0
V	-2455,575199	-2454,892934	-2454,808441	-2455,022373	3,3
TSV-I'	-2455,564145	-2454,888165	-2454,804002	-2455,016518	6,9
I' (I + A)					-0,4
VI	-2147,173606	-2146,609506	-2146,53694	-2146,727269	1,0
TS VI-VII	-2147,147381	-2146,587815	-2146,516131	-2146,703774	15,8
VII	-2147,148663	-2146,589197	-2146,516445	-2146,706633	14,0
VIII	-2145,966675	-2145,42286	-2145,351454	-2145,541617	2,9
IX	-2145,969391	-2145,422165	-2145,352089	-2145,533791	7,8
TSIX-I''	-2145,949621	-2145,409133	-2145,33946	-2145,521958	15,3
I'' (I + B)					13,3
TSI''-XI	-2031,392349	-2030,887606	-2030,822758	-2030,994186	40,9
XII	-2493,637868	-2492,956112	-2492,868949	-2493,090574	5,0
XIII	-2493,639427	-2492,957597	-2492,870613	-2493,090823	7,6
TSXIII-XIV	-2493,636692	-2492,956079	-2492,870468	-2493,083936	11,9
XIV	-2493,65287	-2492,968182	-2492,881826	-2493,100467	1,5
XV	-2494,831116	-2494,130197	-2494,041807	-2494,264352	13,2
TSXV-XVI	-2494,82551	-2494,126831	-2494,039141	-2494,2621	14,6
XVI	-2494,844177	-2494,139696	-2494,05129	-2494,276625	5,5
I''' (I + E)					3,1
I''' (I + F)					10,3
XVI	-2494,875371	-2494,170721	-2494,082428	-2494,307128	-13,6
TSXVI-XVII	-2494,866971	-2494,162555	-2494,076181	-2494,290454	-3,1
XVII	-2494,88713	-2494,17744	-2494,09101	-2494,305907	-12,8
XVIII	-2496,06195	-2495,337898	-2495,248574	-2495,473642	-3,5
TSXVIII-XIX	-2496,057238	-2495,334823	-2495,246533	-2495,469084	-0,6
XIX	-2496,082556	-2495,3552	-2495,266088	-2495,492655	-15,4
2a	-425,3097251	-425,124247	-425,103958	-425,17195	
A	-424,1055017	-423,942659	-423,923599	-423,989985	
B	-114,4888435	-114,462812	-114,457206	-114,486911	
C	-538,6183135	-538,423042	-538,399469	-538,476058	
D	-462,173823	-462,00695	-461,986054	-462,056676	
E	-463,3801597	-463,190912	-463,168615	-463,242341	
F	-463,4050402	-463,214727	-463,192915	-463,264773	
3a	-464,6130713	-464,400182	-464,37728	-464,450683	

Ruthenium catalyzed  $\beta$ -methylation of alcohols using MeOH as a C1 source

<b>H<sub>2</sub></b>	-1,1831508	-1,173224	-1,168536	-1,182599
<b>H<sub>2</sub>O</b>	-76,435733	-76,415055	-76,409663	-76,433421
<b>MeOH</b>	-115,7151951	-115,66526	-115,658501	-115,691295

[a] B97D3-BJ/def2-TZVP(ECP), SMD,  $p = 603$  atm,  $T = 423$  K.  $\Delta G_r = -13.1$  kcal/mol

**Table 2.7:** DFT-computed energies (Hartree) and relative Gibbs free energies (kcal/mol) of compounds shown in Figure 2.4.<sup>[a]</sup>

<b>Compd.</b>	<b><i>E</i></b>	<b><i>E<sub>zpe</sub></i></b>	<b><i>H</i></b>	<b><i>G</i></b>	<b><i>G<sub>rel</sub></i></b>
<b>A</b>	-424,1082302	-423,945614	-423,926565	-423,992504	0,0
<b>B</b>	-114,4900619	-114,464045	-114,458437	-114,488147	0,0
<b>C</b>	-538,6228207	-538,427622	-538,403868	-538,481902	-0,8
<b>D</b>	-462,1756188	-462,008764	-461,987865	-462,058506	-8,9
<b>XXI</b>	-423,6026873	-423,453886	-423,434942	-423,500708	-3,4
<b>XXIII</b>	-538,1220561	-537,940943	-537,917917	-537,994414	-6,9
<b>XXV</b>	-538,1190909	-537,938401	-537,914551	-537,992342	-5,6
<b>TSXX</b>	-657,2337262	-656,955796	-656,922653	-657,021696	12,4
<b>TSXXII</b>	-538,1049116	-537,927011	-537,903786	-537,979732	2,3
<b>TSXXIV</b>	-771,7465077	-771,436438	-771,398554	-771,508003	13,6
<b>TSXXVI</b>	-538,1034854	-537,925888	-537,901684	-537,980414	1,9
<b>I</b>	-2031,4491293	-2030,936031	-2030,871253	-2031,04295	
<b>XIX</b>	-2496,0890281	-2495,361683	-2495,272551	-2495,499395	
<b>2a</b>	-425,3120165	-425,126588	-425,106275	-425,174358	
<b>MeOH</b>	-115,7173188	-115,667409	-115,660645	-115,693452	
<b>H<sub>2</sub>O</b>	-76,4384261	-76,417776	-76,412384	-76,436144	
<b>HO<sup>t</sup>Bu</b>	-233,6411077	-233,509026	-233,494839	-233,546155	
<b>O<sup>t</sup>Bu<sup>-</sup></b>	-233,1321351	-233,012896	-232,999727	-233,048962	

[a] B97D3-BJ/def2-TZVPD(ECP), SMD,  $p = 603$  atm,  $T = 423$  K.

## References

- [1] a) E. J. Barreiro, A. E. Kummerle, C. A. Fraga, *Chem. Rev.* **2011**, *111*, 5215-5246; b) R. L. Wingad, E. J. E. Bergström, M. Everett, K. J. Pellow, D. F. Wass, *Chem. Commun.* **2016**, *52*, 5202-5204; c) Q. Liu, G. Xu, X. Wang, X. Mu, *Green Chem.* **2016**, *18*, 2811-2818; d) K. Natte, H. Neumann, M. Beller, R. V. Jagadeesh, *Angew. Chem. Int. Ed.* **2017**, *56*, 6384-6394.
- [2] H. Schonherr, T. Cernak, *Angew. Chem. Int. Ed. Engl.* **2013**, *52*, 12256-12267.
- [3] a) K. Maruoka, A. B. Concepcion, H. Yamamoto, *Synthesis* **1994**, 1283-1290; b) Y. Yokoyama, K. Mochida, *J. Organomet. Chem.* **1995**, *499*; c) J.-S. Chang, Y.-D. Lee, L. C.-S. Chou, T.-R. Ling, T.-C. Chou, *Ind. Eng. Chem. Res.* **2012**, *51*, 655-661.
- [4] a) J. V. Price, L. Chen, W. B. Whitaker, E. Papoutsakis, W. Chen, *Proc. Natl. Acad. Sci.* **2016**; b) S. Wesselbaum, T. Vom Stein, J. Klankermayer, W. Leitner, *Angew. Chem. Int. Ed. Engl.* **2012**, *51*, 7499-7502; c) J. A. Rodriguez, P. Liu, D. J. Stacchiola, S. D. Senanayake, M. G. White, J. G. Chen, *ACS Catal.* **2015**, *5*, 6696-6706.
- [5] A. Corma, J. Navas, M. J. Sabater, *Chem. Rev.* **2018**, *118*, 1410-1459.
- [6] a) C. Carlini, M. D. Girolamo, A. Macinai, M. Marchionna, M. Noviello, A. M. R. Galletti, G. Sbrana, *J. Mol. Catal. A: Chem.* **2003**, *204-205*, 721-728; b) R. L. Wingad, E. J. E. Bergstrom, M. Everett, K. J. Pellow, D. F. Wass, *Chem. Commun.* **2016**, *52*, 5202-5204.
- [7] a) M. Nielsen, E. Alberico, W. Baumann, H. J. Drexler, H. Junge, S. Gladiali, M. Beller, *Nature* **2013**, *495*, 85-89; b) J. F. Bower, I. S. Kim, R. L. Patman, M. J. Krische, *Angew. Chem. Int. Ed. Engl.* **2009**, *48*, 34-46; c) Q. Wang, K. Wu, Z. Yu, *Organometallics* **2016**, *35*, 1251-1256; d) R. Cano, M. Yus, D. J. Ramon, *Chem. Commun.* **2012**, *48*, 7628-7630; e) T. Suzuki, *Chem. Rev.* **2011**, *111*, 1825-1845; f) E. Balaraman, E. Khaskin, G. Leitius, D. Milstein, *Nat. Chem* **2013**, *5*, 122-125; g) A. Sarbajna, I. Dutta, P. Daw, S. Dinda, S. M. W. Rahaman, A. Sarkar, J. K. Bera, *ACS Catal.* **2017**, *7*, 2786-2790; h) T. Zweifel, J. V. Naubron, H. Grutzmacher, *Angew. Chem. Int. Ed. Engl.* **2009**, *48*, 559-563; i) S. Thiyagarajan, C. Gunanathan, *ACS Catal.* **2017**, *7*, 5483-5490; j) H. W. Cheung, T. Y. Lee, H. Y. Lui, C. H. Yeung, C. P. Lau, *Adv. Synth. Catal.* **2008**, *350*, 2975-2983; k) W. M. Akhtar, C. B. Cheong, J. R. Frost, K. E. Christensen, N. G. Stevenson, T. J. Donohoe, *J. Am. Chem. Soc.* **2017**, *139*, 2577-2580.
- [8] a) L. K. Chan, D. L. Poole, D. Shen, M. P. Healy, T. J. Donohoe, *Angew. Chem. Int. Ed. Engl.* **2014**, *53*, 761-765; b) S. Ogawa, Y. Obora, *Chem. Commun.* **2014**, *50*, 2491-2493; c) D. Shen, D. L. Poole, C. C. Shotton, A. F. Kornahrens, M. P. Healy, T. J. Donohoe, *Angew. Chem. Int. Ed. Engl.* **2015**, *54*, 1642-1645; d) K. Beydoun, G. Ghattas, K. Thenert, J. Klankermayer, W. Leitner, *Angew. Chem. Int. Ed. Engl.* **2014**, *53*, 11010-11014; e) K. Beydoun, T. vom Stein, J. Klankermayer, W. Leitner, *Angew. Chem. Int. Ed. Engl.* **2013**, *52*, 9554-9557.
- [9] a) G. E. Jorg Sauer, *Chem. Eng. Technol.* **1995**, *18*, 284-291; b) W.-H. Lin, H.-F. Chang, *Catal. Today* **2004**, *97*, 181-188.
- [10] Y. Li, H. Li, H. Junge, M. Beller, *Chem. Commun.* **2014**, *50*, 14991-14994.
- [11] K. Oikawa, S. Itoh, H. Yano, H. Kawasaki, Y. Obora, *Chem. Commun.* **2017**, *53*, 1080-1083.

- [12] Q. Liu, G. Xu, Z. Wang, X. Liu, X. Wang, L. Dong, X. Mu, H. Liu, *ChemSusChem* **2017**, *10*, 4748-4755.
- [13] S. M. A. H. Siddiki, A. S. Touchy, M. A. R. Jamil, T. Toyao, K.-i. Shimizu, *ACS Catal.* **2018**, *8*, 3091-3103.
- [14] a) S. U. Ryota Arai, Masahiro Irie, Kenji Matsuda, *J. Am. Chem. Soc.* **2008**, *130*, 9371-9379; b) P. Daublain, A. K. Thazhathveetil, Q. Wang, A. Trifonov, T. Fiebig, F. D. Lewis, *J. Am. Chem. Soc.* **2009**, *131*, 16790-16797.
- [15] K. Oikawa, S. Itoh, H. Yano, H. Kawasaki, Y. Obora, *Chem. Commun.* **2017**, *53*, 1080-1083.
- [16] M. Hatano, R. Gouzu, T. Mizuno, H. Abe, T. Yamada, K. Ishihara, *Catal. Sci. Technol.* **2011**, *1*, 1149-1158.
- [17] a) D. S. Rao, T. R. Reddy, K. Babachary, S. Kashyap, *Org. Biomol. Chem* **2016**, *14*, 7529-7543; b) R. Fernández, A. Ros, A. Magriz, H. Dietrich, J. M. Lassaletta, *Tetrahedron* **2007**, *63*, 6755-6763.
- [18] a) A. Kišić, M. Stephan, B. Mohar, *Adv. Synth. Catal.* **2015**, *357*, 2540-2546; b) S. Rodríguez, B. Qu, K. R. Fandrick, F. Buono, N. Haddad, Y. Xu, M. A. Herbage, X. Zeng, S. Ma, N. Grinberg, H. Lee, Z. S. Han, N. K. Yee, C. H. Senanayake, *Adv. Synth. Catal.* **2014**, *356*, 301-307.
- [19] J. C. Bardhan, D. N. Mukherji, *J. Chem. Soc.* **1956**, 4629-4633.
- [20] S. Koul, J. L. Koul, B. Singh, M. Kapoor, R. Parshad, K. S. Manhas, S. C. Taneja, G. N. Qazi, *Tetrahedron: Asymmetry* **2005**, *16*, 2575-2591.
- [21] W. J. Jang, S. M. Song, J. H. Moon, J. Y. Lee, J. Yun, *J. Am. Chem. Soc.* **2017**, *139*, 13660-13663.
- [22] J. E. Roque Pena, E. J. Alexanian, *Org. Lett.* **2017**, *19*, 4413-4415.
- [23] J. Cao, P. Perlmutter, *Org. Lett.* **2013**, *15*, 4327-4329.
- [24] S. R. Tamang, M. Findlater, *J. Org. Chem.* **2017**, *82*, 12857-12862.
- [25] T. Chen, S. Y. Li, D. Wang, M. Yao, L. J. Wan, *Angew. Chem. Int. Ed.* **2015**, *54*, 4309-4314.
- [26] P. Wang, D.-L. Wang, H. Liu, X.-L. Zhao, Y. Lu, Y. Liu, *Organometallics* **2017**, *36*, 2404-2411.
- [27] Y. J. Jiang, G. P. Zhang, J. Q. Huang, D. Chen, C. H. Ding, X. L. Hou, *Org. Lett.* **2017**, *19*, 5932-5935.
- [28] M. J. Frisch, G. W. Trucks, H. B. Schlegel, G. E. Scuseria, M. A. Robb, J. R. Cheeseman, G. Scalmani, V. Barone, G. A. Petersson, H. Nakatsuji, X. Li, M. Caricato, A. V. Marenich, J. Bloino, B. G. Janesko, R. Gomperts, B. Mennucci, H. P. Hratchian, J. V. Ortiz, A. F. Izmaylov, J. L. Sonnenberg, Williams, F. Ding, F. Lipparini, F. Egidi, J. Goings, B. Peng, A. Petrone, T. Henderson, D. Ranasinghe, V. G. Zakrzewski, J. Gao, N. Rega, G. Zheng, W. Liang, M. Hada, M. Ehara, K. Toyota, R. Fukuda, J. Hasegawa, M. Ishida, T. Nakajima, Y. Honda, O. Kitao, H. Nakai, T. Vreven, K. Throssell, J. A. Montgomery Jr., J. E. Peralta, F. Ogliaro, M. J. Bearpark, J. J. Heyd, E. N. Brothers, K. N. Kudin, V. N. Staroverov, T. A. Keith, R. Kobayashi, J. Normand, K. Raghavachari, A. P. Rendell, J. C. Burant, S. S. Iyengar, J. Tomasi, M. Cossi, J. M. Millam, M. Klene, C. Adamo, R. Cammi, J. W. Ochterski, R. L. Martin, K. Morokuma, O. Farkas, J. B. Foresman, D. J. Fox, in *Gaussian 16 Rev. C.01*, Wallingford, CT, **2016**.
- [29] G. Stefan, E. Stephan, G. Lars, *J. Comput. Chem.* **2011**, *32*, 1456-1465.

- [30] a) F. Weigend, R. Ahlrichs, *PCCP* **2005**, *7*, 3297-3305; b) F. Weigend, F. Furche, R. Ahlrichs, *J. Chem. Phys.* **2003**, *119*, 12753-12762; c) K. Eichkorn, F. Weigend, O. Treutler, R. Ahlrichs, *Theor. Chem. Acc.* **1997**, *97*, 119-124; d) A. Schäfer, C. Huber, R. Ahlrichs, *J. Chem. Phys.* **1994**, *100*, 5829-5835; e) A. Schäfer, H. Horn, R. Ahlrichs, *J. Chem. Phys.* **1992**, *97*, 2571-2577.
- [31] a) B. Metz, H. Stoll, M. Dolg, *J. Chem. Phys.* **2000**, *113*, 2563-2569; b) D. Andrae, U. Häußermann, M. Dolg, H. Stoll, H. Preuß, *Theor. Chem. Acc* **1990**, *77*, 123-141.
- [32] a) B. I. Dunlap, *J. Mol. Struct.-Theochem* **2000**, *529*, 37-40; b) B. I. Dunlap, *J. Chem. Phys.* **1983**, *78*, 3140-3142.
- [33] a) J. Tomasi, B. Mennucci, R. Cammi, *Chem. Rev.* **2005**, *105*, 2999-3094; b) A. V. Marenich, C. J. Cramer, D. G. Truhlar, *J. Phys. Chem. B* **2009**, *113*, 6378-6396; c) E. Cancès, B. Mennucci, J. Tomasi, *J. Chem. Phys.* **1997**, *107*, 3032-3041.



### 3. Manganese(I) catalyzed selective $\beta$ -methylation of alcohols using MeOH as the C1 source

Parts of this chapter have been published:

A. Kaithal, P. van Bonn, M. Hölscher, W. Leitner, *Angew. Chem. Int. Ed.* **2020**, *59*, 215-220.  
*Angew. Chem.* **2020**, *132*, 221 –226.

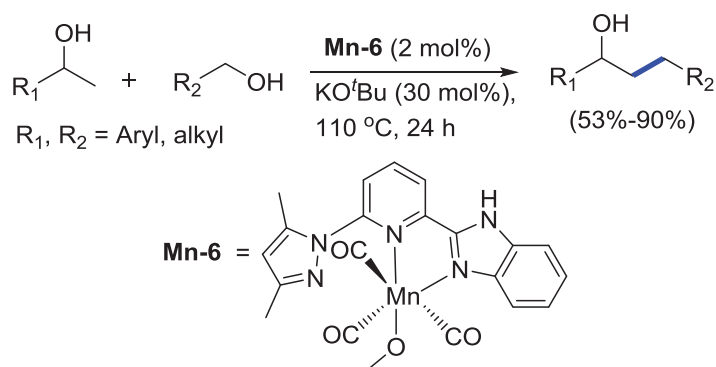
The use of earth-abundant and non-noble metals to substitute noble and rare metals for organic transformations is a topical area in homogeneous catalysis.<sup>[1]</sup> Replacing noble platinum group metals by non-noble 3d metals such as manganese, iron or cobalt could contribute significantly to the conservation of those rare metals and extend the applicability of non-noble metals to a variety of catalytic reactions. In the previous chapter, the Ru(II) catalyzed selective  $\beta$ -methylation of alcohols using methanol as a C1 source was discussed.<sup>[2]</sup> Various alcohols were selectively  $\beta$ -methylated proving the applicability of such reactions in organic synthesis and applied chemistry. DFT calculations revealed the activation energy barriers of all sub-cycles in the whole catalytic cycle, catalyzed by the Ru(II) complex, as being either low or of moderate height. Considering these points, we hypothesized that the selective  $\beta$ -methylation of alcohols might also be achieved using a complex of a cheap earth-abundant metal. Manganese was chosen for this transformation because of its high abundance in the earth's crust. Several transformations were previously reported where using the appropriate ligand, manganese(I) complexes revealed a similar reactivity as ruthenium(II) complexes. Recently, a number of catalytic reactions such as hydrogenation,<sup>[3]</sup> dehydrogenation,<sup>[4]</sup> hydroelementation<sup>[5]</sup> and transfer-hydrogenation<sup>[6]</sup> reactions were reported using manganese complexes. Intrigued by these reports, we assumed that Ru<sup>2+</sup> ions may be substituted by Mn<sup>1+</sup> ions because of diagonal relationship of these two ions in periodic table and same d<sub>6</sub> electronic configuration. Motivated by these studies, for the Mn-MACHO-<sup>i</sup>Pr complex **Mn-2** the Gibbs free activation barrier for the selective  $\beta$ -methylation of 1-phenylpropan-1-ol **1e** using methanol as a C1 source as well as a solvent and NaO<sup>t</sup>Bu as a base at 150 °C temperature was computed. The Gibbs free activation barrier resulted in a value of 30.2 Kcal/mol. This activation barrier is only higher by 1.0 kcal/mol compared to the one computed



for **Ru-20** (see chapter 2.7.5; 29.2 kcal/mol) indicating a reaction, which will be slightly slower, but possible. Accordingly, the DFT computation supported our hypothesis that the reaction can be conducted at similar reaction conditions using Mn-MACHO-*i*Pr as a pre-catalyst.

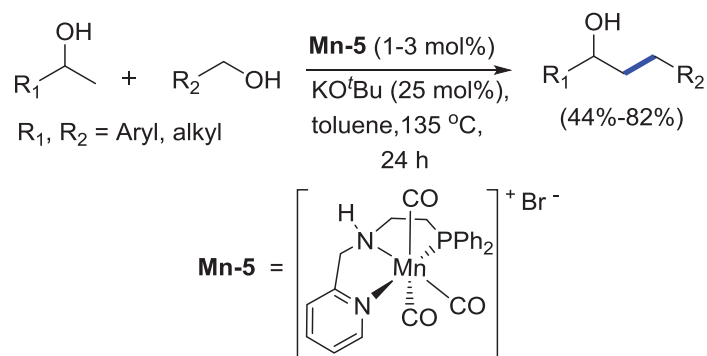
In the last few years, a number of systems were reported where Mn(I) complexes were used for C–C bond formation using hydrogen borrowing reactants.

In 2018, the group of Yu showed an example where the selective  $\beta$ -alkylation of secondary alcohols using primary alcohols as alkylating reagents was performed (Scheme 3.1).<sup>[4b]</sup> The Mn(I) complex consisting of a pyridyl-supported pyrazolyl-imidazolyl ligand was used as a pre-catalyst **Mn-6** with a base as a co-catalyst and toluene as a solvent at 120 °C for 24 h. A variety of aromatic and aliphatic secondary alcohols were selectively  $\beta$ -alkylated, using several aliphatic and aromatic primary alcohols. However, no selective alkylation of alcohols was shown using MeOH as the alkylating reagent.



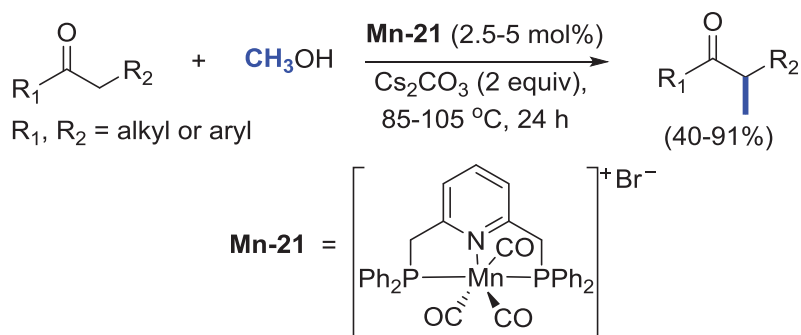
**Scheme 3.1:** Selective  $\beta$ -alkylation of secondary alcohols reported by Yu *et. al.*<sup>[4b]</sup>

In 2018, the group of Rueping also showed the alkylation of secondary alcohols using primary alcohols applying the Mn(I)-PNN pincer complex **Mn-5** (Scheme 3.2).<sup>[7]</sup> The reaction was performed using Mn(I) complex as a pre-catalyst, KO<sup>t</sup>Bu as a co-catalyst and toluene as a solvent at 135 °C for 24 h. Several aliphatic and aromatic secondary alcohols were alkylated using a number of aliphatic and aromatic primary alcohols. The catalytic cycle showed that the reaction is proceeding via “hydrogen borrowing pathways” where N–H functionality in the metal complex used for the proton-shuffling and metal center worked as a hydride transfer confirming the metal-ligand cooperation in the reaction framework.



**Scheme 3.2:** Selective  $\beta$ -alkylation of secondary alcohols reported by Rueping *et. al.*<sup>[7]</sup>

When the present work was stated, there was no report known where the methylation of alcohols was carried out using a manganese complex or other earth-abundant metal complex. However, while we submitted the work concerning the selective  $\beta$ -methylation of alcohols, the selective  $\alpha$ -methylation of ketones using Mn(I)-pincer complexes was reported in 2019 by Rueping *et. al.* (Scheme 3.3).<sup>[8]</sup> The transformation was carried out using a well-established lutidine based Mn(I)-PNP pincer complex **Mn-21**. The  $-\text{CD}_3$  labeled methylated ketones were also synthesized using  $\text{CD}_3\text{OD}$  as a C1 and deuterium source as well as a solvent.

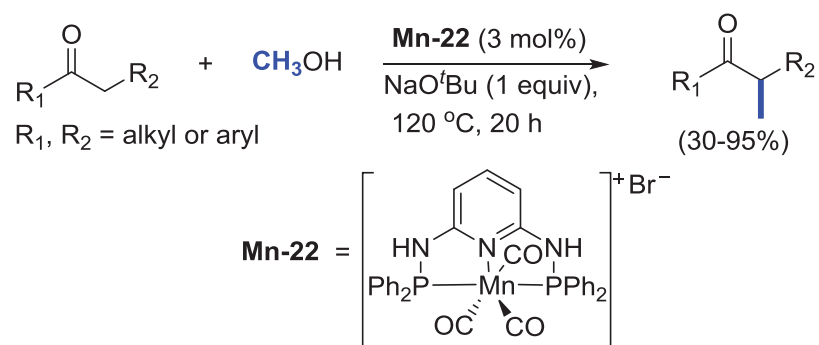


**Scheme 3.3:** Selective  $\alpha$ -methylation of ketones reported by Rueping *et. al.*<sup>[8]</sup>

In the same year, the group of Sortais also published this transformation using Mn(I)-P<sup>N</sup>N<sup>P</sup> pincer complex and methanol as a C1 source (Scheme 3.4).<sup>[9]</sup> A number of aromatic and aliphatic ketones were selective  $\alpha$ -methylated using a Mn(I) pincer complex with a stoichiometric amount of base at 120  $^\circ\text{C}$  for 20 h. Interestingly, this reaction also revealed the selective  $\alpha$ -methylation of esters.

Manganese(I) catalyzed selective  $\beta$ -methylation of alcohols using MeOH as the C1 source

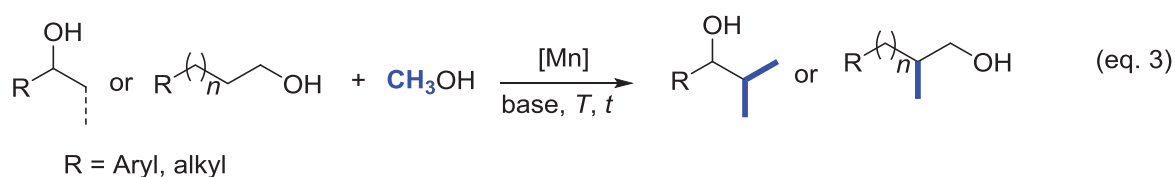
---



**Scheme 3.4:** Selective  $\alpha$ -methylation of ketones reported by Sortais *et. al.*<sup>[9]</sup>

### 3.1. Objective

Substituting a noble and rare metal complex by an earth-abundant metal complex is a dynamic field in modern catalysis. Especially, the formation of C–C bonds via activation of  $sp^3$  C–H bonds is an important transformation in organic synthesis. The objective of this part is to perform the selective  $\beta$ -methylation of alcohols using an earth-abundant metal complex and methanol as a C1 source (eq. 3). Manganese was selected as a metal to perform this transformation because of its high abundance in earth-crust and also the diagonal relationship between the ruthenium(II) and manganese(I) ions in the periodic table. Furthermore, DFT studies of our group had shown that a manganese(I) pincer complex such as Mn-MACHO-<sup>i</sup>Pr **Mn-2** should be active in methylation reaction with methanol. Several manganese(I) pincer complexes will be investigated to perform this transformation. The catalytic cycle will be evaluated based on the control experiments and mechanistic studies.



### 3.2. Reaction optimization

Various manganese pincer complexes were investigated for the selective  $\beta$ -methylation of alcohols. For the optimization, 2-phenyl ethanol **8a** was chosen as a model substrate (Table 3.1). Based on the previous investigation on the ruthenium-catalyzed  $\beta$ -methylation work, the first catalysis attempt was carried out using the Mn-MACHO-*t*Pr complex **Mn-2**. Interestingly, the reaction of **8a** with MeOH in the presence of complex **Mn-2** at 150 °C for 24 h resulted in 97% conversion with a yield of 92% to the corresponding mono-methylated product (Table 3.1, entry 1). Considering these very encouraging results, we studied the effect of different ligands at the manganese center for this particular transformation. Various tridentate Mn(I) complexes such as lutidine based PNP complexes **Mn-21** and **Mn-23**, imidazole based PNN pincer complex **Mn-16** and silane incorporated PNP pincer complex **Mn-24** were prepared and applied in the transformation. Using the same reaction conditions, complexes **Mn-21** and **Mn-23** showed moderate activity and revealed low product formation with the yields of 21% and 24%, respectively (Table 3.1, entry 2 and 3). However, the reaction using Mn(I) PNN complex **Mn-16** and silane-based Mn(I) complex **Mn-24** revealed almost no reactivity (Table 3.1, entry 4 and 5). Based on these results, we concluded that complex **Mn-2** is the best catalyst to perform this organic transformation which was further used for optimization.

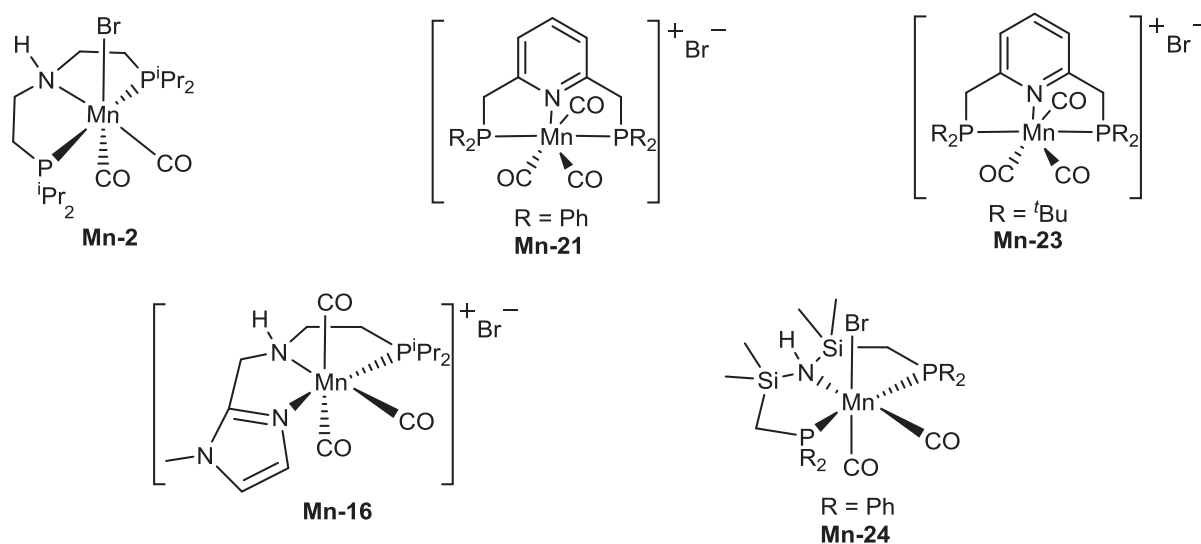


**Figure 3.1:** Tested complexes for the reaction optimization.

Decreasing the amount of complex **Mn-2** from 0.5 mol% to 0.2 mol% decreased the product formation with a yield of 52% (Table 3.1, entry 6). Similarly, while limiting the amount of methanolate from 2 equiv. to 1 equiv. and also the temperature from 150 °C to 125 °C decreased the product formation and showed 70% yield in both cases (Table 3.1, entry 7 and 8). The best optimized reaction condition was found using Mn complex **Mn-2** (0.5 mol%) and NaOMe (2 equiv) at 150 °C for 24 h.

**Table 3.1:**  $\beta$ -methylation of 1-phenyl ethanol **8a** with various manganese precatalysts.<sup>[a, b]</sup>

#	Catalyst	Conv. (%)	Yield <b>9a</b> (%)
1	<b>Mn-2</b> (0.5 mol%)	97	92
2	<b>Mn-21</b> (0.5 mol%)	42	21
3	<b>Mn-23</b> (0.5 mol%)	51	24
4	<b>Mn-16</b> (0.5 mol%)	23	6
5	<b>Mn-24</b> (0.5 mol%)	10	0
6	<b>Mn-2</b> (0.2 mol%)	66	52
7*	<b>Mn-2</b> (0.5 mol%)	76	70
8 <sup>#</sup>	<b>Mn-2</b> (0.5 mol%)	77	70

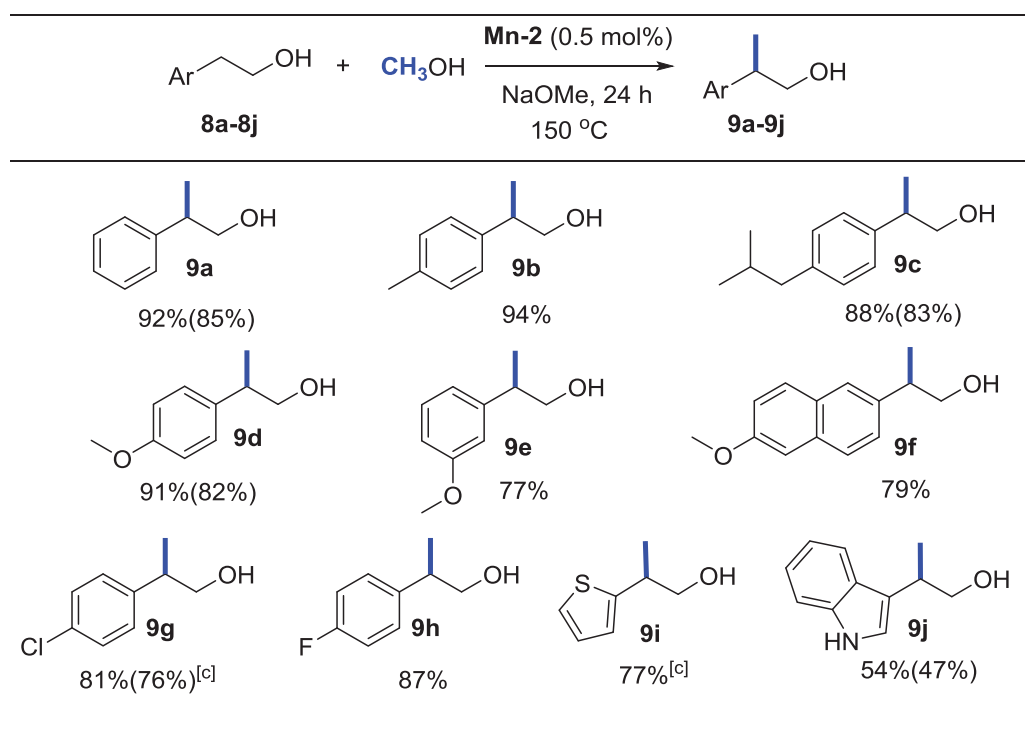
Conditions: [a] **8a** (1 mmol), MeOH (1 mL as a reagent and solvent), Mn precatalyst (0.5 mol%), and NaOMe (2 mmol) at 150 °C for 24 h. [b] Conversion and yield were measured by <sup>1</sup>H NMR and mesitylene was used as an internal standard. \*Reaction was carried out at 125 °C. <sup>#</sup>1 mmol of NaOMe was used.

### 3.3. Mn(I) catalyzed $\beta$ -methylation of 2-arylethanols with methanol

Based on the optimized condition, various 2-arylethanols **8** were investigated for the selective mono-methylation using MeOH as a C1 source and complex **Mn-2** as a pre-catalyst (Table 3.2). The reaction of substituted 2-aryl ethanols bearing electron-donating groups, such as 2-(*p*-tolyl)ethanol **8b** and 2-(4-methoxyphenyl)ethanol **8d**, showed very good activity and resulted in the formation of the corresponding products with yields of 94% and 90%, respectively. The reaction with substrate **8e** bearing a methoxy substituent in *meta* position

revealed 77% yield to the corresponding methylated product. Interestingly, electron-poor substrates such as 2-(4-chlorophenyl)ethanol **8g** and 2-(4-fluorophenyl)ethanol **8h** were also converted to the corresponding mono-methylated products with yields of 81% and 87%, respectively. Heterocyclic alcohols such as thiophene substituted ethanol **8i** and indole substituted ethanol **8j** were well-tolerated and resulted in 77% and 54% yields, respectively to the corresponding methylated products. However, the reaction with pyridine substituted ethanol showed a mixture of products (not shown). Notably, the pharmaceutical important molecules such as ibuprofen alcohol **9c** and naproxen alcohol **9f** were also obtained with very good selectivity comprising the yields of 88% and 79%, respectively.

**Table 3.2:** Mn(I) catalyzed  $\beta$ -methylation of 2-arylethanol with methanol<sup>[a, b]</sup>



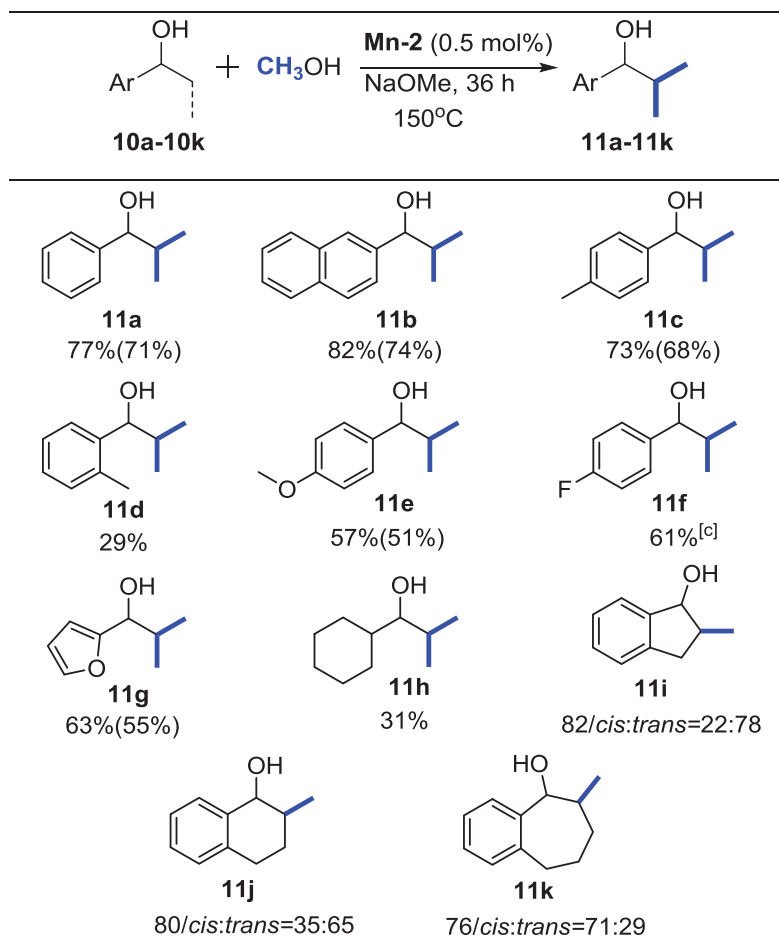
[a] **8** (1 mmol), MeOH (1 mL as a reagent and solvent), Mn precatalyst **Mn-2** (0.5 mol%), and NaOMe (2 mmol) at 150 °C for 24 h. [b] Yields were determined by  $^1\text{H}$ NMR analysis using mesitylene as an internal standard. Yields in parenthesis correspond to the isolated yield after performing column chromatography. [c] Reaction time: 14 h

### 3.4. Mn(I) catalyzed $\beta$ -methylation of secondary alcohols with methanol

Next, the focus was on the selective  $\beta$ -methylation of the secondary alcohols (Table 3.3). For this class, 1-phenyl ethanol **10a** was selected as a benchmark substrate. Using the optimized reaction conditions, a mixture of products was obtained. When the base amount and time was increased to 4 equiv. and 36 h, respectively, the reaction showed the selective formation of the di-methylated product **11a** with yields up to 77%. Surprisingly, this reaction did not generate any monomethylated product, instead >99% selectivity to the di-methylated product **11a** was observed. Using the optimized conditions, various secondary alcohols were tested in the selective  $\beta$ -methylation. The reaction of 1-(naphthalen-2-yl)ethan-1-ol **10b** and 1-(*p*-tolyl)ethanol **10c** showed 82% and 73% yield for the di-methylated products, respectively. However, the substrate with a methyl substituent in the *ortho*-position of the alcohol moiety **10d** revealed very low activity. The low product formation can be explained by a non-favorable influence of the steric hindrance due to the methyl group. The reaction with methoxy-substituent in *para*-position of 1-phenyl ethanol **10e** resulted in a 57% yield of the di-methylated product **11e**. Electron withdrawing groups such as the fluoro substituent in *para*-position in **10f** yielded 44% of the di-methylated product under standard reaction conditions. Interestingly, when the reaction time was increased to 42 h, the yield of the di-methylated product **11f** increased to 61%. Furan as a substituent in ethanol **10g** was tolerated furnishing the di-methylated product **11g** in 63% yield. However, 1-cyclohexylethan-1-ol **10h** revealed lower reactivity with 31% yield of the di-methylated product **11h**.

Furthermore, the selective  $\beta$ -methylation of cyclic secondary alcohols was studied. For these substrates only the mono-methylation was possible. Applying the same reaction conditions, the phenyl substituted five-membered ring containing 2,3-dihydro-1H-inden-1-ol **10i** revealed 82% yield to the mono-methylated product. In this case, majorly the *trans*-isomer was observed. Similarly, phenyl substituted six- **10j** and seven-membered **10k** rings were also tolerated. Both were converted to the corresponding product with the yields of 80% and 76%, respectively. The methylation of 6-membered cyclic alcohols showed the *trans*-isomer as a major product. However 7-membered cyclic alcohols resulted in the predominant formation of *cis*-isomer as a major product.



**Table 3.3:** Mn(I) catalyzed  $\beta$ -methylation of secondary alcohols with methanol.<sup>[a,b]</sup>

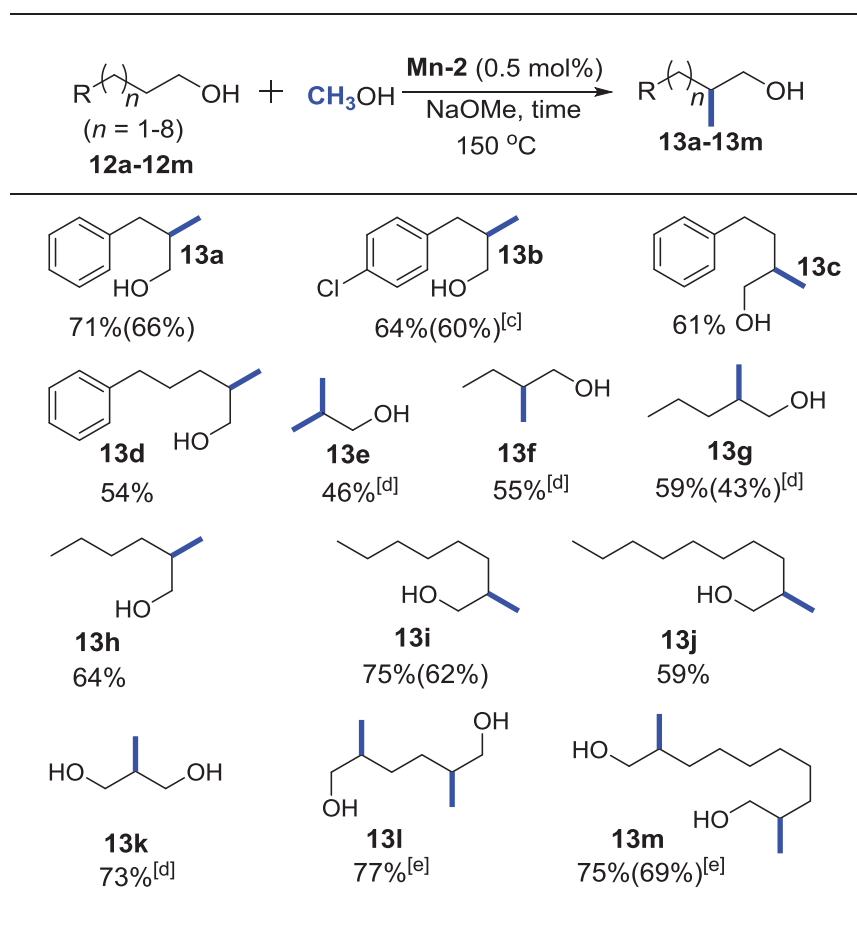
[a] **10** (1 mmol), MeOH (1 mL as a reagent and solvent), Mn precatalyst **Mn-2** (0.5 mol%), and NaOMe (4 mmol) at  $150^\circ\text{C}$  for 36 h. [b] Yields were determined by  $^1\text{H NMR}$  using mesitylene as an internal standard. Yields in parenthesis correspond to the isolated yield after performing column chromatography. [c] Reaction time was increased to 42 h.

### 3.5. Mn(I) catalyzed $\beta$ -methylation of aliphatic alcohols and diols with methanol

Encouraged by these results, the selective  $\beta$ -methylation of aliphatic alcohols was investigated (Table 3.4). At first, aliphatic alcohols substituted with the aromatic substituent distant from the  $-\text{OH}$  group were selected. As a start, 3-phenylpropan-1-ol **12a** was chosen as a benchmark substrate. Reaction parameters showed that the transformation required two equivalents of methanolate to accomplish this transformation. Using the optimized reaction conditions, **12a** was

selectively  $\beta$ -methylated in 71% yield. Similarly, the reaction with the chloro-substituent in *para*-position of 3-phenylpropan-1-ol **12b** also resulted in 64% yield of the desired methylated product **13b**. Furthermore, aryl substituted longer chain aliphatic alcohols were investigated. However, increasing the chain length somehow showed lower reactivity. Compounds 4-phenylbutan-1-ol **12c** and 5-phenylpentan-1-ol **12d** yielded 61% and 54%, respectively of the corresponding mono-methylated product.

**Table 3.4:** Mn(I) catalyzed  $\beta$ -methylation of aliphatic alcohols and diols with methanol.<sup>[a, b]</sup>



[a] **12** (1 mmol), MeOH (1 mL as a reagent and solvent), Mn precatalyst **Mn-2** (0.5 mol%), and NaOMe (2 mmol) at 150 °C for 24 h. [b] Yields were determined by <sup>1</sup>HNMR using mesitylene as an internal standard. Yields in parenthesis correspond to the isolated yield after performing column chromatography. [c] Reaction time: 14 h. [d] Reaction time: 36 h. [e] 4 mmol of NaOMe was used and reaction time was increased to 48 h.

Furthermore, biomass generated pure aliphatic alcohols and diols were inspected for this transformation. Using the standard reaction conditions, the reaction of ethanol with methanol

showed the selective formation of *iso*-butanol **13e** with a yield of 46% after 36 h. Alike, other short chain aliphatic alcohols such as 1-butanol **12f** and 1-pentanol **12g** were also selectively methylated and showed 55% and 59% yield, respectively. Interestingly, the longer chain aliphatic alcohols revealed better reactivity than small chain aliphatic alcohols and required only 24 h to perform this process. The reaction of 1-hexanol **12h** and 1-octanol **12i** with methanol confirmed the product yield of 64% and 75%, respectively. 1-Decanol affirmed slightly lower yield and gave 59% of to the corresponding product **13j**.

Appealingly, these reaction conditions were also applicable to the selective  $\beta$ -methylation of aliphatic diols. The reaction was extended for the preparation of 2-methyl-1,3-propanediol (MPO, **13k**) with 73% yield under standard reaction conditions. MPO is an important and large volume chemical product which is used for the preparation of polyesters. At present, MPO is prepared via four reaction steps from petrochemical propene (oxidation, isomerization, hydroformylation and hydrogenation). Using this process, MPO can be prepared from biomass generated propanediol and green methanol in one step. Similarly, other diols such as 1,6-hexanediol **12l** and 1,10-decanediol **12m** were also selectively methylated and revealed excellent activity with a yield of 77% and 75%, respectively. Entry **12l** and **12m** required an extended reaction time of 48 h and 4 equiv. of methanolate, as the methylation was carried out twice to achieve the final product.

### 3.6. Mechanistic investigation

#### 3.6.1. Conversion/time profile

To explore the reaction pathway, a conversion/time profile was mapped out. Compound **8a** was chosen as a model substrate for this study by performing the individual experiments at different time intervals (Figure 3.2). At the initial reaction phase, the reaction was slow which can be explained due to the slow formation of the Mn(I) active species in the beginning. After ca. 30 min, the reaction accelerates and shows 70% conversion with 41% yield to the mono-methylated product. However, after 2 h the reaction slows down but reaches a conversion of up to 97% with a yield of 92% to the product **9a** in 24 h.

The conversion/time profile appears analogous to the case of the ruthenium-catalyzed  $\beta$ -methylation work (for comparison see 2.7.1). The slow conversion after 2 h can be explained because of the high availability of hydrogen in the reaction mixture due to the excess amount of

methanol being dehydrogenated. At the initial phase of the reaction, complex **Mn-2** catalyzes the de-hydrogenation of **8a** and methanol to the corresponding phenylacetaldehyde **8a'** and formaldehyde, respectively with the liberation of hydrogen. As time passes, the excess hydrogen produced from methanol helps to hydrogenate the aldol coupled product but also reverses the equilibrium from phenylacetaldehyde **8a'** to **8a** which decreases the overall reaction rate. The intermediates formed from the aldol-condensation such as alkene-type aldol intermediates were observed in the  $^1\text{H-NMR}$  spectra while performing the time-conversion profile.

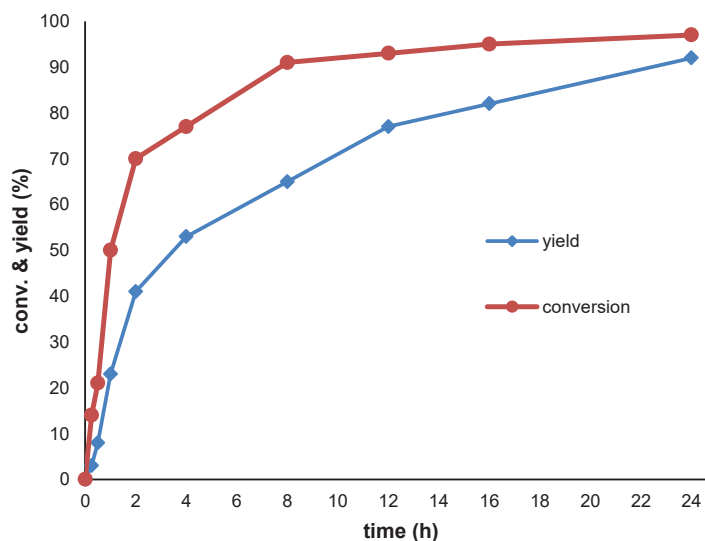
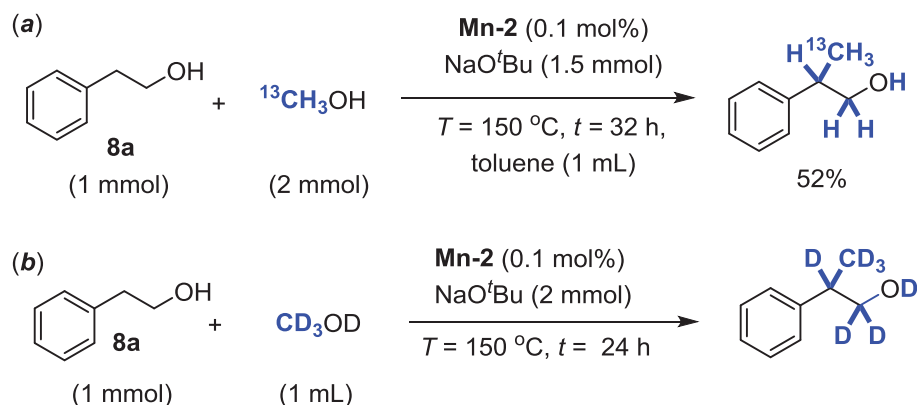


**Figure 3.2:** Reaction progress based on  $^1\text{H NMR}$ . **8a** (1 mmol), MeOH (1 mL as a reagent and solvent), Mn precatalyst **Mn-2** (0.5 mol%), and NaOMe (2 mmol),  $150\text{ }^\circ\text{C}$ .

### 3.6.2. Labeling experiments

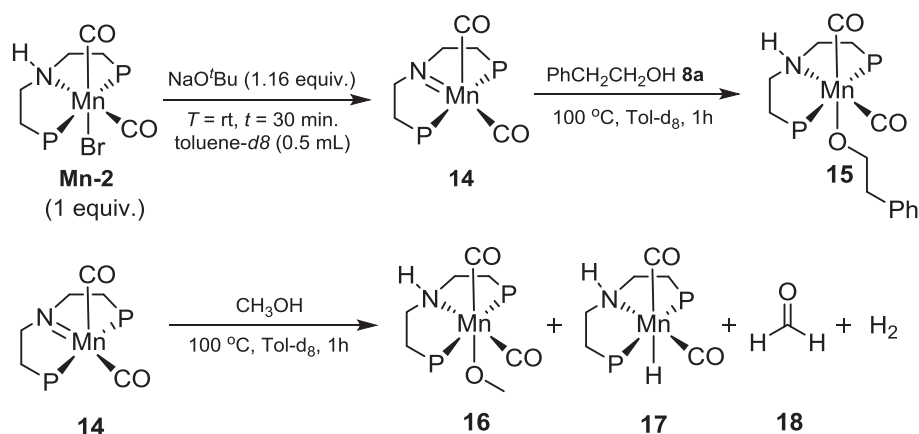
Next, to verify the individual reaction steps and their interconnection, labeling experiments were performed (Scheme 3.5). The reaction of **8a** with  $^{13}\text{C}$ -labeled methanol in toluene showed the corresponding  $^{13}\text{C}$ -labeled methylated product with a yield of 52%. The  $^{13}\text{C}$ -labeled characteristic peak of the methyl group showed a doublet of doublets in the  $^1\text{H NMR}$  spectrum at  $\delta = 1.46\text{ ppm}$  (dd,  $J_1 = 129\text{ Hz}$ ,  $J_2 = 9\text{ Hz}$ ). Similarly, applying the same standard reaction conditions, the reaction of **8a** with  $\text{CD}_3\text{OD}$  revealed the methylated product with a high degree of incorporation of deuterium in the newly formed methyl group as well as in the  $\alpha$ - and  $\beta$ -position of the alcohol. These data clearly indicate that the reaction proceeds via several de-hydrogenation and re-hydrogenation pathways as intermediate reactions.



**Scheme 3.5:** Labeling experiments with  $^{13}\text{C}$  and  $^2\text{H}$  labeled methanol.

### 3.6.3. Stoichiometric reaction of complex Mn-2 with alcohols

Furthermore, to get extended reaction insights, stoichiometric reactions were performed using complex **Mn-2** (Scheme 3.6). The reaction of complex **Mn-2** with the base in  $[\text{D}_8]$ -toluene revealed the formation of active species **14**. Upon reaction of species **14** with 1 equiv. of **8a** resulted in the formation of Mn(I) alcoholate species **15** at  $100\text{ }^\circ\text{C}$  after 1 h. The species **15** was characterized using NMR spectroscopy. Similarly, at  $100\text{ }^\circ\text{C}$ , the reaction of species **14** with methanol also confirmed the formation of Mn(I) methanolate species **16** which upon dehydrogenation revealed the formation of Mn-hydride species **17**, formaldehyde and  $\text{H}_2$  after 1 h (details are described in the experimental section).



**Scheme 3.6:** Spectroscopically identified Mn(I) intermediates obtained by stoichiometric reaction with Mn complex **Mn-2**.

### 3.7. Proposed catalytic cycle

Considering the above-discussed results and previously reported experiments, a reaction mechanism can be proposed (Figure 3.3). The first step involves the formation of Mn(I) active species **XX** by reaction of Mn(I) complex **Mn-2** with a base. This species was depicted experimentally and corresponds to the complex **14**. Next, complex **XX** reacts with the alcohol substrate, which leads to the activation of the O–H bond and forms the Mn(I) alcoholate species **XXI**. The formation of alcoholate species was confirmed spectroscopically and corresponds to the observed species **15** and **16**. Subsequently, species **XXI** passes through  $\beta$ -hydride elimination which causes the formation of the corresponding aldehydes and Mn monohydride complex **XXII**. The generation of complex **XXII** and formaldehyde was observed experimentally and corresponds to the species **17** and **18**, respectively. Next, in the presence of a base, aldol condensation takes place between *in situ* formed phenylacetaldehyde **A** (from **8a**) and formaldehyde **B** (from methanol), this generates the corresponding enone **D**. The generation of complex **XXII** and formaldehyde was observed experimentally and corresponds to the species **17** and **18**, respectively. Next, in the presence of a base, aldol condensation takes place between *in situ* formed phenylacetaldehyde **A** (from **8a**) and formaldehyde **B** (from methanol), this generates the corresponding enone **D**.

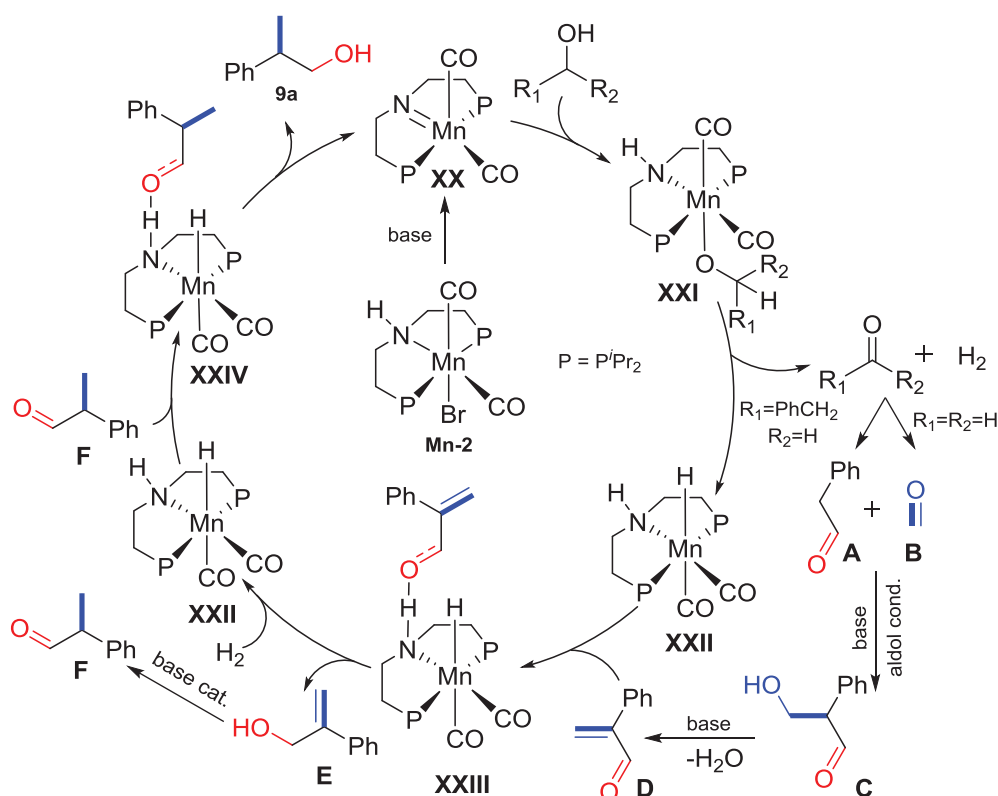


**Figure 3.3:** Postulated catalytic cycle for the selective  $\beta$ -methylation of **8a**.

Afterwards, enone **D** interacts with the N–H proton of Mn-hydride species **XXII** and yields the intermediate species **XXIII**, where the hydride transfers from Mn center to the carbon of C=O functionality and the proton transfers from N–H to the oxygen of C=O group leading to the formation of phenyl substituted allyl alcohol **E** and regenerating the active species **XX**. Furthermore, molecule **E** undergoes a base-catalyzed allyl isomerization to the corresponding aldehyde **F**. Subsequently, the *in situ* formed hydrogen reacts with the active species **XX** and regenerates the Mn monohydride complex **XXII**. Aldehyde **F** reacts with the species **XXII** and generates the final  $\beta$ -methylated product to close the catalytic cycle. Alternatively, apart from isomerization of allyl alcohol **E** to aldehyde **F**, there is also a possibility for the direct hydrogenation of the C=C bond from the *in situ* formed hydrogen. However, previously discussed DFT calculation revealed that the hydrogenation of C=C bond requires more energy in comparison to the base mediated isomerization from **E** to **F**.

### 3.8. Conclusion and outlook

In conclusion, the selective  $\beta$ -methylation of alcohols was achieved using an earth-abundant metal complex. In this catalytic process, a noble-metal ruthenium could be successfully exchanged with manganese. Biomass generated aliphatic alcohols and diols were selectively  $\beta$ -methylated using this approach and showed a pathway to prepare renewable and high-value chemicals. Industrially valuable chemical MPO was prepared from biomass generated 1,3-propanediol and green methanol. A time-conversion profile and mechanistic studies showed that the reaction is proceeding via a “hydrogen-borrowing pathway”. Based on the DFT calculations and mechanistic studies, a catalytic cycle was proposed.

At present, the reaction required a stoichiometric amount of a base in reaction. However, in theory, the reaction should be feasible with the catalytic amount of base. Further optimization and a detailed mechanistic investigation are required to find out the reaction networks and the factors that are controlling the individual reaction steps.

### 3.9. Experimental

#### 3.9.1. General experimental

All catalytic and stoichiometric reactions were performed under argon atmosphere using a combination of Schlenk and glove box techniques. Chemicals were purchased from

Sigma-Aldrich, Alfa-Aesar, TCI chemicals and used without further purification. Dry solvents were prepared according to standard procedures. Glasswares were dried under vacuum at high temperatures, evacuated, and refilled with argon at least three times.  $^1\text{H}$ ,  $^{13}\text{C}$ , and  $^{31}\text{P}$  NMR spectra were recorded with spectrometers Bruker AV300 or AV400 at room temperature. The solvent signals were used as references and the chemical shifts converted to the TMS scale ( $\text{CDCl}_3$ :  $\delta_{\text{H}} = 7.26$  ppm,  $\delta_{\text{C}} = 77.3$  ppm;  $\text{C}_6\text{D}_6$ :  $\delta_{\text{H}} = 7.16$  ppm,  $\delta_{\text{C}} = 127.6$  ppm;  $[\text{D}_8]$ -THF:  $\delta_{\text{H}} = 1.72$  ppm,  $\delta_{\text{C}} = 24.2$  ppm;  $[\text{D}_8]$ -toluene:  $\delta_{\text{H}} = 2.1$  ppm,  $\delta_{\text{C}} = 21.4$  ppm). Chemical shifts for  $^{31}\text{P}$  are reference against  $\text{H}_3\text{PO}_4$  as external standard. Multiplicity is abbreviated as: s, singlet; d, doublet; t, triplet; q, quartet; sext, sextet; m, multiplet; br, broad.

Catalytic reactions involving high pressure gases were carried out in home built stainless steel reactors equipped with pressure transducer and external electrical heating.

**Safety advice:** High-pressure experiments represent a significant risk and must be conducted with appropriate safety procedures and in conjunction with the use of suitable equipment.

### 3.9.2. Synthesis of manganese pincer complexes

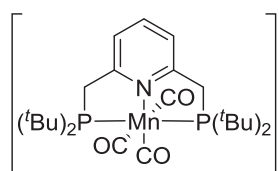
**[Mn(CO) $_2$ (Br)[HN(C $_2$ H $_4$ P $^i$ Pr $_2$ ) $_2$ ] (Mn-2).** A solution of Bis(2-(diisopropylphosphanyl)ethyl)amine (2.26 mL, 10 wt.% in THF, 0.66 mmol, 1.1 equiv.) was added to a solution of [Mn(CO) $_5$ Br] (163.7 mg, 0.60 mmol, 1.0 equiv.) in toluene (8 mL) and stirred for 24 h at 100 °C under argon atmosphere. The volatiles were removed in vacuo and the residue was washed with pentane (3 x 5 mL). Upon drying in vacuo, the residue was solidified and complex **Mn-2** was obtained as a bright yellow powder (267.4 mg, 0.54 mmol, 91%). The analytical data of complex are consistent with those previously reported in the literature.<sup>[3a]</sup>

**[Mn(Ph $_2$ PCH $_2$ ) $_2$ (C $_5$ H $_3$ N)(CO) $_3$ ]Br (Mn-21).** A solution of 2,6-Bis((diphenylphosphanyl)methyl)-pyridine (190.2 mg, 0.40 mmol, 1.1 equiv.) in toluene was added to a solution of [Mn(CO) $_5$ Br] (100.0 mg, 0.36 mmol, 1.0 equiv.) in toluene (8 mL) and stirred for 17 h at 100 °C under argon atmosphere. The volatiles were removed in vacuo and the residue was washed with pentane (3 x 5 mL) and  $\text{CHCl}_3$  (1 x 3 mL). Upon drying in vacuo, the residue was solidified and complex **Mn-21** was obtained as a bright yellow powder (163.7 mg, 0.24 mmol, 65%).  $^1\text{H}$  NMR (300 MHz,  $[\text{D}_6]$ -DMSO, 298 K)  $\delta = 8.17$  (t,  $J = 7.7$  Hz, 1H, ArCH), 7.87 (d,  $J =$



7.7 Hz, 2H, ArCH), 7.70 – 7.56 (m, 20H, ArCH), 4.87 (d,  $J = 8.9$  Hz, 4H, CH<sub>2</sub>) ppm.  
<sup>31</sup>P{<sup>1</sup>H} NMR (121.29 MHz, [D<sub>6</sub>]-DMSO)  $\delta = 69.62$  (s) ppm.

**[Mn(<sup>t</sup>Bu<sub>2</sub>PCH<sub>2</sub>)<sub>2</sub>(C<sub>5</sub>H<sub>3</sub>N)(CO)<sub>3</sub>]Br (Mn-23).** A solution of 2,6-Bis((di-tert-butylphosphaneyl)

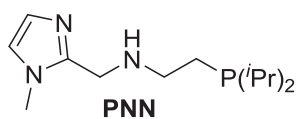


methyl) -pyridine (158.2 mg, 0.40 mmol, 1.1 equiv.) in toluene (1 mL) was added to a solution of [Mn(CO)<sub>5</sub>Br] (100.0 mg, 0.36 mmol, 1.0 equiv.) in toluene (8 mL) and stirred for 17 h at 100 °C under argon atmosphere. The volatiles were removed in vacuo and

the residue was washed with pentane (3 x 5 mL) and CHCl<sub>3</sub> (1 x 3 mL). Upon drying in vacuo, the residue was solidified and complex **Mn-23** was obtained as a bright yellow powder (123.0 mg, 0.20 mmol, 55%). The analytical data of complex are consistent with those previously reported in the literature.<sup>[10]</sup>

**[Mn(CO)<sub>3</sub>(2-(diisopropylphosphanyl)-N-[(1-methyl-1H-imidazol-2-yl)methyl]ethan-1-amine)Br (Mn-16).**

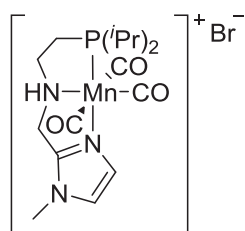
**Preparation of PNN ligand:** A solution of 2-(diisopropylphosphaneyl)ethan-1-amine (2.29 mL,



10 wt.% in THF, 1.24 mmol, 1.0 equiv.) in methanol (3.0 mL) was added drop wise to a solution of 1-methyl-1H-imidazole-2-carbaldehyde (136.6 mg, 1.24 mmol, 1.0 equiv.) in methanol (5.0 mL).

The resulting solution was stirred for 6 h at room temperature. The reaction mixture was cooled to 0 °C and NaBH<sub>4</sub> (70.4 mg, 1.86 mmol, 1.5 equiv.) was added in one portion. The solution was stirred for 12 h and concentrated under reduced pressure. The residue was dissolved in water (5 mL) and the resulting solution was extracted with DCM (3 x 5 mL). The combined organic phases were dried over Na<sub>2</sub>SO<sub>4</sub> and filtered through a short pad of basic alumina. The solvent was removed under reduced pressure to give 2-(diisopropylphosphaneyl)-N-((1-methyl-1H-imidazol-2-yl)methyl)ethan-1-amine (262.1 mg, 1.03 mmol, 83%) as a transparent oil. The analytical data of ligand is consistent with those previously reported in the literature.<sup>[11]</sup>

**Preparation of complex Mn-16:** A solution of PNN ligand (100.0 mg, 0.39 mmol, 1.1 equiv.) in ethanol (1 mL) was added to [MnBr(CO)<sub>5</sub>] (97.9 mg, 0.36 mmol, 1.0 equiv.) dissolved in ethanol (8 mL) and stirred for 24 h at 65 °C. The volatiles were removed in vacuo and the residue was washed with toluene (2 x 3 mL). Upon drying in vacuo, the residue was solidified and complex



**Mn-16** was obtained as a bright yellow powder (123.2 mg, 0.26 mmol, 73%). The analytical data of complex are consistent with those previously reported in the literature.<sup>[11]</sup>

**[Mn(Ph<sub>2</sub>PCH<sub>2</sub>SiMe<sub>2</sub>)<sub>2</sub>NH(CO)<sub>2</sub>Br] (Mn-24)**: Manganese pincer complex **24** was prepared according to the reported literature: A. Kaithal, S. Sen, C. Erken, T. Weyhermüller, M. Hölscher, C. Werlé, W. Leitner. Manganese-catalyzed hydroboration of carbon dioxide and other challenging carbonyl groups. *Nat. Commun.*, DOI: 10.1038/s41467-018-06831-9.<sup>[5a]</sup>

### 3.9.3. General procedure for screening of Mn-catalysts

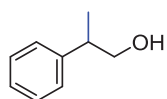
Mn-precursor and NaOMe (108.04 mg, 2 mmol) were weighed into a glass inlet equipped with a stirring bar inside a glovebox. The glass inlet was closed with a septum and transferred into the bottom part of the 10 mL stainless steel autoclave, where it was opened under a stream of argon. After sealing, the autoclave was purged with argon three times. 2-phenyl ethanol **8a** (122.2 mg, 1 mmol) and methanol (1 mL) were added at room temperature through a valve under argon. The autoclave was sealed and heated to at certain temperature. After 24 h, the autoclave was cooled to room temperature and slowly vented while stirring continued. Mesitylene was added as an internal standard to the reaction mixture that was then passed through a short path of acidic alumina before the composition was analyzed by NMR spectroscopy.

### 3.9.4. General procedure for the catalytic selective $\beta$ -methylation of 2-aryl ethanols

Mn-MACHO-<sup>*i*</sup>Pr **Mn-2** (2.48 mg, 0.5 mol%) and NaOMe (108.04 mg, 2 mmol) were weighed into a glass inlet equipped with a stirring bar inside a glovebox. The glass inlet was closed with a septum and transferred into the bottom part of the 10 mL stainless steel autoclave, where it was opened under a stream of argon. After sealing, the autoclave was purged with argon three times. 2-aryl ethanol **8** (1 mmol) and methanol (1 mL) were added at room temperature through a valve under argon. The autoclave was sealed and heated to 150 °C temperature for 24 h. After completion of the reaction, the autoclave was cooled to room temperature and slowly vented while stirring continued. Mesitylene was added as an internal standard to the reaction mixture

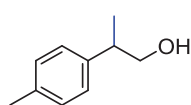
that was then passed through a short path of acidic alumina before the composition was analyzed by NMR spectroscopy. The isolation of pure product was carried out using column chromatography over silica gel (100-200 mesh) using ethyl acetate/petroleum ether (12 : 88) mixture as eluent.

**2-phenylpropan-1-ol (9a):** Prepared by following the general experimental procedure with:



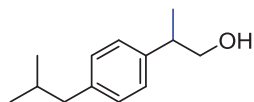
**Mn-2** (2.48 mg, 0.5 mol%), 2-phenylethan-1-ol **8a** (122.2 mg, 1 mmol), NaOMe (108.04 mg, 2 mmol), MeOH (1 mL). Yield was determined by  $^1\text{H NMR}$  spectrum using mesitylene (120 mg, 1 mmol) as an internal standard ( $\delta_{\text{Mesitylene(standard)}} = 6.84$  (s, 3H),  $\delta_{\text{product}} = 3.74$  (d, 2H)).  $^1\text{H NMR}$  (400 MHz,  $\text{CDCl}_3$ , 298 K)  $\delta = 7.27$ -7.38 (m, 5H, ArCH), 3.74 (d, 2H,  $J = 8$  Hz,  $\text{CH}_2$ ), 2.96-3.01 (m, 1H, CH), 1.30 (d, 3H,  $J = 8$  Hz,  $\text{CH}_3$ ).  $^{13}\text{C}\{^1\text{H}\}$ -NMR (101 MHz,  $\text{CDCl}_3$ , 298 K)  $\delta = 143.77$  (quat-C), 128.77 (ArCH), 127.61 (ArCH), 126.81 (ArCH), 68.85 ( $\text{CH}_2$ ), 42.57 (CH), 17.71 ( $\text{CH}_3$ ). Yield of the product after isolation: 85%. The obtained analytical data is consistent with those previously reported in the literature.<sup>[12]</sup>

**2-(*p*-tolyl)propan-1-ol (9b):** Prepared by following the general experimental procedure with:



**Mn-2** (2.48 mg, 0.5 mol%), 2-(*p*-tolyl)ethan-1-ol **8b** (136.2 mg, 1 mmol), NaOMe (108.04 mg, 2 mmol), MeOH (1 mL). Yield was determined by  $^1\text{H NMR}$  spectrum using mesitylene (120 mg, 1 mmol) as an internal standard ( $\delta_{\text{Mesitylene(standard)}} = 6.82$  (s, 3H),  $\delta_{\text{product}} = 3.69$  (d, 2H)).  $^1\text{H NMR}$  (300 MHz,  $\text{CDCl}_3$ , 298 K)  $\delta = 7.15$  (s, 4H, ArCH), 3.69 (d, 2H,  $J = 9$  Hz,  $\text{CH}_2$ ), 2.90-2.97 (m, 1H, CH), 2.35 (s, 3H,  $\text{CH}_3$ ), 1.27 (d, 3H,  $J = 9$  Hz,  $\text{CH}_3$ ) ppm. The obtained analytical data is consistent with those previously reported in the literature.<sup>[12]</sup>

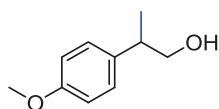
**2-(4-*iso*-butylphenyl)propan-1-ol. (9c):** Prepared by following the general experimental



procedure with: **Mn-2** (2.48 mg, 0.5 mol%), 2-(4-*iso*butylphenyl)ethan-1-ol **8c** (178.3 mg, 1 mmol), NaOMe (108.04 mg, 1 mmol), MeOH (1 mL). Yield was determined by  $^1\text{H NMR}$  spectrum using mesitylene (120 mg, 1 mmol) as an internal standard ( $\delta_{\text{Mesitylene(standard)}} = 6.73$  (s, 3H),  $\delta_{\text{product}} = 3.60$  (d, 2H)).  $^1\text{H NMR}$  (300 MHz,  $\text{CDCl}_3$ , 298 K)  $\delta = 7.01$ -7.08 (m, 4H, ArCH), 3.60 (d, 2H,  $J = 6$  Hz,  $\text{CH}_2$ ), 2.78-2.90 (m, 1H, CH), 2.37 (d, 2H,  $J = 6$  Hz,  $\text{CH}_2$ ), 1.70-1.84 (m, 1H, CH), 1.18 (d, 3H,  $J = 9$  Hz,  $\text{CH}_3$ ), 0.82 (d, 6H,  $J = 6$  Hz,  $\text{CH}_3$ ) ppm.  $^{13}\text{C}\{^1\text{H}\}$ -NMR (101 MHz,  $\text{CDCl}_3$ , 298 K)  $\delta = 140.83$  (quat-C), 140.20 (quat-C), 129.51 (ArCH), 127.29 (ArCH), 68.93 ( $\text{CH}_2$ ), 45.17 ( $\text{CH}_2$ ),

42.17 (CH), 30.35 (CH), 22.55 (CH<sub>3</sub>), 17.75 (CH<sub>3</sub>). Yield of the product after isolation: 83%. The obtained analytical data is consistent with those previously reported in the literature.<sup>[13]</sup>

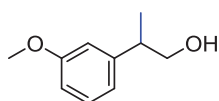
**2-(4-methoxyphenyl)propan-1-ol (9d):** Prepared by following the general experimental



procedure with: **Mn-2** (2.48 mg, 0.1 mol%), 2-(4-methoxyphenyl)ethan-1-ol **8d** (152.2 mg, 1 mmol), NaOMe (108.04 mg, 2 mmol), MeOH (1 mL). Yield was determined by <sup>1</sup>H NMR spectrum using mesitylene (120 mg, 1 mmol) as

an internal standard ( $\delta_{\text{Mesitylene(standard)}} = 2.31$  (s, 9H),  $\delta_{\text{product}} = 1.27$  (d, 3H)). <sup>1</sup>H NMR (300 MHz, CDCl<sub>3</sub>, 298 K)  $\delta = 7.18$  (d, 2H,  $J = 9$  Hz, ArCH), 6.90 (d, 2H,  $J = 9$  Hz, ArCH), 3.82 (s, 3H, CH<sub>3</sub>), 3.68 (d, 2H,  $J = 6$  Hz, CH<sub>2</sub>), 2.89-2.95 (m, 1H, CH), 1.28 (d, 3H,  $J = 9$  Hz, CH<sub>3</sub>) ppm. <sup>13</sup>C{<sup>1</sup>H}-NMR (101 MHz, CDCl<sub>3</sub>, 298 K)  $\delta = 158.48$  (quat-C), 135.70 (quat-C), 128.52 (ArCH), 114.19 (ArCH), 68.95 (CH<sub>2</sub>), 55.41 (OCH<sub>3</sub>), 41.71 (CH), 17.87 (CH<sub>3</sub>). Yield of the product after isolation: 82%. The obtained analytical data is consistent with those previously reported in the literature.<sup>[12]</sup>

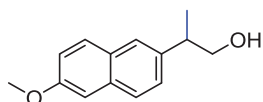
**2-(3-methoxyphenyl)propan-1-ol (9e):** Prepared by following the general experimental



procedure with: **Mn-2** (2.48 mg, 0.5 mol%), 2-(3-methoxyphenyl)ethan-1-ol **8e** (152.2 mg, 1 mmol), NaOMe (108.04 mg, 2 mmol), MeOH (1 mL). Yield

was determined by <sup>1</sup>H NMR spectrum using mesitylene (120 mg, 1 mmol) as an internal standard ( $\delta_{\text{Mesitylene(standard)}} = 2.30$  (s, 9H),  $\delta_{\text{product}} = 1.29$  (d, 3H)). <sup>1</sup>H NMR (300 MHz, CDCl<sub>3</sub>, 298 K)  $\delta = 7.24$ -7.30 (m, 1H, ArCH), 6.78-6.87 (m, 3H, ArCH), 3.82 (s, 3H, CH<sub>3</sub>), 3.71 (d, 2H,  $J = 6$  Hz, CH<sub>2</sub>), 2.86-2.95 (m, 1H, CH), 1.28 (d, 3H,  $J = 9$  Hz, CH<sub>3</sub>) ppm. The obtained analytical data is consistent with those previously reported in the literature.<sup>[13]</sup>

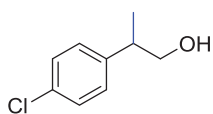
**2-(6-methoxynaphthalen-2-yl)propan-1-ol (9f):** Prepared by following the general



experimental procedure with: **Mn-2** (2.48 mg, 0.5 mol%), 2-(6-methoxynaphthalen-2-yl)ethan-1-ol **8f** (202.3 mg, 1 mmol), NaOMe (108.04 mg, 1 mmol), MeOH (1 mL). Yield was determined by <sup>1</sup>H NMR

spectrum using mesitylene (120 mg, 1 mmol) as an internal standard ( $\delta_{\text{Mesitylene(standard)}} = 6.72$  (s, 3H),  $\delta_{\text{product}} = 1.26$  (d, 3H)). <sup>1</sup>H NMR (300 MHz, CDCl<sub>3</sub>, 298 K)  $\delta = 7.60$ -7.64 (m, 2H, ArCH), 7.52 (s, 1H, ArCH), 7.24-7.26 (m, 1H, ArCH), 7.02-7.07 (m, 2H, ArCH), 3.68 (d, 2H,  $J = 6$  Hz, CH<sub>2</sub>), 2.96-3.03 (m, 1H, CH), 1.26 (d, 3H,  $J = 6$  Hz, CH<sub>3</sub>). The obtained analytical data is consistent with those previously reported in the literature.<sup>[14]</sup>

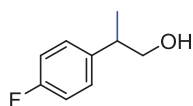
**2-(4-chlorophenyl)propan-1-ol (9g):** Prepared by following the general experimental procedure



with: **Mn-2** (2.48 mg, 0.5 mol%), 2-(4-chlorophenyl)ethan-1-ol **8g** (156.6 mg, 1 mmol), NaOMe (108.04 mg, 2 mmol), MeOH (1 mL). Reaction time: 14 h. Yield was determined by  $^1\text{H}$  NMR spectrum using mesitylene

(120 mg, 1 mmol) as an internal standard ( $\delta_{\text{Mesitylene(standard)}} = 6.83$  (s, 3H),  $\delta_{\text{product}} = 3.68$  (dd, 2H)).  $^1\text{H}$  NMR (400 MHz,  $\text{CDCl}_3$ , 298 K)  $\delta = 7.30$  (d, 2H,  $J = 8.41$  Hz, ArCH), 7.17 (d, 2H,  $J = 8.40$  Hz, ArCH), 3.68 (dd, 2H,  $J = 6.79$  Hz, 2.14 Hz,  $\text{CH}_2$ ), 2.93 (sext, 1H,  $J = 6.95$  Hz, CH), 1.55 (br. s, 1H, OH), 1.25 (d, 3H,  $J = 6.99$  Hz,  $\text{CH}_3$ ).  $^{13}\text{C}\{^1\text{H}\}$ -NMR (101 MHz,  $\text{CDCl}_3$ , 298 K)  $\delta = 142.35$  (quat-C), 132.44 (quat-C), 128.96 (ArCH), 128.86 (ArCH), 68.61 ( $\text{CH}_2$ ), 41.98 (CH), 17.67 ( $\text{CH}_3$ ). Yield of the product after isolation: 76%. The obtained analytical data is consistent with those previously reported in the literature.<sup>[15]</sup>

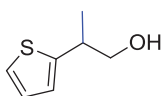
**2-(4-fluorophenyl)propan-1-ol (9h):** Prepared by following the general experimental procedure



with: **Mn-2** (0.59 mg, 0.5 mol%), 2-(4-fluorophenyl)ethan-1-ol **8h** (140.2 mg, 1 mmol), NaOMe (108.04 mg, 2 mmol), MeOH (1 mL). Yield was determined by  $^1\text{H}$  NMR spectrum using mesitylene (124 mg, 1.03 mmol) as an internal

standard ( $\delta_{\text{Mesitylene(standard)}} = 6.83$  (s, 3H),  $\delta_{\text{product}} = 3.68$  (d, 2H)).  $^1\text{H}$  NMR (300 MHz,  $\text{CDCl}_3$ , 298 K)  $\delta = 7.19$ -7.26 (m, 2H, ArCH), 6.83-7.06 (m, 2H, ArCH), 3.68 (d, 2H,  $J = 9$  Hz,  $\text{CH}_2$ ), 2.91-2.98 (m, 1H, CH), 1.28 (d, 3H,  $J = 6$  Hz,  $\text{CH}_3$ ) ppm. The obtained analytical data is consistent with those previously reported in the literature.<sup>[16]</sup>

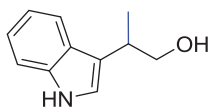
**2-(thiophen-2-yl)propan-1-ol (9i):** Prepared by following the general experimental procedure



with: **Mn-2** (2.48 mg, 0.5 mol%), 2-(thiophen-2-yl)ethan-1-ol **8i** (128.2 mg, 1 mmol), NaOMe (108.04 mg, 2 mmol), MeOH (1 mL). Yield was determined by

$^1\text{H}$  NMR spectrum using mesitylene (122 mg, 1.02 mmol) as an internal standard ( $\delta_{\text{Mesitylene(standard)}} = 6.82$  (s, 3H),  $\delta_{\text{product}} = 1.37$  (d, 3H)).  $^1\text{H}$  NMR (300 MHz,  $\text{CDCl}_3$ , 298 K)  $\delta = 7.20$  (dd, 1H,  $J = 5.02, 1.20$ , ArCH), 6.97-6.99 (m, 1H, ArCH), 6.90-6.91 (m, 1H, ArCH), 3.70 (dd, 2H,  $J = 6.39, 2.46$ ,  $\text{CH}_2$ ), 3.21-3.28 (m, 1H, CH), 1.37 (d, 3H,  $J = 6.96$  Hz,  $\text{CH}_3$ ), 1.36.<sup>[17]</sup>

**2-(1H-indol-3-yl)propan-1-ol (9j):** Prepared by following the general experimental procedure



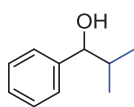
with: **Mn-2** (2.48 mg, 0.5 mol%), 2-(1H-indol-3-yl)ethan-1-ol **8j** (161.2 mg, 1 mmol), NaOMe (108.04 mg, 2 mmol), MeOH (1 mL). Yield was determined

by  $^1\text{H}$  NMR spectrum using mesitylene (120 mg, 1 mmol) as an internal standard ( $\delta_{\text{Mesitylene(standard)}} = 6.83$  (s, 3H),  $\delta_{\text{product}} = 3.32$  (sext, 1H)).  $^1\text{H}$  NMR (300 MHz,  $\text{CDCl}_3$ , 298 K)  $\delta = 8.06$  (br. s, 1H, NH), 7.67 (dt, 1H,  $J = 7.82$ , 0.95 Hz, ArCH), 7.38 (dt, 1H,  $J = 8.13$ , 0.99 Hz, ArCH), 7.21 (ddd, 1H,  $J = 8.15$ , 6.99, 1.28 Hz, ArCH), 7.13 (ddd, 1H,  $J = 7.99$ , 7.01, 1.11 Hz, ArCH), 7.06 (br s, 1H, ArCH), 3.77-3.88 (m, 2H,  $\text{CH}_2$ ), 3.32 (sext, 1H,  $J = 6.78$  Hz, CH), 1.52 (br. s, 1H, OH), 1.41 (d, 3H,  $J = 7.06$  Hz,  $\text{CH}_3$ ).  $^{13}\text{C}\{^1\text{H}\}$ -NMR (75 MHz,  $\text{CDCl}_3$ , 298 K)  $\delta = 136.71$  (quat-C), 126.88 (quat-C), 122.37 (ArCH), 121.37 (quat-C), 119.56 (ArCH), 119.39 (ArCH), 118.15 (ArCH), 111.42 (ArCH), 68.05 ( $\text{CH}_2$ ), 34.07 (CH), 17.42 ( $\text{CH}_3$ ). Yield of the product after isolation: 47%. The obtained analytical data is consistent with those previously reported in the literature.<sup>[17]</sup>

### 3.9.5. General procedure for the catalytic selective $\beta$ -methylation of secondary alcohols

Mn-MACHO **Mn-2** (2.48 mg, 0.5 mol%) and NaOMe (216.08 mg, 4 mmol) were weighed into a glass inlet equipped with a stirring bar inside a glovebox. The glass inlet was closed with a septum and transferred into the bottom part of the 10 mL stainless steel autoclave, where it was opened under a stream of argon. After sealing, the autoclave was purged with argon three times. Secondary alcohol **10** (1 mmol) and methanol (1 mL) were added at room temperature through a valve under argon. The autoclave was sealed and heated to 150 °C temperature. After 36 h, the autoclave was cooled to room temperature and slowly vented while stirring continued. Mesitylene was added as an internal standard to the reaction mixture that was then passed through a short path of acidic alumina before the composition was analyzed by NMR spectroscopy.

**2-methyl-1-phenylpropan-1-ol (11a)**: Prepared by following the general experimental procedure with: **Mn-2** (2.48 mg, 0.5 mol%), 1-phenylethan-1-ol **10a** (122.2 mg,



1 mmol), NaOMe (216.08 mg, 4 mmol), MeOH (1 mL). Yield was determined by  $^1\text{H}$  NMR spectrum using mesitylene (120 mg, 1 mmol) as an internal standard ( $\delta_{\text{Mesitylene(standard)}} = 6.84$  (s, 3H),  $\delta_{\text{product}} = 1.03$  (d, 3H)).  $^1\text{H}$  NMR (400 MHz,  $\text{CDCl}_3$ , 298 K)  $\delta = 7.28$ -7.39 (m, 5H, ArCH), 4.38 (d, 1H,  $J = 6$  Hz, CH), 1.94-2.03 (m, 1H, CH), 1.03 (d, 3H,  $J = 6$  Hz,  $\text{CH}_3$ ), 0.83 (d, 3H,  $J = 6$  Hz,  $\text{CH}_3$ ) ppm.  $^{13}\text{C}\{^1\text{H}\}$ -NMR (101 MHz,  $\text{CDCl}_3$ , 298 K)  $\delta =$



143.76 (quat-C), 128.31 (ArCH), 127.53 (ArCH), 126.69 (ArCH), 80.17 (CH), 35.38 (CH), 19.12 (CH<sub>3</sub>), 18.37 (CH<sub>3</sub>). Yield of the product after isolation: 71%. The obtained analytical data is consistent with those previously reported in the literature.<sup>[12]</sup>

**2-methyl-1-(naphthalen-2-yl)propan-1-ol (11b):** Prepared by following the general experimental procedure with: **Mn-2** (2.48 mg, 0.5 mol%), 1-(naphthalen-2-yl)ethan-1-ol **10b** (172.2 mg, 1 mmol), NaOMe (216.08 mg, 4 mmol), MeOH (1 mL). Yield was determined by <sup>1</sup>H NMR spectrum using mesitylene (120 mg, 1 mmol) as an internal standard ( $\delta_{\text{Mesitylene(standard)}} = 6.84$  (s, 3H),  $\delta_{\text{product}} = 4.54$  (d, 1H)).

<sup>1</sup>H NMR (400 MHz, CDCl<sub>3</sub>, 298 K)  $\delta = 7.81\text{--}7.85$  (m, 3H, ArCH), 7.75-7.76 (m, 1H, ArCH), 7.45-7.50 (m, 3H, ArCH), 4.54 (d, 1H,  $J = 6.84$  Hz, CH), 2.02-2.16 (m, 1H, CH), 1.90 (br. s, 1H, OH), 1.05 (d, 3H,  $J = 6.69$  Hz, CH<sub>3</sub>), 0.84 (d, 3H,  $J = 6.80$  Hz, CH<sub>3</sub>) ppm. <sup>13</sup>C{<sup>1</sup>H}-NMR (101 MHz, CDCl<sub>3</sub>, 298 K)  $\delta = 141.24$  (ArCH), 133.29 (quat-C), 133.08 (ArCH), 128.09 (ArCH), 128.06 (ArCH), 127.79 (ArCH), 126.19 (ArCH), 125.87 (ArCH), 125.54 (ArCH), 124.76 (quat-C), 80.30 (CH), 35.34 (CH), 19.29 (CH<sub>3</sub>), 18.38 (CH<sub>3</sub>). Yield of the product after isolation: 74%. The obtained analytical data is consistent with those previously reported in the literature.<sup>[2]</sup>

**2-methyl-1-(*p*-tolyl)propan-1-ol (11c):** Prepared by following the general experimental procedure with: **Mn-2** (2.48 mg, 0.5 mol%), 1-(*p*-tolyl)ethan-1-ol **10c** (136.1 mg, 1 mmol), NaOMe (216.08 mg, 4 mmol), MeOH (1 mL). Yield was determined by <sup>1</sup>H NMR spectrum using mesitylene (125 mg, 1.04 mmol) as an internal standard

( $\delta_{\text{Mesitylene(standard)}} = 6.86$  (s, 3H),  $\delta_{\text{product}} = 1.05$  (d, 3H)). <sup>1</sup>H NMR (400 MHz, CDCl<sub>3</sub>, 298 K)  $\delta = 7.20\text{--}7.26$  (m, 4H, ArCH), 4.34 (d, 1H,  $J = 6$  Hz, CH), 2.39 (s, 3H, CH<sub>3</sub>), 1.96-2.01 (m, 1H, CH), 1.05 (d, 3H,  $J = 6$  Hz, CH<sub>3</sub>), 0.83 (d, 3H,  $J = 6$  Hz, CH<sub>3</sub>) ppm. <sup>13</sup>C{<sup>1</sup>H}-NMR (75 MHz, CDCl<sub>3</sub>, 298 K)  $\delta = 140.82$  (quat-C), 137.17 (quat-C), 129.01 (ArCH), 126.63 (ArCH), 80.10 (CH), 35.35 (CH), 21.26 (CH<sub>3</sub>), 19.15 (CH<sub>3</sub>), 18.51 (CH<sub>3</sub>). Yield of the product after isolation: 73%. The obtained analytical data is consistent with those previously reported in the literature.<sup>[12]</sup>

**2-methyl-1-(*o*-tolyl)propan-1-ol (11d):** Prepared by following the general experimental procedure with: **Mn-2** (2.48 mg, 0.5 mol%), 1-(*o*-tolyl)ethan-1-ol **10d** (136.1 mg, 1 mmol), NaOMe (216.08 mg, 4 mmol), MeOH (1 mL). Yield was determined by <sup>1</sup>H NMR spectrum using mesitylene (120 mg, 1 mmol) as an internal standard

( $\delta_{\text{Mesitylene(standard)}} = 6.82$  (s, 3H),  $\delta_{\text{product}} = 1.05$  (d, 3H)). <sup>1</sup>H NMR (300 MHz, CDCl<sub>3</sub>, 298 K)  $\delta =$

7.53–7.12 (m, 4H, ArCH), 4.63 (d,  $J = 6$  Hz, 1H, CH), 2.35 (s, 3H, CH<sub>3</sub>), 2.04–1.93 (m, 1H, CH), 1.05 (d, 3H,  $J = 6$  Hz, CH<sub>3</sub>), 0.87 (d, 3H,  $J = 6$  Hz, CH<sub>3</sub>) ppm. The obtained analytical data is consistent with those previously reported in the literature.<sup>[18]</sup>

**1-(4-methoxyphenyl)-2-methylpropan-1-ol (11e):** Prepared by following the general experimental procedure with: **Mn-2** (2.48 mg, 0.5 mol%), 1-(4-methoxyphenyl)ethan-1-ol **10e** (152.2 mg, 1 mmol), NaOMe (216.08 mg, 4 mmol), MeOH (1 mL). Yield was determined by <sup>1</sup>H NMR spectrum using mesitylene (120 mg, 1 mmol) as an internal standard ( $\delta_{\text{Mesitylene(standard)}} = 6.81$  (s, 3H),  $\delta_{\text{product}} = 4.30$  (d, 1H)). <sup>1</sup>H NMR (400 MHz, CDCl<sub>3</sub>, 298 K)  $\delta = 7.23$  (d, 2H,  $J = 8.62$  Hz, ArCH), 6.87 (d, 2H,  $J = 8.66$  Hz, ArCH), 4.30 (d, 1H,  $J = 7.13$  Hz, CH), 3.81 (s, 3H, OCH<sub>3</sub>), 1.89–1.97 (m, 1H, CH), 1.79 (br. s, 1H, OH), 1.01 (d, 3H,  $J = 6.64$  Hz, CH<sub>3</sub>), 0.77 (d, 3H, 6.79 Hz, CH<sub>3</sub>). <sup>13</sup>C{<sup>1</sup>H}-NMR (101 MHz, CDCl<sub>3</sub>, 298 K)  $\delta = 159.06$  (quat-C), 135.98 (quat-C), 127.84 (ArCH), 113.70 (ArCH), 79.90 (CH), 55.40 (OCH<sub>3</sub>), 35.42 (CH), 19.10 (CH<sub>3</sub>), 18.65 (CH<sub>3</sub>). Yield of the product after isolation: 51%. The obtained analytical data is consistent with those previously reported in the literature.<sup>[19]</sup>

**1-(4-fluorophenyl)-2-methylpropan-1-ol (11f):** Prepared by following the general experimental procedure with: **Mn-2** (2.48 mg, 0.5 mol%), 1-(4-fluorophenyl)ethan-1-ol **10f** (140.2 mg, 1 mmol), NaOMe (216.1 mg, 4 mmol), MeOH (1 mL). Reaction time: 42 h. Yield was determined by <sup>1</sup>H NMR spectrum using mesitylene (117 mg, 0.97 mmol) as an internal standard ( $\delta_{\text{Mesitylene(standard)}} = 6.82$  (s, 3H),  $\delta_{\text{product}} = 4.31$  (d, 1H)). <sup>1</sup>H NMR (400 MHz, CDCl<sub>3</sub>, 298 K)  $\delta = 7.24$  (d, 2H,  $J = 8.64$  Hz, ArCH), 6.88 (d, 2H,  $J = 8.60$  Hz, ArCH), 4.29 (d, 1H,  $J = 7.15$  Hz, CH), 1.86–1.99 (m, 1H, CH), 1.02 (d, 3H,  $J = 6.61$  Hz, CH<sub>3</sub>), 0.78 (d, 3H,  $J = 6.76$  Hz, CH<sub>3</sub>). The obtained analytical data is consistent with those previously reported in the literature.<sup>[20]</sup>

**1-(furan-2-yl)-2-methylpropan-1-ol (11g):** Prepared by following the general experimental procedure with: **Mn-2** (2.48 mg, 0.5 mol%), 1-(furan-2-yl)ethan-1-ol **10g** (112.10 mg, 1 mmol), NaOMe (216.08 mg, 4 mmol), MeOH (1 mL). Yield was determined by <sup>1</sup>H NMR spectrum using mesitylene (116 mg, 0.96 mmol) as an internal standard ( $\delta_{\text{Mesitylene(standard)}} = 6.81$  (s, 3H),  $\delta_{\text{product}} = 0.86$  (d, 3H)). <sup>1</sup>H NMR (400 MHz, CDCl<sub>3</sub>, 298 K)  $\delta = 7.37$  (br. s, 1H, ArCH), 6.33 (dd, 1H,  $J = 3.22$  Hz, 1.83 Hz, ArCH), 6.22 (d, 1H,  $J = 3.23$  Hz),



4.37 (d, 1H,  $J = 7.06$  hz, CH), 2.06-2.15 (m, 1H, CH), 1.84 (br. s, 1H, OH), 1.02 (d, 3H,  $J = 6.75$  Hz,  $CH_3$ ), 0.86 (d, 3H,  $J = 6.75$  Hz,  $CH_3$ ).  $^{13}C\{^1H\}$ -NMR (101 MHz,  $CDCl_3$ , 298 K)  $\delta = 156.28$  (quat-C), 141.82 (ArCH), 110.17 (ArCH), 106.60 (ArCH), 73.67 (CH), 33.49 (CH), 18.85 ( $CH_3$ ), 18.36 ( $CH_3$ ). Yield of the product after isolation: 55%. The obtained analytical data is consistent with those previously reported in the literature.<sup>[21]</sup>

**1-cyclohexyl-2-methylpropan-1-ol (11h):** Prepared by following the general experimental procedure with: **Mn-2** (2.48 mg, 0.5 mol%), 1-cyclohexylethan-1-ol **10h** (128.21 mg, 1 mmol), NaOMe (216.08 mg, 4 mmol), MeOH (1 mL). Yield was determined by  $^1H$  NMR (400 MHz,  $CDCl_3$ , 298 K) spectrum using mesitylene (120 mg, 1 mmol) as an internal standard ( $\delta_{Mesitylene(standard)} = 6.82$  (s, 3H),  $\delta_{product} = 3.05$  (t, 1H)). The obtained analytical data is consistent with those previously reported in the literature.<sup>[22]</sup>

**2-methyl-2,3-dihydro-1H-inden-1-ol (11i):** Prepared by following the general experimental procedure with: **Mn-2** (2.48 mg, 0.5 mol%), 2,3-dihydro-1H-inden-1-ol **10i** (134.2 mg, 1 mmol), NaOMe (216.08 mg, 4 mmol), MeOH (1 mL). Yield was determined by  $^1H$  NMR (400 MHz,  $CDCl_3$ , 298 K) spectrum using mesitylene (120 mg, 1 mmol) as an internal standard ( $\delta_{Mesitylene(standard)} = 6.72$  (s, 3H),  $\delta_{product} = 4.63$  (d, 1H),  $\delta_{product} = 4.91$  (d, 1H)). The obtained analytical data is consistent with those previously reported in the literature.<sup>[23]</sup>

**2-methyl-1,2,3,4-tetrahydronaphthalen-1-ol (11j):** Prepared by following the general experimental procedure with: **Mn-2** (2.48 mg, 0.5 mol%), 1,2,3,4-tetrahydronaphthalen-1-ol **10j** (148.2 mg, 1 mmol), NaOMe (216.08 mg, 4 mmol), MeOH (1 mL). Yield was determined by  $^1H$  NMR (300 MHz,  $CDCl_3$ , 298 K) spectrum using mesitylene (120 mg, 1 mmol) as an internal standard ( $\delta_{Mesitylene(standard)} = 6.82$  (s, 3H),  $\delta_{product} = 4.33$  (d, 1H),  $\delta_{product} = 4.56$  (d, 1H)). The obtained analytical data is consistent with those previously reported in the literature.<sup>[24]</sup>

**6-methyl-6,7,8,9-tetrahydro-5H-benzo[7]annulen-5-ol (11k):** Prepared by following the general experimental procedure with: **Mn-2** (1.24 mg, 0.5 mol%), 6,7,8,9-tetrahydro-5H-benzo[7]annulen-5-ol **10k** (81.1 mg, 0.5 mmol), NaOMe (108.04 mg, 2 mmol), MeOH (0.5 mL). Yield was determined by  $^1H$  NMR

(300 MHz, CDCl<sub>3</sub>, 298 K) spectrum using mesitylene (120 mg, 1 mmol) as an internal standard ( $\delta_{\text{Mesitylene(standard)}} = 6.82$  (s, 3H),  $\delta_{\text{product}} = 4.60$  (d, 1H),  $\delta_{\text{product}} = 4.95$  (d, 1H)). The obtained analytical data is consistent with those previously reported in the literature.<sup>[2, 23b]</sup>

### 3.9.6. General procedure for catalytic selective $\beta$ -methylation of aliphatic alcohols

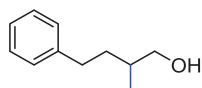
Mn-MACHO **Mn-2** (2.48 mg, 0.5 mol%) and NaOMe (108.04 mg, 2 mmol) were weighed into a glass inlet equipped with a stirring bar inside a glovebox. The glass inlet was closed with a septum and transferred into the bottom part of the 10 mL stainless steel autoclave, where it was opened under a stream of argon. After sealing, the autoclave was purged with argon three times. Aliphatic alcohol **12** (1 mmol) and methanol (1 mL) were added at room temperature through a valve under argon. The autoclave was sealed and heated to 150 °C temperature. After the desired reaction time, the autoclave was cooled to room temperature and slowly vented while stirring continued. Mesitylene was added as an internal standard to the reaction mixture that was then passed through a short path of acidic alumina before the composition was analyzed by NMR spectroscopy.

**2-methyl-3-phenylpropan-1-ol (13a):** Prepared by following the general experimental procedure with: **Mn-2** (2.48 mg, 0.5 mol%), 3-phenylpropan-1-ol **12a** (136.2 mg, 1 mmol), NaOMe (108.04 mg, 2 mmol), MeOH (1 mL), reaction time: 24 h. Yield was determined by <sup>1</sup>H NMR spectrum using mesitylene (120 mg, 1 mmol) as an internal standard ( $\delta_{\text{Mesitylene(standard)}} = 6.82$  (s, 3H),  $\delta_{\text{product}} = 0.93$  (d, 3H)). <sup>1</sup>H NMR (300 MHz, CDCl<sub>3</sub>, 298 K)  $\delta = 7.18$ -7.33 (m, 5H, ArCH), 3.46-3.58 (m, 2H, CH<sub>2</sub>), 2.40-2.80 (dq, 2H,  $J = 93$  Hz, 6 Hz, CH<sub>2</sub>), 1.91-2.02 (m, 1H, CH), 0.93 (d, 3H,  $J = 6$  Hz, CH<sub>3</sub>) ppm. <sup>13</sup>C{<sup>1</sup>H}-NMR (101 MHz, CDCl<sub>3</sub>, 298 K)  $\delta = 140.75$  (quat-C), 129.27 (ArCH), 128.39 (ArCH), 126.00 (ArCH), 67.79 (CH<sub>2</sub>), 39.84 (CH<sub>2</sub>), 37.92 (CH), 16.60 (CH<sub>3</sub>). Yield of the product after isolation: 66%. The obtained analytical data is consistent with those previously reported in the literature.<sup>[25]</sup>

**3-(4-chlorophenyl)-2-methylpropan-1-ol (13b):** Prepared by following the general experimental procedure with: **Mn-2** (2.48 mg, 0.5 mol%), 3-(4-chlorophenyl)propan-1-ol **12b** (170.6 mg, 1 mmol), NaOMe (108.04 mg, 2 mmol), MeOH (1 mL), reaction time: 14 h. Yield was determined by <sup>1</sup>H NMR spectrum using

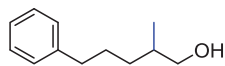
mesitylene (120 mg, 1 mmol) as an internal standard ( $\delta_{\text{Mesitylene(standard)}} = 6.72$  (s, 3H),  $\delta_{\text{product}} = 0.83$  (d, 3H)).  $^1\text{H NMR}$  (400 MHz,  $\text{CDCl}_3$ , 298 K)  $\delta = 7.12$ -7.24 (m, 3H, ArCH), 7.01-7.05 (m, 1H, ArCH), 3.38-3.46 (m, 2H,  $\text{CH}_2$ ), 2.68 (dd, 1H,  $J = 13.50$  Hz, 6.17 Hz, CH), 2.32 (dd, 1H,  $J = 13.49$  Hz, 8.13 Hz, CH), 1.83-1.87 (m, 1H, CH), 1.42 (br. s, 1H, OH), 0.83 (d, 3H,  $J = 6.74$  Hz,  $\text{CH}_3$ ).  $^{13}\text{C}\{^1\text{H}\}$ -NMR (75 MHz,  $\text{CDCl}_3$ , 298 K)  $\delta = 139.19$  (quat-C), 130.61 (ArCH), 130.27 (quat-C), 128.49 (ArCH), 67.55 ( $\text{CH}_2$ ), 39.05 ( $\text{CH}_2$ ), 37.82 (CH), 16.43 ( $\text{CH}_3$ ). Yield of the product after isolation: 60%. The obtained analytical data is consistent with those previously reported in the literature.<sup>[26]</sup>

**2-methyl-4-phenylbutan-1-ol (13c):** Prepared by following the general experimental procedure



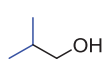
with: **Mn-2** (2.48 mg, 0.5 mol%), 4-phenylbutan-1-ol **12c** (150.2 mg, 1 mmol), NaOMe (108.04 mg, 2 mmol), MeOH (1 mL), reaction time: 24 h. Yield was determined by  $^1\text{H NMR}$  spectrum using mesitylene (120 mg, 1 mmol) as an internal standard ( $\delta_{\text{Mesitylene(standard)}} = 6.82$  (s, 3H),  $\delta_{\text{product}} = 1.0$  (d, 3H)).  $^1\text{H NMR}$  (300 MHz,  $\text{CDCl}_3$ , 298 K)  $\delta = 7.17$ -7.32 (m, 5H, ArCH), 3.54- 3.46 (m, 2H,  $\text{CH}_2$ ), 2.77-2.58 (m, 2H,  $\text{CH}_2$ ), 1.65-1.82 (m, 2H,  $\text{CH}_2$ ), 1.49-1.41 (m, 1H, CH), 1.00 (d,  $J = 6.7$  Hz, 3H,  $\text{CH}_3$ ) ppm. The obtained analytical data is consistent with those previously reported in the literature.<sup>[27]</sup>

**2-methyl-5-phenylpentan-1-ol (13d):** Prepared by following the general experimental



procedure with: **Mn-2** (2.48 mg, 0.5 mol%), 5-phenylpentan-1-ol **12d** (164.2 mg, 1 mmol), NaOMe (108.04 mg, 2 mmol), MeOH (1 mL), reaction time: 24 h. Yield was determined by  $^1\text{H NMR}$  spectrum using mesitylene (120 mg, 1 mmol) as an internal standard ( $\delta_{\text{Mesitylene(standard)}} = 6.72$  (s, 3H),  $\delta_{\text{product}} = 0.83$  (d, 3H)).  $^1\text{H NMR}$  (400 MHz,  $\text{CDCl}_3$ , 298 K)  $\delta = 6.72$ -7.21 (m, 5H, ArCH), 3.30-3.43 (m, 2H,  $\text{CH}_2$ ), 2.50-2.56 (m, 2H,  $\text{CH}_2$ ), 1.48-1.62 (m, 3H,  $\text{CH}_2$  & CH), 1.28-1.42 (m, 2H,  $\text{CH}_2$ ), 0.83 (d, 3H,  $J = 6$  Hz,  $\text{CH}_3$ ). The obtained analytical data is consistent with those previously reported in the literature.<sup>[28]</sup>

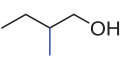
**2-methylpropan-1-ol (13e):** Prepared by following the general experimental procedure with:



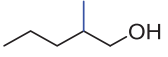
**Mn-2** (4.95 mg, 0.5 mol %), ethanol **12e** (92.1 mg, 2 mmol), NaOMe (216.08 mg, 4 mmol), MeOH (1 mL), reaction time: 36 h. Yield was determined by  $^1\text{H NMR}$  spectrum using mesitylene (120 mg, 1 mmol) as an internal standard ( $\delta_{\text{Mesitylene(standard)}} = 6.82$  (s, 3H),  $\delta_{\text{product}} = 0.94$  (d, 6H)).  $^1\text{H NMR}$  (300 MHz,  $\text{CDCl}_3$ , 298 K)  $\delta = 3.42$  (d,  $J = 6$  Hz, 2H,

$CH_2$ ), 1.85-1.71 (m, 1H,  $CH$ ), 0.94 (d,  $J = 6$  Hz, 6H,  $CH_3$ ) ppm. The obtained analytical data is consistent with those previously reported in the literature.<sup>[29]</sup>

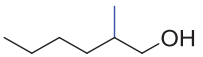
**2-methylbutan-1-ol (13f):** Prepared by following the general experimental procedure with:

 **Mn-2** (2.48 mg, 0.5 mol%), 1-butanol **12f** (74.1 mg, 1 mmol), NaOMe (108.04 mg, 2 mmol), MeOH (1 mL), reaction time: 36 h. Yield was determined by  $^1H$  NMR spectrum using mesitylene (120 mg, 1 mmol) as an internal standard ( $\delta_{\text{Mesitylene(standard)}} = 6.82$  (s, 3H),  $\delta_{\text{product}} = 3.42-3.55$  (m, 2H)).  $^1H$  NMR (300 MHz,  $CDCl_3$ , 298 K)  $\delta = 3.48$  (m, 2H,  $CH_2$ ), 1.61-1.51 (m, 1H,  $CH$ ), 1.51-1.38 (m, 1H,  $CH_2$ ), 0.98-0.92 (m, 6H,  $CH_3$ ). The obtained analytical data is consistent with those previously reported in the literature.<sup>[30]</sup>

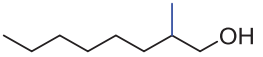
**2-methylpentan-1-ol (13g):** Prepared by following the general experimental procedure with:

 **Mn-2** (2.48 mg, 0.5 mol%), 1-pentanol **12g** (88.2 mg, 1 mmol), NaOMe (108.04 mg, 2 mmol), MeOH (1 mL), reaction time: 36 h. Yield was determined by  $^1H$  NMR spectrum using mesitylene (120 mg, 1 mmol) as an internal standard ( $\delta_{\text{Mesitylene(standard)}} = 6.82$  (s, 3H),  $\delta_{\text{product}} = 3.38-3.54$  (m, 2H)).  $^1H$  NMR (300 MHz,  $CDCl_3$ , 298 K)  $\delta = 3.38-3.54$  (dq, 2H,  $J = 33, 6$  Hz,  $CH_2$ ), 1.07-1.68 (m, 5H,  $CH$  &  $CH_2$ ) 0.90-0.97 (m, 6H,  $CH_3$ ) ppm.  $^{13}C\{^1H\}$ -NMR (75 MHz,  $CDCl_3$ , 298 K)  $\delta = 68.42$  ( $CH_2$ ), 35.58 ( $CH$ ), 35.53 ( $CH_2$ ), 20.18 ( $CH_2$ ), 16.64 ( $CH_3$ ), 14.43 ( $CH_3$ ). Yield of the product after isolation: 43%. The obtained analytical data is consistent with those previously reported in the literature.<sup>[31]</sup>

**2-methylhexan-1-ol (13h):** Prepared by following the general experimental procedure with:

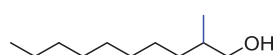
 **Mn-2** (2.48 mg, 0.5 mol%), 1-hexanol **12h** (102.2 mg, 1 mmol), NaOMe (108.04 mg, 2 mmol), MeOH (1 mL), reaction time: 24 h. Yield was determined by  $^1H$  NMR spectrum using mesitylene (120 mg, 1 mmol) as an internal standard ( $\delta_{\text{Mesitylene(standard)}} = 6.72$  (s, 3H),  $\delta_{\text{product}} = 3.29-3.44$  (dq, 2H)).  $^1H$  NMR (300 MHz,  $CDCl_3$ , 298 K)  $\delta = 3.29-3.44$  (dq, 2H,  $J = 30, 6$  Hz,  $CH_2$ ), 1.14-1.53 (m, 7H,  $CH_2$  &  $CH$ ), 0.79-0.86 (m, 6H,  $CH_3$ ). The obtained analytical data is consistent with those previously reported in the literature.<sup>[32]</sup>

**2-methyloctan-1-ol (13i):** Prepared by following the general experimental procedure with:

 **Mn-2** (2.48 mg, 0.5 mol%), 1-octanol **12i** (130.2 mg, 1 mmol), NaOMe (108.04 mg, 2 mmol), MeOH (1 mL), reaction time: 24 h. Yield was

determined by  $^1\text{H}$  NMR spectrum using mesitylene (120 mg, 1 mmol) as an internal standard ( $\delta_{\text{Mesitylene(standard)}} = 6.73$  (s, 3H),  $\delta_{\text{product}} = 3.31\text{-}3.46$  (dq, 2H)).  $^1\text{H}$  NMR (300 MHz,  $\text{CDCl}_3$ , 298 K)  $\delta = 3.31\text{-}3.46$  (dq, 2H,  $J = 30, 6$  Hz,  $\text{CH}_2$ ), 1.47-1.56 (m, 1H,  $\text{CH}$ ), 1.21-1.26 (m, 9H,  $\text{CH}_2$ ), 1-1.07 (m, 1H,  $\text{CH}$ ), 0.79-0.85 (m, 6H,  $\text{CH}_3$ ). The obtained analytical data is consistent with those previously reported in the literature.<sup>[33]</sup>

**2-Methyldecan-1-ol (13j):** Prepared by following the general experimental procedure with:

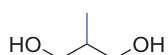


**Mn-2** (2.48 mg, 0.5 mol%), 1-decanol **12j** (158.3 mg, 1 mmol), NaOMe (108.04 mg, 2 mmol), MeOH (1 mL), reaction time: 24 h. Yield was determined by  $^1\text{H}$  NMR spectrum using mesitylene (120 mg, 1 mmol) as an internal standard ( $\delta_{\text{Mesitylene(standard)}} = 6.72$  (s, 3H),  $\delta_{\text{product}} = 3.29\text{-}3.45$  (dq, 2H)).  $^1\text{H}$  NMR (300 MHz,  $\text{CDCl}_3$ , 298 K)  $\delta = 3.29\text{-}3.45$  (dq, 2H,  $J = 30, 6$  Hz,  $\text{CH}_2$ ), 1.43-1.51 (m, 1H,  $\text{CH}$ ), 0.99-1.37 (m, 14H,  $\text{CH}_2$ ), 0.78-0.84 (m, 6H,  $\text{CH}_3$ ). The obtained analytical data is consistent with those previously reported in the literature.<sup>[34]</sup>

### 3.9.7. General procedure for the catalytic selective $\beta$ -methylation of diols

Mn-MACHO **Mn-2** (2.48 mg, 0.5 mol%) and NaOMe were weighed into a glass inlet equipped with a stirring bar inside a glovebox. The glass inlet was closed with a septum and transferred into the bottom part of the 10 mL stainless steel autoclave, where it was opened under a stream of argon. After sealing, the autoclave was purged with argon three times. Diol (**12k-12m**) (1 mmol) and methanol (1 mL) were added at room temperature through a valve under argon. The autoclave was sealed and heated to 150 °C temperature. After the desired reaction time, the autoclave was cooled to room temperature and slowly vented while stirring continued. Mesitylene was added as an internal standard to the reaction mixture which was further analyzed by NMR spectroscopy.

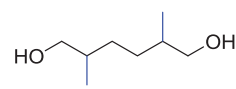
**2-methylpropane-1,3-diol (13k):** Prepared by following the general experimental procedure



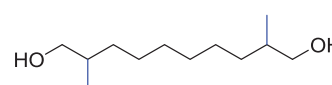
with: **Mn-2** (2.48 mg, 0.5 mol%), propane-1,3-diol **12k** (76.0 mg, 1 mmol), NaOMe (108.04 mg, 2 mmol), MeOH (1 mL), reaction time: 24 h. Yield was determined by  $^1\text{H}$  NMR spectrum using mesitylene (118 mg, 0.97 mmol) as an internal standard ( $\delta_{\text{Mesitylene(standard)}} = 6.76$  (s, 3H),  $\delta_{\text{product}} = 0.84$  (d, 3H)).  $^1\text{H}$  NMR (300 MHz,  $[\text{D}_6]\text{-DMSO}$ , 298 K)

$\delta = 3.44\text{-}3.51$  (m, 4H,  $\text{CH}_2$ ),  $1.58\text{-}1.68$  (m, 1H,  $\text{CH}$ ),  $0.83$  (d, 3H,  $J = 9$  Hz,  $\text{CH}_3$ ). The obtained analytical data are consistent with those previously reported in the literature.<sup>[35]</sup>

**2,5-dimethylhexane-1,6-diol (13l):** Prepared by following the general experimental procedure

 with: **Mn-2** (2.48 mg, 0.5 mol%), hexane-1,6-diol **12l** (118.0 mg, 1 mmol), NaOMe (216.08 mg, 4 mmol), MeOH (1 mL), reaction time: 48 h. Yield was determined by  $^1\text{H}$  NMR spectrum using mesitylene (111 mg, 0.93 mmol) as an internal standard ( $\delta_{\text{Mesitylene(standard)}} = 6.77$  (s, 3H),  $\delta_{\text{product}} = 0.82$  (d, 3H)).  $^1\text{H}$  NMR (400 MHz,  $[\text{D}_6]\text{-DMSO}$ , 298 K)  $\delta = 3.20\text{-}3.24$  (m, 4H,  $\text{CH}_2$ ),  $1.30\text{-}1.43$  (m, 4H,  $\text{CH}_2$  &  $\text{CH}$ ),  $0.93\text{-}1.05$  (m, 2H,  $\text{CH}_2$ ),  $0.82$  (d, 3H,  $J = 3$  Hz,  $\text{CH}_3$ ),  $0.80$  (d, 3H,  $J = 3$  Hz,  $\text{CH}_3$ ). The obtained analytical data are consistent with those previously reported in the literature.<sup>[36]</sup>

**2,9-dimethyldecane-1,10-diol (13m):** Prepared by following the general experimental procedure

 with: **Mn-2** (2.48 mg, 0.5 mol%), decane-1,10-diol **12m** (174.0 mg, 1 mmol), NaOMe (216.08 mg, 4 mmol), MeOH (1 mL), reaction time: 48 h. Yield was determined by  $^1\text{H}$  NMR spectrum using mesitylene (117 mg, 0.97 mmol) as an internal standard ( $\delta_{\text{Mesitylene(standard)}} = 6.76$  (s, 3H),  $\delta_{\text{product}} = 0.82$  (d, 6H)).  $^1\text{H}$  NMR (400 MHz,  $[\text{D}_6]\text{-DMSO}$ , 298 K)  $\delta = 3.14\text{-}3.28$  (m, 4H,  $\text{CH}_2$ ),  $1.40\text{-}1.50$  (m, 2H,  $\text{CH}$ ),  $1.13\text{-}1.28$  (m, 10H,  $\text{CH}_2$ ),  $0.96\text{-}1.03$  (m, 2H,  $\text{CH}_2$ ),  $0.82$  (d, 6H,  $J = 6.64$  Hz,  $\text{CH}_3$ ).  $^{13}\text{C}\{^1\text{H}\}\text{-NMR}$  (101 MHz,  $\text{DMSO-}d_6$ , 298 K)  $\delta = 66.73$  ( $\text{CH}_2$ ),  $35.82$  ( $\text{CH}$ ),  $33.37$  ( $\text{CH}_2$ ),  $29.95$  ( $\text{CH}_2$ ),  $26.98$  ( $\text{CH}_2$ ),  $17.19$  ( $\text{CH}_3$ ). HRMS (ESI-) found  $[\text{M-H}]^- = 201.185960$ ;  $\text{C}_{12}\text{H}_{25}\text{O}_2$  requires 201.186005.

### 3.9.8. Conversion/time profile from experiments for the $\beta$ -methylation of **8a** with MeOH at different time intervals

Nine reactions were performed for the reaction progress experiments at different time intervals. Mn-MACHO **Mn-2** (2.48 mg, 0.5 mol%) and NaOMe (108.04 mg, 2 mmol) were weighed into a glass inlet equipped with a stirring bar inside a glovebox. The glass inlet was closed with a septum and transferred into the bottom part of the 10 mL stainless steel autoclave, where it was opened under a stream of argon. After sealing, the autoclave was purged with argon three times. **8a** (122.1 mg, 1 mmol), and MeOH (1 mL) were added at room temperature through a valve under argon. The autoclave was sealed and heated to 150 °C temperature. After the certain



reaction time, the autoclave was fast cooled, brings it to room temperature and slowly vented while stirring continued. Mesitylene was added as an internal standard to the reaction mixture that was then passed through a short path of acidic alumina before the composition was analyzed by NMR spectroscopy. Yield was determined by  $^1\text{H}$  NMR spectrum using mesitylene as an internal standard ( $\delta_{\text{Mesitylene(standard)}} = 6.72$  (s, 3H),  $\delta_{\text{product}} = 3.58$  (d, 2H)).

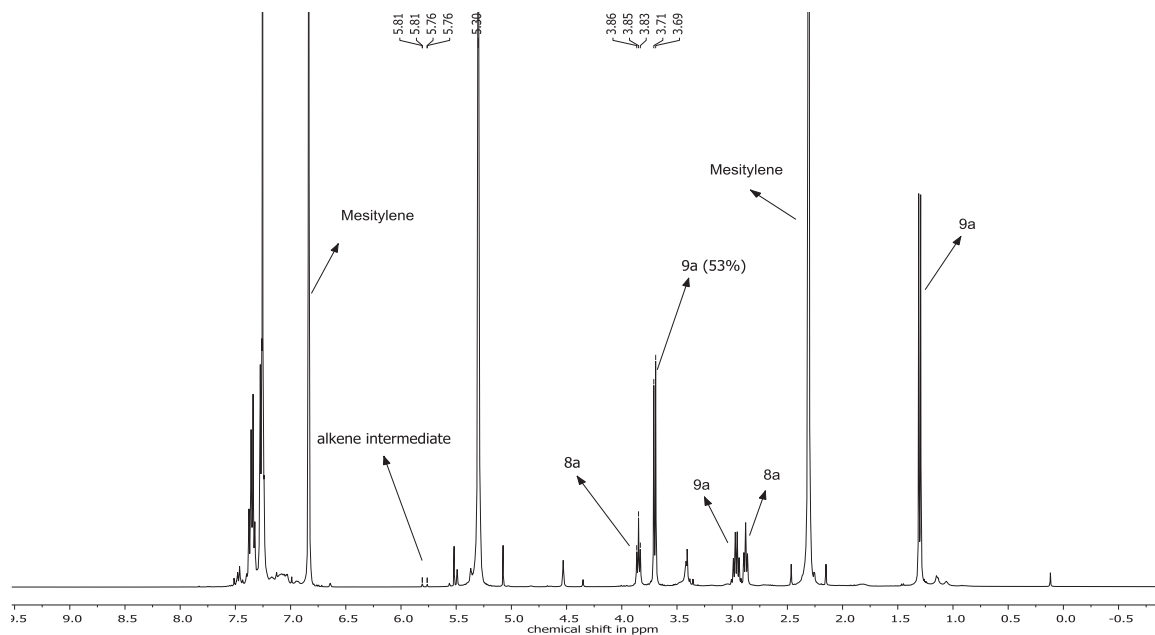
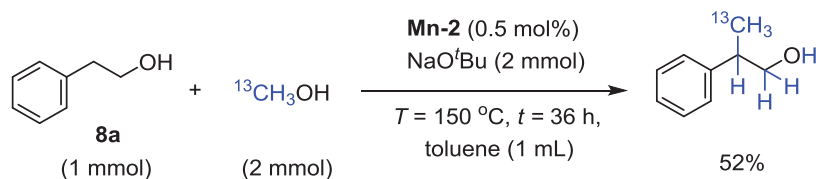


**Figure 3.4:**  $^1\text{H}$  NMR (300 MHz,  $\text{CDCl}_3$ , 298 K) spectrum of reacting of **8a** with MeOH using **Mn-2** after 4 h as example.

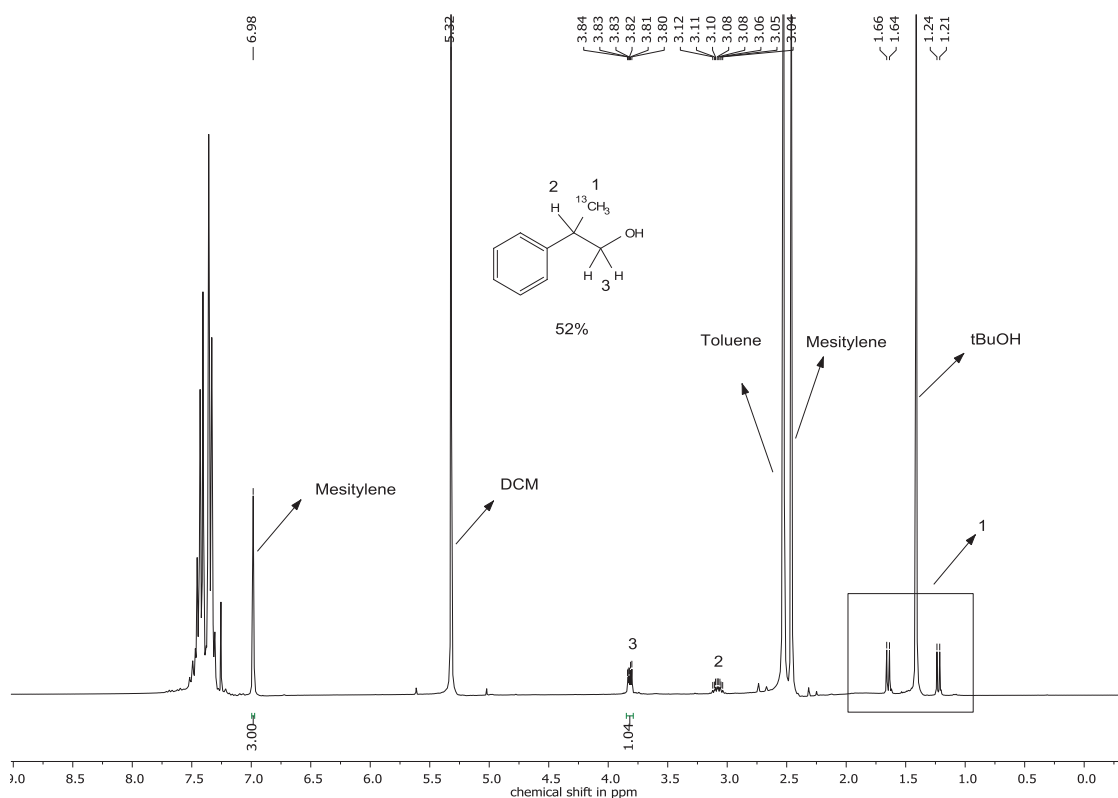
### 3.9.9. Labeling experiments and observation of potential intermediates

#### 3.9.9.1 Procedure for $\beta$ -methylation of **8a** with $^{13}\text{CH}_3\text{OH}$



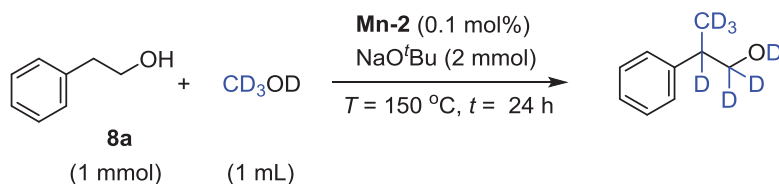
Mn-MACHO **Mn-2** (2.48 mg, 0.5 mol%) and  $\text{NaO}^t\text{Bu}$  (192.3 mg, 2 mmol) were weighed into a glass inlet equipped with a stirring bar inside a glovebox. The glass inlet was closed with a septum and transferred into the bottom part of the 10 mL stainless steel autoclave, where it was opened under a stream of argon. After sealing, the autoclave was purged with argon three times. **8a** (122.1 mg, 1 mmol),  $^{13}\text{CH}_3\text{OH}$  (66.06 mg, 2 mmol) and toluene (1 mL) were added at room

temperature through a valve under argon. The autoclave was sealed and heated to 150 °C temperature for 36 h. After completion of the reaction, the autoclave was cooled to room temperature and slowly vented while stirring continued. Mesitylene (120 mg, 1 mmol) was added as an internal standard to the reaction mixture that was then passed through a short path of acidic alumina before the composition was analyzed by NMR spectroscopy. Yield was determined by  $^1\text{H}$  NMR spectrum using mesitylene as an internal standard ( $\delta_{\text{Mesitylene(standard)}} = 6.98$  (s, 3H),  $\delta_{\text{product}} = 3.80\text{-}3.84$  (m, 2H)).

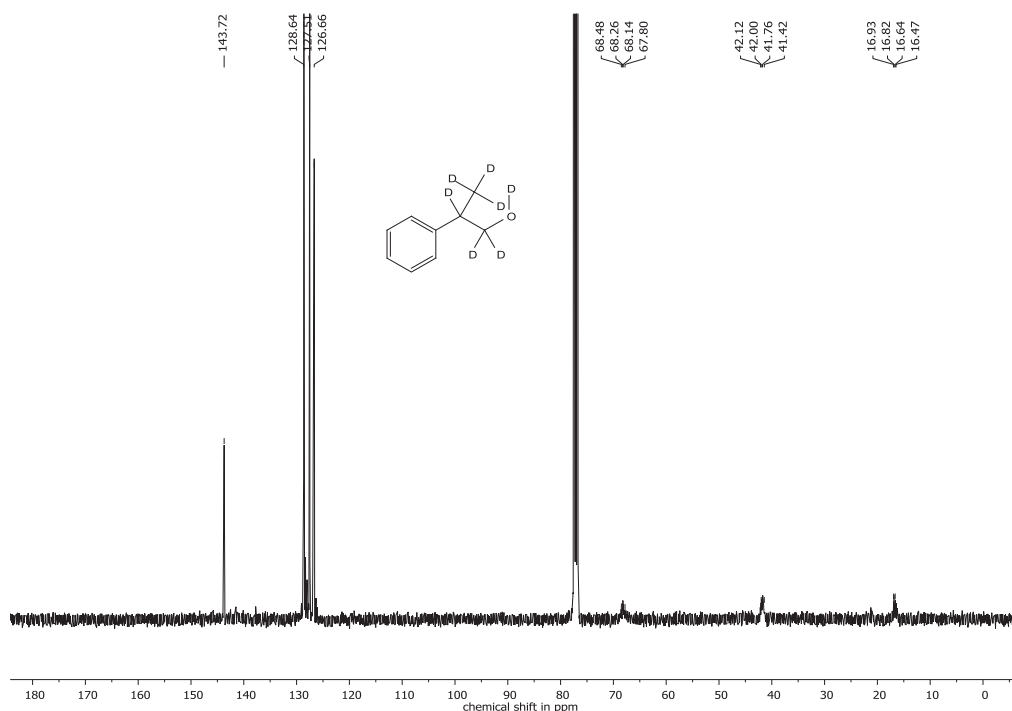


**Figure 3.5:**  $^1\text{H}$  NMR (300 MHz,  $\text{CDCl}_3$ , 298 K) spectrum for the  $\beta$ -methylation of **8a** with  $^{13}\text{CH}_3\text{OH}$ .

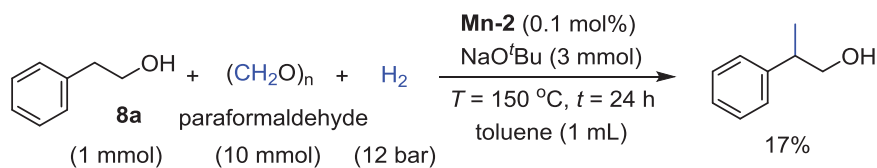


3.9.9.2 Procedure for selective  $\beta$ -methylation of **8a** with  $\text{CD}_3\text{OD}$ 

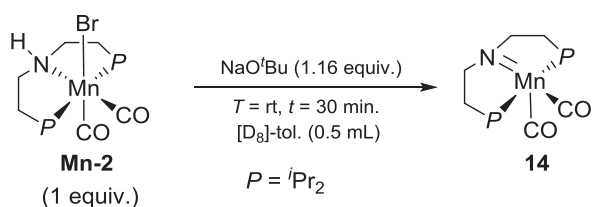
Mn-MACHO **Mn-2** (2.48 mg, 0.5 mol%) and  $\text{NaO}^t\text{Bu}$  (192.3 mg, 2 mmol) were weighed into a glass inlet equipped with a stirring bar inside a glovebox. The glass inlet was closed with a septum and transferred into the bottom part of the 10 mL stainless steel autoclave, where it was opened under a stream of argon. After sealing, the autoclave was purged with argon three times. **8a** (122.1 mg, 1 mmol) and  $\text{CD}_3\text{OD}$  (1 mL) were added at room temperature through a valve under argon. The autoclave was sealed and heated to 150  $^\circ\text{C}$  temperature for 24 h. After 24 h, the autoclave was cooled to room temperature and slowly vented while stirring continued. Mesitylene (120 mg, 1 mmol) was added as an internal standard to the reaction mixture that was then passed through a short path of acidic alumina before the composition was analyzed by NMR spectroscopy.  $^{13}\text{C}\{^1\text{H}\}$ -NMR (101 MHz,  $\text{CDCl}_3$ , 298 K)  $\delta = 143.72$  (quat-C), 128.64 (ArCH), 127.51 (ArCH), 126.66 (quat-C), 67.80-68.48 (m,  $\text{CD}_2$ ), 41.42-42.12 (m, CD), 16.47-16.93 (m,  $\text{CD}_3$ ).



**Figure 3.6:**  $^{13}\text{C}\{^1\text{H}\}$  NMR (75 MHz,  $\text{CDCl}_3$ , 298 K) spectrum for the  $\beta$ -Methylation of **8a** with  $\text{CD}_3\text{OD}$ .

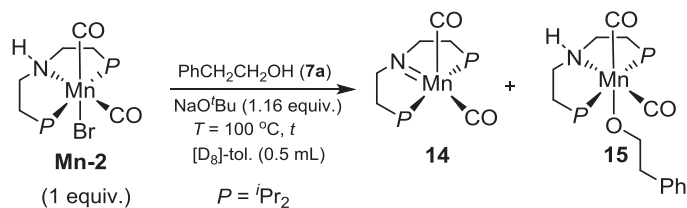
**3.9.9.3 Procedure for  $\beta$ -methylation of **8a** with paraformaldehyde and  $H_2$** 

Mn-MACHO **Mn-2** (2.48 mg, 0.5 mol%), NaO<sup>t</sup>Bu (192.3 mg, 2 mmol) and paraformaldehyde (300.3 mg, 10 mmol) were weighed into a glass inlet equipped with a stirring bar inside a glovebox. The glass inlet was transferred to a 10 mL stainless steel autoclave that was evacuated and refilled with argon at least three times. **8a** (122.1 mg, 1 mmol) and toluene (1 mL) were added at room temperature through a valve under argon. The autoclave was sealed and pressurized with 12 bar of hydrogen. The autoclave was heated to 150 °C temperature for 24 h. After 24 h, the autoclave was cooled to room temperature and slowly vented while stirring continued. Mesitylene (120 mg, 1 mmol) was added as an internal standard to the reaction mixture that was then passed through a short path of acidic alumina before the composition was analyzed by NMR spectroscopy. Yield was determined by <sup>1</sup>H NMR spectrum using mesitylene as an internal standard ( $\delta_{\text{Mesitylene(standard)}}=6.84$  (s, 3H),  $\delta_{\text{product}}=3.71$  (d, 2H)).

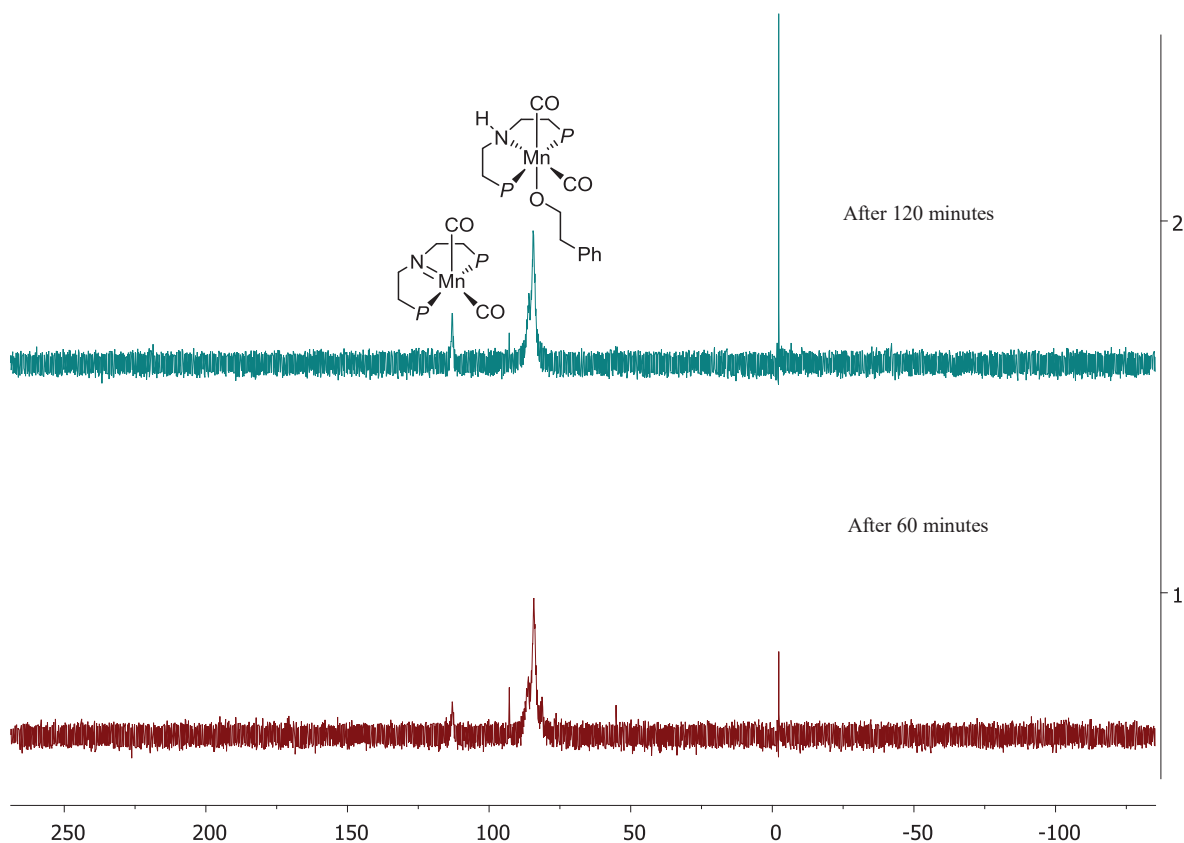
**3.9.9.4 Preparation of complex **14****

A high pressure NMR tube was charged with complex **Mn-2** (15 mg, 0.03 mmol), NaO<sup>t</sup>Bu (3.36 mg, 0.035 mmol) and [D<sub>8</sub>]-toluene (0.4 mL). The resulting solution was stirred for 30 minutes at room temperature leading to a color change from yellow to orange red. <sup>1</sup>H NMR (300 MHz, [D<sub>8</sub>]-toluene, 298 K) and <sup>31</sup>P{<sup>1</sup>H} NMR (121 MHz, [D<sub>8</sub>]-toluene, 298 K) spectroscopies are consistent with the formation of complex **14**.<sup>[37]</sup>

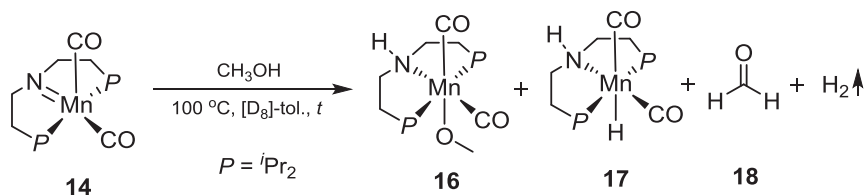
## 3.9.9.5 Reaction of complex Mn-2 with 8a in presence of a base



**8a** (1.22 mg, 0.01 mmol), Mn-complex **Mn-2** (4.95 mg, 0.01 mmol) and  $[\text{D}_8]$ -toluene (0.5 ml as a solvent) were charged in a Teflon tapped NMR tube under argon atmosphere. The NMR tube was heated at 100 °C temperature.  $^{31}\text{P}\{^1\text{H}\}$  NMR of the reaction mixture of **Mn-2** and **8a** were measured at different time intervals which confirmed the formation of Mn(I) intermediate **14** and **15**.<sup>[37]</sup>



**Figure 3.7:** Superposed  $^{31}\text{P}\{^1\text{H}\}$ -NMR spectrum of Mn-intermediates **14** and **15** at different time intervals.

3.9.9.6 Reaction of Mn-complex **14** with methanol

**14** (4.15 mg, 0.01 mmol), MeOH (1.6 mg, 0.05 mmol) and  $[\text{D}_8]$ -toluene (0.4 ml as a solvent) were charged in Teflon capped NMR tube under argon atmosphere. The NMR tube was heated at  $100\text{ }^\circ\text{C}$  temperature.  $^1\text{H}$  NMR of the reaction mixture of **14** and methanol were measured at different time intervals which confirmed the formation of formaldehyde,  $\text{H}_2$  and Mn(I) intermediates **16** and **17** respectively.<sup>[37]</sup>

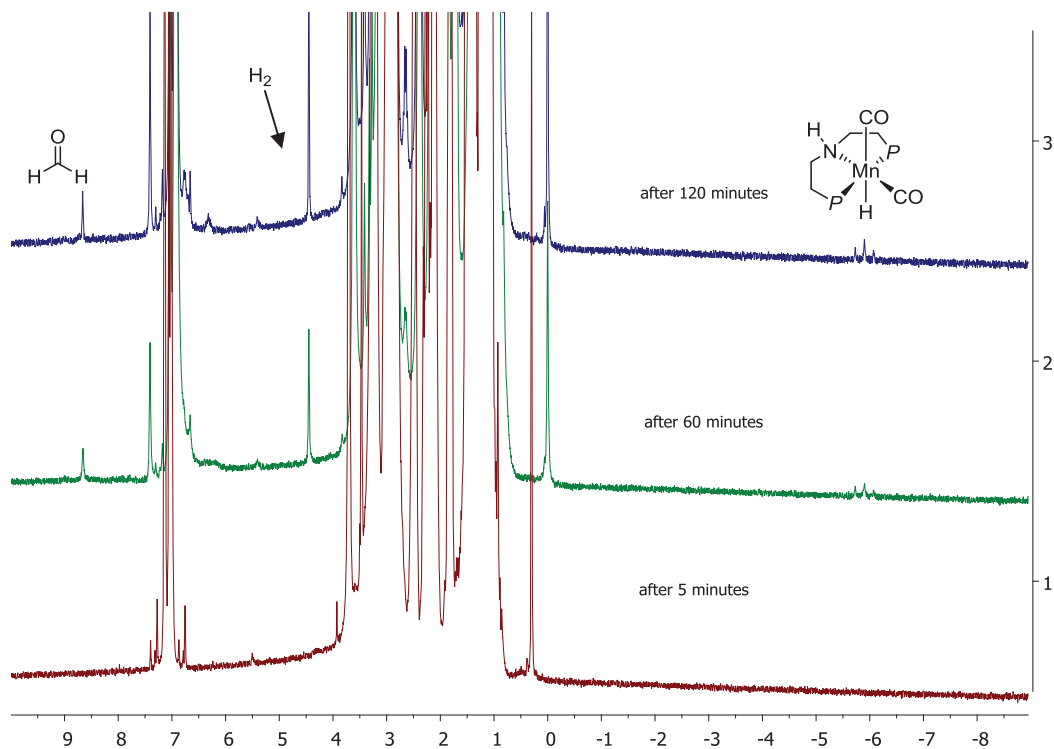


**Figure 3.8:** Superposed  $^1\text{H}$  NMR spectra (300 MHz,  $[\text{D}_8]$ -tol., 298 K) of formaldehyde,  $\text{H}_2$  and intermediate **17** at different time intervals.

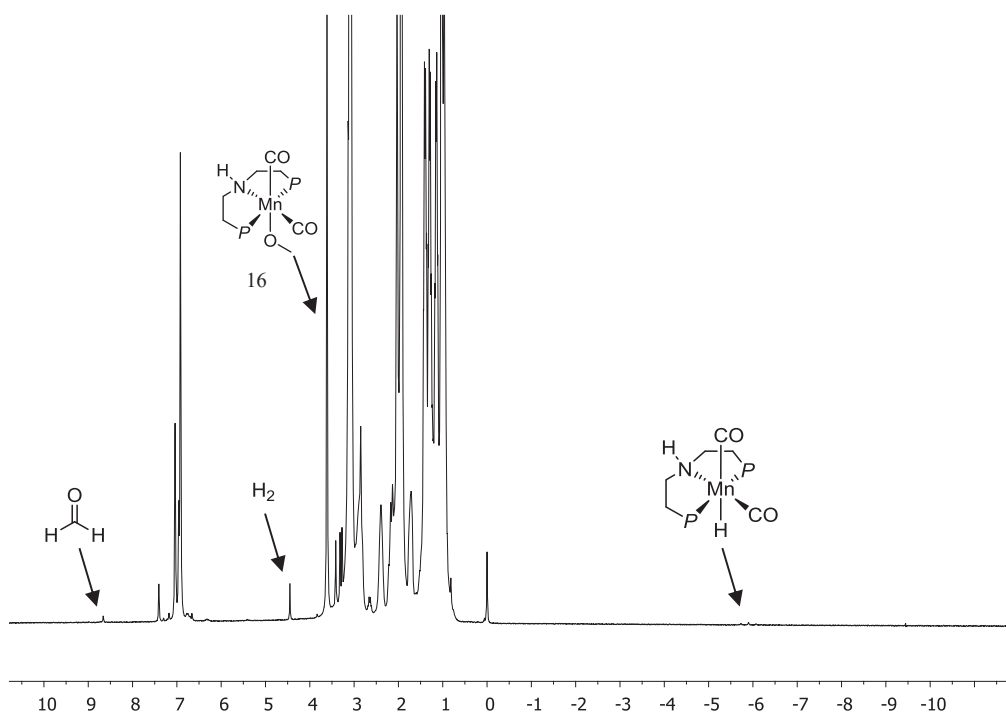


**Figure 3.9:**  $^1\text{H}$  NMR (300 MHz,  $[\text{D}_8]$ -tol., 298 K) spectrum of intermediates **16**, **17**, and formaldehyde after 120 min. at  $100^\circ\text{C}$ .

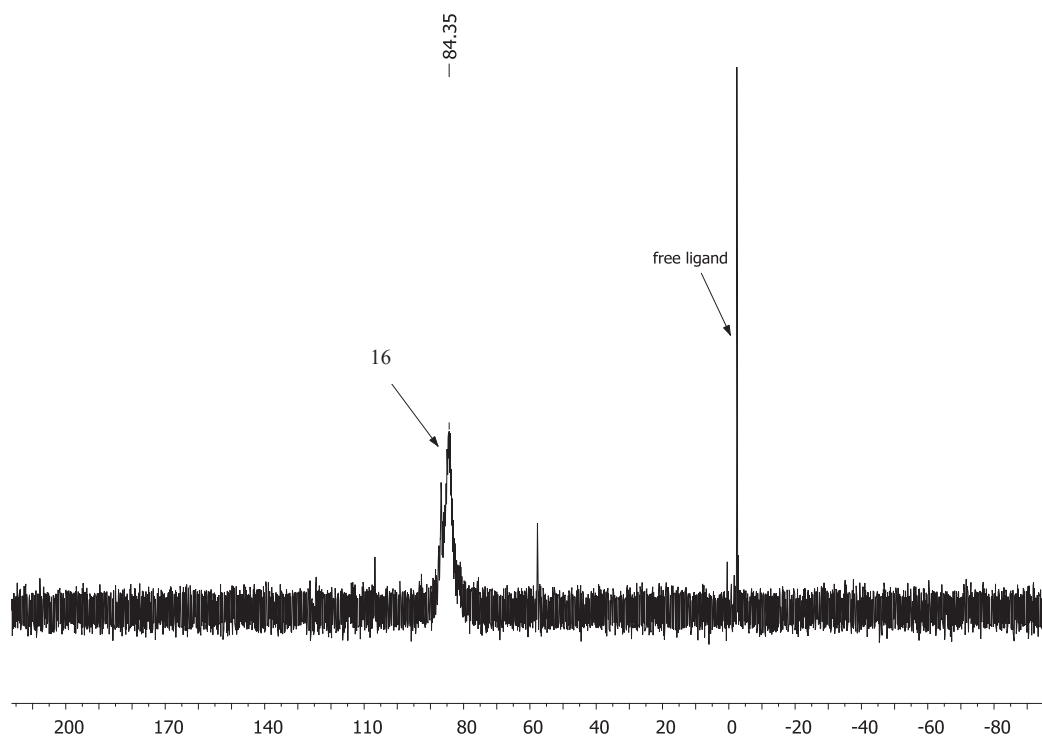


**Figure 3.10:**  $^{31}\text{P}\{^1\text{H}\}$ -NMR (121 MHz,  $[\text{D}_8]$ -tol., 298 K) spectrum of the reaction between complex **14** with MeOH in presence of a base.

## References

- [1] a) A. Mukherjee, D. Milstein, *ACS Catal.* **2018**, *8*, 11435-11469; b) S. Murugesan, K. Kirchner, *Dalton Trans.* **2016**, *45*, 416-439; c) G. Bauer, X. Hu, *Inorg. Chem. Front.* **2016**, *3*, 741-765.
- [2] A. Kaithal, M. Schmitz, M. Hölscher, W. Leitner, *ChemCatChem* **2019**, DOI: 10.1002/cctc.201900788.
- [3] a) S. Elangovan, C. Topf, S. Fischer, H. Jiao, A. Spannenberg, W. Baumann, R. Ludwig, K. Junge, M. Beller, *J. Am. Chem. Soc.* **2016**, *138*, 8809-8814; b) A. Kaithal, M. Hölscher, W. Leitner, *Angew. Chem. Int. Ed.* **2018**, *130*, 13637-13641; c) A. Kumar, T. Janes, N. A. Espinosa-Jalapa, D. Milstein, *Angew. Chem. Int. Ed.* **2018**, *57*, 12076-12080; d) V. Zubar, Y. Lebedev, L. M. Azofra, L. Cavallo, O. El-Sepelgy, M. Rueping, *Angew. Chem. Int. Ed.* **2018**, *57*, 13439-13443; e) R. van Putten, E. A. Uslamin, M. Garbe, C. Liu, A. Gonzalez-de-Castro, M. Lutz, K. Junge, E. J. M. Hensen, M. Beller, L. Lefort, E. A. Pidko, *Angew. Chem. Int. Ed.* **2017**, *56*, 7531-7534; f) U. K. Das, A. Kumar, Y. Ben-David, M. A. Iron, D. Milstein, *J. Am. Chem. Soc.* **2019**, *141*, 12962-12966; g) N. A. Espinosa-Jalapa, A. Nerush, L. J. W. Shimon, G. Leitus, L. Avram, Y. Ben-David, D. Milstein, *Chem. Eur. J.* **2017**, *23*, 5934-5938; h) M. B. Widegren, M. L. Clarke, *Org. Lett.* **2018**, *20*, 2654-2658.
- [4] a) S. Elangovan, J. Neumann, J.-B. Sortais, K. Junge, C. Darcel, M. Beller, *Nat. Commun.* **2016**, *7*, 12641; b) T. Liu, L. Wang, K. Wu, Z. Yu, *ACS Catal.* **2018**, *8*, 7201-7207; c) S. Chakraborty, P. Daw, Y. Ben David, D. Milstein, *ACS Catal.* **2018**, *8*, 10300-10305; d) J. C. Borghs, M. A. Tran, J. Sklyaruk, M. Rueping, O. El-Sepelgy, *J. Org. Chem.* **2019**, *84*, 7927-7935; e) J. Rana, V. Gupta, E. Balaraman, *Dalton Trans.* **2019**, *48*, 7094-7099; f) Y. K. Jang, T. Krückel, M. Rueping, O. El-Sepelgy, *Org. Lett.* **2018**, *20*, 7779-7783; g) M. K. Barman, A. Jana, B. Maji, *Adv. Synth. Catal.* **2018**, *360*, 3233-3238.
- [5] a) A. Kaithal, S. Sen, C. Erken, T. Weyhermüller, M. Hölscher, C. Werlé, W. Leitner, *Nat. Commun.* **2018**, *9*, 4521; b) V. Vasilenko, C. K. Blasius, H. Wadepohl, L. H. Gade, *Angew. Chem. Int. Ed.* **2017**, *56*, 8393-8397; c) X. Ma, Z. Zuo, G. Liu, Z. Huang, *ACS Omega* **2017**, *2*, 4688-4692.
- [6] a) O. Martínez-Ferraté, C. Werlé, G. Franciò, W. Leitner, *ChemCatChem* **2018**, *10*, 4514-4518; b) M. Perez, S. Elangovan, A. Spannenberg, K. Junge, M. Beller, *ChemSusChem* **2017**, *10*, 83-86; c) C. Zhang, B. Hu, D. Chen, H. Xia, *Organometallics* **2019**, *38*, 3218-3226; d) K. Z. Demmans, M. E. Olson, R. H. Morris, *Organometallics* **2018**, *37*, 4608-4618; e) D. Wei, A. Bruneau-Voisine, M. Dubois, S. Bastin, J.-B. Sortais, *ChemCatChem* **2019**, *11*, 5256-5259.
- [7] O. El-Sepelgy, E. Matador, A. Brzozowska, M. Rueping, *ChemSusChem* **2019**, *12*, 3099-3102.
- [8] J. Sklyaruk, J. C. Borghs, O. El-Sepelgy, M. Rueping, *Angew. Chem. Int. Ed.* **2019**, *58*, 775-779.
- [9] A. Bruneau-Voisine, L. Pallova, S. Bastin, V. César, J.-B. Sortais, *Chem. Commun.* **2019**, *55*, 314-317.
- [10] A. Mukherjee, A. Nerush, G. Leitus, L. J. W. Shimon, Y. Ben David, N. A. Espinosa Jalapa, D. Milstein, *J. Am. Chem. Soc.* **2016**, *138*, 4298-4301.

- [11] V. Papa, J. R. Cabrero-Antonino, E. Alberico, A. Spanneberg, K. Junge, H. Junge, M. Beller, *Chem Sci* **2017**, *8*, 3576-3585.
- [12] K. Oikawa, S. Itoh, H. Yano, H. Kawasaki, Y. Obora, *Chem. Commun.* **2017**, *53*, 1080-1083.
- [13] J. C. Bardhan, D. N. Mukherji, *J. Chem. Soc.* **1956**, 4629-4633.
- [14] S. Koul, J. L. Koul, B. Singh, M. Kapoor, R. Parshad, K. S. Manhas, S. C. Taneja, G. N. Qazi, *Tetrahedron: Asymmetry* **2005**, *16*, 2575-2591.
- [15] A. Gansäuer, M. Klatte, G. M. Brändle, J. Friedrich, *Angew. Chem. Int. Ed.* **2012**, *51*, 8891-8894.
- [16] Y. Li, H. Li, H. Junge, M. Beller, *Chem. Commun.* **2014**, *50*, 14991-14994.
- [17] K. Polidano, J. M. J. Williams, L. C. Morrill, *ACS Catal.* **2019**, *9*, 8575-8580.
- [18] T. Slagbrand, T. Kivijärvi, H. Adolfsson, *ChemCatChem* **2015**, *7*, 3445-3449.
- [19] G. V. M. Sharma, K. L. Reddy, P. S. Lakshmi, R. Ravi, A. C. Kunwar, *J. Org. Chem.* **2006**, *71*, 3967-3969.
- [20] K. Polidano, B. G. Reed-Berendt, A. Basset, A. J. A. Watson, J. M. J. Williams, L. C. Morrill, *Org. Lett.* **2017**, *19*, 6716-6719.
- [21] G. Zhao, R. Tong, *Green Chem.* **2019**, *21*, 64-68.
- [22] M. Garbe, Z. Wei, B. Tannert, A. Spannenberg, H. Jiao, S. Bachmann, M. Scalone, K. Junge, M. Beller, *Adv. Synth. Catal.* **2019**, *361*, 1913-1920.
- [23] a) D. S. Rao, T. R. Reddy, K. Babachary, S. Kashyap, *Org. Biomol. Chem* **2016**, *14*, 7529-7543; b) R. Fernández, A. Ros, A. Magriz, H. Dietrich, J. M. Lassaletta, *Tetrahedron* **2007**, *63*, 6755-6763.
- [24] a) A. Kišić, M. Stephan, B. Mohar, *Adv. Synth. Catal.* **2015**, *357*, 2540-2546; b) S. Rodríguez, B. Qu, K. R. Fandrick, F. Buono, N. Haddad, Y. Xu, M. A. Herbage, X. Zeng, S. Ma, N. Grinberg, H. Lee, Z. S. Han, N. K. Yee, C. H. Senanayake, *Adv. Synth. Catal.* **2014**, *356*, 301-307.
- [25] W. J. Jang, S. M. Song, J. H. Moon, J. Y. Lee, J. Yun, *J. Am. Chem. Soc.* **2017**, *139*, 13660-13663.
- [26] Q. Wang, X. Liu, X. Liu, B. Li, H. Nie, S. Zhang, W. Chen, *Chem. Commun.* **2014**, *50*, 978-980.
- [27] J. E. Roque Pena, E. J. Alexanian, *Org. Lett.* **2017**, *19*, 4413-4415.
- [28] J. Cao, P. Perlmutter, *Org. Lett.* **2013**, *15*, 4327-4329.
- [29] G. R. Dowson, M. F. Haddow, J. Lee, R. L. Wingad, D. F. Wass, *Angew. Chem. Int. Ed.* **2013**, *52*, 9005-9008.
- [30] P. H. Galebach, D. J. McClelland, N. M. Eagan, A. M. Wittrig, J. S. Buchanan, J. A. Dumesic, G. W. Huber, *ACS Sustain. Chem. Eng.* **2018**, *6*, 4330-4344.
- [31] S. R. Tamang, M. Findlater, *J. Org. Chem.* **2017**, *82*, 12857-12862.
- [32] I. Burkhardt, J. S. Dickschat, *Eur. J. Org. Chem.* **2018**, *2018*, 3144-3157.
- [33] P. Wang, D.-L. Wang, H. Liu, X.-L. Zhao, Y. Lu, Y. Liu, *Organometallics* **2017**, *36*, 2404-2411.
- [34] B. Cao, X. Chen, Y. Yamaro-Botte, M. B. Richardson, K. L. Martin, G. N. Khairallah, T. W. T. Rupasinghe, R. M. O'Flaherty, R. A. J. O'Hair, J. E. Ralton, P. K. Crellin, R. L. Coppel, M. J. McConville, S. J. Williams, *J. Org. Chem.* **2013**, *78*, 2175-2190.
- [35] H. Ohta, H. Tetsukawa, N. Noto, *J. Org. Chem.* **1982**, *47*, 2400-2404.
- [36] K. Shin, S. Joung, Y. Kim, S. Chang, *Adv. Synth. Catal.* **2017**, *359*, 3428-3436.

[37] A. Kaithal, M. Hölscher, W. Leitner, *Angew. Chem. Int. Ed.* **2018**, *57*, 13449-13453.



#### 4. Direct synthesis of cycloalkanes from diols and secondary alcohols or ketones using a homogeneous manganese catalyst

Parts of this chapter have been published:

A. Kaithal, L. L. Gracia, C. Camp, E. A. Quadrelli, W. Leitner, *J. Am. Chem. Soc.* **2019**, *141*, 17487–1749.

Cycloalkanes are important compounds and form structural motifs that are found in several natural products, pharmaceuticals, and materials.<sup>[1]</sup> Carbocycles consisting of saturated carbon–carbon bonds have versatile properties such as high boiling points, high melting points, and high densities compared to linear alkanes which make them possible additives for motor fuel, and many other heavy oils.<sup>[1]</sup> In the past, considerable efforts have been made to synthesize these molecules, specifically on methods in which the regio- and stereo- selectivity of the molecule can be controlled.<sup>[2]</sup>

Known approaches for the preparation of substituted cycloalkanes, consists of Diels Alder-(4+2)-cycloaddition followed by reduction,<sup>[1d, 3]</sup> cyclization of dihalides via Wurtz reactions,<sup>[2b, 4]</sup> hydrogenation of aromatic six-membered rings,<sup>[5]</sup> Michael reaction on enolizable reagents<sup>[6]</sup> and dimerization of cyclopropanes<sup>[7]</sup> (Figure 4.1). However, all these approaches have some serious drawbacks which comprise the use of high-pressure reaction setup, multi-step procedures, narrow substrate scopes, poor regio- or stereo-selectivities and also some of the reactions generate a stoichiometric amount of chemical waste.

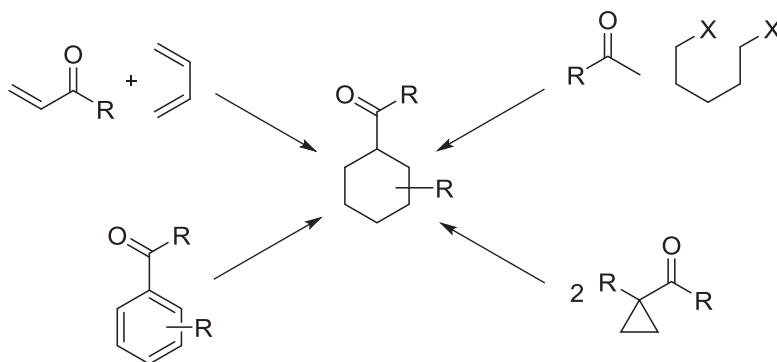


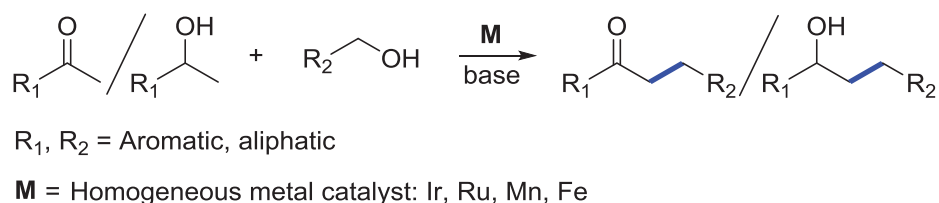
**Figure 4.1:** Currently established strategies for the synthesis of substituted cyclohexanes.

The synthesis of substituted cycloheptane rings is an even bigger challenge in organic synthesis. At present, very few processes are known which can accomplish these molecules from non-cyclic common chemicals. In general, non-substituted cycloheptane rings are produced via the direct reduction of cycloheptanone or cycloheptenes.<sup>[8]</sup> However, multistep procedures such as the synthesis of substituted cycloheptane-1,3-dione is carried out from 1,2-di-ketones and the ring expansion of cyclopentanones which upon reduction can lead to the synthesis of cycloheptane rings.<sup>[9]</sup>

The well-established catalytic methods such as ring-closing metathesis (RCM) followed by reduction or hydrogenation have also a significant impact on the synthesis of medium-sized aliphatic rings.<sup>[10]</sup> Cycloisomerisation followed by reduction is another method that can be a possible route for cycloalkane preparation.<sup>[11]</sup> However, these processes always require a discrete synthesis of the particular starting materials containing a specific functional group in a certain position to perform the cyclization process.

Developing an easy, sustainable, and one-step process to construct these important cycloalkanes from readily available and cheap feedstocks is an attractive target for metal-catalysis. Considering this, alcohols and diols can be envisaged as feedstocks as they are prevalent in nature, sometimes derived from biomass which makes them an attractive and cheap source for the preparation of essential and otherwise difficult obtainable building blocks.

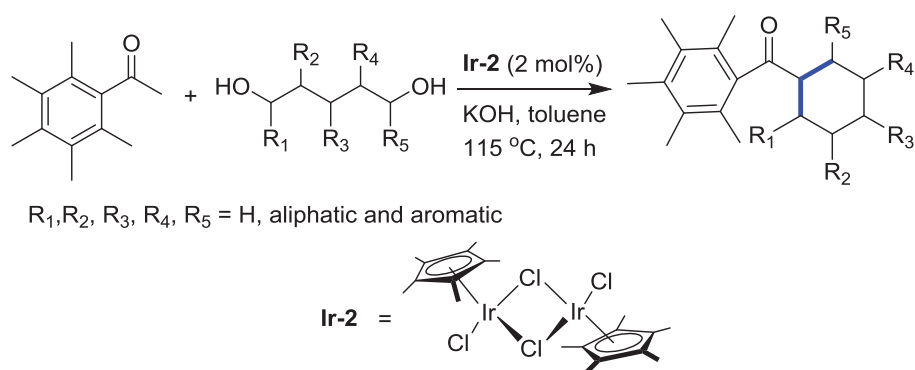
Recently, the formation of C–C bonds via hydrogen borrowing syntheses has gained significant interest in green chemistry.<sup>[12]</sup> Both noble and non-noble metal-catalyzed selective  $\beta$ -alkylation of secondary alcohols and  $\alpha$ -alkylation of ketones is well established (Scheme 4.1).<sup>[13]</sup> In the previous chapters, we discussed the selective  $\beta$ -methylation of alcohols using methanol as a C1 source and alkylating reagent using Ru and Mn as metal precursors (see chapter 2 and chapter 3).<sup>[14]</sup>



**Scheme 4.1:** Metal-catalyzed alkylation of alcohols and secondary alcohols.

## Direct synthesis of cycloalkanes from diols and secondary alcohols or ketones using a homogeneous manganese catalyst

Recently, Donohoe and coworkers reported a catalytic system where they showed the formation of various substituted cyclohexanes using a series of substituted diols (Scheme 4.2).<sup>[15]</sup> The transformation was performed using a sterically hindered ketone 1-(2,3,4,5,6-pentamethylphenyl)ethanone, iridium as a metal precursor and a stoichiometric amount of KOH as a base. However, the reaction was limited to a specific sterically hindered ketone. The reaction was performed under argon atmosphere using  $[(\text{IrCp}^*\text{Cl}_2)_2]$  **Ir-2** as a metal precursor, stoichiometric amount of KOH as a base and 2 equiv. of a diol with respect to ketone at 115 °C for 24 h. Excess amount of diol was used to suppress lactone formation as a side reaction. This whole process follows a (5+1) strategy to prepare the substituted cyclohexane rings.

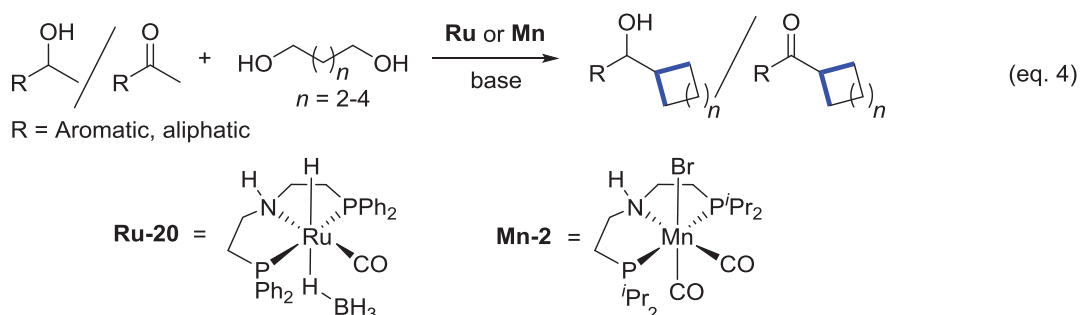


**Scheme 4.2:** Preparation of substituted cyclohexanes reported by Donohoe *et. al.*<sup>[15]</sup>

## 4.1. Objective

Alkylations using a “hydrogen borrowing reactions” are developing into an important methodology in organic synthesis and can be widely used for the formation of C–C bonds. In this chapter, we will focus on the synthesis of substituted cycloalkanes using alcohols or ketones and diols via a hydrogen borrowing reaction network.

The investigation will be carried out using Ru-MACHO-BH **Ru-20** and Mn-MACHO-*i*Pr **Mn-2** complexes due to their known reactivity for the hydrogen borrowing reactions. Based on the previous studies and mechanistic investigation, we assumed that such catalyst systems could be applicable for the synthesis of substituted cycloalkanes using diols as a double alkylating reagent. The focus will be on the synthesis of compounds with five, six and seven membered rings (eq. 4). Control and labeling experiments will be carried out to obtain insight into the reaction intermediates. Based on these results and previous investigations, a postulated catalytic pathway will be proposed.



## 4.2. Reaction optimization

The Ru-MACHO-BH **Ru-20** pincer complex was investigated to perform this transformation as a starting pre-catalyst. 1-Phenylethanol **19a** and 1,5-pentanediol **20a** were selected as benchmark substrates for the optimization reaction. The reaction of **19a** (1 equiv.) with **20a** (2 equiv.) using **Ru-20** (2 mol%) as a pre-catalyst and KO<sup>t</sup>Bu (4 equiv. with respect to **19a**) in toluene (2 mL) at 150 °C showed the desired six-member cyclic product cyclohexyl(phenyl)methanol **21a** with a yield of 35% with >99% conversion after 24 h. A number of side products such as a secondary alcohol self-coupled product, aldol-coupled intermediate products, and dehydrogenated products were observed. Interestingly, when the same reaction was performed using the Mn-MACHO-<sup>i</sup>Pr complex **Mn-2**, an increased formation of the corresponding product **21a** with a yield of 47% was observed (Table 4.1, entry 2). The results confirmed the presence of only a very low amount of side products and showed mainly the unreacted starting materials and the oxidized product of **21a**, acetophenone, as a side product. In this work, the **Mn-2** complex exhibited better reactivity in comparison to the closely related **Ru-20** complex. As manganese is an earth-abundant and non-noble metal, further optimizations were carried out using the **Mn-2** complex (Table 4.1).

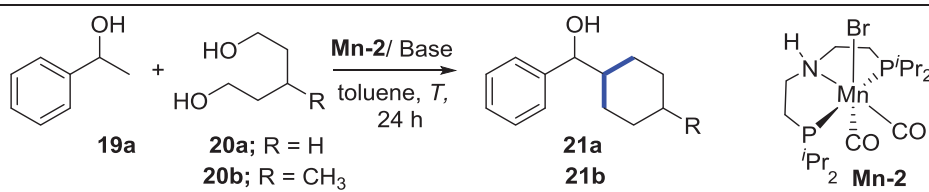
First, the diol concentration was optimized. Under the same reaction conditions, with only 1 equiv. of diol **20a** only a very small amount of product was formed (Table 4.1, entry 1). This low yield can be explained by the self-condensation of the diol. The formation of lactone as a side product was confirmed using GC-MS analysis. Gratifyingly, when the amount of diol was increased to 3 equiv., the amount of desired six-membered cyclic product increased to 60% product yield with >99% conversion after 24 h (Table 4.1, entry 3). The optimized reaction conditions were found by increasing the diol amount further to 4 equiv. The reaction led to the selective formation of **21a** (62% yield) with 82% conversion of **19a** (Table 4.1, entry 4). A small amount of side products formed from the secondary alcohol such as aldol and the self-coupled products was observed. A further increase of the amount of diol to 5 equiv. substantially decreased the catalytic activity and showed limited product formation (Table 4.1, entry 5).

Next, the focus was on the temperature optimization. Decreasing the reaction temperature from 150 °C to 120 °C diminished the product formation and revealed only 10% yield to the corresponding product (Table 4.1, entry 6). Appealingly, increasing the temperature to 170 °C,

Direct synthesis of cycloalkanes from diols and secondary alcohols or ketones using a homogeneous manganese catalyst

showed the desired product **21a** with a yield of 74% while the selectivity remained constant as compared to the reaction at 150 °C (Table 4.1, entry 7).

**Table 4.1:** Reaction optimization for the synthesis of substituted cyclohexane **21a**.<sup>[a]</sup>



#	Diol (equiv.)	Base (equiv.)	Temp (°C)	Conv. (%) <sup>b</sup>	Yield <b>21</b> (%) <sup>c</sup>
1	<b>20a</b> (1)	KO <sup>t</sup> Bu (4)	150	70	16
2	<b>20a</b> (2)	KO <sup>t</sup> Bu (4)	150	89	47
3	<b>20a</b> (3)	KO <sup>t</sup> Bu (4)	150	>99	60
4	<b>20a</b> (4)	KO <sup>t</sup> Bu (4)	150	82	62
5	<b>20a</b> (5)	KO <sup>t</sup> Bu (4)	150	84	35
6	<b>20a</b> (4)	KO <sup>t</sup> Bu (4)	120	60	10
7	<b>20a</b> (4)	KO <sup>t</sup> Bu (4)	170	98	74
8 <sup>S</sup>	<b>20a</b> (4)	KO <sup>t</sup> Bu (4)	150	86	36
9	<b>20a</b> (4)	Cs <sub>2</sub> CO <sub>3</sub> (2)	150	78	2
10	<b>20a</b> (4)	NaO <sup>t</sup> Bu (4)	150	69	12
11*	<b>20a</b> (4)	KO <sup>t</sup> Bu (4)	150	>99	80
12*	<b>20b</b> (4)	KO <sup>t</sup> Bu (4)	150	>99	92; 90:10 d.r.

Conditions: [a] 1-phenylethanol **19a** (0.5 mmol), diol **3a** or **3b**, Mn-complex **Mn-2** (2 mol%), KO<sup>t</sup>Bu and toluene (2 mL) were heated in a closed vessel. <sup>b,c</sup>Conversion and yield were calculated using gas chromatography analysis. <sup>S</sup>1 mol% of Mn-complex **Mn-2** was used. \*Reaction time was extended to 32 h.

On decreasing the catalyst loading from 2 mol% to 1 mol% the reactivity was reduced resulting in a yield of 36% of **21a** at a conversion of 86% (Table 4.1, entry 8). Similarly, changing the base from KO<sup>t</sup>Bu to Cs<sub>2</sub>CO<sub>3</sub> or NaO<sup>t</sup>Bu also diminished the product formation (Table 4.1, entry 9 and 10). The best reaction conditions were found when the reaction time was prolonged to 32 h. The reaction of **19a** (1 equiv.) with **20a** (4 equiv.) and KO<sup>t</sup>Bu (4 equiv.) at 150 °C in toluene (2 mL) after 32 h led to **21a** with a good yield of 80% (Table 4.1, entry 11). Isolation by column chromatography gave 72% yield. Under, these optimized reaction conditions, when **20a** was

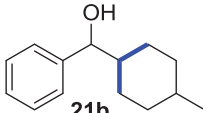
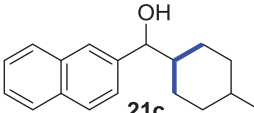
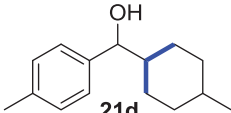
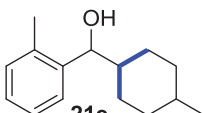
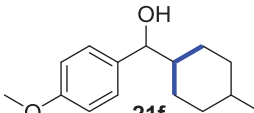
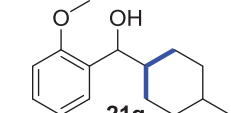
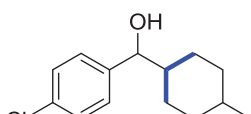
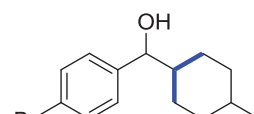
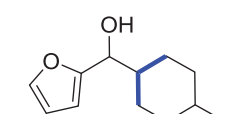
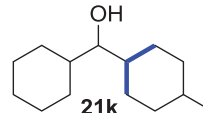
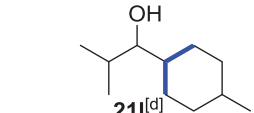
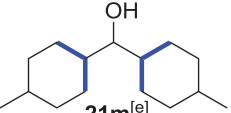
changed to the methyl-substituted 3-methylpentane-1,5-diol **20b**, the reactivity was even better and showed the formation of the desired cyclized product (4-methylcyclohexyl)(phenyl)methanol **21b** with 92% GC yield and 81% yield of the isolated product (Table 4.1, entry 12). In general, the reaction with a substituted diol can lead to a mixture of diastereomeric products. In this case the diastereomeric ratio of 90:10 was observed in favor of the *trans* isomer as a major diastereomeric product which was characterized using NMR spectroscopy and confirmed by DFT calculations (details are described in the experimental section). To verify that the reaction is metal catalyzed, control experiments were carried out. The reaction in the absence of complex **Mn-2** and base did not reveal any product formation. Similarly, the reaction only in the presence of a base and without metal catalyst or vice versa also failed to result in any product formation. These results clearly confirmed that the reaction requires both the metal complex and the base to achieve the final cyclic product.

### 4.3. Selective preparation of substituted cyclohexanes from 3-methylpentane-1,5-diol **20b**

In order to prepare different substituted cyclohexane rings and increase the substrate scope of the reaction, various secondary alcohols were reacted with 3-methylpentane-1,5-diol **20b** (Table 4.2). Based on the established reaction conditions, a number of secondary alcohols embedded with different functionalities and sterically hindered groups were explored. Using the standard reaction conditions, the transformation of a naphthyl-substituted secondary alcohol led to the corresponding substituted six-member ring **21c** with 86% yield (82% yield of the isolated product) as an 87:13 diastereomeric ratio. Likewise, the reaction of methyl substituted 1-phenylethanols such as 1-(*p*-tolyl)ethan-1-ol **19d** and 1-(*o*-tolyl)ethan-1-ol **19e** also revealed good activities and generated the corresponding products **21d** and **21e** with yields of 93% and 79%, respectively. Isolation of the products gave yields of 78% and 72%, respectively. In both cases, the reaction showed mainly the *trans*-diastereomer. Similarly, the reaction of a *p*-methoxy substituted secondary alcohol afforded the desired product **21f** with 78% yield. However, the *o*-methoxy substituted secondary alcohol showed a low product formation with a 52% yield to **21g**. The low reactivity might be a result of the steric hindrance of the methoxy group near the alcohol functionality.

## Direct synthesis of cycloalkanes from diols and secondary alcohols or ketones using a homogeneous manganese catalyst

**Table 4.2:** Manganese-catalyzed selective preparation of substituted cyclohexanes from 3-methylpentane-1,5-diol **20b**.<sup>[a, b]</sup>

$  \begin{array}{c}  \text{R}-\text{CH}(\text{OH})-\text{CH}_3 + \text{HO}-\text{CH}_2-\text{CH}_2-\text{CH}(\text{CH}_3)-\text{CH}_2-\text{OH} \\  \text{19b-19m} \quad \quad \quad \text{20b} \\  \text{R = aryl, alkyl}  \end{array}  \xrightarrow[\text{toluene, 150 }^\circ\text{C, 32 h}]{\text{Mn-2 (2 mol\%), KO}^t\text{Bu (4 equiv.)}}  \begin{array}{c}  \text{R}-\text{CH}(\text{OH})-\text{C}_6\text{H}_{10} \\  \text{21b-21m}  \end{array}  $		
Conversion (%) / GC Yield (Isolated Yield)		
 <p><b>21b</b> &gt;99/92(81) 90:10 <i>d.r.</i></p>	 <p><b>21c</b> &gt;99/86(83) 87:13 <i>d.r.</i></p>	 <p><b>21d</b> 96/93(78) 92:8 <i>d.r.</i></p>
 <p><b>21e</b> &gt;99/79(72) 89:11 <i>d.r.</i></p>	 <p><b>21f</b> &gt;99/78(71) 87:13 <i>d.r.</i></p>	 <p><b>21g</b> &gt;99/52(44) 88:12 <i>d.r.</i></p>
 <p><b>21h</b><sup>[c]</sup> &gt;99/70(61) 93:7 <i>d.r.</i></p>	 <p><b>21i</b><sup>[c]</sup> &gt;99/n.d.(40) 89:11 <i>d.r.</i></p>	 <p><b>21j</b><sup>[d]</sup> &gt;99/n.d.(61) 87:13 <i>d.r.</i></p>
 <p><b>21k</b> 98/71(60) 62:38 <i>d.r.</i></p>	 <p><b>21l</b><sup>[d]</sup> &gt;99/n.d.(67) 88:12 <i>d.r.</i></p>	 <p><b>21m</b><sup>[e]</sup> &gt;99/n.d.(51) 78:22:0 <i>d.r.</i></p>

Conditions: [a] Secondary alcohol **19** (0.5 mmol), 3-methylpentane-1,5-diol **20b** (236 mg, 2 mmol), Mn-complex **Mn-2** (4.96 mg, 2 mol%), KO<sup>t</sup>Bu (224 mg, 2 mmol) and toluene (2 mL) were heated in a closed vessel. [b] Conversion and yield were calculated using gas chromatography analysis. Yield in the parentheses shows the isolated yield after performing the column chromatography. [c] Reaction time: 14 h. [d] 1.5 mmol of **20b** was used. [e] 3 mmol of diol and 4 mmol of KO<sup>t</sup>Bu was used. n.d.: not determined.

Interestingly, the reaction of electron-withdrawing chloro- substituted secondary alcohol with **20b** revealed a high conversion with a mixture of products. However, when the reaction time was decreased to 14 h, the reaction showed 70% yield for the corresponding product **21h** (61% yield of the isolated product) as a 93:7 diastereomeric ratio. Substitution of bromo-group in



*para*-position of 1-phenyl ethanol resulted in 40% yield of the desired cyclohexyl product **21i**. However, 33% of the de-brominated cyclohexyl product was also observed in the reaction mixture showing that the actual cyclization reaction was very effective. The heterocyclic secondary alcohol 1-(furan-2-yl)ethan-1-ol was tolerated to the corresponding product **21j** was obtained after isolation with 61% yield.

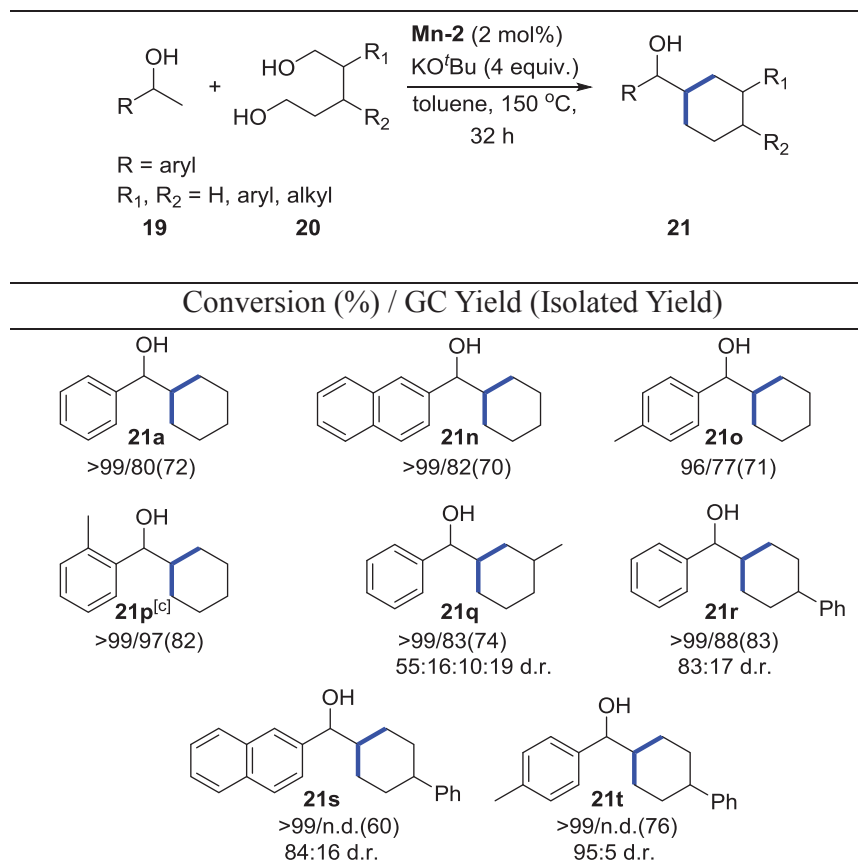
Aliphatic alcohols comprising less acidic  $\beta$ -CH protons with respect to aromatic secondary alcohols also reacted smoothly. The reaction of 1-cyclohexylethanol with **20b** showed the selective formation of cyclohexyl(4-methylcyclohexyl)methanol **21k** with 71% yield (60% yield after isolation). However, the final product **21k** showed a low diastereomeric selectivity of 62:38, while the major isomer observed remained the *trans* isomer. Small aliphatic alcohols such as 3-methylbutan-2-ol and *iso*-propanol also reacted with **21b** smoothly forming the corresponding cyclohexyl products with a major selectivity to the *trans*-diastereomer. Interestingly, employing *iso*-propanol as a substrate resulted in the selective formation of two cyclohexyl rings in one molecule, thus possibly paving the way for even more complex molecules.

#### 4.4. Selective preparation of substituted cyclohexanes from a variety of secondary alcohols and substituted pentanediols

A number of alkyl and aryl-substituted diols were selectively coupled with a variety of secondary alcohols as well (Table 4.3). At first, using the optimized reaction conditions, various secondary alcohols were coupled with **20a**. Naphthyl ring and methyl-substituted secondary alcohols were selectively coupled with **20a** and revealed the selective formation of cycloalkanes **21n**, **21o** and **21p** with very good yields and selectivities. Interestingly, **19a** was also coupled with 2-methylpentane-1,5-diol **20c** and yielded 83% of **21q** (74% yield after isolation). However, the final product showed a mixture of diastereomers with a ratio of 55:16:10:19. The reaction of **19a** with phenyl substituted diol **20d** showed the formation of **21r** with a yield of 88% (83% yield after isolation) in 83:17 ratio diastereomeric mixture. Similarly, other secondary alcohols such as 1-(naphthalen-2-yl)ethan-1-ol and 1-(*p*-tolyl)ethan-1-ol were transformed with good yields to the substituted cyclohexyl products **21s** and **21t**, respectively with the *trans*-diastereomer being the major product.

## Direct synthesis of cycloalkanes from diols and secondary alcohols or ketones using a homogeneous manganese catalyst

**Table 4.3:** Manganese-catalyzed selective preparation of substituted cyclohexanes from a variety of secondary alcohols and diols.<sup>[a, b]</sup>



Conditions: [a] Secondary alcohol **19** (0.5 mmol), diol **20** (2 mmol), Mn-complex **Mn-2** (4.96 mg, 2 mol%), KO<sup>t</sup>Bu (224 mg, 2 mmol) and toluene (2 mL) were heated in a closed vessel. [b] Conversion and yield were calculated using gas chromatography analysis. Yields in parentheses correspond to isolated yields after purification via column chromatography. [c] 1.5 mmol of diol was used.

### 4.5. Selective preparation of substituted cycloalkanes from ketones and diols

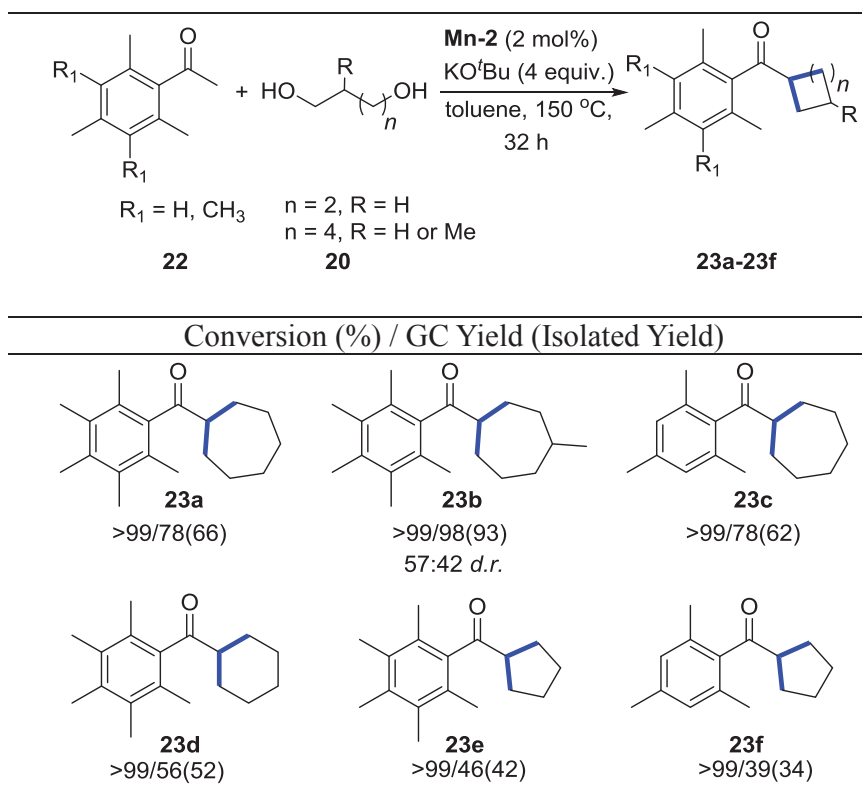
The synthesis of a variety of substituted cyclohexanes using the substituted pentanediols could be established. Accordingly, the preparation of different sizes of cycloalkanes using diols with different chain lengths was focused. There are limited reports concerning the formation of cycloheptane rings. Therefore, the formation of a seven-membered ring was investigated (Table 4.4). Using the optimized reaction conditions, the reaction of 1-phenyl ethanol **19a** with 1,6-hexanediol **20e** led to a mixture of products. When the same reaction was performed using

## Direct synthesis of cycloalkanes from diols and secondary alcohols or ketones using a homogeneous manganese catalyst

the bulky ketone **22a** instead of secondary alcohol **19a**, the reaction showed the formation of a substituted seven-membered ring with very good yield and selectivity. The reaction of 1-(2,3,4,5,6-pentamethylphenyl)ethanone **22a** with **20e** in the presence of Mn complex **Mn-2** yielded the corresponding substituted cycloheptane **23a** with 78% yield (66% yield after isolation). The reaction showed only the formation of the corresponding ketone as a main product, no formation of the corresponding alcohol was observed. Appealingly, methyl substituted 1,6-hexanediol **20f** was also selectively coupled with **22a** and showed very high reactivity with 98% yield to **23b**.

**Table 4.4:** Manganese-catalyzed selective preparation of substituted cycloalkanes from sterically hindered ketones.

[a, b]



Conditions: [a] 1-(methylpolysubstituted-phenyl)-ethanone **22** (0.5 mmol), diol **20** (2 mmol), Mn-complex **Mn-2** (4.96 mg, 2 mol%),  $\text{KO}^t\text{Bu}$  (224 mg, 2 mmol) and toluene (2 mL) were heated in a closed vessel. [b] Conversion and yield were calculated using gas chromatography analysis. Yields in parentheses correspond to isolated yields after purification via column chromatography.

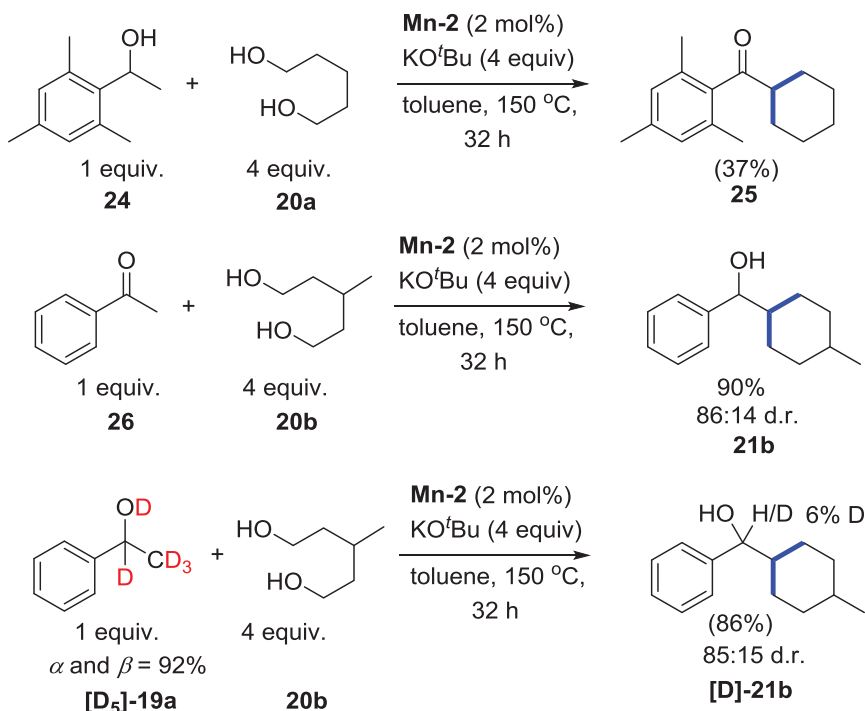
Next, 1-mesitylethan-1-one **22b** was reacted with **20e**. The reaction of **22b** showed a similar reactivity as **22a**. The conversion of **22b** was high (>99%) and the yield of the isolated product

**23c** amounted to 62% (72% GC yield). Similarly, when substrate **22a** and 1,5-pentanediol **20a** were used for the formation of a six-membered ring, the reaction afforded the corresponding six member cyclic product **23d** with a yield of 56% (52% yield after isolation).

Furthermore, the preparation of substituted five-membered rings was investigated. For this case, a mixture of products was obtained when **19a** was reacted with 1,4-butanediol **20g**. The reaction of bulky ketone **22a** with **20g** confirmed the formation of substituted cyclopentane ring **23e** with a 46% yield (42% isolated yield). Similarly, 1-mesitylethan-1-one **22b** was also reacted with **20g** and showed the formation to the corresponding desired product **23f** with a yield of 39% (34% yield after isolation).

#### 4.6. Observation of in situ formed intermediates and labeling experiments

To confirm the individual reaction steps involved in the reaction pathways, a number of control experiments were performed (Scheme 4.3). Using the optimized reaction conditions, the reaction of 1-mesitylethanol **24** with 1,5-pentanediol **20a** selectively formed cyclohexyl(mesityl)methanone **25** with a yield of 37%. The selectivity to the ketone product can be explained with the steric hindrance of the mesityl unit in the substrate which hampered the last hydrogenation step of the ketone to the corresponding final alcohol product and stopped the reaction at this intermediate step. Next, to verify this hypothesis, the reaction of acetophenone **26** with 3-methylpentane-1,5-diol **20b** was carried out. Interestingly, the final alcohol product **21b** was obtained with a yield of 90% as an 86:14 diastereomeric ratio. Similar results were also obtained when the reaction was performed with a secondary alcohol **19a** and **20b** (Table 4.1, entry 12). Next, labeling experiments were performed. Deuterium labeled 1-phenyl ethanol [**D**<sub>5</sub>]-**19a** was synthesized using the established procedure.<sup>[16]</sup> Under the standard reaction conditions, the reaction of deuterium labeled [**D**<sub>5</sub>]-**19a** with **20b** gave the corresponding [**D**]-**21b** with excellent selectivity. Only a small amount of deuterium incorporation was observed in the final product confirming the high H/D scrambling in the reaction and supporting the hydrogen borrowing mechanism.



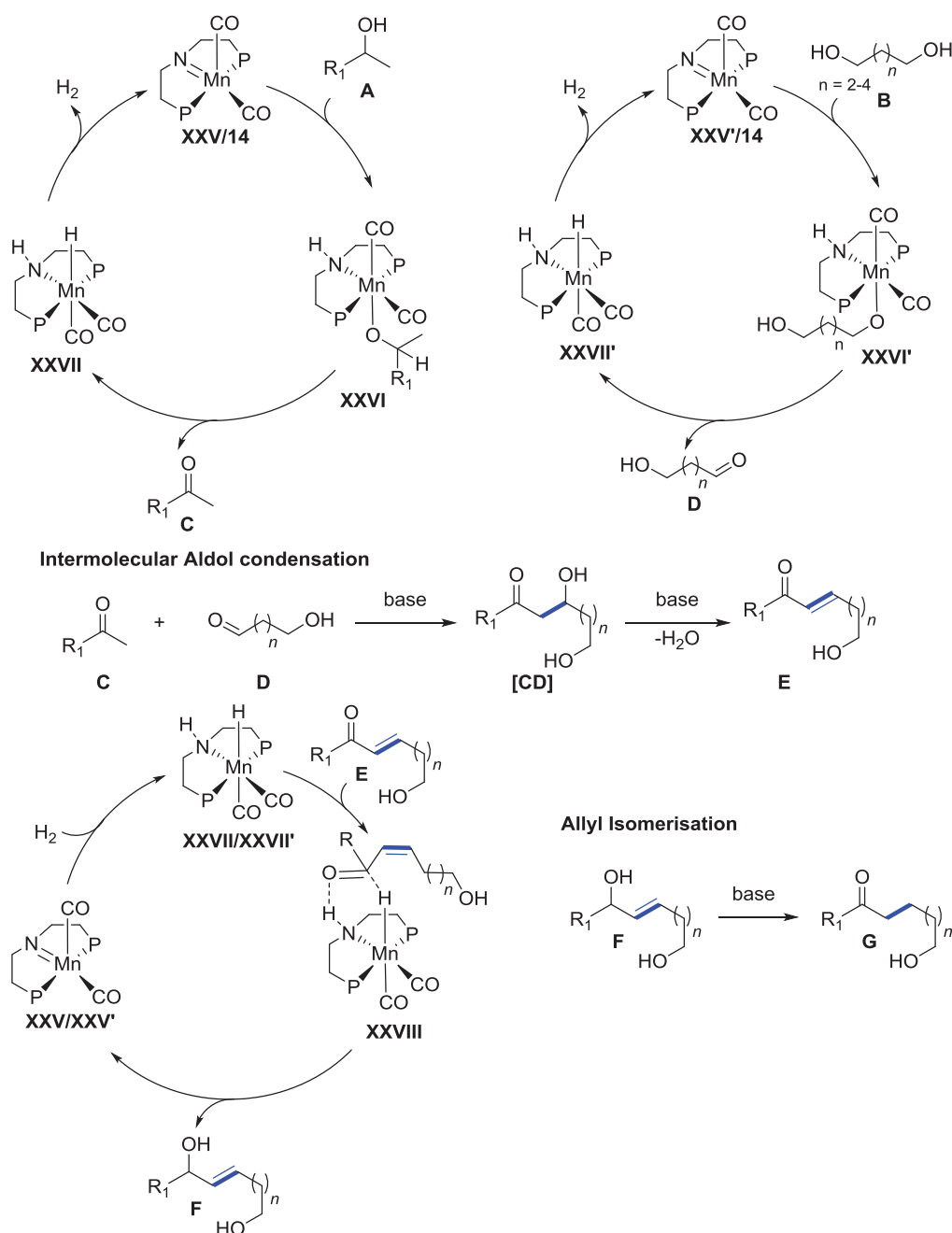
**Scheme 4.3:** Mechanistic studies for the cross-coupling of secondary alcohol and diol.

#### 4.7. Proposed catalytic pathway

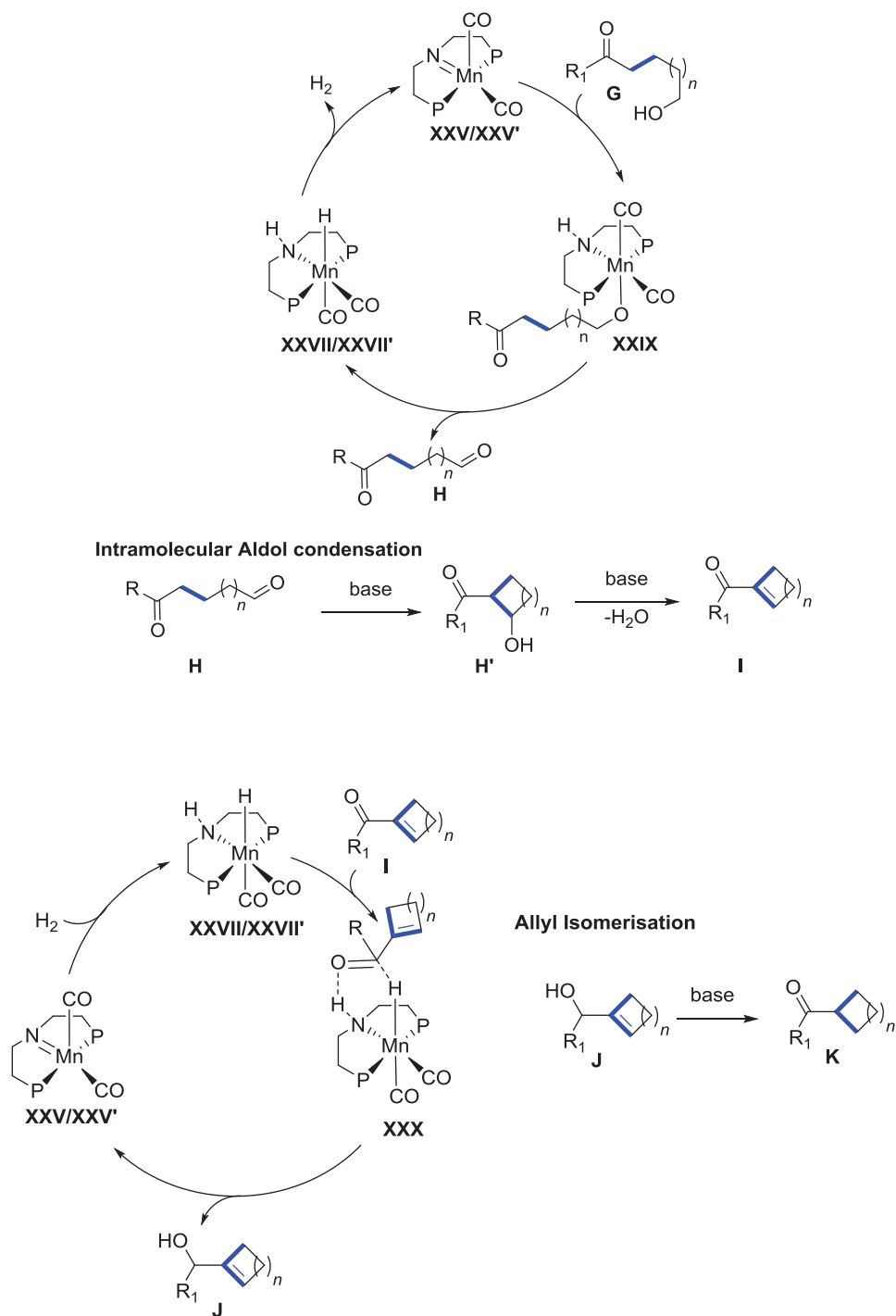
Based on the above-mentioned experiments and previously reported studies, a plausible catalytic cycle was proposed (Figure 4.2). At first, in presence of a base, complex **Mn-2** reacts to the active species **14** (**XXV**). The characterization and observation of the catalytic active species was already discussed in earlier chapters. Next, the alcohol and diols interact with the Mn=N center where the proton from the OH group transfers to the nitrogen center of complex and the alkoxide moiety of the alcohols transfer to the manganese center. The alcoholate complex from secondary alcohol is denoted as **XXVI** and from diol, it is denoted as **XXVI'**.  $\beta$ -hydride elimination in complex **XXVI** and complex **XXVI'** leads to the formation of the corresponding ketone **C** and aldehyde **D**, respectively and generates the subsequent Mn-hydride species **XXVII/XXVII'**. Next, a base-catalyzed aldol-condensation takes place between the molecules **C** and **D** which leads to the formation of the corresponding enone **E**. Furthermore, the *in situ* formed enone **E** interacts with the N-H proton of the complex **XXVII/XXVII'** and the nucleophilic attack of hydride from the Mn center attacks the carbon of the carbonyl functionality which generates the corresponding enol **F** and generates active species **XXV/XXV'**. Subsequently, the base-mediated

Direct synthesis of cycloalkanes from diols and secondary alcohols or ketones using a homogeneous manganese catalyst

allyl-isomerization in the molecule **F** takes place and generates the corresponding ketone **G**. One more time, the same catalytic cycle repeats. However in this catalytic cycle the reaction proceeds via intra-molecular aldol condensation where the formation of intermediates **H**, **I**, and **J** occur and generates the corresponding cyclized ketone product **K**. Based on the substrate, the reaction can be stopped at the ketone product **K** or it can also be proceed for further hydrogenation to the alcohol product **L**.



Direct synthesis of cycloalkanes from diols and secondary alcohols or ketones using a homogeneous manganese catalyst



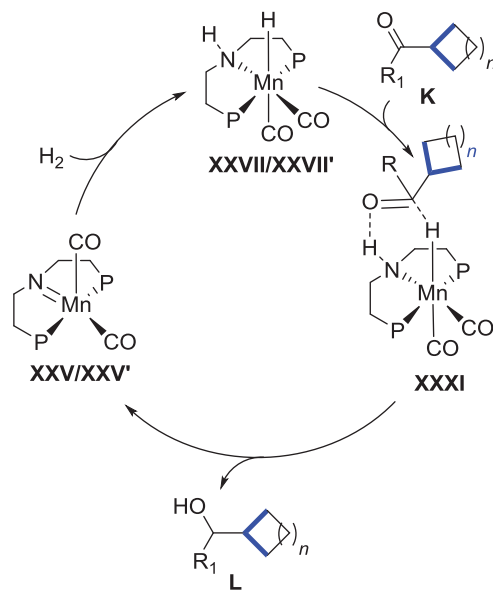


**Figure 4.2:** Detailed postulated catalytic cycle for the preparation of cycloalkanes

#### 4.8. Conclusion and outlook

In conclusion, a novel, and a versatile synthetic strategy was developed for the synthesis of substituted cycloalkanes via the catalytic coupling of secondary alcohols/ketones and diols. The earth-abundant and air-stable manganese pincer complex was used to perform this transformation. A number of aromatic and aliphatic secondary alcohols were coupled with substituted 1,5-pentandiol to generate the corresponding substituted cyclohexane rings with high yields and moderate to high selectivities to *trans* diastereomeric products. Moreover, this methodology was also extended to the synthesis of substituted cycloheptane and cyclopentane rings via changing the carbon length in the diol moiety, reaching moderate to high yields to the corresponding cycloalkane rings. The reaction showed the stoichiometric amount of water as a by-product. However, the excess amount of diol was used due to the formation of lactone as a side product of the reaction. While the manganese catalyst mediates the de- and re-hydrogenation steps and base performs probably the C–C bond formation via aldol condensation and isomerization. Further optimization and mechanistic studies are required to suppress the lactone formation which can be facilitated by the detailed study of the individual reaction step and rate-determining reaction step in the reaction network.



## 4.9. Experimental

### 4.9.1. General experimental

All reactions involving air sensitive compounds were carried out under Argon in flame-dried glassware, ensuring rigorously inert conditions. The solvents were purified using solvent purification-systems and were stored and handled under Argon. Chemicals were purchased from Sigma-Aldrich, Alfa-Aesar, abcr, Acros Organics, TCI chemicals and used without further purification. NMR-spectra were recorded on Bruker AV-300, AV-400, DPX-300 spectrometers at the indicated temperatures with the chemical shifts ( $\delta$ ) given in ppm relative to TMS and the coupling constants ( $J$ ) in Hz. The solvent signals were used as references and the chemical shifts converted to the TMS scale ([D<sub>3</sub>]-Acetonitrile:  $\delta_{\text{H}} = 1.94$  ppm and  $\delta_{\text{C}} = 118.3, 1.3$  ppm; CDCl<sub>3</sub>:  $\delta_{\text{H}} = 7.26$  ppm and  $\delta_{\text{C}} = 77.1$  ppm; CD<sub>2</sub>Cl<sub>2</sub>:  $\delta_{\text{H}} = 5.32$  ppm and  $\delta_{\text{C}} = 54.00$  ppm; C<sub>6</sub>D<sub>6</sub>:  $\delta_{\text{H}} = 7.16$  ppm and  $\delta_{\text{C}} = 128.1$  ppm; [D<sub>8</sub>]-THF:  $\delta_{\text{H}} = 1.72$  ppm, 3.58 ppm and  $\delta_{\text{C}} = 67.2, 25.3$  ppm; [D<sub>8</sub>]-Toluene:  $\delta_{\text{H}} = 2.08, 6.97, 7.01, 7.09$  ppm and  $\delta_{\text{C}} = 137.5, 128.9, 127.9, 125.1, 20.4$  ppm. [D<sub>6</sub>]-DMSO:  $\delta_{\text{H}} = 2.50$  ppm and  $\delta_{\text{C}} = 39.5$  ppm).<sup>[17]</sup> HRMS spectra were recorded on a Bruker ESQ3000 spectrometer.

**Note:** All catalytic reactions were carried out in 15 mL ace pressure tubes. In reaction, the reaction temperature corresponds to the temperature of heating bath.

### 4.9.2. Synthesis of manganese pincer complex

Synthesis of manganese pincer complex **Mn-2** was discussed in Chapter 3 (see chapter 3.9.2).<sup>[18]</sup>

### 4.9.3. Preparation of starting materials

**2-methylpentane-1,5-diol (20c):** At 0 °C, a solution of 2-methylglutaric acid (1.00 g, 6.9 mmol) in THF (20 mL) was added to a stirred suspension of LiAlH<sub>4</sub> (0.90 g, 24.0 mmol). The resulting solution was warmed to rt and then further refluxed for 16 h. After 16 h, the reaction mixture was cooled to 0 °C and then THF (20 mL) was added. The reaction mixture was quenched by sequential dropwise addition of water (1 mL), aq. NaOH (15 % w/v, 1 mL) and water (2 mL). MgSO<sub>4</sub> was added to the reaction mixture at rt and

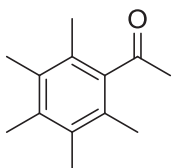
stirred for 30 minutes. The reaction mixture was filtered, concentrated *in vacuo* and characterized. The spectral data are in agreement with the reported literature.<sup>[15]</sup> <sup>1</sup>H NMR (300 MHz, CD<sub>2</sub>Cl<sub>2</sub>, 298 K)  $\delta$  = 3.57-3.62 (m, 2H, CH<sub>2</sub>), 3.41-3.44 (m, 2H, CH<sub>2</sub>), 1.69-1.76 (br s, 2H, OH), 1.42-1.67 (m, 4H, CH<sub>2</sub>), 1.09-1.21 (m, 1H, CH), 0.91 (d, 3H, <sup>3</sup>J<sub>HH</sub> = 6 Hz, CH<sub>3</sub>). Isolated yield: 0.73 g, 93%. Physical state: Colorless oil.

**3-phenylpentane-1,5-diol (20d):** At 0 °C, a solution of 3-phenylglutaric acid (3 g, 14.4 mmol) in THF (25 mL) was added to a stirred suspension of LiAlH<sub>4</sub> (1.64 g, 43.2 mmol). The resulting solution was cooled to rt and further reflux for 16 h. After 16 h, at 0 °C, Et<sub>2</sub>O (150 mL) was added to the resulting solution and quenched by sequential dropwise addition of water (2 mL), aq. NaOH (15% w/v, 2 mL) and water (5.5 mL). MgSO<sub>4</sub> was added to the reaction mixture at rt and stirred for 30 minutes. The reaction solution was filtered, concentrated *in vacuo* and further preceded for characterization. The spectral data is according to the reported literature.<sup>[15]</sup> <sup>1</sup>H NMR (300 MHz, CD<sub>2</sub>Cl<sub>2</sub>, 298 K)  $\delta$  = 7.19-7.24 (m, 2H, ArCH), 7.10-7.13 (m, 3H, ArCH), 3.29-3.46 (m, 4H, CH<sub>2</sub>), 2.73-2.86 (m, 1H, CH), 1.68-1.87 (m, 6H, CH<sub>2</sub> and OH). Isolated yield: 90%.

**3-methylhexane-1,6-diol (20f):** At 0 °C, a solution of 3-methyladipic acid (5 g, 31 mmol) in THF (50 mL) was added to a stirred suspension of LiAlH<sub>4</sub> (3.5 g, 93 mmol). The resulting solution was cooled to rt and further reflux for 16 h. At 0 °C, THF (100 mL) was added to the resulting solution and quenched by sequential drop wise addition of water (3 mL), aq. NaOH (15% w/v, 3 mL) and water (10 mL). MgSO<sub>4</sub> was added to the reaction mixture at rt and stirred for 30 minutes. The reaction solution was filtered, concentrated *in vacuo* and further preceded for characterization. <sup>1</sup>H NMR (300 MHz, CD<sub>2</sub>Cl<sub>2</sub>, 298 K)  $\delta$  = 3.55-3.66 (m, 4H, CH<sub>2</sub>), 2.07 (br s, 2H, OH), 1.46-1.64 (m, 4H, CH<sub>2</sub>), 1.33-1.44 (m, 2H, CH<sub>2</sub>), 1.15-1.22 (m, 1H, CH), 0.90 (d, 3H, J = 6 Hz, CH<sub>3</sub>). <sup>13</sup>C{<sup>1</sup>H}-NMR (75 MHz, Tol-*d*<sub>8</sub>, 298 K):  $\delta$  = 63.45 (CH<sub>2</sub>), 61.31 (CH<sub>2</sub>), 40.37 (CH<sub>2</sub>), 33.41 (CH<sub>2</sub>), 30.63 (CH), 29.79 (CH<sub>2</sub>), 19.95 (CH<sub>2</sub>). Isolated yield: 64%.

**1-(2,3,4,5,6-pentamethylphenyl)ethanone (22a):** In a round bottom flask, at 0 °C, pentamethylbenzene (5 g, 33.7 mmol) and acetyl chloride (2.6 mL, 37.1 mmol) was dissolved in DCM (200 mL) under argon atmosphere. Aluminium Chloride (5.6 g, 42.3 mmol) was added

portion wise over 10 minutes to the reaction mixture. Next, the reaction mixture was warmed to



rt which was further stirred for 5 h. The resulting solution was poured into crushed ice and the organic layer was extracted with DCM (2 x 100 mL). Further, the organic layer was washed with brine (40 mL). MgSO<sub>4</sub> was added to the solution and stirred for 10 minutes. The reaction mixture was filtered and

concentrated in *vacuo*. Purification using column chromatography afforded the corresponding compound **5a** as a white solid. The spectral data is according to the reported literature.<sup>[15]</sup>

<sup>1</sup>H NMR (300 MHz, CD<sub>2</sub>Cl<sub>2</sub>, 298 K)  $\delta$  = 2.16 (s, 3H, CH<sub>3</sub>), 2.02 (s, 3H, CH<sub>3</sub>), 1.98 (s, 6H, CH<sub>3</sub>), 1.96 (s, 6H, CH<sub>3</sub>). Isolated yield: 96%.

#### 4.9.4. General procedure for reaction optimization

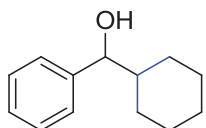
To an ace pressure tube, Mn-MACHO-<sup>i</sup>Pr **Mn-2**, base, 1-phenylethanol **19a** (61.10 mg, 0.50 mmol) and 1,5-pentanediol **20a** were introduced under an argon atmosphere. Toluene (2 mL) was added as a solvent. The pressure tube was sealed and heated to a certain temperature for 24 h. After completion of the reaction, the pressure tube was cooled down and slowly vented while stirring continued. Mesitylene was added as an internal standard to the crude reaction mixture. 1N HCl was added dropwise to the crude reaction mixture until the pH of the solution becomes close to 7 and then the reaction mixture was extracted with DCM (3 x 5 mL) and the organic fraction was washed with water (1 x 5 mL). The organic layer was dried using MgSO<sub>4</sub> and filtered before the composition was analyzed by GC.

#### 4.9.5. General procedure for the preparation of substituted cyclohexanes from secondary alcohols and diols

To an ace pressure tube, Mn-MACHO-<sup>i</sup>Pr **Mn-2** (4.96 mg, 2 mol%), KO<sup>t</sup>Bu (224 mg, 2 mmol), secondary alcohol **19** (0.5 mmol) and diol **20** (2 mmol) were measured under argon atmosphere. Toluene (2 mL) was added as a solvent. The pressure tube was sealed and heated to a 150 °C for a 32 h. After completion of the reaction, the pressure tube was cooled down and slowly vented while stirring continued. Mesitylene was used as an internal standard to the crude reaction mixture. 1N HCl was added drop wise to the crude reaction mixture until the solution becomes neutral. The reaction mixture was further extracted with DCM and water. Organic layer was

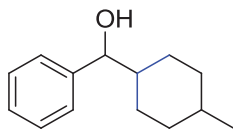
dried using  $\text{MgSO}_4$  and filtered before the composition was analyzed by GC spectrometry. The isolation of pure product was carried out using column chromatography.

**Cyclohexyl(phenyl)methanol (21a):** Prepared by following the general experimental procedure



with: **Mn-2** (4.96 mg, 2 mol%), 1-Phenylethanol **19a** (61.10 mg, 0.50 mmol), 1,5-Pentanediol **20a** (208.0 mg, 2.0 mmol),  $\text{KO}^t\text{Bu}$  (224.0 mg, 2.0 mmol) and toluene (2 mL). Conversion and yield were determined by gas chromatography analysis using mesitylene (61.0 mg, 0.51 mmol) as an internal standard. Isolated yield was also reported after performing column chromatography. The spectral data are in agreement with the reported literature.<sup>[19]</sup>  $^1\text{H NMR}$  (300 MHz,  $\text{CD}_2\text{Cl}_2$ , 298 K)  $\delta$  = 7.25-7.35 (m, 5H, ArCH), 4.35 (d, 1H,  $J$  = 9 Hz, CH), 1.92-1.96 (m, 2H, CH and OH), 1.56-1.74 (m, 4H,  $\text{CH}_2$ ), 0.87-1.38 (m, 6H,  $\text{CH}_2$ );  $^{13}\text{C}\{^1\text{H}\}$ -NMR (75 MHz, toluene- $d_8$ , 298 K):  $\delta$  = 139.54 ( $C_{\text{Ar}}$ ), 123.11 ( $\text{CH}_{\text{Ar}}$ ), 122.21 ( $\text{CH}_{\text{Ar}}$ ), 121.82 ( $\text{CH}_{\text{Ar}}$ ), 74.06 (CH), 40.47 (CH), 24.61 ( $\text{CH}_2$ ), 23.83 ( $\text{CH}_2$ ), 21.82 ( $\text{CH}_2$ ), 21.49 ( $\text{CH}_2$ ), 21.41 ( $\text{CH}_2$ ). HRMS (ESI+) found  $[\text{M}+\text{Na}]^+ = 213.1250$ ;  $\text{C}_{13}\text{H}_{18}\text{ONa}$  requires 213.1250. Isolated yield: 72%.

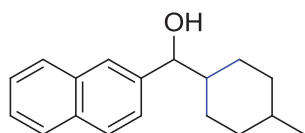
**(4-methylcyclohexyl)(phenyl)methanol (21b):** Prepared by following the general experimental



procedure with: **Mn-2** (4.96 mg, 2.0 mol%), 1-Phenylethanol **19a** (61.10 mg, 0.50 mmol), 3-methylpentane-1,5-diol **20b** (236.34 mg, 2.0 mmol),  $\text{KO}^t\text{Bu}$  (224.0 mg, 2.0 mmol) and toluene (2 mL). Conversion and yield were determined by gas chromatography analysis using mesitylene (63.0 mg, 0.52 mmol) as an internal standard. Isolated yield was also reported after performing column chromatography.  $^1\text{H NMR}$  (300 MHz,  $\text{CD}_2\text{Cl}_2$ , 298 K) (mixture of diastereoisomers)  $\delta$  = 7.23-7.36 (m, 5H, ArCH), 4.50 (d, 1H,  $J$  = 9 Hz, CH)-minor, 4.34 (d, 1H,  $J$  = 9 Hz, CH)-major, 1.93-1.99 (m, 2H, CH & OH), 1.51-1.76 (m, 4H,  $\text{CH}_2$ ), 1.26-1.38 (m, 1H, CH), 0.81-1.09 (m, 7H,  $\text{CH}_2$  &  $\text{CH}_3$ );  $^{13}\text{C}\{^1\text{H}\}$ -NMR (75 MHz,  $\text{CD}_2\text{Cl}_2$ , 298 K) (mixture of diastereoisomers):  $\delta$  = 144.62 ( $C_{\text{Ar}}$ )-minor, 144.41 ( $C_{\text{Ar}}$ )-major, 128.52 ( $\text{CH}_{\text{Ar}}$ )-minor, 128.40 ( $\text{CH}_{\text{Ar}}$ )-major, 127.68 ( $\text{CH}_{\text{Ar}}$ )-minor, 127.56 ( $\text{CH}_{\text{Ar}}$ )-major, 127.01 ( $\text{CH}_{\text{Ar}}$ )-minor, 126.96 ( $\text{CH}_{\text{Ar}}$ )-major, 79.53 (CH)-major, 77.31 (CH)-minor, 45.21 (CH)-major, 43.82 (CH)-minor, 35.27 ( $\text{CH}_2$ )-major, 35.22 ( $\text{CH}_2$ )-major, 33.07 (CH)-major, 31.44 ( $\text{CH}_2$ )-minor, 31.18 ( $\text{CH}_2$ )-minor, 30.74 (CH)-minor, 29.68 ( $\text{CH}_2$ )-major, 29.03 ( $\text{CH}_2$ )-major, 25.33 ( $\text{CH}_2$ )-minor, 24.52 ( $\text{CH}_2$ )-minor, 22.71 ( $\text{CH}_3$ )-

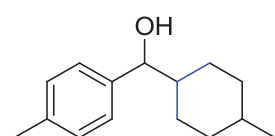
major, 19.63 (CH<sub>3</sub>)-minor. **HRMS** (ESI<sup>+</sup>) found [M+Na]<sup>+</sup> = 227.1408; C<sub>14</sub>H<sub>20</sub>ONa requires 227.1406. Isolated yield: 81%, 90:10 d.r.

**(4-methylcyclohexyl)(naphthalen-2-yl)methanol (21c)**: Prepared by following the general



experimental procedure with: **Mn-2** (4.96 mg, 2.0 mol%), 1-(naphthalen-2-yl)ethanol **19b** (86.10 mg, 0.50 mmol), 3-methylpentane-1,5-diol **20b** (236.34 mg, 2.0 mmol), KO<sup>t</sup>Bu (224.0 mg, 2.0 mmol) and toluene (2 mL). Conversion and yield were determined by gas chromatography analysis using mesitylene (62.0 mg, 0.52 mmol) as an internal standard. Isolated yield was also reported after performing column chromatography. <sup>1</sup>H NMR (300 MHz, CD<sub>2</sub>Cl<sub>2</sub>, 298 K) (mixture of diastereoisomers) δ = 7.60-7.64 (m, 3H, ArCH), 7.52 (s, 1H, ArCH), 7.24-7.30 (m, 3H, ArCH), 4.46 (d, 1H, *J* = 9 Hz, CH)-minor, 4.30 (d, 1H, *J* = 9 Hz, CH)-major, 1.96 (br. s, 1H, OH), 1.76-1.82 (dt, 1H, *J* = 15 Hz, *J* = 3 Hz, CH), 1.38-1.56 (m, 4H, CH<sub>2</sub>), 1.13-1.20 (dt, 1H, *J* = 15 Hz, *J* = 3 Hz, CH), 0.60-0.93 (m, 7H, CH<sub>2</sub>& CH<sub>3</sub>). <sup>13</sup>C{<sup>1</sup>H}-NMR (75 MHz, CD<sub>2</sub>Cl<sub>2</sub>, 298 K) (mixture of diastereoisomers): δ = 142.04 (CH<sub>Ar</sub>)-minor, 141.89 (CH<sub>Ar</sub>)-major, 133.60 (C<sub>Ar</sub>)-minor, 133.56 (C<sub>Ar</sub>)-major, 133.39 (C<sub>Ar</sub>)-minor, 133.32 (C<sub>Ar</sub>)-major, 128.32 (CH<sub>Ar</sub>)-minor, 128.22 (CH<sub>Ar</sub>)-major, 128.12 (CH<sub>Ar</sub>)-major, 127.97 (CH<sub>Ar</sub>)-major, 126.40 (CH<sub>Ar</sub>)-major, 126.04 (CH<sub>Ar</sub>)-major, 125.92 (C<sub>Ar</sub>)-minor, 125.74 (C<sub>Ar</sub>)-major, 125.20 (CH<sub>Ar</sub>)-major, 79.65 (CH)-major, 77.45 (CH)-minor, 45.13 (CH)-major, 43.68 (CH)-minor, 35.27 (CH<sub>2</sub>)-major, 35.24 (CH<sub>2</sub>)-major, 33.08 (CH)-major, 31.46 (CH<sub>2</sub>)-minor, 31.22 (CH<sub>2</sub>)-minor, 29.77 (CH<sub>2</sub>)-major, 29.09 (CH<sub>2</sub>)-major, 25.43 (CH<sub>2</sub>)-minor, 24.59 (CH<sub>2</sub>)-minor, 22.76 (CH<sub>3</sub>)-major. **HRMS** (ESI<sup>+</sup>) found [M+Na]<sup>+</sup> = 277.1558; C<sub>18</sub>H<sub>22</sub>ONa requires 277.1563. Isolated yield: 83%, 87:13 d.r.

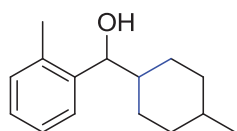
**(4-methylcyclohexyl)(*p*-tolyl)methanol (21d)**: Prepared by following the general experimental



procedure with: **Mn-2** (4.96 mg, 2.0 mol%), 1-(*p*-tolyl)ethanol **19c** (68.1 mg, 0.50 mmol), 3-methylpentane-1,5-diol **20b** (236.34 mg, 2.0 mmol), KO<sup>t</sup>Bu (224.0 mg, 2.0 mmol) and toluene (2 mL). Conversion and yield were determined by gas chromatography analysis using mesitylene (61.0 mg, 0.51 mmol) as an internal standard. Isolated yield was also reported after performing column chromatography. <sup>1</sup>H NMR (300 MHz, CD<sub>2</sub>Cl<sub>2</sub>, 298 K) (mixture of diastereoisomers) δ = 7.03-7.12 (m, 4H, ArCH), 4.37 (d, 1H, *J* = 9 Hz, CH)-minor, 4.20 (d, 1H, *J* = 9 Hz, CH)-major, 2.24

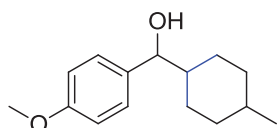
(s, 3H,  $CH_3$ ), 1.79-1.91 (m, 2H,  $CH$  &  $OH$ ), 1.36-1.67 (m, 4H,  $CH_2$ ), 1.05-1.28 (m, 4H,  $CH_2$ ), 0.71-0.94 (m, 4H,  $CH$  &  $CH_3$ );  $^{13}C\{^1H\}$ -NMR (75 MHz,  $CD_2Cl_2$ , 298 K) (mixture of diastereoisomers):  $\delta$  = 141.38 ( $C_{Ar}$ )-minor, 140.87 ( $C_{Ar}$ )-major, 137.41 ( $C_{Ar}$ )-minor, 137.29 ( $C_{Ar}$ )-major, 129.19 ( $CH_{Ar}$ )-minor, 129.07 ( $CH_{Ar}$ )-major, 126.87 ( $CH_{Ar}$ )-major, 79.41 (CH)-major, 77.08 (CH)-minor, 45.16 (CH)-major, 43.72 (CH)-minor, 35.26 ( $CH_2$ )-major, 35.22 ( $CH_2$ )-major, 33.08 (CH)-major, 31.41 ( $CH_2$ )-minor, 31.16 ( $CH_2$ )-minor, 30.09 (CH)-minor, 29.76 ( $CH_2$ )-minor, 29.67 (CH)-major, 29.16 ( $CH_2$ )-major, 22.74 ( $CH_3$ )-major, 21.19 ( $CH_3$ )-major. **HRMS** (ESI+) found  $[M+Na]^+ = 241.1568$ ;  $C_{15}H_{22}ONa$  requires 241.1563. Isolated yield: 78%, 92:8 d.r.

**(4-methylcyclohexyl)(*o*-tolyl)methanol (21e)**: Prepared by following the general experimental



procedure with: **Mn-2** (4.96 mg, 2.0 mol%), 1-(*o*-tolyl)ethanol **19d** (61.1 mg, 0.50 mmol), 3-methylpentane-1,5-diol **20b** (236.34 mg, 2.0 mmol),  $KO^tBu$  (224.0 mg, 2.0 mmol) and toluene (2 mL). Conversion and yield were determined by gas chromatography analysis using mesitylene (55.0 mg, 0.46 mmol) as an internal standard. Isolated yield was also reported after performing column chromatography.  $^1H$  NMR (300 MHz,  $CD_2Cl_2$ , 298 K) (mixture of diastereoisomers)  $\delta$  = 7.39 (d, 1H,  $J$  = 6 Hz,  $ArCH$ ), 7.18-7.23 (m, 1H,  $ArCH$ ), 7.12-7.16 (m, 2H,  $ArCH$ ), 4.76 (d, 1H,  $J$  = 6 Hz,  $CH$ )-minor, 4.64 (d, 1H,  $J$  = 6 Hz,  $CH$ )-major, 2.36 (s, 3H,  $CH_3$ )-minor, 2.33 (s, 3H,  $CH_3$ )-major, 1.94-2.03 (dq, 1H,  $J$  = 15 Hz,  $J$  = 3 Hz,  $CH$ ), 1.88 (br. s, 1H,  $OH$ ), 1.71-1.79 (dq, 1H,  $J$  = 12 Hz,  $J$  = 3 Hz,  $CH$ ), 1.50-1.68 (m, 2H,  $CH_2$ ), 1.29-1.38 (m, 2H,  $CH_2$ ), 1.09-1.19 (m, 2H,  $CH_2$ ), 0.83-0.92 (m, 5H,  $CH_3$  &  $CH_2$ ).  $^{13}C\{^1H\}$ -NMR (75 MHz,  $CD_2Cl_2$ , 298 K)  $\delta$  = 142.92 ( $C_{Ar}$ ), 135.68 ( $C_{Ar}$ ), 130.69 ( $CH_{Ar}$ ), 127.36 ( $CH_{Ar}$ ), 126.79 ( $CH_{Ar}$ ), 126.40 ( $CH_{Ar}$ ), 75.38 (CH), 44.79 (CH), 35.55 ( $CH_2$ ), 35.39 ( $CH_2$ ), 33.28 (CH), 30.05 ( $CH_2$ ), 28.88 ( $CH_2$ ), 22.94 ( $CH_3$ ), 19.75 ( $CH_3$ ). **HRMS** (EI+) found  $[M]^+ = 218.1663$ ;  $C_{15}H_{22}O$  requires 218.1665. Isolated yield: 72%, 89:11 d.r.

**(4-methoxyphenyl)(4-methylcyclohexyl)methanol (21f)**: Prepared by following the general

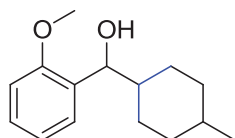


experimental procedure with: **Mn-2** (4.96 mg, 2.0 mol%), 1-(4-methoxyphenyl)ethanol **19e** (76.0 mg, 0.50 mmol), 3-methylpentane-1,5-diol **20b** (236.34 mg, 2.0 mmol),  $KO^tBu$  (224.0 mg, 2.0 mmol) and toluene (2 mL). Conversion and yield were determined by gas chromatography



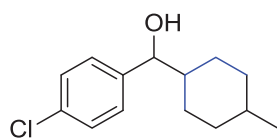
analysis using mesitylene (59.0 mg, 0.49 mmol) as an internal standard. Isolated yield was also reported after performing column chromatography.  $^1\text{H NMR}$  (300 MHz,  $\text{CD}_2\text{Cl}_2$ , 298 K) (mixture of diastereoisomers)  $\delta = 7.18$  (d, 2H,  $J = 9$  Hz, ArCH), 6.84 (d, 2H,  $J = 9$  Hz, ArCH), 4.43 (d, 1H,  $J = 9$  Hz, CH)-minor, 4.25 (d, 1H,  $J = 6$  Hz, CH)-major, 3.77 (s, 3H,  $\text{CH}_3$ ), 1.94-1.99 (m, 1H, CH), 1.86 (br s, 1H, -OH), 1.68-1.74 (m, 1H, CH), 1.58-1.63 (m, 2H,  $\text{CH}_2$ ), 1.17-1.34 (m, 2H,  $\text{CH}_2$ ), 0.75-1.09 (m, 7H,  $\text{CH}_2$  &  $\text{CH}_3$ ).  $^{13}\text{C}\{^1\text{H}\}$ -NMR (75 MHz,  $\text{CD}_2\text{Cl}_2$ , 298 K)  $\delta = 159.50$  ( $\text{C}_{\text{Ar}}$ ), 136.68 ( $\text{C}_{\text{Ar}}$ ), 128.27 ( $\text{CH}_{\text{Ar}}$ ), 113.95 ( $\text{CH}_{\text{Ar}}$ ), 79.27 (CH), 55.74 ( $\text{CH}_3$ ), 45.37 (CH), 35.40 ( $\text{CH}_2$ ), 33.27 (CH), 29.81 ( $\text{CH}_2$ ), 29.50 ( $\text{CH}_2$ ), 22.91 ( $\text{CH}_3$ ). HRMS (ESI+) found  $[\text{M}+\text{Na}]^+ = 257.1518$ ;  $\text{C}_{15}\text{H}_{22}\text{Na}_1\text{O}_2$  requires 257.1512. Isolated yield: 71%, 87:13 d.r.

**(2-methoxyphenyl)(4-methylcyclohexyl)methanol (21g):** Prepared by following the general



experimental procedure with: **Mn-2** (4.96 mg, 2.0 mol%), 1-(2-methoxyphenyl)ethanol **19f** (76.0 mg, 0.50 mmol), 3-methylpentane-1,5-diol **20b** (236.34 mg, 2.0 mmol),  $\text{KO}^t\text{Bu}$  (224.0 mg, 2.0 mmol) and toluene (2 mL). Conversion and yield were determined by gas chromatography analysis using mesitylene (63.0 mg, 0.52 mmol) as an internal standard. Isolated yield was also reported after performing column chromatography.  $^1\text{H NMR}$  (300 MHz,  $\text{CD}_2\text{Cl}_2$ , 298 K) (mixture of diastereoisomers)  $\delta = 7.20$ -7.25 (m, 2H, ArCH), 6.88-6.95 (m, 2H, ArCH), 4.66 (t, 1H,  $J = 9$  Hz, CH)-minor, 4.48 (t, 1H,  $J = 9$  Hz, CH), 3.82 (s, 3H,  $\text{CH}_3$ ), 2.46-2.48 (m, 1H, OH), 1.97-2.05 (dq, 1H,  $J = 15$  Hz,  $J = 3$  Hz, CH), 1.69-1.77 (dq, 1H,  $J = 12$  Hz,  $J = 3$  Hz, CH), 1.56-1.65 (m, 2H,  $\text{CH}_2$ ), 1.23-1.34 (m, 2H,  $\text{CH}_2$ ), 1.00-1.09 (m, 2H,  $\text{CH}_2$ ), 0.79-0.90 (m, 5H,  $\text{CH}_3$  &  $\text{CH}_2$ ).  $^{13}\text{C}\{^1\text{H}\}$ -NMR (75 MHz,  $\text{CD}_2\text{Cl}_2$ , 298 K)  $\delta = 157.39$  ( $\text{C}_{\text{Ar}}$ ), 132.34 ( $\text{C}_{\text{Ar}}$ ), 128.65 ( $\text{CH}_{\text{Ar}}$ ), 128.53 ( $\text{CH}_{\text{Ar}}$ ), 120.89 ( $\text{CH}_{\text{Ar}}$ ), 111.14 ( $\text{CH}_{\text{Ar}}$ ), 76.52 (CH), 55.77 ( $\text{CH}_3$ ), 44.24 (CH), 35.59 ( $\text{CH}_2$ ), 35.49 ( $\text{CH}_2$ ), 33.30 (CH), 30.29 ( $\text{CH}_2$ ), 29.50 ( $\text{CH}_2$ ), 22.96 ( $\text{CH}_3$ ). HRMS (ESI+) found  $[\text{M}+\text{Na}]^+ = 257.1518$ ;  $\text{C}_{15}\text{H}_{22}\text{NaO}_2$  requires 257.1512. Isolated yield: 44%, 88:12 d.r.

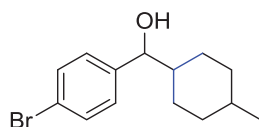
**(4-chlorophenyl)(4-methylcyclohexyl)methanol (21h):** Prepared by following the general



experimental procedure with: **Mn-2** (4.96 mg, 2.0 mol%), 1-(4-chlorophenyl)ethanol **19g** (78.3 mg, 0.50 mmol), 3-methylpentane-1,5-diol **20b** (236.34 mg, 2.0 mmol),  $\text{KO}^t\text{Bu}$  (224.0 mg, 2.0 mmol) and toluene (2 mL),  $t = 14$  h. Conversion and yield were determined by gas chromatography analysis using mesitylene (60.0 mg, 0.50 mmol) as an internal standard. Isolated

yield was also reported after performing column chromatography.  $^1\text{H NMR}$  (300 MHz,  $\text{CD}_2\text{Cl}_2$ , 298 K) (mixture of diastereoisomers)  $\delta = 7.20\text{-}7.24$  (m, 3H, ArCH), 7.14-7.17 (m, 1H, ArCH), 4.42 (d, 1H,  $J = 6$  Hz, CH)-minor, 4.27 (d, 1H,  $J = 6$  Hz, CH)-major, 1.79-1.87 (m, 2H, OH & CH), 1.51-1.67 (m, 3H, CH &  $\text{CH}_2$ ), 1.23-1.54 (m, 4H,  $\text{CH}_2$ ), 0.83- 0.86 (m, 2H,  $\text{CH}_2$ ), 0.76 (d, 3H,  $J = 6$  Hz,  $\text{CH}_3$ ).  $^{13}\text{C}\{^1\text{H}\}$ -NMR (75 MHz,  $\text{CD}_2\text{Cl}_2$ , 298 K)  $\delta = 142.95$  ( $\text{C}_{\text{Ar}}$ )-major, 139.76 ( $\text{C}_{\text{Ar}}$ )-minor, 133.03 ( $\text{C}_{\text{Ar}}$ ), 128.47 ( $\text{CH}_{\text{Ar}}$ )-major, 128.42 ( $\text{CH}_{\text{Ar}}$ )-major, 128.07 ( $\text{CH}_{\text{Ar}}$ )-minor, 78.74 (CH)-major, 77.78 (CH)-minor, 45.23 (CH), 35.19 ( $\text{CH}_2$ )-major, 35.14 ( $\text{CH}_2$ )-major, 34.01 ( $\text{CH}_2$ )-minor, 33.89 ( $\text{CH}_2$ )-minor, 33.07 (CH)-minor, 33.03 (CH)-major, 31.15 ( $\text{CH}_2$ )-minor, 31.02 ( $\text{CH}_2$ )-minor, 29.53 ( $\text{CH}_2$ )-major, 28.80 ( $\text{CH}_2$ )-major, 24.04 ( $\text{CH}_3$ )-minor, 22.66 ( $\text{CH}_3$ )-major. HRMS (EI+) found  $[\text{M}]^+ = 238.1085$ ;  $\text{C}_{14}\text{H}_{19}\text{ClO}$  requires 238.1119. Isolated yield: 62%, 93:7 d.r.

**(4-bromophenyl)(4-methylcyclohexyl)methanol (21i)**: Prepared by following the general

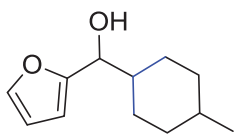


experimental procedure with: **Mn-2** (4.96 mg, 2.0 mol%), 1-(4-bromophenyl)ethan-1-ol **19h** (100.5 mg, 0.50 mmol), 3-methylpentane-1,5-diol **20b** (236.34 mg, 2.0 mmol),  $\text{KO}^t\text{Bu}$  (224.0 mg, 2.0 mmol) and toluene (2 mL),  $t = 14$  h. Conversion and yield were determined by gas chromatography analysis using mesitylene (59.0 mg, 0.49 mmol) as an internal standard. Isolated

yield was also reported after performing column chromatography.  $^1\text{H NMR}$  (300 MHz,  $\text{CDCl}_3$ , 298 K) (mixture of diastereoisomers)  $\delta = 7.38$  (d, 2H,  $J = 8.41$  Hz, ArCH), 7.09 (d, 2H,  $J = 8.42$  Hz, ArCH), 4.43 (t, 1H,  $J = 8.35$  Hz, CH)-minor, 4.27 (dd, 1H,  $J = 7.02, 5.35$  Hz, CH)-major, 1.82-1.97 (m, 1H, CH), 1.77 (br s, 1H, OH), 1.61-1.70 (m, 2H,  $\text{CH}_2$ ), 1.51-1.60 (m, 1H, CH), 1.36-1.49 (m, 1H, CH), 1.24-1.33 (m, 1H, CH), 1.12-1.22 (m, 1H, CH), 0.93-1.02 (m, 1H, CH), 0.81-0.89 (m, 2H,  $\text{CH}_2$ ), 0.78 (d, 3H,  $J = 6.53$  Hz,  $\text{CH}_3$ ).  $^{13}\text{C}\{^1\text{H}\}$ -NMR (75 MHz,  $\text{CD}_2\text{Cl}_2$ , 298 K)  $\delta = 142.63$  ( $\text{C}_{\text{Ar}}$ ), 131.26 ( $\text{CH}_{\text{Ar}}$ ), 128.34 ( $\text{CH}_{\text{Ar}}$ ), 126.62 ( $\text{C}_{\text{Ar}}$ ), 78.71 (CH), 44.72 (CH), 34.77 ( $\text{CH}_2$ ), 34.72 ( $\text{CH}_2$ ), 32.62 ( $\text{CH}_2$ ), 28.80 ( $\text{CH}_2$ ), 28.55 ( $\text{CH}_2$ ), 22.57 ( $\text{CH}_3$ ). HRMS for **21i** (ESIpos+neg) found  $[\text{M}-\text{H}]^- = 281.054960$ ;  $\text{C}_{14}\text{H}_{18}\text{Br}_1\text{O}_1$  requires 281.054665. HRMS for the de-brominated product **21b** (ESIpos+neg) found  $[\text{M}+\text{Na}]^+ = 227.140630$ ;  $\text{C}_{14}\text{H}_{20}\text{O}_1\text{Na}_1$  requires 227.140634. Isolated Yield for **21i**: 40% (33% of de-brominated product **21b** was also obtained), 89:11 d.r.

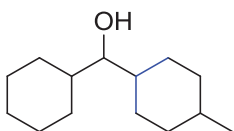


**Furan-2-yl(4-methylcyclohexyl)methanol (21j):** Prepared by following the general experimental procedure with: **Mn-2** (4.96 mg, 2.0 mol%), 1-(furan-2-yl)ethan-1-ol **19i** (56.1 mg, 0.50 mmol), 3-methylpentane-1,5-diol **20b** (177.25 mg, 1.5 mmol), KO<sup>t</sup>Bu (224.0 mg, 2.0 mmol) and toluene (2 mL).



Conversion and yield were determined by gas chromatography analysis using mesitylene (60.0 mg, 0.50 mmol) as an internal standard. Isolated yield was also reported after performing column chromatography. <sup>1</sup>H NMR (300 MHz, CDCl<sub>3</sub>, 298 K) (mixture of diastereoisomers)  $\delta$  = 7.36-7.37 (m, 1H, ArCH), 6.32 (dd, 1H,  $J$  = 3.21, 1.83, ArCH), 6.20-6.24 (m, 1H, ArCH), 4.57 (d, 1H,  $J$  = 8.96 Hz, CH)-minor, 4.37 (d, 1H,  $J$  = 7.45 Hz, CH)-major, 1.99 (dq, 1H,  $J$  = 11.65, 2.75 Hz, CH), 1.64-1.78 (m, 3H, CH<sub>2</sub> & CH), 1.39-1.46 (m, 1H, CH), 1.22-1.34 (m, 1H, CH), 0.90-1.08 (m, 4H, CH<sub>2</sub>), 0.87 (d, 3H,  $J$  = 6.50 Hz, CH<sub>3</sub>). <sup>13</sup>C{<sup>1</sup>H}-NMR (101 MHz, CDCl<sub>3</sub>, 298 K)  $\delta$  = 156.29 (C<sub>Ar</sub>)-minor, 156.25 (C<sub>Ar</sub>)-major, 141.94 (CH<sub>Ar</sub>)-minor, 141.85 (CH<sub>Ar</sub>)-major, 110.15 (CH<sub>Ar</sub>)-major, 106.82 (CH<sub>Ar</sub>)-minor, 106.68 (CH<sub>Ar</sub>)-major, 72.97 (CH)-major, 70.40 (CH)-minor, 42.81 (CH)-major, 41.08 (CH)-minor, 34.87 (CH<sub>2</sub>)-major, 34.83 (CH<sub>2</sub>)-major, 34.44 (CH)-minor, 32.77 (CH)-major, 31.05 (CH<sub>2</sub>)-minor, 30.71 (CH<sub>2</sub>)-minor, 29.15 (CH<sub>2</sub>)-major, 28.90 (CH<sub>2</sub>)-major, 25.18 (CH<sub>2</sub>)-minor, 24.40 (CH<sub>2</sub>)-minor, 22.72 (CH<sub>3</sub>)-minor. HRMS (ESI<sup>+</sup>) found [M+Na]<sup>+</sup> = 217.120000; C<sub>12</sub>H<sub>18</sub>O<sub>2</sub>Na<sub>1</sub> requires 217.119899, Isolated yield: 64%, 87:13 d.r.

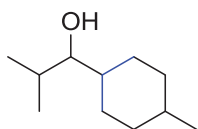
**Cyclohexyl(4-methylcyclohexyl)methanol (21k):** Prepared by following the general experimental procedure with: **Mn-2** (4.96 mg, 2.0 mol%), 1-cyclohexylethanol **19j** (64.1 mg, 0.50 mmol), 3-methylpentane-1,5-diol **20b** (236.34 mg, 2.0 mmol), KO<sup>t</sup>Bu (224.0 mg, 2.0 mmol) and toluene (2 mL).



Conversion and yield were determined by gas chromatography analysis using mesitylene (63.0 mg, 0.52 mmol) as an internal standard. Isolated yield was also reported after performing column chromatography. <sup>1</sup>H NMR (300 MHz, CD<sub>2</sub>Cl<sub>2</sub>, 298 K) (mixture of diastereoisomers)  $\delta$  = 3.50 (t, 1H,  $J$  = 6 Hz, CH)-minor, 2.93 (t, 1H,  $J$  = 6 Hz, CH)-major, 1.53-1.74 (m, 8H, CH<sub>2</sub>), 1.45-1.49 (m, 3H, CH), 1.03-1.21 (m, 8H, CH<sub>2</sub>), 0.86-0.88 (m, 2H, CH<sub>2</sub>), 0.78 (d, 3H,  $J$  = 9 Hz, CH<sub>3</sub>). <sup>13</sup>C{<sup>1</sup>H}-NMR (75 MHz, CD<sub>2</sub>Cl<sub>2</sub>, 298 K)  $\delta$  = 80.73 (CH), 40.65 (CH), 40.13 (CH), 35.80 (CH<sub>2</sub>), 35.53 (CH<sub>2</sub>), 33.36 (CH), 30.59 (CH<sub>2</sub>), 30.45 (CH<sub>2</sub>), 27.90 (CH<sub>2</sub>), 27.78 (CH<sub>2</sub>), 27.19

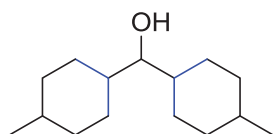
(CH<sub>2</sub>), 27.09 (CH<sub>2</sub>), 26.79 (CH), 23.01 (CH<sub>3</sub>). **HRMS** (EI+) found [M-H<sub>2</sub>O]<sup>+</sup> = 192.1860; C<sub>14</sub>H<sub>24</sub> requires 192.1878,. Isolated yield: 60%, 62:38 d.r.

**2-methyl-1-(4-methylcyclohexyl)propan-1-ol (21l):** Prepared by following the general experimental procedure with: **Mn-2** (4.96 mg, 2.0 mol%), 3-methylbutan-2-ol **19k** (44.1 mg, 0.50 mmol), 3-methylpentane-1,5-diol **20b** (177.25 mg, 1.5 mmol), KO<sup>t</sup>Bu (224.0 mg, 2.0 mmol) and toluene (2 mL). Conversion and



yield were determined by gas chromatography analysis using mesitylene (62.0 mg, 0.52 mmol) as an internal standard. Isolated yield was also reported after performing column chromatography. <sup>1</sup>H NMR (300 MHz, CDCl<sub>3</sub>, 298 K) (mixture of diastereoisomers) δ = 3.25 (t, 1H, J = 4.95 Hz, CH)-minor, 3.03 (t, 1H, J = 5.74 Hz, CH), 1.83-1.92 (m, 1H, CH), 1.68-1.79 (m, 3H, CH<sub>2</sub> & OH), 1.54-1.63 (m, 1H, CH), 1.21-1.40 (m, 4H, CH<sub>2</sub>), 0.96-1.18 (m, 2H, CH<sub>2</sub>), 0.85-0.95 (m, 10H, CH<sub>3</sub> & CH<sub>2</sub>). <sup>13</sup>C{<sup>1</sup>H}-NMR (75 MHz, CDCl<sub>3</sub>, 298 K) δ = 81.19 (CH)-major, 40.42 (CH)-major, 39.50 (CH)-minor, 35.30 (CH<sub>2</sub>)-major, 35.04 (CH<sub>2</sub>)-major, 34.21 (CH<sub>2</sub>)-minor, 33.83 (CH<sub>2</sub>)-minor, 32.86 (CH)-major, 32.13 (CH)-minor, 31.46 (CH<sub>2</sub>)-minor, 31.10 (CH<sub>2</sub>)-minor, 30.08 (CH<sub>2</sub>)-major, 29.91 (CH<sub>2</sub>)-major, 28.62 (CH)-minor, 27.70 (CH)-major, 22.81 (CH<sub>3</sub>)-major, 20.03 (CH<sub>3</sub>)-major, 16.67 (CH<sub>3</sub>)-major. **HRMS** (ESI+) found [M+Na]<sup>+</sup> = 193.156360; C<sub>11</sub>H<sub>22</sub>O<sub>1</sub>Na<sub>1</sub> requires 193.156284. Isolated yield: 67%, 88:12 d.r.

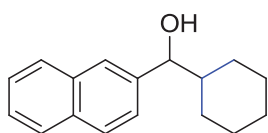
**Bis(4-methylcyclohexyl)methanol (21m):** Prepared by following the general experimental procedure with: **Mn-2** (4.96 mg, 2.0 mol%), *iso*-propanol **19l** (30.0 mg, 0.50 mmol), 3-methylpentane-1,5-diol **20b** (354.5 mg, 3.0 mmol), KO<sup>t</sup>Bu (448.8 mg, 4.0 mmol) and toluene (2 mL). Conversion and yield



were determined by gas chromatography analysis using mesitylene (60.0 mg, 0.50 mmol) as an internal standard. Isolated yield was also reported after performing column chromatography. <sup>1</sup>H NMR (300 MHz, CDCl<sub>3</sub>, 298 K) (mixture of diastereoisomers) δ = 3.17 (t, 1H, J = 6 Hz, CH)-minor, 2.99 (t, 1H, J = 5.65 Hz, CH)-major, 1.72-1.79 (m, 2H, CH), 1.62-1.70 (m, 4H, CH<sub>2</sub>), 1.45-1.52 (m, 2H, CH), 1.42 (br s, 1H, OH), 1.14-1.37 (m, 6H, CH<sub>2</sub>), 0.92-1.11 (m, 4H, CH<sub>2</sub>), 0.85-0.88 (m, 2H, CH<sub>2</sub>), 0.80 (d, 6H, J = 6.46 Hz, CH<sub>3</sub>). <sup>13</sup>C{<sup>1</sup>H}-NMR (75 MHz, CDCl<sub>3</sub>, 298 K) δ = 80.49 (CH)-major, 78.40 (CH)-minor, 39.87 (CH)-major, 39.47 (CH)-minor, 39.06 (CH)-minor, 35.46 (CH<sub>2</sub>)-minor, 35.36 (CH<sub>2</sub>)-major, 35.10 (CH<sub>2</sub>)-minor, 35.06 (CH<sub>2</sub>)-major, 32.91 (CH)-minor, 32.87 (CH)-major, 31.54 (CH)-minor, 31.15 (CH)-minor, 30.38 (CH<sub>2</sub>)-minor,

30.00 (CH<sub>2</sub>)-major, 28.99 (CH<sub>2</sub>)-minor, 27.35 (CH<sub>2</sub>)-major, 26.24 (CH<sub>2</sub>)-minor, 25.18 (CH<sub>2</sub>)-minor, 23.14 (CH<sub>3</sub>)-minor, 22.82 (CH<sub>3</sub>)-major, 19.18 (CH<sub>3</sub>)-minor. **HRMS** (ESI+) found [M+Na]<sup>+</sup> = 247.203200; C<sub>15</sub>H<sub>28</sub>O<sub>1</sub>Na<sub>1</sub> requires 247.203234. Isolated yield: 51%, 78:22:0 d.r.

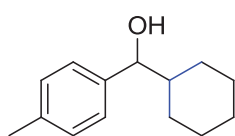
**Cyclohexyl(naphthalen-2-yl)methanol (21n):** Prepared by following the general experimental



procedure with: **Mn-2** (4.96 mg, 2.0 mol%), 1-(naphthalen-2-yl)ethanol **19b** (86.10 mg, 0.50 mmol), 1,5-Pentanediol **20a** (208.0 mg, 2.0 mmol), KO<sup>t</sup>Bu (224.0 mg, 2.0 mmol) and toluene (2 mL). Conversion and yield

were determined by gas chromatography analysis using mesitylene (60.0 mg, 0.50 mmol) as an internal standard. Isolated yield was also reported after performing column chromatography. The spectral data are in agreement with the reported literature.<sup>[20]</sup> **<sup>1</sup>H NMR** (300 MHz, CD<sub>2</sub>Cl<sub>2</sub>, 298 K) δ = 7.72-7.76 (m, 3H, ArCH), 7.64 (s, 1H, ArCH), 7.35-7.39 (m, 3H, ArCH), 4.44 (d, 1H, *J* = 9 Hz, CH), 1.87-1.95 (m, 2H, CH & OH), 1.47-1.70 (m, 4H, CH<sub>2</sub>), 0.87-1.32 (m, 6H, CH<sub>2</sub>); **<sup>13</sup>C{<sup>1</sup>H}-NMR** (75 MHz, CD<sub>2</sub>Cl<sub>2</sub>, 298 K): δ = 142.00 (C<sub>Ar</sub>), 133.77 (C<sub>Ar</sub>), 133.52 (C<sub>Ar</sub>), 128.39 (C<sub>Ar</sub>), 128.29 (C<sub>Ar</sub>), 128.14 (C<sub>Ar</sub>), 126.57 (C<sub>Ar</sub>), 126.21 (C<sub>Ar</sub>), 125.94 (C<sub>Ar</sub>), 125.39 (C<sub>Ar</sub>), 79.78 (CH), 45.62 (CH), 30.06 (CH<sub>2</sub>), 29.31 (CH<sub>2</sub>), 27.08 (CH<sub>2</sub>), 26.75 (CH<sub>2</sub>), 26.69 (CH<sub>2</sub>). **HRMS**(ESI+) found [M+Na]<sup>+</sup> = 263.1409; C<sub>17</sub>H<sub>20</sub>ONa requires 263.1406. Isolated yield: 70%.

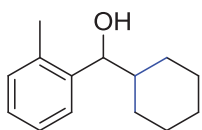
**Cyclohexyl(*p*-tolyl)methanol (21o):** Prepared by following the general experimental procedure with: **Mn-2** (4.96 mg, 2.0 mol%), 1-(*p*-tolyl)ethanol **19c** (68.10 mg, 0.50 mmol), 1,5-Pentanediol



**20a** (208.0 mg, 2.0 mmol), KO<sup>t</sup>Bu (224.0 mg, 2.0 mmol) and toluene (2 mL). Conversion and yield were determined by gas chromatography analysis using mesitylene (62.0 mg, 0.52 mmol) as an internal standard.

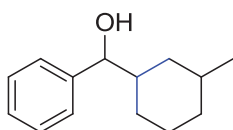
Isolated yield was also reported after performing column chromatography. The spectral data are in agreement with the reported literature.<sup>[21]</sup> **<sup>1</sup>H NMR** (300 MHz, CD<sub>2</sub>Cl<sub>2</sub>, 298 K) δ = 7.13-7.19 (m, 4H, ArCH), 4.30 (d, 1H, *J* = 9 Hz, CH), 2.33 (s, 3H, CH<sub>3</sub>), 1.87-1.97 (m, 2H, CH & OH), 1.51-1.77 (m, 4H, CH<sub>2</sub>), 0.86-1.37 (m, 6H, CH<sub>2</sub>); **<sup>13</sup>C{<sup>1</sup>H}-NMR** (75 MHz, CD<sub>2</sub>Cl<sub>2</sub>, 298 K): δ = 141.52 (C<sub>Ar</sub>), 137.50 (C<sub>Ar</sub>), 129.28 (C<sub>Ar</sub>), 127.11 (C<sub>Ar</sub>), 79.55 (CH), 45.65 (CH), 29.96 (CH<sub>2</sub>), 29.42 (CH<sub>2</sub>), 27.10 (CH<sub>2</sub>), 26.75 (CH<sub>2</sub>), 26.68 (CH<sub>2</sub>), 21.38 (CH<sub>3</sub>). **HRMS**(ESI+) found [M+Na]<sup>+</sup> = 227.1402; C<sub>14</sub>H<sub>20</sub>ONa requires 227.1406. Isolated yield: 71%.

**Cyclohexyl(*o*-tolyl)methanol (21p):** Prepared by following the general experimental procedure



with: **Mn-2** (4.96 mg, 2.0 mol%), 1-(*o*-tolyl)ethanol **19d** (61.10 mg, 0.50 mmol), 1,5-Pentanediol **20a** (156.0 mg, 1.50 mmol), KO<sup>t</sup>Bu (224.0 mg, 2.0 mmol) and toluene (2 mL). Conversion and yield were determined by gas chromatography analysis using mesitylene (59.0 mg, 0.49 mmol) as an internal standard. Isolated yield was also reported after performing column chromatography. The spectral data are in agreement with the reported literature.<sup>[22]</sup> <sup>1</sup>H NMR (300 MHz, CD<sub>2</sub>Cl<sub>2</sub>, 298 K)  $\delta$  = 7.28-7.31 (m, 1H, ArCH), 7.08-7.13 (m, 1H, ArCH), 7.02-7.06 (m, 2H, ArCH), 4.54 (d, 1H,  $J$  = 6 Hz, CH<sub>2</sub>), 2.23 (s, 3H, CH<sub>3</sub>), 1.86-1.90 (m, 1H, CH), 1.66-1.73 (m, 2H, CH<sub>2</sub>), 1.46-1.60 (m, 4H, CH<sub>2</sub>), 1.24-1.29 (m, 1H, OH), 0.94-1.20 (m, 4H, CH<sub>2</sub>). <sup>13</sup>C{<sup>1</sup>H}-NMR (75 MHz, CD<sub>2</sub>Cl<sub>2</sub>, 298 K):  $\delta$  = 142.82 (C<sub>Ar</sub>), 135.73 (C<sub>Ar</sub>), 130.69 (CH<sub>Ar</sub>), 127.36 (CH<sub>Ar</sub>), 126.81 (CH<sub>Ar</sub>), 126.39 (CH<sub>Ar</sub>), 75.42 (CH), 45.07 (CH), 30.17 (CH<sub>2</sub>), 28.96 (CH<sub>2</sub>), 27.07 (CH<sub>2</sub>), 26.89 (CH<sub>2</sub>), 26.67 (CH<sub>2</sub>), 19.74 (CH<sub>2</sub>). HRMS (EI<sup>+</sup>) found [M]<sup>+</sup> = 204.1510; C<sub>14</sub>H<sub>20</sub>O requires 204.1509. Isolated yield: 82%.

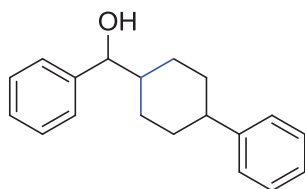
**(3-methylcyclohexyl)(phenyl)methanol (21q):** Prepared by following the general experimental



procedure with: **Mn-2** (4.96 mg, 2 mol%), 1-Phenylethanol **19a** (61.10 g, 0.50 mmol), 2-methylpentane-1,5-diol **20c** (236.34 mg, 2.0 mmol), KO<sup>t</sup>Bu (224.0 mg, 2.0 mmol) and toluene (2 mL). Conversion and yield were determined by gas chromatography analysis using mesitylene (60.0 mg, 0.50 mmol) as an internal standard. Isolated yield was also reported after performing column chromatography. <sup>1</sup>H NMR (300 MHz, CD<sub>2</sub>Cl<sub>2</sub>, 298 K) (mixture of diastereoisomers)  $\delta$  = 7.14-7.27 (m, 5H, ArCH), 4.46 (dd, 1H,  $J$  = 6 Hz,  $J$  = 2.1 Hz, CH), 4.37-4.42 (dt, 1H,  $J$  = 9 Hz,  $J$  = 3 Hz, CH), 4.30-4.34 (m, 1H, CH), 4.23-4.26 (m, 1H, CH), 1.74-1.92 (m, 2H, CH & OH), 1.43-1.65 (m, 4H, CH<sub>2</sub>), 1.02-1.37 (m, 3H, CH & CH<sub>2</sub>), 0.83-0.94 (m, 1H, CH), 0.71-0.82 (m, 3H, CH<sub>3</sub>), 0.51-0.69 (m, 1H, CH). <sup>13</sup>C{<sup>1</sup>H}-NMR (75 MHz, CD<sub>2</sub>Cl<sub>2</sub>, 298 K) (mixture of diastereoisomers)  $\delta$  = 144.39 (C<sub>Ar</sub>), 144.37 (C<sub>Ar</sub>), 144.31 (C<sub>Ar</sub>), 143.68 (C<sub>Ar</sub>), 128.51 (CH<sub>Ar</sub>), 128.43 (CH<sub>Ar</sub>), 127.59 (CH<sub>Ar</sub>), 127.48 (CH), 127.03 (CH<sub>Ar</sub>), 126.98 (CH<sub>Ar</sub>), 126.88 (CH<sub>Ar</sub>), 126.69 (CH<sub>Ar</sub>), 122.48 (CH<sub>Ar</sub>), 121.24 (CH<sub>Ar</sub>), 79.56 (CH), 79.47 (CH), 78.36 (CH), 77.63 (CH), 45.46 (CH), 43.84 (CH), 43.65 (CH), 38.34 (CH<sub>2</sub>), 37.66 (CH<sub>2</sub>), 35.52 (CH), 32.86 (CH<sub>2</sub>), 32.80 (CH<sub>2</sub>), 30.50 (CH), 29.30 (CH<sub>2</sub>), 28.63 (CH<sub>2</sub>), 26.38 (CH<sub>2</sub>), 26.30 (CH<sub>2</sub>), 24.21 (CH<sub>2</sub>), 24.14 (CH<sub>2</sub>), 23.77 (CH<sub>2</sub>), 23.11 (CH<sub>2</sub>), 23.04 (CH<sub>2</sub>), 22.33(CH<sub>3</sub>), 22.00 (CH<sub>3</sub>), 21.93 (CH<sub>3</sub>) 21.75 (CH<sub>3</sub>).

**HRMS** (EI<sup>+</sup>) found  $[M]^+$  = 204.1506; C<sub>14</sub>H<sub>20</sub>O requires 204.1509. Isolated yield: 74%. 55:16:10:19 d.r.

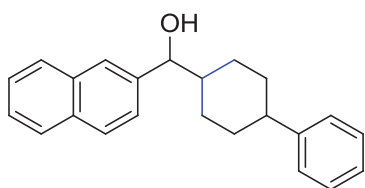
**Phenyl(4-phenylcyclohexyl)methanol (21r):** Prepared by following the general experimental



procedure with: **Mn-2** (4.96 mg, 2.0 mol%), 1-Phenylethanol **19a** (61.10 mg, 0.50 mmol), 3-phenylpentane-1,5-diol **20d** (360.50 mg, 2.0 mmol), KO<sup>t</sup>Bu (224.0 mg, 2.0 mmol) and toluene (2 mL).

Conversion and yield were determined by gas chromatography analysis using mesitylene (62.0 mg, 0.51 mmol) as an internal standard. Isolated yield was also reported after performing column chromatography. <sup>1</sup>H NMR (300 MHz, CD<sub>2</sub>Cl<sub>2</sub>, 298 K) (mixture of diastereoisomers)  $\delta$  = 7.05-7.27 (m, 5H, ArCH), 4.41 (d, 1H, *J* = 9 Hz, CH)-minor, 4.31 (d, 1H, *J* = 9 Hz, CH)-major, 2.29-2.41 (m, 2H, CH & OH), 1.70-2.06 (m, 4H, CH<sub>2</sub>), 1.48-1.65 (m, 1H, CH), 1.03-1.44 (m, 4H, CH<sub>2</sub>); <sup>13</sup>C{<sup>1</sup>H}-NMR (75 MHz, CD<sub>2</sub>Cl<sub>2</sub>, 298 K) (mixture of diastereoisomers)  $\delta$  = 148.06 (C<sub>Ar</sub>)-major, 144.27 (C<sub>Ar</sub>) -major, 144.18 (C<sub>Ar</sub>)-minor, 142.52 (C<sub>Ar</sub>)-minor, 128.61 (CH<sub>Ar</sub>)-major, 128.51 (CH<sub>Ar</sub>)-major, 127.90 (CH<sub>Ar</sub>)-minor, 127.85 (CH<sub>Ar</sub>)-minor, 127.15 (CH<sub>Ar</sub>)-major, 127.06 (CH<sub>Ar</sub>)-minor, 127.01 (CH<sub>Ar</sub>)-major, 126.18 (CH<sub>Ar</sub>)-major, 125.29 (CH<sub>Ar</sub>)-major, 124.16 (CH<sub>Ar</sub>)-minor, 123.89 (CH<sub>Ar</sub>)-minor, 79.43 (CH)-major, 78.81 (CH)-minor, 45.01 (CH)-major, 44.71 (CH)-major, 41.18 (CH)-minor, 41.14 (CH)-minor, 34.29 (CH<sub>2</sub>)-major, 34.25 (CH<sub>2</sub>)-major, 29.90 (CH<sub>2</sub>)-major, 29.32 (CH<sub>2</sub>)-major, 28.65 (CH<sub>2</sub>)-minor, 27.64 (CH<sub>2</sub>)-minor, 26.11 (CH<sub>2</sub>)-minor, 25.61 (CH<sub>2</sub>)-minor. **HRMS** (ESI<sup>+</sup>) found  $[M+Na]^+$  = 289.1567; C<sub>19</sub>H<sub>22</sub>ONa requires 289.1563. Isolated yield: 83%, 83:17 d.r.

**Naphthalen-2-yl(4-phenylcyclohexyl)methanol (21s):** Prepared by following the general

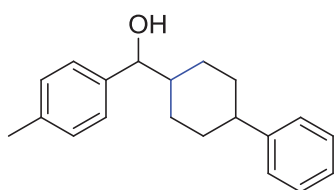


experimental procedure with: **Mn-2** (4.96 mg, 2.0 mol%), 1-(naphthalen-2-yl)ethanol **19b** (86.0 mg, 0.50 mmol), 3-phenylpentane-1,5-diol **20d** (360.50 mg, 2.0 mmol), KO<sup>t</sup>Bu (224.0 mg, 2.0 mmol) and toluene (2 mL). Conversion and yield

were determined by gas chromatography analysis using mesitylene (61.0 mg, 0.51 mmol) as an internal standard. Isolated yield was also reported after performing column chromatography. <sup>1</sup>H NMR (300 MHz, CD<sub>2</sub>Cl<sub>2</sub>, 298 K) (mixture of diastereoisomers)  $\delta$  = 7.74-7.77 (m, 3H, ArCH), 7.67 (s, 1H, ArCH), 7.37-7.41 (m, 2H, ArCH), 7.04-7.27 (m, 6H, ArCH), 4.59 (d, 1H, *J* = 6 Hz, CH)-minor, 4.48 (d, 1H, *J* = 9 Hz, CH)-major, 2.31-2.40 (m, 1H, CH),

2.02-2.08 (m, 1H, CH), 1.81-1.87 (m, 1H, CH), 1.69-1.76 (m, 1H, CH), 1.09-1.47 (m, 6H, CH<sub>2</sub>). <sup>13</sup>C{<sup>1</sup>H}-NMR (75 MHz, CD<sub>2</sub>Cl<sub>2</sub>, 298 K) (mixture of diastereoisomers): δ = 148.05 (C<sub>Ar</sub>), 141.72 (C<sub>Ar</sub>), 133.58 (CH<sub>Ar</sub>), 133.37 (CH<sub>Ar</sub>), 128.61 (CH<sub>Ar</sub>), 128.22 (CH<sub>Ar</sub>), 127.99 (CH<sub>Ar</sub>), 127.16 (CH<sub>Ar</sub>), 126.46 (C<sub>Ar</sub>), 126.19 (CH<sub>Ar</sub>), 126.11 (C<sub>Ar</sub>), 125.78 (CH<sub>Ar</sub>), 125.30 (CH<sub>Ar</sub>), 125.16 (CH<sub>Ar</sub>), 79.47 (CH), 44.93 (CH), 44.71 (CH), 34.28 (CH<sub>2</sub>), 34.26 (CH<sub>2</sub>), 29.98 (CH<sub>2</sub>), 29.33 (CH<sub>2</sub>). HRMS (EI+) found [M+Na]<sup>+</sup> = 316.1830; C<sub>23</sub>H<sub>24</sub>O requires 316.1822. Isolated yield: 60%, 84:16 d.r.

**(4-phenylcyclohexyl)(*p*-tolyl)methanol (21t):** Prepared by following the general experimental



procedure with: **Mn-2** (4.96 mg, 2.0 mol%), 1-(*p*-tolyl)ethanol **19c** (68.0 mg, 0.50 mmol), 3-phenylpentane-1,5-diol **20d** (360.50 mg, 2.0 mmol), KO<sup>t</sup>Bu (224.0 mg, 2.0 mmol) and toluene (2 mL).

Conversion and yield were determined by gas chromatography analysis using mesitylene (59.0 mg, 0.49 mmol) as an internal standard. Isolated yield was also reported after performing column chromatography. <sup>1</sup>H NMR (300 MHz, CD<sub>2</sub>Cl<sub>2</sub>, 298 K) (mixture of diastereoisomers) δ = 7.06-7.20 (m, 9H, ArCH), 4.64 (d, 1H, *J* = 9 Hz, CH)-minor, 4.27 (d, 1H, *J* = 9 Hz, CH)-major, 2.31-2.40 (m, 1H, CH), 2.25 (s, 3H, CH<sub>3</sub>), 2.01-2.07 (m, 1H, CH), 1.71-1.87 (m, 2H, CH<sub>2</sub>), 1.28-1.44 (m, 3H, CH), 1.02-1.19 (m, 3H, CH). <sup>13</sup>C{<sup>1</sup>H}-NMR (75 MHz, CD<sub>2</sub>Cl<sub>2</sub>, 298 K) (mixture of diastereoisomers): δ = 148.09 (C<sub>Ar</sub>), 141.24 (C<sub>Ar</sub>), 137.45 (C<sub>Ar</sub>), 129.16 (CH<sub>Ar</sub>), 128.60 (CH<sub>Ar</sub>), 127.15 (CH<sub>Ar</sub>), 126.90 (CH<sub>Ar</sub>), 126.16 (CH<sub>Ar</sub>), 79.28 (CH), 44.97 (CH), 44.72 (CH), 34.28 (CH<sub>2</sub>), 34.25 (CH<sub>2</sub>), 29.89 (CH<sub>2</sub>), 29.42 (CH<sub>2</sub>), 21.21 (CH<sub>3</sub>). HRMS (EI+) found [M-H<sub>2</sub>O]<sup>+</sup> = 262.1714; C<sub>20</sub>H<sub>22</sub> requires 262.1716. Isolated yield: 76%, 95:5 d.r.

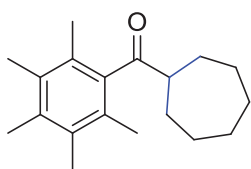
#### 4.9.6. General procedure for the preparation of substituted cycloheptanes from ketone and diols

To an ace pressure tube, Mn-MACHO-<sup>i</sup>Pr **Mn-2** (4.96 mg, 2.0 mol%), KO<sup>t</sup>Bu (224.0 mg, 2.0 mmol), ketone **22** (0.50 mmol) and diol **20** (2.0 mmol) were introduced under an argon atmosphere. Toluene (2 mL) was added as a solvent. The pressure tube was sealed and introduced in an oil heat bath set to 150 °C for 32 h. After completion of the reaction, the pressure tube was cooled down and slowly vented while stirring continued. Mesitylene was



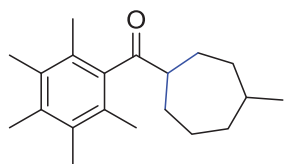
introduced as an internal standard to the crude reaction mixture. 1N HCl was added dropwise to the crude reaction mixture until the pH of the solution becomes close to 7. The reaction mixture was then extracted with DCM (3 x 5 mL) and the organic layer was washed with water (1 x 5 mL). The organic layer was then dried using MgSO<sub>4</sub> and filtered before the composition was analyzed by GC. Purification was carried out using column chromatography over silica gel (100-200 mesh) using ethyl acetate/petroleum ether (7 : 93) mixture as eluent to isolate the pure product.

**Cycloheptyl(2,3,4,5,6-pentamethylphenyl)methanone (23a):** Prepared by following the general experimental procedure with: **Mn-2** (4.96 mg, 2.0 mol%), 1-(2,3,4,5,6-pentamethylphenyl)ethanone **22a** (95.10 mg, 0.50 mmol), 1,6-hexanediol **20e** (236.30 mg, 2.0 mmol), KO<sup>t</sup>Bu (224.0 mg, 2.0 mmol) and toluene (2 mL). Conversion and yield were determined by gas chromatography analysis using mesitylene (58.0 mg, 0.48 mmol) as an internal standard.



Isolated yield was also reported after performing column chromatography. <sup>1</sup>H NMR (300 MHz, CD<sub>2</sub>Cl<sub>2</sub>, 298 K) δ = 2.75-2.84 (m, 1H, CH), 2.24 (s, 3H, CH<sub>3</sub>), 2.18 (s, 6H, CH<sub>3</sub>), 2.07 (s, 6H, CH<sub>3</sub>), 1.89-1.98 (m, 2H, CH<sub>2</sub>), 1.69-1.78 (m, 2H, CH<sub>2</sub>), 1.60-1.66 (m, 2H, CH<sub>2</sub>), 1.51-1.59 (m, 4H, CH<sub>2</sub>), 1.38-1.49 (m, 2H, CH<sub>2</sub>). <sup>13</sup>C{<sup>1</sup>H}-NMR (75 MHz, CD<sub>2</sub>Cl<sub>2</sub>, 298 K) δ = 215.15 (CO), 140.78 (C<sub>Ar</sub>), 135.79 (C<sub>Ar</sub>), 133.54 (C<sub>Ar</sub>), 128.76 (C<sub>Ar</sub>), 55.19 (CH), 29.92 (CH<sub>2</sub>), 29.03 (CH<sub>2</sub>), 27.05 (CH<sub>2</sub>), 18.23 (CH<sub>3</sub>), 16.98 (CH<sub>3</sub>), 16.32 (CH<sub>3</sub>). HRMS (ESI<sup>+</sup>) found [M+Na]<sup>+</sup> = 295.2029; C<sub>19</sub>H<sub>28</sub>NaO requires 295.2032. Isolated yield: 62%.

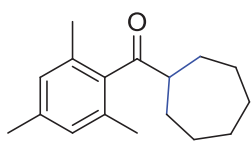
**(4-methylcycloheptyl)(2,3,4,5,6-pentamethylphenyl)methanone (23b):** Prepared by following the general experimental procedure with: **Mn-2** (4.96 mg, 2.0 mol%), 1-(2,3,4,5,6-pentamethylphenyl)ethanone **22a** (95.10 mg, 0.50 mmol), 3-methylhexane-1,6-diol **20f** (264.40 mg, 2.0 mmol), KO<sup>t</sup>Bu (224.0 mg, 2.0 mmol) and toluene (2 mL). Conversion and yield were



determined by gas chromatography analysis using mesitylene (61.0 mg, 0.51 mmol) as an internal standard. Isolated yield was also reported after performing column chromatography. <sup>1</sup>H NMR (300 MHz, CD<sub>2</sub>Cl<sub>2</sub>, 298 K) (mixture of diastereoisomers) δ = 2.75-2.89 (m, 1H, CH), 2.24 (s, 3H, CH<sub>3</sub>), 2.18 (s, 6H, CH<sub>3</sub>), 2.06 (s, 6H, CH<sub>3</sub>), 1.93-2.01 (m, 1H, CH), 1.72-1.85 (m, 4H, CH<sub>2</sub>), 1.55-1.63 (m, 4H, CH<sub>2</sub>), 1.02-1.35 (m, 2H, CH<sub>2</sub>), 0.89-0.92 (m, 3H, CH<sub>3</sub>).

$^{13}\text{C}\{^1\text{H}\}$ -NMR (75 MHz,  $\text{CD}_2\text{Cl}_2$ , 298 K) (mixture of diastereoisomers)  $\delta$  = 214.92 (CO), 214.86 (CO), 140.59 (quat-C), 135.60 ( $C_{\text{Ar}}$ ), 133.35 ( $C_{\text{Ar}}$ ), 128.58 ( $C_{\text{Ar}}$ ), 128.56 ( $C_{\text{Ar}}$ ), 55.28 (CH), 38.56 ( $\text{CH}_2$ ), 36.84( $\text{CH}_2$ ), 36.39( $\text{CH}_2$ ), 35.59( $\text{CH}_2$ ), 34.69 (CH), 33.62 (CH), 30.46 ( $\text{CH}_2$ ), 30.41 ( $\text{CH}_2$ ), 29.27 ( $\text{CH}_2$ ), 28.71 ( $\text{CH}_2$ ), 26.72 ( $\text{CH}_3$ ), 26.45 ( $\text{CH}_3$ ), 23.98 ( $\text{CH}_2$ ), 23.91 ( $\text{CH}_2$ ), 18.03 ( $\text{CH}_3$ ), 16.79 ( $\text{CH}_3$ ), 16.13 ( $\text{CH}_3$ ). **HRMS** (EI+) found  $[\text{M}]^+ = 286.2287$ ;  $\text{C}_{20}\text{H}_{30}\text{O}$  requires 286.2291. Isolated yield: 92%. 57:42 d.r.

**Cycloheptyl(mesityl)methanone (23c):** Prepared by following the general experimental



procedure with: **Mn-2** (4.96 mg, 2.0 mol%), 1-mesitylethanone **22b** (81.10 mg, 0.50 mmol), 1,6-hexanediol **20e** (236.30 mg, 2.0 mmol),  $\text{KO}^t\text{Bu}$  (224.0 mg, 2.0 mmol) and toluene (2 mL). Conversion and yield were

determined by gas chromatography analysis using mesitylene (59.0 mg, 0.49 mmol) as an internal standard. Isolated yield was also reported after performing column chromatography.

$^1\text{H}$  NMR (300 MHz,  $\text{CD}_2\text{Cl}_2$ , 298 K)  $\delta$  = 6.85 (s, 2H, ArCH), 2.84-2.94 (m, 1H, CH), 2.28 (s, 3H,  $\text{CH}_3$ ), 2.18 (s, 6H,  $\text{CH}_3$ ), 1.89-1.98 (m, 2H,  $\text{CH}_2$ ), 1.69-1.79 (m, 2H,  $\text{CH}_2$ ), 1.54-1.66 (m, 6H,  $\text{CH}_2$ ), 1.40-1.52 (m, 2H,  $\text{CH}_2$ ).  $^{13}\text{C}\{^1\text{H}\}$ -NMR (75 MHz,  $\text{CD}_2\text{Cl}_2$ , 298 K)  $\delta$  = 213.78 (CO), 139.80 ( $C_{\text{Ar}}$ ), 138.81 ( $C_{\text{Ar}}$ ), 134.01 ( $C_{\text{Ar}}$ ), 129.09 ( $\text{CH}_{\text{Ar}}$ ), 54.20 (CH), 29.99 ( $\text{CH}_2$ ), 29.01 ( $\text{CH}_2$ ), 27.04 ( $\text{CH}_2$ ), 21.29 ( $\text{CH}_3$ ), 20.02 ( $\text{CH}_3$ ). **HRMS** (EI+) found  $[\text{M}]^+ = 244.1808$ ;  $\text{C}_{17}\text{H}_{24}\text{O}$  requires 244.1822. Isolated yield: 59%.

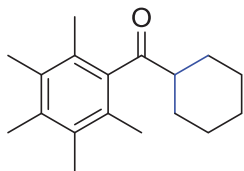
#### 4.9.7. General procedure for the preparation of substituted cyclohexane from ketone and diols

To an ace pressure tube, Mn-MACHO- $^i\text{Pr}$  **Mn-2** (4.96 mg, 2.0 mol%),  $\text{KO}^t\text{Bu}$  (224.0 mg, 2.0 mmol), ketone **22** (0.50 mmol) and 1,5-Pentanediol **20a** (208.0 mg, 2.0 mmol) were introduced under an argon atmosphere. Toluene (2 mL) was added as a solvent. The pressure tube was sealed and introduced in an oil heat bath set to 150 °C for 32 h. After completion of the reaction, the pressure tube was cooled down and slowly vented while stirring continued. Mesitylene was introduced as an internal standard to the crude reaction mixture. 1N HCl was added dropwise to the crude reaction mixture until the pH of the solution becomes close to 7. The reaction mixture was then extracted with DCM (3 x 5 mL) and the organic layer was washed with water (1 x 5 mL). The organic layer was then dried using  $\text{MgSO}_4$  and filtered before the



composition was analyzed by GC. Purification was carried out using column chromatography over silica gel (100-200 mesh) using ethyl acetate/petroleum ether (7 : 93) mixture as eluent.

**Cyclohexyl(2,3,4,5,6-pentamethylphenyl)methanone (23d):** Prepared by following the general



experimental procedure with: **Mn-2** (4.96 mg, 2.0 mol%), 1-(2,3,4,5,6-pentamethylphenyl)ethanone **22a** (95.10 mg, 0.50 mmol), 1,5-Pentanediol **20a** (208.0 mg, 2.0 mmol), KO<sup>t</sup>Bu (224.0 mg, 2.0 mmol) and toluene (2 mL). Conversion and yield were determined by gas chromatography

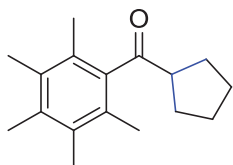
analysis using mesitylene (61.0 mg, 0.51 mmol) as an internal standard. Isolated yield was also reported after performing column chromatography. The spectral data are in agreement with the reported literature.<sup>[15]</sup> <sup>1</sup>H NMR (300 MHz, CD<sub>2</sub>Cl<sub>2</sub>, 298 K)  $\delta$  = 2.52-2.62 (tt, 1H,  $J$  = 11.69, 3.31 Hz, CH), 2.23 (s, 3 H, CH<sub>3</sub>), 2.17 (s, 6H, CH<sub>3</sub>), 2.05 (s, 6H, CH<sub>3</sub>), 1.85-1.90 (m, 2H, CH<sub>2</sub>), 1.77-1.82 (m, 2H, CH<sub>2</sub>), 1.66-1.68 (m, 1H, CH), 1.29-1.39 (m, 2H, CH<sub>2</sub>), 1.22-1.26 (m, 3H, CH & CH<sub>2</sub>). Isolated yield: 52%.

#### 4.9.8. General procedure for the preparation of substituted cyclopentanes from ketone and diols

To an ace pressure tube, Mn-MACHO-<sup>i</sup>Pr **Mn-2** (4.96 mg, 2.0 mol%), KO<sup>t</sup>Bu (224.0 mg, 2.0 mmol), ketone **22** (0.50 mmol) and butane-1,4-diol **20g** (2.0 mmol) were introduced under an argon atmosphere. Toluene (2 mL) was added as a solvent. The pressure tube was sealed and introduced in an oil heat bath set to 150 °C for 32 h. After completion of the reaction, the pressure tube was cooled down and slowly vented while stirring continued. Mesitylene was introduced as an internal standard to the crude reaction mixture. 1N HCl was added dropwise to the crude reaction mixture until the pH of the solution becomes close to 7. The reaction mixture was then extracted with DCM (3 x 5 mL) and the organic layer was washed with water (1 x 5 mL). The organic layer was then dried using MgSO<sub>4</sub> and filtered before the composition was analyzed by GC. Purification was carried out using column chromatography over silica gel (100-200 mesh) using ethyl acetate/petroleum ether (7 : 93) mixture as eluent.

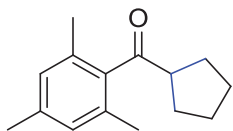
**Cyclopentyl(2,3,4,5,6-pentamethylphenyl)methanone (23e):** Prepared by following the general experimental procedure with: **Mn-2** (4.96 mg, 2.0 mol%),

1-(2,3,4,5,6-pentamethylphenyl)ethanone **22a** (95.10 mg, 0.50 mmol), butane-1,4-diol **20g** (180.0 mg, 2.0 mmol), KO<sup>t</sup>Bu (224.0 mg, 2.0 mmol) and toluene (2 mL).



Conversion and yield were determined by gas chromatography analysis using mesitylene (64.0 mg, 0.53 mmol) as an internal standard. Isolated yield was also reported after performing column chromatography. <sup>1</sup>H NMR (300 MHz, CD<sub>2</sub>Cl<sub>2</sub>, 298 K) δ = 3.09-3.20 (quint, 1H, CH), 2.24 (s, 3H, CH<sub>3</sub>), 2.18 (s, 6H, CH<sub>3</sub>), 2.08 (s, 6H, CH<sub>3</sub>), 1.80-1.87 (m, 4H, CH<sub>2</sub>), 1.70-1.78 (m, 2H, CH<sub>2</sub>), 1.57-1.63 (m, 2H, CH<sub>2</sub>). <sup>13</sup>C{<sup>1</sup>H}-NMR (75 MHz, CD<sub>2</sub>Cl<sub>2</sub>, 298 K) δ = 215.13 (CO), 141.68 (C<sub>Ar</sub>), 135.72 (C<sub>Ar</sub>), 133.54 (C<sub>Ar</sub>), 128.17 (C<sub>Ar</sub>), 54.86 (CH), 30.01 (CH<sub>2</sub>), 26.39 (CH<sub>2</sub>), 18.09 (CH<sub>3</sub>), 16.96 (CH<sub>3</sub>), 16.30 (CH<sub>3</sub>). HRMS (EI<sup>+</sup>) found [M]<sup>+</sup> = 244.1819; C<sub>17</sub>H<sub>24</sub>O requires 244.1822. Isolated yield: 42%.

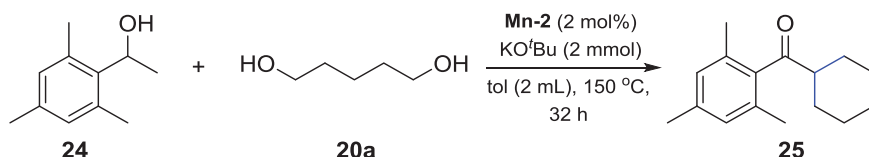
**Cyclopentyl(mesityl)methanone (23f):** Prepared by following the general experimental procedure with: **Mn-2** (4.96 mg, 2.0 mol%), 1-mesitylethanone **22b** (81.10 mg, 0.50 mmol), butane-1,4-diol **20g** (180.0 mg, 2.0 mmol), KO<sup>t</sup>Bu (224.0 mg, 2.0 mmol) and toluene (2 mL). Conversion and yield were



determined by gas chromatography analysis using mesitylene (66.0 mg, 0.55 mmol) as an internal standard. Isolated yield was also reported after performing column chromatography. <sup>1</sup>H NMR (300 MHz, CD<sub>2</sub>Cl<sub>2</sub>, 298 K) δ = 6.84 (s, 2H, ArCH), 3.21 (quint., 1H, J = 9 Hz, CH), 2.27 (s, 3H, CH<sub>3</sub>), 2.17 (s, 6H, CH<sub>3</sub>), 1.80-1.87 (m, 4H, CH<sub>2</sub>), 1.58-1.74 (m, 4H, CH<sub>2</sub>). <sup>13</sup>C{<sup>1</sup>H}-NMR (75 MHz, CD<sub>2</sub>Cl<sub>2</sub>, 298 K) δ = 213.98 (CO), 140.74 (C<sub>Ar</sub>), 138.76 (C<sub>Ar</sub>), 133.47 (C<sub>Ar</sub>), 129.04 (CH<sub>Ar</sub>), 53.84 (CH), 30.24 (CH<sub>2</sub>), 26.53 (CH<sub>2</sub>), 21.31 (CH<sub>3</sub>), 19.91 (CH<sub>3</sub>). HRMS (EI<sup>+</sup>) found [M]<sup>+</sup> = 216.1505; C<sub>15</sub>H<sub>20</sub>O requires 216.1509. Isolated yield: 39%.

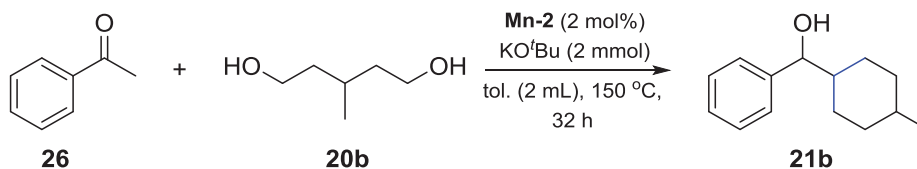
## 4.9.9. Control experiments and labeling studies

### 4.9.9.1 Reaction of 1-mesitylethanol **24** with **20a** in the presence of complex Mn-2



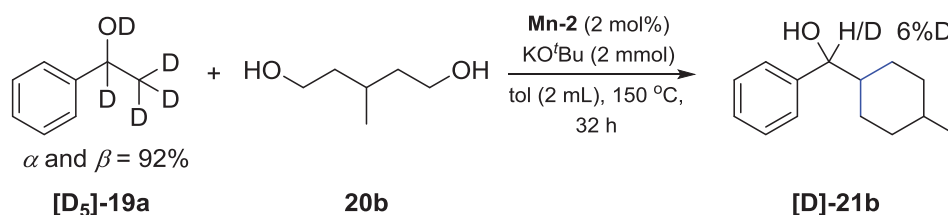
To an ace pressure tube, Mn-MACHO-<sup>*i*</sup>Pr **Mn-2** (4.96 mg, 2.0 mol%), KO<sup>t</sup>Bu (224.0 mg, 2.0 mmol), 1-mesitylethanol **24** (82.10 mg, 0.50 mmol) and 1,5-Pentanediol **20a** (208.0 mg, 2.0 mmol) were measured under argon atmosphere. Toluene (2 mL) was added as a solvent. The pressure tube was sealed and introduced in an oil heat bath set to 150 °C for 32 h while stirring. After completion of the reaction, the pressure tube was cooled down and slowly vented while stirring continued. Mesitylene (57.0 mg, 0.47 mmol) was introduced as an internal standard to the crude reaction mixture. 1N HCl was added drop wise to the crude reaction mixture until the pH of the solution becomes close to 7. The reaction mixture was then extracted with DCM (3 x 5 mL) and the organic layer was washed with water (1 x 5 mL). The organic layer was then dried using MgSO<sub>4</sub> and filtered before the composition was analyzed by GC spectrometry. The isolation of pure product was carried out using column chromatography over silica gel (100-200 mesh) using ethyl acetate/petroleum ether (7 : 93) mixture as eluent. <sup>1</sup>H NMR (300 MHz, CD<sub>2</sub>Cl<sub>2</sub>, 298 K) δ = 6.76 (s, 2H, ArCH), 2.59 (tt, 1H, *J* = 9 Hz, *J* = 3 Hz, CH), 2.19 (s, 3H, CH<sub>3</sub>), 2.08 (s, 6H, CH<sub>3</sub>), 1.78-1.82 (m, 2H, CH<sub>2</sub>), 1.70-1.73 (m, 2H, CH<sub>2</sub>), 1.13-1.35 (m, 6H, CH<sub>2</sub>). <sup>13</sup>C{<sup>1</sup>H}-NMR (75 MHz, CD<sub>2</sub>Cl<sub>2</sub>, 298 K) δ = 213.68 (CO), 139.81 (quat-C), 138.77 (quat-C), 133.81 (quat-C), 129.01 (ArCH), 52.71 (CH), 28.79 (CH<sub>2</sub>), 26.52 (CH<sub>2</sub>), 26.46 (CH<sub>2</sub>), 21.29 (CH<sub>2</sub>), 19.96 (CH<sub>2</sub>). HRMS (EI<sup>+</sup>) C<sub>16</sub>H<sub>22</sub>O found = 230.1673; requires 230.1665. Isolated yield: 31%.

#### 4.9.9.2 Reaction of acetophenone **26** with **20b** in the presence of complex Mn-2



To an ace pressure tube, Mn-MACHO-<sup>*i*</sup>Pr **Mn-2** (4.96 mg, 2.0 mol%), KO<sup>t</sup>Bu (224.0 mg, 2.0 mmol), acetophenone **26** (60.10 mg, 0.50 mmol) and 3-methylpentane-1,5-diol **20b** (236.34 mg, 2.0 mmol) were measured under argon atmosphere. Toluene (2 mL) was added as a solvent. The pressure tube was sealed and introduced in an oil heat bath set to 150 °C for 32 h while stirring. After completion of the reaction, the pressure tube was cooled down and slowly vented while stirring continued. Mesitylene (59.0 mg, 0.49 mmol) was introduced as an internal standard to the crude reaction mixture. 1N HCl was added drop wise to the crude reaction mixture until the pH of the solution becomes close to 7. The reaction mixture was then extracted with DCM (3 x 5 mL) and the organic layer was washed with water (1 x 5 mL). The organic layer was then dried using MgSO<sub>4</sub> and filtered before the composition was analyzed by GC. GC conv.: >99%, GC yield: 90%, 86:14 d.r.

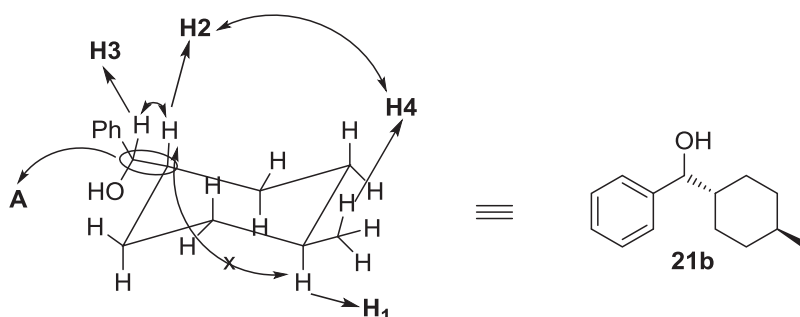
#### 4.9.9.3 Reaction of 1-phenyl ethanol-d<sub>5</sub> [**D**<sub>5</sub>]-**19a** with **20b** in the presence of complex Mn-2



To an ace pressure tube, Mn-MACHO-<sup>*i*</sup>Pr **Mn-2** (4.96 mg, 2.0 mol%), KO<sup>t</sup>Bu (224.0 mg, 2.0 mmol), deuterium labeled 1-phenylethanol-1-d<sub>5</sub> [**D**<sub>5</sub>]-**19a** (64.10 mg, 0.50 mmol) and 3-methylpentane-1,5-diol **20b** (236.34 mg, 2.0 mmol) were measured under argon atmosphere. Toluene (2 mL) was added as a solvent. The pressure tube was sealed and introduced in an oil heat bath set to 150 °C for 32 h while stirring. After completion of the reaction, the pressure tube was cooled down and slowly vented while stirring continued. Mesitylene (62.0 mg, 0.52 mmol) was introduced as an internal standard to the crude reaction mixture. 1N HCl was added drop

wise to the crude reaction mixture until the pH of the solution becomes close to 7. The reaction mixture was then extracted with DCM (3 x 5 mL) and the organic layer was washed with water (1 x 5 mL). The organic layer was then dried using MgSO<sub>4</sub> and filtered before the composition was analyzed by GC spectrometry. The isolation of pure product was carried out using column chromatography over silica gel (100-200 mesh) using ethyl acetate/petroleum ether (7 : 93) mixture as eluent. <sup>1</sup>H NMR (300 MHz, CD<sub>2</sub>Cl<sub>2</sub>, 298 K) (mixture of diastereoisomers) δ = 7.16-7.26 (m, 5H, ArCH), 4.42 (d, 1H, *J* = 6 Hz, CH)-minor, 4.23 (d, 1H, *J* = 6 Hz, CH)-major, 1.87 (br s, 2H, CH & OH), 1.42-1.67 (m, 4H, CH<sub>2</sub>), 1.18-1.28 (m, 1H, CH), 0.75-0.88 (m, 7H, CH<sub>2</sub> & CH<sub>3</sub>). <sup>13</sup>C{<sup>1</sup>H}-NMR (75 MHz, CD<sub>2</sub>Cl<sub>2</sub>, 298 K) (mixture of diastereoisomers) δ = 144.83 (quat-C)-minor, 144.62 (quat-C)-major, 128.73 (ArCH)-minor, 128.62 (ArCH)-major, 127.89 (ArCH)-minor, 127.78 (ArCH)-major, 127.22 (ArCH)-minor, 127.17 (ArCH)-major, 79.73 (CH)-major, 77.49 (CH)-minor, 45.39 (CH)-major, 45.30 (CH)-minor, 35.45 (CH<sub>2</sub>), 35.40 (CH<sub>2</sub>), 33.26 (CH)-major, 33.17 (CH)-minor, 29.86 (CH<sub>2</sub>)-major, 29.76 (CH<sub>2</sub>)-minor, 29.22 (CH<sub>2</sub>)-major, 29.12 (CH<sub>2</sub>)-minor, 22.92 (CH<sub>3</sub>). Isolated yield: 86%, 85:15 d.r.

#### 4.9.10. Characterization of major diastereomer in compound **21b**



To determine the major diastereomer of **21b**, COSY and NOESY 2D NMR spectra were recorded at room temperature using a 600 MHz NMR spectrometer and CD<sub>2</sub>Cl<sub>2</sub> as deuterated solvent.

Using the <sup>1</sup>H-<sup>1</sup>H COSY NMR spectrum, protons **H1**, **H2** and **H3** were unambiguously identified. The **H1** proton showed strong <sup>3</sup>*J*<sub>HH</sub> coupling with the CH<sub>3</sub> proton (see figure 4.4). Similarly, the <sup>3</sup>*J*<sub>HH</sub> coupling between protons **H2** and **H3** was also seen in the COSY NMR spectrum (see figure 4.5).

The NOESY spectrum confirmed the cross peak between the **H2** and the **H4** proton of CH<sub>3</sub> (see figure 4.7). This spatial interaction is possible when the **H2** proton and the **H4** proton of CH<sub>3</sub> are in the same plane. No cross peaks were observed between the **H1** and **H2** protons which confirmed that the **H1** and **H2** protons are not in the same plane (see figure 4.8). Small spatial interaction between **H2** and **H3** protons were also observed which indicates also that the **H2** and **H3** protons are in the same plane.

Summing all these results, it can be stated that the major diastereomer is a *trans*-diastereomer as **H2** proton and CH<sub>3</sub> protons are in the same plane and it is only possible when the C–C bond **A** will be *trans* to the CH<sub>3</sub> functionality in the molecule. The spectral data are in agreement with the reported literature.<sup>[23]</sup> Based on these observations, the stereochemistry of other substituted alcohols was also assigned.

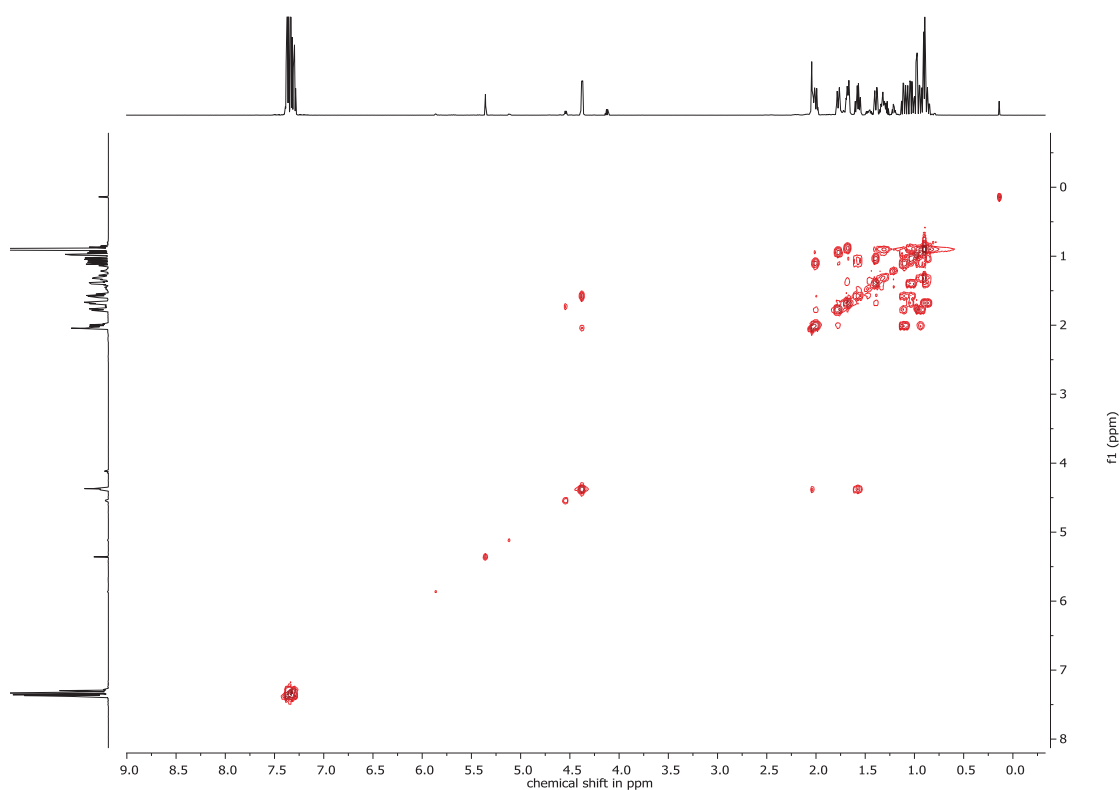


**Figure 4.3:** <sup>1</sup>H-<sup>1</sup>H COSY (600 MHz, CD<sub>2</sub>Cl<sub>2</sub>, 298 K) NMR spectrum of compound **21b**.

Direct synthesis of cycloalkanes from diols and secondary alcohols or ketones using a homogeneous manganese catalyst

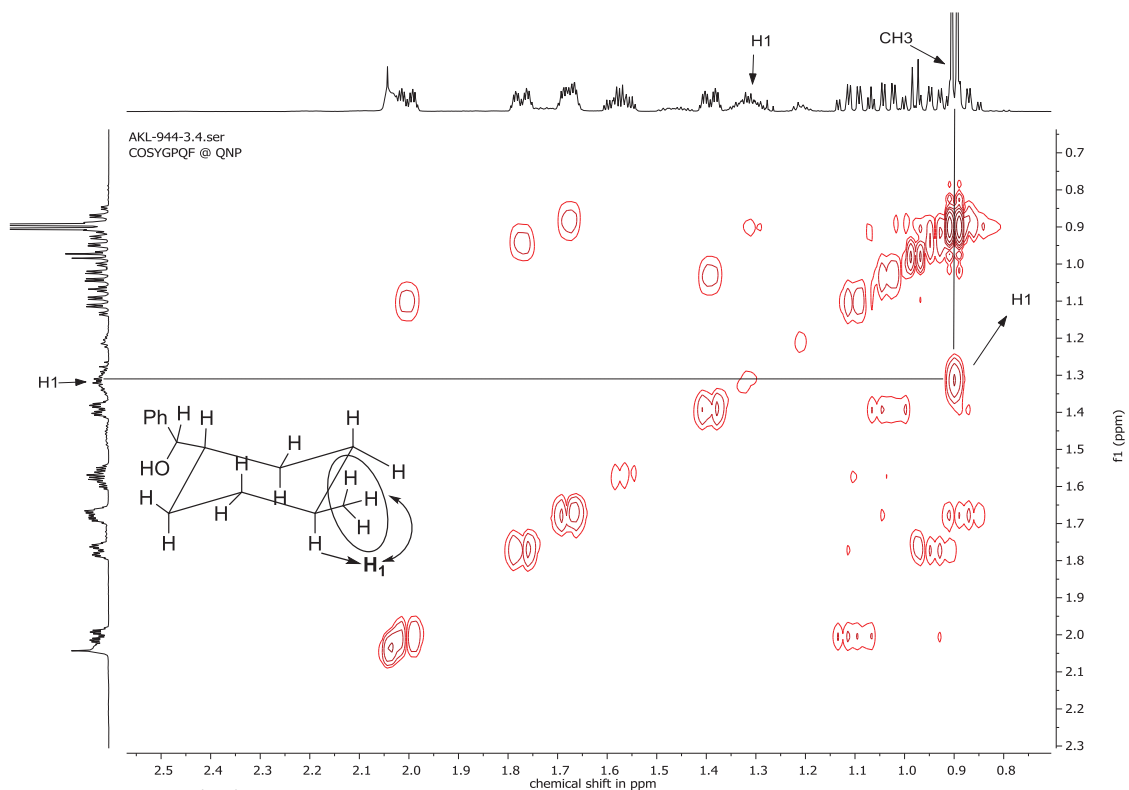


Figure 4.4: Expanded  $^1\text{H}$ - $^1\text{H}$  COSY (600 MHz,  $\text{CD}_2\text{Cl}_2$ , 298 K) NMR spectrum of compound **21b** to attribute proton H1.

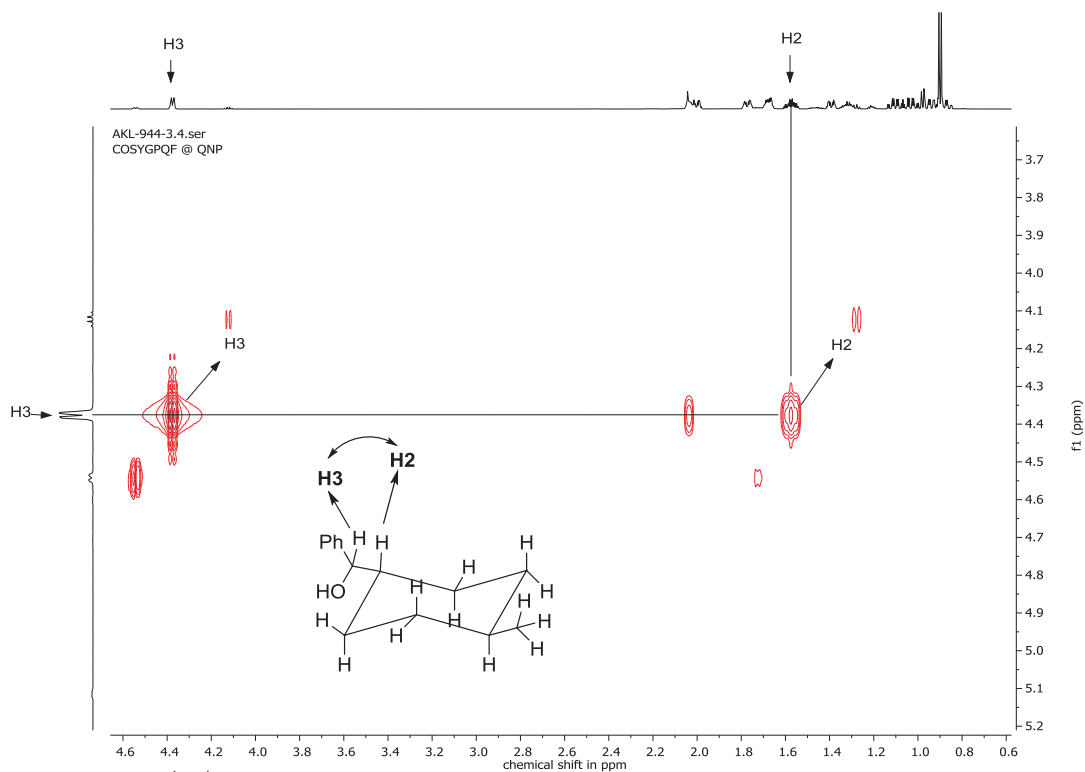


Figure 4.5: Expanded  $^1\text{H}$ - $^1\text{H}$  COSY (600 MHz,  $\text{CD}_2\text{Cl}_2$ , 298 K) NMR spectrum of compound **21b** to attribute proton H2.

Direct synthesis of cycloalkanes from diols and secondary alcohols or ketones using a homogeneous manganese catalyst

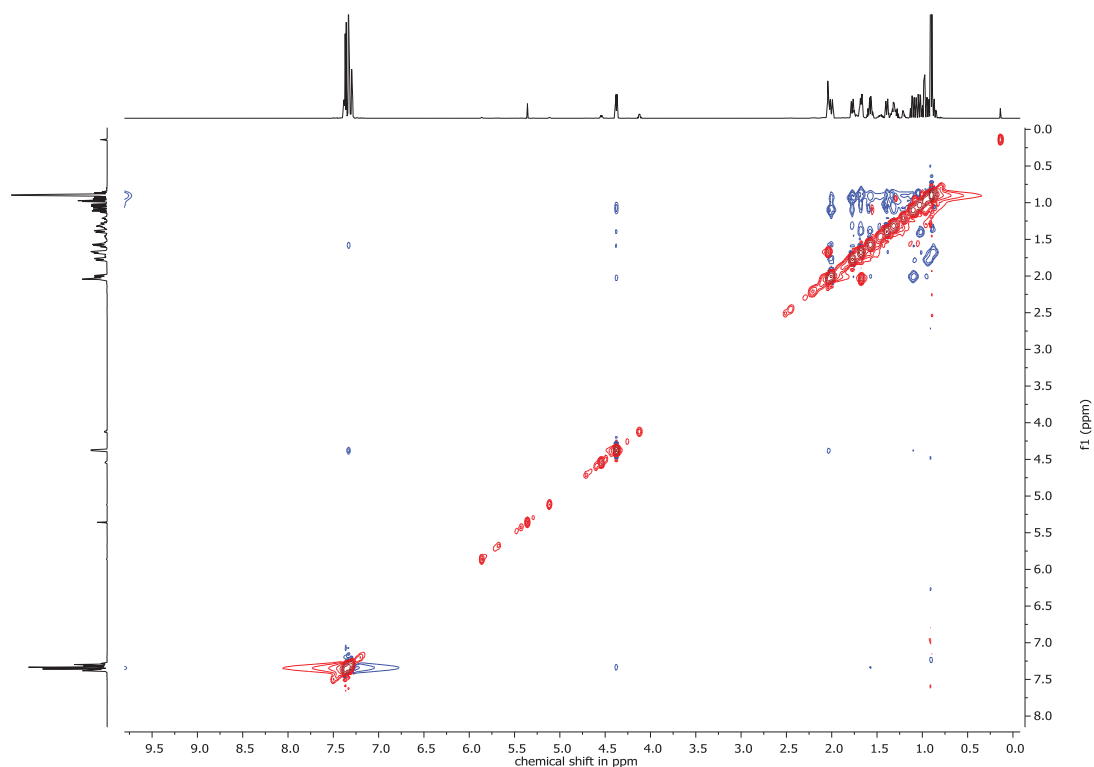


Figure 4.6: NOESY (600 MHz, CD<sub>2</sub>Cl<sub>2</sub>, 298 K) NMR spectrum of compound **21b**; mixing time: 0.5 seconds.

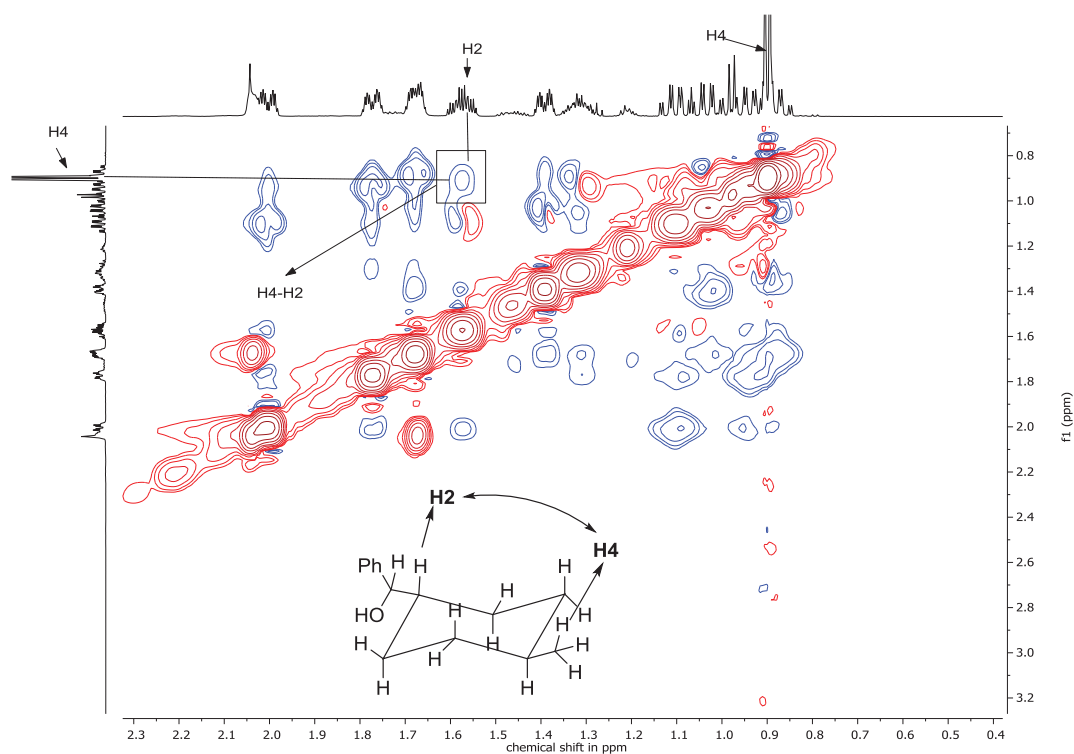
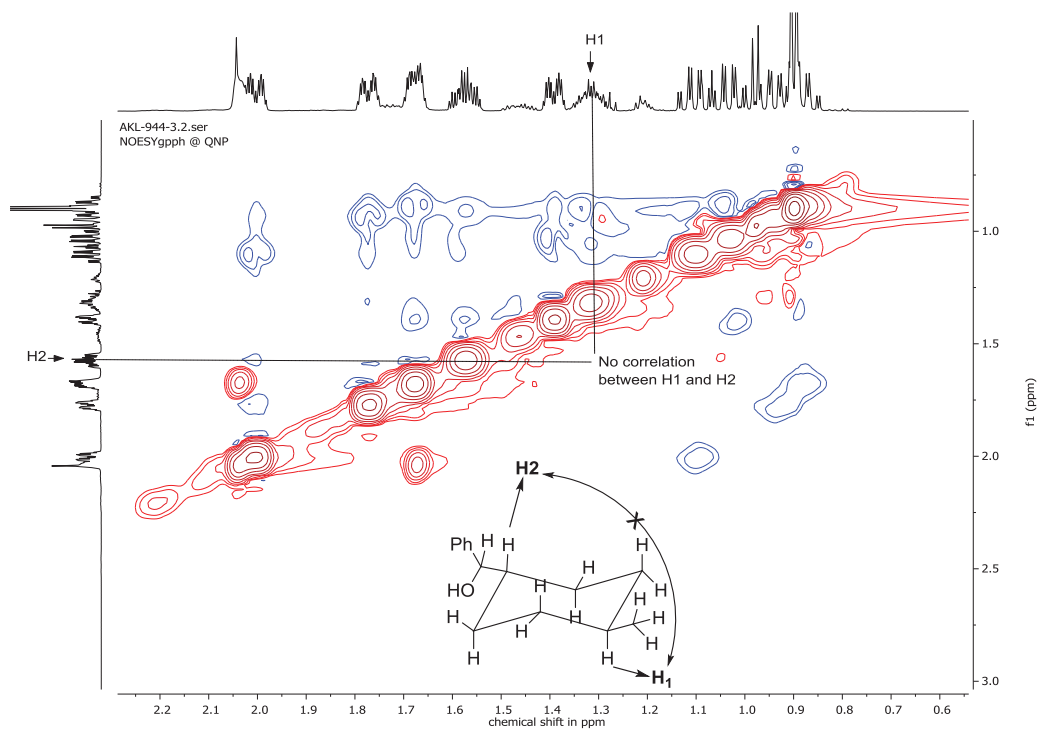


Figure 4.7: Expanded NOESY (600 MHz, CD<sub>2</sub>Cl<sub>2</sub>, 298 K) NMR spectrum of compound **21b** showing a correlation between protons H2 and H4.



Direct synthesis of cycloalkanes from diols and secondary alcohols or ketones using a homogeneous manganese catalyst



**Figure 4.8:** Expanded NOESY (600 MHz, CD<sub>2</sub>Cl<sub>2</sub>, 298 K) NMR spectrum of compound **21b** showing no correlations between protons H1 and H2.

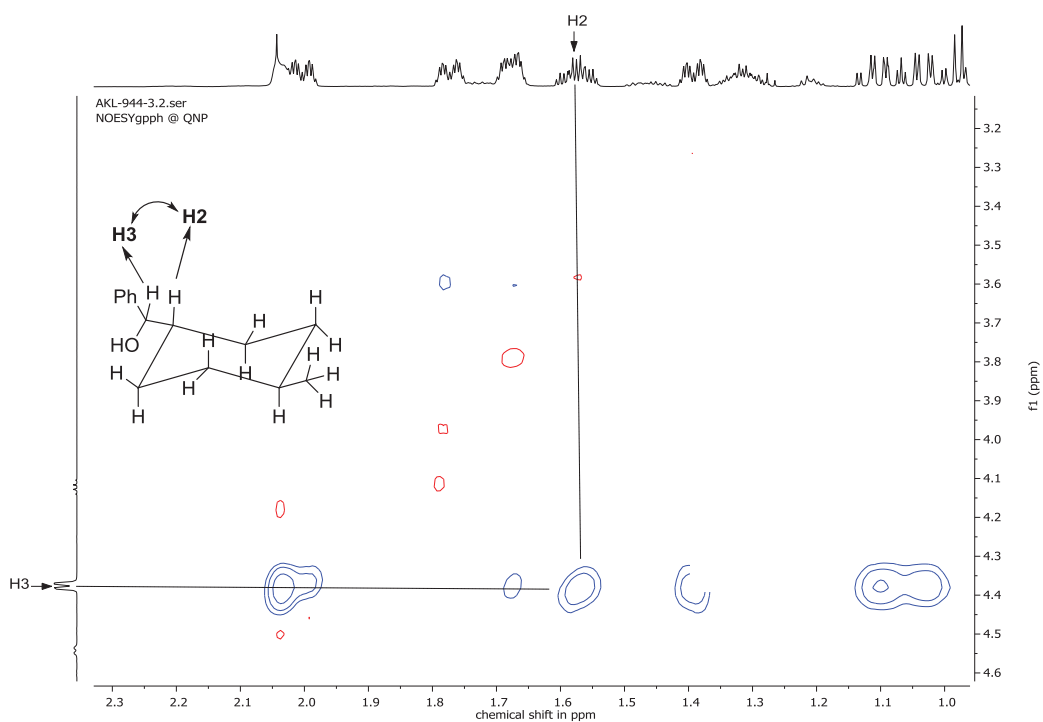
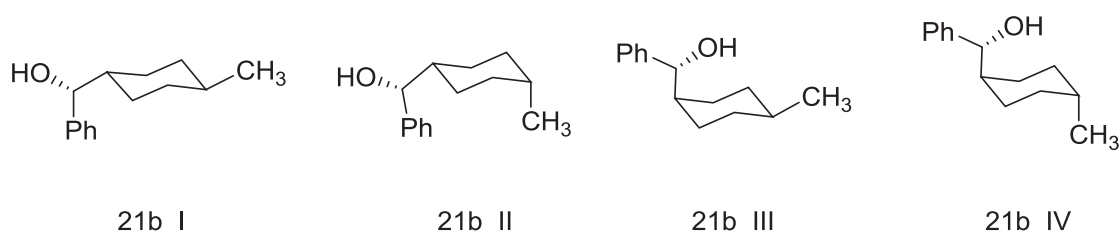


**Figure 4.9:** Expanded NOESY (600 MHz, CD<sub>2</sub>Cl<sub>2</sub>, 298 K) NMR spectrum of compound **21b** showing a correlation between protons H2 and H3.

#### 4.9.11. Computation of the relative stability for different isomers of **21b**

The computational study was performed by David A Kuß. The stability of the four possible isomers was calculated with DFT methods using the program Gaussian<sup>[24]</sup> together with the B3-LYP functional<sup>[25]</sup> and dispersion correction with Becke-Johnson damping by Grimme<sup>[26]</sup> and the def2-TZVP basis set<sup>[27]</sup>. The energies tabulated refer to the gas phase. Frequency calculations confirmed that all structures correspond to local minima.



The isomer with both sterically demanding groups in an equatorial position (21b\_I) is the thermodynamically most stable product. The corresponding isomer with an axial methyl group (21b\_II) is 1.9 kcal mol<sup>-1</sup> less stable. Similarly, the bulky residue containing the alcohol and phenyl moiety situated in the axial position and the methyl group in equatorial position (21b\_III), the stability is decreased by 3.6 kcal mol<sup>-1</sup>. In consequence, the most unstable product is the one with both groups in an axial position (21b\_IV) (5.7 kcal mol<sup>-1</sup>) (Table 4.5). This suggests that the formation of the product **21b** is under the thermodynamic control which also supports the experimental data and the reported literature.<sup>[5d, 28]</sup>

**Table 1:** Comparison of the relative stability of the possible isomers of compound **21b**.

Compound	Electronic energy [Hartree]	Gibbs free energy [Hartree]	$\Delta G$ relative to 21b_I [kcal/mol]
21b_I	-621.073680	-620.803378	$\pm 0.0$
21b_II	-621.071135	-620.800420	+1.9
21b_III	-621.068885	-620.797594	+3.6
21b_IV	-621.066028	-620.794340	+5.7

## References

- [1] a) G. Xia, X. Han, X. Lu, *Org. Lett.* **2014**, *16*, 2058-2061; b) A. Banerjee, S. Sarkar, B. K. Patel, *Org. Biomol. Chem.* **2017**, *15*, 505-530; c) L. Bravo, J. A. Mico, E. Berrocoso, *Expert Opin. Drug Dis* **2017**, *12*, 1281-1291; d) S. Gouedranche, W. Raimondi, X. Bugaut, T. Constantieux, D. Bonne, J. Rodriguez, *Synthesis* **2013**, *45*, 1909-1930; e) M. F. Ansell, *Supplements to the 2nd Edition of Rodd's Chemistry of Carbon Compounds. A Modern Comprehensive Treatise* **2008**, *2*; f) R. A. Holton, C. Somoza, H. B. Kim, F. Liang, R. J. Biediger, P. D. Boatman, M. Shindo, C. C. Smith, S. Kim, *J. Am. Chem. Soc.* **1994**, *116*, 1597-1598; g) J. A. Dabrowski, D. C. Moebius, A. J. Wommack, A. F. Kornahrens, J. S. Kingsbury, *Org. Lett.* **2010**, *12*, 3598-3601.
- [2] a) K. I. Booker-Milburn, A. Sharpe, *J. Chem. Soc., Perkin Trans. 1* **1998**, 983-1006; b) M. B. Smith, J. March, *Vol. March's Advanced Organic Chemistry: Reactions, Mechanisms, and Structure, Sixth Edition*, **2006**.
- [3] a) X. Ding, H. Wang, J. Wang, S. Wang, D. Lin, L. Lv, Y. Zhou, X. Luo, H. Jiang, J. L. Aceña, V. A. Soloshonok, H. Liu, *Amino Acids* **2013**, *44*, 791-796; b) S. Danishefsky, T. Kitahara, *J. Am. Chem. Soc.* **1974**, *96*, 7807-7808; c) E. J. Corey, *Angew. Chem. Int. Ed.* **2002**, *41*, 1650-1667.
- [4] a) A. Wurtz, *Justus Liebigs Ann. Chem.* **1855**, *96*, 364-375; b) G. M. Lampman, J. C. Aumiller, *Org. Synth.* **1971**, *51*, 55.
- [5] a) M. M. Stalzer, C. P. Nicholas, A. Bhattacharyya, A. Motta, M. Delferro, T. J. Marks, *Angew. Chem. Int. Ed.* **2016**, *55*, 5263-5267; b) B. K. Peters, J. Liu, C. Margarita, W. Rabten, S. Kerdphon, A. Orebom, T. Morsch, P. G. Andersson, *J. Am. Chem. Soc.* **2016**, *138*, 11930-11935; c) Y. Wang, X. Cui, Y. Deng, F. Shi, *RSC Adv.* **2014**, *4*, 2729-2732; d) M. P. Wiesenfeldt, Z. Nairoukh, T. Dalton, F. Glorius, *Angew. Chem. Int. Ed.* **2019**, *58*, 10460-10476; e) D.-S. Wang, Q.-A. Chen, S.-M. Lu, Y.-G. Zhou, *Chem. Rev.* **2012**, *112*, 2557-2590.
- [6] a) H. Schick, B. Roatsch, H. Schwarz, A. Hauser, S. Schwarz, *Liebigs Ann. Chem.* **1992**, *1992*, 419-422; b) M. E. Jung, in *Comprehensive Organic Synthesis* (Eds.: B. M. Trost, I. Fleming), Pergamon, Oxford, **1991**, pp. 1-67.
- [7] a) T. F. Schneider, J. Kaschel, D. B. Werz, *Angew. Chem. Int. Ed.* **2014**, *53*, 5504-5523; b) W. Ma, J. Fang, J. Ren, Z. Wang, *Org. Lett.* **2015**, *17*, 4180-4183.
- [8] a) W. Oppolzer, *Acc. Chem. Res.* **1982**, *15*, 135-141; b) P. De Mayo, *Acc. Chem. Res.* **1971**, *4*, 41-47.
- [9] a) R. Haraguchi, Y. Takada, S. Matsubara, *Org. Biomol. Chem.* **2015**, *13*, 241-247; b) Y. Takada, K. Nomura, S. Matsubara, *Org. Lett.* **2010**, *12*, 5204-5205; c) J. A. Ragan, T. W. Makowski, D. J. am Ende, P. J. Clifford, G. R. Young, A. K. Conrad, S. A. Eisenbeis, *Org. Process Res. Dev.* **1998**, *2*, 379-381.
- [10] a) J. Renaud, S. G. Ouellet, *J. Am. Chem. Soc.* **1998**, *120*, 7995-7996; b) A. Jana, K. Misztal, A. Žak, K. Grela, *J. Org. Chem.* **2017**, *82*, 4226-4234; c) O. M. Ogba, N. C. Warner, D. J. O'Leary, R. H. Grubbs, *Chem. Soc. Rev.* **2018**, *47*, 4510-4544; d) M. E. Maier, *Angew. Chem. Int. Ed.* **2000**, *39*, 2073-2077.

- [11] a) V. Michelet, P. Y. Toullec, J.-P. Genêt, *Angew. Chem. Int. Ed.* **2008**, *47*, 4268-4315; b) C. Böing, G. Franciò, W. Leitner, *Chem. Commun.* **2005**, 1456-1458; c) S. M. Stevenson, E. T. Newcomb, E. M. Ferreira, *Org. Chem. Front.* **2016**, *3*, 1228-1235; d) A. Fürstner, *Chem. Soc. Rev.* **2009**, *38*, 3208-3221; e) C. I. Stathakis, P. L. Gkizis, A. L. Zografos, *Nat. Prod. Rep.* **2016**, *33*, 1093-1117.
- [12] a) A. Corma, J. Navas, M. J. Sabater, *Chem. Rev.* **2018**, *118*, 1410-1459; b) B. G. Reed-Berendt, K. Polidano, L. C. Morrill, *Org. Biomol. Chem.* **2019**, *17*, 1595-1607.
- [13] a) M. H. S. A. Hamid, P. A. Slatford, J. M. J. Williams, *Adv. Synth. Catal.* **2007**, *349*, 1555-1575; b) T. D. Nixon, M. K. Whittlesey, J. M. J. Williams, *Dalton Trans.* **2009**, 753-762; c) T. Liu, L. Wang, K. Wu, Z. Yu, *ACS Catal.* **2018**, *8*, 7201-7207; d) S. Elangovan, J.-B. Sortais, M. Beller, C. Darcel, *Angew. Chem. Int. Ed.* **2015**, *54*, 14483-14486; e) J. Yang, X. Liu, D.-L. Meng, H.-Y. Chen, Z.-H. Zong, T.-T. Feng, K. Sun, *Adv. Synth. Catal.* **2012**, *354*, 328-334; f) K.-i. Fujita, C. Asai, T. Yamaguchi, F. Hanasaka, R. Yamaguchi, *Org. Lett.* **2005**, *7*, 4017-4019; g) S. Chakraborty, P. Daw, Y. Ben David, D. Milstein, *ACS Catal.* **2018**, *8*, 10300-10305; h) F.-X. Yan, M. Zhang, X.-T. Wang, F. Xie, M.-M. Chen, H. Jiang, *Tetrahedron* **2014**, *70*, 1193-1198.
- [14] a) A. Kaithal, M. Schmitz, M. Hölscher, W. Leitner, *ChemCatChem* **2019**, DOI: 10.1002/cctc.201900788; b) A. Kaithal, P. v. Bonn, M. Hölscher, W. Leitner, *Angew. Chem. Int. Ed.* **2019**, DOI: 10.1002/anie.201909035.
- [15] W. M. Akhtar, R. J. Armstrong, J. R. Frost, N. G. Stevenson, T. J. Donohoe, *J. Am. Chem. Soc.* **2018**, *140*, 11916-11920.
- [16] B. Chatterjee, C. Gunanathan, *Org. Lett.* **2015**, *17*, 4794-4797.
- [17] G. R. Fulmer, A. J. M. Miller, N. H. Sherden, H. E. Gottlieb, A. Nudelman, B. M. Stoltz, J. E. Bercaw, K. I. Goldberg, *Organometallics* **2010**, *29*, 2176-2179.
- [18] A. Kaithal, M. Hölscher, W. Leitner, *Angew. Chem. Int. Ed.* **2018**, *57*, 13449-13453.
- [19] M. Kuriyama, R. Shimazawa, R. Shirai, *J. Org. Chem.* **2008**, *73*, 1597-1600.
- [20] J. G. Kim, P. J. Walsh, *Angew. Chem. Int. Ed.* **2006**, *45*, 4175-4178.
- [21] Y.-X. Liao, J. Dong, Q.-S. Hu, *Tetrahedron Lett.* **2018**, *59*, 1548-1550.
- [22] G. W. Kabalka, Z. Wu, Y. Ju, *Tetrahedron* **2002**, *58*, 3243-3248.
- [23] K. Iwasaki, K. K. Wan, A. Oppedisano, S. W. Crossley, R. A. Shenvi, *J. Am. Chem. Soc.* **2014**, *136*, 1300-1303.
- [24] M. J. Frisch, G. W. Trucks, H. B. Schlegel, G. E. Scuseria, M. A. Robb, J. R. Cheeseman, G. Scalmani, V. Barone, G. A. Petersson, H. Nakatsuji, X. Li, M. Caricato, A. V. Marenich, J. Bloino, B. G. Janesko, R. Gomperts, B. Mennucci, H. P. Hratchian, J. V. Ortiz, A. F. Izmaylov, J. L. Sonnenberg, Williams, F. Ding, F. Lipparini, F. Egidi, J. Goings, B. Peng, A. Petrone, T. Henderson, D. Ranasinghe, V. G. Zakrzewski, J. Gao, N. Rega, G. Zheng, W. Liang, M. Hada, M. Ehara, K. Toyota, R. Fukuda, J. Hasegawa, M. Ishida, T. Nakajima, Y. Honda, O. Kitao, H. Nakai, T. Vreven, K. Throssell, J. A. Montgomery Jr., J. E. Peralta, F. Ogliaro, M. J. Bearpark, J. J. Heyd, E. N. Brothers, K. N. Kudin, V. N. Staroverov, T. A. Keith, R. Kobayashi, J. Normand, K. Raghavachari, A. P. Rendell, J. C. Burant, S. S. Iyengar, J. Tomasi, M. Cossi, J. M. Millam, M. Klene, C. Adamo, R. Cammi, J. W. Ochterski, R. L. Martin, K. Morokuma, O. Farkas, J. B. Foresman, D. J. Fox, in *Gaussian 16 Rev. C.01*, Wallingford, CT, **2016**.

- [25] a) A. D. Becke, *J. Chem. Phys.* **1993**, *98*, 5648-5652; b) C. Lee, W. Yang, R. G. Parr, *Phys. Rev. B* **1988**, *37*, 785-789; c) S. H. Vosko, L. Wilk, M. Nusair, *Can. J. Phys.* **1980**, *58*, 1200-1211; d) P. J. Stephens, F. J. Devlin, C. F. Chabalowski, M. J. Frisch, *J. Phys. Chem.* **1994**, *98*, 11623-11627.
- [26] a) S. Grimme, *Wiley Interdisciplinary Reviews: Computational Molecular Science* **2011**, *1*, 211-228; b) S. Grimme, S. Ehrlich, L. Goerigk, *J. Comput. Chem.* **2011**, *32*, 1456-1465.
- [27] F. Weigend, R. Ahlrichs, *PCCP* **2005**, *7*, 3297-3305.
- [28] a) J. Härtner, U. M. Reinscheid, *J. Mol. Struct.* **2008**, *872*, 145-149; b) V. Dragojlovic, *ChemTexts* **2015**, *1*, 14.

## 5. Manganese catalyzed selective $\alpha$ - and $\alpha$ , $\beta$ -deuteration of primary alcohols using deuterium oxide

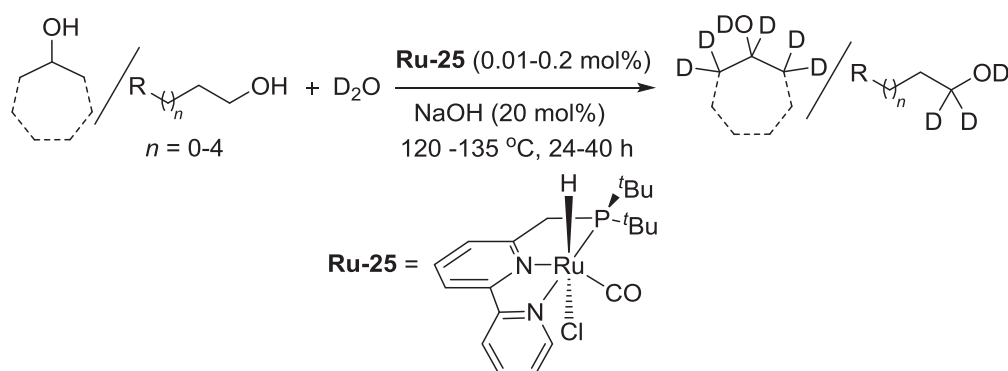
In the previous chapter, various methylation and ring closing reactions of alcohols by the manganese pincer complex using hydrogen borrowing pathways were discussed. Mechanistic studies and DFT calculations revealed that alcohols can be easily de-hydrogenated/re-hydrogenated using complex **Mn-2**. Based on the previous studies and the observed reactivity concerning the dehydrogenation of alcohols, the selective deuteration of alcohols using complex **Mn-2** and D<sub>2</sub>O as a deuterium source were investigated.

The synthesis of deuterium-labeled alcohols is an important transformation in organic synthesis. Deuterium labeled compounds has a range of applications in pharmaceuticals and is used for the study of biological compounds and their modes of action.<sup>[1]</sup> They can play an important role in the analysis of metabolism and enzymes. In general, the strength of deuterium-carbon bonds is six to ten times higher than the simple hydrogen-carbon bonds. The study of these bonds could lead us to a better understanding of many drugs, where the biological effects for the scission of hydrogen and carbon bonds are examined.<sup>[2]</sup> Additionally, the deuterium-labeled compounds are also used as solvents in NMR spectroscopy, as probes in mass spectrometry, as raw materials for labeled compounds and polymers.<sup>[1a, 3]</sup> At present, the synthesis of deuterium-labeled alcohols is carried out in a multistep procedure.<sup>[4]</sup> Generally, carbonyl compounds are reduced using deuterium-labeled reducing reagents such as LiAlD<sub>4</sub>, NaBD<sub>4</sub>, or SiDMe<sub>2</sub>Ph/F<sup>-</sup>. These processes require a stoichiometric amount of reducing agents and generate a hazardous and stoichiometric amount of chemical waste which requires repetitive workup procedures to produce the final deuterated product.<sup>[5]</sup> Therefore, the usage of a catalytic method and a cheap deuterium source is highly appealing in the chemical industry, as the direct preparation of deuterium-labeled alcohols can much easier be undertaken. Concerning this, deuterium oxide can be a good option to use as a deuterium source for the deuteration of alcohols.

To synthesize the deuterium-labeled alcohols, significant efforts were made using mainly noble metal complexes such as iridium, ruthenium, palladium, and osmium complexes.<sup>[1c, 6]</sup> However, in many cases, the reaction required a high catalyst loading and also, in some reports, D<sub>2</sub>O was not used as a deuterium source. For example, in the case of an iridium catalyzed deuteration of

alcohols, the reaction was performed using  $[D_6]$ -benzene as a deuterium source. Similarly, some of the reports, such as the ruthenium and osmium catalyzed deuteration reactions, required the use of deuterated *iso*-propyl alcohol as a deuterium source.<sup>[7]</sup>

In 2013, the group of Milstein reported a catalytic system capable of the selective deuteration of alcohols, by using a ruthenium pincer complex **Ru-25** and  $D_2O$  as a deuterium source (Scheme 5.1).<sup>[8]</sup> The reaction was performed employing a lutidine based Ru-PNN pincer complex as a precatalyst, NaOH as a co-catalyst and  $D_2O$  as a deuterium source at moderate temperatures for 24 h to 40 h. A variety of alcohols such as primary and secondary alcohols were selectively deuterated at the  $\alpha$ -position or at the  $\alpha$ ,  $\beta$ -positions, respectively. Interestingly, the reaction showed also a good reactivity under air atmosphere. Important NMR deuterated solvents such as  $[D_6]$ -ethanol and  $[D_8]$ -*iso*-propanol were also prepared using this methodology.

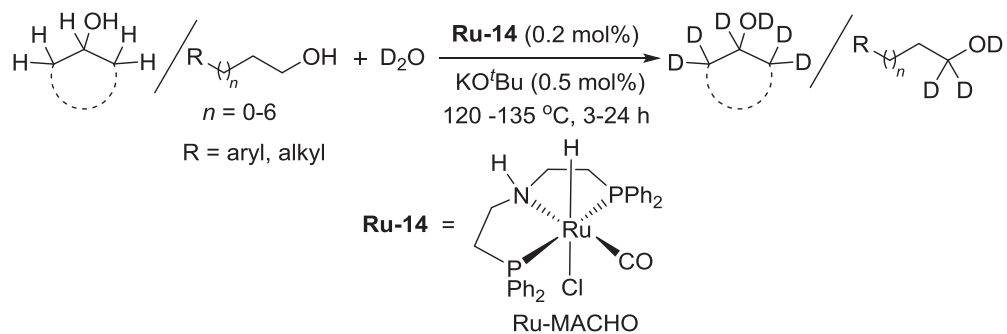


**Scheme 5.1:** Selective deuteration of alcohols reported by Milstein *et al.*<sup>[8]</sup>

In 2015, the group of Gunanathan also showed the selective deuteration of alcohols using a ruthenium PNP pincer (Ru-MACHO, **Ru-14**) complex (Scheme 5.2).<sup>[6b]</sup> The reaction revealed the selective  $\alpha$ -deuteration to primary alcohols using 0.2 mol% of the ruthenium complex and a catalytic amount of base. The use of secondary alcohols as substrates resulted in the selective deuteration at both, the  $\alpha$ - and  $\beta$ - position. The catalyst showed a very high reactivity towards a variety of alcohols. The transformation was performed at moderate temperature (60-100 °C) and 24 h time. Mechanistic studies revealed that the activation of the O-D (D/R) bond was necessary, benefiting from metal-ligand incorporation and dehydrogenation of alcohol took place to the corresponding carbonyl compound.

Manganese catalyzed selective  $\alpha$ - and  $\alpha, \beta$ -deuteration of primary alcohols using deuterium oxide

---

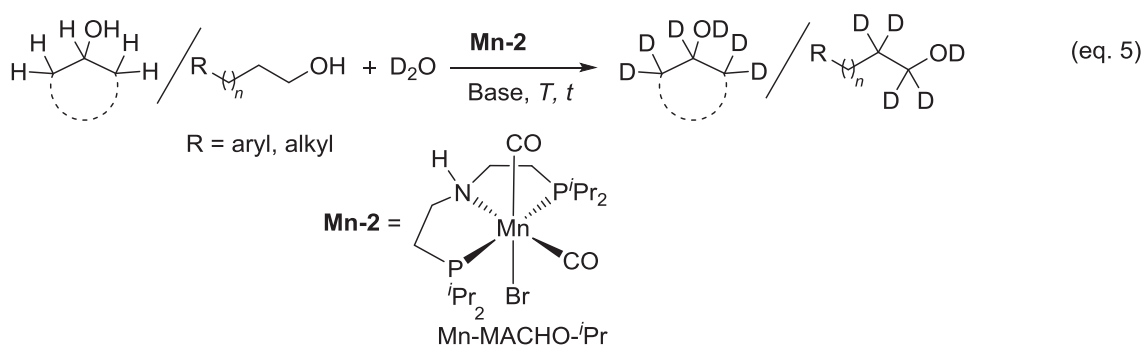


**Scheme 5.2:** Selective deuteration of alcohols reported by Gunanathan *et. al.*<sup>[6b]</sup>



## 5.1. Objective

Deuterium compounds have numerous applications in pharmaceutical and biological chemistry. At present, very few catalytic methods were reported where the selective deuteration of organic molecules were carried out using an earth-abundant metal complex. The objective of this work is to perform the selective deuteration of alcohols using the earth-abundant metal complex (eq. 5). Based on the previous studies, Mn-MACHO-*i*Pr complex **Mn-2** will be investigated for this transformation. Mechanistic studies will be carried out and the de-hydrogenation of the alcohols will be studied using complex **Mn-2**. A catalytic cycle will be proposed based on control experiments, kinetic studies and DFT calculations.



## 5.2. Reaction optimization

The reaction optimization was performed using 4-methyl benzyl alcohol **27b** as a model substrate (Table 5.1). Deuterium oxide was chosen as a deuteration agent for the reaction. Initially, the reaction of **27b** with deuterium oxide in the presence of Mn-MACHO-<sup>i</sup>Pr complex **Mn-2** (0.35 mol%) as a pre-catalyst and NaO<sup>t</sup>Bu (1.1 mol%) as a co-catalyst at 100 °C already gave selective 57% deuteration at the  $\alpha$ -position after 10 h. Further optimization was focused on the concentration of the catalyst and the base as a co-catalyst. Increasing the catalyst amount from 0.35 mol% to 0.75 mol% and the base amount from 1.1 mol% to 2 mol% at 100 °C led to higher reactivity and confirmed the selective deuteration (85%) at the  $\alpha$ -position of **27b**. The optimized conditions resulted in nearly complete deuteration (96%) at the  $\alpha$ -position after 10 h using 1.5 mol% of complex **Mn-2** and 3 mol% of the base at 100 °C. To confirm that the reaction is metal-catalyzed, control experiments were performed. The reaction in the absence of metal-catalyst **Mn-2** and base did not show any deuteration of **27b**. Similarly, the reaction only in the presence of a base and without metal-catalyst revealed no reactivity either. Based on these reactions, we concluded that the reaction required both metal and base to accomplish this transformation.

**Table 5.1:** Optimization for the deuteration of **27b** using complex **Mn-2**<sup>[a]</sup>

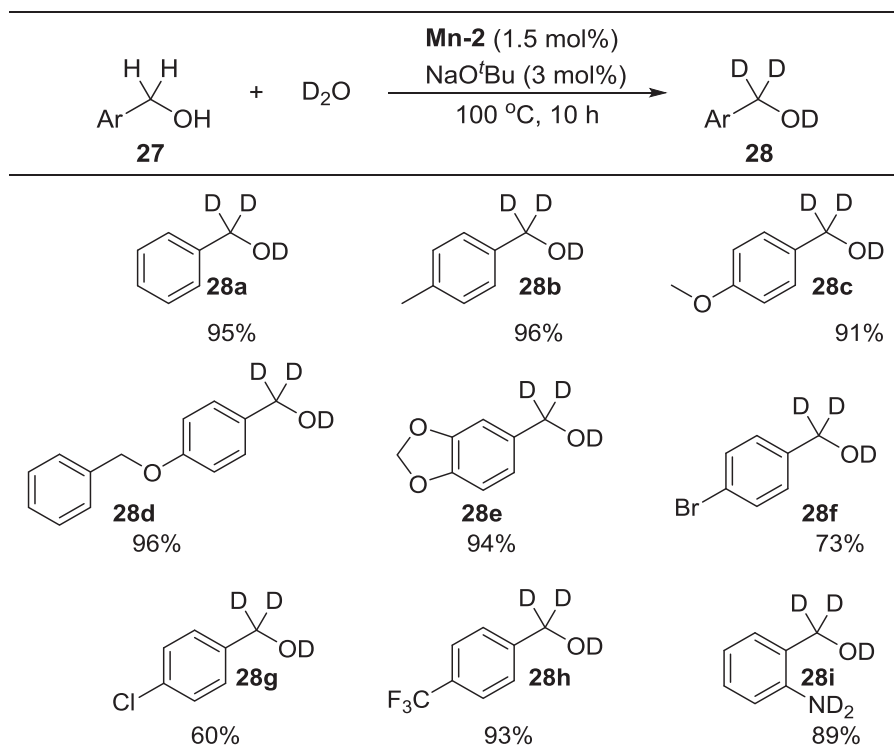
#	Catalyst (mol%)	NaO <sup>t</sup> Bu (mol%)	$\alpha$ -Deuteration (%)
1	0.35	1.1	57
2	0.75	2	85
3	1.5	3	96
4	-	-	0
5	-	3	0

Conditions: [a] **27b** (0.5 mmol), Mn catalyst **Mn-2**, NaO<sup>t</sup>Bu and D<sub>2</sub>O (0.4 mL) were charged in a schlenk tube under the argon atmosphere and the reaction mixture was heated at 100 °C for 10 h. The percentage of deuteration was measured by <sup>1</sup>H NMR spectroscopy.

### 5.3. Selective $\alpha$ -deuteration of aryl Methanols

Based on the optimized reaction conditions, various aryl methanols were investigated for selective  $\alpha$ -deuteration (Table 5.2). Benzyl alcohol **27a** was selectively deuterated in high yield (95%) at the  $\alpha$ -position. Next, in order to confirm the electronic effects, various aryl methanols substituted with electron-donating groups (EDGs) and electron-withdrawing groups (EWGs) were investigated. Aryl methanols embedded with EDGs such as *p*-methoxy benzyl alcohol **27c** and (4-(benzyloxy)phenyl)methanol **27d** showed a 91% and 96% deuteration-level at the  $\alpha$ -position, respectively. Piperonyl alcohol **27e** also revealed the selective 96% deuteration at the  $\alpha$ -position without any deuteration at the acidic CH<sub>2</sub> position of the ether functionality.

**Table 5.2:** Selective  $\alpha$ -Deuteration of aryl methanols catalyzed by Mn-precatalyst **Mn-2**<sup>[a]</sup>



Conditions: [a] **27** (0.5 mmol), Mn catalyst **Mn-2** (1.5 mol%), NaO<sup>t</sup>Bu (3 mol%) and D<sub>2</sub>O (0.4 mL) were charged in a schlenk tube under the argon atmosphere and the reaction mixture was heated at 100 °C for 10 h. The percentage of deuteration was measured by <sup>1</sup>H NMR spectroscopy.

In the next screening process, alcohols bearing halogen functionality and EWGs were investigated. The reaction of chloro- and bromo- substituted at *para*- position of benzyl alcohol showed moderate reactivity with 63% and 70% deuteration to  $\alpha$ -position, respectively. The low

reactivity can be explained due to the existence of halogen functionality in the molecule. However, unlike in the case of ruthenium-catalyzed deuteration, this system was able to perform the selective deuteration of bromo-substituted alcohol. (4-(trifluoromethyl)-phenyl)-methanol **27h** with a high activity showed a selective 93% deuteration at the  $\alpha$ -position. Next, an amine incorporated benzyl alcohol **27i** was investigated. The reaction of 2-amino benzyl alcohol with D<sub>2</sub>O showed an 89% deuteration. These results affirmed that the reaction is feasible with both electron-donating and electron-withdrawing functionalities.

#### 5.4. Selective $\alpha$ -, and $\beta$ - deuteration of 2-aryl ethanols

Next, the selective deuteration of 2-aryl ethanols (Table 5.3, entry 5a-5e) was studied. In this class, 2-phenyl ethanol **29a** was chosen as a benchmark substrate for optimization. Applying the previously optimized reaction conditions affirmed a low degree of deuteration. The reaction also revealed the deuteration at the  $\beta$ -position, which can be attributed to the base-catalyzed keto-enol tautomerization. As the deuteration at the  $\beta$ -position is not detrimental for most of the applications, the optimization was performed for both  $\alpha$ - and  $\beta$ -position. Reaction optimization studies confirmed that 3 mol% of catalyst **Mn-2** and 4 mol% of a base are best for this class of substrate. Using the optimized reaction conditions, **29a** was formed with 81% and 96% deuteration at the  $\alpha$ - and  $\beta$ -position, respectively. Similarly, other substituted aryl ethanols associated with different EDGs and EWGs also showed good reactivity. Electron donating groups in the *para*-position of 2-aryl ethanols such as methyl and methoxy substituted aryl ethanols showed selective deuteration to the  $\alpha$ - and  $\beta$ -position (94:96%, 95:96%, respectively). Similarly, electron-withdrawing groups such as *para*- substituted chloro- and fluoro- aryl ethanol affirmed the selective deuteration to  $\alpha$ - and  $\beta$ -position (94:96%, 95:96%, respectively).

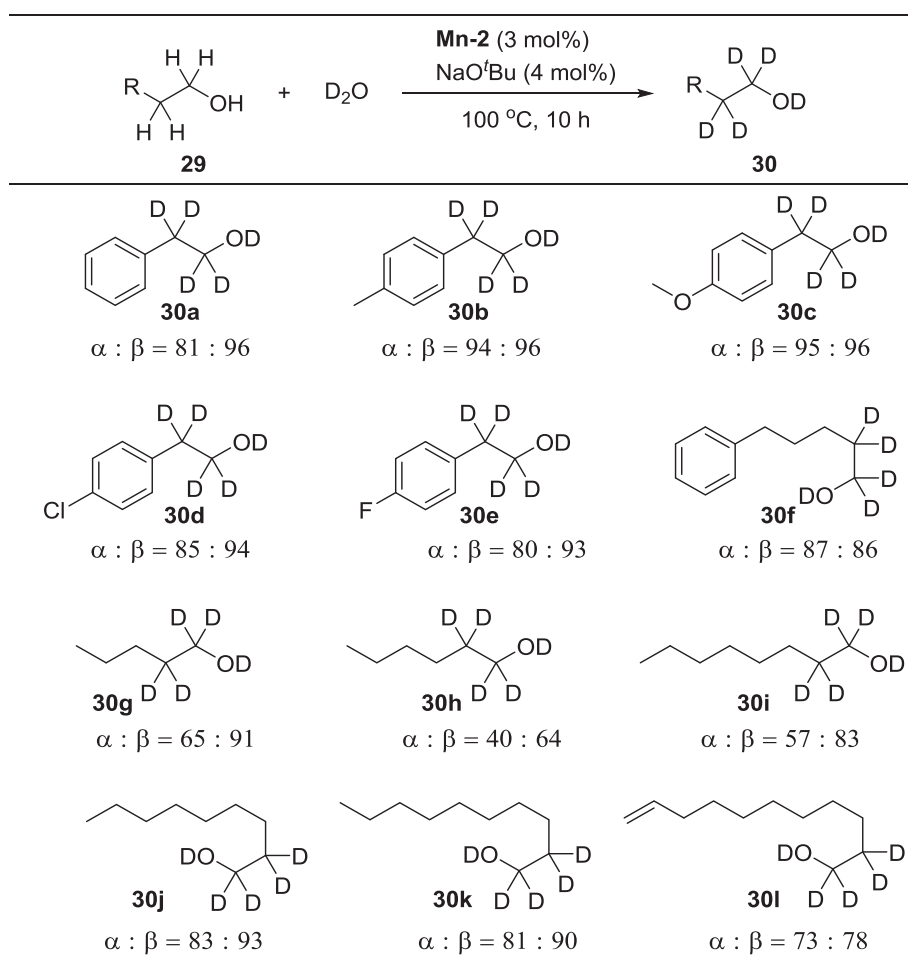
#### 5.5. Selective $\alpha$ -, and $\beta$ - deuteration of aliphatic alcohols

Furthermore, the deuteration of aliphatic alcohols was also investigated (Table 5.3, entry 5f-5l). Using the same optimized conditions phenyl substituted aliphatic alcohol such as 5-phenylpentan-1-ol **29f** led to 87% and 86% deuteration at the  $\alpha$ - and  $\beta$ -positions, respectively. The short-chain aliphatic alcohol 1-pentanol **29g** showed low activity towards the  $\alpha$ -position giving 65% deuteration and high reactivity towards the  $\beta$ -position showing an excellent grade of

Manganese catalyzed selective  $\alpha$ - and  $\beta$ -deuteration of primary alcohols using deuterium oxide

deuteration (91%). Interestingly, applying the same reaction conditions, longer chain aliphatic alcohols such as 1-octanol **29i**, 1-nonanol **29j**, and 1-decanol **29k** revealed good reactivities. 1-hexanol **29h** exhibited only low reactivity. Longer chain alcohols such as 1-nonanol, and 1-decanol were selectively deuterated at the  $\alpha$ - and  $\beta$ -position with 83:93 % and 81:90 % deuteration, respectively. Next, the effect of an alkene functionality in the aliphatic alcohol was also examined. The reaction of 10-undecen-1-ol showed 100% chemo-selectivity with 73% and 78% deuteration at the  $\alpha$ - and  $\beta$ -position, respectively. No deuteration was observed in the alkene moiety, thus paving the way to the selective deuteration of more complex molecules.

**Table 5.3:** Selective  $\alpha$ -, and  $\beta$ -deuteration of 2-aryl ethanol and aliphatic alcohols catalyzed by **Mn-2**.<sup>[a]</sup>

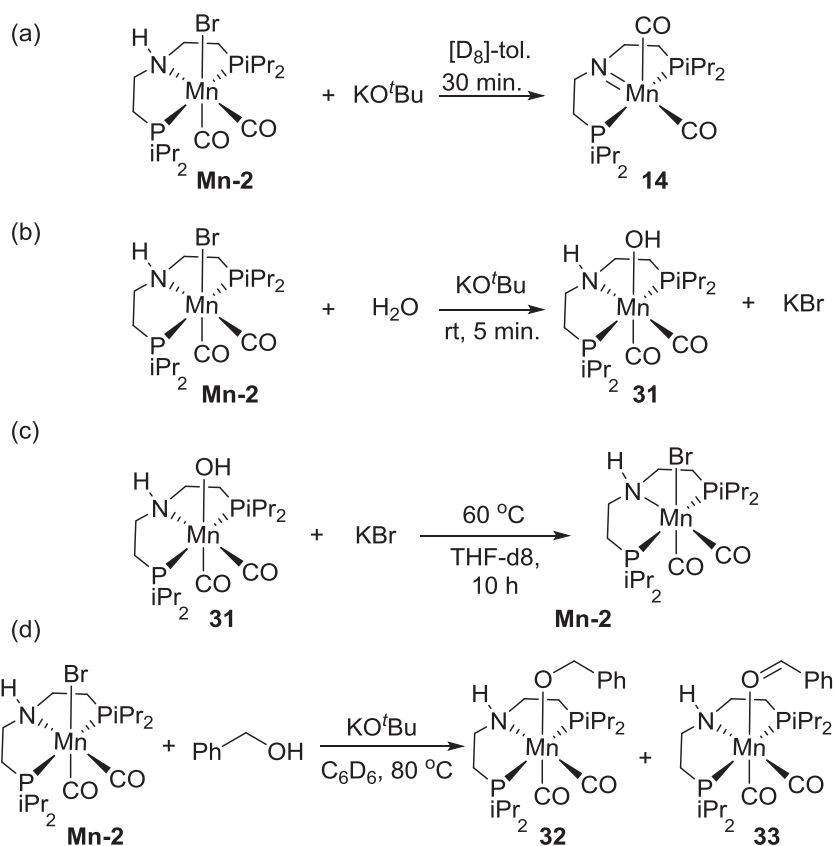


Conditions: [a] **29** (0.5 mmol), Mn catalyst **Mn-2** (3 mol%), NaO<sup>t</sup>Bu (4 mol%) and D<sub>2</sub>O (0.4 mL) were charged in a schlenk tube under the argon atmosphere and the reaction mixture was heated at 100 °C for 10 h. The percentage of deuteration was measured by <sup>1</sup>H NMR spectroscopy.

## 5.6. Mechanistic Studies

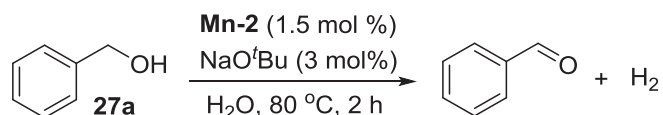
### 5.6.1. Stoichiometric reaction of complex Mn-2 with water and alcohols

Several stoichiometric reactions were performed to investigate the reaction mechanism (Scheme 5.3). The reaction of complex **Mn-2** with a base revealed the formation of the unsaturated Mn(I) species **14**. The formation of active species **14** was already discussed in earlier chapters. The reaction of complex **Mn-2** with water in the presence of a base leads to the Mn-hydroxy species **31** within 5 minutes.<sup>[9]</sup> The formation of species **31** was confirmed using NMR spectroscopy. Species **31** showed a reversible relation with complex **Mn-2**. On heating the reaction mixture of species **31** at 60 °C, an interconversion between species **31** and starting complex **Mn-2** could be confirmed using <sup>31</sup>P NMR spectroscopy. The stoichiometric reaction of complex **Mn-2** with benzyl alcohol **27a** in the presence of a base at 80 °C affirmed the formation of benzyloxy ligated Mn(I) complex **32** and benzaldehyde co-ordinated Mn(I) complex **33**.



**Scheme 5.3:** Observed *in situ* formed Mn(I) intermediates.

Additionally, the catalytic reaction of benzyl alcohol **27a** with complex **Mn-2** and base in water at 80 °C showed the formation of benzaldehyde (Scheme 5.4). These reactions confirm that the de-hydrogenation of alcohol to the corresponding carbonyl moiety is the intermediate step in the catalytic cycle.



**Scheme 5.4:** Dehydrogenation of benzyl alcohol by **Mn-2**.

### 5.6.2. Kinetic experiments

To obtain detailed information about the catalytic cycle, kinetic experiments and DFT studies (Density functional theory) were carried out using 4-methyl benzyl alcohol **27b** as a model substrate. The activation barrier of this reaction was determined experimentally. To calculate the activation energy, the Eyring equation was used. At first, the reaction order for the whole reaction was determined. After that, the rate constants ( $k$ ) were calculated by performing several reactions at four different temperatures. The temperatures were selected in a narrow range to exclude mass transfer limitations at high reaction rates. At one temperature, five reactions were performed with different reaction times to determine the value of  $k$ .

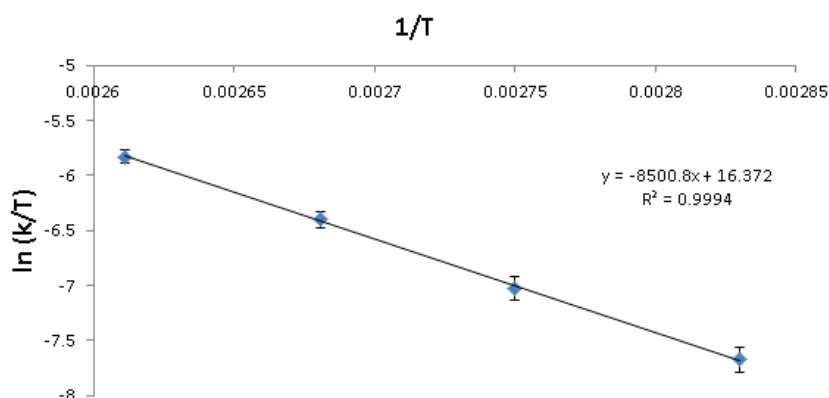


**Figure 5.1:** Eyring plot for the deuteriation of 4-methyl benzyl alcohol **27b** with **Mn-2** at four different temperatures (80-110 °C).

To obtain a reliable Eyring plot, every experiment was repeated at least two times. Once the  $k$  values were calculated at different temperatures, an Eyring plot was generated (Figure 5.1)

(details are described in the experimental section) to obtain the value of the Gibbs free activation energy. From the Eyring plot, the Gibbs free activation energy was calculated to be  $\Delta G^\ddagger = 20.9 \pm 0.5$  kcal/mol.

## 5.7. Catalytic cycle based on DFT calculation

Based on the experimental and kinetic results, a plausible catalytic cycle was proposed and subsequently calculated using DFT methods (Figure 5.2). In the presence of a base, complex **Mn-2** reacts to the active catalyst species **XXXII** (14). Intermediate **XXXII** reacts with the alcohol substrate where O–H functionality of alcohol interacts with the nitrogen centre of **XXXII** and C–H group of alcohol reacts to the Mn-center of **XXXII** and form the complex **XXXIII**.  $\beta$ -hydride elimination takes place leading to the release of aldehyde from complex **XXXIII** (the formation of aldehyde-coordinated manganese intermediate **IV** and free aldehyde was confirmed by  $^1\text{H-NMR}$  spectroscopy, Scheme 5.1 & Scheme 5.2) and to the formation of Mn- monohydride

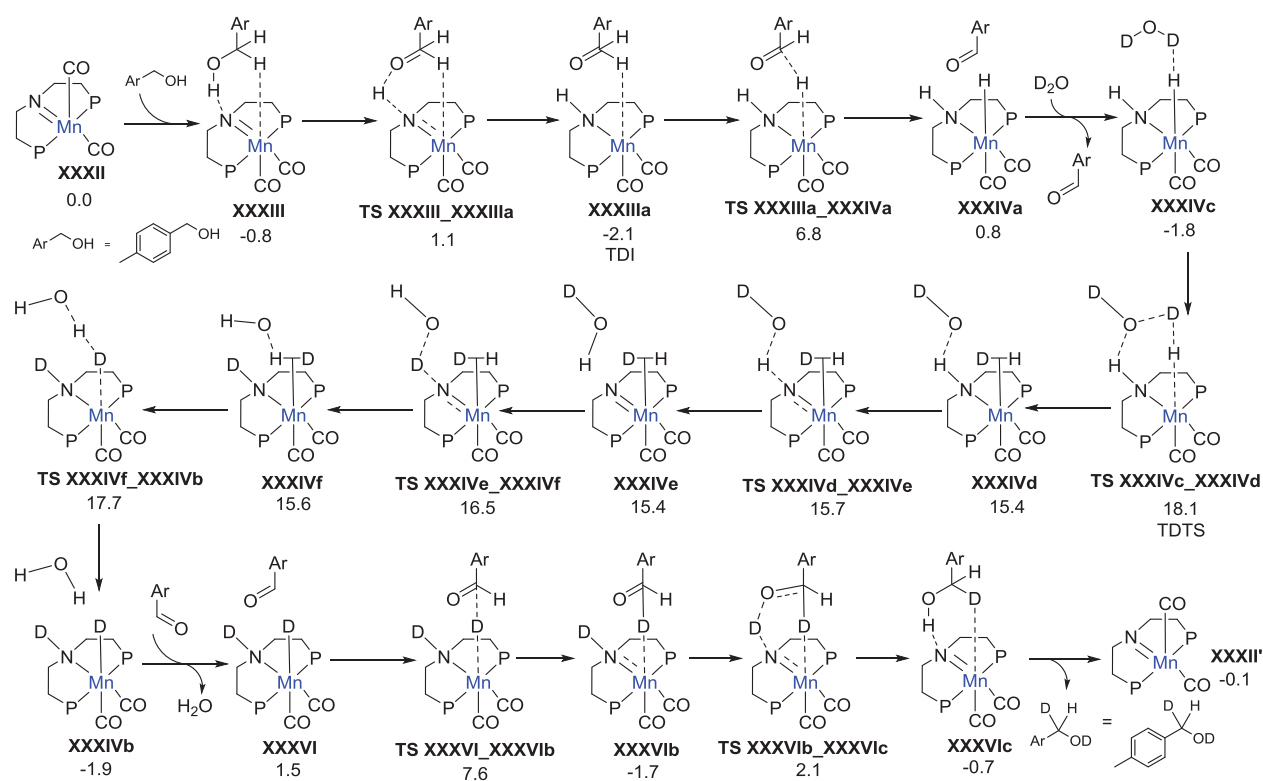


Figure 5.2: DFT calculated catalytic cycle for the selective deuteration of **27b**.



**XXXIVa**. Next Mn-H/D exchange occurs on **XXXIVa** with solvent ( $D_2O$ ), which generates intermediate **XXXIVb**. In the following step, the *in situ* generated aldehyde inserts into the Mn-D bond of **XXXIVb**, subsequently generating the monodeuterated alkoxy-ligated intermediate **XXXVIb**. A reductive elimination of the formed alcohol from **XXXVIb** provides the mono-deuterated alcohol, deuteration at the  $\alpha$ -position, and regenerates the active species **XXXII** to complete one cycle.

## 5.8. Conclusion

In conclusion, a highly selective and efficient deuteration of assorted primary aromatic and aliphatic alcohols was achieved using an earth-abundant manganese complex and  $D_2O$  as the cheapest deuterium source. Aryl methyl alcohols predominantly underwent selective  $\alpha$ -deuteration and aliphatic alcohols showed the deuteration both at the  $\alpha$ - and  $\beta$ -position. To study the catalytic cycle, DFT calculations and kinetic studies were carried out. Experiments and DFT studies confirmed that the reaction proceeds by the activation of the O-D bond and alcohol by Mn-unsaturated species **XXXII**. Formation of the aldehyde proceeds via amine-amide metal-ligand cooperation. Deuterated complex interacts with aldehyde and leads to the deuteration of alcohol. The computed Gibbs free activation energy of 20.2 kcal/mol for the overall reaction is very close to the experimentally estimated value of  $20.9 \pm 0.5$  kcal/mol. This process revealed an excellent activity towards deuteration of alcohols and can open new routes for both academia and industry for the preparation of useful deuterated compounds using a cheap earth-abundant metal catalyst under mild conditions and good selectivity.

## 5.9. Experimental

### 5.9.1. General experimental

All catalytic and stoichiometric reactions were performed under argon atmosphere using a combination of Schlenk and glove box techniques. Chemicals were purchased from Sigma Aldrich, Alfa-Aesar, TCI chemicals and used without further purification. Dry solvents were prepared according to standard procedures. Glasswares were dried under vacuum at high temperatures, evacuated, and refilled with argon at least three times.  $^1H$ ,  $^{13}C$ , and  $^{31}P$  NMR spectra were recorded with spectrometers Bruker AV300 or AV400 at room temperature. The

solvent signals were used as references and the chemical shifts converted to the TMS scale (CDCl<sub>3</sub>:  $\delta_{\text{H}} = 7.26$  ppm,  $\delta_{\text{C}} = 77.3$  ppm; C<sub>6</sub>D<sub>6</sub>:  $\delta_{\text{H}} = 7.16$  ppm,  $\delta_{\text{C}} = 127.6$  ppm; [D<sub>8</sub>]-THF:  $\delta_{\text{H}} = 1.72$  ppm,  $\delta_{\text{C}} = 24.2$  ppm; [D<sub>8</sub>]-Toluene:  $\delta_{\text{H}} = 2.1$  ppm,  $\delta_{\text{C}} = 21.4$  ppm). Chemical shifts for <sup>31</sup>P are reference against H<sub>3</sub>PO<sub>4</sub> as external standard. Multiplicity is abbreviated as: s, singlet; d, doublet; t, triplet; q, quartet; m, multiplet; br, broad.

### 5.9.2. General procedure for catalytic H/D exchange reaction for aryl methyl alcohol

To a schlenk tube, Mn-MACHO-<sup>i</sup>Pr complex **Mn-2** (1.5 mol%), NaO<sup>t</sup>Bu (2 mol%), alcohol (0.5 mmol), were introduced inside the glove-box. Degassed D<sub>2</sub>O (0.4 mL) was added under argon atmosphere. The schlenk tube was closed and heated to 100 °C temperature for 10 h. The reaction mixture was extracted with dichloromethane (3 x 5 mL) and the organic fraction was washed with water (1 x 5 mL). The organic layer was dried using MgSO<sub>4</sub> and filtered. The removal of solvent under reduced pressure provided the deuterated product which was further analysed using NMR spectroscopy.

### 5.9.3. General procedure for catalytic H/D exchange reaction for aliphatic alcohol

To a schlenk tube, Mn-MACHO-<sup>i</sup>Pr complex **Mn-2** (3 mol%), NaO<sup>t</sup>Bu (4 mol%), alcohol (0.5 mmol), were introduced inside the glove-box. Degassed D<sub>2</sub>O (0.4 mL) was added under argon atmosphere. The schlenk tube was closed and heated to 100 °C temperature for 10 h. The reaction mixture was extracted with dichloromethane (3 x 5 mL) and the organic fraction was washed with water (1 x 5 mL). The organic layer was dried using MgSO<sub>4</sub> and filtered. The removal of solvent under reduced pressure provided the deuterated product which was further analysed using NMR spectroscopy.

### 5.9.4. Stoichiometric reaction of complex **Mn-2** with $\text{H}_2\text{O}$ in the presence of a base

A J-young type NMR tube was charged with complex **Mn-2** (0.025 mmol, 12.375 mg),  $\text{H}_2\text{O}$  (0.25 mmol, 4.5  $\mu\text{l}$ ),  $\text{KO}^t\text{Bu}$  (0.0275 mmol) and  $[\text{D}_8]$ -THF (0.4 mL) under argon atmosphere. The NMR tube was stirred using centrifuge for 5 minutes at room temperature. The  $^{31}\text{P}$  NMR spectrum was recorded which indicates the formation of a new peak at  $\delta$ : 86.48 ppm corresponds to the complex **31**. The formation of complex **31** is in agreement with the reported literature.<sup>[10]</sup>

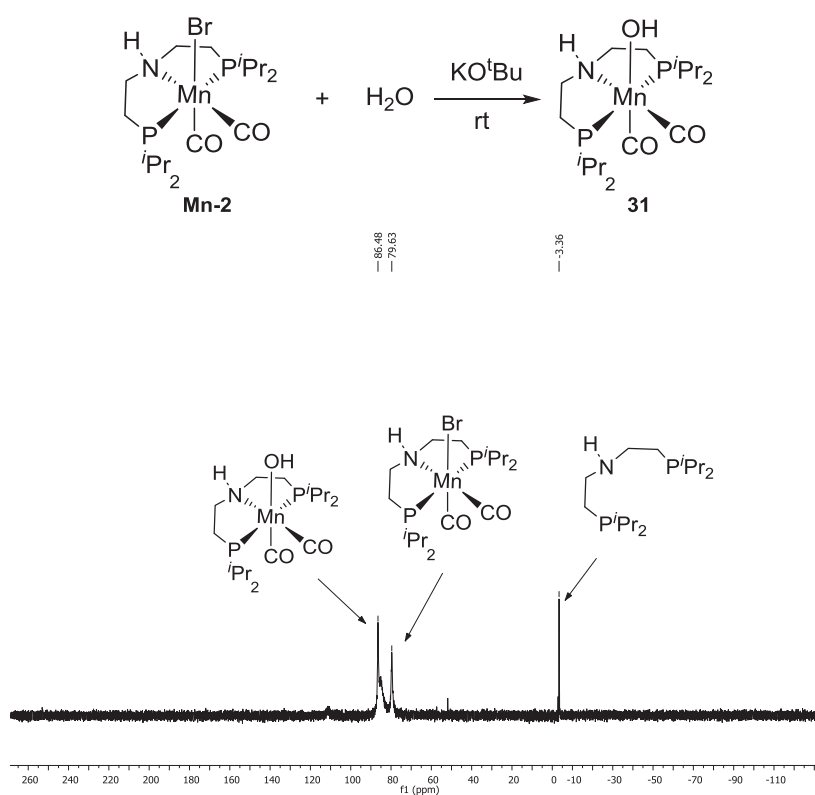


**Figure 5.3:**  $^{31}\text{P}\{^1\text{H}\}$ -NMR (162 MHz,  $[\text{D}_8]$ -toluene, 298 K) spectrum of **Mn-2** and **31**.

### 5.9.5. Reaction after 10 h at 60 °C temperature

The above discussed same reaction mixture was heated at 60 °C for 10 h. The  $^{31}\text{P}$  NMR showed the disappearance of the complex **31** and regeneration of the complex **Mn-2**.

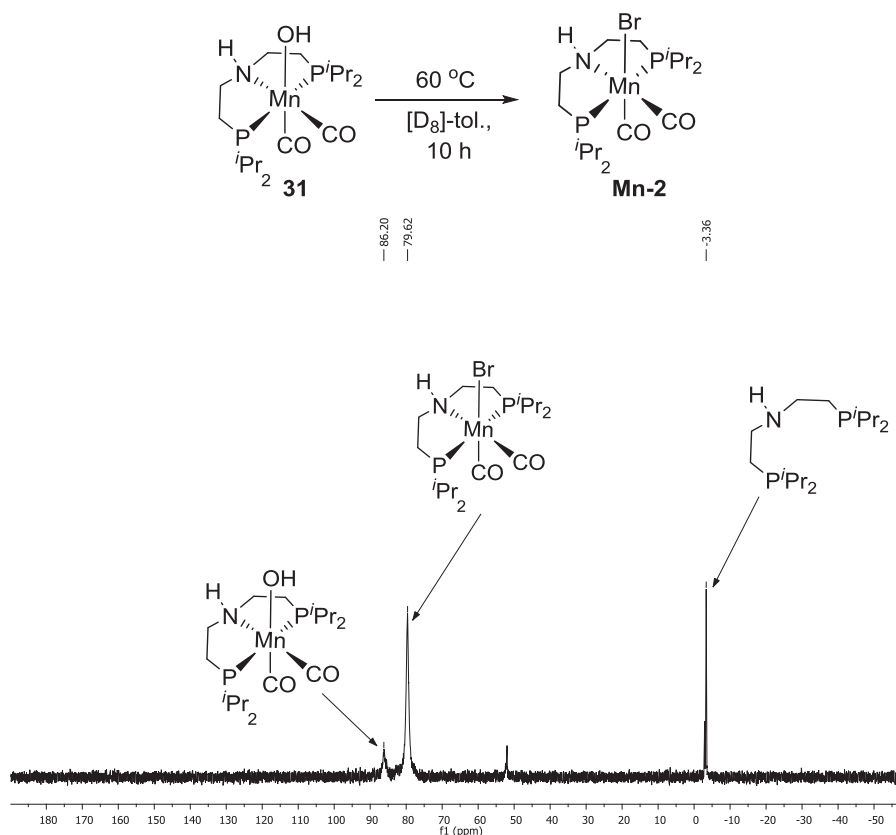
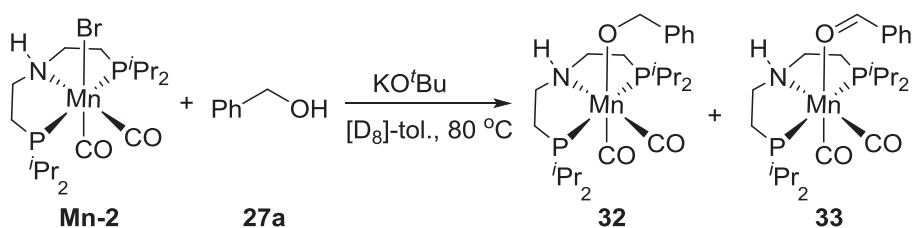


Figure 5.4:  $^{31}\text{P}\{^1\text{H}\}$ -NMR (162 MHz,  $[\text{D}_8]$ -toluene, 298 K) spectrum of **Mn-2** and **31** after 10 h at 60 °C

### 5.9.6. Stoichiometric reaction of complex **Mn-2** with benzyl alcohol **27a**



Under an argon atmosphere, a J-young type NMR tube was charged with complex **Mn-2** (0.025 mmol, 12.375 mg), benzyl alcohol **27a** (0.031 mmol, 3.2  $\mu\text{l}$ ),  $\text{KO}^t\text{Bu}$  (0.0275 mmol) and  $[\text{D}_8]$ -toluene (0.4 mL). The resulting solution was stirred using centrifuge for 5 minutes at room temperature and further recorded for  $^{31}\text{P}$  NMR spectrum. The NMR tube was further heated to 100 °C for 10 h and  $^{31}\text{P}$  NMR spectrum was recorded for one more time.

Manganese catalyzed selective  $\alpha$ - and  $\alpha$ ,  $\beta$ -deuteration of primary alcohols using deuterium oxide

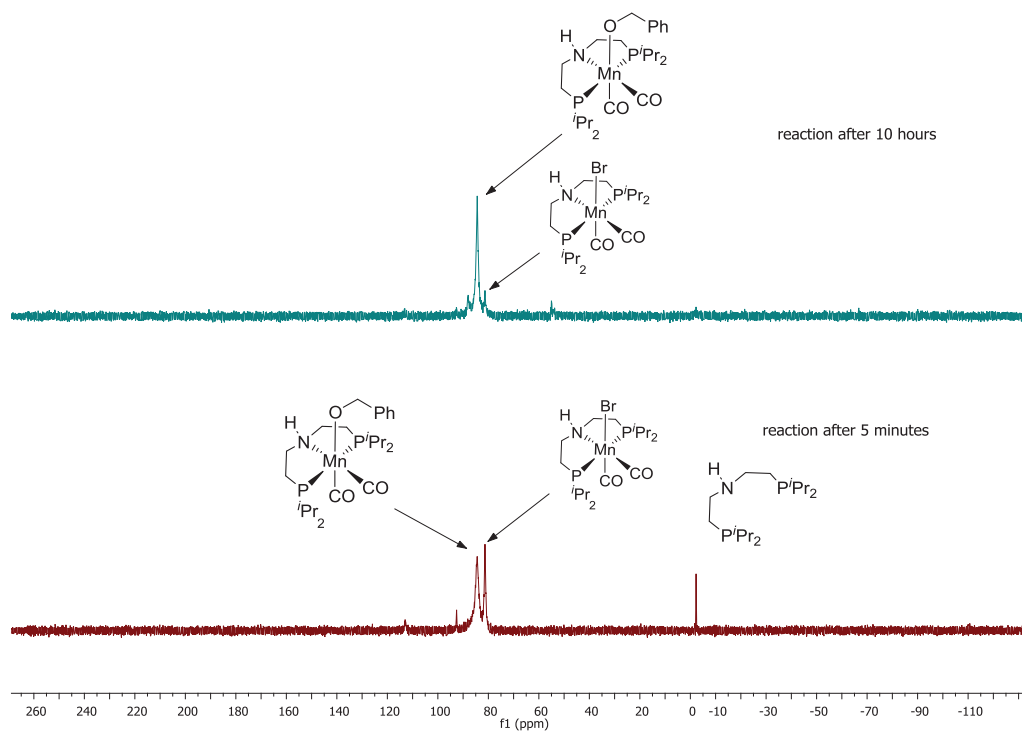


Figure 5.5:  $^{31}\text{P}\{^1\text{H}\}$ -NMR (162 MHz,  $[\text{D}_8]$ -toluene, 298 K) spectrum of **32** and **33** at different time interval.

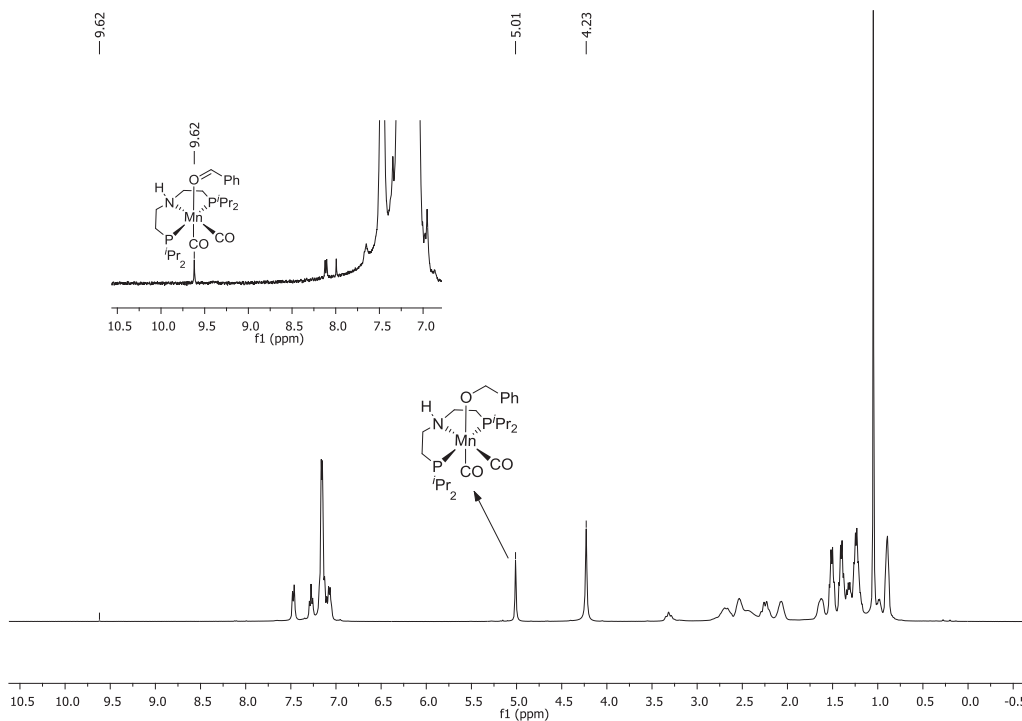
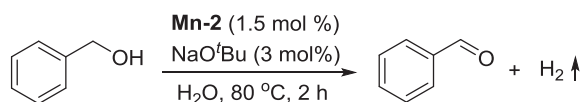
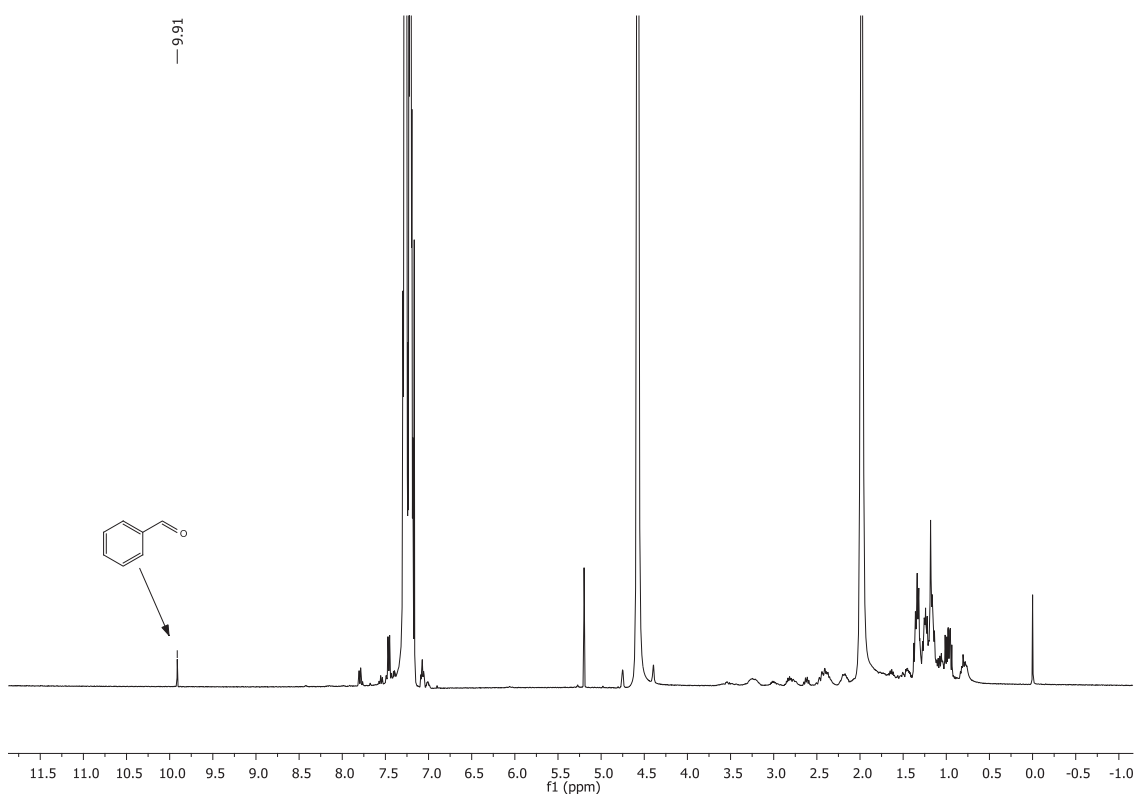


Figure 5.6:  $^1\text{H}$  NMR (300 MHz,  $[\text{D}_8]$ -toluene, 298 K) spectrum of **32** and **33**.

### 5.9.7. Dehydrogenation of benzyl alcohol **27a** using complex **Mn-2**



To a schlenk tube, Mn-MACHO-<sup>i</sup>Pr complex **Mn-2** (0.005 mmol, 2.48 mg), KO<sup>t</sup>Bu (0.01 mmol, 1.12 mg), and benzyl alcohol **27a** (0.5 mmol, 0.051 mL) were introduced inside the glove-box. Degassed water (0.4 mL) was added under argon atmosphere. The schlenk tube was closed and heated to 80 °C temperature for 2 h. The reaction mixture was extracted with dichloromethane (3 x 5 mL) and the organic fraction was washed with water (1 x 5 mL). The organic layer was dried over MgSO<sub>4</sub> and filtered. The solvent was removed under reduced pressure. <sup>1</sup>H NMR spectrum confirmed the formation of benzaldehyde in the reaction mixture.



**Figure 5.7:** <sup>1</sup>H NMR (300 MHz, CDCl<sub>3</sub>, 298 K) spectrum for the reaction of benzyl alcohol **27a** in the presence of complex **Mn-2** and base.

### 5.9.8. Eyring-Plot

Exemplary for the  $\alpha$ -deuteration of 4-methyl benzyl alcohol **27b** with precatalyst **Mn-2**.

#### Determination of the order of the reaction

To calculate the order of a reaction, two different sets of experiments were performed. In the first set of experiments, the order was examined based on the different concentration of **27b**. For this particular investigation, several experiments were performed at 100 °C using a constant concentration of D<sub>2</sub>O (0.4 ml), manganese complex **Mn-2** (1.5 mol%), NaO<sup>t</sup>Bu (2 mol%) with different concentration of 4-methyl benzyl alcohol **27b**. By obtaining the result from <sup>1</sup>H-NMR spectroscopy, the reaction rates were calculated which was further plotted with respect to the concentration of alcohol. The results revealed that the concentration of alcohol showed first order dependency in the overall reaction.

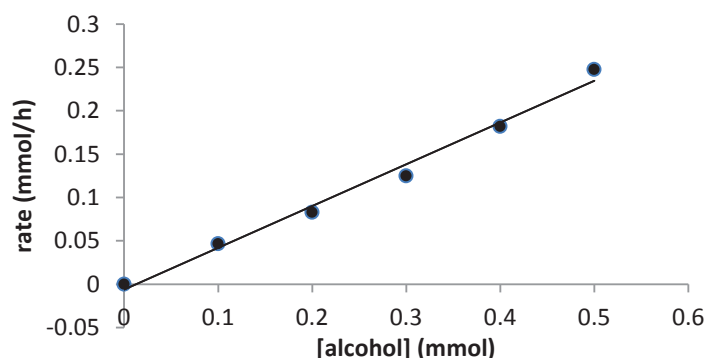


**Figure 5.8:** Plot between reaction rate (mmol/h) vs. [alcohol] (first order)

Similarly other sets of experiments were performed by varying the concentration of catalyst **Mn-2**. For this set of experiments, several experiments were performed at 100 °C using constant concentration of D<sub>2</sub>O (0.4 ml), 4-methyl benzyl alcohol **27b** (0.5 mmol), NaO<sup>t</sup>Bu (2 equiv. with respect to complex **Mn-2**) with different concentration of complex **Mn-2**. Using the <sup>1</sup>H NMR spectroscopy, the reaction rate was calculated which was further plotted against the concentration of the catalyst. In this case also, the reaction confirmed the first order dependency for the concentration of catalyst.

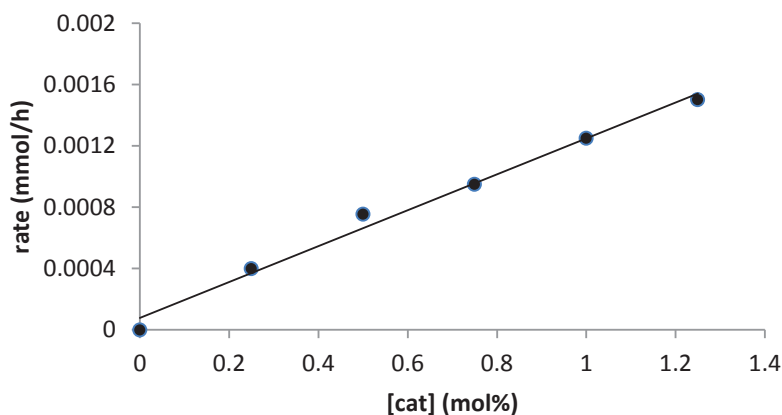


**Figure 5.9:** Plot of rate (mmol/h) Vs. [catalyst] (first order).

The concentration the  $D_2O$  was not considered for the calculation of the reaction order. As it was used in a large amount and also acted as a reaction solvent.

Overall rate equation for the deuteration of the **27b**:

$$d[P]/dt = K_{obs} [\text{catalyst}]^1 [\text{Alcohol}]^1$$

The overall reaction follows 2<sup>nd</sup> order kinetic.

### Calculation of $k$ -value at different temperature

Four different temperatures were chosen to calculate the value of  $k$ . The reactions were performed at 80 °C, 90 °C, 100 °C, and 110 °C temperature. At one temperature, five reactions were performed and monitored at different times to find the exact value of  $k$ . All reactions were performed at least two times to get the exact value of  $k$ .

### Reaction procedure for calculating the value of $k$ at 80 °C temperatures

Five reactions were performed at 80 °C which was analyzed at different times. To a schlenk tube, Mn-MACHO-<sup>*i*</sup>Pr complex **Mn-2** (1.5 mol%), NaO<sup>*i*</sup>Bu (3 mol%), 4-methyl benzyl alcohol **27b** (0.5 mmol) were introduced inside the glove-box. Degassed  $D_2O$  (0.4 mL) was added under argon atmosphere. The schlenk tube was closed and heated to 80 °C temperature for a certain time. The reaction mixture was extracted with dichloromethane (3 x 5 mL) and the organic fraction was washed with water (1 x 5 mL). The organic layer was dried over  $MgSO_4$  and filtered. The solvent was removed under reduced pressure and analyzed by NMR spectroscopy.



Manganese catalyzed selective  $\alpha$ - and  $\beta$ -deuteration of primary alcohols using deuterium oxide

The above-mentioned procedure was also applied to other experiments which were performed at 90, 100 and 110 °C temperature and the values of  $k$  were calculated from the slope.

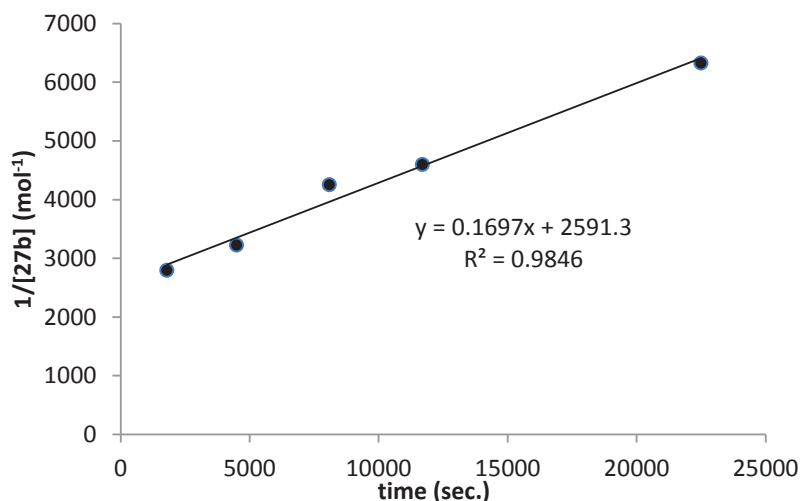


Figure 5.10: Plot of 1/[27b] vs time at 80 °C temperature.

### Eyring Equation

$$k = \frac{k_B \cdot T}{h} \cdot e^{\frac{-\Delta G^\ddagger}{R \cdot T}}$$

$$\Delta G^\ddagger = \Delta H^\ddagger - T \Delta S^\ddagger$$

$$\ln\left(\frac{k}{T}\right) = \frac{-\Delta H^\ddagger}{R} \frac{1}{T} + \ln \frac{k_B}{h} + \frac{\Delta S^\ddagger}{R}$$

$h$  = Plank's constant =  $6.6262 \cdot 10^{-34}$  Js

$k_B$  = Boltzmann's constant =  $1,3807 \cdot 10^{-23}$  JK<sup>-1</sup>

$R$  = Gas constant =  $0.00198588$  kcalK<sup>-1</sup>mol<sup>-1</sup>

$T$  = Temperature = 423 K

Table 2: Average k-values for the deuteration of 27b with precatalyst Mn-2

Temp. (°C)	Average k	1/T	ln (k/T)
80	0.1638	0.002833	-7.675511293
90	0.3216	0.00275	-7.030233261
100	0.6196	0.00268	-6.400269564
110	1.1284	0.00261	-5.827215141

## Experimental error

The experimental error was calculated by as the sum of errors from the temperature curves, linear fit of the Eyring-plot, the weighing error and the measuring error when using syringes.

### 5.9.9. Computational Details

The DFT calculations in this work were carried out by Dr. Markus Hölscher using the Gaussian09 program package (Revision E.01).<sup>[11]</sup> All compounds shown in Figure 5.2 were optimized using the B97 density functional augmented with Grimmes D3 dispersion correction in combination with the Becke-Johnson (BJ) damping (B97D3-BJ).<sup>[12]</sup> The def2-TZVP basis set<sup>[13]</sup> was used for all elements together with the associated ECP for ruthenium.<sup>[14]</sup> The automatic density fitting approximation was activated.<sup>[15]</sup> The optimizations were carried out using an implicit solvent model (IEF-PCM) with the SMD radii model.<sup>[16]</sup> The solvent used was D<sub>2</sub>O. Corrections for standard state were applied by setting the pressure to 603 atm, while the thermochemical parameters were computed for a temperature of  $T = 373$  K. The nature of all local minima and all transition states was characterized by performing frequency calculations showing no ( $i = 0$ ) or one ( $i = 1$ ) imaginary frequencies, respectively. In selected cases intrinsic reaction coordinate (IRC) computations were carried out to prove the localized transition states to connect the independently optimized preceding/following minima. Energy values reported in figures and text are Gibbs free energies unless otherwise noted. The energies are listed in Table 5.5.

Manganese catalyzed selective  $\alpha$ - and  $\alpha$ ,  $\beta$ -deuteration of primary alcohols using deuterium oxide

**Table 5.4:** DFT-computed energies (Hartree) and relative Gibbs free energies (kcal/mol) of compounds shown in Figure 5.5 of the main text.

Compd.	<i>E</i>	<i>Ezpe</i>	<i>H</i>	<i>G</i>	<i>Grel</i>
XXXII	-2746.90531	-2746.39741	-2746.34881	-2746.475943	0.0
XXXIII	-3132.93101	-3132.26361	-3132.20041	-3132.358059	-0.8
TSXXIII-XXIIIa	-3132.92778	-3132.26373	-3132.2016	-3132.354988	1.1
XXXIIIa	-3132.93571	-3132.26819	-3132.20551	-3132.360111	-2.1
TS_XXIIIa_XXXIVa	-3132.91834	-3132.2543	-3132.19173	-3132.346002	6.8
XXXIVa	-2748.11073	-2747.58195	-2747.53277	-2747.658462	0.8
XXXIVc	-2824.56836	-2824.0177	-2823.96392	-2824.099247	-1.8
TS_XXXIVc-XXXIVd	-2824.53357	-2823.98852	-2823.93557	-2824.067562	18.1
XXXIVd	-2824.53745	-2823.99118	-2823.93752	-2824.071374	15.4
TS_XXXIVd-XXXIVe	-2824.53235	-2823.99171	-2823.9386	-2824.071443	15.7
XXXIVe					15.4
TS_XXXIVe-XXXIVf	-2824.53235	-2823.99066	-2823.93765	-2824.070067	16.5
XXXIVf	-2824.53745	-2823.99177	-2823.93821	-2824.071562	15.6
TS_XXXIVf-XXXIVb	-2824.53357	-2823.98955	-2823.93678	-2824.068243	17.7
XXXIVb	-2824.56836	-2824.01805	-2823.96424	-2824.099342	-1.9
XXXVI	-2748.11073	-2747.58748	-2747.53771	-2747.664395	1.5
TSXXXVI-XXXVIb	-3132.91834	-3132.25957	-3132.19642	-3132.351664	7.6
XXXVIb	-3132.93571	-3132.27424	-3132.21112	-3132.366437	-1.7
TS_XXXVIb-XXXII	-3132.92778	-3132.26901	-3132.20647	-3132.360498	2.1
	-3132.93101	-3132.27018	-3132.20656	-3132.36489	-0.7
XXXII'					-0.1
	-385.999007	-385.842245	-385.827425	-385.88087	
	-385.999008	-385.848759	-385.833536	-385.887939	
	-384.79459	-384.660555	-384.646999	-384.697025	
H <sub>2</sub> O	-76.43566	-76.414981	-76.41024	-76.429622	
D <sub>2</sub> O	-76.43566	-76.420611	-76.415824	-76.436594	
HOD	-76.2287488	-76.223748	-76.21885	-76.239127	

## References

- [1] a) J. Atzrodt, V. Derdau, T. Fey, J. Zimmermann, *Angew. Chem. Int. Ed.* **2007**, *46*, 7744-7765; b) T. Junk, W. J. Catallo, *Chem. Soc. Rev.* **1997**, *26*, 401-406; c) M. H. G. Pechtl, M. Hölscher, Y. Ben-David, N. Theyssen, D. Milstein, W. Leitner, *Eur. J. Inorg. Chem.* **2008**, *2008*, 3493-3500; d) L. Neubert, D. Michalik, S. Bähn, S. Imm, H. Neumann, J. Atzrodt, V. Derdau, W. Holla, M. Beller, *J. Am. Chem. Soc.* **2012**, *134*, 12239-12244; e) B. Chatterjee, C. Gunanathan, *Org. Lett.* **2015**, *17*, 4794-4797; f) B. Chatterjee, C. Gunanathan, *Chem. Commun.* **2016**, *52*, 4509-4512; g) *Synthesis and Application of Isotopically Labeled Compounds*, Pleiss, U., Voges, R., Eds.; Wiley: New York, 2001; Vol. 2007; h) M. Saljoughian, P. G. Williams, *Curr. Pharm. Des.* **2000**, *6*, 1029-1056.
- [2] R. P. Bell, *Chem. Soc. Rev.* **1974**, *3*.
- [3] a) A. Di Giuseppe, R. Castarlenas, J. J. Pérez-Torrente, F. J. Lahoz, V. Polo, L. A. Oro, *Angew. Chem. Int. Ed.* **2011**, *50*, 3938-3942; b) T. H. Lowry., K. S. Richardson, *Mechanism and Theory in Organic Chemistry*, Harper and Row, New York **1987**.
- [4] a) M. Orfanopoulos, I. Smonou, C. S. Foote, *J. Am. Chem. Soc.* **1990**, *112*, 3607-3614; b) F.-D. Kopinke, G. Zimmermann, J. Aust, K. Scherzer, *Chem. Ber.* **1989**, *122*, 721-725; c) J.-L. Abad., G. Villorbina., G. Fabria`s., F. Camps, *J. Org. Chem.* **2004**, *69*, 7108-7113; d) R. C. Todd, M. M. Hossain, K. V. Josyula, P. Gao, J. Kuo, C. T. Tan, *Tetrahedron Lett.* **2007**, *48*, 2335-2337; e) I. N. Lykakis, C. Tanielian, R. Seghrouchni, M. Orfanopoulos, *J. Mol. Catal. A: Chem.* **2007**, *262*, 176-184.
- [5] a) D. Klomp, T. Maschmeyer, U. Hanefeld, J. A. Peters, *Chem. Eur. J.* **2004**, *10*, 2088-2093; b) D. R. Jensen, M. J. Schultz, J. A. Mueller, M. S. Sigman, *Angew. Chem. Int. Ed.* **2003**, *42*, 3810-3813; c) P. L. Polavarapu, L. P. Fontana, H. F. Smith, *J. Am. Chem. Soc.* **1986**, *108*, 94-99; d) Q. Wang, X. Sheng, J. H. Horner, M. Newcomb, *J. Am. Chem. Soc.* **2009**, *131*, 10629-10636; e) P. G. Andersson, *J. Org. Chem.* **1996**, *61*, 4154-4156; f) L. Xu, N. P. Price, *Carbohydr. Res.* **2004**, *339*, 1173-1178; g) M. Fujita, T. Hiyama, *J. Org. Chem.* **1988**, *53*, 5405-5415; h) D. Miyazaki, K. Nomura, H. Ichihara, Y. Ohtsuka, T. Ikeno, T. Yamada, *New J. Chem.* **2003**, *27*, 1164-1166.
- [6] a) C. M. Yung, M. B. Skaddan, R. G. Bergman, *J. Am. Chem. Soc.* **2004**, *126*, 13033-13043; b) B. Chatterjee, C. Gunanathan, *Org. Lett.* **2015**, *17*, 4794-4797; c) W. Bai, K.-H. Lee, S. K. S. Tse, K. W. Chan, Z. Lin, G. Jia, *Organometallics* **2015**, *34*, 3686-3698; d) S. R. Klei, J. T. Golden, T. D. Tilley, R. G. Bergman, *J. Am. Chem. Soc.* **2002**, *124*, 2092-2093; e) C. Balzarek., T. J. R. Weakley., D. R. Tyler, *J. Am. Chem. Soc.* **2000**, *122*, 9427-9434; f) K. L. Breno., D. R. Tyler, *Organometallics* **2001**, *20*, 3864-3868.
- [7] G. Bossi, E. Putignano, P. Rigo, W. Baratta, *Dalton Trans.* **2011**, *40*, 8986-8995.
- [8] E. Khaskin, D. Milstein, *ACS Catal.* **2013**, *3*, 448-452.
- [9] S. Fu, Z. Shao, Y. Wang, Q. Liu, *J. Am. Chem. Soc.* **2017**, *139*, 11941-11948.
- [10] S. Fu, Z. Shao, Y. Wang, Q. Liu, *J. Am. Chem. Soc.* **2017**, *139*, 11941-11948.
- [11] M. J. Frisch, G. W. Trucks, H. B. Schlegel, G. E. Scuseria, M. A. Robb, J. R. Cheeseman, G. Scalmani, V. Barone, G. A. Petersson, H. Nakatsuji, X. Li, M. Caricato, A. V. Marenich, J. Bloino, B. G. Janesko, R. Gomperts, B. Mennucci, H. P. Hratchian, J. V. Ortiz, A. F. Izmaylov, J. L. Sonnenberg, Williams, F. Ding, F. Lipparini, F. Egidi, J. Goings, B. Peng, A.

- Petrone, T. Henderson, D. Ranasinghe, V. G. Zakrzewski, J. Gao, N. Rega, G. Zheng, W. Liang, M. Hada, M. Ehara, K. Toyota, R. Fukuda, J. Hasegawa, M. Ishida, T. Nakajima, Y. Honda, O. Kitao, H. Nakai, T. Vreven, K. Throssell, J. A. Montgomery Jr., J. E. Peralta, F. Ogliaro, M. J. Bearpark, J. J. Heyd, E. N. Brothers, K. N. Kudin, V. N. Staroverov, T. A. Keith, R. Kobayashi, J. Normand, K. Raghavachari, A. P. Rendell, J. C. Burant, S. S. Iyengar, J. Tomasi, M. Cossi, J. M. Millam, M. Klene, C. Adamo, R. Cammi, J. W. Ochterski, R. L. Martin, K. Morokuma, O. Farkas, J. B. Foresman, D. J. Fox, in *Gaussian 16 Rev. C.01*, Wallingford, CT, **2016**.
- [12] G. Stefan, E. Stephan, G. Lars, *J. Comput. Chem.* **2011**, *32*, 1456-1465.
- [13] a) F. Weigend, R. Ahlrichs, *PCCP* **2005**, *7*, 3297-3305; b) K. Eichkorn, F. Weigend, O. Treutler, R. Ahlrichs, *Theor. Chem. Acc.* **1997**, *97*, 119-124.
- [14] a) D. Andrae, U. Häußermann, M. Dolg, H. Stoll, H. Preuß, *Theor. Chem. Acc.* **1990**, *77*, 123-141; b) F. Weigend, F. Furche, R. Ahlrichs, *J. Chem. Phys.* **2003**, *119*, 12753-12762; c) A. Schäfer, C. Huber, R. Ahlrichs, *J. Chem. Phys.* **1994**, *100*, 5829-5835; d) A. Schäfer, H. Horn, R. Ahlrichs, *J. Chem. Phys.* **1992**, *97*, 2571-2577; e) B. Metz, H. Stoll, M. Dolg, *J. Chem. Phys.* **2000**, *113*, 2563-2569.
- [15] a) B. I. Dunlap, *J. Mol. Struct.-Theochem* **2000**, *529*, 37-40; b) B. I. Dunlap, *J. Chem. Phys.* **1983**, *78*, 3140-3142.
- [16] a) A. V. Marenich, C. J. Cramer, D. G. Truhlar, *J. Phys. Chem. B* **2009**, *113*, 6378-6396; b) J. Tomasi, B. Mennucci, R. Cammi, *Chem. Rev.* **2005**, *105*, 2999-3094; c) E. Cancès, B. Mennucci, J. Tomasi, *J. Chem. Phys.* **1997**, *107*, 3032-3041.

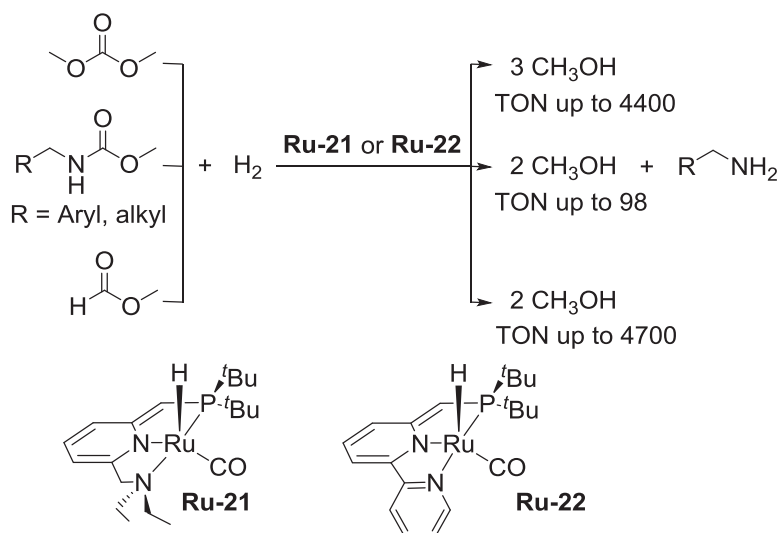
## 6. Catalytic hydrogenation of cyclic carbonates using manganese complexes

Parts of this chapter have been published:

**A. Kaithal**, M. Hölscher, W. Leitner, *Angew. Chem. Int. Ed.* **2018**, *57*, 13449-13453. *Angew. Chem.* **2018**, *130*, 13637-13641.

The reduction of carbonyl functionalities is an ongoing topic in organic synthesis and among all of the organic carbonyl functionalities, carbonic acid derivatives are the most challenging substrates to hydrogenate.<sup>[1]</sup> Organic carbonates are one of the classes of carbonic acid derivatives and can be made directly from the reaction of CO<sub>2</sub> and alcohols or cyclic ethers. These molecules have a great potential in industry as they are environmentally benign, sustainable and can be used as solvents and reagents. As these molecules can directly be derived from CO<sub>2</sub> and as their direct hydrogenation can lead to the formation of methanol and the corresponding valuable organic molecules such as alcohols, diols, and amine, at present, there is a strong interest in the hydrogenation of these molecules.<sup>[2]</sup> Methanol itself is an attractive compound in the chemical industry because of its use in the fuel industry,<sup>[3]</sup> as a C1 source in organic transformation,<sup>[4]</sup> or as an organic precursor for the production of higher hydrocarbons.<sup>[5]</sup> In the chemical industry, the synthesis of methanol is carried out converting synthesis gas (CO, H<sub>2</sub>, and CO<sub>2</sub>) catalyzed by Cu/ZnO/Al<sub>2</sub>O<sub>3</sub>-based heterogeneous catalyst at high temperature and high pressure.<sup>[6]</sup> Several studies were also reported where methanol was directly synthesized from CO<sub>2</sub> using a heterogeneous catalyst.<sup>[7]</sup> Presently, the direct hydrogenation of CO<sub>2</sub> to methanol using a homogeneous molecular catalyst is still a great challenge. The high thermodynamic stability of inert CO<sub>2</sub><sup>[8]</sup> where one equivalent of CO<sub>2</sub> is reduced employing three equivalents of hydrogen results in high activation barriers to produce one equivalent of methanol and one equivalent of water. In the last few years, a couple of investigations were reported where homogeneous molecular catalysts were used for the hydrogenation of CO<sub>2</sub> to MeOH.<sup>[3f, 3g, 9]</sup>

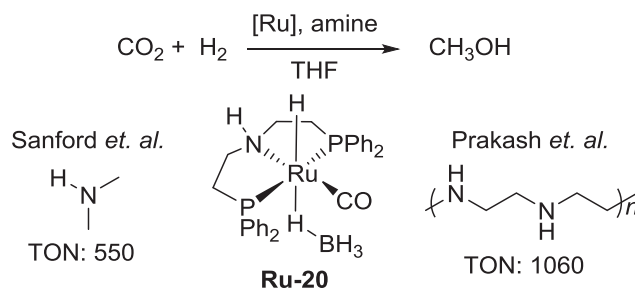
In 2011, the group of Milstein reported the catalytic hydrogenation of CO<sub>2</sub> indirectly via the reduction of isolated CO<sub>2</sub> derivatives such as carbonates, formates, and carbamates using Ru-PNN pincer complexes under relatively mild conditions (Scheme 6.1).<sup>[2]</sup> Lutidine based Ru-PNN pincer complexes (**Ru-21** and **Ru-22**) and hydrogen as a reducing agent was used to accomplish this transformation. The reaction showed a maximum TON of 4400 for the hydrogenation of methyl carbonate to methanol at 50 bar of H<sub>2</sub> and 145 °C in THF as a solvent. Similarly, formates and carbamates were also reduced. Using the same ruthenium PNN pincer complexes, the reduction of methyl formate to methanol afforded the maximum TON of 4700 after 14 h at 50 bar of H<sub>2</sub> and 110 °C in THF. However, carbamates showed low reactivity and resulted in low TONs (up to 98) to methanol after 48 h at 10 bar of H<sub>2</sub> and 110 °C in THF as a solvent.



**Scheme 6.1:** Hydrogenation of carbonates, carbamates and formate reported by Milstein *et al.*<sup>[2]</sup>

Seminal contributions were also reported by the groups of Sanford, and Prakash and Olah (Scheme 6.2).<sup>[3g, 9a]</sup> Both individual groups performed the hydrogenation of CO<sub>2</sub> in a one-pot reaction sequence, comprising two individual reaction steps. In the first step, the hydrogenation of CO<sub>2</sub> to formamide was performed in the presence of an amine at a lower temperature (80 to 95 °C). In the second step, the temperature was increased to 155-165 °C and the hydrogenation of formamide to methanol was performed with the subsequent regeneration of the amine. Both groups used the well-established Ru-MACHO-BH catalyst **Ru-20** for the hydrogenation in combination with various amines. The group of Sanford reported their highest TONs (550) of

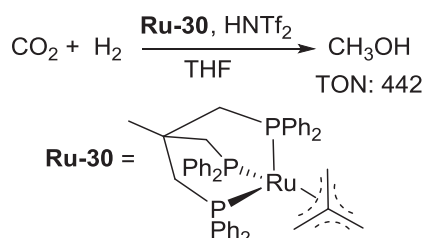
methanol formation by starting with CO<sub>2</sub> (2.5 bar), H<sub>2</sub> (50 bar) and dimethylamine as an additive in THF as a solvent. However, a significant amount of other C1 products such as dimethylformamide (DMF) and dimethylammonium formate (DMFA) was also generated. Similarly, the group of Prakash reported maximum TONs of 1060 to CH<sub>3</sub>OH using CO<sub>2</sub>, H<sub>2</sub> with the ratio of 1:3 (total 75 bar) and pentaethylenhexamine (PEHA) as an additive in an etherial solvent.



**Scheme 6.2:** Hydrogenation of CO<sub>2</sub> reported by Sanford and Prakash *et. al.*.<sup>[3g, 9a]</sup>

In 2012, the groups of Klankermayer and Leitner reported the hydrogenation of CO<sub>2</sub> to CH<sub>3</sub>OH by using a well-defined Ru-triphos-TMM molecular complex as a pre-catalyst **Ru-30** and HNTf<sub>2</sub> as a co-catalyst (Scheme 6.3).<sup>[9b]</sup> The hydrogenation of CO<sub>2</sub> (20 bar) using H<sub>2</sub> (60 bar) at 140 °C, employing **Ru-30** (25 μmol), HNTf<sub>2</sub> (1 equiv. with respect to Ru) and EtOH (10 mmol) in THF showed the formation of methanol with a TON of 221. It was assumed that the reaction was passing through the intermediate formation of ethyl formate as ethanol was used as an additive in the reaction. The reaction of formic acid generated from CO<sub>2</sub> and H<sub>2</sub> and ethanol leads to the generation of formate which on hydrogenation produces MeOH as a final product.

Interestingly in 2015, the group of Klankermayer and Leitner also reported the direct hydrogenation of CO<sub>2</sub> to methanol.<sup>[3f]</sup> In this case, no additive was used. The reaction of CO<sub>2</sub> (20 bar), H<sub>2</sub> (60 bar) at 140 °C using **Ru-30** (6.3 μmol), HNTf<sub>2</sub> (1 equiv. with respect to Ru) in THF as a solvent resulted in increase in TON of up to 442 for methanol.

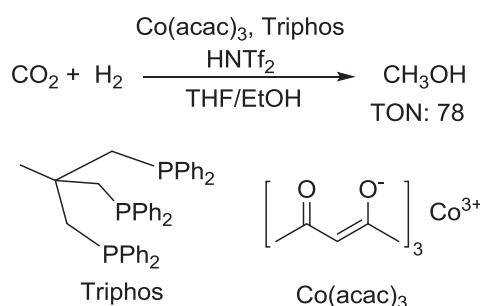


**Scheme 6.3:** Hydrogenation of CO<sub>2</sub> reported by Klankermayer and Leitner *et. al.*.<sup>[3f, 9b]</sup>



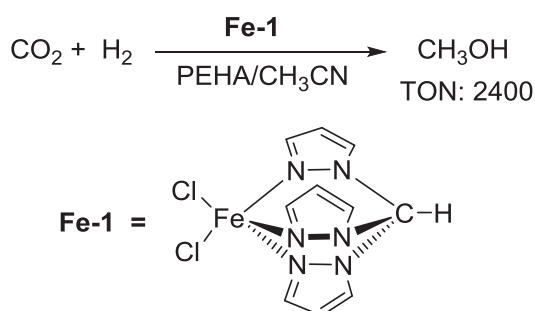
The reported transformations so far were performed using the noble and rare metal complexes. However, very few examples are known where the catalytic hydrogenation of CO<sub>2</sub> to methanol was performed employing a non-noble and earth-abundant metal complex.

In 2017, the group of Beller reported a catalytic system for the hydrogenation of CO<sub>2</sub> using the triphos ligand with the incorporation of Co(acac)<sub>3</sub> as a metal salt with the catalytic amount of HNTf<sub>2</sub> (Scheme 6.4).<sup>[3h]</sup> The reaction was performed in a mixture of THF and ethanol as a solvent. The reaction showed a maximum TON of 78 after a prolonged reaction time of 96 h. As discussed earlier, ethanol was used as a solvent in the reaction to form ethyl formate as an intermediate by the reaction of ethanol. Apart from methanol, other C1 products such as formic acid and ethyl formate were also found as intermediate products in the reaction mixture.



**Scheme 6.4:** Hydrogenation of CO<sub>2</sub> reported by Beller *et. al.*<sup>[3h]</sup>

In the same year, the group of Pombeiro reported a catalytic system for the hydrogenation of CO<sub>2</sub> to methanol by using an iron base metal catalyst **Fe-1** (Scheme 6.5).<sup>[10]</sup> The reaction revealed an outstanding reactivity using Pentaethylenhexamine (PEHA) as a solvent and amine as an additive at 80 °C and resulted in 2400 TONs to methanol.

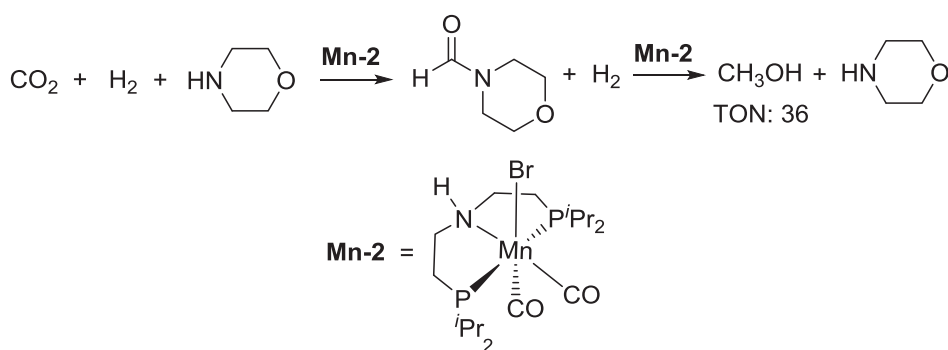


**Scheme 6.5:** Hydrogenation of CO<sub>2</sub> reported by Pombeiro *et. al.*<sup>[10]</sup>

The direct hydrogen of CO<sub>2</sub> to methanol comprising TONs of 1450 TONs was also shown using acetonitrile (CH<sub>3</sub>CN) as a solvent. However, several iron complexes are reported for the

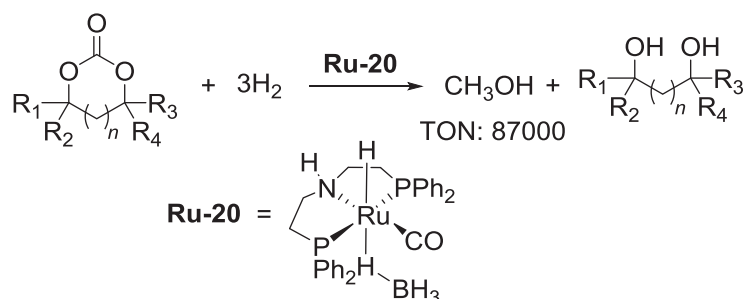
hydrogenation of the acetonitrile to the corresponding amine.<sup>[11]</sup> Unfortunately, no reaction was shown in other solvents and therefore it is still possible that the *in situ* formed amine may be an assisted additive in the reaction.

In 2018, Prakash *et. al.* also showed the sequential hydrogenation of CO<sub>2</sub> to methanol by using the Mn-MACHO-*i*Pr complex **Mn-2** (Scheme 6.6).<sup>[12]</sup> However, the reaction was carried out in two separate steps. In the first step, formamide was produced using CO<sub>2</sub>, H<sub>2</sub>, and amine in the presence of the Mn-complex. In the second step, the reaction was cooled down to room temperature and the system was depressurized. The last step needed re-pressurisation with H<sub>2</sub> to further hydrogenate the formamide and subsequently produce methanol as a final product. The maximum TON for methanol achieved was 36.



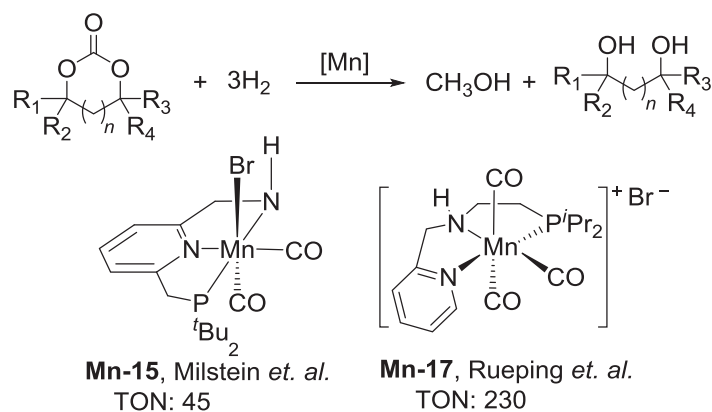
**Scheme 6.6:** Sequential hydrogenation of CO<sub>2</sub> reported by Prakash *et. al.*<sup>[12]</sup>

In 2012, the group of Ding reported the maximum TONs to methanol by the hydrogenation of cyclic carbonates (Scheme 6.7).<sup>[13]</sup> The hydrogenation of cyclic carbonates was performed using the Ru-MACHO-BH complex **Ru-20** at 140 °C and 60 bar of hydrogen pressure where the maximum TON of 87000 was found to the corresponding methanol and diol. Reports concerning the hydrogenation of cyclic carbonate using the non-noble metal complexes are very limited.



**Scheme 6.7:** Hydrogenation of cyclic carbonates reported by Ding *et. al.*<sup>[13]</sup>

During our own studies to the Mn-catalyzed hydrogenation of cyclic carbonates, the group of Milstein and Rueping individually reported the catalytic systems for the same transformation using Mn(I) pincer complexes (Scheme 6.8).<sup>[14]</sup> A variety of carbonates were hydrogenated and showed good yields to the corresponding diols and methanol with up to >99% using 1 to 2 mol% of the Mn-complexes. The maximum TONs for the hydrogenation of carbonates to methanol reported by Milstein and Rueping group achieved were 45 and 230, respectively.

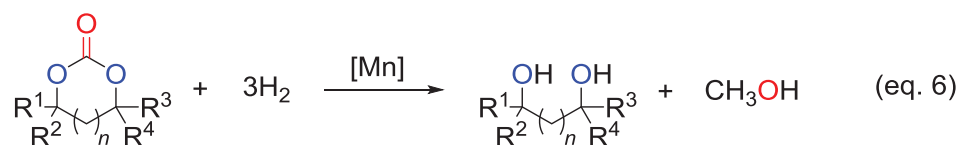


**Scheme 6.8:** Hydrogenation of cyclic carbonates reported by Milstein and Rueping *et. al.*<sup>[14]</sup>

## 6.1. Objective

Noble metal molecular complexes are able to facilitate the hydrogenation of CO<sub>2</sub> to methanol via direct or indirect methods. However, very few catalytic methods were established where this process was achieved using non-noble metal complexes. Cyclic carbonates are an attractive structural motif that can be produced from CO<sub>2</sub> and epoxide or oxetane which on reduction can lead to the formation of methanol and the corresponding diols. Thus this route resembles an indirect path for the hydrogenation of CO<sub>2</sub> to methanol formation employing non-noble metal complexes.

The objective of this work is to perform the hydrogenation of cyclic carbonates using the manganese pincer complexes (eq. 6). In the previous chapters, we discussed about the Mn-complexes reactivity towards hydrogen borrowing reactions such as hydrogenation and de-hydrogenation. A number of Mn-pincer complexes will be investigated for the hydrogenation of cyclic carbonates. Based on the control experiments and previously reported literature, a catalytic cycle will be proposed.



## 6.2. Catalyst screening

Initially, the focus was on catalyst optimization employing various ligands at the Mn metal centre (Table 6.1). Therefore, a variety of well-defined manganese (I) pincer complexes were synthesized and applied for hydrogenation. Initial studies were carried out using ethylene carbonate **34a** as a benchmark substrate with various Mn-complexes as pre-catalysts, and NaO<sup>t</sup>Bu as co-catalyst. The reductions were performed in THF as a solvent at 120 °C under 30 bar of H<sub>2</sub> pressure for 24 h. Using these reaction conditions, the reaction with pyridine based Mn-PNP pincer complexes **Mn-21** and **Mn-23** revealed very low activity to the corresponding products, ethylene glycol **35a** and methanol **36**. Similarly, the reaction using a substituted imidazole based PNN pincer complex **Mn-16** also showed very low product formation.

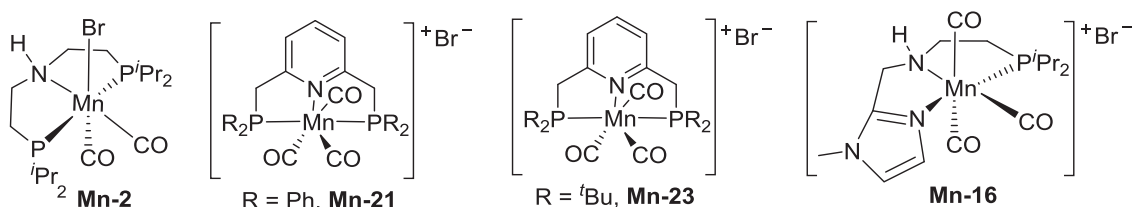


**Figure 6.1:** Used Mn(I) complexes for reaction optimization.

**Table 6.1:** Manganese catalyzed hydrogenation of **34a**: Influence of catalyst precursors.<sup>[a, b]</sup>

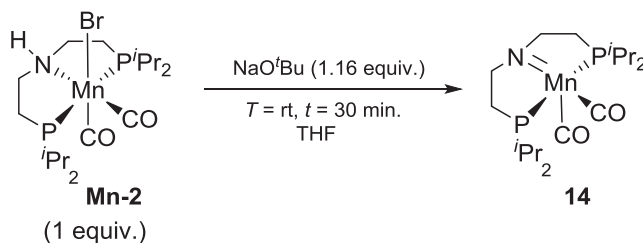
#	Reaction Conditions			H <sub>2</sub> (bar)	t (h)	X (%)	35a (%) (TON)	36 (%) (TON)
	[Mn] No.	[Mn] (mol%)	NaO <sup>t</sup> Bu (mol%)					
1	<b>Mn-2</b>	1	2	30	26	86	86 (86)	62 (62)
2	<b>Mn-21</b>	1	2	30	26	23	10 (10)	4 (4)
3	<b>Mn-23</b>	1	2	30	26	23	14 (14)	3 (3)
4	<b>Mn-16</b>	1	2	30	26	10	11 (11)	5 (5)

Conditions: [a] **34a** (44 mg, 0.5 mmol), H<sub>2</sub>, T = 120 °C, THF (0.7 mL). [b] Yield was calculated using gas chromatography, ethyl heptanoate (25 μL, 0.15 mmol) was used as an internal standard.

Notably, the reaction using Mn-MACHO-<sup>i</sup>Pr complex **Mn-2** revealed a good activity and showed the formation of ethylene glycol **35a** with a yield of 86% and methanol with a 62%

yield. The characterization and calculation of the yield for these molecules was carried out using gas chromatography. The reaction showed a high selectivity to ethylene glycol, although the lower yield of methanol with respect to diol can be explained because of low boiling point of methanol and also the formation of formate ester as a side product in the reaction.

Based on these results, further optimization was performed using complex **Mn-2** (Table 6.2). Complex **Mn-2** revealed good catalytic activity even at a low temperature. The reaction at 100 °C showed a good conversion of 74% with 71% yield to **35a** and a 62% yield to methanol after 24 h. Next, we focused on the influence of the pre-catalyst and co-catalyst loading in the reaction. When the amount of **Mn-2** and the base were increased to 2 mol% and 3 mol%, respectively, the reaction proceeded with 98% conversion and with 90% yield to **35a** and 75% yield to methanol at 120 °C. Decreasing the amount of complex **Mn-2** to 0.5 mol% and base amount to 1 mol% led to the 70% conversion and 66% yield to **35a** which corresponds to a TON of 132. The reaction even at a low loading of **Mn-2** with only 0.2 mol% and 0.5 mol% of base confirmed the formation of **35a** and methanol with the TONs of 240 and 175, respectively. Increasing the pressure from 30 bar to 60 bar of H<sub>2</sub> showed 240 TON to **35a**. However, the methanol TON was reduced to 145.



**Scheme 6.9:** Synthesis of complex **14**.

The catalyst was highly reactive when it was preactivated. Complex **Mn-2** was activated by treatment with a base in THF for 30 min. at room temperature (Scheme 6.1). The reaction showed the quantitative formation of **14** after removal of all volatiles. The formation of the active species **14** was verified by <sup>1</sup>H NMR and <sup>31</sup>P NMR spectroscopy. After the removal of all volatiles, the stock solution of complex **14** was prepared using a known amount of THF which was further used in catalysis. Using 0.2 mol% of complex **14** at 60 bar of H<sub>2</sub> pressure, the reaction showed 38% conversion with a 187 TON for **35a** and 129 TON for MeOH after 14 h. Increasing the reaction time to 40 h, showed 70% conversion with a TON of 336 TON for **35a**

and a TON of 220 for MeOH. The best results were found when the loading of complex **14** was decreased to 0.1 mol%. The reaction resulted in 66% conversion with a TON of 620 for **35a** and TON of 400 for methanol.

**Table 6.2:** Reaction optimization using complex **Mn-2** and **14** for hydrogenation of **34a**.<sup>[a, b]</sup>

C1OC(=O)OC1 + 3 H<sub>2</sub>  $\xrightarrow[\text{NaO}^t\text{Bu, } T = 120\text{ }^\circ\text{C}]{[\text{Mn}]}$  OCCO + CO

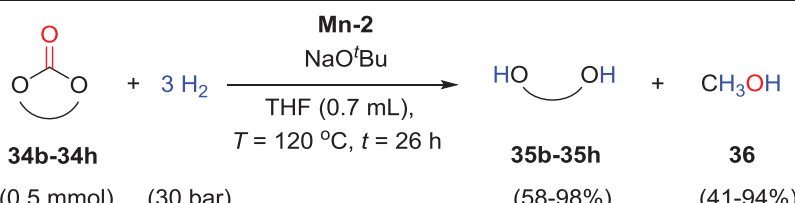
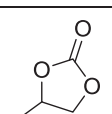
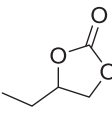
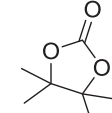
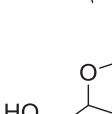
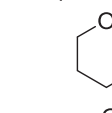
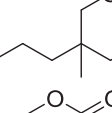
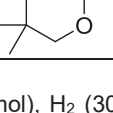
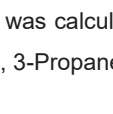
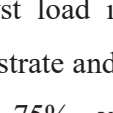
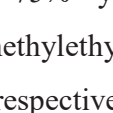
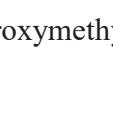
entry	[Mn] No.	[Mn] (mol%)	NaO <sup>t</sup> Bu (mol%)	H <sub>2</sub> (bar)	t (h)	X (%)	<b>35a</b> (%) (TON)	<b>36</b> (%) (TON)
1 <sup>§</sup>	<b>Mn-2</b>	1	2	30	26	74	71 (71)	62 (62)
2	<b>Mn-2</b>	2	3	30	26	98	90 (45)	75 (38)
3	<b>Mn-2</b>	0.5	1	30	26	70	66 (132)	46 (92)
4 <sup>#</sup>	<b>Mn-2</b>	0.2	0.5	30	40	56	48 (240)	35 (175)
5 <sup>#</sup>	<b>Mn-2</b>	0.2	0.5	60	40	60	52 (260)	30 (147)
6 <sup>#</sup>	<b>14</b>	0.2	-	60	14	38	37 (187)	26 (129)
7 <sup>#</sup>	<b>14</b>	0.2	-	60	40	70	67 (336)	44 (220)
8 <sup>#</sup>	<b>14</b>	0.1	-	60	40	66	62 (620)	40 (400)

Conditions: [a] **34a** (44 mg, 0.5 mmol), H<sub>2</sub>, Mn complex, NaO<sup>t</sup>Bu, temp. (120 °C), THF (0.7 mL). [b] Yield was calculated using gas chromatography, ethyl heptanoate (25 μL, 0.15 mmol) was used as an internal standard. <sup>§</sup>T=100 °C. <sup>#</sup>**34a** (440 mg, 5 mmol), H<sub>2</sub>, Mn complex, NaO<sup>t</sup>Bu, temp. (120 °C), THF (2 mL).

### 6.3. Mn(I) catalyzed hydrogenation of various cyclic Carbonates

After the successful identification of a suitable catalyst system, different cyclic carbonates were investigated for the hydrogenation to the corresponding diol and methanol (Table 6.3). The hydrogenation of various 5- and 6-membered cyclic carbonates was performed with the established reaction condition using complex **Mn-2** without pre-activation. The reaction of propylene carbonate **34b** (0.5 mmol) with H<sub>2</sub> (30 bar) using complex **Mn-2** (1 mol%) and NaO<sup>t</sup>Bu (1.1 equiv. with respect to Mn) gave 89% conversion with yields of 75% for **35b** and 66% for methanol.

**Table 6.3:** Hydrogenation of cyclic carbonates using Mn complex **Mn-2** as a pre-catalyst.<sup>[a, b]</sup>

					
#	Carbonate	[Mn] (mol%)	Conv. (%)	Diol ( <b>35</b> , %)	Methanol ( <b>36</b> , %)
1	 <b>34b</b>	1	89	75	66
2	 <b>34c</b>	2	>99	82	75
3	 <b>34d</b>	1	86	82	65
4	 <b>34e</b>	2	>99	97	74
5	 <b>34f</b>	1	82	76	66
6*	 <b>34g</b>	1	67	59	43
7*	 <b>34h</b>	2	77	71	60
8	 <b>34b</b>	1	79	58	41
9	 <b>34c</b>	2	97	80	75
10	 <b>34d</b>	1	>99	98	94
11	 <b>34e</b>	1	80	73	57

Conditions: [a] **34** (0.5 mmol), H<sub>2</sub> (30 bar), complex **Mn-2**, NaO<sup>t</sup>Bu (1.1 equiv. with respect to **Mn-2**), THF (0.7 mL), T = 120 °C, 26 h. [b] Yield was calculated using gas chromatography, ethyl heptanoate (25 μL, 0.15 mmol) was used as an internal standard. \*1, 3-Propanediol (25 μL, 0.34 mmol) was used as an internal standard.

Increasing the catalyst load into 2 mol% and the base amount accordingly, resulted in full conversion of the substrate and thus increased the product formation and showed a good yield of 82% of **35b** and 75% yield of methanol. Similarly, butylene carbonate **34c** and 1,1-dimethyl 2, 2-dimethylethylene carbonate **34d** was also well-tolerated and showed a yield of up to 97% and 76%, respectively to the corresponding diol and 74% and 66% yield to methanol, respectively. 4-(hydroxymethyl)-1,3-dioxolan-2-one **34e** which is directly produced from



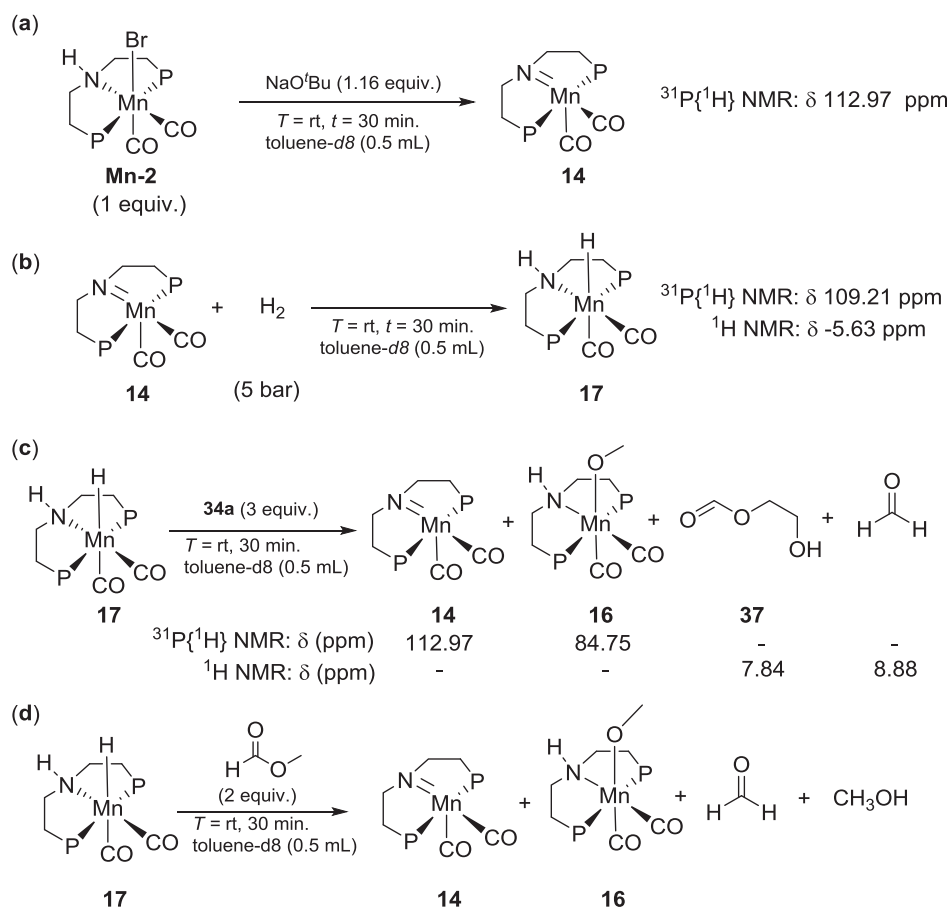
vegetable oils, was also selectively hydrogenated to the corresponding triol and methanol with a yield of 71% and 60%, respectively. Thus, the system is able to tolerate free hydroxyl groups in the substrate, further validating its broad applicability.

Interestingly, six member cyclic carbonates showed even higher activity with respect to the five membered cyclic carbonates. The reaction of 1,3-dioxan-2-one **34f** with H<sub>2</sub> (30 bar) using the complex **Mn-2** (1 mol%) and NaO<sup>t</sup>Bu (1.1 mol%) generated the corresponding diol and methanol with yields of 58% and 41%, respectively. Increasing the catalyst amount to 2 mol% and the base amount to 2.2 mol% enhanced the product formation and confirmed the formation of diol with 80% and methanol with a 75% yield. Similarly, other six-membered cyclic carbonates such as 5-methyl-5-propyl-1,3-dioxan-2-one **34g** and 5,5-dimethyl-1,3-dioxan-2-one **34h** were also reacted smoothly and confirmed the formation of the corresponding diol 98% and 73%, respectively and methanol yields of 94% and 57%, respectively.

#### 6.4. Mechanistic Investigation

To get insight into the possible catalytic cycle and possible intermediates formed from Mn complex **Mn-2** and carbonates, a series of control reactions were performed (Scheme 6.10). The reaction of complex **Mn-2** with the base generates the intermediate unsaturated manganese active species **14**. The catalytic active species **14** was already discussed in the previous chapters. The catalytic active species **14** was also used directly as a catalyst as discussed in table 2, and confirmed as a kinetically competent intermediate in the catalytic cycle. The reaction of intermediate species **14** with H<sub>2</sub> (5 bar) in [D<sub>8</sub>]-toluene at room-temperature confirmed the formation of manganese mono-hydride species **17** within 30 minutes. Species **17** was characterized using <sup>1</sup>H-NMR and <sup>31</sup>P{<sup>1</sup>H}-NMR spectroscopy which showed the characteristic hydride peak at  $\delta$ : -5.63 ppm (t,  $J$  = 51 Hz, Mn-H) and 109.21 ppm, respectively. The addition of 3 equivalents of ethylene carbonate to the solution of **17** regenerated the active species **14** along with the formation of a small amount of methoxy coordinated manganese complex **16** as confirmed by <sup>31</sup>P{<sup>1</sup>H} NMR spectroscopy. The formation of species **16** and **17** was also discussed in chapter 3 (see chapter 3.9.9.6). The organic products such as the formate ester of ethylene glycol **37** and formaldehyde were also observed in <sup>1</sup>H-NMR spectrum with a ratio of 75:25. Similarly, the reaction of complex **17** with methyl formate also revealed the formation of manganese complex **14** and **16** together with free formaldehyde and methanol. These results

clearly confirmed the excellent reactivity of Mn-MACHO-*i*Pr complex **Mn-2** towards the activation of H<sub>2</sub> to the corresponding H<sup>-</sup> and H<sup>+</sup> and their transfer to the C=O functionality of the CO<sub>2</sub> derivatives which leads to the final reduced product.



**Scheme 6.10:** Formation of presumed Mn(I) intermediates and their reactivity towards organic substrates; P = P<sup>i</sup>Pr<sub>2</sub>.

## 6.5. Catalytic Cycle

Considering these observed intermediates, *in situ* formed intermediate products and reported literature, the catalytic cycle shown in Figure 6.2 is proposed.

At first, in the presence of a base, complex **Mn-2** reacts to the catalytic active species **XXXVII**. The catalytic active species **XXXVII** was observed experimentally and resemble complex **14**. The reaction of complex **XXXVII** with H<sub>2</sub> leads to the heterolytic cleavage of H<sub>2</sub> on the Mn=N center and leads to the formation of manganese monohydride species **XXXVIII** which was observed experimentally as complex **17**.

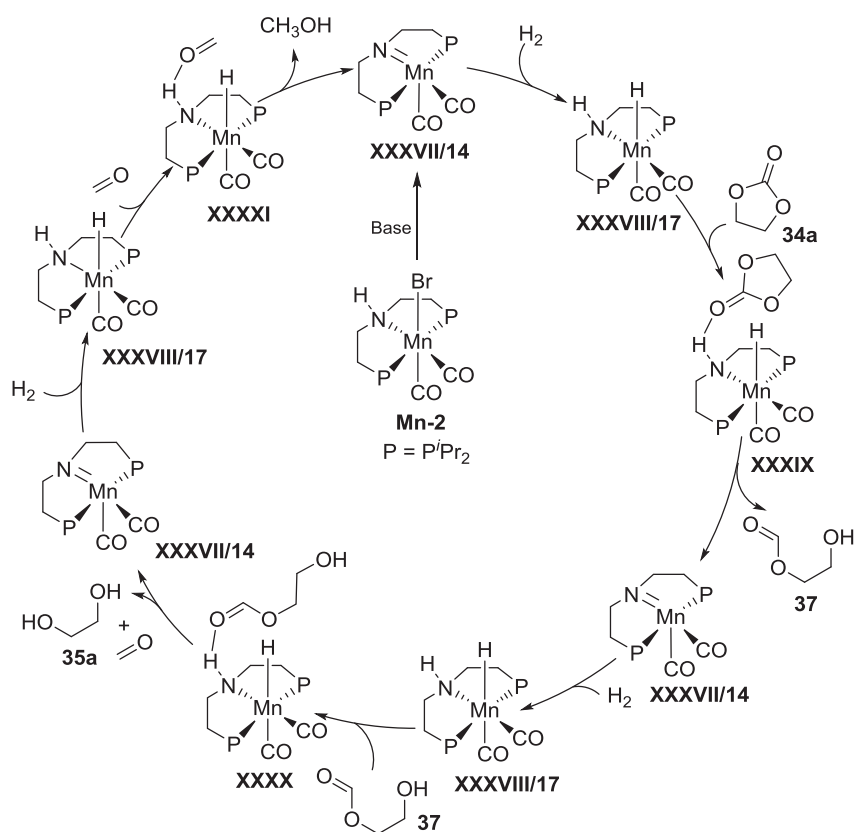


**Figure 6.2:** Possible catalytic for catalytic hydrogenation of cyclic carbonates using the Mn-MACHO-<sup>i</sup>Pr complex **Mn-2** as a pre-catalyst.

Next, the protic N–H hydrogen of complex **XXXVIII** interacts with the carbonyl functionality of the substrate which causes the activation of C=O bond. The nucleophilic attack of hydride from manganese center to the carbon of the C=O unit generates the cyclic ortho ester as a first reduced product and regenerates the active species **XXXVII**. In general, cyclic ortho ester is more stable in their open isomeric form of the formate ester and alcohol which is in line with the observation of this species in control experiments. One more time, the hydrogen reacts with the complex **XXXVII** and regenerates the manganese monohydride species **XXXVIII**. This hydride species interacts with the carbonyl functionality of formate ester and alcohols and in the same previously discussed manner, they produce the corresponding formaldehyde and diol and regenerate the active species **XXXVII**. The formaldehyde and diol was detected using NMR spectroscopy. The same process repeats one more time where formaldehyde reduced to their final methanol product using the same catalytic steps.

## 6.6. Conclusion

In conclusion, the selective hydrogenation of cyclic carbonates was performed using the cheap, earth-abundant and benign manganese as a metal component. The Mn-MACHO-<sup>i</sup>Pr complex **Mn-2** was identified as highly active catalyst for this transformation. For the hydrogenation of cyclic carbonates, the complex **Mn-2** afforded with maximal TONs of 620 for the corresponding diol and 400 TONs for methanol. Thus, this system outnumbers previous and parallel reported non-noble metal complexes for this transformation. Furthermore, first steps to a potential catalytic cycle were established by performing control experiments accordingly. Two crucial intermediates, complex **14** and complex **17** were identified and isolated and could be employed as kinetically competent intermediate in catalysis. Complex **Mn-2** revealed a high reactivity towards the cleavage of H<sub>2</sub> by the Mn=N/ Mn-N centre and forms the Mn complex **17**. The hydride and proton transfer from the complex **17** to the C=O unit of the substrate performs the stepwise hydrogenation of cyclic carbonate and generates methanol and diol as a final product. Overall, this chapter showed the possibility for the hydrogenation of CO<sub>2</sub> derived cyclic carbonates using the manganese pincer complexes and revealed the indirect way to prepare methanol.

## 6.7. Experimental

### 6.7.1. General experimental

All catalytic and stoichiometric reactions were performed under argon atmosphere using standard Schlenk and glove box techniques. Glassware was dried under vacuum at high temperatures, evacuated and refilled with argon at least three times. Commercially available chemicals were purchased from Sigma-Aldrich, Alfa-Aesar, or TCI chemicals and used without further purification. Dry and deoxygenated solvents were prepared according to standard procedures. NMR spectra were recorded with spectrometers Bruker AV300 or AV400 at room temperature. The solvent signals were used as internal references for <sup>1</sup>H and <sup>13</sup>C{<sup>1</sup>H} spectra and the chemical shifts converted to the TMS scale (CDCl<sub>3</sub> δ<sub>H</sub> = 7.26 ppm, δ<sub>C</sub> = 77.3 ppm; C<sub>6</sub>D<sub>6</sub> δ<sub>H</sub> = 7.16 ppm, δ<sub>C</sub> = 127.6 ppm; [D<sub>8</sub>]-THF δ<sub>H</sub> = 1.72 ppm, δ<sub>C</sub> = 24.2 ppm; [D<sub>8</sub>]-toluene

$\delta_{\text{H}} = 2.1$  ppm,  $\delta_{\text{C}} = 21.4$  ppm).  $^{31}\text{P}\{^1\text{H}\}$  spectra are reference against  $\text{H}_3\text{PO}_4$  as external standard. Multiplicity is abbreviated as: s, singlet; d, doublet; t, triplet; q, quartet; m, multiplet; br, broad. GC analyses were performed on a Trace GC Ultra (Thermo Scientific) using a packed CP-WAX-52-CB column (length = 60 m, diameter = 0.25 mm) isothermally at 50 °C for 10 min, then heated to 250 °C at 8 °C min<sup>-1</sup>. A constant 1.5 bar pressure of He was applied. The gas chromatograph was equipped with a FID detector.

Catalytic hydrogenations involving pressurized hydrogen were carried out in home built stainless steel reactors equipped with pressure transducer and external electrical heating. **Safety advice:** High-pressure experiments represent a significant risk and must be conducted with appropriate safety procedures and in conjunction with the use of suitable equipment.

### 6.7.2. Synthesis of manganese complexes

Synthesis of manganese pincer complexes **Mn-2**, **Mn-21**, **Mn-23** and **Mn-16** were discussed in Chapter 3 (see chapter 3.9.2).<sup>[15]</sup>

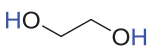
### 6.7.3. General procedure for screening of Mn-catalysts

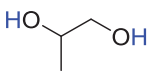
Mn-precursor and NaO<sup>t</sup>Bu were weighed into a glass inlet equipped with a stirring bar inside a glovebox. The glass inlet was transferred to a 20 mL stainless steel autoclave that was sealed, evacuated, and refilled with argon at least three times. Ethylene Carbonate **34a** (44 mg, 0.5 mmol) (dissolved in 0.7 mL THF) was added at room temperature by syringe through a needle valve under argon flow. The autoclave was sealed, pressurized with hydrogen gas, and heated to the reaction temperature. After the given reaction time, the autoclave was cooled to room temperature and carefully vented under continuous stirring. Ethyl heptanoate (25  $\mu\text{L}$ , 0.14 mmol) was added as an internal standard and the resulting solution was diluted in ethanol for analysis by gas chromatography.

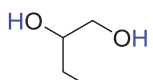
### 6.7.4. General procedure for the hydrogenation of cyclic carbonates 6 using complex MN-2

Mn complex **Mn-2** and NaO<sup>t</sup>Bu were weighed into a glass inlet equipped with a stirring bar inside a glovebox. The glass inlet was transferred to a 20 mL stainless steel autoclave that was

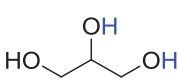
sealed, evacuated, and refilled with argon at least three times. Cyclic Carbonate **34** (0.5 mmol) (dissolved in 0.7 mL THF) was added by syringe through a needle valve under argon flow at room temperature. The autoclave was sealed and pressurized with hydrogen gas (30 bar) and heated to 120 °C. After 26 h, the autoclave was cooled to room temperature and carefully vented under continuous stirring. Ethyl heptanoate (25  $\mu$ L, 0.14 mmol) was added as an internal standard and the resulting solution was diluted in ethanol for analysis by gas chromatography.

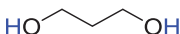
**Ethane-1,2-diol (35a):** Prepared by following the general experimental procedure with: **Mn-2**  (2.48 mg, 1 mol% or 4.94 mg, 2 mol%), **34a** (44 mg, 0.5 mmol), H<sub>2</sub> (30 bar) and NaO<sup>t</sup>Bu (0.6 mg, 1.1 mol% or 1.1 mg, 2.2 mol%) for 26 h. **GC analysis data:** retention time for **35a**: 27.655, methanol: 7.015.

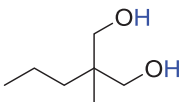
**Propane-1,2-diol (35b):** Prepared by following the general experimental procedure with: **Mn-2**  (2.48 mg, 1 mol% or 4.95 mg, 2 mol%), **34b** (51.05 mg, 0.5 mmol), H<sub>2</sub> (30 bar) and NaO<sup>t</sup>Bu (0.6 mg, 1.1 mol% or 1.1 mg, 2.2 mol%) for 26 h. **GC analysis data:** retention time for **35b**: 26.9, methanol: 6.99.


**Butane-1,2-diol (35c):** Prepared by following the general experimental procedure with: **Mn-2**  (2.48 mg, 1 mol% or 4.95 mg, 2 mol%), **35c** (58.05 mg, 0.5 mmol), H<sub>2</sub> (30 bar) and NaO<sup>t</sup>Bu (0.6 mg, 1.1 mol% or 1.1 mg, 2.2 mol%) for 26 h. **GC analysis data:** retention time for **35c**: 28.5, methanol: 6.97.

**2,3-dimethylbutane-2,3-diol (35d):** Prepared by following the general experimental procedure with: **Mn-2** (2.48 mg, 1 mol%), **34d** (72.1 mg, 0.5 mmol), H<sub>2</sub> (30 bar) and NaO<sup>t</sup>Bu (0.6 mg, 1.1 mol%) for 26 h. **GC analysis data:** retention time for **35d**: 24.717, methanol: 6.898.

**Propane-1,2,3-triol (35e):** Prepared by following the general experimental procedure with: **Mn-2** (2.48 mg, 1 mol% or 4.95 mg, 2 mol%), **34e** (59.05 mg, 0.5 mmol), H<sub>2</sub>  (30 bar) and NaO<sup>t</sup>Bu (0.6 mg, 1.1 mol% or 1.1 mg, 2.2 mol%) for 26 h. 1, 3-Propanediol (25  $\mu$ L, 0.34 mmol) was used as an internal standard. **GC analysis data:** retention time for **35e**: 26.6 methanol: 7.01.

**Propane-1,3-diol (35f):** Prepared by following the general experimental procedure with:  **Mn-2** (2.48 mg, 1 mol% or 4.95 mg, 2 mol%), **34f** (51.05 mg, 0.5 mmol), H<sub>2</sub> (30 bar) and NaO<sup>t</sup>Bu (1.1 mg, 1.1 mol%) for 26 h. **GC analysis data:** retention time for **35f**: 30.1, methanol: 6.93.

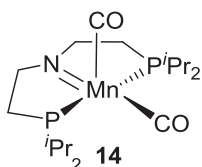
**2-methyl-2-propylpropane-1,3-diol (35g):** Prepared following the general experimental procedure with:  **Mn-2** (2.48 mg, 1 mol%), **34g** (79.1 mg, 0.5 mmol), H<sub>2</sub> (30 bar) and NaO<sup>t</sup>Bu (0.6 mg, 1.1 mol%) for 26 h. **GC analysis data:** retention time for **35g** : 30.17, methanol: 6.87.

**2,2-dimethylpropane-1,3-diol (35h):** Prepared following the general experimental procedure with:  **Mn-2** (2.48 mg, 1 mol%), **34h** (65.1 mg, 0.5 mmol), H<sub>2</sub> (30 bar) and NaO<sup>t</sup>Bu (1.1 mg, 1.1 mol%) for 26 h. **GC analysis data:** retention time for **35h** : 33.494, methanol: 6.83.

## 6.7.5. General procedure for the hydrogenation of ethylene carbonate **34a** using the pre-activated complex **14**

### 6.7.5.1. Synthesis of complex **14**

Inside a glove box, a PTFE sample vial was charged with complex **Mn-2** (50 mg, 0.1 mmol), NaO<sup>t</sup>Bu (11.53 mg, 0.12 mmol) and THF (0.4 mL). The resulting solution was stirred for half an hour at room temperature leading to a color change from yellow to orange red. <sup>1</sup>H-NMR and <sup>31</sup>P{<sup>1</sup>H}-NMR spectroscopies are consistent with the formation of complex **14**. Filtration of the reaction mixture over celite followed by removal of the solvent under vacuo led to the isolation of complex **14** (38.5 mg, 0.092 mmol, 92%) as a dark red solid. The analytical data of complex are consistent with those previously reported in the literature.<sup>[16]</sup>



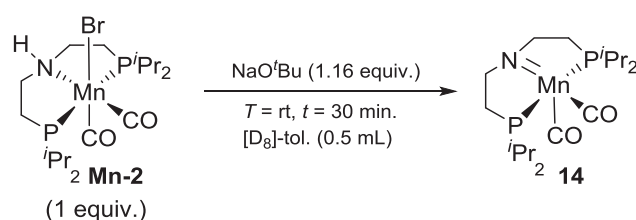
### 6.7.5.2. General procedure

To a 20 mL stainless autoclave, ethylene Carbonate **34a** (440 mg, 5 mmol) (dissolved in 1.5 mL THF) and stock solution of Mn complex **14** in THF (0.5 mL) were added by syringe through a needle valve under argon flow at room temperature. The autoclave was sealed and pressurized

with hydrogen gas (60 bar) and heated to 120 °C. After the given reaction time, the autoclave was cooled to room temperature and carefully vented under continuous stirring. Ethyl heptanoate (25  $\mu$ L, 0.14 mmol) was added as internal standard and the resulting solution was diluted in ethanol for analysis by gas chromatography.

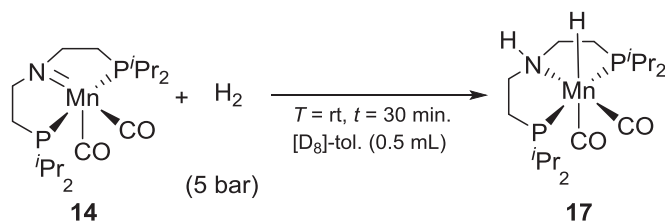
### 6.7.5.3. Generation of potential intermediates and their reactivity towards organic substrates

#### Generation of complex **14** / intermediate XXXVII



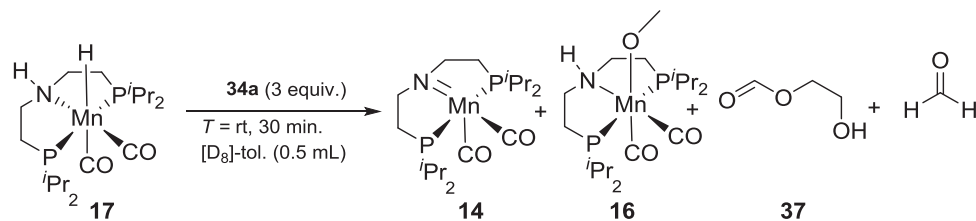
A high pressure NMR tube was charged with complex **Mn-2** (15 mg, 0.03 mmol), NaO<sup>t</sup>Bu (3.36 mg, 0.035 mmol) and [D<sub>8</sub>]-toluene (0.4 mL). The resulting solution was stirred for 30 minutes at room temperature leading to a color change from yellow to orange red. <sup>1</sup>H-NMR (300 MHz, [D<sub>8</sub>]-toluene, 298 K) and <sup>31</sup>P{<sup>1</sup>H}-NMR (121 MHz, [D<sub>8</sub>]-toluene, 298 K) spectroscopies are consistent with the formation of complex **14**.<sup>[16]</sup>

#### Generation of complex **17** / intermediate XXXVIII



The reaction mixture produced from the stoichiometric reaction of **Mn-2** and NaO<sup>t</sup>Bu was pressurized with H<sub>2</sub> (5 bar) at room temperature and carefully shaken. After half an hour, the <sup>1</sup>H NMR (300 MHz, [D<sub>8</sub>]-toluene, 298 K) spectrum of the mixture showed a new hydride peak at  $\delta$ : -5.63 ppm (t,  $J$ = 51 ppm, Mn-H) and a corresponding signal in <sup>31</sup>P{<sup>1</sup>H} NMR (121 MHz, [D<sub>8</sub>]-tol, 298 K) at  $\delta$ : 109.21 ppm confirming formation of complex **17**.<sup>[16]</sup>



Reaction of complex **17** with ethylencarbonate **34a**

A solution of complex **17** was treated with ethylene carbonate **34a** (7.92 mg, 0.09 mmol). After half an hour at room temperature, the formation of complexes **14** and **16** together with the formate ester of ethylene glycol **37** and free formaldehyde was observed by  $^1\text{H}$  NMR (300 MHz,  $[\text{D}_8]\text{-toluene}$ , 298 K) and  $^{31}\text{P}\{^1\text{H}\}$  NMR (121 MHz,  $[\text{D}_8]\text{-toluene}$ , 298 K) spectra. Ratio of (**37**:formaldehyde = 75:25)

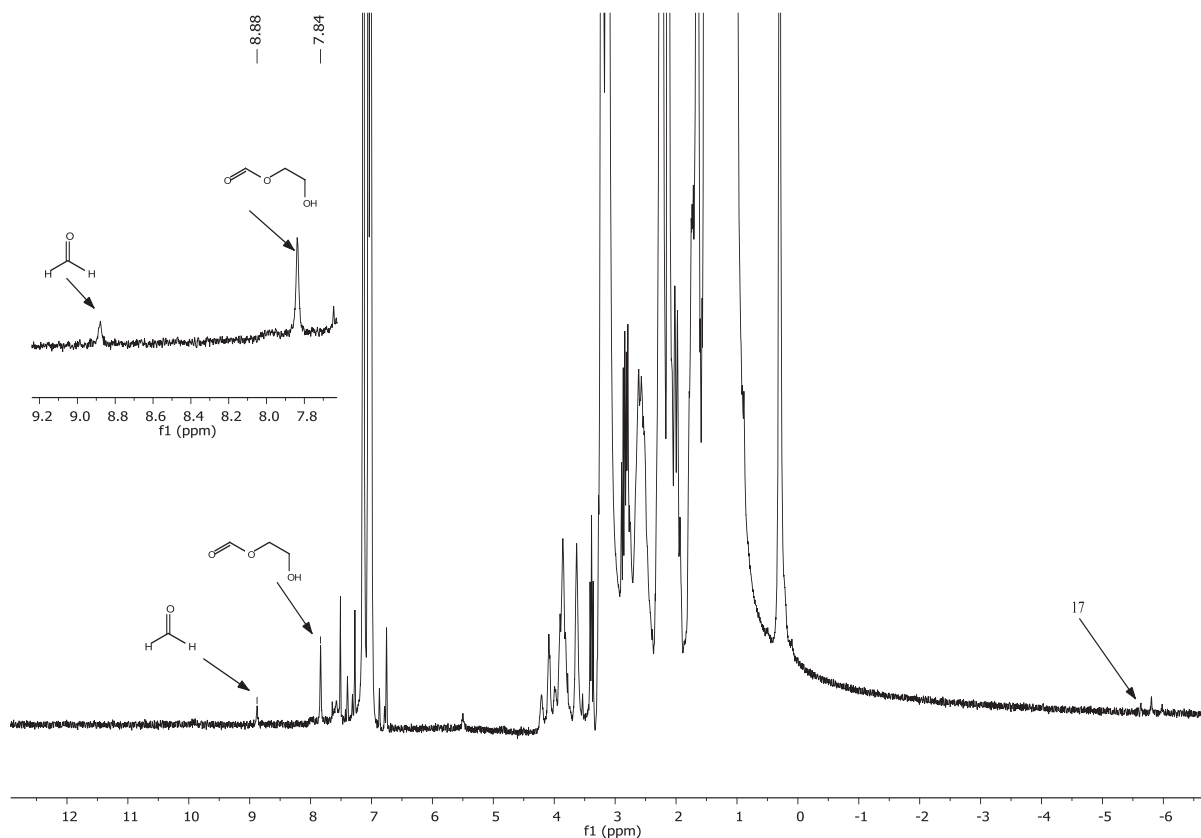


**Figure 6.3:**  $^1\text{H}$ -NMR (300 MHz,  $[\text{D}_8]\text{-tol.}$ , 298 K) reaction mixture spectrum of the reaction between complex **17** with **34a**.

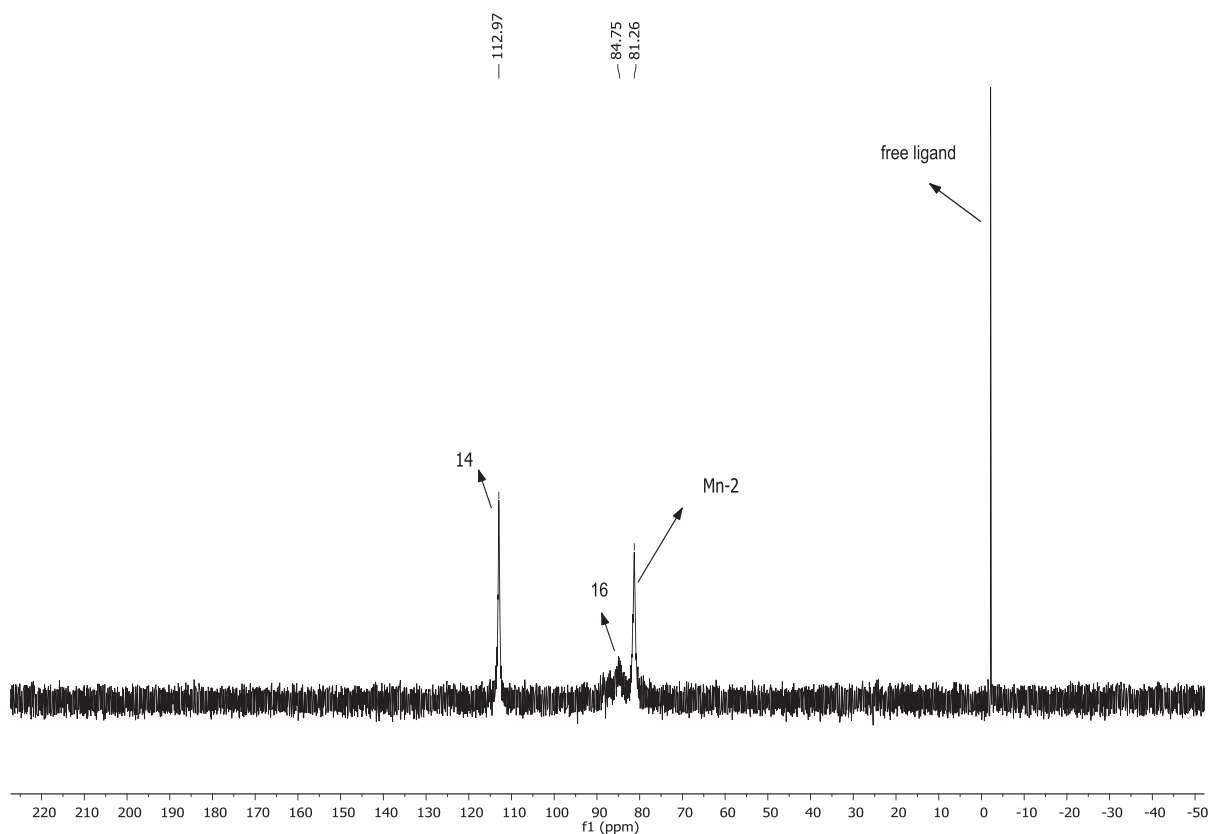
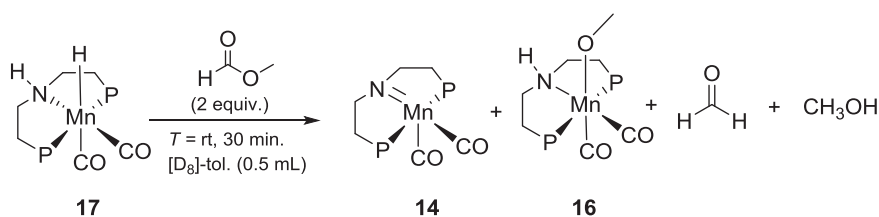


**Figure 6.4:**  $^{31}\text{P}\{^1\text{H}\}$ -NMR (121 MHz,  $[\text{D}_8]$ -tol., 298 K) reaction mixture spectrum of the reaction between complex **17** with **34a**.

### Reaction of complex **17** with methyl formate



A solution of complex **17** was treated with methyl formate (3.6 mg, 0.06 mmol). After half an hour at room temperature, the formation of complex **14** and **16** together with formaldehyde and methanol was revealed by  $^1\text{H}$  NMR (300 MHz,  $[\text{D}_8]$ -toluene, 298 K) and  $^{31}\text{P}\{^1\text{H}\}$  NMR (121 MHz,  $[\text{D}_8]$ -toluene, 298 K) spectra and gas chromatography.

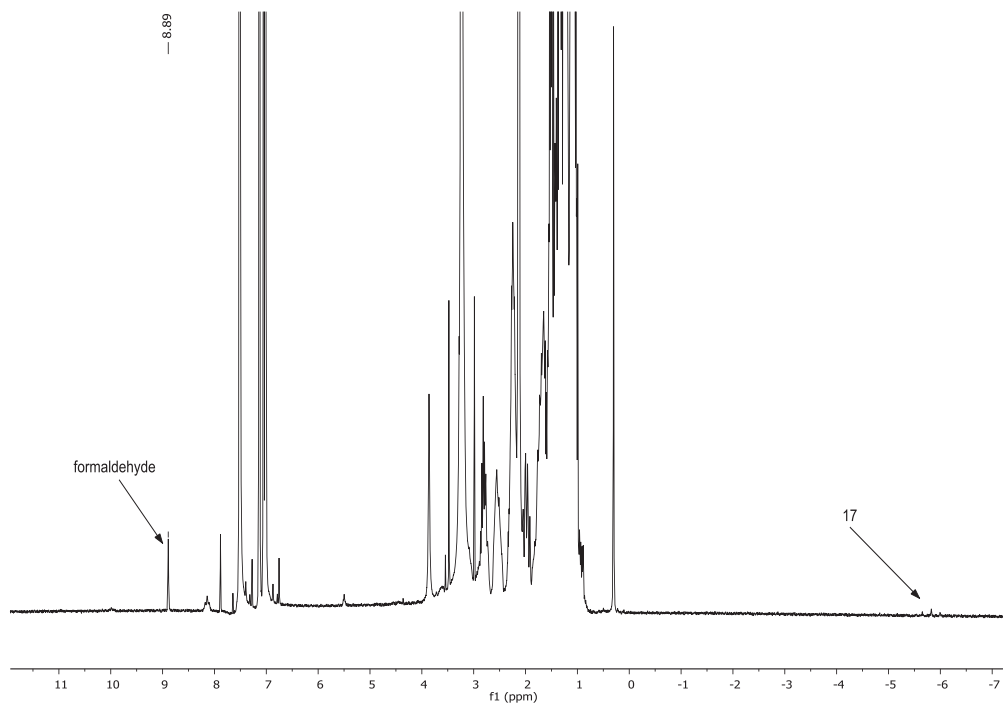


**Figure 6.5:**  $^1\text{H-NMR}$  (300 MHz,  $[\text{D}_8]\text{-tol.}$ , 298 K) reaction mixture spectrum of the reaction between complex **17** with methyl formate.

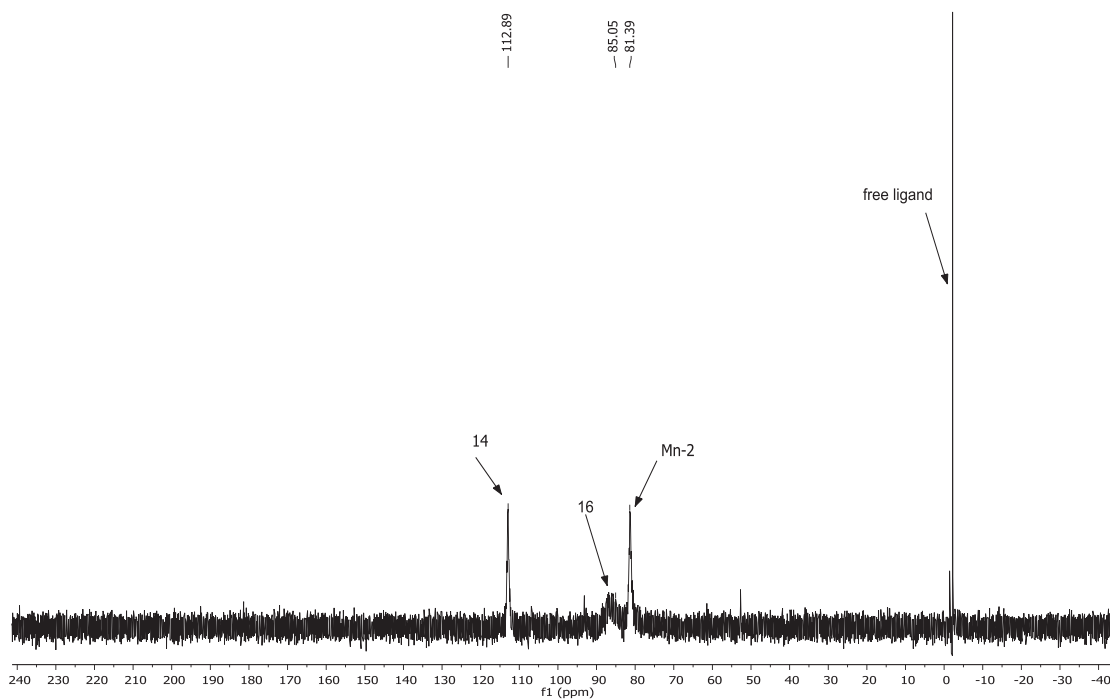


**Figure 6.6:**  $^{31}\text{P}\{^1\text{H}\}\text{-NMR}$  (121 MHz,  $[\text{D}_8]\text{-tol.}$ , 298 K) reaction mixture spectrum of the reaction between complex **17** with methyl formate.

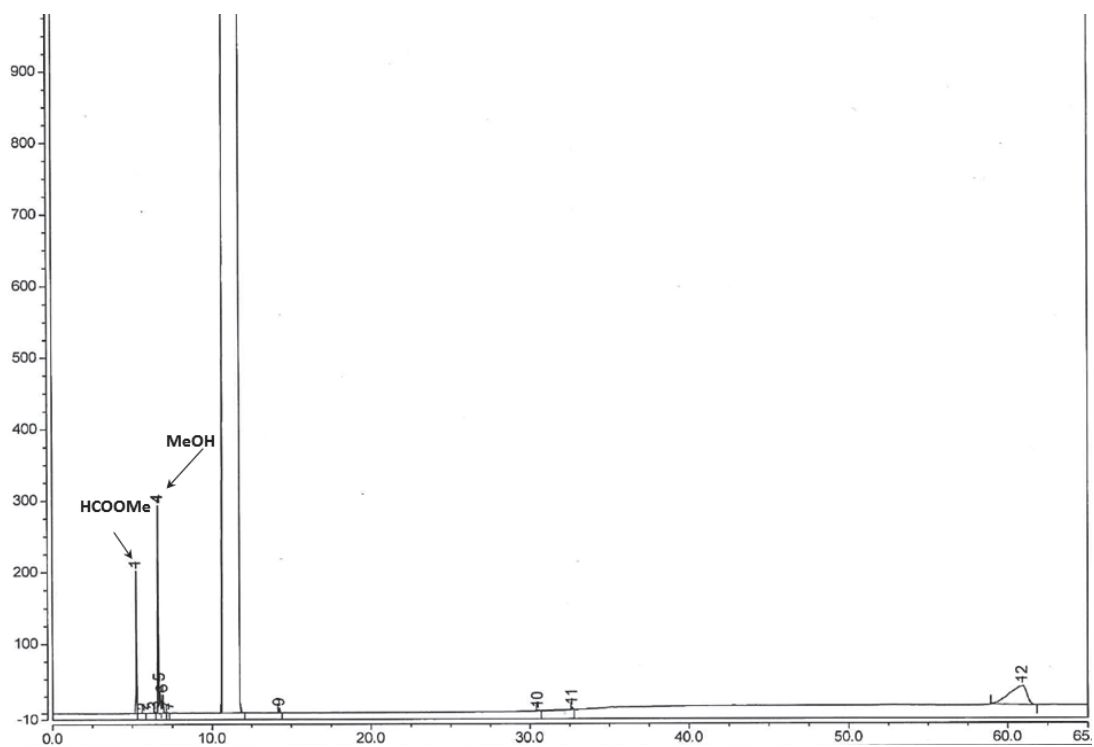


**Figure 6.7:** GC reaction mixture spectrum of the reaction between complex **17** with methyl formate after 24 h.

## References

- [1] M. Ito, T. Ootsuka, R. Watari, A. Shiibashi, A. Himizu, T. Ikariya, *J. Am. Chem. Soc.* **2011**, *133*, 4240-4242.
- [2] E. Balaraman, C. Gunanathan, J. Zhang, L. J. W. Shimon, D. Milstein, *Nat. Chem* **2011**, *3*, 609.
- [3] a) J. Klankermayer, W. Leitner, *Science* **2015**, *350*, 629-630; b) K. Jürgen, W. Sebastian, B. Kassem, L. Walter, *Angew. Chem. Int. Ed.* **2016**, *55*, 7296-7343; c) Q. Liu, L. Wu, R. Jackstell, M. Beller, *Nat. Commun.* **2015**, *6*, 5933; d) C. A. Huff, M. S. Sanford, *J. Am. Chem. Soc.* **2011**, *133*, 18122-18125; e) W. Sebastian, v. S. Thorsten, K. Jürgen, L. Walter, *Angew. Chem. Int. Ed.* **2012**, *51*, 7499-7502; f) S. Wesselbaum, V. Moha, M. Meuresch, S. Brosinski, K. M. Thenert, J. Kothe, T. v. Stein, U. Englert, M. Hölscher, J. Klankermayer, W. Leitner, *Chem Sci* **2015**, *6*, 693-704; g) N. M. Rezayee, C. A. Huff, M. S. Sanford, *J. Am. Chem. Soc.* **2015**, *137*, 1028-1031; h) J. Schneidewind, R. Adam, W. Baumann, R. Jackstell, M. Beller, *Angew. Chem. Int. Ed.* **2017**, *56*, 1890-1893; i) M. Matzen, M. Alhajji, Y. Demirel, *Energy* **2015**, *93*, 343-353; j) J. Wilhelm, H. Janßen, J. Mergel, D. Stolten, *J. Power Sources* **2011**, *196*, 5299-5308; k) J. M. Ogden, M. M. Steinbugler, T. G. Kreutz, *J. Power Sources* **1999**, *79*, 143-168; l) K. Räuchle, L. Plass, H.-J. Wernicke, M. Bertau, *Energy Technol.* **2016**, *4*, 193-200; m) A. Kowalewicz, *Proc. Inst. Mech. Eng. D* **1993**, *207*, 43-52.
- [4] a) A. Kaithal, M. Schmitz, M. Hölscher, W. Leitner, *ChemCatChem* **2019**, DOI: 10.1002/cctc.201900788; b) K. Natte, H. Neumann, M. Beller, R. V. Jagadeesh, *Angew. Chem. Int. Ed.* **2017**, *56*, 6384-6394.
- [5] a) J. F. Haw, W. Song, D. M. Marcus, J. B. Nicholas, *Acc. Chem. Res.* **2003**, *36*, 317-326; b) B. Liu, L. France, C. Wu, Z. Jiang, V. L. Kuznetsov, H. A. Al-Megren, M. Al-Kinany, S. A. Aldrees, T. Xiao, P. P. Edwards, *Chem. Sci.* **2015**, *6*, 5152-5163.
- [6] M. Behrens, F. Studt, I. Kasatkin, S. Köhl, M. Hävecker, F. Abild-Pedersen, S. Zander, F. Girgsdies, P. Kurr, B.-L. Kniep, M. Tovar, R. W. Fischer, J. K. Nørskov, R. Schlögl, *Science* **2012**, *336*, 893-897.
- [7] J. Graciani, K. Mudiyansele, F. Xu, A. E. Baber, J. Evans, S. D. Senanayake, D. J. Stacchiola, P. Liu, J. Hrbek, J. F. Sanz, J. A. Rodriguez, *Science* **2014**, *345*, 546-550.
- [8] W. Leitner, *Angewandte Chemie International Edition in English* **1995**, *34*, 2207-2221.
- [9] a) J. Kothandaraman, A. Goepfert, M. Czaun, G. A. Olah, G. K. S. Prakash, *J. Am. Chem. Soc.* **2016**, *138*, 778-781; b) S. Wesselbaum, T. vom Stein, J. Klankermayer, W. Leitner, *Angew. Chem. Int. Ed.* **2012**, *51*, 7499-7502.
- [10] A. P. C. Ribeiro, L. M. D. R. S. Martins, A. J. L. Pombeiro, *Green Chemistry* **2017**, *19*, 4811-4815.
- [11] a) S. Chakraborty, D. Milstein, *ACS Catal.* **2017**, *7*, 3968-3972; b) S. Chakraborty, G. Leitner, D. Milstein, *Chem. Commun.* **2016**, *52*, 1812-1815.
- [12] S. Kar, A. Goepfert, J. Kothandaraman, G. K. S. Prakash, *ACS Catal.* **2017**, *7*, 6347-6351.
- [13] Z. Han, L. Rong, J. Wu, L. Zhang, Z. Wang, K. Ding, *Angew. Chem. Int. Ed.* **2012**, *51*, 13041-13045.

- [14] a) A. Kumar, T. Janes, N. A. Espinosa-Jalapa, D. Milstein, *Angew. Chem. Int. Ed.* **2018**, *57*, 12076-12080; b) V. Zubar, Y. Lebedev, L. M. Azofra, L. Cavallo, O. El-Sepelgy, M. Rueping, *Angew. Chem. Int. Ed.* **2018**, *57*, 13439-13443.
- [15] A. Kaithal, M. Hölscher, W. Leitner, *Angew. Chem. Int. Ed.* **2018**, *57*, 13449-13453.
- [16] S. Fu, Z. Shao, Y. Wang, Q. Liu, *J. Am. Chem. Soc.* **2017**, *139*, 11941-11948.

## 7. Manganese(I) catalyzed selective hydroboration of organic carbonates and carbon dioxide

Parts of this chapter have been published:

A. Kaithal,<sup>‡</sup> S. Sen,<sup>‡</sup> C. Erken,<sup>‡</sup> T. Weyhermüller, M. Hölscher, C. Werlé, W. Leitner, *Nat. Commun.* **2018**, *9*, 4521. (<sup>‡</sup>Equal contribution. In the manuscript, the sequence of the authors are in alphabetical order, however, the original sequence is described in author contributions.)

Functional reduction of the C=O unit in carbonic acid derivatives, including in particular carbon dioxide is a challenging process of key importance for the synthesis of value-added chemicals.<sup>[1]</sup> It can enable novel synthetic pathways for the preparation of fine chemicals, pharmaceuticals, and materials through the manipulation of functional groups in agreement with the principles of Green Chemistry. In particular, these transformations are important in the utilization of alternative feedstocks derived from biomass or from carbon dioxide.<sup>[3-5]</sup> Catalysts based on earth-abundant, cheap, and benign metals would greatly contribute to the development of sustainable synthetic processes derived from this concept.

In the last chapter, we have discussed the selective hydrogenation of cyclic carbonates using the manganese pincer complex **Mn-2** as a pre-catalyst and hydrogen as a reducing agent. Based on previous studies, we hypothesized that the boron-hydrogen bond could be activated in a similar way using manganese pincer complex which can be further used for the activation of small molecule and difficult carbonyl substrates.

Hydroboration is a well-known and established methodology for the reduction of a variety of carbonyl functionality such as aldehydes, ketones, esters, and amides.<sup>[1-2]</sup> The use of 3d-transition metal complexes is well-established to perform these transformations. However, the reduction of carbonic acid derivatives such as organic carbonates and CO<sub>2</sub> using borane-hydride is still not well explored. At present, the selective reduction of organic carbonates and CO<sub>2</sub> is a great challenge as these compounds are highly stable and require a large

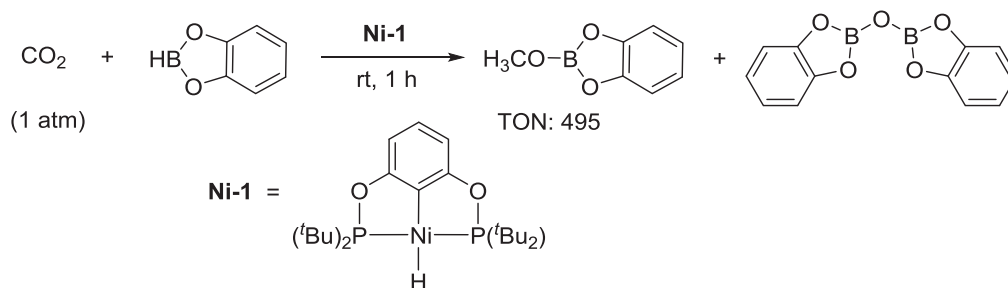
amount of energy to activate. The selective reduction of organic carbonates is a challenging process as they are kinetically stable towards the addition of hydride.<sup>[3]</sup> In fact, in some processes, these compounds are used as an organic solvent in catalytic reduction reactions. At present, organic carbonates have gained ample interest as they can be directly prepared from CO<sub>2</sub> and CO, which upon reduction leads to the methanol derivatives. Additionally, these compounds can also be used as a synthetic precursor or a protecting group for the diols which can be liberated upon reductive cleavage from cyclic carbonates.

Moreover, as already discussed in the previous chapter, the direct reduction of CO<sub>2</sub> to methanol or its derivatives is an important process as CO<sub>2</sub> is an abundant, inexpensive, and renewable C1-carbon feedstock. While many processes were reported for the reduction of carbonyl compounds such as reduction via hydrogenation, transfer hydrogenation and stoichiometric alkali metal hydrides reduction,<sup>[4]</sup> these methods always require high-pressure reaction setup, elevated temperature or a stoichiometric amount of reducing reagents which generate a considerable amount of waste and show poor selectivity.<sup>[5]</sup>

In this context, catalytic hydroelementation reactions such as hydroboration and hydrosilylation reactions can be used for reduction reactions as they are non-toxic, stable and can be excellent surrogates over the other organometallic compounds.<sup>[6]</sup> Notably, in the past years, various hydrosilylation and hydroboration based reductions of aldehydes, ketones, and esters were reported using noble metal catalysts.<sup>[7]</sup> At the same time, 3d-metals such as Zn, Fe, and Mn also showed good reactivity for hydrosilylation and hydroboration reactions.<sup>[8]</sup> <sup>[2, 9]</sup> However reports on hydroboration of carbonates are still missing. Interestingly, the hydroboration of the challenging substrate CO<sub>2</sub> has been explored using both, noble and non-noble metal complexes.<sup>[10]</sup>

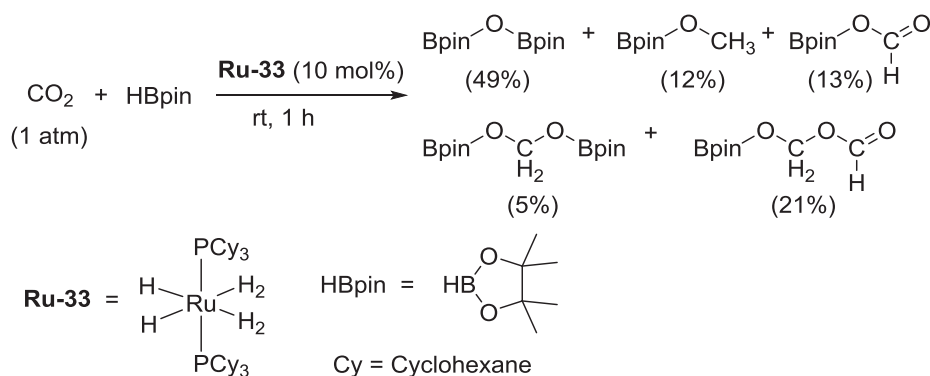
In 2010, Guan *et. al.* reported a catalytic system where they performed the hydroboration of CO<sub>2</sub> to the corresponding methoxy borane using the P<sup>O</sup>C<sup>O</sup>P nickel pincer complex (Scheme 7.1).<sup>[11]</sup> Catecholborane was used as a reducing reagent in the reaction to obtain the reduced C1 product. The reaction showed maximum TONs of up to 495 at room temperature after one hour. The mechanistic studies confirmed that a nickel hydride is the catalytically active species in the catalytic cycle and the reaction proceeds via the intermediates such as formate and formaldehyde.





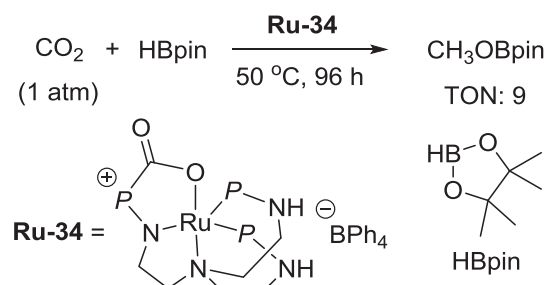
**Scheme 7.1:** Hydroboration of  $\text{CO}_2$  to methoxy-borane reported by Guan *et. al.*<sup>[11]</sup>

In 2012, the group of Sabo-Etienne showed a system for the hydroboration of  $\text{CO}_2$  using a molecular ruthenium complex (Scheme 7.2).<sup>[12]</sup> The reaction was investigated using the bis(dihydrogen) ruthenium complex  $[\text{RuH}_2(\text{H}_2)_2(\text{PCy}_3)_2]$  and pinacolborane as a reducing agent at room temperature. The catalytic system revealed a poor selectivity towards the formation of  $\text{C}_1$  and  $\text{C}_2$  products. Apart from the formation of methoxy borane, other  $\text{C}_1$  and  $\text{C}_2$  product such as pinBOCHO, pinBOCH<sub>2</sub>OBpin and pinBOCH<sub>2</sub>OCHO were observed in the reaction mixture.



**Scheme 7.2:** Hydroboration of  $\text{CO}_2$  reported by Sabo-Etienne *et. al.*<sup>[12]</sup>

In 2012, the group of Stephan also reported the hydroboration of  $\text{CO}_2$  to methoxy borane using a ruthenium tris(aminophosphine) complex (Scheme 7.3).<sup>[13]</sup> The combined approach of transition-metal system and the concept of frustrated Lewis pairs (FLPs) were proposed for the activation of  $\text{CO}_2$  using pinacolborane as a reducing reagent. However, the reaction revealed only a poor productivity (TON = 9) to methoxy borane after heating the reaction mixture of atmospheric  $\text{CO}_2$  and pinacolborane at 50 °C for 96 h.

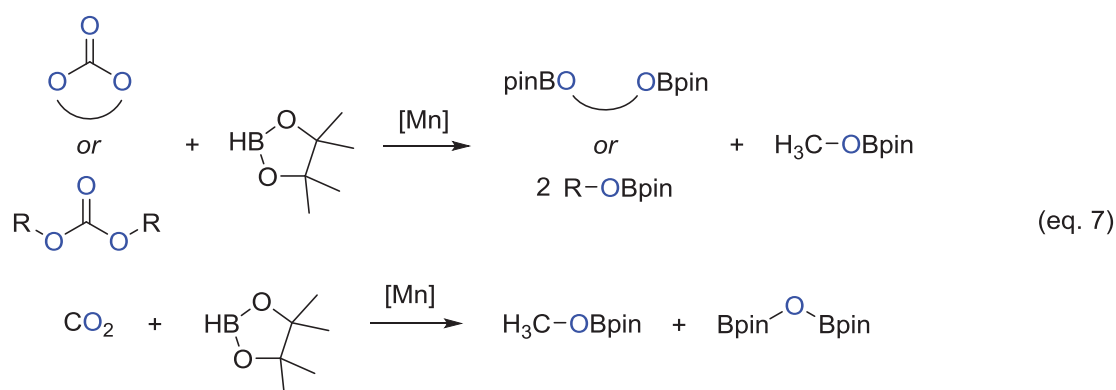


**Scheme 7.3:** Hydroboration of  $\text{CO}_2$  to methoxy-borane reported by Stephan *et. al.*<sup>[13]</sup>

## 7.1. Objective

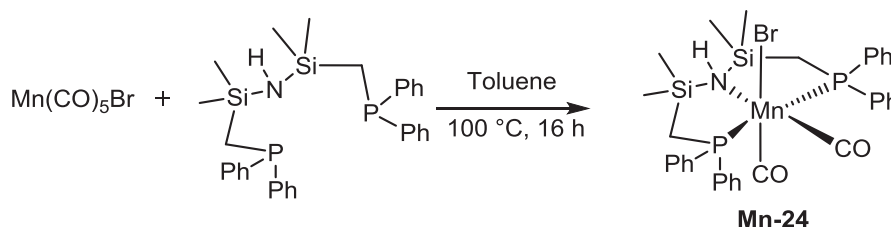
The selective catalytic reduction of carbon dioxide ( $\text{CO}_2$ ) to methanol is considered to be a promising way that might solve the problem of depletion of fossil fuel and greenhouse gas control, respectively. Several processes were established where  $\text{CO}_2$  can be directly reduced to methanol. The straightforward process includes the direct hydrogenation of  $\text{CO}_2$  to methanol using hydrogen gas. However, these systems showed low selectivity to convert  $\text{CO}_2$  to MeOH and revealed other C1 products such as formates and formamides. Very few molecular noble metal complexes are known which can accomplish this transformation selectively with good performance. Alternate to this method, the reduction of  $\text{CO}_2$  using preactivated reducing agents such as borane or silane hydrides is also possible.

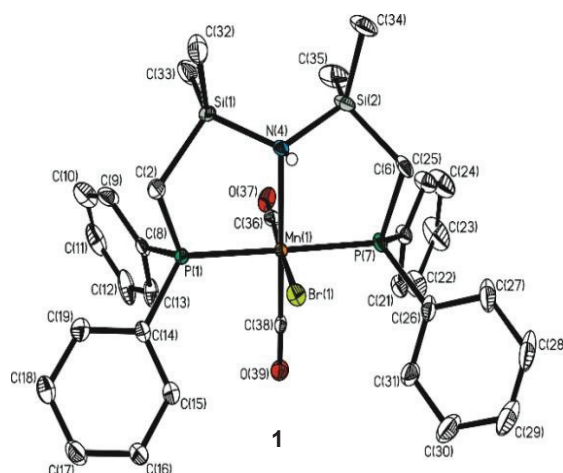
In this chapter, we investigated the selective reduction of carbonic acid derivative ( $\text{O}=\text{C}(\text{OR})_2$ ) (which can be easily prepared from carbon dioxide) and carbon dioxide ( $\text{CO}_2$ ) using pinacolborane as a reducing agent (eq. 7). Very few reports are present in the literature capable to perform these transformations using noble and non-noble metal complexes. The objective of this work is to identify and prepare a suitable new manganese catalyst to accomplish this transformation and investigate the reaction mechanism by performing the control experiments.

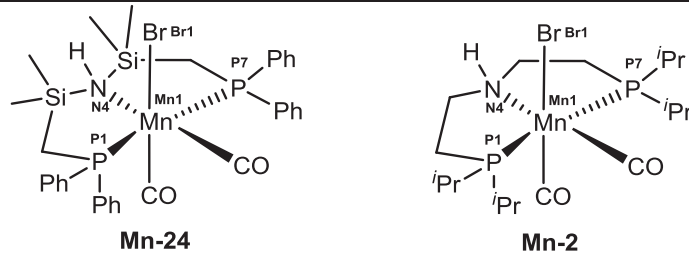


## 7.2. Synthesis of a manganese precatalyst

For this particular transformation, a new silane-based Mn-MACHO complex **Mn-24** was synthesized. The synthesis of a ligand used for the preparation of complex **Mn-24** is straightforward and requires only two steps to reach the final product. Alike, the synthesis of well-established MACHO-ligand, no protection and deprotection of amine is required for the silane-based MACHO ligand. The starting material used for this synthesis is commercially available and can be used under ambient argon environment. The main motivation to prepare this ligand is to exchange the established MACHO ligand to another type of MACHO ligand which can be easily accessible, easy to prepare and reveal similar reactivity. Interestingly, in the past, silane based PNP complexes were established towards the activation of hydrogen while coordinating with a metal-center.<sup>[14]</sup> The preparation of organic ligand (**Si-PNP**) is discussed in the experimental section.<sup>[15]</sup> The synthesis of manganese pincer complex  $[\text{Mn}(\text{Ph}_2\text{PCH}_2\text{SiMe}_2)_2\text{NH}(\text{CO})_2\text{Br}]$  **Mn-24** was carried out by the treatment of manganese precursor ( $\text{Mn}(\text{CO})_5\text{Br}$ ) with one equivalent of 1,3-bis((diphenyl-phosphino) methyl)tetramethyl-di-silazane in toluene at 100 °C for 16 h. The complex was isolated as yellow solid with 90% yield. The complex was fully characterized by Suman Sen. Various spectroscopic techniques were used and showed the data in the expected range. Single crystals suitable for X-ray crystal diffraction were obtained by the slow diffusion of hexane into a concentrated solution of complex **Mn-24** in dichloromethane. The crystal structure of the complex revealed the distorted octahedral structure. It was shown that the coordination of the metal center with ligand was in comparison with the previously established Mn-MACHO complexes.<sup>[16]</sup> The brief comparison between the complex **Mn-24** and Mn-MACHO-*i*-Pr **Mn-2** complex is shown in the Table 7.1.




**Scheme 7.4:** Synthesis and crystal structure of Manganese complex **Mn-24**.

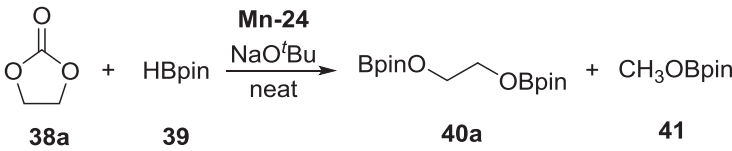
**Table 7.1:** Structure similarity between complex **Mn-24** and Mn-MACHO-*i*Pr **Mn-2**.


Selected bond length [pm] for Mn-24		Selected bond length for Mn-2	
Mn(1)-N(4)	227.4 pm	Mn(1)-N(4)	212.2 pm
Mn(1)-P(1)	230.0 pm	Mn(1)-P(1)	230.0 pm
Mn(1)-P(7)	230.2 pm	Mn(1)-P(7)	230.0 pm
Mn(1)-Br(1)	253.0 pm	Mn(1)-Br(1)	257.7 pm
Selected bond angle [deg] for Mn-24		Selected bond angle [deg] for Mn-2	
[P(1)-Mn(1)-P(7)]	173.5	[P(1)-Mn(1)-P(7)]	165.8
[P(1)-Mn(1)-Br(1)]	87.6	[P(1)-Mn(1)-Br(1)]	90.2
[P(7)-Mn(1)-Br(1)]	86.6	[P(7)-Mn(1)-Br(1)]	90.5
[N(4)-Mn(1)-Br(1)]	82.2	[N(4)-Mn(1)-Br(1)]	84.8

### 7.3. Reaction optimization for the reduction of organic carbonates using Mn complex Mn-24

For the reaction optimization, ethylene carbonate **38a** was chosen as a model substrate to screen the catalytic reaction and to identify the standard reaction conditions using the manganese complex **Mn-24** (Table 7.2). The reaction of **38a** (1 mmol) with the stoichiometric amount of pinacolborane (3 mmol) using the Mn(I) complex **Mn-24** (0.25 mol%) and a base (0.4 mol%) at 90 °C showed the formation of boronate diol ester **40a** with a yield of 97% after 4 h. Methyl boronate **41**, the reduction product from the central carbon of **38a** was observed in 62% yield. Decreasing the pre-catalyst load and base to 0.1 mol% and 0.3 mol%, respectively revealed lower reactivity and showed 77% yield of the corresponding product **40a** after 4 h.

**Table 7.2:** Optimization studies for the hydroboration of ethylene carbonate **38a**.<sup>[a, b]</sup>

					
Entry	Catalyst (mol%)	NaO <sup>t</sup> Bu (mol%)	Temp. (°C)	Time (h)	Yield <b>40a</b> (%) <sup>a</sup>
1	0.25	0.4	90	4	97
2	0.1	0.3	90	4	77
3	0.1	0.3	100	4	88
4	0.1	0.3	90	8	95
5	-	-	110	12	12
6	-	0.3	110	12	13

Conditions: [a] **38a** (1 mmol), **39** (3 mmol), **Mn-24**, NaO<sup>t</sup>Bu, *T*. [b] Yields were determined by <sup>1</sup>H NMR spectroscopy using mesitylene as an internal standard.

Interestingly, the yield was increased when the reaction was performed at 100 °C temperature. At this temperature, **40a** was obtained with a yield of 88% after 4 h. The best-optimized conditions were obtained when the reaction was performed using 0.1 mol% of **Mn-24** and 0.3 mol% of the base at 90 °C for 8 h. The reaction showed 95% yield to the corresponding product **40a**. Based on these optimized conditions, several organic carbonates were investigated for selective reduction

to their respective hydroboronate product. Control experiments revealed that the reaction in the absence of manganese complex or base, a small amount of product was obtained.

#### 7.4. Mn(I)-catalyzed selective hydroboration of Organic carbonates

Using the standard reaction conditions, various cyclic and linear carbonates were reduced to the corresponding hydroboration product (Table 7.3). All reactions were performed under solvent-free conditions. Initially, five-membered cyclic carbonates were chosen for this transformation. Propylene and 1,2-butylene carbonates (**38b** and **38c**) were well tolerated and showed the reduced boronate diol esters (**40b** and **40c**) with a yield of 95% and 97%, respectively. Interestingly, 1,2-carbonate glycerol **38d** which is a byproduct of the vegetable industry was also reduced to the corresponding boronate-ester **40d** with a yield of 88%. Next, the reduction of six-membered cyclic carbonates was carried out. 1,3-dioxan-2-one **38e** and 5-methyl-5-propyl-1,3-dioxan-2-one **38f** showed 98% and 94% yield, respectively to the corresponding reduced boronate diol ester on reaction with pinacolborane. Low yield was observed for the hydroboration of 5,5-dimethyl-1,3-dioxan-2-one **38g**, this can be explained due to the low solubility of **38g** in pinacolborane.

Further, linear carbonates, substantially more difficult as substrates for reduction were tested. Using the same optimized reaction conditions, the reaction of benzyl carbonate **38h** with pinacolborane in presence of complex **Mn-24** and base revealed the corresponding product formation **40h** with a yield of 95%. Diphenyl carbonate **38i** also showed a 71% yield to the corresponding boronate diol ester product. However, the reduction of pure aliphatic linear carbonates such as dimethyl and ethyl methyl carbonate (**38j** and **38k**) showed lower product formation. The lower yield in the case of **38j** and **38k** can be explained due to the low electron density in the carbonyl functionality of carbonates compared to aromatic carbonates and the absence of strain compared to cyclic structures.

**Table 7.3:** Hydroboration of carbonates using Mn complex **Mn-24** as catalyst.<sup>[a, b]</sup>

Entry	Carbonate	Conv. (%)	Boronate Ester (%)	Yield <b>4</b> (%)
a	<b>38a</b>	96	BpinO-CH <sub>2</sub> -CH <sub>2</sub> -OBpin <b>40a</b>	95
b	<b>38b</b>	>99	BpinO-CH(CH <sub>3</sub> )-CH <sub>2</sub> -OBpin <b>40b</b>	95
c	<b>38c</b>	>99	BpinO-CH(CH <sub>2</sub> CH <sub>3</sub> )-CH <sub>2</sub> -OBpin <b>40c</b>	97
d <sup>[d]</sup>	<b>38d</b>	95	BpinO-CH(CH <sub>2</sub> OH)-CH <sub>2</sub> -OBpin <b>40d</b>	88
e	<b>38e</b>	>99	BpinO-(CH <sub>2</sub> ) <sub>3</sub> -OBpin <b>40e</b>	98
f	<b>38f</b>	43	BpinO-C(CH <sub>3</sub> ) <sub>2</sub> -CH <sub>2</sub> -OBpin <b>40f</b>	39
g	<b>38g</b>	>99	BpinO-C(CH <sub>3</sub> ) <sub>2</sub> -CH <sub>2</sub> -CH <sub>2</sub> -OBpin <b>40g</b>	94
H	<b>38h</b>	98	Ph-CH <sub>2</sub> -OBpin <b>40h</b>	95
i <sup>[d]</sup>	<b>38i</b>	-	Ph-OBpin <b>40i</b>	71
j <sup>[d]</sup>	<b>38j</b>	57	OBpin (3 equiv.) <b>40j</b>	54
k	<b>38k</b>	46	OBpin 6k:4a = 1:2 <b>40k</b>	42



Conditions: [a] **38** (88 mg, 1 mmol), **39** (0.435 mL, 3 mmol), **Mn-24** (0.73 mg, 0.1 mol%) and NaO<sup>t</sup>Bu (0.3 mg, 0.3 mol%) at 90 °C for 8 h. [b] Yields of **40** were determined by <sup>1</sup>H NMR analysis using mesitylene as internal standard. [c] 4 mmol of **39** was used. [d] Yield of **41** was determined by <sup>1</sup>H NMR analysis using mesitylene as internal standard.

## 7.5. Catalytic reactivity of complex **Mn-24** in CO<sub>2</sub> hydroboration

The high reactivity of complex **Mn-24** towards the reduction of organic carbonates prompted us to investigate the challenging reduction of carbon dioxide to methyl boronate under similar conditions (Table 7.4). Interestingly, the manganese complex **Mn-24** also showed a very good reactivity towards the hydroboration of CO<sub>2</sub> to the corresponding methyl boronate ester. Control experiments confirmed that the reaction required both the manganese complex and base to perform this transformation. Initial experiments were carried out using a manganese complex **Mn-24** (0.036 mol%) and NaO<sup>t</sup>Bu (0.1 mol%) in pinacolborane under ambient pressure of CO<sub>2</sub> at 90 °C. The reaction revealed the selective formation of methyl boronate ester **41** with a 76% yield at 90 °C after 14 h. The formation of methyl boronate was verified by NMR spectroscopy. This data corresponds to a TON of 697 under non-optimized conditions, thus outnumbering the highest TONs reported for this transformation. The reaction showed high selectivity towards the synthesis of methyl boronate ester and showed no other C<sub>1</sub> products such as formaldehyde, CO or methane. To verify the reactivity of this transformation in different solvents, the reaction was also performed in toluene and THF. Complex **Mn-24** showed reactivity in both solvents, however with lower yields. Doubling the catalyst and base amount, increased the overall yield to 83%, albeit on expense of the productivity (TON = 380). The best-optimized reaction conditions were found at a slightly higher temperature of 100 °C. Using this reaction condition with Mn complex **Mn-24** (0.036 mol%), NaO<sup>t</sup>Bu (0.1 mol%), pinacolborane (2.76 mmol) and 1 atm of CO<sub>2</sub> at 100 °C confirmed the formation of methyl boronate ester with the yield of 96% and a maximal TON of 883 after 14 h.

**Table 7.4:** Hydroboration of CO<sub>2</sub> using Mn complex **Mn-24** as catalyst.<sup>[a, b]</sup>

Entry	Temp. (°C)	Solvent (mL)	Yield <b>41</b> (%)	TON ( <b>41</b> )
1	90	-	76	697
2	rt	-	5	46
3	90	Toluene (0.5)	52	480
4	90	THF (0.5)	12	110
5 <sup>[c]</sup>	90	-	91	380
6	100	-	96	883

Conditions: [a] CO<sub>2</sub> (1 atm, balloon), **39** (353.2 mg, 2.76 mmol), **Mn-24** (0.73 mg, 0.036 mol%), NaO<sup>t</sup>Bu (0.3 mg, 0.1 mol%), *T*, *t* = 14 h. [b] Yields were determined by <sup>1</sup>H NMR analysis using mesitylene as an internal standard. [c] CO<sub>2</sub> (1 atm), **Mn-24** (1.46 mg, 0.072 mol%), NaO<sup>t</sup>Bu (0.6 mg, 0.2 mol%) and **39** (353.2 mg, 2.76 mmol) at 90 °C for 14 h.

## 7.6. Mechanistic Studies

Next, to understand the reactivity of complex **Mn-24** and its interaction with pinacolborane to reduce the challenging substrates, stoichiometric reactions were performed (Figure 7.1). The reaction of complex **Mn-24** with KO<sup>t</sup>Bu at room temperature in [D<sub>8</sub>]-THF showed the immediate color change from yellow to dark violet. The spectroscopic studies verified the formation of Mn(I)-unsaturated species **42** in line with the previously reported Mn(I)-unsaturated PNP species **14**. <sup>31</sup>P{<sup>1</sup>H} NMR showed the formation of complex **42** at δ 61.26 ppm. Several attempts were made to obtain the crystalline material of complex **42**, however, all attempts remained unsuccessful. The stoichiometric reaction of species **42** with pinacolborane at room temperature restored the yellow color and revealed the formation of a new species **43a**. The species **43a** was confirmed with <sup>1</sup>H NMR and <sup>31</sup>P{<sup>1</sup>H} NMR spectrum and showed new signals at δ -6.56 ppm (broad, half-width: 88 Hz) and 65.21 ppm, respectively. Over time, the species **43a** converts slowly to the newly formed Mn-hydride **43**. The hydride complex **43** exhibited the new peak at δ: -7.67 ppm (*t*, *J* = 32 Hz) and 57.87 ppm in <sup>1</sup>H NMR and <sup>31</sup>P NMR, respectively. Heating the solution of **43a** at 50 °C for 30 minutes showed the ratio of **43a/43** of 90:10, full conversion to **43** was achieved after storing the solution at room temperature for 48 h.

The single crystal for the intermediate active species **43a** suitable for X-ray diffraction was obtained by slow diffusion of hexane into a concentrated solution of **43a** in DCM. The crystal structure of **43a** showed an important feature. It contained a four-membered Mn–H–B–N ring, which confirms a vital intermediate by the heterolytic cleavage of the B–H bond across the Mn=N bond. The complex **43a** showed shorter distance between the Mn and N bond in comparison to the complex **Mn-24**.

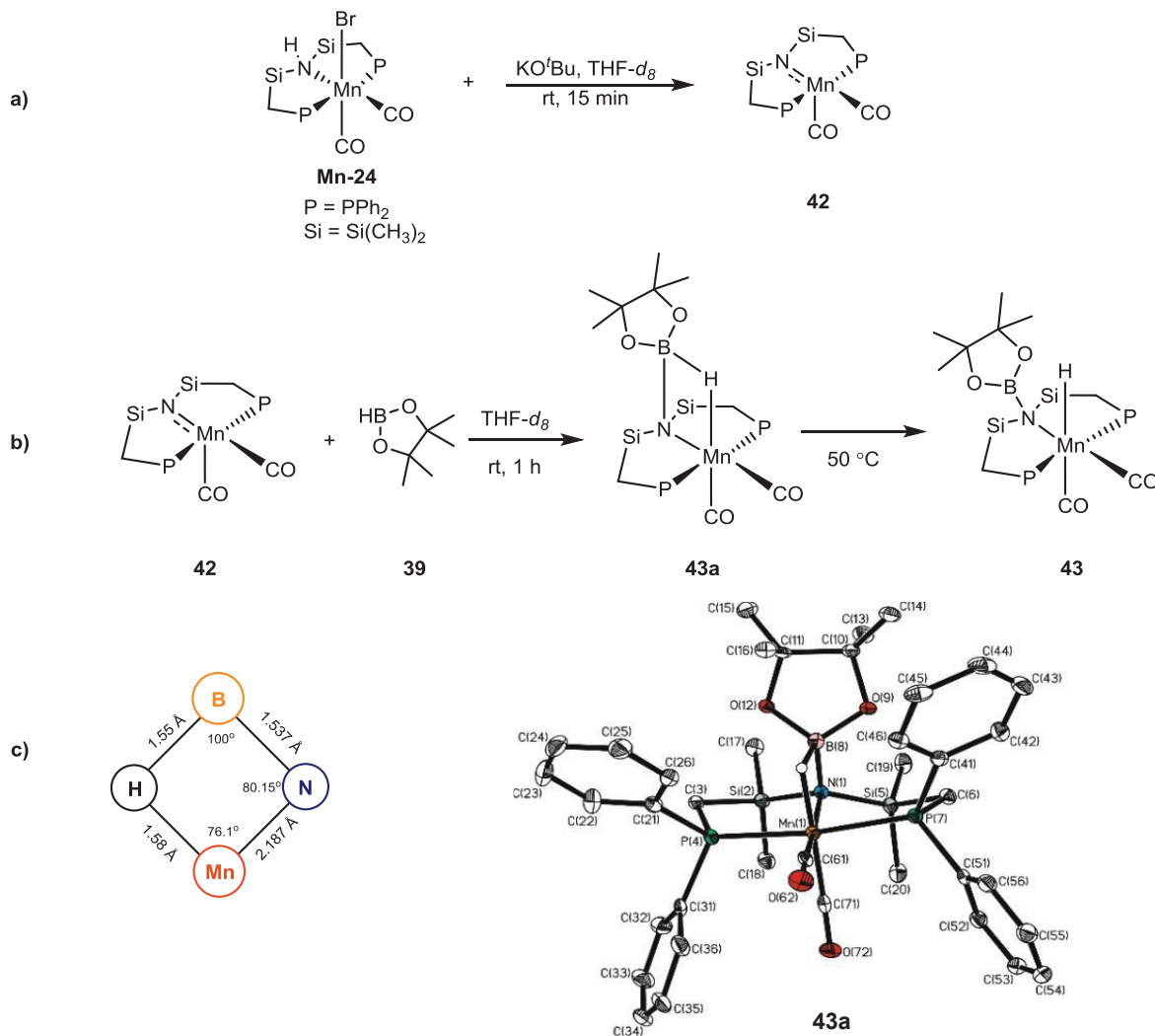


**Figure 7.1:** Generation and molecular structure of potential intermediate Mn complexes. Overall geometry for **43a**: Distorted Octahedral. Selected angles and atom distances : [P(4)-Mn(1)-P(7) = 172.38°], [C(61)-Mn(1)-C(71) = 86.73°], [N(1)-Mn(1)-P(4) = 88.85°], [N(1)-Mn(1)-P(7) = 88.90°], (Mn(1)-N(1) = 218.7 pm), (Mn(1)-P(4) = 226.93 pm), (Mn(1)-P(7) = 226.95 pm), (N(1)-Si(2) = 178.1 pm), (N(1)-Si(5) = 177.9 pm).

## 7.7. Catalytic Cycle

Based on the experimental observations and previous studies reported by our and other groups, a catalytic cycle was proposed for the hydroboration of CO<sub>2</sub> (Figure 7.2). In the presence of a base, complex **Mn-24** reacts to the catalytic Mn(I)-unsaturated active species **XXXXII**. The formation of active species **XXXXII** was confirmed using <sup>1</sup>H-NMR and <sup>31</sup>P-NMR spectroscopy and corresponds to the complex **42**. The reaction of species **XXXXII** with pinacolborane afforded the formation of complex **XXXXIIa** (**43a**) via B-H bond activation which slowly forms hydride complex **XXXXIIa'** (**43**). From this state, two routes are possible for the attack of CO<sub>2</sub>, one was the direct attack of CO<sub>2</sub> at species **XXXXIIa** and the second route includes the formation of hydride species **XXXXIIa'** from species **XXXXIIa** and subsequent attack of CO<sub>2</sub> to complex **XXXXIIa'**.

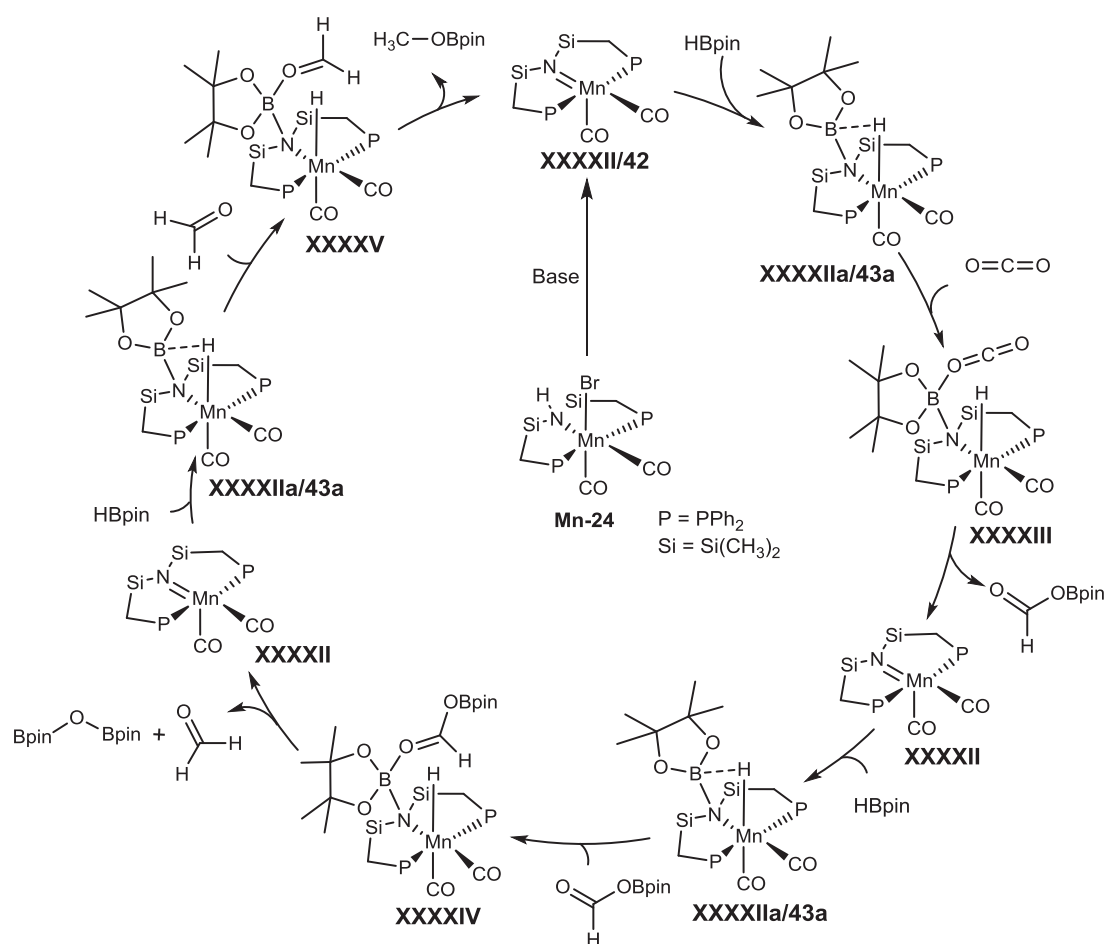


**Figure 7.2:** Suggested reaction mechanism for the hydroboration of carbon dioxide by complex **Mn-24**.

However, due to the slow formation of hydride complex **XXXXIIa'**, we favor the direct attack of CO<sub>2</sub> to the active species **XXXXIIa**. Next, the carbonyl group of CO<sub>2</sub> interact with the Lewis acidic boron center which destabilizes the four membered ring and opens up the possibility for a hydride to attack the carbonyl functionality of CO<sub>2</sub> and form the complex **XXXXIII**. This transformation leads to the formation of formoxyborane and regeneration of the complex **XXXXII**. The formation of formoxyborane was observed by <sup>1</sup>H-NMR while performing the CO<sub>2</sub> hydroboration experiments. Afterwards, pinacolborane reacts to the active species **XXXXII** and regenerates the species **XXXXIIa** another time. The *in situ* formed formoxyborane afforded the formation of acetal H<sub>2</sub>C(O)OBpin on reaction with the complex **XXXXIIa**. Due to the low stability of the acetal intermediate, it cleaved to the corresponding formaldehyde and BpinOBpin. The whole cycle repeats and the carbonyl group of formaldehyde reacts with **XXXXIIa** until it reaches to the final methoxy borane product, regenerates the active species **XXXXII** and closes the catalytic cycle. In a similar manner, carbonates can also be reacted and generate the final diboronate ester and methoxy borane product.

## 7.8. Conclusion

In conclusion, the new manganese pincer complex **Mn-24** was synthesized and used as precatalyst for the hydroboration of organic carbonates and CO<sub>2</sub>. Complex **Mn-24** showed remarkable activity for the hydroboration of organic carbonates and CO<sub>2</sub> using pinacolborane as a reducing reagent. A variety of organic carbonates were reduced using this methodology and showed the corresponding boronate ester formation in yields up to 97%. Similarly, CO<sub>2</sub> was reduced to the corresponding methoxy boronate ester with >99% selectivity, up to 96% yield and showed a maximal TON of 883 which is the highest TON for this transformation reported till now. This work opens a new pathway for the functionalization of the challenging substrates and enlarge the scope of earth-abundant and non-toxic metal catalyst to employ in organic transformations. The mechanistic insight and synthetic protocol from this chapter may devote to the development of new and benign catalytic systems for sustainable processes including the use of non-fossil fuels originated from biomass or CO<sub>2</sub>.

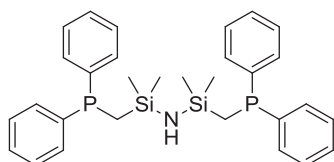
## 7.9. Experimental

### 7.9.1. General experimental

All reactions involving air sensitive compounds were carried out under argon in flame-dried glassware, ensuring rigorously inert conditions. The solvents were purified using solvent purification-systems and were stored and handled under Argon. Chemicals were purchased from Sigma-Aldrich, Alfa-Aesar, abcr, Acros Organics, TCI chemicals and used without further purification. NMR-spectra were recorded on Bruker AV-300, AV-400, DPX-300 spectrometers at the indicated temperatures with the chemical shifts ( $\delta$ ) given in ppm relative to TMS and the coupling constants ( $J$ ) in Hz. The solvent signals were used as references and the chemical shifts converted to the TMS scale ([D<sub>3</sub>]-Acetonitrile:  $\delta_{\text{H}}$  = 1.94 ppm and  $\delta_{\text{C}}$  = 118.3, 1.3 ppm; CDCl<sub>3</sub>:  $\delta_{\text{H}}$  = 7.26 ppm and  $\delta_{\text{C}}$  = 77.1 ppm; C<sub>6</sub>D<sub>6</sub>:  $\delta_{\text{H}}$  = 7.16 ppm and  $\delta_{\text{C}}$  = 128.1 ppm; [D<sub>8</sub>]-THF:  $\delta_{\text{H}}$  = 1.72 ppm, 3.58 ppm and  $\delta_{\text{C}}$  = 67.2, 25.3 ppm; [D<sub>8</sub>]-toluene:  $\delta_{\text{H}}$  = 2.08, 6.97, 7.01, 7.09 ppm and  $\delta_{\text{C}}$  = 137.5, 128.9, 127.9, 125.1, 20.4 ppm. [D<sub>6</sub>]-DMSO:  $\delta_{\text{H}}$  = 2.50 ppm and  $\delta_{\text{C}}$  = 39.5 ppm).<sup>[17]</sup> HRMS spectra were recorded on an Bruker ESQ3000 spectrometer.

### 7.9.2. Synthesis of the ligand (Si-PNP)

**1,3-bis((diphenyl-phosphino)methyl)tetramethyldi-silazane.** The organic ligand (**Si-PNP**)



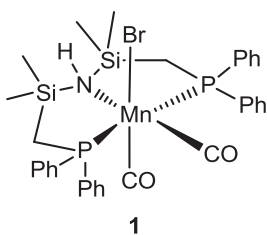
was prepared by following a modified literature procedure.<sup>[15]</sup> *n*-BuLi (2.5 M in hexane, 6.65 mmol, 2.7 mL) was added dropwise to a solution of Ph<sub>2</sub>PH (1.24 g, 6.65 mmol) in THF (10 mL) at -78 °C, leading to a bright yellow solution. The resulting mixture

was stirred at -78 °C for 30 min and then slowly warmed up to room temperature where it was stirred for another 30 min to ensure full conversion of the starting material. Subsequently, the mixture was cooled down to -78 °C and added via cannula transfer to a pre-cooled solution (-78 °C) of 1,3-Bis(chloromethyl)-1,1,3,3-tetramethyldisilazane (0.76 g, 3.33 mmol) in THF (8 mL) leading to a color change from bright yellow to light pale. After warming up to room temperature, the resulting solution was stirred for another 12 h. The volatiles were then removed in vacuo. The residue was extracted with pentane (15 mL) and filtered over fritted glass to remove undissolved LiCl. Removals of the solvent in vacuo lead to the targeted ligand **Si-PNP**

as a colourless oil (1.3 g, 2.45 mmol, 74%) which was used without further purification.  $^1\text{H-NMR}$  (300 MHz,  $\text{C}_6\text{D}_6$ , 298 K):  $\delta = 7.52\text{-}7.47$  (m, 8H), 7.09-7.04 (m, 12H), 1.30 (s, 4H), 0.06 (s, 12H);  $^{31}\text{P}\{^1\text{H}\}\text{-NMR}$  (300 MHz,  $\text{C}_6\text{D}_6$ , 298 K):  $\delta = -22.51$ .

### 7.9.3. Synthesis of manganese complex Mn-24

**Mn(Ph<sub>2</sub>PCH<sub>2</sub>SiMe<sub>2</sub>)<sub>2</sub>NH(CO)<sub>2</sub>Br (Mn-24)**. A solution of **Si-PNP** (0.210 g, 0.396 mmol) in



toluene (1 mL) was added to a suspension of  $\text{Mn}(\text{CO})_5\text{Br}$  (0.109 g, 0.395 mmol) in toluene (4 mL). The reaction mixture was stirred at 100 °C for 12 h. The volatiles were removed in vacuo and the residue was washed with hexane ( $2 \times 5$  mL). Upon drying in vacuo, the residue solidified and complex **Mn-24** was obtained as a bright yellow powder

(0.265 g, 0.367 mmol, 93%). Bright yellow crystals suitable for X-ray diffraction were grown by layering a solution of complex **Mn-24** (20 mg, 0.0028 mmol) in dichloromethane (0.5 mL) with hexane (5 mL).  $^1\text{H NMR}$  (300 MHz,  $[\text{D}_8]\text{-THF}$ , 298 K):  $\delta = 7.88\text{-}7.79$  (m, 8H), 7.34-7.22 (m, 12H), 1.92 (s, 4H), 0.41 (s, 6H), 0.13 (s, 6H);  $^{31}\text{P}\{^1\text{H}\}\text{ NMR}$  (23 MHz,  $[\text{D}_8]\text{-THF}$ , 298 K):  $\delta = 48.46$ ;  $^{13}\text{C}\{^1\text{H}\}\text{ NMR}$  (100.1 MHz,  $\text{CD}_2\text{Cl}_2$ , 298 K):  $\delta = 138.8, 138.6, 137.7, 137.5, 137.4, 132.7, 132.6, 132.6, 131.6, 129.5, 128.8, 128.3, 14.7, 3.6, 0.7$ ; **HRMS (ESI<sup>+</sup>)**:  $m/z$ : calcd. for  $\text{C}_{32}\text{H}_{37}\text{BrMnNP}_2\text{Si}_2$   $[\text{M}]^+$ : 719.03964; found: 719.03961.

### 7.9.4. Optimization of the reaction conditions for the hydroboration of ethylene carbonate

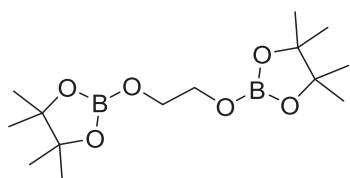
To a schlenk tube, ethylene carbonate **38a** (0.088 g, 1 mmol) was added at room temperature to a mixture of  $[\text{Mn}]$ -precatalyst **Mn-24**,  $\text{NaO}^t\text{Bu}$  and pinacolborane **39** (0.435 mL, 3 mmol) under argon atmosphere. The schlenk tube was closed and reaction mixture was then heated at the indicated temperature. After reaction time was reached, reaction medium was cooled down to room temperature, mesitylene was added as an internal standard. Subsequently, a sample (10  $\mu\text{L}$ ) of the reaction mixture in  $\text{CDCl}_3$  (0.4 mL) was subjected to  $^1\text{H NMR}$  spectroscopy to determine the yield in alkyl boronate ester.



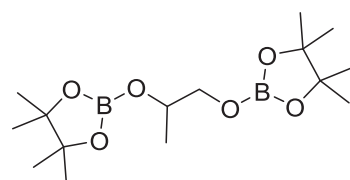
### 7.9.5. General procedure for the hydroboration of carbonates

To a schlenk tube, carbonate **38** (1 mmol) was added at room temperature to a mixture of [Mn]-precatalyst **Mn-24** (0.1 mol%), NaO<sup>t</sup>Bu (0.3 mol%) and pinacolborane (3 mmol). The schlenk tube was closed and reaction mixture was then heated at 90 °C for 8 h. Afterwards, the reaction medium was cooled down to room temperature, and mesitylene was added as an internal standard. Subsequently, a sample (10 μL) of the reaction mixture in CDCl<sub>3</sub> (0.4 mL) was subjected to <sup>1</sup>H NMR spectroscopy to determine the yield in alkyl boronate ester.

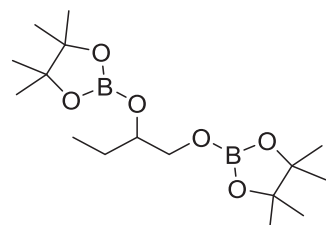
**1,2-bis((4,4,5,5-tetramethyl-1,3,2-dioxaborolan-2-yl)oxy)ethane (40a)**: Prepared by following the general experimental procedure with: **Mn-24** (0.73 mg, 0.1 mol%), **38a** (88.06 mg, 1 mmol), **39** (0.435 mL, 3 mmol) and NaO<sup>t</sup>Bu (0.288 mg, 0.3 mol%). <sup>1</sup>H NMR (300 MHz, CDCl<sub>3</sub>, 298 K): δ = 3.87 (s, 4H, CH<sub>2</sub>), 1.18 (s, 24H, CH<sub>3</sub>); <sup>13</sup>C{<sup>1</sup>H} NMR (75 MHz, CDCl<sub>3</sub>, 298 K): δ = 82.8, 65.1, 24.6; <sup>11</sup>B{<sup>1</sup>H} NMR (96 MHz, CDCl<sub>3</sub>, 298 K): δ = 22.27.



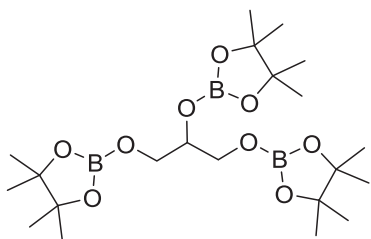
**2,2'-(propane-1,2-diylbis(oxy))bis(4,4,5,5-tetramethyl-1,3,2-dioxaborolane) (40b)**: Prepared by following the general experimental procedure with: **Mn-24** (0.73 mg, 0.1 mol%), **38b** (102.0 mg, 1 mmol), **39** (0.435 mL, 3 mmol) and NaO<sup>t</sup>Bu (0.288 mg, 0.3 mol%). The obtained analytical data are consistent with those previously reported in the literature.<sup>[18]</sup>



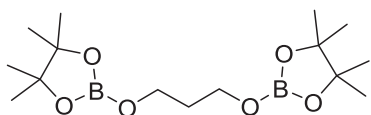
**2,2'-(butane-1,2-diylbis(oxy))bis(4,4,5,5-tetramethyl-1,3,2-dioxaborolane) (40c)**: Prepared by following the general experimental procedure with: **Mn-24** (0.73 mg, 0.1 mol%), **38c** (116.12 mg, 1 mmol), **39** (0.435 mL, 3 mmol) and NaO<sup>t</sup>Bu (0.288 mg, 0.3 mol%). <sup>1</sup>H NMR (300 MHz, CDCl<sub>3</sub>, 298 K): δ = 3.96-4.04 (m, 1H), 3.65-3.77 (m, 2H), 1.37-1.50 (m, 2H, CH<sub>2</sub>), 1.19 (s, 12H, CH<sub>3</sub>), 1.18 (s, 12H, CH<sub>3</sub>), 0.85 (t, J = 9 Hz, 3H, CH<sub>3</sub>); <sup>13</sup>C{<sup>1</sup>H} NMR (75 MHz, CDCl<sub>3</sub>, 298 K): δ = 82.8, 82.7, 75.5, 67.8, 25.4, 24.7, 24.6, 9.6; <sup>11</sup>B{<sup>1</sup>H} NMR (128 MHz, CDCl<sub>3</sub>, 298 K): δ = 22.14.



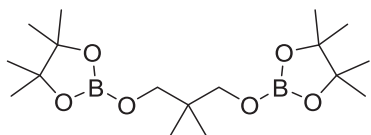


**2,2',2''-(propane-1,2,3-triyltris(oxy))tris(4,4,5,5-tetramethyl-1,3,2-dioxaborolane) (40d):**

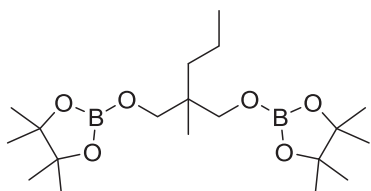
Prepared by following the general experimental procedure with: **Mn-24** (0.73 mg, 0.1 mol%), **38d** (118.00 mg, 1 mmol), **39** (0.580 mL, 4 mmol) and NaO<sup>t</sup>Bu (0.288 mg, 0.3 mol%). <sup>1</sup>H NMR (101 MHz, CDCl<sub>3</sub>, 298 K): δ = 4.15-4.23 (quin, *J* = 6 Hz, 1H, CH), 3.74-3.88 (m, 4H, CH<sub>2</sub>), 1.19 (s, 12H, CH<sub>3</sub>), 1.17 (s, 24H, CH<sub>3</sub>); <sup>13</sup>C{<sup>1</sup>H} NMR (101 MHz, CDCl<sub>3</sub>, 298 K): δ = 82.9, 82.8, 73.7, 65.2, 24.6, 24.5; <sup>11</sup>B{<sup>1</sup>H} NMR (128 MHz, CDCl<sub>3</sub>, 298 K): δ = 22.16.

**1,3-bis((4,4,5,5-tetramethyl-1,3,2-dioxaborolan-2-yl)oxy)propane (40e):** Prepared by

following the general experimental procedure with: **Mn-24** (0.73 mg, 0.1 mol%), **38e** (102.10 mg, 1 mmol), **39** (0.435 mL, 3 mmol) and NaO<sup>t</sup>Bu (0.288 mg, 0.3 mol%). <sup>1</sup>H NMR (300 MHz, CDCl<sub>3</sub>, 298 K): δ = 3.86 (t, *J* = 6 Hz, 4H, CH<sub>2</sub>), 1.77 (quin, *J* = 6 Hz, 2H, CH<sub>2</sub>), 1.17 (s, 24H, CH<sub>3</sub>); <sup>13</sup>C{<sup>1</sup>H} NMR (101 MHz, CDCl<sub>3</sub>, 298 K): δ = 82.8, 61.6, 33.4, 24.7; <sup>11</sup>B{<sup>1</sup>H} NMR (128 MHz, CDCl<sub>3</sub>, 298 K): δ = 22.19.

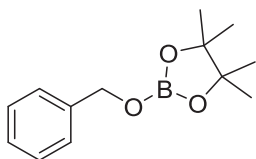
**2,2'-((2,2-dimethylpropane-1,3-diyl)bis(oxy))bis(4,4,5,5-tetramethyl-1,3,2-dioxaborolane) (40f):**

Prepared by following the general experimental procedure with: **Mn-24** (0.73 mg, 0.1 mol%), **38f** (130.10 mg, 1 mmol), **39** (0.435 mL, 3 mmol) and NaO<sup>t</sup>Bu (0.288 mg, 0.3 mol%). <sup>1</sup>H NMR (300 MHz, CDCl<sub>3</sub>, 298 K): δ = 3.57 (s, 4H, CH<sub>2</sub>), 1.20 (s, 24H, CH<sub>3</sub>), 0.81 (s, 6H, CH<sub>3</sub>); <sup>13</sup>C{<sup>1</sup>H} NMR (101 MHz, CDCl<sub>3</sub>, 298 K): δ = 82.9, 70.4, 36.8, 21.3, 21.2. <sup>11</sup>B{<sup>1</sup>H} NMR (128 MHz, CDCl<sub>3</sub>, 298 K): δ = 22.03.

**2,2'-((2-methyl-2-propylpropane-1,3-diyl)bis(oxy))bis(4,4,5,5-tetramethyl-1,3,2-**

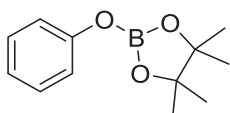
**dioxaborolane) (40g):** Prepared by following the general experimental procedure with: **Mn-24** (0.73 mg, 0.1 mol%), **38g** (158.19 mg, 1 mmol), **39** (0.435 mL, 3 mmol) and NaO<sup>t</sup>Bu (0.288 mg, 0.3 mol%). <sup>1</sup>H-NMR (300 MHz, CDCl<sub>3</sub>, 298 K): δ = 3.59 (d, *J* = 2.4 Hz, 4H, CH<sub>2</sub>), 1.17 (s, 28H, CH<sub>2</sub> and CH<sub>3</sub>), 0.76-0.81 (m, 6H, CH<sub>3</sub>); <sup>13</sup>C{<sup>1</sup>H} NMR (101 MHz, CDCl<sub>3</sub>, 298 K): δ = 82.7, 68.9, 39.2, 36.1, 24.7, 18.4, 16.5, 15.0; <sup>11</sup>B{<sup>1</sup>H} NMR (128 MHz, CDCl<sub>3</sub>, 298 K): δ = 22.21.

**2-(benzyloxy)-4,4,5,5-tetramethyl-1,3,2-dioxaborolane (40h):** Prepared by following the



general experimental procedure with: **Mn-24** (0.73 mg, 0.1 mol%), **38h** (242.10 mg, 1 mmol), **39** (0.435 mL, 3 mmol) and NaO<sup>t</sup>Bu (0.288 mg, 0.3 mol%). The obtained analytical data are consistent with those previously reported in the literature.<sup>[19]</sup>

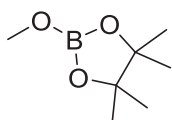
**4,4,5,5-tetramethyl-2-phenoxy-1,3,2-dioxaborolane (40i):** Prepared by following the general



experimental procedure with: **Mn-24** (0.73 mg, 0.1 mol%), **38i** (214.10 mg, 1 mmol), **39** (0.435 mL, 3 mmol) and NaO<sup>t</sup>Bu (0.288 mg, 0.3 mol%). The obtained analytical data are consistent with those previously reported in the

literature.<sup>[20]</sup>

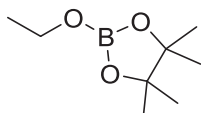
**2-methoxy-4,4,5,5-tetramethyl-1,3,2-dioxaborolane (40j):** Prepared by following the general



experimental procedure with: **Mn-24** (0.73 mg, 0.1 mol%), **38j** (90.00 mg, 1 mmol), **39** (0.435 mL, 3 mmol) and NaO<sup>t</sup>Bu (0.288 mg, 0.3 mol%). The obtained analytical data are consistent with those previously reported in the

literature.<sup>[21]</sup>

**2-ethoxy-4,4,5,5-tetramethyl-1,3,2-dioxaborolane (40k):** Prepared by following the general



experimental procedure with: **Mn-24** (0.73 mg, 0.1 mol%), **38k** (104.11 mg, 1 mmol), **39** (0.435 mL, 3 mmol) and NaO<sup>t</sup>Bu (0.288 mg, 0.3 mol%). The obtained analytical data are consistent with those previously reported in the

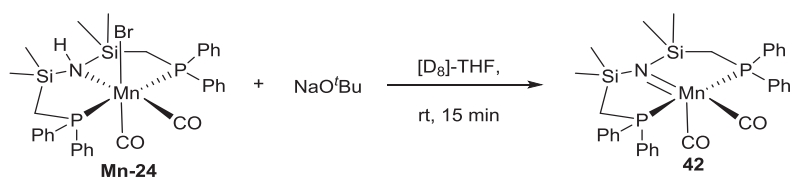
literature.<sup>[22]</sup>

## 7.9.6. General procedure for catalytic hydroboration of carbon dioxide

Carbon dioxide was purged three times through a schlenk containing a mixture of Mn-precatalyst **Mn-24** (0.73 mg, 0.036 mol%), NaO<sup>t</sup>Bu (0.288 mg, 0.1 mol%) and pinacolborane (353.2 mg, 2.76 mmol) in the indicated solvent. Afterwards, the schlenk tube was equipped with a CO<sub>2</sub> balloon and the reaction mixture was heated at the indicated temperatures. The reaction medium was then cooled down to room temperature, and mesitylene was added as an internal standard. Subsequently, a sample (10 μL) of the reaction mixture in CDCl<sub>3</sub> (0.4 mL) was subjected to <sup>1</sup>H NMR spectroscopy to determine the yield in alkyl boronate ester.

## 7.9.7. Observation of catalytic intermediates

### 7.9.7.1. Observation of complex 42



Sodium *tert*-butoxide (2.40 mg, 0.025 mmol) was added to a THF (0.4 mL) solution of complex **Mn-24** (15 mg, 0.021 mmol). The resulting mixture was stirred for fifteen minutes at room temperature leading to a colour change from yellow to dark violet. Subsequent filtration over celite, followed by removal of the solvent in vacuo led to complex **42** (9.8 mg, 0.015 mmol, 74%) as a dark violet solid. Several attempts were performed to obtain single crystals of complex **42**, but were proven so far unsuccessful. <sup>1</sup>H NMR (300 MHz, [D<sub>8</sub>]-THF, 298 K): δ = 7.66-7.74 (m, 8H), 7.35-7.36 (m, 12H), 1.84 (t, 4H, *J* = 6 Hz), -0.02 (s, 12H). <sup>13</sup>C{<sup>1</sup>H} NMR<sup>a</sup> (75 MHz, [D<sub>8</sub>]-THF, 298 K): δ = 133.6 (vt, *J* = 5.4 Hz), 130.4 (br s), 129.8 (s), 129.1 (vt, *J* = 4.4 Hz), 8.1 (s), 5.9 (s). <sup>31</sup>P{<sup>1</sup>H} NMR (121 MHz, [D<sub>8</sub>]-THF, 298 K) δ = 61.26. HRMS (ESI<sup>+</sup>): *m/z*: calcd. for C<sub>32</sub>H<sub>37</sub>MnNP<sub>2</sub>Si<sub>2</sub> [M+H]<sup>+</sup>: 640.12131; found: 640.12119. The presumably broad <sup>13</sup>C signals of the carbonyl groups could not be located even after increasing the acquisition time or using two-dimensional NMR experiments.

## Manganese(I) catalyzed selective hydroboration of organic carbonates and carbon dioxide

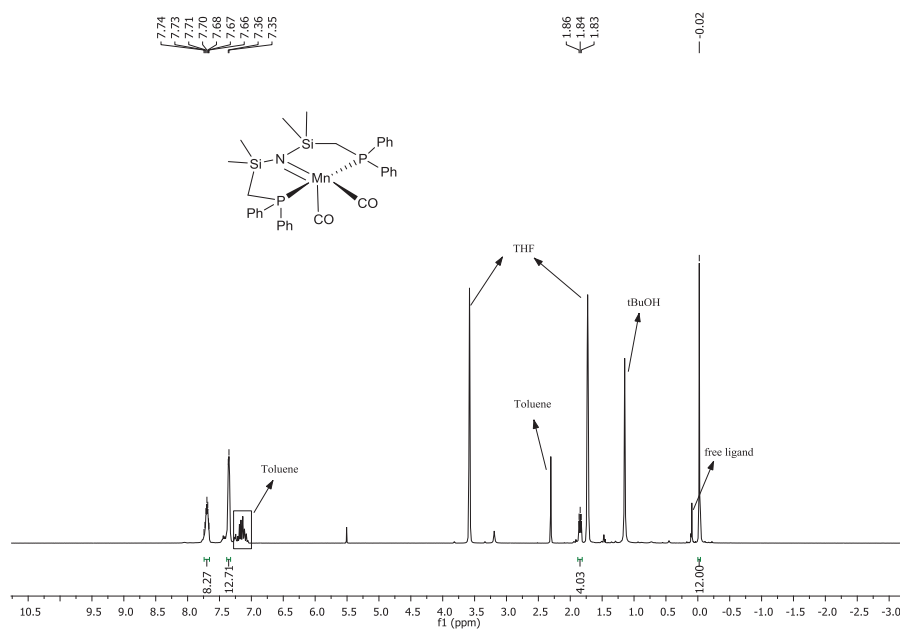


Figure 7.3:  $^1\text{H}$  NMR (300 MHz,  $[\text{D}_8]$ -THF, 298 K) spectrum of complex 42.

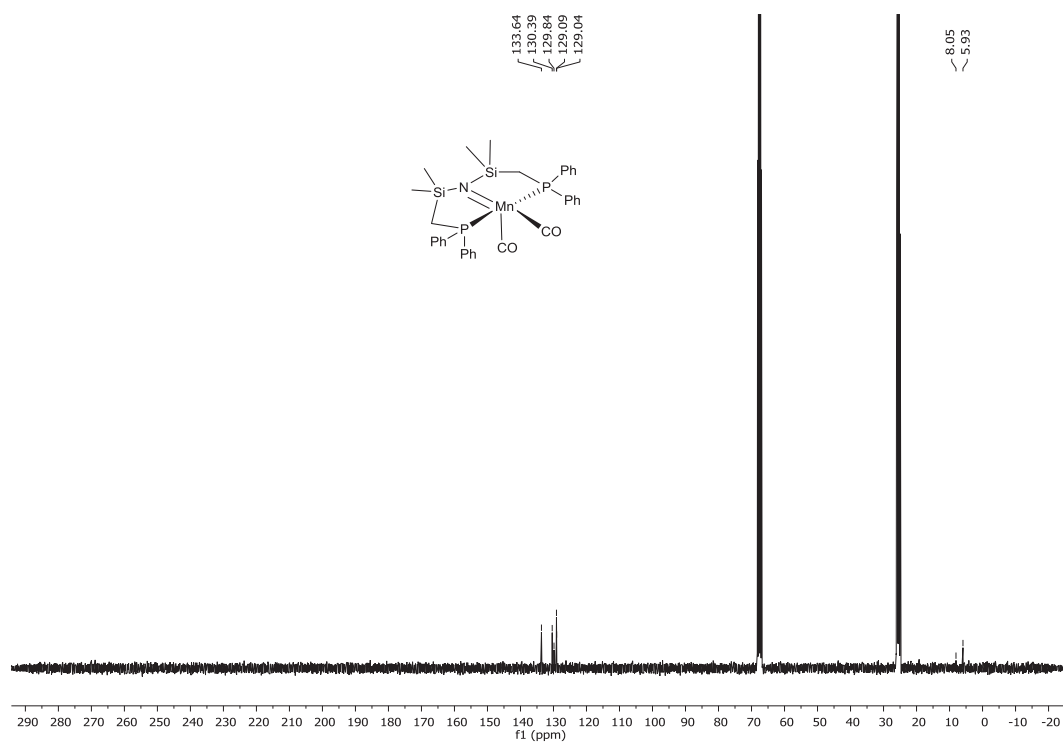


Figure 7.4:  $^{13}\text{C}\{^1\text{H}\}$  NMR (75 MHz,  $[\text{D}_8]$ -THF, 298 K) spectrum of complex 42.

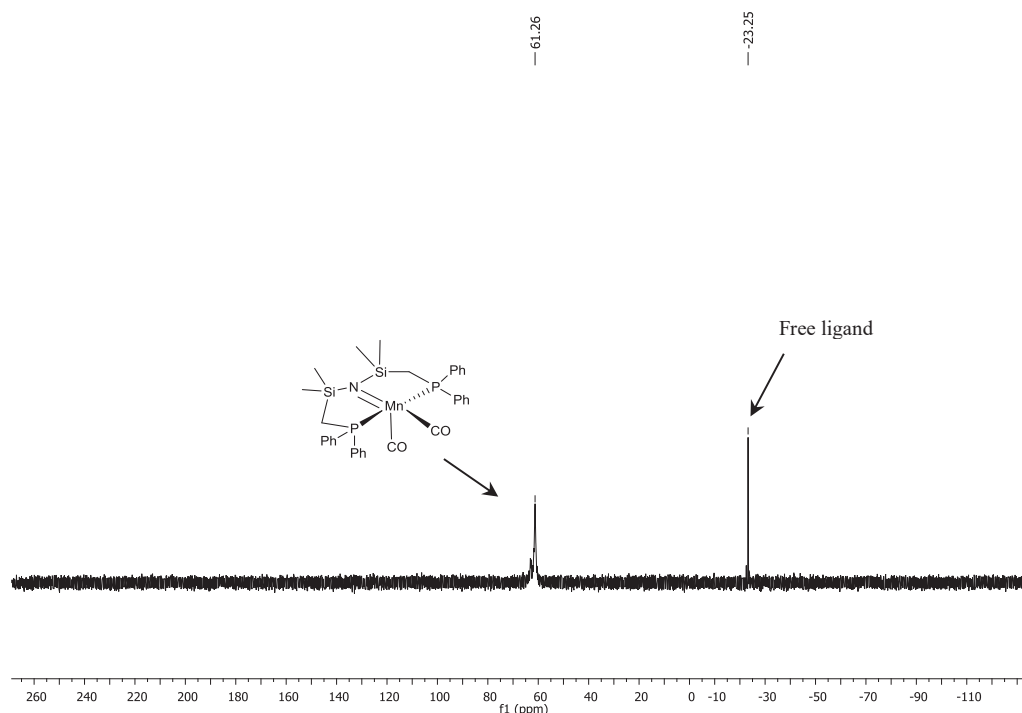
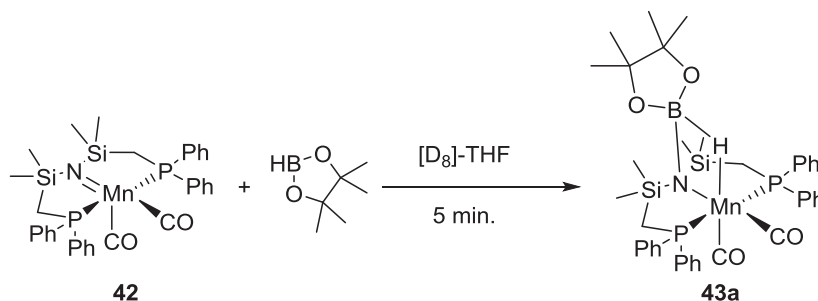
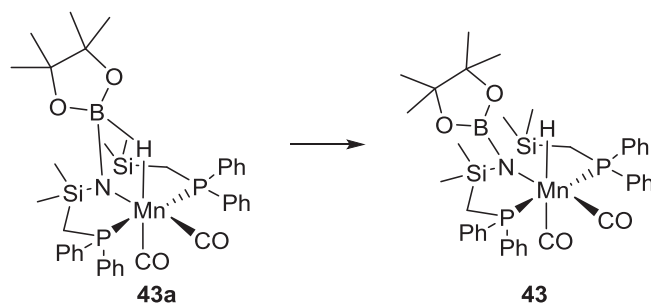


Figure 7.5:  $^{31}\text{P}\{^1\text{H}\}$  NMR (121 MHz,  $[\text{D}_8]$ -THF, 298 K) spectrum of complex **42**.

### 7.9.7.2. Stoichiometric reaction of complex **42** with pinacolborane



The addition of complex **42** (13.5 mg, 0.021 mmol) to a solution of pinacolborane (3.9 mg, 0.030 mmol) in  $[\text{D}_8]$ -THF (0.4 mL) lead to a concomitant color change from dark violet to yellow.  $^1\text{H}$ -NMR analysis revealed a broad signal at  $\delta -6.57$  ppm that can be attributed to complex **43a**, where a pinacolborane bridges the manganese atom with the nitrogen from the ligand framework. This results in the formation of a metal hydride. Furthermore,  $^{31}\text{P}\{^1\text{H}\}$  and  $^{11}\text{B}\{^1\text{H}\}$ -NMR analysis revealed a new peak at  $\delta 65.20$  ppm and 21.35 ppm, respectively. The formation of complex **43a**, could be confirmed by X-Ray analysis of single crystals grown by the slow diffusion of hexane into a concentrated solution of **43a** in dichloromethane.



When complex **43a** is heated at 50°C for 30 min, a new signal in the hydride region of the  $^1\text{H}$ -NMR spectrum is observed ( $\delta$ : -8.14 ppm, t,  $J = 32$  Hz). The associated  $^{31}\text{P}\{^1\text{H}\}$ -NMR spectrum also revealed the apparition of a new signal at  $\delta$ : 62.31 ppm. These signals can be attributed to the formation of **43**. Interestingly, after 2 days of reaction, most of **43a** converts into **43**.

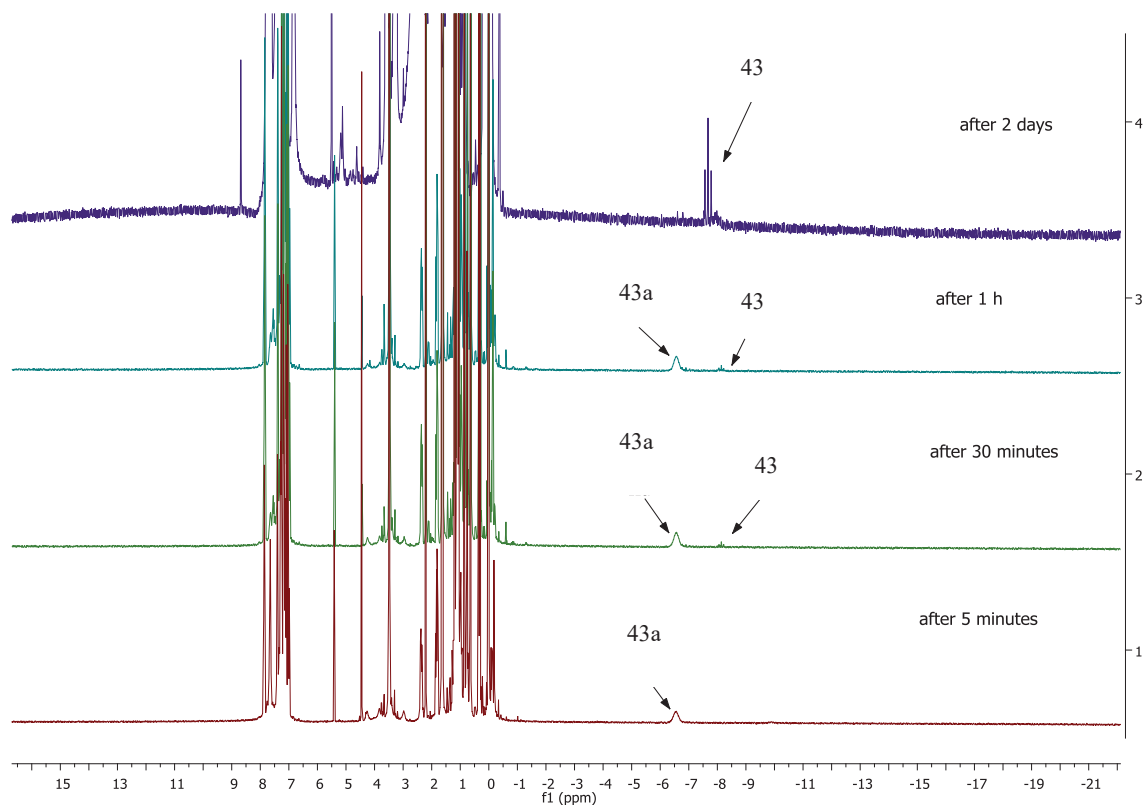


**Figure 7.6:** Superposed  $^1\text{H}$  NMR spectra (300 MHz,  $[\text{D}_8]$ -THF, 298 K) of intermediates **43a** and **43** at different time intervals.

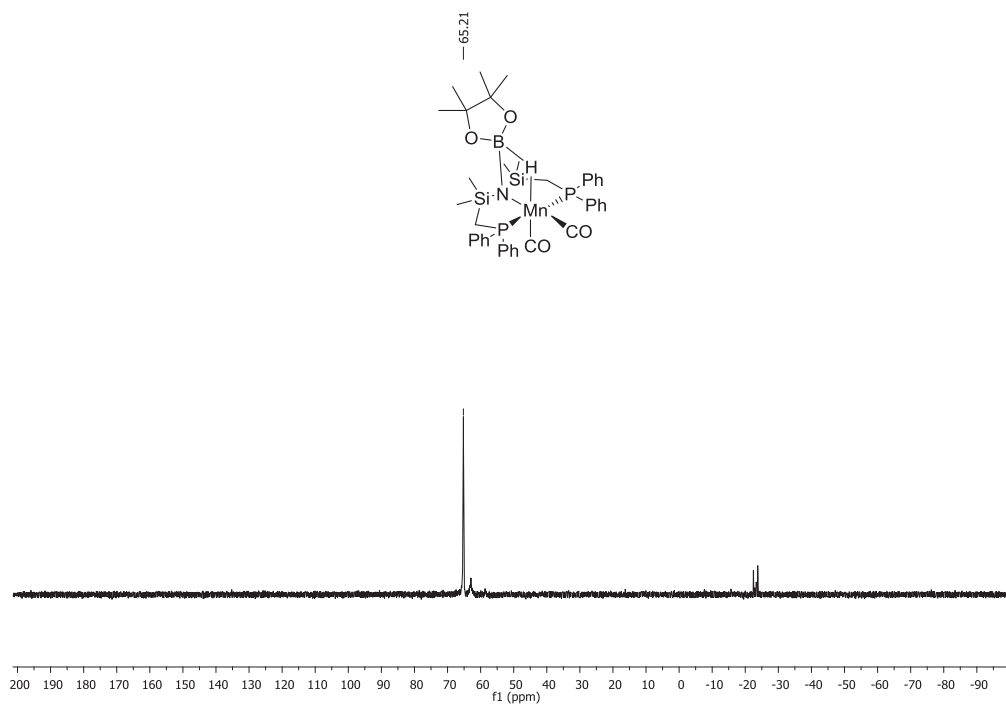


Figure 7.7:  $^{31}\text{P}\{^1\text{H}\}$ -NMR (162 MHz,  $[\text{D}_8]$ -THF, 298 K) spectrum of complex **43a**.

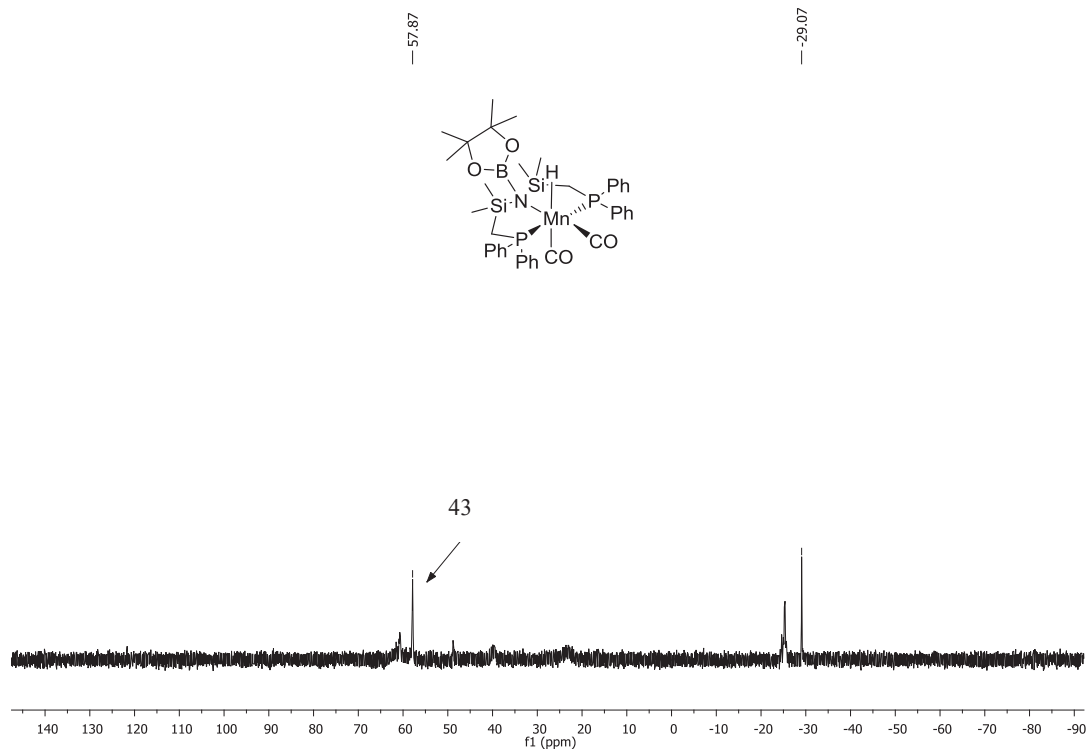


Figure 7.8:  $^{31}\text{P}\{^1\text{H}\}$  NMR (121 MHz,  $[\text{D}_8]$ -THF, 298 K) spectrum of reaction mixture of complex **43** after 48 h.

## References

- [1] M. L. Shegavi, S. K. Bose, *Catal. Sci. Technol.* **2019**, *9*, 3307-3336.
- [2] C. C. Chong, R. Kinjo, *ACS Catal.* **2015**, *5*, 3238-3259.
- [3] E. Balaraman, C. Gunanathan, J. Zhang, L. J. W. Shimon, D. Milstein, *Nat. Chem* **2011**, *3*, 609.
- [4] a) S. Werkmeister, K. Junge, M. Beller, *Org. Process Res. Dev.* **2014**, *18*, 289-302; b) J. Pritchard, G. A. Filonenko, R. van Putten, E. J. M. Hensen, E. A. Pidko, *Chem. Soc. Rev.* **2015**, *44*, 3808-3833; c) H. C. Maytum, B. Tavassoli, J. M. J. Williams, *Org. Lett.* **2007**, *9*, 4387-4389; d) D. Wang, D. Astruc, *Chem. Rev.* **2015**, *115*, 6621-6686; e) M. Aresta, A. Dibenedetto, *Dalton Trans.* **2007**, 2975-2992.
- [5] a) C. Gunanathan, M. Hölscher, W. Leitner, *Eur. J. Inorg. Chem.* **2011**, *2011*, 3381-3386; b) S. Elangovan, M. Garbe, H. Jiao, A. Spannenberg, K. Junge, M. Beller, *Angew. Chem. Int. Ed.* **2016**, *55*, 15364-15368; c) Z. Lu, T. J. Williams, *Chem. Commun.* **2014**, *50*, 5391-5393; d) K. Soai, A. Ookawa, *J. Org. Chem.* **1986**, *51*, 4000-4005.
- [6] a) A. J. J. Lennox, G. C. Lloyd-Jones, *Chem. Soc. Rev.* **2014**, *43*, 412-443; b) M. M. Midland, *Chem. Rev.* **1989**, *89*, 1553-1561; c) K. Burgess, M. J. Ohlmeyer, *Chem. Rev.* **1991**, *91*, 1179-1191.
- [7] a) G. Du, M. M. Abu-Omar, *Organometallics* **2006**, *25*, 4920-4923; b) B. Chatterjee, C. Gunanathan, *Chem. Commun.* **2014**, *50*, 888-890; c) D. Youngshil, H. Junghoon, R. Y. Ho, P. Jaiwook, *Adv. Synth. Catal.* **2011**, *353*, 3363-3366; d) K. Riener, M. P. Högerl, P. Gigler, F. E. Kühn, *ACS Catal.* **2012**, *2*, 613-621.
- [8] a) Y. Jian, T. T. Don, *Angew. Chem. Int. Ed.* **2010**, *49*, 10186-10188; b) N. S. Shaikh, K. Junge, M. Beller, *Org. Lett.* **2007**, *9*, 5429-5432; c) T. Bleith, L. H. Gade, *J. Am. Chem. Soc.* **2016**, *138*, 4972-4983; d) S. Marcin, B. Agata, M. Jacek, *ChemCatChem* **2016**, *8*, 3575-3579; e) P. Shaofeng, P. Jiajian, L. Jiayun, B. Ying, X. Wenjun, L. Guoqiao, *Chirality* **2013**, *25*, 275-280; f) J. Kathrin, M. Konstanze, W. Bianca, D. Shoubhik, G. Dirk, T. Kerstin, B. Matthias, *Chemistry – An Asian Journal* **2012**, *7*, 314-320; g) F. S. Wekesa, R. Arias-Ugarte, L. Kong, Z. Sumner, G. P. McGovern, M. Findlater, *Organometallics* **2015**, *34*, 5051-5056; h) A. Raya-Baron, C. P. Galdeano-Ruano, P. Ona-Burgos, A. Rodriguez-Dieguez, R. Langer, R. Lopez-Ruiz, R. Romero-Gonzalez, I. Kuzu, I. Fernandez, *Dalton Trans.* **2018**, *47*, 7272-7281; i) X. Ma, Z. Zuo, G. Liu, Z. Huang, *ACS Omega* **2017**, *2*, 4688-4692; j) V. K. Chidara, G. Du, *Organometallics* **2013**, *32*, 5034-5037.
- [9] a) D. Yan, P. Dai, S. Chen, M. Xue, Y. Yao, Q. Shen, X. Bao, *Org. Biomol. Chem* **2018**, *16*, 2787-2791; b) V. K. Jakhar, M. K. Barman, S. Nembenna, *Org. Lett.* **2016**, *18*, 4710-4713; c) A. Kaithal, B. Chatterjee, C. Gunanathan, *Org. Lett.* **2015**, *17*, 4790-4793; d) V. L. Weidner, C. J. Barger, M. Delferro, T. L. Lohr, T. J. Marks, *ACS Catal.* **2017**, *7*, 1244-1247; e) D. Mukherjee, A. Ellern, A. D. Sadow, *Chem Sci* **2014**, *5*, 959-964; f) M. K. Barman, A. Baishya, S. Nembenna, *Dalton Trans.* **2017**, *46*, 4152-4156; g) A. Kaithal, B. Chatterjee, C. Gunanathan, *J. Org. Chem.* **2016**, *81*, 11153-11161; h) C. Weetman, M. D. Anker, M. Arrowsmith, M. S. Hill, G. Kociok-Kohn, D. J. Liptrot, M. F. Mahon, *Chem Sci* **2016**, *7*, 628-641; i) M. Arrowsmith, M. S. Hill, T. Hadlington, G. Kociok-Köhn, C. Weetman, *Organometallics* **2011**, *30*, 5556-5559; j) A. Kaithal, B. Chatterjee, C. Gunanathan, *Org.*

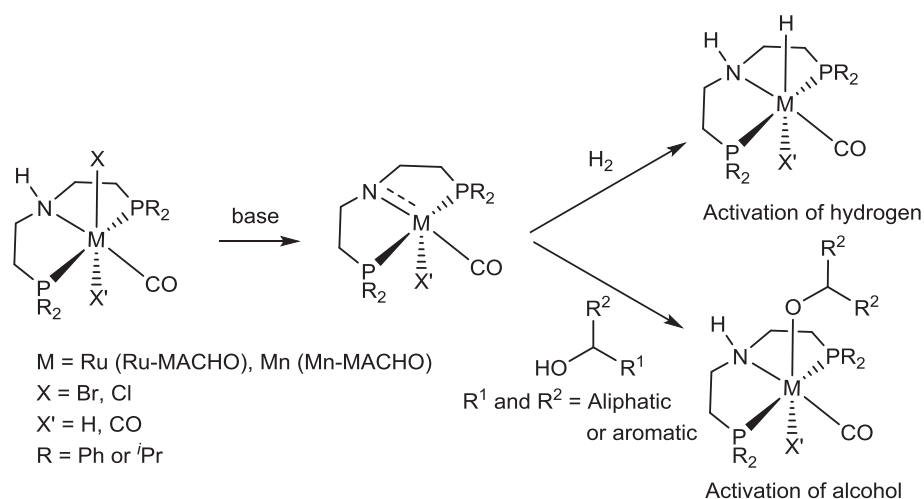


- Lett.* **2016**, *18*, 3402-3405; k) A. A. Oluyadi, S. Ma, C. N. Muhoro, *Organometallics* **2013**, *32*, 70-78; l) Z. Huang, D. Liu, J. Camacho-Bunquin, G. Zhang, D. Yang, J. M. López-Encarnación, Y. Xu, M. S. Ferrandon, J. Niklas, O. G. Poluektov, J. Jellinek, A. Lei, E. E. Bunel, M. Delferro, *Organometallics* **2017**, *36*, 3921-3930.
- [10] a) L. J. Murphy, H. Hollenhorst, R. McDonald, M. Ferguson, M. D. Lumsden, L. Turculet, *Organometallics* **2017**, *36*, 3709-3720; b) R. Shintani, K. Nozaki, *Organometallics* **2013**, *32*, 2459-2462; c) T. Liu, W. Meng, Q.-Q. Ma, J. Zhang, H. Li, S. Li, Q. Zhao, X. Chen, *Dalton Trans.* **2017**, *46*, 4504-4509; d) L. Li, H. Zhu, L. Liu, D. Song, M. Lei, *Inorg. Chem.* **2018**, *57*, 3054-3060; e) S. Bontemps, L. Vendier, S. Sabo-Etienne, *Angew. Chem. Int. Ed.* **2012**, *51*, 1671-1674.
- [11] S. Chakraborty, J. Zhang, J. A. Krause, H. Guan, *J. Am. Chem. Soc.* **2010**, *132*, 8872-8873.
- [12] S. Bontemps, L. Vendier, S. Sabo-Etienne, *J. Am. Chem. Soc.* **2014**, *136*, 4419-4425.
- [13] M. J. Sgro, D. W. Stephan, *Angew. Chem. Int. Ed.* **2012**, *51*, 11343-11345.
- [14] M. D. Fryzuk, C. D. Montgomery, S. J. Rettig, *Organometallics* **1991**, *10*, 467-473.
- [15] M. D. Fryzuk, P. A. MacNeil, S. J. Rettig, A. S. Secco, J. Trotter, *Organometallics* **1982**, *1*, 918-930.
- [16] S. Elangovan, C. Topf, S. Fischer, H. Jiao, A. Spannenberg, W. Baumann, R. Ludwig, K. Junge, M. Beller, *J. Am. Chem. Soc.* **2016**, *138*, 8809-8814.
- [17] G. R. Fulmer, A. J. M. Miller, N. H. Sherden, H. E. Gottlieb, A. Nudelman, B. M. Stoltz, J. E. Bercaw, K. I. Goldberg, *Organometallics* **2010**, *29*, 2176-2179.
- [18] D. Mukherjee, A. Ellern, A. D. Sadow, *Chem. Sci.* **2014**, *5*, 959-964.
- [19] A. Kaithal, B. Chatterjee, C. Gunanathan, *Org. Lett.* **2015**, *17*, 4790-4793.
- [20] B. Chattopadhyay, J. E. Dannatt, I. L. Andujar-De Sanctis, K. A. Gore, R. E. Maleczka, Jr., D. A. Singleton, M. R. Smith, 3rd, *J. Am. Chem. Soc.* **2017**, *139*, 7864-7871.
- [21] S. Chakraborty, J. Zhang, J. A. Krause, H. Guan, *J. Am. Chem. Soc.* **2010**, *132*, 8872-8873.
- [22] S. Kisan, V. Krishnakumar, C. Gunanathan, *ACS Catal.* **2018**, *8*, 4772-4776.

## 8. General Conclusion

In this dissertation, we have investigated catalytic systems based on ruthenium(II) and manganese(I) pincer complexes for hydrogen transfer reactions. Various hydrogen borrowing reactions and reduction reactions were examined.

The results from this dissertation confirmed that all hydrogen transfer reactions were preceded by metal-ligand cooperation in the pincer complex where the formation of a hydride at a metal center plays an important role for catalysis and activation of organic molecules. All transformations were performed using the MACHO ligand incorporated metal complex. The N–H functionality in the MACHO complexes mediates the proton shuffling and the metal center promotes the hydride transfer. This methodology promotes the de-hydrogenation and hydrogenation reactions and performs the whole catalytic reactions.



**Scheme 8. 1:** Metal-ligand cooperation to activate hydrogen and organic molecules.

Initially, hydrogen borrowing reactions were investigated. Selective  $\beta$ -methylation of alcohols using methanol as a C1 source was performed where Ru-MACHO-BH **Ru-20** pincer complex was found to be the highly active catalyst. Complex **Ru-20** performed the de-hydrogenation and re-hydrogenation reaction while the base was used to perform the aldol condensation in the reaction.

The  $\beta$ -methylation of alcohols using methanol as a C1 source was also carried out using a non-noble manganese metal precursor. Manganese was chosen as a metal precursor, as we assumed that the substitution of  $\text{Ru}^{2+}$  into  $\text{Mn}^{1+}$  is particularly favorable because of the diagonal

relationship between the two ions in the periodic table. Mn-MACHO-*i*Pr **Mn-2** complex resulted in similar reactivity in comparison with the **Ru-20** complex. Mechanistic investigations were performed. Alike **Ru-20** complex, **Mn-2** complex also showed reactivity towards de-hydrogenation and re-hydrogenation reactions.

Similarly, employing the hydrogen borrowing reaction mechanism, we performed the preparation of substituted cycloalkanes from secondary alcohols or ketones and diols using complex **Mn-2** and a stoichiometric amount of a base. Interestingly, it was found that the **Mn-2** complex revealed better reactivity in comparison to the closely related **Ru-20** complex. Various substituted cycloalkane rings such as cyclopentane, cyclohexane and cycloheptane rings were prepared using this process.

In the other transformation, selective deuteration of alcohol was performed where D<sub>2</sub>O was employed as a deuterium source; **Mn-2** complex as a precatalyst and catalytic amount of a base as a cocatalyst.

Based on these results, reduction reactions employing manganese(I) pincer complexes were also investigated. Using the Mn(I) pincer complexes, the hydrogenation of cyclic carbonates to the corresponding diols and methanol were examined. Various Mn(I) pincer complexes were investigated for this transformation. Among all chosen complexes, Mn-MACHO-*i*Pr complex **Mn-2** revealed the best catalytic activity resulting in TONs of 620 and 400 to diol and methanol, respectively.

Likewise, the reduction of other challenging substrates such as carbon dioxide, linear carbonates, and cyclic carbonates was performed using pinacolborane as a reducing reagent. For this process, a new silane-based Mn(I) pincer complex **Mn-24** was synthesized and used for the catalysis. The new manganese complex showed very good reactivity for the reduction reactions and resulted in 883 TONs to the methoxy borane for the reduction of CO<sub>2</sub>. Similarly, linear and cyclic carbonates were also reduced employing pinacolborane as a reducing agent, **Mn-24** as a precatalyst and catalytic amount of a base as a cocatalyst.

These results indicate that employing an adequate ligand, the metal-complex comprising Ru<sup>2+</sup> ion can be substituted to Mn<sup>1+</sup> ions and employed for various hydrogen transfer reactions. Mn(I) pincer complexes revealed good reactivity towards hydride formation on reaction with hydrogen or hydride source which can easily be transferred to the other organic molecules. Formation of hydride into the metal complex led to the various hydrogen transfer reactions and

resulted in various hydrogen borrowing and reduction reactions in this dissertation. Overall, manganese(I) pincer complexes revealed a broad scope and even in some cases the activities and productivities are competitive and better to the well-established Ru(II) complexes. For future developments, a fine-tuning in the ligand structure of the manganese(I) complexes is necessary which can make them as competitive as the early established noble metal complexes. Additionally, enantioselective catalysis and asymmetric hydrogenation reactions need to be investigated using the manganese complexes.

## 9. Summary

### Motivation and structure of the thesis (Chapter 1)

#### Pincer complexes and their reactivity in hydrogen transfer reactions

The hydrogen transfer reactions have received great interest in recent decades, and substantial researches have been made in past. Employing this strategy, the inert  $sp^3$  C–H bond can be activated and functionalized into various important bonds such as C–C, C–N, C–O and C–S bonds.<sup>[1]</sup>

In this chapter, we focused on the recent developments made by manganese(I) pincer complexes and their similar reactivities with the ruthenium(II) pincer complexes for the hydrogen transfer reactions.

In the past, several works were reported for hydrogen transfer reactions using pincer complexes. Pincer ligand has a tridentate site which on coordinating with a metal-center provides a well-coordinated tridentate stable molecular complex.<sup>[2]</sup>



**Figure 9.1:** Common structure for pincer complexes.

Lastly, hydrogen transfer reactions were reported by using noble metal complexes such as ruthenium, iridium or palladium pincer complexes.<sup>[1, 3]</sup> In general, these complexes are activated by base which in hydrogen environment generates the metal-hydride complex and used as a hydrogen transfer catalyst. Recently, earth-abundant 3d-metals such as iron, manganese, cobalt and nickel pincer complexes were also used for these transformations.<sup>[4]</sup> Especially, Mn(I) pincer complexes revealed very similar reactivity with the early established Ru(II) complexes because of its diagonal relationship, same electronic configuration and isoelectronic nature with the Ru(II) complexes.<sup>[5]</sup>

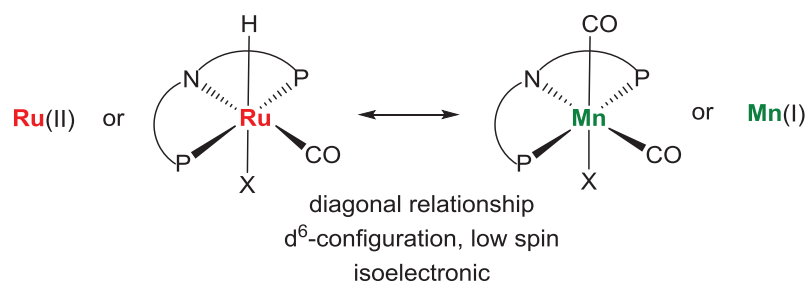


**Figure 9.2:** Similar properties between Ru(II) and Mn(I) complexes.

In the last few decades, Ru(II) complexes are well-established for alkylation and hydrogenation reactions via hydrogen borrowing methods.<sup>[6] [3b]</sup> In the recent years, alike Ru(II) complexes, various Mn(I) complexes were investigated and showed good reactivity for the alkylation reactions using primary alcohols as an alkylating reagent.<sup>[5b, 5c]</sup> Several alkylation reactions such as alkylation of ketones, alcohols, nitriles, esters and amides were reported using the manganese(I) pincer complexes. Similarly, hydrogenation of carbonyl functionalities were also shown using the Mn(I) complexes.<sup>[5b, 5c]</sup> A variety of carbonyl functionalities such as aldehydes, ketones, esters, amides, carbonates, carbamates and urea were hydrogenated using the Mn(I) pincer complexes. However, as the comparison aspect of Mn(I) versus Ru(II), manganese(I) complexes showed lower reactivity in comparison to the closely related ruthenium(II) complexes for hydrogenation reactions.

In conclusion, Mn(I) pincer complexes have shown good reactivity towards the hydrogen transfer reactions alike Ru(II) complexes. Various alkylation reactions using alcohols as an alkylating reagent and hydrogenation of carbonyl functionalities using hydrogen were reported employing Mn(I) pincer complexes. However, the present drawback of manganese complexes consists of the incorporation of an expensive phosphorous backbone. At present, most of these transformations were shown using the phosphorous incorporated ligands as a backbone in Mn(I) complexes. Therefore, the ligand with more modular structure, easy to synthesize and non-phosphorous ligands has to be investigated for future applications.

### Structure of the thesis

This dissertation focuses on the hydrogen transfer reactions accompanied by Ru(II) and Mn(I) pincer complexes. The dissertation is divided into two sections. In the first section, reports on ruthenium(II) and manganese(I) catalyzed hydrogen borrowing reactions were studied. Using the Ru(II) and Mn(I) complexes, selective  $\beta$ -methylation of alcohols was investigated. Similarly,

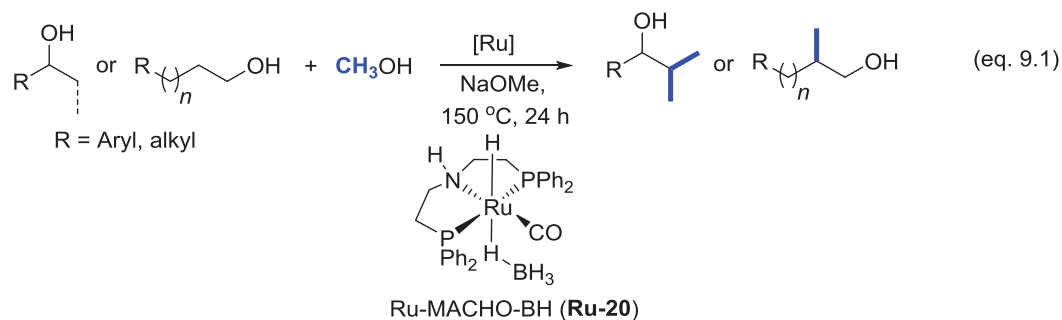
selective deuteration of alcohols using D<sub>2</sub>O as a deuterium source and synthesis of substituted cycloalkanes from diols and alcohols or ketones was studied employing Mn(I) pincer complexes via “Hydrogen borrowing methods”.

In the second section, reduction of organic carbonates and CO<sub>2</sub> was explored using hydrogen or pinacolborane as a reducing agents and manganese(I) pincer complexes as pre-catalysts.

### **Ruthenium catalyzed $\beta$ -methylation of alcohols using MeOH as a C1 source (Chapter 2)**

The methyl group is one of the fundamental and ubiquitous functionality in all sorts of chemicals, biomolecules and pharmaceuticals.<sup>[7]</sup> The selective insertion of methyl group into the alkyl chain to form new C–C bond is an important methodology.<sup>[7-8]</sup> In general, the methylation is performed using a toxic and highly flammable reagents such as Grignard reagent or methylation reagents (e.g. methyl iodide, methyl sulfate or diazomethane).<sup>[9]</sup> To ease these problems, the use of methanol as a methylation reagent can be a good option, as it is less toxic and can be produce from biomass or CO<sub>2</sub> and H<sub>2</sub>.<sup>[10]</sup> By applying the hydrogen borrowing methods, methanol can be used an alkylating reagent.

In this chapter, the selective  $\beta$ -methylation of alcohols was investigated using the various ruthenium precursors and methanol as a methylating reagent. Ruthenium complexes were chosen for this transformation because of their known reactivity towards the hydrogen borrowing reactions. For the optimization, 1-phenyl ethanol was chosen as a benchmark substrate. A number of monodentate, bidentate and tridentate (pincer) complexes were investigated for this transformation. Among all, Ru-MACHO-BH complex showed the best catalytic activity for the selective  $\beta$ -methylation of 1-phenyl ethanol. Based on the optimized reaction conditions, several secondary alcohols, 2-aryl ethanols and aliphatic alcohols were chosen and selective methylated to  $\beta$ -position (eq. 9.1). The selective  $\beta$ -methylation of various alcohols was achieved in the range of 54-94% yield.



**Scheme 9.1:**  $\beta$ -methylation of alcohols using **Ru-20** complex.

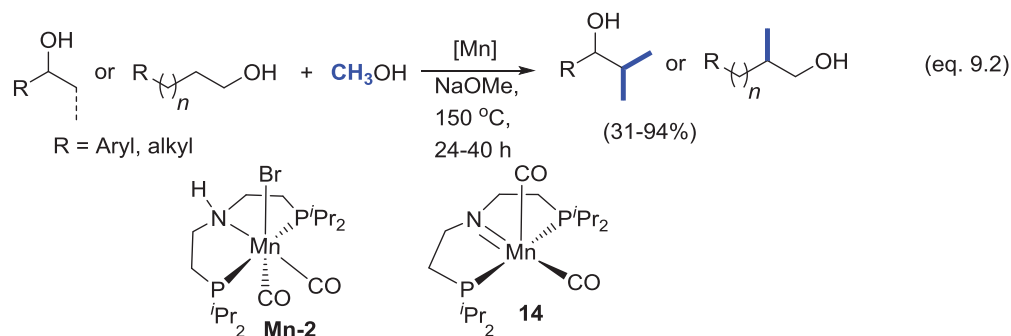
Next detailed investigations were performed to get the reaction insight. To verify that the reaction proceeds via hydrogen borrowing pathways, several labeling and intermediate studies were performed. The activation of complex and reactivity of alcohols was also checked by performing the stoichiometric reactions of complex with alcohols.

Based on the mechanistic studies, a detailed DFT calculation was performed and catalytic cycle was proposed accordingly. The catalytic cycle follows a hydrogen borrowing pathways where the metal ligand cooperation plays an important role for the activation of alcohols and base was used for the formation of C–C bond. The calculated catalytic cycle showed the Gibbs free activation energy of 29.2 kcal/mol which showed close relation to the experimental calculated value of 26.2  $\pm$  0.5 kcal/mol.

### Manganese(I) catalyzed selective $\beta$ -methylation of alcohols using MeOH as the C1 source (Chapter 3)

As in the chapter 2, it was shown that the energies for the subcycles in whole catalytic cycles are either in low or in moderate height. We postulated that using the same base, the reaction maybe performed using the earth-abundant metal complex. Manganese was chosen as a metal-precursor because of its abundance in the earth-crust and also the diagonal relationship between the ruthenium(II) and manganese(I) ions. Several manganese complexes were synthesized and employed for the selective  $\beta$ -methylation of 2-phenylethanol where Mn-MACHO-*i*Pr resulted in the best catalytic activity. Next, optimization was performed using the Mn-MACHO-*i*Pr as a pre-catalyst and NaOMe as a base. Based on the optimized reaction conditions, a variety of 2-aryl ethanols, secondary alcohols and aliphatic alcohols were selective  $\beta$ -methylated (eq 9.2). Interestingly, this process also afforded the selective  $\beta$ -methylation of biomass-generated diols.



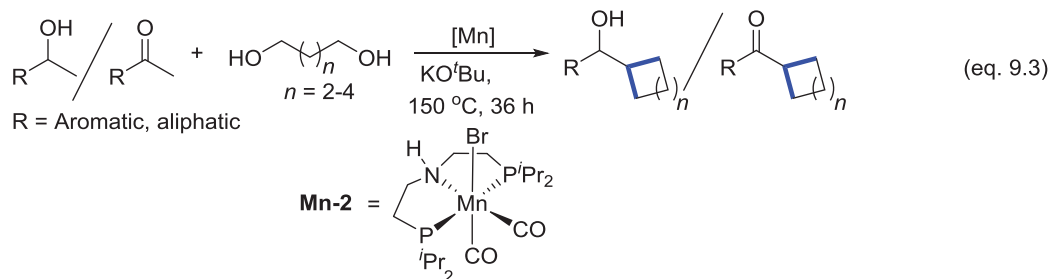


**Scheme 9.2:**  $\beta$ -methylation of alcohols using **Mn-2** complex.

Next to investigate the catalytic cycle, labeling experiments were performed. Labeling experiments confirmed that the reaction is proceeding via hydrogen borrowing pathways and methanol is acting as a C1 source. Stoichiometric reactions using complex **Mn-2** and base showed the formation of active species **14** which on reaction with alcohols resulted in Mn-alkoxy and Mn-hydride species. Based on the mechanistic studies and previous reports, a catalytic cycle was proposed which revealed the metal ligand cooperation in the manganese metal center and hydrogen borrowing reaction to achieve the final methylated product.

### Direct synthesis of cycloalkanes from diols and secondary alcohols or ketones using a homogeneous manganese catalyst (Chapter 4)

Substituted cycloalkanes such as cyclopentanes, cyclohexanes and cycloheptanes are ubiquitous structural motifs and present in many pharmaceuticals, natural products and materials.<sup>[11]</sup> Presently, these molecules are synthesized in multistep procedures and sometimes require high pressure reaction steps to achieve final cycloalkyl product.<sup>[11d, 12]</sup> In general, these processes show narrow substrates scope, poor regio- and stereo-selectives and also generate a stoichiometric amount of chemical waste. At present, the direct and one-step synthesis of these molecules is one of the aspirations of catalysis. Based on the previous investigations on selective  $\beta$ -methylation of alcohols, we assumed that employing the MACHO-type ligands, the synthesis of substituted cycloalkanes are possible using diols as a double alkylating reagent. For this process, both Ru-MACHO-BH **Ru-20** and Mn-MACHO-*i*-Pr **Mn-2** were investigated using 1-phenylethanol as a benchmark substrate and KO<sup>t</sup>Bu as a base. The catalytic reaction showed better reactivity with complex **Mn-2** in comparison to closely related complex **Ru-20**. Considering this, further optimization studies were performed using the **Mn-2** complex (eq 9.3).



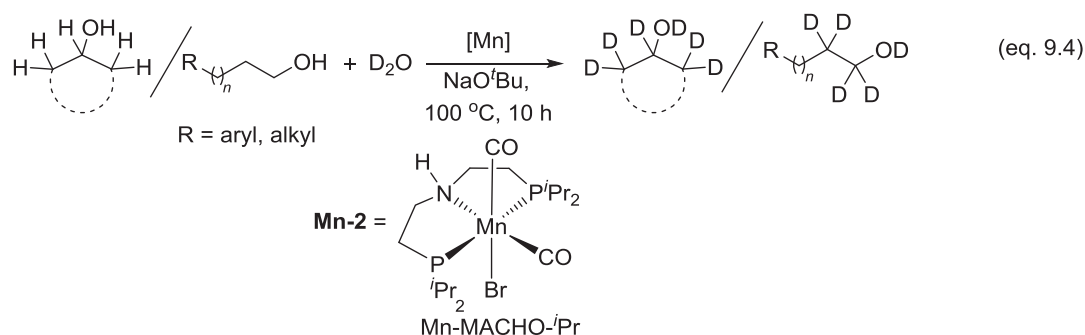
**Scheme 9.3:** Synthesis of substituted cycloalkanes from diols and secondary alcohols or ketones using **Mn-2** complex.

Numerous substituted cyclohexanes were synthesized using the substituted secondary alcohols and substituted diols. The substituted cyclohexanes at the *para*- position revealed good selectivity to the *trans*-product. Next, we focused on the preparation of substituted cyclopentanes and cycloheptanes. Using the optimized reaction conditions, the reaction of 1-phenyl ethanol with 1,4-butanediol and 1,5-hexanediol revealed a mixture of products. However, when the secondary alcohols were substituted with sterically hindered ketones such as 1-(2,3,4,5,6-pentamethylphenyl)ethanone and 1-mesitylethan-1-one, selective formation of substituted cycloheptanes and cyclopentanes was obtained by using substituted 1,6-hexanediol and 1,4-butanediol, respectively. Using the bulky ketones, various substituted cyclopentanes and cycloheptanes were prepared. To confirm that the reaction is proceeding via hydrogen borrowing pathways, labeling experiments and *in situ* reactions were performed. The catalytic cycle was proposed based on the performed experiments and previous studies.

### Manganese catalyzed selective $\alpha$ - and $\alpha, \beta$ -deuteration of primary alcohols using $D_2O$ (Chapter 5)

Deuterium labeled compounds has a wide range of applications in pharmaceuticals, used in the study of biological compounds and plays an important role in the analysis of metabolism and enzymes.<sup>[13]</sup> Previous chapters showed that high reactivity of complex **Mn-2** towards the dehydrogenation of alcohols. Based on this analysis, we speculated whether the deuteration of alcohols can also be performed using **Mn-2** and  $D_2O$  as a deuterium source, as the reaction proceeds via de-hydrogenation of alcohols which subsequently deuterated by deuterium generated from  $D_2O$ . 4-methyl benzyl alcohol was chosen as a benchmark substrate. The reaction showed good reactivity while the reaction of 4-methyl benzyl alcohol with  $D_2O$  in the presence

of complex **Mn-2** and the catalytic amount of base was performed. Using the optimized reaction conditions, various aryl methanols, 2-phenylethanols and aliphatic alcohols were deuterated. Aryl methanols showed selective deuteration at  $\alpha$ - position and 2-aryl ethanol and aliphatic alcohols resulted in deuteration at  $\alpha$ - and  $\beta$ - positions both (eq. 9.4).



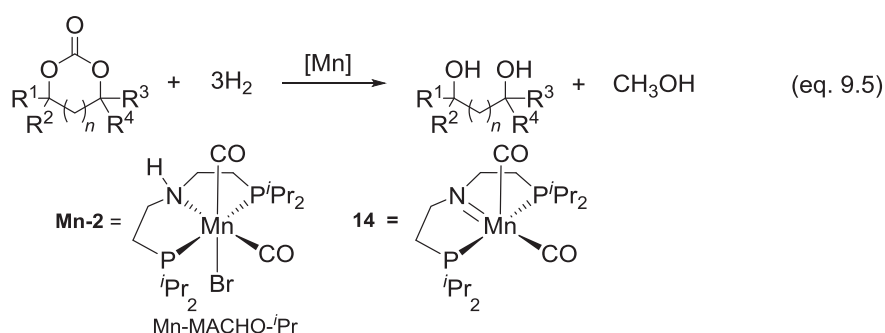
**Scheme 9.4:** Selective deuteration of alcohols by D<sub>2</sub>O using complex **Mn-2**.

A detailed mechanistic investigation was carried out to propose the catalytic cycle. To analyze the reaction insight, several stoichiometric reactions of complex **Mn-2** with alcohols and water in the presence of a base were performed. Gibbs free activation energy was calculated by performing the kinetic experiments. Eyring equation was used to calculate the Gibbs free activation energy. From the Eyring plot, the Gibbs free activation was calculated with a value of  $\Delta G^\ddagger = 20.9 \pm 0.5$  kcal/mol. Based on the mechanistic studies, DFT calculations were also performed to propose the catalytic cycle. The Gibbs free activation energy calculated by DFT calculation was shown to be  $\Delta G^\ddagger = 20.1$  kcal/mol which showed close correlation with the experiment calculated value.

## Catalytic Hydrogenation of Cyclic Carbonates using Manganese Complexes (Chapter 6)

Among all the families of carbonyl functionalities, carbonic acid derivatives are the most challenging substrates to hydrogenate.<sup>[14]</sup> Organic carbonates are one of the classes of carbonic acid derivatives and can be generated by the reaction of CO or CO<sub>2</sub> with alcohols or cyclic ethers. Direct hydrogenation of these molecules leads to the synthesis of methanol and the corresponding diols and alcohols. Methanol itself is an important industrial molecule and used as a fuel, as a C1 source for organic transformations and as a precursor for the synthesis of higher hydrocarbons.<sup>[15]</sup> In this chapter, we investigated the hydrogenation of cyclic carbonates using

manganese pincer complexes as catalyst precursor and hydrogen as a reducing agent. Several manganese pincer complexes were prepared and investigated for the hydrogenation of ethylene carbonate where Mn-MACHO-*i*Pr **Mn-2** complex showed to be the best catalytic activity for the hydrogenation of ethylene carbonate to methanol and the corresponding diol. Interestingly, it was found that when complex **Mn-2** was preactivated with a base and used for the catalysis, the hydrogenation reactivity increased and revealed the maximum TONs of 400 to methanol and 620 TON to diol. Based on the optimization conditions, various five and six membered cyclic carbonates were hydrogenated using the complex **Mn-2** and a catalytic amount of a base (eq. 9.5).



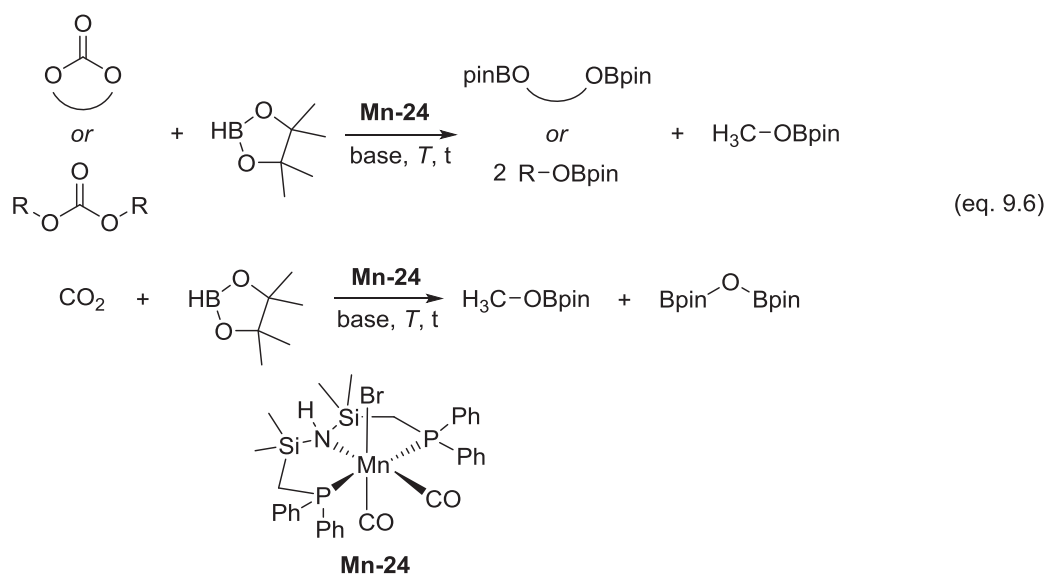
**Scheme 9.5:** Hydrogenation of cyclic carbonates using complex **Mn-2**.

To get insight the possible catalytic cycle, a series of controls experiments were performed. The reaction of complex **Mn-2** with a base showed a formation of activated species **14** which on reaction with hydrogen showed the formation of Mn-hydride complex. The stoichiometric reaction of *in situ* generated Mn-hydride complex with the ethylene carbonate resulted in several crucial intermediates such as the formation of manganese unsaturated complex **14**, methoxy coordinated manganese complex, formate ester of ethylene carbonate and free formaldehyde. Based on the observed intermediates and previous studies, a catalytic cycle was proposed.

### Manganese(I) catalyzed selective hydroboration of organic carbonates and CO<sub>2</sub> (Chapter 7)

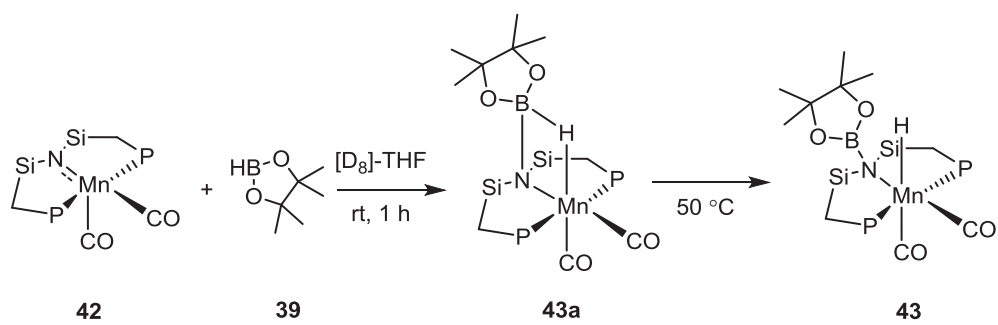
In this chapter, the catalytic reduction of CO<sub>2</sub> and organic carbonates was performed using pinacolborane as a reducing reagent and manganese(I) as a catalyst precursor. Considering the previous chapter studies, alike the activation of hydrogen, the activation of boron hydrogen bond was investigated. Pinacolborane was chosen as a reducing agent. A new silane based manganese PNP pincer complex was synthesized and investigated for this particular transformation. At first,

organic carbonates were chosen for the catalytic reduction. Ethylene carbonate was selected as a benchmark substrate for the optimization. Using the pre-catalyst **Mn-24** and catalytic amount of base, manganese complex showed good reactivity towards the hydroboration of ethylene carbonates. Based on the optimized conditions, several cyclic and non-cyclic organic carbonates were selectively reduced with high yield to the corresponding methyl boronate ester and diol or alcohol boronate ester (eq. 9.6). Encouraged by these results, selective hydroboration of CO<sub>2</sub> to methoxy boronate ester was also investigated. Interestingly, the catalyst revealed high reactivity for the hydroboration of CO<sub>2</sub> to methoxy boronate ester. The best optimized conditions for the hydroboration of CO<sub>2</sub> confirmed the TON of 883 to the corresponding methoxy boronate ester (eq. 9.6).



**Scheme 9.6:** Hydroboration of organic carbonates and CO<sub>2</sub> by pinacoleborane using complex **Mn-24**.

Next the mechanistic investigations were carried out. Alike the activation of Mn-MACHO-<sup>*i*</sup>Pr complex **Mn-2**, this complex also revealed the formation of unsaturated Mn active species **42** on reaction with a base. The stoichiometric reaction of active species **42** with pinacolborane showed the formation of a new intermediate species **43a**. The crystal structure of species **43a** contained a four-membered Mn–H–B–N ring as an intermediate in the reaction. The species **43a** on heating revealed the formation Mn–hydride species. Based on the experimental results and previous studies, a catalytic cycle was proposed for the hydroboration of CO<sub>2</sub>.



**Scheme 9.7:** Generation and molecular structure of potential intermediate Mn complexes.

## 9. Sommaire

### Motivation et structure de la thèse (Chapitre 1)

#### Les complexes en pince et leur réactivité dans les réactions de transferts d'hydrogène

Les réactions de transferts d'hydrogène ont été d'un grand intérêt dans les précédentes années et des avancées considérables ont été récemment apportées. Dans cet esprit, la liaison inerte  $sp_3$  C-H peut être activée et fonctionnalisée en liaisons plus intéressantes comme C-C, C-N, C-O and C-S. <sup>[1]</sup>

Dans ce chapitre, on s'est concentré sur les récents développements apportés par des complexes de manganèse(I) en pince et leur réactivité similaire avec des complexes de ruthénium(II) pour des réactions de transferts d'hydrogène.

Précédemment, plusieurs travaux ont été reportés pour ces réactions de transferts d'hydrogène en utilisant des complexes en pince. Le ligand en pince possède un site tridenté qui en se coordonnant au métal offre un complexe moléculaire stable. <sup>[2]</sup>

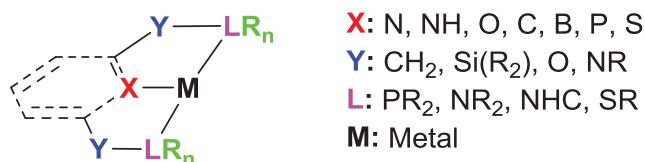


**Figure 9.1:** Structure commune pour les complexes en pince.

Récemment, ces réactions de transferts d'hydrogène ont été reportées utilisant des complexes en pince à base de métaux nobles comme du ruthénium, de l'iridium, ou du palladium. <sup>[1, 3]</sup> En général, ces complexes sont activés par une base qui, avec un environnement riche en hydrogène, génère le complexe métal-hydrure utilisé pour la réaction de transfert d'hydrogène. Dernièrement, des complexes à base de métaux 3d abondants comme le fer, manganèse, cobalt et nickel ont aussi été utilisés pour ces transformations. <sup>[4]</sup> Un complexe Mn(I) a révélé une réactivité similaire établie pour le complexe Ru(II) grâce à sa position diagonale dans le tableau périodique et sa même configuration électronique en comparaison avec le complexe Ru(II). <sup>[5]</sup>

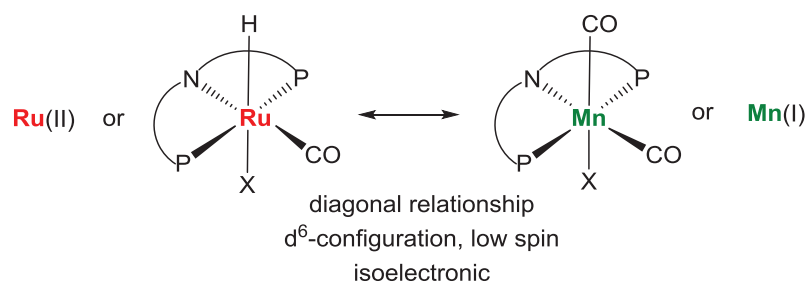


**Figure 9.2:** Propriété similaire entre les complexes Ru(II) and Mn(I).

Les complexes Ru(II) sont depuis bien connus pour les réactions d'alkylation et d'hydrogénations via transferts d'hydrogènes.<sup>[6] [3b]</sup> De même, différents complexes Mn(I) ont été investigués et ont montrés des réactivités intéressantes pour des réactions d'alkylation en utilisant des alcools primaires comme agent alkylant.<sup>[5b, 5c]</sup> Diverse réactions d'alkylation comme l'alkylation de cétones, d'alcools, de nitriles, d'esters et d'amides ont été reportées en utilisant le complexe en pince Mn(I). Similairement, des hydrogénations de fonctions carbonyle ont été conduites grâce au complexe Mn(I). Cependant, le complexe Mn(I) a montré une réactivité plus faible que le complexe Ru(II) pour les réactions d'hydrogénations.

En conclusion, les complexes en pince Mn(I) ont montré une bonne réactivité pour des réactions de transferts d'hydrogènes comme les complexes Ru(II). Différentes réactions d'alkylation, utilisant des alcools comme agent alkylant, et d'hydrogénation de fonctions carbonyle ont été reportées avec un complexe en pince Mn(I). Cependant, l'utilisation de complexes nécessite l'incorporation de ligands phosphorés très couteux. C'est pourquoi un ligand plus facile à synthétiser et non-phosphoré doit être investigué pour des applications futures.

### Structure de la thèse

Cette dissertation se focalise sur des réactions de transferts d'hydrogènes en utilisant des complexes en pince Mn(I) et Ru(II) et est divisée en deux parties. Dans la première, on reporte des réactions de transferts d'hydrogènes catalysées par des complexes Ru(II) et Mn(I). Grâce à ces complexes, la  $\beta$ -méthylation sélective d'alcools a été étudiée. Similairement la deutération sélective d'alcools utilisant D<sub>2</sub>O comme source de deutérium et la synthèse de cycloalcanes substitués à partir de diols et d'alcools ou cétones ont été étudiées en utilisant des complexes en pince Mn(I) et via transferts d'hydrogène ou « Hydrogen borrowing methods ».



Dans la deuxième partie, la réduction de carbonates organiques et de CO<sub>2</sub> a été exploré en utilisant de l'hydrogène ou du pinacolborane comme agents réducteurs et des complexes en pince Mn(I) comme pré-catalyseurs.

### ***β*-méthylation d'alcools catalysée par du Ruthénium utilisant MeOH comme C1 source (Chapitre 2)**

Le groupement méthyle est l'une des fonctions fondamentales et des plus répandues dans toutes sortes de produits chimiques, biologiques et pharmaceutiques.<sup>[7]</sup> L'insertion sélective d'un groupement méthyle dans une chaîne alkyle pour former une nouvelle liaison C–C est une transformation importante.<sup>[7-8]</sup> En général, la méthylation est conduite grâce à des réactifs toxiques et hautement inflammables comme des réactifs de Grignard ou de méthylation ((e.g. méthyle iodure, méthyle sulfate ou diazométhane).<sup>[9]</sup> Pour pallier à ce problème, l'utilisation du méthanol comme agent de méthylation est une option, étant moins toxique et pouvant être synthétisé à partir de la biomasse, de CO<sub>2</sub> et d'H<sub>2</sub>. En se servant de la méthode de transferts d'hydrogène, le méthanol peut être utilisé comme agent alkylant.

Dans ce chapitre, la *β*-méthylation sélective d'alcools a été investiguée en variant les précurseurs catalytiques à base de ruthénium et avec du méthanol comme agent alkylant. Les complexes de ruthénium ont été choisis pour cette transformation pour leur réactivité bien connue envers les réactions de transfert d'hydrogène. Pour l'optimisation, 1-phényl éthanol a été choisi comme substrat de référence. Des complexes en pince monodentés, bidentés et tridentés ont été testés pour cette transformation. Le complexe Ru-MACHO-BH a montré la meilleure réactivité concernant la *β*-méthylation sélective du 1-phényl éthanol. Avec les conditions de réactions optimisées, différents alcools secondaires, 2-aryl éthanol et des alcools aliphatiques ont été choisis et méthylés sélectivement en *β* (eq. 9.1). La *β*-méthylation sélective de différents alcools a été conduit avec succès avec rendements dans une plage de 54-94%.

Différentes autres investigations ont été menées pour comprendre le mécanisme de la réaction. Pour vérifier que la réaction procède bien par transfert d'hydrogène, plusieurs marquages et études d'intermédiaires ont été étudiés. L'activation du complexe et la réactivité des alcools ont aussi été testés par réactions stœchiométriques entre complexe et alcools.

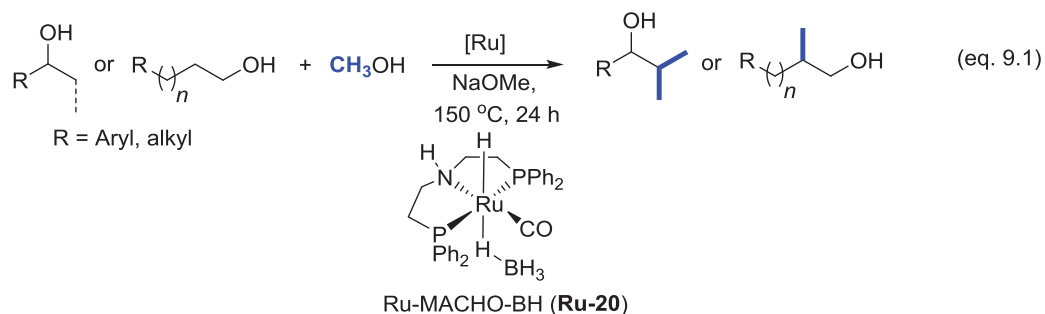


**Schéma 9.1:**  $\beta$ -méthylation d'alcools en utilisant le complexe **Ru-20**.

Grâce à des études mécanistiques, des calculs DFT détaillés ont été faits et un cycle catalytique a été proposé en accord avec ceux-ci. Le cycle catalytique suit une méthode de transferts d'hydrogène où la coopération métal-ligand joue un rôle important pour l'activation des alcools et où une base est utilisée pour la formation de la liaison C–C. Le cycle catalytique proposé montre une énergie libre d'activation de Gibbs de 29.2 kcal/mol, très proche de celle expérimentale de 26.2  $\pm$  0.5 kcal/mol.

### **$\beta$ -méthylation d'alcools catalysée sélectivement par un complexe Manganèse(I) utilisant MeOH comme C1 source (Chapitre 3)**

Dans le chapitre 2, il a été montré que les énergies pour les sous-cycles du cycle catalytique global sont soit basses soit modérément hautes, on a postulé qu'en utilisant la même base, la réaction peut aussi être conduite avec des complexes à base de métaux abondants et non nobles. Le manganèse a été choisi comme métal-précurseur pour son abondance sur terre et pour sa position en diagonale comparé au ruthénium dans le tableau périodique des éléments. Plusieurs complexes de manganèse ont été synthétisés et employés pour la  $\beta$ -méthylation sélective du 2-phényléthanol où le complexe Mn-MACHO-<sup>i</sup>Pr a montré la meilleure activité catalytique. Puis, l'optimisation a été conduite en utilisant Mn-MACHO-<sup>i</sup>Pr comme pré-catalyseur et NaOMe comme base. Avec les conditions de réactions optimisées, une variété de 2-aryl éthanols, d'alcools secondaires et alcools aliphatiques ont été sélectivement  $\beta$ -méthylé (eq 9.2).

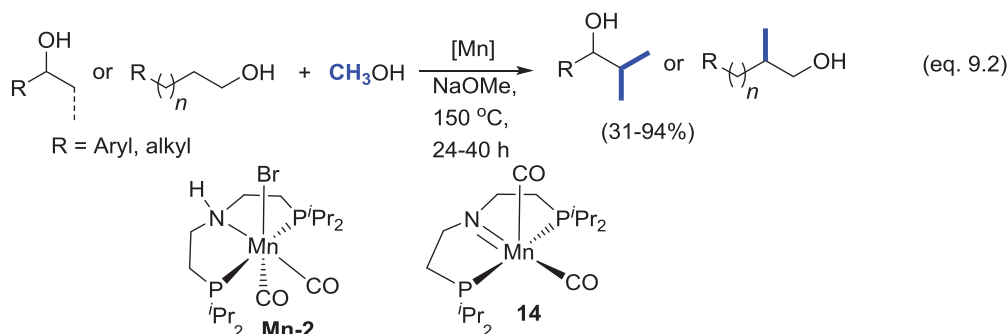


**Schéma 9.2:**  $\beta$ -méthylation d'alcools en utilisant le complexe **Mn-2**.

Ensuite, pour compléter le cycle catalytique, des marquages ont été réalisés. Ceux-ci ont confirmé que la réaction procède via transferts d'hydrogène et que le méthanol est la source de carbone C1. Des réactions stœchiométriques utilisant le complexe **Mn-2** et une base ont montré la formation de l'espèce active **14** qui en réagissant avec l'alcool génère les espèces Mn-alkoxy et Mn-hydrure. Un cycle catalytique a été proposé en partant des études mécanistiques menées et des travaux antérieurs, et a révélé la coopération métal-ligand dans le complexe de manganèse et les transferts d'hydrogène pour produire le produit final méthylé.

### Synthèse de cycloalcanes à partir de diols et d'alcools secondaires ou cétones en utilisant un catalyseur homogène à base de manganèse (Chapitre 4)

Les cycloalcanes substitués comme les cyclopentanes, cyclohexanes et cycloheptanes sont des motifs structuraux omniprésents, présents dans de nombreux produits pharmaceutiques et naturels.<sup>[11]</sup> Aujourd'hui, ces molécules sont synthétisées par des procédures comportant plusieurs étapes et qui nécessitent de dures conditions de réactions pour certaines étapes de réaction.<sup>[11d, 12]</sup> En général, ces procédés montrent un domaine de substrats possibles restreints, une faible régio- et stéréo-sélectivité et génère aussi une quantité stœchiométrique de déchets. La synthèse directe et en une seule étape de ces molécules est donc l'un des défis en catalyse. Grâce aux travaux précédents sur la  $\beta$ -méthylation sélective des alcools, il a été présumé qu'employer le ligand type MACHO pour la synthèse de cycloalcanes substitués serait possible, en utilisant des diols comme un agent doublement alkylant. Pour ce procédé, les deux complexes Ru-MACHO-BH **Ru-20** et Mn-MACHO-<sup>i</sup>Pr **Mn-2** ont été testés en utilisant le 1-phényléthanol comme substrat de référence et KO<sup>t</sup>Bu comme base. La réaction catalytique a montré de meilleurs résultats avec le complexe **Mn-2** en comparaison avec le complexe **Ru-20**.

En s'appuyant sur ces résultats, les études d'optimisation ont été accomplies avec le complexe **Mn-2** (eq 9.3).

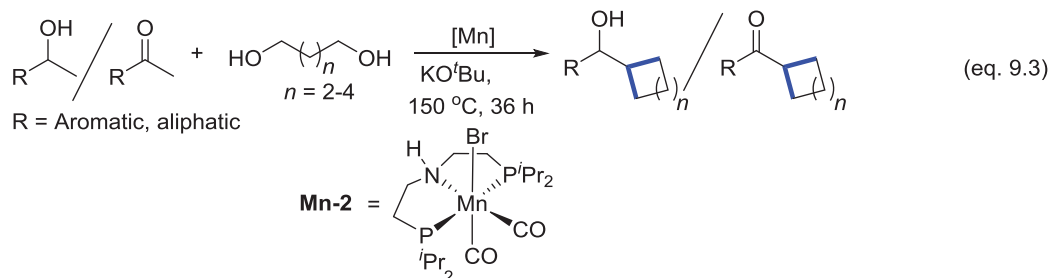


**Schéma 9.3:** Synthèse de cycloalcanes substitués à partir de diols et alcools secondaires ou cétones en utilisant le complexe **Mn-2**.

De nombreux cycloalcanes substitués ont été synthétisés en utilisant des alcools secondaires et diols substitués. Les cyclohexanes substitués en position para- ont révélé une bonne sélectivité pour le produit trans-. De plus, la préparation de cyclopentanes et cyclopentanes substitués ont aussi été un succès. En utilisant les conditions de réactions optimisées, la réaction entre le 1-phényl éthanol avec 1,4-butanediol et 1,5-hexanediol ont révélé un mélange de produits. Mais, quand les alcools secondaires utilisés sont remplacés par des cétones très encombrées stériquement comme la 1-(2,3,4,5,6-pentaméthylphényl)éthanone et la 1-mésityléthan-1-one, la formation sélective de cycloheptanes et cyclopentanes substitués a été obtenue en utilisant le 1,6-hexanediol et le 1,4-butnaediol, respectivement. Grâce au cétones encombrées, de nombreux cyclopentanes et cycloheptanes ont été synthétisés. Pour confirmer que ces réactions procèdent via transferts d'hydrogène, des expériences avec marquage ont été faites, ainsi que des expériences avec générations in-situ d'intermédiaires de réaction. Le cycle catalytique a été proposé en s'appuyant sur ces expériences et sur les études précédentes.

### L' $\alpha$ - et $\alpha$ , $\beta$ -deutération sélective catalysée par manganèse d'alcools primaires en utilisant D<sub>2</sub>O (Chapitre 5)

Les composés marqués au deutérium ont de vastes applications en pharmaceutique, utilisés pour l'étude de composés biologiques et jouent un rôle important dans l'analyse de métabolismes et d'enzymes. <sup>[13a-g, 16]</sup> Les chapitres précédents ont montré la grande réactivité du complexe **Mn-2** envers la déshydratation d'alcools. Il a donc été spéculé, que la deutération d'alcools peut aussi

être réalisée avec **Mn-2** et D<sub>2</sub>O comme source de deutérium, puisque la réaction opère par déshydrogénation d'alcools puis deutération par D<sub>2</sub>O. Le 4-méthyl benzyl alcool a été choisi comme substrat de référence. La réaction a montré une bonne réactivité quand le 4-méthyl benzyl alcool avec du D<sub>2</sub>O en présence du complexe **Mn-2** et une quantité catalytique de base ont réagi. En utilisant les conditions de réaction optimisées, différents méthanol-aryles, 2-aryléthanol et alcools aliphatiques ont été deutérés. Les méthanol-aryles ont montré une deutération sélective en position  $\alpha$  et les 2-phényl éthanol et alcools aliphatiques en position  $\alpha$  et  $\beta$  (eq. 9.4).

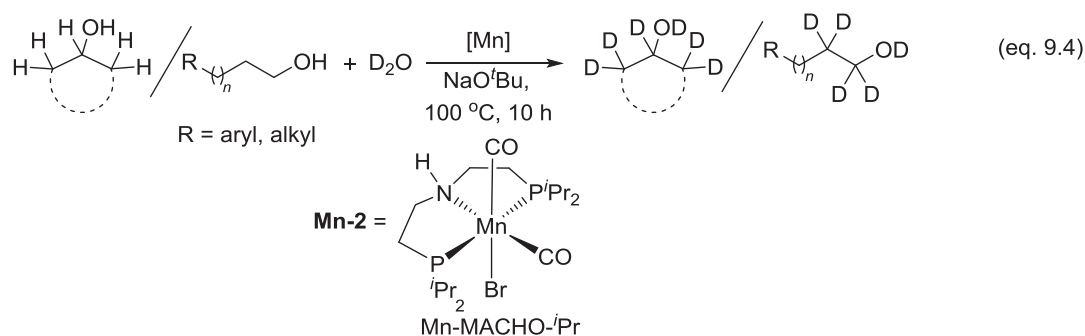


**Schéma 9.4:** Deuteration sélective d'alcools par D<sub>2</sub>O avec le complexe **Mn-2**.

Une investigation détaillée du mécanisme a été effectuée pour proposer un cycle catalytique. Pour analyser le mécanisme, différentes réactions stœchiométriques entre le complexe **Mn-2** avec de l'eau en présence d'une base ont été effectuées. Les énergies libres de réactions ont été calculées en effectuant des expériences cinétiques. L'équation Eyring a été utilisée pour calculer une énergie libre de réaction de  $\Delta G^\ddagger = 20.9 \pm 0.5$  kcal/mol. En se servant des études mécanistiques, des calculs DFT ont aussi été effectués pour proposer un cycle catalytique. L'énergie libre de réaction calculé par DFT de  $\Delta G^\ddagger = 20.1$  kcal/mol montre un très faible écart avec la valeur expérimentale.

### L'hydrogénation Catalytique de Carbonates Cycliques en utilisant des Complexes à base de Manganèse (Chapitre 6)

Dans la famille des fonctions carbonyles, les dérivés acides carboniques sont les substrats les plus difficiles à hydrogéner.<sup>[14]</sup> Les carbonates organiques sont des dérivés d'acides carboniques et peuvent être générés par réaction de CO ou CO<sub>2</sub> avec des alcools ou des éthers cycliques. L'hydrogénation directe de ces molécules s'accompagne de la synthèse de méthanol et des diols

et alcools correspondants. Le méthanol est une molécule industrielle importante, utilisée comme carburant, comme source de carbone C1 pour des transformations organiques et comme précurseur pour la synthèse d'hydrocarbures supérieurs.<sup>[15a-n, 15r, 17]</sup> Dans ce chapitre, l'hydrogénation de carbonates cycliques a été testé, en utilisant les complexes en pince à base de manganèse comme catalyseur et de l'hydrogène comme agent réducteur. Différents complexes en pince de manganèse ont été préparés et testés pour l'hydrogénation de carbonates d'éthylène, où le complexe Mn-MACHO-*i*-Pr **Mn-2** a montré la meilleure activité catalytique. Fait intéressant, lorsque le complexe **Mn-2** a été pré-activé avec une base et utilisé en catalyse, la réactivité concernant l'hydrogénation a augmenté et montré un TON de 400 pour le méthanol et 620 pour le diol. Avec les conditions de réactions optimisées, différents carbonates cycliques à cinq et six chaînons ont été hydrogénés avec le complexe **Mn-2** et une quantité catalytique de base (eq. 9.5).

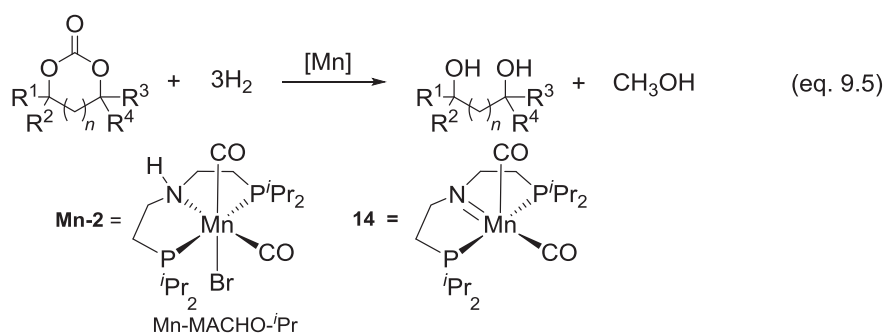


**Schéma 9.5:** Hydrogénation de carbonates cycliques avec le complexe **Mn-2**.

Pour comprendre davantage le cycle catalytique, une série d'expériences de contrôle a été effectuée. La réaction entre le complexe **Mn-2** avec une base a montré la formation de l'espèce activée **14** qui, par réaction avec de l'hydrogène a montré la formation du complexe Mn-hydrure. La réaction de ce complexe généré *in-situ* avec le carbonate d'éthylène a montré la formation d'intermédiaires cruciaux comme le complexe insaturé **14**, le complexe où le manganèse est coordonné à un groupe méthoxy, l'ester formate et le formaldéhyde libéré. Grâce à ces intermédiaires observés et aux études précédentes, un cycle catalytique a pu être proposé.

## Manganese(I) catalyzed selective hydroboration of organic carbonates and CO<sub>2</sub> (Chapter 7)

Dans ce chapitre, la réduction catalytique du CO<sub>2</sub> and des carbonates organiques a été effectuée en utilisant du pinacolborane comme agent réducteur et un complexe manganèse(I) comme précurseur catalytique. A l'aide des études des chapitres précédents, et comme pour l'activation de l'hydrogène, l'activation de la liaison hydrogène-bore a été étudiée. Un nouveau complexe en pince PNP à base de manganèse et de silane a été synthétisé et investigué pour cette transformation particulière. Pour commencer, les carbonates organiques ont été choisis pour la réduction catalytique. Le carbonate d'éthylène a été sélectionné comme substrat de référence pour l'optimisation. En utilisant le pré-catalyseur **Mn-24**, une quantité catalytique de base, le complexe de manganèse a montré une bonne réactivité envers l'hydroboration de carbonates d'éthylène. En se servant des conditions de réaction optimisées, différents carbonates organiques cycliques et non-cycliques ont été réduits sélectivement avec de très bons rendements, en méthyl boronate ester et diol ou alcool boronate ester (eq. 9.6). Encouragés par ces résultats, l'hydrogénation sélective de CO<sub>2</sub> en méthoxyboronate ester a aussi été testée. Le catalyseur a révélé dans ce cas de hautes réactivités. Avec les meilleures conditions de réaction pour l'hydroboration de CO<sub>2</sub>, un TON de 883 a été atteint. (eq. 9.6).

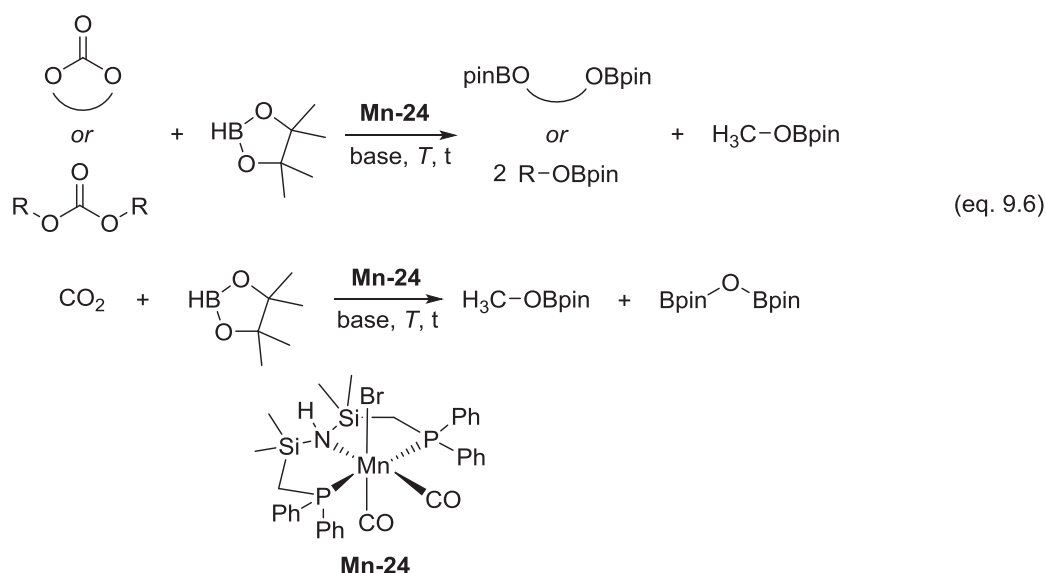


**Schéma 9.6:** Hydroboration de carbonates organiques et de CO<sub>2</sub> par le pinacolborane avec le complexe **Mn-2**.

Ensuite, les études mécanistiques ont été menées. Comme pour l'activation du complexe Mn-MACHO-iPr **Mn-2**, ce complexe a aussi révélé la formation de l'espèce active instaurée **Mn 42** par réaction avec une base. La réaction stœchiométrique entre l'espèce active **42** avec le pinacolborane a montré la formation d'une nouvelle espèce intermédiaire **43a**. La structure cristalline de l'espèce **43a** contient une structure cyclique avec quatre membres Mn-H-B-N comme intermédiaire de réaction. L'espèce **43a**, après chauffage, a révélé la formation de l'espèce Mn-hydrure. En se servant des résultats expérimentaux et des études précédentes, un cycle catalytique a été proposé pour l'hydroboration du CO<sub>2</sub>.

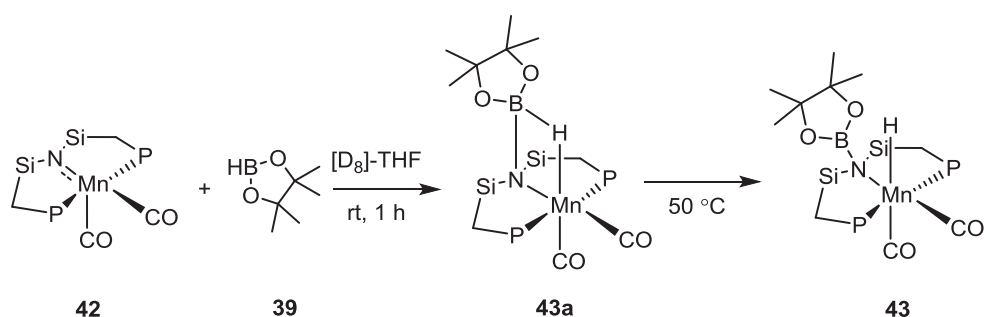


**Schéma 9.7:** Génération et structure moléculaire des complexes intermédiaires potentiels Mn.



## References

- [1] A. Corma, J. Navas, M. J. Sabater, *Chem. Rev.* **2018**, *118*, 1410-1459.
- [2] E. Peris, R. H. Crabtree, *Chem. Soc. Rev.* **2018**, *47*, 1959-1968.
- [3] a) M. H. S. A. Hamid, P. A. Slatford, J. M. J. Williams, *Adv. Synth. Catal.* **2007**, *349*, 1555-1575; b) C. Gunanathan, D. Milstein, *Chem. Rev.* **2014**, *114*, 12024-12087; c) T. Suzuki, *Chem. Rev.* **2011**, *111*, 1825-1845; d) H. Guo, K. Ding, L. Dai, *Chin. Sci. Bull.* **2004**, *49*, 2003-2016; e) P. Etayo, A. Vidal-Ferran, *Chem. Soc. Rev.* **2013**, *42*, 728-754; f) Q.-A. Chen, Z.-S. Ye, Y. Duan, Y.-G. Zhou, *Chem. Soc. Rev.* **2013**, *42*, 497-511; g) O. Saidi, J. M. J. Williams, in *Iridium Catalysis* (Ed.: P. G. Andersson), Springer Berlin Heidelberg, Berlin, Heidelberg, **2011**, pp. 77-106; h) B. Anxionnat, D. Gomez Pardo, G. Ricci, K. Rossen, J. Cossy, *Org. Lett.* **2013**, *15*, 3876-3879; i) J. Muzart, *Eur. J. Org. Chem.* **2015**, *2015*, 5693-5707; j) R. Sariego, I. Carkovic, M. Martínez, M. Valderrama, *J. Mol. Catal.* **1986**, *35*, 161-167; k) N. Westhues, J. Klankermayer, *ChemCatChem* **2019**, *11*, 3371-3375; l) I. Bauer, H.-J. Knölker, *Chem. Rev.* **2015**, *115*, 3170-3387.
- [4] a) E. Balaraman, A. Nandakumar, G. Jaiswal, M. K. Sahoo, *Catal. Sci. Technol.* **2017**, *7*, 3177-3195; b) R. A. Farrar-Tobar, B. Wozniak, A. Savini, S. Hinze, S. Tin, J. G. de Vries, *Angew. Chem. Int. Ed.* **2019**, *58*, 1129-1133; c) G. Wienhöfer, I. Sorribes, A. Boddien, F. Westerhaus, K. Junge, H. Junge, R. Llusar, M. Beller, *J. Am. Chem. Soc.* **2011**, *133*, 12875-12879; d) W. Ai, R. Zhong, X. Liu, Q. Liu, *Chem. Rev.* **2019**, *119*, 2876-2953; e) D. Wang, D. Astruc, *Chem. Rev.* **2015**, *115*, 6621-6686.
- [5] a) N. Gorgas, K. Kirchner, *Acc. Chem. Res.* **2018**, *51*, 1558-1569; b) M. Garbe, K. Junge, M. Beller, *Eur. J. Org. Chem.* **2017**, *2017*, 4344-4362; c) G. A. Filonenko, R. van Putten, E. J. M. Hensen, E. A. Pidko, *Chem. Soc. Rev.* **2018**, *47*, 1459-1483.
- [6] G. Chelucci, *Coord. Chem. Rev.* **2017**, *331*, 1-36.
- [7] E. J. Barreiro, A. E. Kummerle, C. A. Fraga, *Chem. Rev.* **2011**, *111*, 5215-5246.
- [8] a) R. L. Wingad, E. J. E. Bergström, M. Everett, K. J. Pellow, D. F. Wass, *Chem. Commun.* **2016**, *52*, 5202-5204; b) Q. Liu, G. Xu, X. Wang, X. Mu, *Green Chem.* **2016**, *18*, 2811-2818; c) K. Natte, H. Neumann, M. Beller, R. V. Jagadeesh, *Angew. Chem. Int. Ed. Engl.* **2017**, *56*, 6384-6394.
- [9] a) K. Maruoka, A. B. Concepcion, H. Yamamoto, *Synthesis* **1994**, 1283-1290; b) Y. Yokoyama, K. Mochida, *J. Organomet. Chem.* **1995**, *499*; c) J.-S. Chang, Y.-D. Lee, L. C.-S. Chou, T.-R. Ling, T.-C. Chou, *Ind. Eng. Chem. Res.* **2012**, *51*, 655-661.
- [10] a) J. V. Price, L. Chen, W. B. Whitaker, E. Papoutsakis, W. Chen, *Proc. Natl. Acad. Sci.* **2016**; b) S. Wesselbaum, T. Vom Stein, J. Klankermayer, W. Leitner, *Angew. Chem. Int. Ed. Engl.* **2012**, *51*, 7499-7502; c) J. A. Rodriguez, P. Liu, D. J. Stacchiola, S. D. Senanayake, M. G. White, J. G. Chen, *ACS Catal.* **2015**, *5*, 6696-6706.
- [11] a) G. Xia, X. Han, X. Lu, *Org. Lett.* **2014**, *16*, 2058-2061; b) A. Banerjee, S. Sarkar, B. K. Patel, *Org. Biomol. Chem.* **2017**, *15*, 505-530; c) L. Bravo, J. A. Mico, E. Berrocoso, *Expert Opin. Drug Dis* **2017**, *12*, 1281-1291; d) S. Gouedranche, W. Raimondi, X. Bugaut, T. Constantieux, D. Bonne, J. Rodriguez, *Synthesis* **2013**, *45*, 1909-1930; e) M. F. Ansell, *Supplements to the 2nd Edition of Rodd's Chemistry of Carbon Compounds. A Modern Comprehensive Treatise* **2008**, *2*; f) R. A. Holton, C. Somoza, H. B. Kim, F. Liang, R. J. Biediger, P. D. Boatman, M. Shindo, C. C. Smith, S. Kim, *J. Am. Chem. Soc.* **1994**, *116*,

- 1597-1598; g) J. A. Dabrowski, D. C. Moebius, A. J. Wommack, A. F. Kornahrens, J. S. Kingsbury, *Org. Lett.* **2010**, *12*, 3598-3601.
- [12] a) A. Wurtz, *Justus Liebigs Ann. Chem.* **1855**, *96*, 364-375; b) M. B. Smith, J. March, *Vol. March's Advanced Organic Chemistry: Reactions, Mechanisms, and Structure, Sixth Edition*, **2006**; c) G. M. Lampman, J. C. Aumiller, *Org. Synth.* **1971**, *51*, 55; d) X. Ding, H. Wang, J. Wang, S. Wang, D. Lin, L. Lv, Y. Zhou, X. Luo, H. Jiang, J. L. Aceña, V. A. Soloshonok, H. Liu, *Amino Acids* **2013**, *44*, 791-796; e) S. Danishefsky, T. Kitahara, *J. Am. Chem. Soc.* **1974**, *96*, 7807-7808; f) E. J. Corey, *Angew. Chem. Int. Ed.* **2002**, *41*, 1650-1667; g) M. M. Stalzer, C. P. Nicholas, A. Bhattacharyya, A. Motta, M. Delferro, T. J. Marks, *Angew. Chem. Int. Ed.* **2016**, *55*, 5263-5267; h) B. K. Peters, J. Liu, C. Margarita, W. Rabten, S. Kerdpchon, A. Orebom, T. Morsch, P. G. Andersson, *J. Am. Chem. Soc.* **2016**, *138*, 11930-11935; i) Y. Wang, X. Cui, Y. Deng, F. Shi, *RSC Adv.* **2014**, *4*, 2729-2732; j) M. P. Wiesenfeldt, Z. Nairoukh, T. Dalton, F. Glorius, *Angew. Chem. Int. Ed.* **2019**, *58*, 10460-10476; k) D.-S. Wang, Q.-A. Chen, S.-M. Lu, Y.-G. Zhou, *Chem. Rev.* **2012**, *112*, 2557-2590; l) T. F. Schneider, J. Kaschel, D. B. Werz, *Angew. Chem. Int. Ed.* **2014**, *53*, 5504-5523; m) W. Ma, J. Fang, J. Ren, Z. Wang, *Org. Lett.* **2015**, *17*, 4180-4183.
- [13] a) J. Atzrodt, V. Derdau, T. Fey, J. Zimmermann, *Angew. Chem. Int. Ed.* **2007**, *46*, 7744-7765; b) T. Junk, W. J. Catallo, *Chem. Soc. Rev.* **1997**, *26*, 401-406; c) M. H. G. Pechtl, M. Hölscher, Y. Ben-David, N. Theyssen, D. Milstein, W. Leitner, *Eur. J. Inorg. Chem.* **2008**, *2008*, 3493-3500; d) L. Neubert, D. Michalik, S. Bähn, S. Imm, H. Neumann, J. Atzrodt, V. Derdau, W. Holla, M. Beller, *J. Am. Chem. Soc.* **2012**, *134*, 12239-12244; e) B. Chatterjee, C. Gunanathan, *Org. Lett.* **2015**, *17*, 4794-4797; f) B. Chatterjee, C. Gunanathan, *Chem. Commun.* **2016**, *52*, 4509-4512; g) *Synthesis and Application of Isotopically Labeled Compounds*, Pleiss, U., Voges, R., Eds.; Wiley: New York, 2001; Vol. 2007; h) M. Saljoughian, P. G. Williams, *Curr. Pharm. Des.* **2000**, *6*, 1029-1056.
- [14] M. Ito, T. Ootsuka, R. Watari, A. Shiibashi, A. Himizu, T. Ikariya, *J. Am. Chem. Soc.* **2011**, *133*, 4240-4242.
- [15] a) J. Klankermayer, W. Leitner, *Science* **2015**, *350*, 629-630; b) Q. Liu, L. Wu, R. Jackstell, M. Beller, *Nat. Commun.* **2015**, *6*, 5933; c) C. A. Huff, M. S. Sanford, *J. Am. Chem. Soc.* **2011**, *133*, 18122-18125; d) S. Wesselbaum, V. Moha, M. Meuresch, S. Brosinski, K. M. Thenert, J. Kothe, T. v. Stein, U. Englert, M. Hölscher, J. Klankermayer, W. Leitner, *Chem Sci* **2015**, *6*, 693-704; e) N. M. Rezayee, C. A. Huff, M. S. Sanford, *J. Am. Chem. Soc.* **2015**, *137*, 1028-1031; f) J. Schneidewind, R. Adam, W. Baumann, R. Jackstell, M. Beller, *Angew. Chem. Int. Ed.* **2017**, *56*, 1890-1893; g) M. Matzen, M. Alhajji, Y. Demirel, *Energy* **2015**, *93*, 343-353; h) J. Wilhelm, H. Janßen, J. Mergel, D. Stolten, *J. Power Sources* **2011**, *196*, 5299-5308; i) X. Zhen, Y. Wang, *Renewable and Sustainable Energy Reviews* **2015**, *52*, 477-493; j) J. M. Ogden, M. M. Steinbugler, T. G. Kreutz, *J. Power Sources* **1999**, *79*, 143-168; k) A. Kaithal, M. Schmitz, M. Hölscher, W. Leitner, *ChemCatChem* **2019**, DOI: 10.1002/cctc.201900788; l) K. Natte, H. Neumann, M. Beller, R. V. Jagadeesh, *Angew. Chem. Int. Ed.* **2017**, *56*, 6384-6394; m) J. F. Haw, W. Song, D. M. Marcus, J. B. Nicholas, *Acc. Chem. Res.* **2003**, *36*, 317-326; n) B. Liu, L. France, C. Wu, Z. Jiang, V. L. Kuznetsov, H. A. Al-Megren, M. Al-Kinany, S. A. Aldrees, T. Xiao, P. P. Edwards, *Chem. Sci.* **2015**, *6*, 5152-5163; o) J. Klankermayer, S. Wesselbaum, K. Beydoun, W. Leitner, *Angew. Chem. Int. Ed.* **2016**, *55*, 7296-7343; p) S. Wesselbaum, T. vom Stein, J. Klankermayer, W.

- Leitner, *Angew. Chem. Int. Ed.* **2012**, *51*, 7499-7502; q) K. Räuchle, L. Plass, H.-J. Wernicke, M. Bertau, *Energy Technol.* **2016**, *4*, 193-200; r) A. Kowalewicz, *Proc. Inst. Mech. Eng. D* **1993**, *207*, 43-52.
- [16] M. Saljoughian, P. G. Williams, *Current pharmaceutical design* **2000**, *6*, 1029-1056.
- [17] a) K. Jürgen, W. Sebastian, B. Kassem, L. Walter, *Angew. Chem. Int. Ed.* **2016**, *55*, 7296-7343; b) W. Sebastian, v. S. Thorsten, K. Jürgen, L. Walter, *Angew. Chem. Int. Ed.* **2012**, *51*, 7499-7502; c) R. Konstantin, P. Ludolf, W. Hans-Jürgen, B. Martin, *Energy Technology* **2016**, *4*, 193-200.

## **Acknowledgements**

The following thesis has been performed in a combined project as a part of the SINCHEM program between two research institutes. The home institute is the Institut für Technische und Makromolekulare Chemie (ITMC) of RWTH Aachen University and the host institute is Laboratory of Chemistry, Catalysis, Polymers, and Processes, C2P2 UMR 5265, Université de Lyon. I've spent two and a half years in my home institute and six months in the host institute. This is the reason that I had the best opportunity to work in different labs and different environments.

I would like to express my deepest gratitude to my Ph.D. supervisors, Prof. Dr. Walter Leitner, Dr. Markus Hölscher, Prof. Alessandra Quadrelli, and Dr. Clement Camp for their guidance, caring, patience and supporting me during my whole Ph.D. study. It was a very good experience working under four different supervisors and gaining different ideas and perspectives which helped me to improve my research work and my studies.

First and foremost I would like to thank my home institute supervisor Prof. Dr. Walter Leitner, a person with an amiable and positive nature. It has been an honor for me to be his Ph.D. student. My warm thanks to him for accepting me as his Ph.D. student and guiding and supporting me in my whole Ph.D. studies. I wish that I could be as energetic and enthusiastic as him and one day be in a position to guide people as he can. In a daily life, he is a very busy person; nevertheless, he always assisted me in my whole studies and my research work and gave me a lot of freedom to perform my research work.

I will forever be grateful to Dr. Markus Hölscher who was my advisor in my whole Ph.D. studies. He was always been supportive, friendly and always assisted me in a friendly manner in my whole research work. He always encouraged me and gave his precious time for the good discussions and suggestions for tackling the research problems which helped me throughout in my whole studies. I always enjoyed his guidance either in research or while going out with the whole group or traveling from Aachen to Mülheim via car rides for one and a half hours. We always discussed the German and Indian politics, discussion about sustainability and old best western movies which I enjoyed a lot.

Concerning my stay in Lyon, I was in Lyon only for six months; nevertheless, these six months were very enjoyable, productive and knowledgeable for me. I want to express my deepest thank

to Prof. Alessandra Quadrelli for her all-time positive support and guidance. She was always helpful to me in my whole Ph.D. studies. She always encouraged me and provides her precious time for insightful discussions and valuable advice which assist me and guide me in my whole studies.

I want to thank Dr. Clement Camp who was my teacher, and supervisor in Lyon. He always suggested me how should I proceed and be more productive during my short stay in Lyon. He was always open for discussions and allowed me to talk about my research whenever I feel suitable. He was always friendly and supportive and arranges everything which I require for my research during my small stay. I still remember the bowling game which I played with the whole group in Lyon and I was good but Dr. Camp didn't perform well. So he challenges the whole group to compete with him in bouldering as he was good at bouldering. However, we didn't get further chance to compete with him in bouldering but it was a real fun.

Next, I would like to express my deepest gratitude to my SINCEM program for providing me the fellowship in my whole doctoral studies and arranging all the possible mobility and paperwork throughout my studies.

My deepest thanks go to Prof. Stefania Albonetti for taking care of the whole SINCEM program. I am grateful to her for accepting my application as a Ph.D. student and allowed me to perform my doctoral studies under the SINCEM program. I never forget the moments that we had memorable and friendly discussions while in every SINCEM meeting about research, daily life and your support in my whole Ph.D. study.

I thank Dr. Stefanie Gottuck for helping me in my whole Ph.D. and taking care of my all paperwork, financial and traveling stuff. It will be a really tough for me to handle all paperwork without you. I am very grateful for your all support.

I would like to thank all the jury members: Prof. Carmen Claver, Prof. Carsten Bolm, Prof. David Cole-Hamilton, Dr. Hélène Bourbigou, Prof. Regina Palkovits, Prof. Bruno Andrioletti, and Prof. Dieter Vogt for giving their valuable time in reading my dissertation.

My special thanks to my Master Supervisor Dr. Chidambaram Gunanathan and Dr. Basujit Chatterjee who suggested me that I should go to the lab of Prof. Leitner and continue my Ph.D. in his group. Their support and encouragement made me to focus on the research and allowed me to join Ph.D in Aachen.

## Acknowledgements

---

Thanks a lot to my laboratory colleagues in Aachen, Benjamin Schieweck, Marc Schmitz, Thomas Diehl, Karolin Schenk, and Max Kliemann, for the good discussions and all the fun which we had in last three years.

My special thanks to my laboratory colleagues in Lyon, Pooja Gaval, Marc, Valeria, Clement, Martin, Pauline, Ravi and Sebastian for making my stay in Lyon very joyful and helping me in my research as well as in my daily life. I especially thank to Pooja for preparing the best Indian food and inviting me all the time.

I also thank my researchers Pit von Bonn, Lisa-Lou Gracia, and Christian Martin Condras. Working with you all was always fun and special to me. I wish them all the best for their future.

I would like to emphasize some more and repetitive names which I discussed earlier that I would like to thank them. My special thanks to Benjamin Schieweck, Thomas Diehl, Niklas F. Westhues, Anne-Christine, Gregor Voit, Stefan Westhues, Marc Schmitz, Celine Jung, David A. Kuß, Christian Westhues, Hannah Schumacher, Dennis Weidner, Philipp Jüring-Will, Jan Wiesenthal, Jasmine Idel, Meria Ronge, and Martin Schwarzer for the beautiful moments, Friday's night out and memorable drinking stories. I think that I'll never forget those beautiful moments which I've spent with all of you.

I thank Niklas and Benni for beautiful holidays and trips to India and USA which was memorable and funny at the same time. My special thanks go to Gregor Voit for giving me a swimming lesson and making me a good swimmer. I thank Anne-Christine and Thomas Diehl for a great time, discussions, stories and inviting me for tasty Indian dinners.

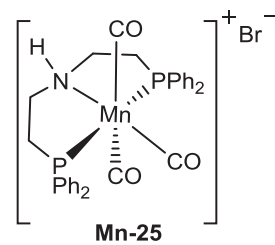
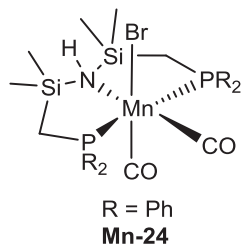
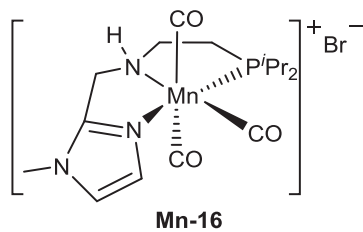
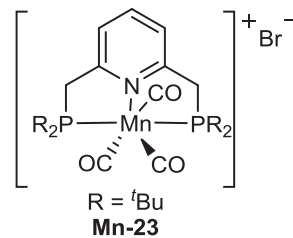
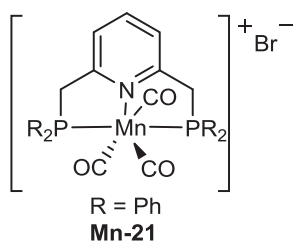
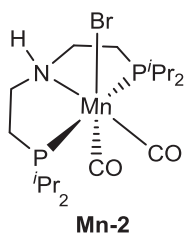
I am grateful to my whole SINCHEM family, especially from the 2016 batch, Sonia, Ravi, Valeria, Daniel, Ulisse, Marcelo, and Tran for the good time and valuable discussions.

I would like to thank to my all Indian friends, Vicky, Amit, Ravi, Basujit, Nitish, Pooja and Steffi for spending a great time together and making memorable trip to several places in Europe.

Lastly, I would like to thank my whole family: my parents, brothers and my cousins for their continued support and unconditional love in my whole study.

## Annexes

## List of synthesized complexes





## List of publications

### List of publications arising from the dissertation

- [1] **A. Kaithal**, M. Schmitz, M. Hölscher, W. Leitner, *ChemCatChem*. **2020**, *12*, 781-787. *On the mechanism of the Ruthenium-catalyzed  $\beta$ -Methylation of Alcohols with methanol.*  
“Published in a special issue: Pincer Chemistry and Catalysis”
- [2] **A. Kaithal**, P. van Bonn, M. Hölscher, W. Leitner, *Angew. Chem. Int. Ed.* **2020**, *59*, 215-220. *Angew. Chem.* **2020**, *132*, 221–226. *Manganese (I)-Catalyzed  $\beta$ -Methylation of Alcohols using Methanol as C<sub>1</sub> source.*
- [3] **A. Kaithal**, L. L. Gracia, C. Camp, E. A. Quadrelli, W. Leitner, *J. Am. Chem. Soc.* **2019**, *141*, 17487–1749. *Direct Synthesis of Cycloalkanes from Diols and Secondary Alcohols or Ketones Using a Homogeneous Manganese Catalyst.*  
“Selected as a cover feature in the Issue 44, Volume 141, and Number 44”.
- [4] **A. Kaithal**, M. Schmitz, M. Hölscher, W. Leitner *ChemCatChem*, **2019**, *11*, 5287-5291. *Ruthenium(II)-Catalyzed  $\beta$ -Methylation of Alcohols using Methanol as C<sub>1</sub> Source.*  
“Published in a special issue: New Concepts in Homogeneous catalysis”
- [5] **A. Kaithal**,<sup>‡</sup> S. Sen,<sup>‡</sup> C. Erken,<sup>‡</sup> T. Weyhermüller, M. Hölscher, C. Werlé, W. Leitner, *Nat. Commun.* **2018**, *9*, 4521. *Manganese-catalyzed hydroboration of carbon dioxide and other challenging carbonyl groups.*  
(<sup>‡</sup>Equal contribution. In the manuscript, the sequence of the authors are in the alphabetical order, however, the original sequence is described in authors contribution.)
- [6] **A. Kaithal**, M. Hölscher, W. Leitner, *Angew. Chem. Int. Ed.* **2018**, *57*, 13449-13453. *Angew. Chem.* **2018**, *130*, 13637-13641. *Catalytic Hydrogenation of Cyclic Carbonates using Manganese Complexes.*

### List of publications not including in the dissertation

- [7] **A. Kaithal**,<sup>†</sup> B. Chatterjee,<sup>†</sup> C. Gunanathan, *J. Org. Chem.*, **2016**, *81*, 11153-11161. *Ruthenium-Catalyzed Selective Hydroboration of Nitriles and Imines.*  
“Highlights: *Synfacts* **2017**, *13*, 0078.” (<sup>†</sup> Equal Contribution)
- [8] **A. Kaithal**,<sup>†</sup> B. Chatterjee,<sup>†</sup> C. Gunanathan, *Org. Lett.* **2016**, *18*, 3402-3405. *Ruthenium-Catalyzed Regioselective 1,4-Hydroboration of Pyridines.*  
“Highlights: *Synfacts* **2016**, *12*, 0956.” (<sup>†</sup> Equal Contribution)



- [9] **A. Kaithal**,<sup>†</sup> B.Chatterjee,<sup>†</sup> C. Gunanathan, *Org. Lett.* **2015**, *17*, 4790-4793. *Ruthenium Catalyzed Selective Hydroboration of Carbonyl Compounds.* (<sup>†</sup> Equal Contribution)
- [10] B.Chatterjee, D. Kalsi, **A. Kaithal**, A. Bordet, W. Leitner, C. Gunanathan, **2020**, *One-Pot Dual Catalysis for the Hydrogenation of Heteroarenes and Arenes.* (Manuscript is submitted)
- [11] **A. Kaithal**, M. Hölscher, W. Leitner, **2020**, *Manganese(I) Catalyzed  $\beta$ -Methylation of alcohols Using Carbon Monoxide and Hydrogen.* (Manuscript is submitted)

Akash Kaithal

## Curriculum Vitae

Date of Birth: 13.04.1993  
Place of Birth: Kanpur, India  
Citizenship: Indian  
Current Address: Bahnhofstraße 13, 52064 Aachen, DE  
Phone: (+49)15257685522  
E-Mail: kaithal@itmc.rwth-aachen.de

## University Education

Since 10/2016      Doctoral studies under supervision of Univ.-Prof. Dr. Walter Leitner and Univ. Prof. Elsje Alessandra Quadrelli in Chemistry, RWTH Aachen University and Université Lyon 1.

06/2011 – 06/2016      Integrated master of sciences (Int. M.Sc. 5 yr. course) in Chemistry, National Institute of Science Education and Research (NISER), Bhubaneswar, India.

06/2014 – 06/2016      Master theses in the group of Dr. Chidambaram Gunanathan.  
**Title of thesis:** *“Ruthenium catalyzed hydroboration reactions”*

05/2014 – 07/2014      Research Project under the supervision of Dr. G. V. Madhava Sharma in Chemistry, Indian Institute of Chemical Technology (IICT), Hyderabad, India.  
**Title of the project:** *“Synthesis of structural analogue of Rolipram”*

05/2013 – 07/2013      Research project under the supervision of Prof. Jitendra Kumar Bera in Chemistry, Indian Institute of Technology (IIT), Kanpur, India.  
**Title of the project:** *“Synthesis and characterization of Napthyridine-based tetra-dentate Ligands”*

05/2012 – 07/2012      Research project under the supervision of Dr. Sanjib Kar in Chemistry, National Institute of Science Education and Research (NISER), Bhubaneswar, India.

**Title of the project:** *“Synthesis and characterization of Silver Corrole Complexes.”*

### **Fellowship and Academic Distinctions**

10/2016 – 10/2019      Erasmus+ (the European Doctoral Programme on Sustainable Industrial Chemistry (SINCHEM)) Scholarship for Doctoral Studies.

06/2011 – 06/2016      Innovation in Science Pursuit for Inspired Research (INSPIRE) Scholarship for Masters Studies.

06/2011 – 06/2015      Gas Authority of India Limited (GAIL) Scholarship for Masters Studies.

04/2010 – 04/2011      Student of the Super-30 Kanpur, India.

### **School Education**

1996 – 2010      Seth Moti Lal Khedia Inter College, Kanpur, India (primary and grammar school)

### **Language Skill**

Hindi      Mother Tongue

English      Fluent

### **Personal Interest**

Cricket, Drawing, Drummer